Check Dam Construction for Sustainable Watershed Management and Planning

@seismicisolation
@seismicisolation

Check Dam Construction for Sustainable Watershed Management and Planning

Edited by

Zhanbin Li
State Key Laboratory of Eco-hydraulics in Northwest Arid Region, Xi'an University of Technology, China.

Peng Li
State Key Laboratory of Eco-hydraulics in Northwest Arid Region, Xi'an University of Technology, China.

Yang Yu
Jixian National Forest Ecosystem Observation and Research Station, CNERN, School of Soil and Water Conservation, Beijing Forestry University, China.

Peng Shi
State Key Laboratory of Eco-hydraulics in Northwest Arid Region, Xi'an University of Technology, China.

Guillaume Piton
University Grenoble Alpes, The French National Institute for Agriculture, Food and Environment (INRAE), Torrent Control, Snow and Avalanche Research Unit (ETNA), Grenoble, France.

WILEY

@seismicisolation

This first edition first published 2022
© 2022 John Wiley & Sons, Inc.

All rights reserved. No part of this publication may be reproduced, stored in a retrieval system, or transmitted, in any form or by any means, electronic, mechanical, photocopying, recording or otherwise, except as permitted by law. Advice on how to obtain permission to reuse material from this title is available at http://www.wiley.com/go/permissions.

The right of Zhanbin Li, Peng Li, Yang Yu, Peng Shi, and Guillaume Piton to be identified as the authors of the editorial material in this work has been asserted in accordance with law.

Registered Office
John Wiley & Sons, Inc., 111 River Street, Hoboken, NJ 07030, USA

Editorial Office
Boschstr. 12, 69469 Weinheim, Germany

For details of our global editorial offices, customer services, and more information about Wiley products visit us at www.wiley.com.

Wiley also publishes its books in a variety of electronic formats and by print-on-demand. Some content that appears in standard print versions of this book may not be available in other formats.

Limit of Liability/Disclaimer of Warranty
In view of ongoing research, equipment modifications, changes in governmental regulations, and the constant flow of information relating to the use of experimental reagents, equipment, and devices, the reader is urged to review and evaluate the information provided in the package insert or instructions for each chemical, piece of equipment, reagent, or device for, among other things, any changes in the instructions or indication of usage and for added warnings and precautions. While the publisher and authors have used their best efforts in preparing this work, they make no representations or warranties with respect to the accuracy or completeness of the contents of this work and specifically disclaim all warranties, including without limitation any implied warranties of merchantability or fitness for a particular purpose. No warranty may be created or extended by sales representatives, written sales materials or promotional statements for this work. The fact that an organization, website, or product is referred to in this work as a citation and/or potential source of further information does not mean that the publisher and authors endorse the information or services the organization, website, or product may provide or recommendations it may make. This work is sold with the understanding that the publisher is not engaged in rendering professional services. The advice and strategies contained herein may not be suitable for your situation. You should consult with a specialist where appropriate. Further, readers should be aware that websites listed in this work may have changed or disappeared between when this work was written and when it is read. Neither the publisher nor authors shall be liable for any loss of profit or any other commercial damages, including but not limited to special, incidental, consequential, or other damages.

Library of Congress Cataloging-in-Publication Data
Names: Li, Zhanbin, editor. | Li, Peng (Hydrology), editor. | Yu, Yang (Hydrology), editor. | Shi, Peng (Hydrology), editor. | Piton, Guillaume, editor.
Title: Check dam construction for sustainable watershed management and planning / edited by Zhanbin Li, Peng Li, Yang Yu, Peng Shi, and Guillaume Piton
Description: First edition | Hoboken, NJ, USA : Wiley, 2022. | Includes bibliographical references and index.
Identifiers: LCCN 2022009090 (print) | LCCN 2022009091 (ebook) | ISBN 9781119742401 (cloth) | ISBN 9781119742432 (adobe pdf) | ISBN 9781119742425 (epub)
Subjects: LCSH: Dams. | Soil conservation. | Watershed management.
Classification: LCC TC540 .C46 2022 (print) | LCC TC540 (ebook) | DDC 627/.8–dc23/eng/20220321
LC record available at https://lccn.loc.gov/2022009090
LC ebook record available at https://lccn.loc.gov/2022009091

Cover Design: Wiley
Cover Image: Courtesy of Peng Shi, Xi'An University of Technology

Set in 10/12pt TimesNewRoman by Straive, Pondicherry, India

@seismicisolation

CONTENTS

Notes on Contributors ..... **vii**

Preface ..... **xi**

Section I Dam Development **1**

1. **The Formation and Development of a Dam System in a Small Watershed in the Loess Plateau**
   Peng Li, Yang Yu, Peng Shi, Zhanbin Li, Hong Yan, Rui Wang, and Beilei Liu 3

2. **Water and Soil Conservation by Check Dam Construction**
   Peng Shi, Yang Yu, Lulu Bai, Zongping Ren, Kunxia Yu, Lie Xiao, Hong Yan, and Yan Zhang 23

3. **Regulating the Effect of a Check Dam System on Sediment Redistribution**
   Guoce Xu, Tanbao Li, Jibin Wang, Zongping Ren, Kunxia Yu, Zhanbin Li, Lie Xiao, Zhihai Wei, Dejun Wang, and Yan Zhang 41

4. **An Analysis of Sediment Sources and Water–Sediment Retarding Effects of Check Dams**
   Guoce Xu, Tanbao Li, Jibin Wang, Lulu Bai, Kunxia Yu, Peng Li, Jingmei Sun, Ying Jiang, and Miaoxia Wen 53

5. **The Regulation of Check Dam System in Erosion Dynamic Process**
   Tian Wang, Jingming Hou, Shuilong Yuan, Guoce Xu, Zhanbin Li, Dejun Wang, Jingmei Sun, Zhiqiang Min, Zhi Yang, and Zhengyan Ren 91

Section II Dam Erosion Processes and Dynamics **115**

6. **The Mechanism of Erosion Reduction by Check Dam**
   Qihua Ran, Honglei Tang, Peng Li, Feng Wang, Tian Wang, Zhihai Wei, Jingmei Sun, Miaoxia Wen, and Zhiqiang Min 117

7. **The Mechanism of Water Damage of Check Dam**
   Wen Wang, Guoqiang Yu, Shengdong Cheng, Mengjing Guo, Tanbao Li, Jibin Wang, and Dejun Wang 141

8. **Flood Control Risk Assessment on Warping Dam Systems**
   Shengdong Cheng, Tanbao Li, Jibin Wang, Zhihai Wei, Ying Jiang, Kunxia Yu, Binhua Zhao, Wen Wang, Penglei Hang, and Ganggang Ke 177

9. **Development and Utilization Model of a Check Dam System**
   Peng Shi, Peng Li, Shengdong Cheng, Lulu Bai, Laizhang Zhang, Daxiang Wang, Anli Ma, and Yan Zhang 189

10. **The Safety Distribution of Check Dam System and Potential of Check Dam Construction**
    Peng Li, Zhanbin Li, Laizhang Zhang, Binhua Zhao, Shuilong Yuan, Peng Shi, Daxiang Wang, Anli Ma, Ying Jiang, Miaoxia Wen, Zhiqiang Min, and Yan Zhang 209

Section III Check Dams and Open Check Dams in Debris-flows and Debris-flood Catchements **233**

11. **Design of Torrential Barriers: An Austrian Perspective**
    Johannes Hübl, Jürgen Suda, and Georg Nagl 235

@seismicisolation

12. Effect of Check Dams on Sediment Connectivity
Tomáš Galia, Václav Škarpich, and Ivan Smažák 245

13. French Experience With Open Check Dams: Inventory and Lessons Learnt Through Adaptive Management
Simon Carladous, Guillaume Piton, Damien Kuss, Gilles Charvet, Romain Paulhe, Maxime Morel, and Yann Quefféléan 253

14. Design of Open Check Dams and Their Application in the Wenchuan Earthquake Area
Jiangang Chen, Huayong Chen, Xi'an Wang, and Xiaoqing Chen 273

15. Prevention and Mitigation Against Debris Flow and Woody Debris in Japanese Design Using a Steel Pipe Open Sabo Dam
Toshiyuki Horiguchi and Hiroshi Kokuryo 285

16. Determining the Optimal Distance of Check Dams, Case Study: Shirkuh River, Iran
Mohammad Ebrahim Banihabib, Ali Mohammadi, and Mahmoud Piri Ardakani 297

Index **303**

@seismicisolation

NOTES ON CONTRIBUTORS

Mahmoud Piri Ardakani
Department of Rangeland and Watershed Management
Faculty of Natural Resources and Desert Studies
Yazd University
Yazd, Iran

Lulu Bai
Institute of Water Resources and Hydro-electric Engineering
Xi'an University of Technology
Xi'an, China

Mohammad Ebrahim Banihabib
Department of Water Engineering
College of Aburaihan, University of Tehran
Pakdasht, Iran

Simon Carladous
Isère, ONF
Direction Nationale Risques Naturels
Grenoble, France

Gilles Charvet
Savoie, ONF-RTM, Agence Alpes du Nord
Service de Savoie
Chambéry, France

Jiangang Chen
CAS Key Laboratory of Mountain Hazards and Earth Surface Process
Institute of Mountain Hazards and Environment
Chinese Academy of Sciences (CAS)
Chengdu, China
Beijing, China

Huayong Chen
CAS Key Laboratory of Mountain Hazards and Earth Surface Process
Institute of Mountain Hazards and Environment
Chinese Academy of Sciences (CAS)
Chengdu, China
Beijing, China

Xiaoqing Chen
CAS Key Laboratory of Mountain Hazards and Earth Surface Process
Institute of Mountain Hazards and Environment
Chinese Academy of Sciences (CAS)
Chengdu, China
Beijing, China

Shengdong Cheng
State Key Laboratory of Eco-hydraulics in Northwest Arid Region, Institute of Water Resources and Hydro-electric Engineering
Xi'an University of Technology
Xi'an, China

Tomáš Galia
Department of Physical Geography and Geoecology
University of Ostrava
Ostrava, Czechia

Mengjing Guo
Institute of Water Resources and Hydro-electric Engineering
Xi'an University of Technology
Xi'an, China

Penglei Hang
State Key Laboratory of Eco-hydraulics in Northwest Arid Region, Institute of Water Resources and Hydro-electric Engineering
Xi'an University of Technology
Xi'an, China

Toshiyuki Horiguchi
Department of Civil Engineering
National Defense Academy
Youkosuka, Japan

Jingming Hou
Institute of Water Resources and Hydro-electric Engineering
Xi'an University of Technology
Xi'an, China

@seismicisolation

Johannes Hübl
Institute of Mountain Risk Engineering
University of Natural Resources and Life Sciences
Vienna, Austria

Ying Jiang
Northwest Institute of Forest Inventory, Planning and Design, National Forestry and Grassland Administration
Xi'an, China

Ganggang Ke
State Key Laboratory of Eco-hydraulics in Northwest Arid Region, Institute of Water Resources and Hydro-electric Engineering
Xi'an University of Technology
Xi'an, China

Hiroshi Kokuryo
Nippon Steel Metal Product Co., Ltd.
Kiba, Koutouku
Tokyo, Japan

Damien Kuss
Isère, ONF
Direction Nationale Risques Naturels
Grenoble, France

Peng Li
Institute of Water Resources and Hydro-electric Engineering
Xi'an University of Technology
Xi'an, China

Tanbao Li
Northwest Institute of Forest Inventory, Planning and Design, National Forestry and Grassland Administration
Xi'an, China

Zhanbin Li
Institute of Water Resources and Hydro-electric Engineering
Xi'an University of Technology
Xi'an, China

Beilei Liu
Institute of Water Resources and Hydro-electric Engineering
Xi'an University of Technology
Xi'an, China

Anli Ma
Upper and Middle Yellow River Bureau
YRCC
Xi'an, China

Zhiqiang Min
Northwest Institute of Forest Inventory, Planning and Design, National Forestry and Grassland Administration
Xi'an, China

Ali Mohammadi
Department of Water Engineering
College of Aburaihan, University of Tehran
Pakdasht, Iran

Maxime Morel
Isère, University Grenoble Alpes,
INRAE, ETNA
Grenoble, France

Georg Nagl
Institute of Mountain Risk Engineering, Department of Civil Engineering and Natural Hazards
University of Natural Resources and Life Sciences
Vienna, Austria

Romain Paulhe
Savoie, ONF-RTM, Agence Alpes du Nord
Service de Savoie
Chambéry, France

Guillaume Piton
Isère, University Grenoble Alpes, INRAE
UR, ETNA
Grenoble, France

Yann Queffelean
Isère, ONF
Direction Nationale Risques Naturels
Grenoble, France

Qihua Ran
Institute of Hydrology and Water Resources Engineering
Zhejiang University of Technology
Hangzhou, China

Zongping Ren
Institute of Water Resources and Hydro-electric Engineering
Xi'an University of Technology
Xi'an, China

@seismicisolation
@seismicisolation

Zhengyan Ren
Soil and Water Conservation Bureau of Ningxia Water Conservancy
Yinchuan, China

Peng Shi
Institute of Water Resources and Hydro-electric Engineering
Xi'an University of Technology
Xi'an, China

Jürgen Suda
Alpinfra engineering + consulting GmbH
Vienna, Austria

Václav Škarpich
Department of Physical Geography and Geoecology
University of Ostrava
Ostrava, Czechia

Ivan Smažák
Department of Physical Geography and Geoecology
University of Ostrava
Ostrava, Czechia

Jingmei Sun
Northwest Institute of Forest Inventory, Planning and Design, National Forestry and Grassland Administration
Xi'an, China

Honglei Tang
Institute of Hydrology and Water Resources Engineering
Zhejiang University of Technology
Hangzhou, China

Daxiang Wang
Upper and Middle Yellow River Bureau
YRCC
Xi'an, China

Dejun Wang
Northwest Institute of Forest Inventory, Planning and Design, National Forestry and Grassland Administration
Xi'an, China

Feng Wang
Institute of Hydrology and Water Resources Engineering
Zhejiang University of Technology
Hangzhou, China

Jibin Wang
Northwest Institute of Forest Inventory, Planning and Design, National Forestry and Grassland Administration
Xi'an, China

Rui Wang
Institute of Water Resources and Hydro-electric Engineering
Xi'an University of Technology
Xi'an, China

Tian Wang
Institute of Water Resources and Hydro-electric Engineering
Xi'an University of Technology
Xi'an, China

Wen Wang
State Key Laboratory of Eco-hydraulics in Northwest Arid Region, Institute of Water Resources and Hydro-electric Engineering
Xi'an University of Technology
Xi'an, China

Xi′an Wang
CAS Key Laboratory of Mountain Hazards and Earth Surface Process
Institute of Mountain Hazards and Environment
Chinese Academy of Sciences (CAS)
Chengdu, China
Beijing, China

Zhihai Wei
Northwest Institute of Forest Inventory, Planning and Design, National Forestry and Grassland Administration
Xi'an, China

Miaoxia Wen
Northwest Institute of Forest Inventory, Planning and Design, National Forestry and Grassland Administration
Xi'an, China

@seismicisolation

Lie Xiao
Institute of Water Resources and Hydro-electric Engineering
Xi'an University of Technology
Xi'an, China

Guoce Xu
Institute of Water Resources and Hydro-electric Engineering
Xi'an University of Technology
Xi'an, China

Hong Yan
Faculty of Humanities and Foreign Languages
Xi'an University of Technology
Xi'an, China

Zhi Yang
Soil and Water Conservation Bureau of Ningxia Water Conservancy
Yinchuan, China

Guoqiang Yu
Institute of Water Resources and Hydro-electric Engineering
Xi'an University of Technology
Xi'an, China

Kunxia Yu
State Key Laboratory of Eco-hydraulics in Northwest Arid Region
Institute of Water Resources and Hydro-electric Engineering
Xi'an University of Technology
Xi'an, China

Yang Yu
Jixian National Forest Ecosystem Research Network Station
CNERN, Beijing Forestry University
School of Soil and Water Conservation
Beijing, China

Shuilong Yuan
Institute of Water Resources and Hydro-electric Engineering
Xi'an University of Technology
Xi'an, China

Laizhang Zhang
Upper and Middle Yellow River Bureau
YRCC
Xi'an, China

Yan Zhang
College of Urban and Environmental Sciences
Northwest University
Xi'an, China

Binhua Zhao
State Key Laboratory of Eco-hydraulics in Northwest Arid Region, Institute of Water Resources and Hydro-electric Engineering
Xi'an University of Technology
Xi'an, China

@seismicisolation
@seismicisolation

PREFACE

As recalled by a recent IPCC Special Report [1], land degradation, i.e. erosion and associated problems, is occurring over a quarter of the Earth's ice-free land area, thus affecting billions of people. Maintaining and enhancing life quality throughout every regions of the world require the implementation of efficient and cost-effective erosion control master plans. Recently, the influences of climate changes and anthropogenic activities on watershed management and sustainable ecosystems development have been in the spotlight of science. While ecological conservation projects and man-made structures (e.g. check dam or open check dam) naturally aim at increasing vegetation cover, mitigating hydrogeological risks, stabilizing the channel bed, the watershed-scale success of such conservation efforts is not easily quantifiable. Knowledge on how landscapes, i.e. landforms and ecosystems, respond to both of anthropogenic and climate at watershed scale should, however, be the foundation for implementing appropriate measures on watershed design and management. Moreover, it is still unclear if such ecological engineering measurements are able to alleviate the sensitivity of the ecosystem toward climate change (i.e. increase the resilience and resistance). Consequently, it is necessary for us to survey the anthropogenic-environment relationships for watershed management and to summarize the advantages and limitations of ecological engineering efforts during long-term watershed restoration.

This book brings a contribution by summarizing the current knowledge about check dams on a regional and global scale. Among all of the soil and water conservation structures, check dams are widespread and effective soil and water conservation measurements all over the world. It is obvious that watershed management projects require well-designed technique packages that generate income for local communities, overcome water shortage over a certain time period, and protect societies against risks and extreme events. This knowledge is crucial prior to correct restoration project design in the context of water storage as an ecosystem service and to estimate the success of conservation activities. Therefore, our aim is to propose more relevant intervention strategies for a sustainable watershed management and planning via construction of new check dams or adaptations of existing measures. Our forefathers did not wait to get strong scientific knowledge to build check dams and launch ambitious restoration master plans. They progressed by tests and trials, learning from successes and failures. Much knowledge was gained through time and recently thanks to the availability of new technologies and models. We decided to edit this book in order to share the knowledge acquired in China, Austria, France, Czech Republic, Japan, and Iran. We hope it will help readers to progress in the planning, design, and maintenance of check dams and sometimes prevent repetition of mistakes made elsewhere.

The ongoing research on check dams and watershed management, as reported in this book, is dealt with from different points of view. The book is divided into three sections. As discussed in Sections I and II, the development history of the check dams will be reviewed, and its ecological effects during watershed management will be elaborated in the Loess Plateau of China. Section I included four chapters, the main topic is the check dam development in the Loess Plateau of China. After more than 60 years of practice, check dams have gone through the process from scattered construction without scale to the dam system construction with small watershed as the unit. Check dams are an important type of water and soil conservation measure for the soil erosion control in the Loess Plateau. Sedimentation was redistributed with drainage structure. A large amount of natural environmental and humanistic environmental information are explained by the source identification. Section II focused on dam erosion dynamics and processes, six chapters are included, the main topic is the mechanism of flood and sediment reduction. By research, the effects of a check dam system on flood, runoff and peak discharge characteristics, the regulation of check dam system on erosion dynamic process were quantified. Silting patterns were related to runoff and deposition process. Restricted by economic and technical conditions, insufficient design and construction standards of check dams led to many ruined structures during high and extreme rainstorms. The investigation of the forms and causes of dam break and safety status was conducted to simulate and

@seismicisolation

analyze the mechanism of check dam breaking. Flood control risk was assessed in the check dam system watershed to analyze the construction scale suitable for check dam system. Check dams can have various utilization modes, including trapping of sediment and silting up to create agricultural land; flood control and reduction of flood disasters; or combined use of water resources, water diversion irrigation, and fish farming in check dam reservoir. Sections I and II provide a comprehensive perspective of the strong experience gained by Chinese authors working on the key erosion hotspot that is the Loess Plateau. Section III rather gathers elements from other regions, landscape types, and cultures. It is especially more oriented on gravel-bed, steep channels located in mountainous catchments experiencing debris flows and/or debris floods. In such locations, check dams have functions slightly different from the Loess plateau: the aim is not on water conservation and agriculture. In "Alpine" environment, check dams rather seek to influence the bed-load transport (dis)connectivity, to consolidate landslides, to ease artificial and spontaneous reforestation, and, generally speaking, to initiate and drive feedback loops in geomorphic and ecological processes to decrease erosion near headwaters. Two chapters address these topics with examples from Czeck Republic and Iran. Conversely, it is sometimes difficult to work and stabilize headwaters. Then, it is more relevant to trap the fraction of sediment transport that threatens downstream settlements, namely coarse grains and large wood. Open check dams, mechanically dredged after filling, are rather used in this case. Four chapters provide overviews on how open check dams are designed and implemented along with other mitigation structures in Austria, France, China, and Japan. These chapters enable to cross-compare how open check dam techniques were tailored to the peculiarities of these different contexts.

This book is a comprehensive first hand book including several scopes of interests in the field of soil and water conservation, watershed management, sediment connectivity, and ecosystem services. We surely believe that the book will have wide spectrum of readers with a common interest of ecologist, water resources scientist, foresters, risk managers, policy makers, and resources managers. It highlights the current status of check dam/open check dam research and also proposes lines of future research.

Sections I and II were supported by the National Key Research and Development Program of China (2017YFC0504704) and National Natural Science Foundation of China (U2040208, 42077073, 42177310, and 51779204). Section III was supported by the HydroDemo research project funded by the French State through the FNADT-CIMA funds and the European Union through the FEDER-POIA funds (Grant agreement PA0020551). The European Union is committed to the Alpine massif with the European Regional Development Fund (FEDER). The editors warmly thank Prof. Kostadinov, Prof. Lopez, and all anonymous reviewers for their reviews of all chapters during COVID-19.

Zhanbin Li, Peng Li, Yang Yu,
Peng Shi and Guillaume Piton
June 2022

REFERENCE

1. Olsson, L. et al. (2019). Land degradation. In: *Climate Change and Land: An IPCC Special Report on Climate Change, Desertification, Land Degradation, Sustainable Land Management, Food Security, and Greenhouse Gas Fluxes in Terrestrial Ecosystems*. https://www.ipcc.ch/site/assets/uploads/sites/4/2019/11/07_Chapter-4.pdf.

@seismicisolation

Section I
Dam Development

@seismicisolation
@seismicisolation

1

The Formation and Development of a Dam System in a Small Watershed in the Loess Plateau

Peng Li[1], Yang Yu[2,3], Peng Shi[1], Zhanbin Li[1], Hong Yan[4], Rui Wang[1], and Beilei Liu[1]

1.1. INTRODUCTION

Under the influence of climate change and human activities, the water flow and sediment in the Yellow River have undergone significant changes since the mid-1980s, and the amount of water flow entering the Yellow River has dropped sharply, while the sediment has increased. Identifying objective methods to understand water and soil conservation and ecological construction measures' effects and the reasons for the rapid decline of water flow and increased sediment in the Yellow River in recent years have become a focus of attention on the part of both domestic and foreign experts [1]. The channel is the focal point of water and soil erosion in the watershed, and its effective management, development, and use are beneficial for social, economic, and ecological development [2].

Long-term practical evidence in water and soil conservation indicates that a check dam is an important water and soil conservation measure to control soil erosion [3, 4]; it is the most effective measure to reduce the sediment inflow to the Yellow River quickly, reduce the sedimentation in the lower reaches of the Yellow River, and prevent the riverbed from rising [5, 6]. Check dams solve the two major problems of serious soil erosion and drought in the Loess Plateau effectively and unify the relation between ecological environment construction and local people's enrichment organically, which provides significant ecological, economic, and social benefits and plays an irreplaceable role in controlling soil erosion, reducing sediment entering the Yellow River, developing the regional economy, and improving people's living standards, as well as the ecological environment [7–9]. However, from the 1950s to the present, the most fundamental reason for the change in check dam construction is the frequent flood damage check dams suffer [10]. Because of the dams' properties, improper management, and excessive rainstorms, 7347 check dams in Northern Shaanxi Province were destroyed or damaged to varying degrees from July to August 1994, and these dam breaches damaged the largest area and number of dams and caused the most severe damage since the People's Republic of China was founded [11, 12]. Further, extensive floods in 2012 and 2013 caused by continuous rainstorms in Northern Shaanxi posed a great threat to the local check dams' safe operation.

In response to these problems, a large number of scientific and technological workers in China have conducted research on ways to optimize the layout of check dams, create a relatively stable dam system, and achieve the benefits of check dams' water and sediment reduction [13, 14]. After more than 60 years of practice, the check dam has undergone a process from scattered

[1] *Institute of Water Resources and Hydro-electric Engineering, Xi'an University of Technology, Xi'an, China*
[2] *Jixian National Forest Ecosystem Research Network Station, CNERN, Beijing Forestry University, Beijing, China*
[3] *School of Soil and Water Conservation, Beijing Forestry University, Beijing, China*
[4] *Faculty of Humanities and Foreign Languages, Xi'an University of Technology, Xi'an, China*

Check Dam Construction for Sustainable Watershed Management and Planning, First Edition.
Edited by Zhanbin Li, Peng Li, Yang Yu, Peng Shi, and Guillaume Piton.
© 2022 John Wiley & Sons, Inc. Published 2022 by John Wiley & Sons, Inc.

@seismicisolation

construction without scale to dam system construction with a small watershed as the unit, from lack of planning and design to the standardized construction and continuous improvement upon previous work [15]. At the same time, scientific and technological workers gained some successful experience in scientific planning, flood control and harvesting, single dam construction, and dam construction technology and management and realized fully that scientific planning is the foundation of, and engineering quality is the key to, dam system construction, and improving the existing management system guarantees the system's sound operation [16].

1.2. HISTORICAL EVOLUTION OF DAM SYSTEM CONSTRUCTION IN THE LOESS PLATEAU

1.2.1. Western Zhou Dynasty

According to records, sediment was used to improve soil in China during the Western Zhou Dynasty. According to Zhouli Kaogongji Jinagren, "The formation of gully is caused by water flow. Therefore, it is necessary to use terrain to prevent and control." Because water currents wash away the gullies easily, it can be beneficial to mankind only when the water is controlled.

1.2.2. Ming and Qing Dynasty

The first check dam in the Loess Plateau was formed by natural accumulation more than 400 years ago. In 1569, in Wangjiage Cave, Zizhou County, Shaanxi Province, the mountain slid on both sides of the gullies, blocking the channel, and collecting water and mud that formed a natural accumulation, i.e. a check dam, with a height of 62 m, a catchment area of 2.72 km^2, and dam land area of 53 hm^2.

The earliest record indicates that human construction of check dams began in Fenxi County, Shanxi Province, during 1573–1619. At that time, Mao Jiong, the county magistrate, made an announcement to encourage farmers to construct check dams. He stated that "People who can build a check dam can be rewarded, the food received does not need to be handed in, and the government issued a certificate to allow farmers to own the land. In three years, more than 300 families have built the check dam."

In 1877, there was a severe drought and no grains were harvested on the nearby slopes. However, the wheat yield in the dam area of Jia's family was 2100 kg/hm^2. The fact that the dam was rich in yield caused a sensation in the local area. In some surrounding villages, the rich hired people to build the dam, while the poor people built small dams through labor force exchange. Since then, the construction of check dams has developed gradually in this area.

1.2.3. The Period of the Republic of China

During the period of the Republic of China, preliminary investigations were carried out on the construction of check dams in the Loess Plateau, some specific measures for gully management were put forward, and check dams were built in Jingyugou, Xi'an to conduct an experiment. Some check dams were also built in certain local areas, such as Northern Shaanxi, Eastern Gansu, and Southern Ningxia.

The Republic of China government built the first check dam in the Jingyugou in the suburbs of Xi'an in 1945 in the Guanzhong Experimental Zone of the Yellow River Conservancy Commission. The small check dam was completed within two months, with a control area of 2.6 km^2. In the following year, the Guanzhong Soil and Water Conservation Experimental Zone built a second check dam in Jingyugou with 5 million yuan from the US special fund for China's soil and water conservation, with a control area of 6.17 km^2 and a height of 16.2 m.

In 1947, Cheng Fulong, a native of Linxian County, Shanxi, emphasized in his "Treatment of the Yellow River" that "building dams in gullies" is the only strategy to control the Yellow River. He believed that building embankments and dredging seaports downstream are "preventing nature and resisting nature," and "the project is complicated with little effect." "Building dams in the upper reaches of the Yellow River" constitutes "controlling nature and making use of nature" and "projects are easy to make huge profits." General Feng Yuxiang, the patriotic general, wrote to Zhao Shoujue, the Chairman of the Yellow River Water Conservancy Commission, during his inspection in the United States in 1947, stating: "The fundamental plan for the prevention of disasters on the Yellow River is to build large dams and small dams of local limestone and stone with the height of two or three feet, one or two foot at the beginning of each river and in every valley in Qinghai, Gansu, Ningxia, Suiyuan, Shanxi, Shaanxi, and Western Henan. In each province, 10 000 dams are built at most, and 8000 dams at least."

@seismicisolation

Moreover, he emphasized that the important thing is for them to be strong and not leak, so that the water can be retained, and it is easier to plant trees on the mountain. At the same time, he also pointed out that "There must be thirty or fifty talents in every province and county that can understand the importance of damming, and promote water conservancy." These statements showed that Feng Yuxiang had realized the importance of check dam construction in reducing disasters attributable to the Yellow River at that time and believed that the construction of check dams should not only rely on farmers but should include training professional talents to guide the dam construction.

1.3. CONSTRUCTION AND DEVELOPMENT OF CHECK DAMS SINCE THE FOUNDING OF THE PEOPLE'S REPUBLIC OF CHINA

Since the People's Republic of China was founded, the Party Central Committee and the State Council have made soil and water conservation in the Loess Plateau a national priority. The party committees and governments of all provinces (autonomous regions) in the Loess Plateau region regard soil and water conservation as a fundamental measure to change agricultural production conditions, improve rural living standards, govern the Yellow River, and improve the local ecological environment. As an important channel engineering measure for soil and water conservation, check dams have also been developed greatly. During the more than 50 years that check dams have been constructed, their construction in the Loess Plateau has gone through approximately four development stages.

1.3.1. First Stage (1949–1957)

Key trials and demonstrations of check dams were conducted during this stage, and small-scale promotion was also carried out on the basis of practical experience.

In the autumn and winter of 1949, Tao Ke, the cadre of the Department of Agriculture of the Northern Shaanxi Administration, and the water and soil conservation team of Mizhi Farm, built three check dams on a trial basis in Sunjiashan and Shuihuayuanzi on Mizhi Farm. A further 11 dams were built in 1950. In 1951, a survey team composed of more than 80 people of the Northwest Yellow River Engineering Bureau organized investigated the dam and reservoir projects to assess their ability to govern gullies. A total of 26 dam locations was surveyed and provided data for future dam construction. In September of the same year, a dam for flood storage and sediment retention with a height of 11 m was built in Xigou, Xifeng Town, Gansu Province. In the early 1950s, the earliest water and soil conservation test stations in the Loess Plateau, such as Suide, Yan'an, Xifeng, Pingliang, Tianshui, and Lishi, emphasized the importance of governing gullies and damming from the beginning in the small experimental watershed to which they belonged. Further, experimental research was conducted that played a demonstrative role. In 1952, Xifeng Soil and Water Conservation Station built the first dam, Longdong, at Nanxiaohegou. From 1953 to 1954, the Suide Soil and Water Conservation Station built five check dams successively in the Jiuyuangou watershed with a storage capacity of more than 1 million m^3 and a single dam control area of approximately 10 km^2. Later, dams were built in larger branches, which controlled a drainage area of 70.7 km^2 effectively. As these check dams were used in experiments and demonstrations, they included three forms of dam structure: first, the dams in the main gully were composed of earth dams, spillways, and discharge tunnels, which can accomplish water storage and discharge; second, the branch gully dam was composed of two facilities, an earth dam and a discharge tunnel, which block the upstream water and sediment completely; third, the small branch gully dam had only one large earth dam, which relies mainly on storage capacity and full storage retention. By treating slopes and heightening old dams, they could achieve relative stability. Driven by the demonstration and propaganda of Suide Station, Suide, Mizhi, Jiaxian, and Wubao Counties were taken as the key pilot areas. Two hundred and fourteen dams were built within two years, most of which were less than 10 m high with control areas within 0.8 km^2. These dams achieved significant benefits of dam land and higher production, and were well received by the local people.

While all soil and water conservation stations were trying to build gully dams, since 1953, the Northwest Yellow River Engineering Bureau, with the vigorous cooperation of various provinces (regions), had built check dams in the middle and lower reaches of the main gully in small watersheds in Northern Shaanxi, Western Shanxi, Eastern Gansu, and Hohhot through soil and water conservation stations' active demonstration and promotion of check dams' construction.

@seismicisolation

The dams were designed in accordance with the technical regulations of small reservoirs, with an earth dam, spillway, and discharge tunnel, and good construction quality. All of these efforts promoted the development of check dam construction in the Loess Plateau. With the establishment of agricultural cooperatives and people's communes, the citizens' enthusiasm for damming was unprecedentedly high. By the end of 1954, there were more than 3000 check dams with more than 2300 hectares of dam land in Shaanxi Province. By April 1956, more than 1700 dams had been built in the province in Zhongyang County alone. More than 4200 dams were built in Shilou County in 1958 alone. By 1957, more than 9200 check dams were built in the Yulin area of Northern Shaanxi, 29 of which had a storage capacity of more than 1 million m^3. As a result of their widespread success, dam construction technology began to gain popularity among cadres and the public everywhere.

1.3.2. Second Stage (1958–1970)

The concept of a "dam system" was developed at this stage. The success of the previous stage strengthened people's confidence in building check dams. Therefore, soil deposition by dam building technology in the middle reaches of the Yellow River was promoted fully. A leading institution for farmland infrastructure construction that focused on gully dams was established in Shilou County, Shanxi Province, and 4216 dams were built, which *The People's Daily* reported. In the construction of large-scale check dams, major technological innovations and tool reforms were carried out in various regions, and blasting to loosen the soil and rack trucks to transport it began to be used often to hasten construction. The remaining labor force was organized into the basic farmland construction team to carry out dam construction and maintenance throughout the year; during the slack season, most laborers were organized to carry out assault months and assault days that focused on constructing medium-sized dams. In 1958 in particular, the Agricultural Construction Department of Shanxi Province succeeded in blasting and building dams in Zhongyang and other counties, which advanced the speed of dam construction. Although there were natural disasters during the early 1960s and the "Cultural Revolution" after the mid-1960s, dam construction was still promoted widely in the Loess Plateau.

In 1962, the "Regulations on Rewarding People's Communes for Building Soil and Water Conservation Projects" the State Council issued pointed out that for the new dam land of check dams built in waste gullies, all of its output belonged to the production team that participated in the construction. Starting from the benefit year, there was no procurement for three to five years. The successful test of check dams and the State Council's policies stimulated the people's enthusiasm to build dams further. In the first half of 1960, the 4 soil and water conservation stations of the Yellow River Conservancy Commission of the Ministry of Water Resource in Xifeng, Suide, Tianshui, and Huining used directional blasting to build 33 earth dams, which increased work efficiency 40–50 times. During the 12 years from 1958 to 1970, 27 600 check dams were built in the Loess Plateau that covered more than 33 000 hectares of dam land. In the typical small watersheds with well-developed check dam construction in Western Shanxi and Northern Shaanxi, one or several Yaoba should be added at appropriate locations on the dam to intercept upstream floods and form a simple dam system. Hence, the concept of "dam system" was generated.

Since then, with the increase of check dams, the problem of flood control and harvesting in the dams had become more and more prominent. The Suide Water Conservation Station had conducted experiments since 1961 on flood control and harvesting with more dams in the Wangmaogou watershed. A dam with more dam land was used as a production dam to ensure harvest and discharge flood water for farming; dams with less land, such as rush-harvesting dams, and the flood discharged from production dams, was introduced into storage to form "storage and farming"; one of the original production dams was selected and heightened as a flood interception dam to form a "storage and farming in rotation," which unified flood control, sediment retention, and production to build a dam system that achieved good results.

1.3.3. The Third Stage (1971–1985)

Dam systems were built on a large scale during this stage. In 1971, the Yellow River Conservancy Commission of the Ministry of Water Resource, the hydroelectric board of Shaanxi, and the water control bureau of Shanxi, held a joint collaboration meeting and established the Shaanxi-Shanxi Water Dam Test and Research Group to conduct water dam test research, in which they achieved fruitful results. This achievement won the prize at the National Science

@seismicisolation

Conference in 1978. In 1973, the Soil and Water Conservation Conference held in Yan'an required the experience with hydraulic filling method to be summarized and promoted; in 1977, the Yellow River Conservancy Commission of the Ministry of Water Resource and the Shaanxi-Shanxi hydraulic filling test group hosted a scientific research meeting in Linfen; in 1979, the hydroelectric department held a meeting to exchange experience in hydraulic filling in Taiyuan and visited the construction sites of hydraulic filling dams in five counties in Luliang City. These meetings promoted the popularization and application of hydraulic filling in the Loess Plateau further.

The hydraulic filling method for dam construction was characterized by high efficiency, low cost, good quality, and simple construction; further, it was easy for local people to operate, which could generally improve the working efficiency several times or even dozens of times compared with manual ramming and rolling dams. Therefore, in the 1950s, check dams that required the support of plenty of labor could be completed by using the hydraulic filling method with a production team. Since then, the hydraulic filling method for dam construction has been popular in several provinces (autonomous regions) of the Loess Plateau region, and every production team was able to build dams. According to the statistics of 28 counties in the West of Shanxi Province in 1976, there were nearly 1000 production teams using hydraulic filling for dam construction, with a total of 420 sets of special hydraulic filling equipment and 600 sets of simultaneous equipment. The giant hydraulic for earth-moving produced in Xingxian County was popularized throughout the province. In approximately 1972, dams were built in nearly all gullies in Northern Shaanxi, Shanxi, Western Gansu, and Inner Mongolia. According to incomplete statistics in 1977, more than 8000 sluicing-siltation earth dams had been built in Shanxi and Shaanxi provinces. In just a few years, 15 000 dams were built in Yulin alone. In Yan'an and Yulin City, 11 700 hm^2 of dam land were added in the three years from 1973 to 1975, and nearly half of the dam land in Shanxi Province was constructed during this period. Check dams built during this period in the Huangfuchuan Watershed in Inner Mongolia accounted for more than 60% of the total current check dams.

During this period, there was a bias in some places that did not pay attention to science and did not follow the laws of nature. In some places, the planning and engineering design of the dam system was unreasonable, the construction quality was poor, some watersheds were small and clustered without backbone, and water damage threat existed in some dams. During 1973–1978, some dams were damaged to different degrees during the rainstorms. On 25 August 1973, in Yanchuan County, Shaanxi Province, where there was 112.5 mm of rainfall, 3300 of the 7570 check dams suffered water damage of varying degrees; heavy rains in 1975, 1977, and 1987 caused more than 30 000 check dams to be damaged to varying degrees in the Qingyang area of Gansu Province, the Yulin and Yan'an areas of Shaanxi Province, and 28 counties in Western Shanxi Province. The serious damage the check dams suffered led the people to doubt their effectiveness. However, because of continuous summaries of experience, the dam number, dam system layout, and construction technology of check dams during this period had made greater breakthroughs than in the past, and these check dams were effective in retaining sediment and increasing production.

1.3.4. The Fourth Stage (1986–1995)

At this stage, key engineering for gully control was undertaken actively, and the dam system was improved. On the basis of conscientiously summarizing the experience of check dam construction during the previous 30 years, many studies were carried out on dam system planning, engineering structure, design standards, and check dams' construction sequence. The public recognized widely the experience of "making dams and reservoir protected each other," and "small groups with backbones." In the spring of 1984, in accordance with the requirements of the Planning Commission of China and the hydroelectric department, the Yellow River Conservancy Commission of the Ministry of Water Resource drafted the "Reference Materials for the Key Engineering for Gully Control for Water and Soil Conservation in the Middle Reaches of the Yellow River," which demonstrated the necessity and feasibility of the key engineering necessary for gully control, as well as the implementation plan. In the same year, according to the preliminary plan of the key engineering for gully control the Middle Yellow River Bureau proposed, the Yellow River Conservancy Commission of the Ministry of Water Resource asked the hydroelectric department to increase its investment in the construction of the key dam engineering needed to control gullies in the Middle Yellow River area with

@seismicisolation

coarse sediment and include it in the capital construction plan. In 1985, the National Planning Commission approved including a key engineering plan for gully control in the capital construction plan, and it was implemented in the first year of the Seventh Five-Year Plan. In the area of the Loess Plateau with the most serious soil erosion (annual erosion modulus greater than 5000 t/km^2), the key dam for gully control was built, combined with terraces, forests and grasses on the slope, and small gullies and dams in the branch gully with a catchment area of 3–5 km^2. The storage capacity of most dams was 500 000 to 1 million m^3, while the capacity of several was 1–2 million m^3, and the capacity of individual dams that could be used as control projects reached 5 million m^3.

At the end of 1985, the Middle Yellow River Bureau put forward the first draft of the key engineering plan for gully control, which was taken as a part of the "Special Governance Plan for Soil and Water Conservation in the Loess Plateau Region of the Yellow River watershed." After it was approved, the experiment was launched in 1986. In the dam system layout, on the basis of several check dams in the channel, the key dam should be built in the proper place with better dam conditions according to the channel situation to control the flood in the entire watershed, ensure the safe production of dam system engineering, and give full play to its comprehensive function of storage, arresting, infiltration, and drainage. In 1984 and 1986, the hydroelectric department formulated and issued successively the "Interim Regulations on the Design and Construction of hydraulic filling dams" and "Interim Specifications for Key engineering for Gully Control of Soil and Water Conservation," which led to scientific and standardized dam system construction. In 1994, Shanxi Province in Kanghegou of Fenxi County and Zhaojiagou of Yonghe County undertook the pilot project of dam system ecological engineering construction.

1.3.5. The Fifth Stage (After 2000)

In the middle and late 1990s, the development of dam ecological agriculture in the Loess Plateau entered a new stage. During this stage, the Party Central Committee and the State Council were very concerned about controlling soil erosion and improving the ecological environment. On 5 August 1997, General Secretary Jiang Zemin read the report on the "Investigation on the Control of Soil Erosion and Construction of Ecological Agriculture in Northern Shaanxi" by Vice Premier Jiang Chunyun of the State Council and provided important instructions. In his instructions, Jiang Zemin called on the people of the entire country to ". . . place great emphasis on afforestation, greening deserts, and construction of Eco-agriculture," and "create a beautiful northwestern region." From 28 August to 1 September 1997, the State Council held an on-site meeting on "National Soil Erosion Control and Eco-agriculture" in Northern Shaanxi and made arrangements for the national ecological environment governance and construction of Eco-agriculture. This was the highest-level meeting on Eco-agriculture projects held in the northwest region. On 5 October 2000, Huang Ziqiang, Deputy Director of the Yellow River Conservancy Commission of the Ministry of Water Resource, published the "Practice and Plan for Construction of Dam System Ecological Project in Gullies in the Loess Plateau" in the No. 10 of Soil and Water Conservation in China, which promoted the development of dam system ecological projects in the Loess Plateau. On 9 August 2001, Wang Shucheng, Minister of Water Resource, emphasized at a meeting commemorating the tenth anniversary of the promulgation and implementation of the Soil and Water Conservation Law: "In the middle reaches of the Yellow River, check dams should be taken as the main measures for soil erosion control and strengthen the construction of dam systems with the focus on key engineering for gully control." In September 2002, the "Experience Exchange and Commendation Meeting of Soil and Water Conservation Ecological project of Yellow River" the Yellow River Conservancy Commission of the Ministry of Water Resource held in Tianshui City proposed that the construction of the gully dam system must be placed in an outstanding position. After the Soil and Water Conservation Law was revised in 2011, it indicated clearly that check dams are the main measures to control soil erosion.

1.4. CHARACTERISTICS OF CHECK DAM CONSTRUCTION IN THE NEW PERIOD

On 14 July 2002, the "Recent Key governance and Development Plan of Yellow River" the State Council approved pointed out clearly that "The governance measures focus on the construction of the gully dam system and key projects for gully control." At present, the construction of dam system ecological projects in the Loess Plateau has been developed most effectively, with the fastest speed, large scale, and high

@seismicisolation

quality. Dam agriculture was built and the ecological environment was improved because of the following characteristics.

1.4.1. Carrying Out Dam System Construction and Comprehensive Watershed Management Simultaneously

Many good governance models have emerged in the Loess Plateau through the vigorous development of the comprehensive management of soil and water conservation.

1.4.1.1. Wangmaogou Watershed in Northern Shaanxi

After more than 40 years of comprehensive governance and summary, the Yellow River Conservancy Commission of the Ministry of Water Resource Suide Water and Soil Conservation Scientific Experiment Station established a unique comprehensive governance model of Wangmaogou watershed with its "comprehensive planning, comprehensive governance, slope and gully governance, gully control as priority, strengthening management and protection, and dynamic regulation." In the past, the water and soil erosion in the Wangmaogou watershed were extremely serious, and thus, the achievements made after more than 40 years of continuous comprehensive management were of great significance. The degree of watershed treatment has now exceeded 65%, and a large number of gullies have been managed to a basic extent, such that the sand transport modulus has been reduced by 95.8% compared with that before treatment. The cultivated land area has been decreased from 340 hm^2 before treatment to 187 hm^2, and the cultivated land per capita was reduced by 40%. However, per capita grain production increased by approximately three times. Now the per capita farmland area is 0.18 hm^2, of which there is a dam field of 0.04 hm^2. The dam land alone can produce more than 150 kg of grain per capita annually, which lays a solid foundation for controlling soil erosion in the watershed effectively and relieving local people from poverty by increasing their income tremendously.

1.4.1.2 Small Watershed in Zhuanglang County, Gansu

Since 1996, 37 key dams and check dams have been built in 10 key small watersheds of Zhuanglang County. And 350 000 tons of sediment were intercepted by various projects. More than 4.6 million cubic meters of water were intercepted, which was equivalent to the annual water storage capacity of 1 million mu of terraced fields. Fifteen check dams in the Yulingou watershed control two-thirds of the watershed's area. Essentially, the entire watershed has achieved a terraced mountain, irrigated flat land, a gully dam system, watershed ecological restoration, and road networking, which is a typical model of comprehensive governance of small watersheds.

1.4.1.3. Xiheidai Small Watershed of Zhungeer Banner, Inner Mongolia

From 1981 to the present, through 30 years of soil and water conservation and ecological project construction, remarkable governance results have been achieved in the Xiheidai small watershed. The desolate mountain ravine in the past is covered in lush, green vegetation that demonstrates the ecological, economic, and social benefits of the conservation and ecological work there. Xiheidai small watershed governance is a leader in comprehensive governance of soil and water conservation in the loess hilly and gully region. As of 2011, the slope treatment area of the Xiheidai small watershed was 2241.6 hm^2, and the slope treatment degree reached 70.05%; slope measures, as the first defense in the governance of small watersheds, reduce runoff and sediment on slopes, help slow the inflow of sediment, reduce flood control pressure on the dam system, reduce storage capacity and siltation, extend the dam/dam system's service life, and improve its relative stability.

1.4.2. Establish of Typical Demonstration Dam System from Point to Region

Located in the first subregion of the loess hilly and gully region, the Jiuyuangou small watershed, Suide County, Shaanxi Province, has a total area of 70.7 km^2, a gully density of 5.34 km/km^2, and an annual soil erosion modulus of 18120 t/km^2. This small watershed channel project was constructed in the 1950s. As floods damaged the incomplete dam system many times because of its imperfections, the project was destroyed to varying degrees. Later, dam system construction was improved and was designed scientifically and reasonably. By the first half of 2000, 203 large and small dams had been built in the watershed, including seven key engineering dams for gully control, with a total storage capacity of 27.32 million m^3, dam land of 315 hm^2, blocked mud of 18 million m^3 of sediment, and a dam land area of 260 hm^2. Rainstorms have damaged the Jiuyuangou dam system several times in recent years. However, the

@seismicisolation

upper, middle, and lower reaches of the dam system are planned and managed in a unified way because the dam system construction promotes the conversion of farmland to forest and grassland, the vegetation on the gully slope has increased, and the dam supports the system in the gully. With the combination of engineering and biological measures, silting, control, drainage and storage, the crops in the dam are harvested every year. Thus, it has become a typical demonstration watershed for dam system construction in the middle reaches of the Yellow River. The dam system's mud interception and water storage benefits accounted for 66.7 and 70.8% of the total interception benefits of the soil and water conservation measures, respectively, and the sediment in the watershed basically was unable to flow out of the gully. The dam land's benefit of increasing harvest yields is also very prominent, and its output per unit area is more than nine times that of slope farmland.

The small watershed of Dongshiyang, Shilou County, Shanxi Province, covers an area of 103 km^2, with a soil erosion area of 94 km^2. On the basis of years of comprehensive governance, the construction of the channel dam system has increased, and more than 130 large and small dam reservoirs have been built. Many branch gullies in the watershed have realized full storage and full retention of flood and sediment. In the past, it used to be said that ". . . it was characterized by bare mountains, rocks in the gully, and disasters occurring every year, no harvesting for many years." Now it has become a demonstration dam system gully with planned rivers and walls, and a flat dam with a good ecological environment engineering demonstration ditch. The annual net income can exceed 500 000 yuan from the seven key dam projects' dam land alone, as well as protect cultivated land downstream, and breeding. More than 160 hectares of land have been silted in the entire watershed, more than 600 hectares of cultivated land have been converted into forests, and 470 hm^2 of economic forests and 530 hm^2 of water conservation forests have been planted. Food production has doubled compared with that before the governance, per capita income has exceeded 1000 yuan, and the people's quality of life has been improved significantly.

1.4.3. Enriching and Developing the Theory of Check Dams and Standardizing Construction

In recent years, the three systems of "project legal person system, bidding system, and construction supervision system" have been attempted, as required in the ecological engineering construction of the dam system in the Loess Plateau. Further, the construction unit has been clarified and is identified as a unit engaged in organizing project construction and management established or entrusted by the project legal person. The bidding system is a major competitive transaction method for market construction under the market economy system. In the process of bidding, construction, inspection, and approval of key gully control projects, new systems and mechanisms have been created for supervision and management.

With respect to the construction supervision system, all of the provinces (regions) in the Yellow River Watershed entrusted Xi'an Yellow River Engineering Supervision Co., Ltd. to supervise the implementation of the ecological engineering of the dam system in the Yellow River Soil and Water Conservation Ecological Project in 2001 and 2002, to give full play in the role of supervising project construction, controlling project progress, projecting investment and project quality, managing project contracts and information, and coordinating the relation between construction and construction units. The Inner Mongolia Autonomous Region has also established the "Yellow River Soil and Water Conservation Ecological Engineering Project Supervision Department," and Shanxi Province has established soil and water conservation supervision agencies in 11 prefectures (cities). Qinghai, Shaanxi, Shanxi, and Henan have all conducted pilot bidding for key gully control projects. The supervision engineers supervise the engineering construction in an open, fair, just, and realistic manner based largely on the relevant project approval documents, design reports, technical specifications, and industry standards, as well as the "Soil and Water Conservation Comprehensive Treatment Project Construction Supervision Measures" (for trial implementation) and "Soil and Water Conservation Comprehensive Treatment Project Construction Supervision Rules" (for trial implementation), combined with the specific conditions of the project construction. Further, the supervision report and on-site supervision instructions are submitted timely to ensure the project's smooth progress.

A series of rules and regulations has been compiled and issued under the organization of the Ministry of Water Resources, the Yellow River Conservancy Commission, and the Upper and Middle Reaches Administration Bureau of the Yellow River, to promote standardized, normalized, scientific, and systematic dam system projects continuously, such as

@seismicisolation

"Technical Specifications for Key Gully Control Projects for Soil and Water Conservation," "Management Measures for Key Gully Control Projects of Water and Soil Conservation in the Yellow River Watershed," "Paid Investment Methods for Key Gully Control Projects of Water and Soil Conservation," "Financial Management Measures for Key Gully Control Projects of Water and Soil Conservation," and "Flood Control Work Regulations for Key Gully Control Projects of Soil and Water Conservation," etc. Shaanxi Province has issued the "Shaanxi Province Check Dam Management Measures," and the "Shanxi Province Check Dam Engineering Technical Specifications," and many prefectures (cities) have formulated relevant regulations, methods, and implementation rules based on local conditions. This has promoted the standardized construction of dam ecological engineering effectively and laid the foundation for a scientific management system.

The Upper and Middle Reaches Administration Bureau of the Yellow River put forward the design method of using two major structural types of a dam discharge project for the key engineering hub composition after study and discussion by summarizing the successful experience of check dam construction based on the Loess Plateau's characteristics of high flood peaks, small flow, and short duration. The preliminary dam system relative balance theory has been put forward by the majority of dam system engineering professionals based on many years of practice and the fact of the limited project storage capacity and the infinite sediment in the Loess Plateau, and this theory is under intensive study at present and will be applied gradually in the planning and construction of the dam system. In view of the slow dehydration and consolidation of the heavy silty loam with a high content of clay in the Loess Plateau, some experts in the dam system field have explored a method to drain dams with a microporous corrugated pipe recently, which makes water fall dams possible in the Loess area with its high clay content, and has reduced the project cost greatly. The experimental research on the combination of directional blasting and hydraulic filling dams, dam loosening through arsenic blasting, optimized simulation of water release structures, planning to optimize dam systems for key gully control projects, and rapid greening of dam slopes have solved the technical problems in engineering planning and design and enriched and developed the design and construction theory, which will surely promote the dam system's current large-scale ecological engineering construction.

1.5. ACHIEVEMENTS IN THE CONSTRUCTION OF CHECK DAMS IN THE LOESS PLATEAU

1.5.1. Development History of Check Dam Construction in the Loess Plateau

The construction of check dams in the Loess Plateau essentially began in the 1950s, and the two peak periods of construction were from 1968 to 1976 and 2004 to 2008. Statistics show that by the end of 2018, there were 59 154 check dams in the Loess Plateau, including 5877 backbone dams, 12 131 medium-scale dams, and 41 146 small-scale dams. 18 018–24% of the large-scale dams (backbone dams), 68% of the medium-scale dams, and 69% of the small-scale dams – that were built before 1980. The check dams of medium-scale and the scale above occupy a cumulative control area of 48 000 km^2 and hold nearly 5.65 billion tons of sediment. Thirty percent of the backbone dams, 66% of the medium-scale dams, and 69% of the small-scale dams were built before 1980. The peak construction period of backbone dams was from 2000 to 2010, and nearly 50% of these dams were constructed during this period; the peak construction period of medium- and small-scale dams was in the 1970s, when 47% of medium-scale and 48% of small-scale dams were constructed (Figure 1.1).

Based on the data of the first national water conservancy census in 2011, and the quantitative changes caused by the addition of check dams and functional changes from 2012 to 2018, the statistics in November 2019 showed that there are 58 776 check dams in the Loess Plateau, including 5905 large-scale dams, 12 169 medium-scale dams, and 40 702 small-scale dams that account for 10.05, 20.70, and 69.25% of the total number of check dams, respectively (Figure 1.2).

The loess hilly and gully areas and the loess plateau and gully areas are the main types of water and soil erosion areas in the Loess Plateau. Among them, the surface area of hilly and gully areas accounts for approximately one-third of the Plateau's total area, and that of plateau and gully areas accounts for approximately 4% of the total. It can be seen from Table 1.1 that the number of check dams in the hilly and gully areas accounts for 81.23% of the total number of check dams in the Loess Plateau, while the number of check dams in the plateau and gully areas accounts for 2.78% of the total.

@seismicisolation

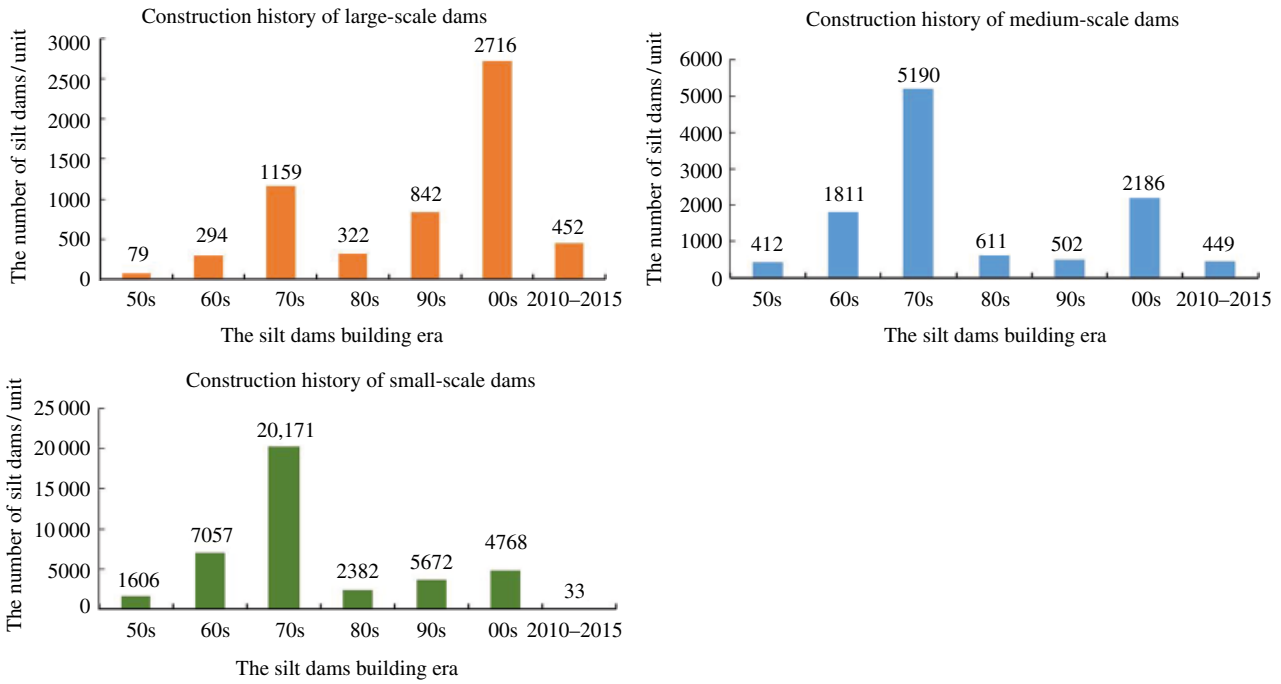

Figure 1.1 Construction history of check dams in the Loess Plateau.

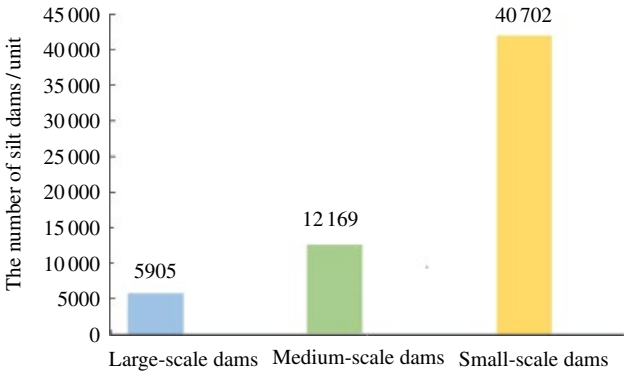

Figure 1.2 The number of different types of check dams.

1.5.2. Distribution According to Key Areas of Water and Soil Erosion

Sand-rich areas, sand-rich areas with coarse sand, and concentrated source areas of coarse sediment are key areas of water and soil erosion in the Loess Plateau [16]. The number of check dams in the areas above are 52 241, 40 876, and 12 072, respectively, which account for 88.88, 69.55, and 20.54% of the total number of check dams in the Loess Plateau, respectively (Table 1.2).

The analysis showed that the distribution density of check dams in the sand-rich areas, sand-rich areas with coarse sand, and the concentrated source areas of coarse sediment are 0.25/km^2, 0.52/km^2, and 0.64/km^2, respectively, which was significantly higher than the average distribution density of 0.09 dams/km^2 in the Loess Plateau [17].

1.6. EVOLUTION AND ITINERARY OF THE DAM SYSTEM IN A TYPICAL SMALL WATERSHED

1.6.1. Historical Analysis of the Evolution of Jiuyuangou Dam System

1.6.1.1. Test and Demonstration Stage (1953–1963)

In 1953, five check dams were built in the main gully and the larger branch gullies first, and then the construction of check dams progressed gradually into the branch gullies. The dam system construction at this stage involved building a dam at the mouth of the main gully or larger branch gullies in the first step, and building the second check dam upstream of the first dam after siltation, which is used to hold the upstream flood and ensure the downstream dam body and the safe operation of the dam land. This is performed from the bottom repeatedly, with the top storing up and the bottom seeding until it is full. The advantage of this layout is that check dams settle quickly, provide benefits early, and the dam system forms rapidly as well. The construction method is primarily manual compaction, and the dams take considerable time to construct.

@seismicisolation

Table 1.1 Statistics of check dams in the water and soil erosion areas of the Loess Plateau.

	Loess hilly and gully areas		Loess Plateau and gully areas		Other areas		
Types	Number (dam)	Ratio (%)	Number (dam)	Ratio (%)	Number (dam)	Ratio (%)	Loess Plateau area
Large dams	4631	78.43	374	6.33	900	15.24	5905
Medium dams	10698	87.91	180	1.48	1291	10.61	12169
Small dams	32416	79.64	1078	2.65	7208	17.71	40702
Total	47745	81.23	1632	2.78	9399	15.99	58776

Note: Other areas include loess terrace areas, alluvial plain areas, windy sand areas, arid grasslands, highland grasslands, and forest areas.

Table 1.2 Statistical of check dams in key areas of water and soil erosion in the Loess Plateau.

Types	Large dams	Medium dams	Small dams	Total	Proportion (%)
Concentrated source areas of coarse sediment	1104	3680	7288	12072	20.54
Sand-rich areas with coarse sand	3174	9652	28050	40876	69.55
Sand-rich areas	4930	11269	36042	52241	88.88
Loess Plateau areas	5905	12169	40702	58776	100

A total of 148 check dams were built during this stage, with a density of 2.1 dams/km^2, a storage capacity of 14.655 million m^3, a sediment retention capacity of 10.943 million m^3, and a silting capacity of 153.61 hm^2. A total of 54 hm^2 of land has been silted, with an annual average of 5.4 hm^2. On 1 August 1961, a heavy rainstorm occurred in the watershed, with an average precipitation of 57.5 mm. The center of the rainstorm is located here once in 86 years, with a mean of once in 20 years. Sixty-eight check dams were destroyed by water, which accounted for 45.9% of the total number of dams. Among them, 30 dams were destroyed completely, which accounted for 44.1% of the number of dams destroyed by water, 23 were largely destroyed which accounted for 33.8% of the number of dams destroyed by water,and 15 spillways were damaged which accounted for 22.1% of the number of dams destroyed by water.

1.6.1.2. Development Stage of the Dam System (1964–1977)

The successful test of hydraulic filling dams' construction technology has accelerated the development of check dams greatly and promoted the full launch of the construction of the dam system in the watershed. During this period, 237 more dams were built, for a total of 333, with a density of 4.7 dams/km^2, a total storage capacity of 12.3886 million m^3, a sediment retention capacity of 9.248 million m^3, and a silting capacity of 123.43 hm^2. The characteristics of the construction of the dam system at this stage were "small and more clusters, small dominated." The operational mode is "storage and seeding in parallel." The "dead gourd dams" were built in the tributary gully, all of which were used to block the flood and sediment from upstream. The advantages of the dam construction and application are small investment, fast formation of the dam system, and high utilization rate of dam land. Its disadvantages are no controlling backbone project in the dam system, low system design standards, poor flood control capacity, unsafe project, unguaranteed production of dam land, and serious flood damage.

1.6.1.3. Backbone Control Stage of the Dam System (1978–1983)

During this stage, the dam system was rebuilt (expanded) based on the experience and lessons of the previous stage according to the principle of merging small dams into large dams, combining large and small dams, and backbone control. The former 333 check dams in the watershed were adjusted and merged into 253, with a density of 3.6 dams/km^2. Backbone projects were added to the 12 larger branch gullies, and the design standards were improved. The production dams were heightened according to a flood once in 20 years plus three years of siltation. The maximum inundation depth of crops on the dam was designed to be 1.0 m,

@seismicisolation

and the maximum siltation thickness in a flood was 0.3 m, with the flooded dam expected to be discharged completely in three days; the backbone project was designed according to a flood every 50 years, and the total amount of one flood plus the five-year siltation amount was used as the flood control storage capacity, equipped with the water discharge structure. At this stage, six new dams were built with a total storage capacity of 427 100 m^3, a sediment retention capacity of 322 000 m^3, and a silting capacity of 4.6 hm^2. Twenty-three dams were rebuilt, and 21 check dams were heightened and reinforced. After these reforms, the dam system in the watershed has retained floods, expanded the area of check land, and improved the dam land's production efficiency effectively.

1.6.1.4. Relatively Stable Development Stage (After 1984)

During this stage, storing up and seeding were alternated, and the supporting facilities were increased in phases to improve the dam's utilization rate and increase the guaranteed crop yield. According to the standard ratio of 1/20 between dam land area and catchment area, those dams up to standard were increased appropriately, and the check dam areas and flood control storage capacity were increased to improve the dam system's flood control capacity; for dams that did not meet the standard, the number of dams was increased, or the old dams were heightened to expand the area of dam land, and flood discharge facilities were built when necessary to ensure the dam system's safety and the dam's production. At this stage, 20 check dams were built, with a total storage capacity of 2.019 million m^3, a sediment retention capacity of 1.494 million m^3, and a silting capacity of 21.39 hm^2. By 1998, there were 202 dams in total with a density of 2.9 dams/km^2. Their utilization rate increased to 81.0%, and the guaranteed yield rate reached 78.7%. From 4 August 1994 to 5 August 1994, there was 124.00 mm of precipitation. According to the data of the past 46 years, the maximum daily precipitation of such heavy rain was once in 80 years. Nonetheless, the dam system in this watershed remained sound, and the crops planted on it yielded a good harvest.

1.6.2. Historical Analysis of Wangmaogou Dam System Evolution

Wangmaogou watershed is one of the water and soil conservation test and demonstration watersheds and is also a small watershed in the major national river basin. The construction of, and research on, check dams in Wangmaogou watershed began with the construction of a check dam at the mouth of the watershed in 1953. To date, nearly 60 years after construction, it has experienced the initial construction stage of the dam system, reconstruction (expansion) stage, adjustment stages, and finally, the relatively stable stage.

1.6.2.1. The Initial Construction Stage of the Dam System (1953–1963)

This stage is an aspect of the exploratory stage. The layout and application of the check dams were carried out according to the principle of comprehensive planning, adjusting measures to local conditions, small domination, small clusters, and top storing up and bottom seeding. The check dams were designed according to a storm flood once in five years, and a check dam system for flood prevention, sediment retention, and siltation was built initially.

In 1953, a medium check dam, Wangmaogou No. 1 dam, was built at the mouth of the main gully first, and a comprehensive treatment that focused on gully management and dam construction began. After the dam was completed, the flood season was at its peak; it was planned to expand it in 1954, but because of topographical conditions, the dam body could not be heightened further. Thus, the No. 2 check dam was built in the middle reaches of Wangmaogou to replace the retention effect of the No. 1 check dam. The upper dam was used to retain flood water and mud, and the lower dam was used for planting, reflecting the concept of top storing up and bottom seeding. At the same time, the branch gullies were also repaired in succession. The dam construction sequence of the main branch gully was to build a check dam at the gully mouth first. When the dam was full, No. 2 dam was built immediately upstream from it, followed by No. 3 dam to build a relatively complete check dam system in the gully gradually. This construction and operation mode has the advantages of fast land siltation, early benefits, and production safety. To hasten the construction of check dams, some branch gullies also adopted the method of building dams in sections simultaneously, but in general, it followed the order of downstream first and upstream later. In this way, 9 check dams were built in the main gully and branch gullies from 1955 to 1956, and 32 check dams were built from 1959 to 1960. A total of 42 check dams were built in the initial construction stage of the dam system, among which 18 were silted up, with 10.5 hm^2 check land and 7.0 hm^2 check land used.

@seismicisolation

1.6.2.2. Reconstruction (Expansion) Stage of the Dam System (1964–1978)

After the initial formation of the Wangmaogou dam system, it was found after repeated test storm floods that the initial design according to the standard of a storm flood once in five years was too short, because as soon as there was a heavy rainstorm, the water destroyed part of the project. To change this situation, the second phase of reconstructing and expanding the dam system was carried out, and the design standards were improved based on Jiuyuangou's rainstorm data from 1954 to 1961. The production dam was designed according to the standard of a storm flood once in 10 years, and the dam was designed according to the standard of a storm flood once in 20 years. In 1964, the entire dam system was rebuilt. This stage happened to take place during a period in which areas in Northern Shaanxi were drought-prone, and the drought-tolerant yield of the dam land was high, which the local people welcomed highly. To silt out more land as soon as possible, some of the check dams in the branch gullies used a combination of natural storage and artificial mountain splitting to build the dam, and a permanent reservoir was built downstream of the No. 2 dam of the main gully to solve the domestic water problem of some farmland and the local people. The number of dams at this time has been adjusted to 35.

After the reconstruction, the check dam system adopted the operation mode of storage and seeding rotation. Most of the check dams were used as production dams for crop planting, and the remaining dams with larger flood retention storage capacity and strong control or dams that were heightened more were used as flood barriers to ensure the downstream dams' safety. During this period, the flood barrier dams of the branch gully and the main gully had no spillway. The branch gully dam had a larger storage capacity for all barriers and full storage. The main gully dam was equipped with a water discharge structure, which was operated in the manner of retention and drainage to solve the problems of clear water sources in permanent reservoirs and to prevent the sediment from flowing out of the watershed. Since the dam system was reconstructed and expanded, the production efficiency has increased continuously, and the people's confidence in dam construction has been strengthened further, such that this period was the peak of dam construction in the watershed.

1.6.2.3. Dam System Adjustment Stage (1979–2002)

In 1977, a heavy rainstorm struck the Wangmaogou watershed. The dam system overall withstood the rainstorm without a major flood accident. However, 9 individual dams were destroyed and 20 were damaged to varying degrees. The permanent reservoir of the main gully also lost its function because of siltation. These phenomena indicated that the flood control standards of the check dam system needed to be improved, particularly to prevent floods and protect downstream dams. The flood control standards of backbone projects were still too low and needed to be improved further. At the same time, most of the check dams had been silted up after heavy rains and floods. Thus, the sediment height of most check dams was less than 1 meter above the dam land, which weakens the retention and siltation capacity of flood sediment significantly. In this situation, in addition to repairing the damaged check dams, a series of adjustment measures was taken for the entire system. Some dams were merged appropriately, and the system's flood control standards were improved further. The production dams were designed and constructed according to the standard of a flood once in 20 years plus three years of siltation storage capacity; the backbone dams were designed according to the standard of a storm flood once in 50 years plus five years sediment storage capacity, and water delivery tunnels were also built.

In 1999, there were 45 check dams in the Wangmaogou watershed, including 5 key dams and 40 small and medium check dams. Five dams had a height of more than 20 m, 6 had a height between 15 and 20 m, 17 had a height between 10 and 15 m, 12 had a height between 5 and 12 m, and 5 had a height less than 5 m. The total storage capacity was 3.2082 million m^3, with a sediment storage capacity of 1 761 800 m^3, and a remaining storage capacity of 1 446 400 m^3. The dam system was adjusted according to the principle of backbone control, small-scale dam merger, and large-scale dam integration. The small branch gullies were no longer reinforced and heightened but merged with the check dams; key dams were built at the main gully upstream and the mouth of larger branch gullies. By the end of 2002, after all of these adjustments, the number of check dams in the Wangmaogou watershed had been adjusted to 23, with a density of 3.85 dams/km^2, a total storage capacity of 2 785 700 m^3, a sediment storage capacity of 2 749 500 m^3, and a sediment retention capacity of 1 504 500 m^3.

@seismicisolation

1.6.2.4. Relatively Stable Stage (2002–Present) At present, there is no clear concept of a dam system's relative stability. This study quotes the meaning of the relative stability of a dam system Cao Wenhong proposed that after the construction of the dam system in small watersheds has reached a certain scale, the joint adjustment, sediment retention, and water storage of large-, medium-, and small-scale dam groups result in the flood sediment's rational use. Under heavy rainstorms (generally once in 200–300 years), the backbone dams in the system can maintain safe operation, while during smaller rainstorms (generally once in 10–20 years), the crop harvest in dam land can be guaranteed.

Since the Wangmaogou watershed was merged and adjusted, it has operated for 10 years thus far, still with 23 check dams in the small watershed, none of which have been destroyed by water. Even after the heavy rainstorm on 15 July 2012, the backbone dams on the main gully remained safe and sound. Through surveys and interviews with local elderly people, the crop planting in the past 10 years has largely yielded good harvests. This shows that the Wangmaogou watershed has basically reached a relatively stable stage.

Throughout the entire evolutionary history of check dams, the most important cause of their water damage is rainstorms and floods, whether in the initial construction stage, the reconstruction (expansion construction) stage, or the adjustment stage. The difference is that the loss attributable to water damage is different when rainstorms of equal magnitude are encountered. In the initial stage of the dam system construction, even smaller rainstorms caused a large number of check dams to break because of the relatively low design standards and the dams' unreasonable location. After the dam system was adjusted and the design standards were improved, some check dams still broke during larger rainstorms. In the relatively stable stage of the dam system, the key dams in the system still play a role in the event of heavy rainstorms and floods, and under the conditions of relatively small rainstorms and floods, the check dams can not only operate normally, but good crops can also be harvested on the dam land.

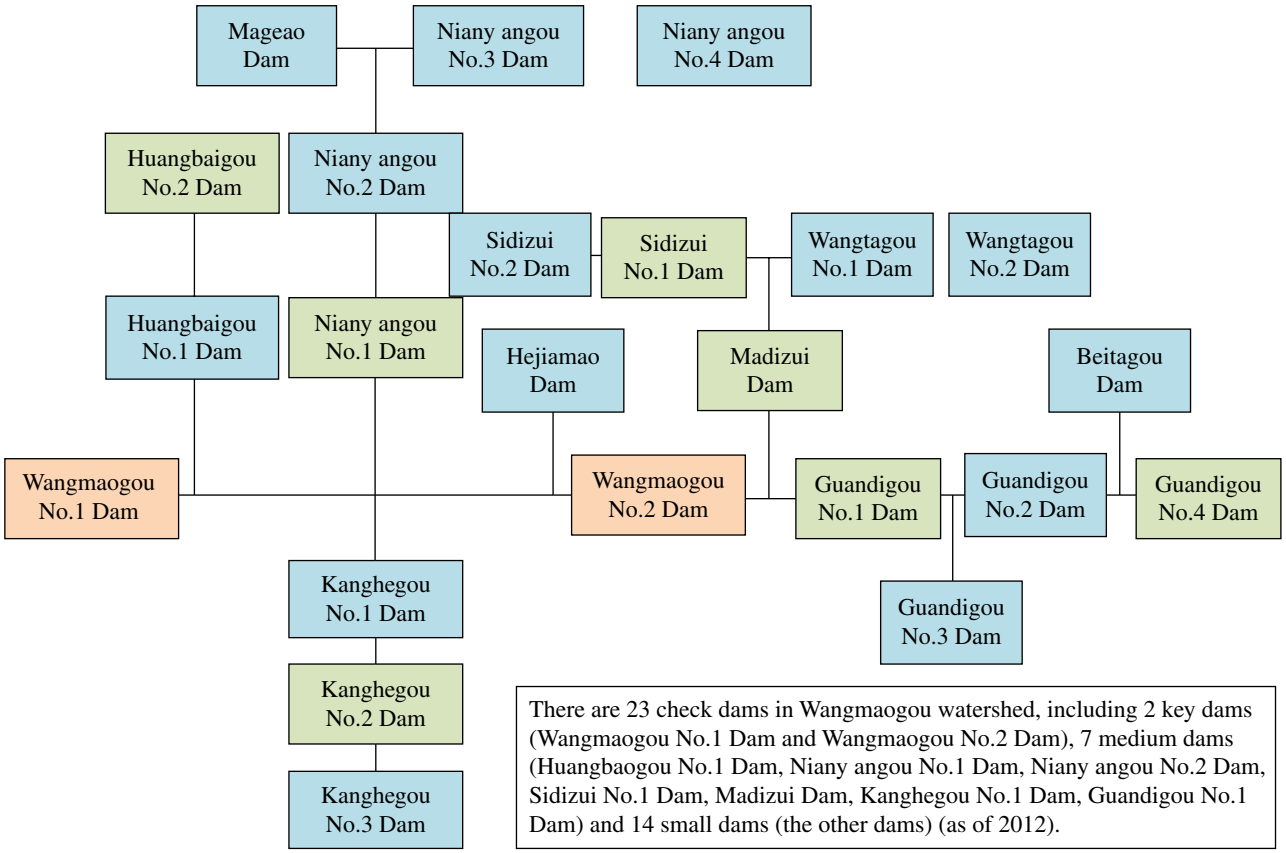

Figure 1.3 The check dam systerm in the Wangmaogou watershed.

@seismicisolation

As of September 2012, there are 23 check dams in the Wangmaogou watershed, including 2 key dams, 7 medium dams, and 14 small dams. There are 2, 4, 10, and 7 dams with a height greater than 20 m, 15–20 m, 10–15 m, and less than 10 m, respectively. The location of the dam system in the Wangmaogou watershed is shown in Figure 1.3.

1.7. CONSTRAINTS ON THE SAFETY AND STABILITY OF DAM SYSTEMS IN SMALL WATERSHEDS IN THE LOESS PLATEAU

Most of the check dams were built in the 1960s and 1970s after the founding of the People's Republic of China, and great achievements have been made in their construction in the Loess Plateau. Limited by various conditions at that time, most of the check dams were not constructed according to an engineering design or the design standards were low, and the layout of the dam system overall had not been planned. In addition, the system has been in use for more than 20 years, and the later management and protection measures cannot keep pace. Therefore, at present, most of the dams have been silted up, the facilities are aging and in disrepair, the capacity for flood and sediment reduction has been reduced greatly, and the difficulties and risks are becoming more and more serious, which restrict the check dams' benefits overall greatly. On the other hand, because of long-term restrictions on capital, investment, and other conditions, check dams' construction scale, speed, and quality have also been affected severely, and the research on check dams has lagged behind relatively, which is inconsistent with the needs for ecological construction and regional economic and social development in the Loess Plateau.

1.7.1. Existing Check Dams' Severe Aging, and Low Capacity for Flood Control and Sediment Reduction

Most of the existing check dams were built during mass movements in the past, and therefore, most of them have no flood control and drainage facilities because of insufficient funds and technical capacity, which has brought many problems to safe production. According to an investigation-relevant department of Shaanxi Province conducted, by the end of 1989, approximately 95% of the more than 30 000 check dams in 25 counties in Northern Shaanxi were built before the 1970s. After decades of operation, these projects have made great contributions to reducing sediment and silting, developing production, and reducing sediment in the Yellow River. However, they have lost their role in flood and sediment reduction because most of these projects are full of silt, aged, and in disrepair. At present, there are 536 large check dams and 4135 medium check dams in Northern Shaanxi that fail to meet the provincial standards and account for 64 and 73.8% of the total, respectively. Among the 185 check dams in the 3 small watersheds of Zizhou County and Mizhi County, the sediment surface in 129, which accounts for 69.7% of the total, is less than 2 m from the top of the dam. All of these dams that are, or are about to be, full need to be reinforced in accordance with the requirements overall of planning a dam system in a small watershed, a task that will be very onerous.

1.7.2. Unreasonable Layout, Unsuitable Facilities, and Low Standards of Dam System

As the local people built most of the check dams in the past spontaneously and blindly, there was a lack of unified planning, and no survey and design. The people took the village as a unit and had no communication, which led to an extremely unreasonable layout of check dams in some gullies and many problems such as "dam in dam," "dam by dam," "upper dam flooding lower dam," and "lower dam cannot be full." At the same time, because of the unreasonable project configuration and lack of controllable key dams, when a dam has an accident in the event of rainstorms and floods, it will cause a chain reaction. For example, in 1977 and 1978, because of several sudden rainstorms in Northern Shaanxi, 70% of the small check dams were destroyed to varying degrees, which taught an extremely profound lesson. Among the more than 110 000 check dams in the Loess Plateau, only 1356 are key dams. According to a survey of Shaanxi Province, more than 400 key dams have been built in the province since 1986, with an average of only 1 key dam per 200 km^2. In addition to their unreasonable configuration, few dam systems have been formed, and there is a particular lack of controllable key dams in many small watersheds. Hence, the flood control capacity is poor overall. In addition, the project's supporting facilities are imperfect, and there is a lack of flood discharge and drainage buildings. Among the existing check dams in Shaanxi Province, the vast majority are small check dams, most of which local people built spontaneously with low standards and poor quality. Sixty percent of

@seismicisolation

check dams have only dam bodies without flood discharge and drainage facilities.

There are various problems in check dams' engineering design, such as low design standards, short siltation period, and small scale of flood discharge facilities.

1.7.3. Severe Salinization and Low Utilization Rate of Dam Land

There are many reasons that dam land becomes salinized [18], which can be summarized as follows:

1.7.3.1. Soluble Saline-Alkali Substances Contained in the Sediment Are Deposited on the Dam Land

The soil of the dam land is silted primarily by erosion materials on the slope of the Loess Plateau, and loess is an alkaline soil. Therefore, the sediment of the dam land contains soluble saline-alkali substances. Generally, the upper part of the dam land has poor drainage and the groundwater level is high. Because of groundwater evaporation, the soluble saline-alkali substances in the sediment rise with the water through capillary action and accumulate on the surface of the dam land, forming saline-alkaline soil.

1.7.3.2. Leakage of Water Storage Project Built at the End or Upstream of the Dam Land

The loess hilly and gully area has been in drought for 10 years, and in response, the local people have built some small water storage ponds and dams at the end or upstream of the dam land for irrigation or to address drinking water shortages. The leakage of these projects' dam bodies and foundations has increased the amount of groundwater recharge of the dam land below, raised the land's groundwater level, and aggravated its salinization, all of which have resulted in a significant reduction in the utilization rate of the dam land. For example, the area downstream of Maliangou in Suide County has a total of 4.67 hm^2 of dam land. The saline-alkali area of the dam land is 2.33 hm^2 because of the water accumulation at the end, which accounts for 50% of the total area of the dam land.

1.7.3.3. Flowing Water Overflows and Accumulated Water Increases in the Dam Land Often

After the dam land was established, the ground gradient changed from 1–2% to 0.07–0.15%. The front parts of some dam lands have a high elevation, which leads to changes in surface runoff drainage conditions. Wide, shallow flow channels form on the land, which prolongs the infiltration rate of water flow, increases the recharge of groundwater, and raises the groundwater level, thus increasing the salinization of the dam land or expanding the area swamped. Water accumulated at the tail of the dam land in Tuoxiang Village, Zhaoshipan Town, Hengshan County, Shaanxi Province, and the swamped area reached 5.87 hm^2, causing overflowing water, overgrown weeds, and barren land.

1.7.3.4. Continuous Seepage of Underground Spring Water at the Dam Site

The larger gullies in Northern Shaanxi are all groundwater drainage areas. The bedrock fissure water on both banks appears in the Mesozoic sandstone in the form of descending springs. Quaternary pore water is also discharged into the gully in the form of spring water on the top surface of the bedrock or the top surface of the laterite layer, where the flow of spring water is generally less than 1.0 l/s, and typically between 0.1 and 0.5 l/s. In the past, some places did not pay attention to ways to protect and use spring water appropriately when building dams, and even pressed the spring water under the dam land, which became a factor in the swamping of the accumulated water in dam land. This is also a reason that the dam land has become salinized.

1.7.3.5. Poor Drainage System of Dam Land

Many dam lands are not equipped with drainage and flood drainage systems, so that the incoming water has no way out. The more water accumulates, the higher the water level. Even if some dam lands are equipped with drainage and flood drainage systems, the elevation at the bottom of the ditch is essentially the same as the ground of the dam land, or even much higher. This method can only drain floods and cannot lower the groundwater level, which leads to salt accumulation or swamping in the dam land. For example, after the flood drainage ditch of the dam land in Sanjiaoping Village, Suide County, Northern Shaanxi was silted, it changed from an underground ditch to an overground ditch, which led to salinization at the end of the dam land. Within a single year, the area of salinization in the dam land had increased from 0.8 to 2.13 hm^2.

1.7.3.6. Unreasonable Water Use for Irrigation

At present, such problems as the layout of irrigation ditch systems, moisture control, the relation between drainage and irrigation, the irrigation system, and the combination of agricultural technical measures in the

@seismicisolation

dam land are still being explored, and there is no long-term experience. Sometimes, excessive irrigation raises the groundwater level on existing irrigable dam land, which aggravates the degree of salinization and expands the swamped area.

The salinization of dam land is an important factor that affects the production utilization rate of dam land and causes resource waste of dam land. For example, 1/3–1/2 of the dam land in some places in Northern Shaanxi and Western Shanxi cannot be cultivated because of salinization. According to a survey by the Suide Soil and Water Conservation Station of the Yellow River Conservancy Commission, as of the end of 1975, there were 35 300 hm^2 of dam land in Yan'an and Yulin, and only 23 300 hm^2 were usable. Because of salinization and swamping, the annual yield has been reduced by approximately 50 000 000 kg.

1.7.4. Lagging Management and Maintenance of Check Dams

1.7.4.1. Body Responsible for Check Dam Management Is Unclear

For many years, the construction of check dams has been funded largely by the state and completed by rural collective economic organizations that mobilize the public. Because of the unclear property rights of the project and the lack of close contact with the public and understanding of their personal interests, the body responsible for the project management is unclear, and the management and maintenance work is weak or is not even implemented. Particularly after the household contract, responsibility system was implemented in rural areas, the dam land is divided among farmers, and the problem that no one is managing the check dam projects has become more prominent. As a result, the more the projects are constructed, the heavier the "burden" of national management, maintenance, and flood prevention.

1.7.4.2. Lack of a Sound Operation and Management Mechanism for Check Dams

Because the establishment of a benign operation and management mechanism was neglected when check dams were constructed in the beginning, their construction, management, and use were inconsistent, and after the project was completed, the responsibility, power, and benefit in management were unclear, and the management and maintenance responsibility system was a mere formality. The increase of check dams without the maintenance funds necessary to support facilities, such as drainage and flood discharge, is a difficult problem to solve and has resulted in a large number of aging dams in disrepair, declining benefits, and more and more dangerous dams, all of which not only restrict the development of check dam construction and the full use of their benefits but also poses a great threat to downstream security. According to the Shaanxi Provincial Bureau of Soil and Water Conservation's census results of check dams in Northern Shaanxi, there are more than 35 000 check dams in the region, of which 24 000, or more than 75%, are dangerous.

1.7.4.3. Backward Operation and Management Technology

In the construction of check dams on the Loess Plateau in the past, the idea of "emphasizing construction and neglecting management" was prominent for a long while. Construction focused instead on solving technical problems in engineering, and ignored research on management technology, thus causing a backward management technology that affected the check dams' safe operation seriously and reduced their normal benefits.

1.7.5. Construction Period and Quality Affected Because of the Lag in Preliminary Work

The preliminary work on a check dam is divided into four stages: planning; project proposal; feasibility study, and preliminary design. The first step is preparing a plan for the check dam. According to the Law of the People's Republic of China on Water and Soil Conservation, the plan must be approved by the people's government at or above the county level to guide the construction of check dams in the next period. The key areas and construction projects identified in the plan should become the basis for project approval in the next phase. The second step is to put forward the proposed project and prepare the project proposal under the guidance of the plan and according to the project's priority. The third step is to carry out a feasibility study of the project and prepare the feasibility study report. Once the report is approved, the project is approved officially. The fourth step is to complete the dam's preliminary design, which is included in the annual plan for construction after approval by the relevant departments.

In the past, it was often the case that the state had confirmed the construction project already before the preliminary work began, and sometimes the state had

@seismicisolation

even issued an investment plan when the design document had not yet been issued. Because of tight working hours, it is difficult to guarantee the quality of the completed planning and design. At the same time, because of the long-term lack of preliminary work funds, there are few reserve projects in various regions, which affects the provinces' ability to apply for projects from the central government, causes delays in the construction period, and influences the project's effectiveness directly.

1.7.6. Imperfect Theory of Dam System Construction and Certain Key Technical Problems Remain Unresolved

Untill now, a complete theoretical system for check dams has not been developed, and certain key technical problems, such as quantitative research on gully gravity erosion, density, scale, and construction timing of dam layout, as well as configuration, design, and construction of the dam system, have not been resolved, which have affected the scientific, efficient, and rapid development of check dam construction [19].

1.7.6.1. Planning

Although relevant units have adopted the empirical planning method successively for more than 60 years – the linear planning method, multi-objective planning method, and nonlinear planning method – to optimize dam systems, and the national "Eighth Five-Year Plan" key project and the Yellow River Basin Soil and Water Conservation Research Fund Project have also set up special subjects to carry out relative stability test research on the dam system and established a physical model based on research on the subject, to date, there is no set of mature and complete dam system construction theoretical systems, and the dam system planning method has continued to use the traditional empirical planning method. The lack of a scientific method to compare and select plans, coupled with the relatively weak planning power, have resulted in the lack of high-tech content in planning results and a certain disconnect from reality.

1.7.6.2. Design

Because of the lack of measures of hydrological data, most of the current check dam systems are designed with traditional empirical methods, and the engineering structural calculation and hydraulic calculation methods are relatively crude. For example, the key links in engineering design, such as the determination of dam height and flood regulation calculations, are calculated typically using empirical formulas, measured data, or community data from similar watersheds. These methods need to be improved, as do the efficiency and automation level of design work. In recent years, although research on the shape design of check dams has been carried out, and the relevant units have developed a computer-aided design (CAD) system, it is still in the development stage and needs to be improved through model tests and actual verification, which cannot yet be promoted fully. Coupled with the uneven design power and level of business departments in various regions, the current design efficiency and quality fall far short of meeting the needs of large-scale check dam construction.

1.7.6.3. Construction

For many years, the construction of check dam projects lacked a complete set of standard construction technical regulations, and many places continued to use traditional construction methods that affected the construction quality seriously. The professional construction technology is weak, particularly because of the lack of professionals, which makes it difficult to guarantee the construction quality and frequent engineering construction changes. An effective quality monitoring and supervision system during the construction process has not yet been established, and the quality supervision stations in various regions and industries are currently insufficiently sound. Further, there are many irregularities in construction management and project quality control, and there is a lack of necessary quality monitoring equipment and methods. Although an engineering supervision system has been implemented in recent years, because of the difference between a check dam project and other construction projects, it is difficult to implement the "three systems (Project legal person responsibility system, bidding contract system, construction supervision system)" of engineering construction fully. Thus, the "three systems" has not yet been implemented fully at present. The project supervision manages only the key gully control projects, and the method of supervision is mainly through touring inspections, which lacks full control of the project quality process. Further, because of the lack of necessary funding, the promotion and incorporation of new construction research results are slow.

@seismicisolation

REFERENCES

1. Liu, X.Y. (2020). The water and sediment situation and countermeasure. *Yellow River 42* (9): 34–40.
2. Yao, W.Y. (2019). Development opportunity and sicentific positioning of soil and water conservation of the Yellow River in the new era. *Yellow River 41* (12): 1–7.
3. Lewis, B. (2002). *Farm Dams: Planning, Construction and Maintenance*. Collingwood: Landlinks Press.
4. Pisaniell, J.D., Burritt, R.L., and Tingey-holyoak, J. (2011). Dam safety management for sustainable farming businesses and catchments agriculture. *Water Management 98*: 507–516.
5. Ai, K.K. and Yang, Y.D. (2018). Development of check dams in the Loess Plateau from the Ming dynasty to the Republic of China: case study of Shaanxi and Shanxi provinces. *Agricultural Archaeology 6*: 134–141.
6. Fan, R.Y. (2004). *Ecological Engineering of Loess Plateau Check Dam System*. Zhengzhou: The yellow water conservancy press.
7. Cao, W.H. (2013). *Optimized Configuration and Construction Technology of Gully Improvement Project in Loess Area*. Shannxi: China Water & Power Press.
8. Han, X.J. (2015). Ministry of water resources actively respond to the work of the safe flooding of silt dams. *Soil and Water Conservation in China 7*: 1.
9. Zhang, Q.L. and Liang, X.W. (2003). The most densely distributed area of silt dams in China - a review of the construction of silt dams in northern Shaanxi. *West China Development 12*: 18–27.
10. Ran, D.C., Luo, Q.H., and Liu, B. (2003). Effect of soil-retaining dams on flood and sediment reduction in middle reaches of Yellow River. *Journal of Hydraulic Engineering 17*: 67–69.
11. Chen, Q. and Zhang, C.Y. (1998). Discussion on the reform of management system of northern Shaanxi check dam. *Yellow River 20* (9): 14–15.
12. Gao, Z.L. and Yang, S.W. (1999). Existing problems of silt arresters on the Loess Plateau. *Bulletin of Soil and Water Conservation 19* (6): 16–19.
13. Li, Z.B. (2016). *Flood Risk Assessment Techniques for Small Basin Silt Dam Systems*. Beijing: Science Press.
14. Yuan, C.Q. (2007). Speeding up warping dam construction of the Loess Plateau and making greater contributions to promoting regional harmonious development. *Soil and Water Conservation in China 11* (11): 1–3.
15. Xu, X.Z. (2004). Development of check-dam system in gullies on the Loess Plateau, China. *Enviromental Science & Policy 7*: 79–86.
16. Zheng, X.M. (2005). Research on management of concentrated coarse sediment source area of the Loess Plateau. *Soil and Water Conservation in China 12*: 5–6.
17. Liang, G.A. (2010). Collaborative distributed GIS framework for check-dams planning and management. *Proceeding of the 18th International Conference on Geoinformatics: GISscience in Change, Geoinformatics 2010* (June 2010). Beijing: Peking University.
18. Liu, N. (2016). Advance the engineering construction of diseased and dangerous silt dams in an orderly manner by solidly carrying out the preliminary work. *Soil and Water Conservation in China 6*: 1–3.
19. Luo, Z.B. (2020). Precipitation recharges the shallow groundwater of check dams in the loessial hilly and gully region of China. *Science of the Total Environment 742*: 140625.

@seismicisolation

2

Water and Soil Conservation by Check Dam Construction

Peng Shi[1], Yang Yu[2,3], Lulu Bai[1], Zongping Ren[1], Kunxia Yu[1], Lie Xiao[1], Hong Yan[4], and Yan Zhang[5]

2.1. INTRODUCTION

In China, the Loess Plateau is a key area for soil conservation and ecological construction [1]. Since the founding of the People's Republic of China in 1949, the state, in response to the two major ecological problems of soil erosion and drought [2], has successively implemented a number of key projects, such as the Yellow River Soil and Water Conservation Ecological Project, the Loess Plateau Check Dam Project, and the Loess Plateau World Bank Loan Project [3]. Meanwhile, a stricter forest-sealing policy has been adopted to restore vegetation via ecological self-rehabilitation [4]. With these efforts, great achievements have been made in improving the ecological environment of the Loess Plateau [5, 6].

As a major soil and water conservation engineering measure (Figure 2.1), check dam systems, through making full use of the natural processes of soil and water losses, supply the collected water for agricultural land nearby the dams, thereby increasing and stabilizing the yield [7]. In addition, check dams have attracted the attention of river management departments for their ability to quickly intercept sediment flowing into the Yellow River and reduce siltation [8]. Check dams are a line of defense in the comprehensive management system of the river basins [9]. They can effectively prevent soil erosion by local retention of the sediment brought by the flood, and they make full use of water and soil resources by forming a dam field [10, 11]. After the sediment is intercepted, check dams raise the base point of erosion, prevent the downward erosion of the channels, lower the gradients of the channels, and delay the retrogressive erosion and channel bank expansion [12]. They are thus of great significance to alleviate gravitational erosion like landslides, collapses, and debris sliding and to stabilize the channel beds. Check dams have significant ecological, economic, and social benefits because they effectively address the two serious problems of soil erosion and drought on the Loess Plateau and achieve a good balance in the relationship between the ecological environment and local prosperity [13]. They also play an irreplaceable role in controlling soil erosion, reducing sediment flowing into the Yellow River, developing regional economies, raising people's living standards, and improving the ecological environment [14]. The Loess Plateau area has a thick, deep soil layer. The widely distributed loess is characterized by its uniform texture, loose structure, strong permeability, easy disintegration, fast

[1] *Institute of Water Resources and Hydro-electric Engineering, Xi'an University of Technology, Xi'an, China*
[2] *Jixian National Forest Ecosystem Research Network Station, CNERN, Beijing Forestry University, Beijing, China*
[3] *School of Soil and Water Conservation, Beijing Forestry University, Beijing, China*
[4] *Faculty of Humanities and Foreign Languages, Xi'an University of Technology, Xi'an, China*
[5] *College of Urban and Environmental Sciences, Northwest University, Xi'an, China*

Check Dam Construction for Sustainable Watershed Management and Planning, First Edition.
Edited by Zhanbin Li, Peng Li, Yang Yu, Peng Shi, and Guillaume Piton.
© 2022 John Wiley & Sons, Inc. Published 2022 by John Wiley & Sons, Inc.

@seismicisolation

Figure 2.1 Check dam on the Loess Plateau.

dehydration, and consolidation, etc., so it is an excellent dam-building material that can be obtained locally [15]. Moreover, the policy of returning farmland to forest and grassland has provided a huge surplus labor market for the construction of check dams [1]. Check dam construction is of great significance to raise the base level of channel erosion, prevent water and soil losses, detain floods, retain sediment and dam land, and reduce sediment flowing into the Yellow River [16].These dams improve local production and living conditions, facilitate high- and stable-yield farmland construction, and accelerate local people in shaking off poverty, and therefore the dams are an important measure for the comprehensive treatment of small watersheds [8].

Since the 1950s, scientific and technological workers have done extensive work on layout optimization of check dams, relative stable of dam systems, and the benefits from water and sediment reduction by check dams [5]. But there are still some deficiencies in the current research on the water and soil conservation functions of check dams, as a complete theoretical system has not yet been formed, especially in the cascade regulation and control of the flood storage, and sediment retention of the check dam system, as well as the water and soil conservation effect of the system [17]. The existing studies do not provide enough scientific and technological support for regional ecological construction and economic development, especially in terms of the cascade control of the flood storage and sediment retention of the check dam system, as well as the water and soil conservation mechanisms of check dams [18]. As one of the three "highlight projects" of the Ministry of Water Resources in 2003, the Check Dam Project has attracted extensive attention from all walks of life [18]. The Administration Bureau of the Upper and Middle Reaches of the Yellow River, the main organizer and implementer of this "highlight project," has done a lot of fruitful work on the planning, roles, functions, benefits, scientific studies, construction, and the management mechanisms of check dams [19]. Furthermore, a series of measures have been taken to publicize the importance of check dam construction in improving the ecological environment of the Loess Plateau, assisting local people to become more prosperous, and reducing the amount of sediment flowing into the Yellow River. For all of the above reasons, it is important to study the mechanisms of water and soil conservation of the check dam system in the small watersheds on the Loess Plateau.

2.2. METHOD

For this study, the Soil & Water Assessment Tool (SWAT) was used to simulate the hydrological responses in the study of watershed. SWAT is a physically based hydrological model developed to predict the impact of land management practices on runoff, sediment, and nutrient loss on the watershed scale [20]. In the hydrological module of SWAT, the Curve Number method was applied to simulated rainfall–runoff processes [21]. In the soil erosion module, the Modified Universal Soil Loss Equation was applied to calculate sediment yield by considering runoff, soil erodibility, coverage and management, topographical factors, support practices, and coarse fragment factors. Check dams are considered reservoirs. If the water level in the reservoirs lies between the emergencyand the principal spillway volumes, then the flow out of the reservoir can be simulated by the following water balance equations:

$$V_{flowout} = V - V_{pr} \quad V - V_{pr} < q_{rel} \times 86400 \tag{2.1}$$

$$V_{flowout} = q_{rel} \times 86\,400 \quad V - V_{pr} < q_{rel} \times 86\,400, \tag{2.2}$$

@seismicisolation

where $V_{flowout}$ represents the flow out of the reservoir, V represents the water storage of the reservoir, V_{pr} represents the water storage at the spillway level, V_{em} represents the reservoir storages when filled to the emergency spillway, and q_{rel} represents the daily discharge flow by the spillway. If the water level in the reservoirs exceeded the emergency spillway, then the flow out of the reservoir was calculated using the following equations:

$$V_{flowout} = (V - V_{em}) + (V_{em} - V_{pr}) \quad V_{em} - V_{pr} < q_{rel} \times 86\,400 \tag{2.3}$$

$$V_{flowout} = (V - V_{em}) + q_{rel} \times 86\,400 \quad V_{em} - V_{pr} > q_{rel} \times 86\,400. \tag{2.4}$$

Sediment trapped in the check dam was calculated as follows:

$$V_L = \frac{\overline{W_{sb}}(1-\eta_s)N}{\gamma_d} \tag{2.5}$$

where $\overline{W_{sb}}$ represents the average sediment yield, η_s represents sediment desilting, N represents the design sedimentation period, and γ_d represents the bulk density of the sediment.

The simulation period was divided into two periods: calibration (1992–1993) and validation (1994–1996). Using the Digital Elevation Model (DEM), the soil map, the land-use map of 1990, and the meteorological data between 1992 and 1996, a SWAT model was run to simulate the monthly flow and sediment yields from 1992 to 1996.

The agreement between simulated and observed values was quantitatively evaluated using the Nash–Sutcliff coefficient of efficiency (NS) and the coefficient of determination (R^2):

$$NS = 1 - \frac{\sum_i (O-S)_i^2}{\sum_i (O_i - \bar{O})^2} \tag{2.6}$$

$$R^2 = \frac{\left[\sum_i (O_i - \bar{O})(S_i - \bar{S})\right]^2}{\sum_i (O_i - \bar{O})^2 \sum_i (S_i - \bar{S})^2}, \tag{2.7}$$

where O represents the observed runoff or sediment and S represents the simulated runoff or sediment. $\bar{O}$ and $\bar{S}$ are the average values of the observed and simulated values, respectively.

Generally, if $NS > 0.5$ and $R^2 > 0.6$, then the simulation results were regarded as credible.

2.3. FLOOD DETENTION AND WATER STORAGE EFFECTS OF THE CHECK DAM SYSTEM

2.3.1. Infiltration Characteristics Under Different Land-Use Conditions

The main factors affecting soil precipitation infiltration are soil properties, such as soil texture, bulk density, moisture content, surface crusts, water-stable aggregate content, and utilization methods. Both land-use methods and soil infiltration rates vary according to the soil texture. In this study, a small field double-ring infiltration test device was used to study the vertical change of soil infiltration rate in Wangmaogou, a small watershed in Suide, Northern Shaanxi, under different land-use methods. This study aims to investigate the spatial variation law of the soil's infiltration rate in small watersheds under various land-use conditions from a microscopic perspective.

2.3.1.1. Variation Law of Soil Infiltration Rate Under Different Land-Use Methods

Figure 2.2 shows that the soil infiltration processes under various land-use methods are different to some extent. The infiltration rates tend to plunge at the beginning of infiltration and then dwindle over time to finally reach stable infiltration. Specifically, the dam land takes the longest time to reach stable infiltration at

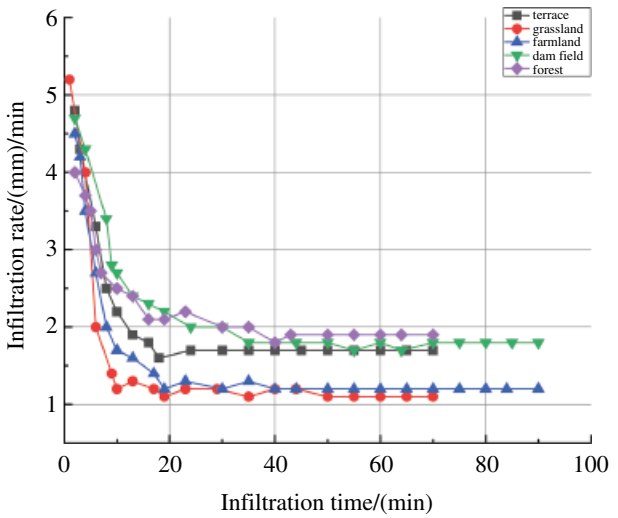

Figure 2.2 Soil infiltration process in land with different use types.

@seismicisolation

70 minutes; the sloping farmland reaches stable infiltration in only 40 minutes, which is the shortest; and the dam land lags 30 minutes on average behind the other four types of land use in reaching stable infiltration. This shows that among the five land-use types in the study area, dam land can enhance soil permeability, delay surface runoff, and reduce the possibility of soil erosion. In contrast, sloping farmland will greatly accelerate the formation of surface runoff, resulting in massive surface soil erosion. Compared with sloping farmland, terraces, grasslands, and woodlands have certain positive effects on soil erosion control.

2.3.1.2. Cumulative Infiltration Volume and Saturated Hydraulic Conductivity

Figure 2.3 illustrates the change process of cumulative soil infiltration volume over time in land with different uses. As time increases, the cumulative infiltration volumes of soil in various land types present an upward trend but with different increments. The cumulative infiltration volumes increase obviously in the first 10 minutes, and then they show a steady increasing trend. After 10 minutes onward, the increasing trends of cumulative infiltration of grassland, sloping farmland, terrace, woodland, and dam land increase successively. The cumulative infiltration volumes of grassland, sloping farmland, terrace, woodland, and dam land are 14.0, 15.3, 16.0, 16.8, and 17.2 cm at 10 minutes, and 28.6, 32.7, 38.3, 42.0, and 42.4 cm at 70 minutes, respectively.

Saturated hydraulic conductivity of soil (Table 2.1): The saturated hydraulic conductivity of soil is related to the soil properties and water quality and reflects the infiltration capacity of soil. It should be a fixed value in case of constant soil structure and texture. There are many calculation methods for this index. In this paper, it is calculated by:

$$K_s = R_s / \left[\frac{H}{C_1 L + C_2 D} + \frac{1}{\alpha \left(C_1 L + C_2 D \right)} + 1 \right] \quad (2.8)$$

where K_s is the saturated hydraulic conductivity of soil (mm/min), R_s is the stable infiltration rate (mm/min), H is the height of water head (cm), L is the depth of the inner ring in the soil (cm), and D is the diameter of the inner ring (cm). C_1 and C_2 are constants at 0.316π and 0.184π, respectively, and α is a constant at 0.05 (1/cm).

The relationship between the saturated hydraulic conductivity and the steady infiltration rate of the soil

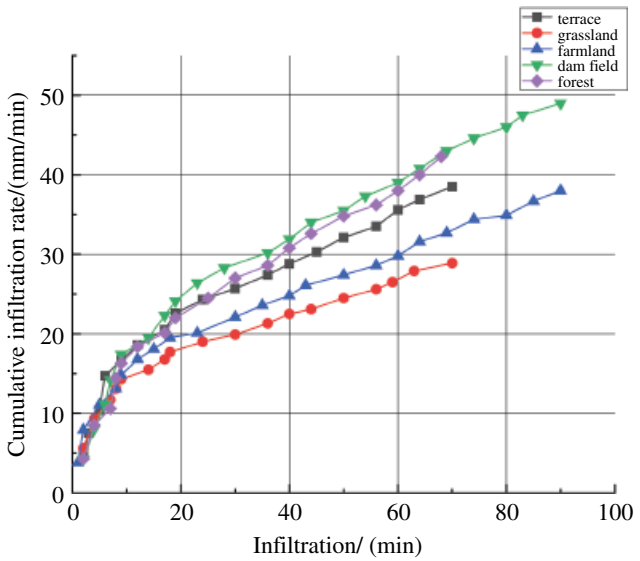

Figure 2.3 Soil accumulative infiltration process in land with different use types.

Table 2.1 Saturated hydraulic conductivity of soil in different land-use types (mm/min).

Land-use types	Terrace	Grassland	Sloping cropland	Dam land	Forestland
Steady infiltration rate	1.60	1.05	1.28	1.75	1.90
Saturated hydraulic conductivity	0.83	0.55	0.66	0.91	0.99

@seismicisolation

has long attracted attention, and the research results of scholars are not the same. In this test, the saturated hydraulic conductivities of different soil types were calculated by the infiltration process as measured by the double-ring infiltration instrument. In terms of saturated hydraulic conductivity, there is grassland<sloping farmland<terraces<dam land<woodland. The average saturated hydraulic conductivity of the five land types is 52% of the average stable infiltration rate, which is consistent with the research results. This suggests that the infiltration process as measured by the double-ring infiltration method is unsuitable for calculating the saturated hydraulic conductivity. The low saturated conductivities may be ascribed to the small value of α in formula (2.1).

2.3.1.3. Soil Infiltration Model

To further explore the infiltration characteristics of different land types in the study area, they were fitted into the Kosgakov model. The results are listed in Table 2.2.

Through the fitted research, it was found that the Kosgakov formula had the highest fitting accuracy. The value of a when fitted with the Kosgakov formula ranges from 4.075 to 4.567. This value is related to the soil's bulk density, and the maximum appears in dam land and the minimum is in sloping farmland. The value of b ranges between 0.199 and 0.363 and is capable of reflecting the decrease in infiltration rate. The larger the b, the faster the infiltration rate decreases with time. It can be seen that the grassland soil infiltration rate declines the fastest, while that of woodland decreases the slowest.

Table 2.2 Regression results of parameters in the infiltration model.

Land-use types	*a*	*b*	R^2
Terrace	4.567	0.279	0.891
Grassland	4.075	0.363	0.827
Sloping cropland	4.085	0.294	0.851
Dam land	4.502	0.228	0.928
Forestland	4.094	0.199	0.942

2.3.2. Impact of Check Dam on the Runoff Process in Watersheds

2.3.2.1. Impact of Check Dam on Runoff Coefficient and Sediment Transport Modulus

The runoff coefficient α is the ratio of the runoff depth (R) to the corresponding precipitation depth (P) in a certain period of time, and it reflects the overall impact of physical and geographic factors in the basin on runoff. The sediment transport modulus refers to the amount of sediment transported per unit area above a certain section of the river. From the actual measurement data of the comparative watersheds of Jiuyuangou, Peijiamao, Wangmaogou, Lijiazhai, Xiangtagou, and Tuanyuangou, it was found that the runoff coefficient of Jiuyuangou was reduced by 29.43% and the sand transport modulus by 28.09% compared with Peijiamao (Table 2.3). Compared to Lijiazhai, the runoff coefficient of Wangmaogou was reduced by 34.63% and the sand transport modulus by 67.75%. Compared with Tuanyuangou watershed, the runoff coefficient of Xiangtagou watershed decreased by 16.78%, and the sand transport modulus decreased by 27.75%.

2.3.2.2. Impact of Check Dam on Flood Lag Time

Flood lag time refers to the interval between the centroid appearance time of the flood process line at the outlet of the watershed and the centroid appearance time of the net rain process, namely, the delay. Flood lag time is an important factor in determining the unit line and peak discharge of a watershed. For an untreated watershed, its area and slope are two major factors affecting the flood lag time. The implementation of soil

Table 2.3 Calculation results of multi-year mean runoff coefficient and sediment transport modulus.

Watershed	Area km²	Ecological management	Period	Runoff coefficient%	Sediment coefficient t/km²	Decrease of runoff coefficient %	Decrease of sediment coefficient %
Jiuyuangou	70.50	Management	1959–1969	8.80	1220.00	29.43	28.09
Peijiamao	41.50	Control	1959–1969	12.47	1696.49		
Wangmaogou	5.97	Management	1962–1963	2.68	232.60	34.63	67.75
Lijiazhai	4.92	Control	1962–1963	4.10	721.19		
Xiangtagou	0.45	Management	1958–1961	18.60	3314.77	16.78	27.75
Tuanyuangou	0.49	Control	1958–1961	22.35	4587.78		

@seismicisolation

Table 2.4 Calculation results of flood lag time for Wangmaogou and Lijiazhai.

Watershed name	Flood number	Precipitation mm	Duration of rainfall min	Rainfall intensity mm/h	Flood duration min	Flood peak discharge m^3/s	Watershed lag time
Wangmaogou watershed	19610801	70.4	231	18.3	3560	21	105
	19610813	47.7	930	3.1	930	0.38	300
	19620715	30.5	533	3.4	1200	1.9	90
	19630706	60.7	701	5.2	1230	0.58	104
	19640712	24.3	751	1.9	477	1.63	60
	19640714	13.1	32	24.6	440	7.04	40
	19640721	32.8	854	2.3	710	0.75	120
	19640907	25.1	900	1.7	475	1.6	148
	19640917	14.1	320	2.6	270	0.95	90
Lijiazhai watershed	19620715	29.6	444	4	1025	3.41	30
	19620723	16	1030	0.9	615	0.038	25
	19620825	32.8	1120	1.8	1120	0.04	40
	19630615	24.5	994	1.5	1100	3.85	40
	19630706	65.4	692	5.7	830	4.35	26
	19630807	9.2	12	45.8	650	8.19	74
	19630829	9.6	568	1.3	529	1.35	32

and water conservation measures, especially the construction of dams and reservoirs, will have a profound impact on the flood lag time. Given that Wangmaogou and Lijiazhai watersheds are similar in area and slope, it is possible to compare the difference in flood lag time between the two basins to study the influence of check dam construction on the confluence process. The results show that the average flood lag time of Wangmaogou watershed is 117 min, about three times that of 38 min in Lijiazhai watershed (Table 2.4). This demonstrates that the check dams greatly delay the appearance of flood peaks.

2.3.2.3. Influence Mechanism of Check Dams on Runoff Process

The impact of check dams on the runoff process is mainly reflected in two aspects. First, with the siltation of the dam land, the channel shape gradually transforms from the original V to U. Consequently, the gradient decreases, and the cross-sectional area of the flow becomes larger. Moreover, the natural channel is originally dominated by sparse grasslands. After the siltation, it turns into agricultural land, on which the main crop is corn, and the underlying surface of the water channel changes accordingly. Second, the check dam serves as an obstacle of natural river channels that affects the runoff process of the basin.

In order to analyze the first impact, the unit flow is introduced to quantify the impact of check dams on the runoff process. The flow of a certain river section below the water level of 1 m is defined as the unit flow of the river section. With the support of ArcGIS, the Wangmaogou–Lijiazhai DEM is used to extract the gradients of 27 natural channels in Wangmaogou, 34 silted channels (dam land), and 25 channels in Lijiazhai, as well as the upper, middle, and lower sections of each channel. Based on the extracted sections, the cross-sectional area and wetted perimeter at unit water level (1 m) are calculated, and the hydraulic radius is obtained. Meanwhile, according to relevant literature, the roughness (n) of natural river channels is determined to be 0.04, and that of silted channels is 0.10. Subsequently, the Xiecai formula is used to calculate the channel flow (Tables 2.5). The results show that the average gradient of natural channel in the Wangmaogou watershed is 12.38% and drops to 0.29% after the siltation turns it into dam land. The cross-sectional area of natural channel at the unit water level is 6.58 m^2, and that of the dam land is 33.14 m^2. Compared with natural channel, the wetted perimeter of the silted channel increases from 10.25 m to 34.97 m, and the average hydraulic radius rises from 0.64 m to 0.95 m. The unit flow of the natural channel is 41.82 m^3/s, and that of the dam land is 17.13 m^3/s. After the siltation of the dam land, the unit flow of the channel declines to only 40% of the original.

In order to analyze the second impact of check dam on runoff process, the river network nodes are divided

@seismicisolation

Table 2.5 Calculation results of unit flow of channels.

Category	Average gradient t/%	Discharge section area m^2	Wetted perimeter m	Hydraulic radius	Unit overflow m^3/s
Channel of Wangmaogou	12.38	6.58	10.25	0.64	41.82
Dam land of Wangmaogou	0.29	33.14	34.97	0.95	17.13
Channel of Lijiazhai	10.22	5.37	8.93	0.59	28.19

into three categories: (i) the confluence of rivers, called the river convergence node; (ii) the check dam, i.e. the obstacle node of the river; and (iii) the transition point from natural channel to silted channel, that is, the tail of the dam land, and this kind of point is herein referred to as the transformation node of the channel feature. The obstructive nodes (check dams) of the river can be further divided into three subcategories according to the types of discharge structures: (i) check dams with a spillway are classified as strongly connected nodes; (ii) check dams with a vertical shaft and horizontal pipe are grouped into weakly connected nodes; and (iii) check dams without a discharge structure, for example, Menhulu Dam, are non-connected nodes.

Similarly, the unit flow of the spillway at unit water level (1 m) can be calculated by the Xiecai formula, and the unit flow of the vertical shaft and horizontal pipe can be calculated by the orifice outflow formula. The results show that the unit flow of the spillway of Guandigou No. 2 Dam is 5.33 m^3/s, and that of Wangmaogou No. 1 Dam is 5.47 m^3/s. The unit flow of vertical shaft and horizontal pipe is 1.65 and 0.55 m^3/s, respectively.

A weight value of 1 is assigned to the river convergence node. The weight of the river's obstacle node can be calculated from the ratio of the unit flow of the water discharge structure to the unit flow of the upstream channel. For large check dams, for instance Menhulu Dam, the unit flow is 0, so the weight is assigned to 0. For the channel feature transformation node, its weight can be determined by the ratio of the unit flow of the downstream silted channel to the unit flow of the upstream natural channel. With the assistance of graph theory, the river network tree map of Wangmaogou watershed is established, as shown in Figure 2.4. The tree has 11 layers, and the aforementioned node weights are assigned to the edges of the tree as the weight of each edge. The farther each node is from the runoff control station, the smaller the "interference" to the flow process. Therefore, for the tree diagram in Figure 2.3, formula (2.1) is used to calculate the weight of the entire tree:

$$q = \frac{\sum_{i=1}^{n}\left(k_i \frac{1}{u_i}\right)}{\sum_{i=1}^{n}\frac{1}{u_i}} \tag{2.9}$$

where k_i is the weight of a certain layer and u_i is the number of the layer.

The tree weight of Wangmaogou watershed is calculated to be 0.21, and for Lijiazhai where no check dam has been built, its tree weight is 1. The runoff coefficient, total runoff amount, flood lag time, and flood peak discharge for a runoff process under similar rainfall conditions (total precipitation, rainfall intensity) are selected to draw a scatter diagram for fitting. The results show that the peak discharge of Wangmaogou and Lijiazhai watersheds can be well distributed on both sides of a straight line with a slope of 0.21, and the coefficient of determination (R^2) is 0.51 (Figure 2.5). It is thus proven that the check dam, as an obstacle node, significantly weakens the peak flow of the basin.

2.4. ANALYSIS OF SEDIMENT RETENTION AND WATER STORAGE BY CHECK DAM SYSTEM

2.4.1. Precipitation Analysis

According to the precipitation data of 27 rainfall stations in a demonstration dam system of 12 small watersheds on the Loess Plateau from 2006 to 2010, and May to October, the annual precipitation is small and concentrated, with large inter-annual variation and uneven monthly distribution; the average annual precipitation ranges from 380 to 567 mm; the precipitation during the flood season (May to October) accounts for 60–70% of the annual precipitation, and it mostly appears in the form of torrential rain with a short duration and high intensity.

@seismicisolation

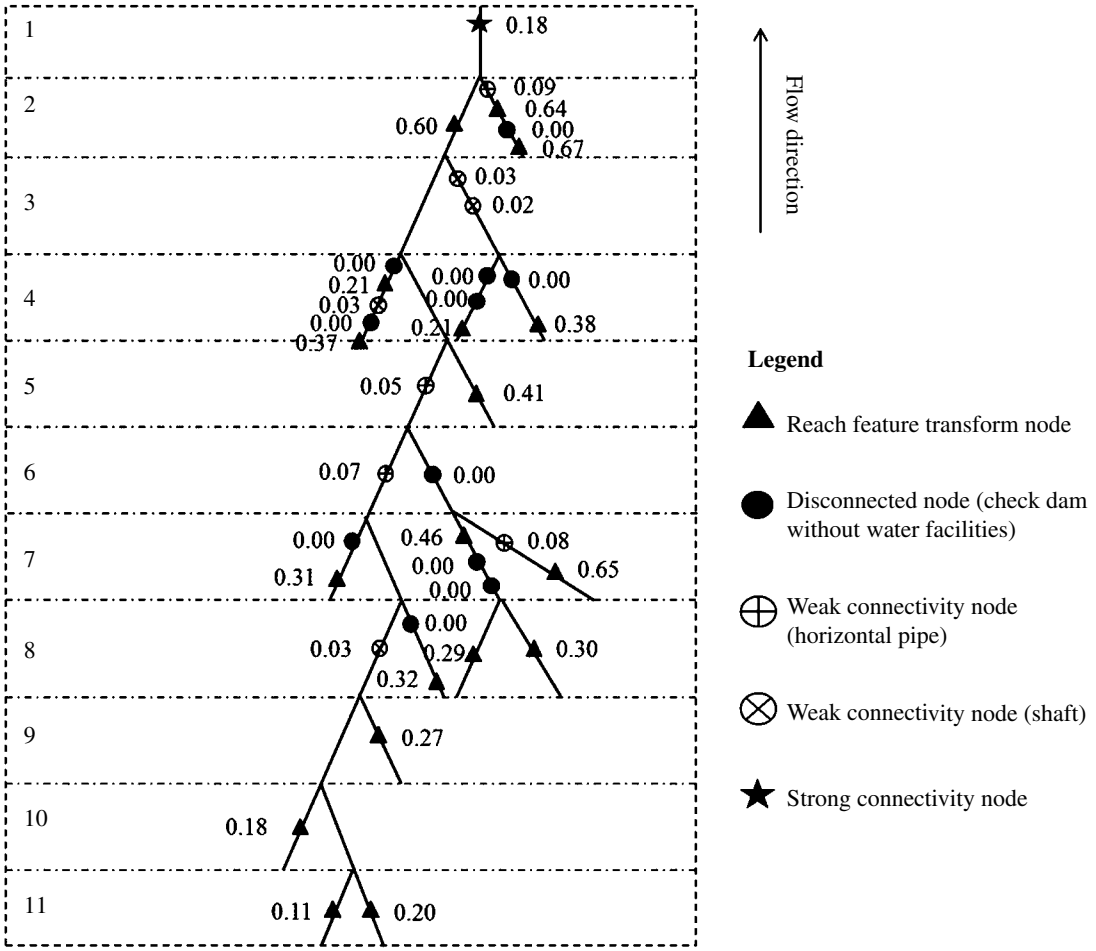

Figure 2.4 The river network tree map of Wangmaogou.

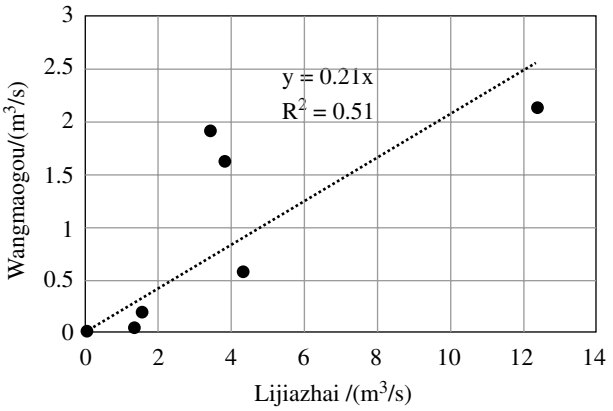

Figure 2.5 Comparison of flood peak discharge between Wangmaogou and Lijiazhai.

Table 2.6 gives the corresponding maximum daily precipitation (mm), number of rainy days (d), annual rainfall, amount of runoff at the runoff control station, and sediment volume during the flood season of the basin between 2006 and 2010. It can be seen from the table that from 2006 to 2010, the change trend of the flood runoff at the control stations in 12 small watersheds is the most similar to that of the maximum daily rainfall during the flood season. When the maximum daily rainfall increases, the flood runoff at the control stations also increases. It indicates that the maximum daily rainfall during the flood season is the dominant factor of the flood runoff.

2.4.2. Sediment Retention of Dam Systems in Small Watersheds

The sediment in the Yellow River mainly comes from the thousands of gullies in the hilly loess area in the middle reaches of the Yellow River. The check dams built in the channels block the way for transporting sediment from the source to downstream, creating an artificial barrier where the sediment collects. According to the statistics, 51 main dams have been built in the

@seismicisolation

Table 2.6 Rainfall, runoff, and sediment discharge in 12 small watersheds during flood seasons from 2006 to 2010.

Time period (flood season)	2006	2007	2008	2009	2010
Maximum daily rainfall during the flood season/mm	52	109.4	52.5	70	98.4
Average number of rainy days in flood season/d	37.6	42.7	38.1	40.3	40.4
Average precipitation during the flood season/mm	324.4	409.7	314.5	278.7	329.8
Gate station flood runoff/$10^4 m^3$	176.52	790.43	235.16	316.36	693.93
The discharge of sand at the mouth/10^4t	19.94	20.38	12.28	5.04	6.89

upper reaches of the Huangfuchuan River Basin in the past 15 years. These dams, with a total storage capacity of 111 million m^3, are capable of controlling a soil erosion area of 460 km^2 and holding back 74.9 million m^3 of sediment. Among them, the dams in the three small watersheds of Chuanzhanggou, Hujitugou, and Budonggou have an average annual sediment retention capacity of 8.7 million t, accounting for 16.4% of the average annual sediment loss of 53 million tons in the whole basin. On 21 July 1989, a heavy rainstorm hit the Huangfuchuan River Basin in Inner Mongolia. The average precipitation in the rainstorm center Chuanzhanggou was 118.9 mm. The 14 large dams that had been completed at that time blocked 5.93 million m^3 of sediment in total during this flood, with a sediment reduction rate of 89.7%. The Wangmaogou watershed (Jiuyuangou influent) in Suide County, Shaanxi Province, covers a drainage area of 5.97 km^2. From 1953 to 1983, 42 check dams were constructed in this region, blocking a total of 1.2 million m^3 of sediment, and forming 24.5 hm^2 of dam land. During the 30 years, these dams roughly blocked all the flood and sediment.

According to relevant survey data, for every 1 hm^2 of dam land, large-scale check dams can hold an average of 130 000 tons of sediment, medium check dams 100 000 t, and small-scale check dams 51 000 t. The sediment blocking effect is even better in typical dam systems. The survey data of typical dam systems show that the well-built dam systems, such as Dongshiyang in Shanxi, Nianzhuanggou and Jiuyuangou in Shaanxi, and Qiligou in Gansu, have intercepted over 80% of the sediment and floods. The dam system of the Xiheidai watershed in Jungar Banner, Inner Mongolia, covers a total drainage area of 32 km^2. Since 1986, measures have been taken to improve the construction of the dam system. By far, 38 check dams have been built to accumulatively block 6.45 million tons of sediment. The Zhaoshipan watershed in Hengshan County, Shaanxi, has a drainage area of 60.68 km^2. The 45 check dams built, including eight large dams, have a total storage capacity of 29.825 million m^3 and have blocked 20.39 million m^3 of sediment.

To monitor the siltation of large, medium-sized, and small check dams, a total of 524 sediment blocking monitoring points have been set up in the watersheds of 12 demonstration dam systems on the Loess Plateau. Due to such factors as the uneven spatial and temporal distribution of rainfall and different channel conditions, the siltation situation of dams varies. Based on the concrete pile number and the excavation siltation section, combined with the original storage capacity curve, the dam system's sediment retention amount is measured.

Sediment retention amount and sediment retention indicators of different types of check dams: The sediment retention capacity and the sediment retention per unit area of large dams and- small and medium-sized dams are classified and calculated according to the monitoring data.

Sediment yield: The sediment yield of the small watershed has three parts: the sediment blocked by the dam system, the sediment held back by the slope project, and the sediment transported by the control station. It is calculated by:

$$W_C = W_S + W_P + W_0 \tag{2.10}$$

where W_C is the annual sediment yield of small watershed, W_S is the annual sediment retention amount of the dam system, W_P is the amount of sediment blocked by the slope project, and W_0 is the amount of sediment transported by the control station.

Sediment retention ratio: The sediment retention rate η (%) of the small watershed dam system is the ratio of

@seismicisolation

Table 2.7 Annual sediment retention by dams in 12 small watersheds.

Year	Main check dams		Large check dams		Small check dams		Dam system combined	Sediment yield in small watershed/10^4 t	Dam system sand retention rate/%
	10^4 t	Proportion/%	10^4 t	Proportion/%	10^4 t	Proportion/%	10^4 t		
2006	547.7	94.1	23.6	4.1	10.9	1.9	581.9	671.9	86.6
2007	428.3	81.2	63.8	12.1	35.6	6.7	527.8	620.5	85.1
2008	104.8	55.2	54.5	28.7	30.4	16.0	189.8	275.9	68.8
2009	143.8	62.0	55.6	23.9	32.5	14.0	232.0	312.7	74.2
2010	172.1	62.8	65.9	24.0	36.1	13.2	274.1	358.2	76.5
Aggregate	1396.9	77.4	263.4	14.6	145.7	8.1	1 805.6	2 239.2	80.6

the annual sediment retention amount to the annual sediment yield. It is calculated by the following formula:

$$\eta = (W_S / W_C) \times 100\% \tag{2.11}$$

According to the monitoring data, from 2006 to 2010, the 12 small watershed dam systems accumulatively retained $1{,}805.56 \times 10^4$ tons of sediment. The sediment yield was 2329.24×10^4 t, and the average sediment retention ratio of the dam system was 80.63%. In 2010, the amount of sediment held by the dam system and the sediment yield in small watersheds both decreased compared with 2006. The reduced sediment yield was attributed to the decrease in the sediment retention amount of the dam system and in the sediment transported at the control station. The change trend of the sediment retention amount of the dam system is opposite to that of the treatment level. This indicates that with the improvement of the treatment level year by year, the amount of sediment blocked by the dam system presents a descending trend. The annual sediment retention amount of each type of dams is shown in Table 2.7.

As shown in Figure 2.6, there is an overall decreasing trend in the 2006–2010 inter-annual change in the sediment retention by the demonstration projects (the dam systems in 12 small watersheds including Jingyanggou watershed) on the Loess Plateau. The dam system has the highest amount of sediment retention of 5819 100 tons in 2006, and the minimum sediment retention of 1897 900 tons appears in 2008. From the relationship between the amount of sediment retention and the treatment level, conclusions can be drawn that, when other influence factors are not considered, the change trend of the amount of sediment retention by the dam system is opposite to that of the treatment level. This again demonstrates that, with the annual improvement of treatment level, the amount of sediment blocked by the dam system shows a decreasing trend. The reason is

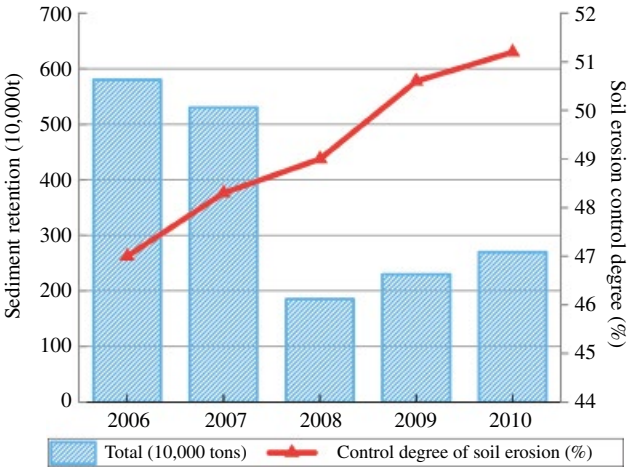

Figure 2.6 Inter-annual variation of sediment retention by 12 small watershed dam systems.

that with the advancement of soil and water conservation and ecological construction, the slope governance and vegetation coverage in the study area have increased, and the areas of sloping farmland, waste grassland, and bare land have declined. In recent years, the benefits from returning farmland to forests have gradually emerged, young forests have grown, canopy density has risen, and sediment retention rates have increased. In addition, the implementation of ecological construction and closure measures on barren hills and slopes (waste grassland and bare land) in the study areas has led to the rapid recovery of vegetation on the slope. Moreover, the soil erosion caused by human activities has been greatly reduced. These efforts together have blocked most of the sediment in the study areas and also significantly reduced the sediment from the slope and the siltation.

From Table 2.7 and Figure 2.7, it can be seen that by the end of 2010, the main dams in the 12 small watersheds constructed on the Loess Plateau are mostly

@seismicisolation

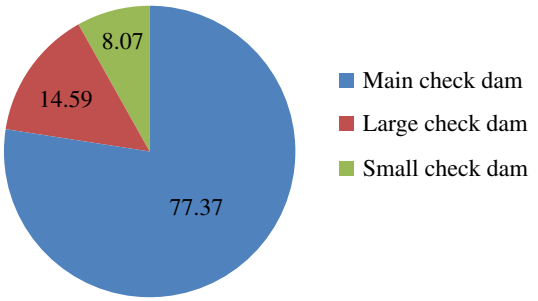

Figure 2.7 Comparison of accumulated sediment retention of check dams in 12 small watersheds at the end of 2010.

large dams. Specifically, the cumulative sediment retention capacity of large dams is 13.9688 million tons, accounting for 77.37% of the entire dam system; that of medium-sized dams is 2633 800 tons, accounting for 14.59% of the entire dam system, and that of small dams is 1456 600 tons, only accounting for 8.07%. Thus, large dams have the largest sediment retention capacity, followed by medium-sized dams and small dams. In the entire dam system, the sediment retention capacity of large dams accounts for a considerable proportion. In 2008, however, the amount of sediment retention by the dam system was the smallest in the 5 years, and there was little difference between the retention amount by large dams and small and medium-sized ones. The dominant factor behind that is that the maximum daily rainfall of 52.5 mm during the flood season in 2008 was significantly smaller than that in 2007–2010. As a result, the soil erosion on the slope was relatively small, and there was less flood and sediment from upstream. Partly being blocked by small and medium-sized dams, the sediment transported to the control area of the downstream large dams decreased. Hence, small and medium-sized dams played a major role.

From 1970 to 1996, the average annual flood and sediment reduction by the check dams in the region of Helong Interval accounted for 59.3 and 64.7% of the total annual reduction by water and soil conservation measures. The average annual flood reduction of check dams in the Jinghe, Beiluo, and Weihe river basins accounted for 33.6, 43.9, and 5.4% of the total annual flood reduction by soil and water conservation measures, respectively. The average annual sediment reduction of check dams in the three basins accounted for 17.2, 29.9, and 27.6% of the total annual sediment reduction by soil and water conservation measures.

The construction of check dams, especially the large dams, in areas with severe soil erosion in the hilly Loess regions has progressed by leaps and bounds in recent years. The number of dams constructed during the "Ninth Five-Year Plan" period was twice that during the "Eighth Five-Year Plan" period. The number of dam projects under construction during the "Tenth Five-Year Plan" period alone exceeded the total number of check dams completed in the past. The 1,585 large dams built on the Loess Plateau are able to control an area of 10133 km^2. With a total storage capacity of 1.375 billion m^3, they are estimated to block 1.065 billion tons of sediment.

In view of the pivotal role of the dam system in blocking sediment, it is suggested to take small watershed as a unit in check dam construction, so as to build a relatively stable check dam system with large dams for channel treatment as the main body, and large, medium-sized, and small check dams as supplements.

2.5. ANALYSIS OF SEDIMENT RETAINING MEASURES ON SLOPES IN SMALL WATERSHEDS

The flood and sediment in the channel mainly come from the slope surface. Generally, the slope is low in treatment level and large in exposed surface. Thus, when heavy rain occurs, a large amount of runoff and sediment converges in a short period, posing a great threat to check dams. In case of high slope treatment level, the slope engineering measures are able to store water and retain soil, thereby reducing floods and sediment in small watersheds. Observation and analysis results show that horizontal terraces can block 35–65% of the water and 60–90% of the sediment. By intercepting rainfall, woodlands and grasslands can reduce raindrop splash erosion, raise ground roughness, decrease runoff, and increase infiltration, thereby reducing water by 20–60% and sediment by 30–50% on average. Practice has shown that the improved treatment of small watersheds decreases slope runoff and soil erosion, and the flood control pressure of the dam system, which enhance the flood control capacity of the dam. Table 2.8 presents the quota standards for sediment retention and erosion reduction by slope surface treatment projects.

The sediment amount is calculated by the formula of water and soil conservation benefit after referring to the method in the *Analysis of Soil and Water Conservation Benefits from Yellow River Management in the Recent 50 Years*. The results show that the accumulative sediment amount blocked by slope treatment

@seismicisolation

Table 2.8 Quota standards for sediment retention and erosion reduction by soil and water conservation measures of the Yellow River.

Project		Unit	Qinhai	Gansu	Ningxia	Inner Mongolia	Shaanxi	Shanxi	Henan
Sediment quota	Terraced fields	t/hm^2	8.4	27.6	21.45	28.8	38.4	28.2	9.15
	Afforestation	t/hm^2	4.35	14.4	11.25	15	20.1	14.7	4.8
	Seeding	t/hm^2	2.4	8.1	6.3	8.4	11.25	8.25	2.7

Table 2.9 Sediment retention by slope management measures in dam systems in small watersheds.

Year	Terraced fields/10^{4}t	Afforestation/10^{4}t	Grass-planting/10^{4}t	Total/10^{4}t
2006	29.85	35.99	4.23	70.06
2007	30.73	37.07	4.53	72.33
2008	31.4	37.77	4.72	73.88
2009	31.81	39.07	4.78	75.67
2010	33.17	39.26	4.78	77.21
Slope measures for sediment containment/10^{4}t	156.95	189.16	23.04	369.15

Table 2.10 Monitoring results of water storage and utilization of dam systems in small watersheds.

Year	Year-end storage (10^{4}m^3)	Additional surface area (hm^2)	Water consumption (10^{4}m^3)	Rate of change of water consumption (%)
2006	387.69	37.2	23.39	5.69
2007	570.47	43.73	32.7	5.42
2008	501.2	–4.74	43.67	8.02
2009	503.01	24.85	43.1	7.89
2010	578.49	27.65	37.65	6.11

measures in the 12 small watersheds from 2006 to 2010 reached 369.15×10^4 tons, of which 156.95×10^4 tons were blocked by terraces, 189.16×10^4 tons by afforestation, and 23.04×10^4 tons by grass planting. Among the slope treatment measures, afforestation and terraces blocked most of the sediment, while grass planting retained a relatively small part (see Table 2.9).

Slope management measures such as terraces, afforestation, and grass planting reduce ineffective evaporation by transforming the ineffective evaporation of soil water from land previously bare or with low vegetation coverage into effective transpiration of plants. At the same time, though intercepting part of the runoff, increasing rainfall infiltration, and improving the utilization rate of precipitation and land production capacity, they reduce slope erosion and nutrient loss induced by rainfall, thereby improving the ecological environment.

2.6. ANALYSIS OF WATER STORAGE AND UTILIZATION OF DAM SYSTEMS IN SMALL WATERSHEDS

From 2006 to 2010, the change in water storage capacity of the 12 dam systems showed an annually increasing trend. At the end of 2006, the water storage capacity of the dam systems was 387.69×10^4 m^3. By the end of 2010, it increased by 49.2% to 578.49×10^4 m^3, an increase of 190.80×10^4 m^3. The increased water storage can be used for irrigation, for drinking water, to supplement groundwater through soil infiltration, and also to change the local microclimate (Table 2.10).

Wangmaogou watershed is compared with Lijiazhai watershed, which has similar natural conditions but fewer dams. In the two torrential rains on 19 August 1959 and 1 August 1961, the peak discharge of Wangmaogou watershed was 4.0 and

@seismicisolation

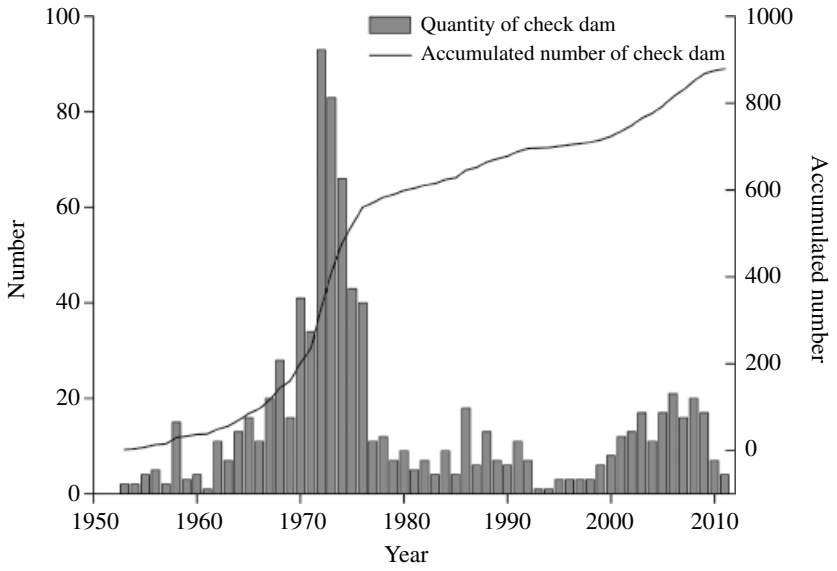

Figure 2.8 Check dams constructed from 1953 to 2010 in the Wuding River watershed.

2.1 m^3/s, respectively, while that of Lijiazhai watershed was 43.0 and 18.0 m^3/s, respectively,. The Wangmaogou dam system reduced flood peaks by up to 90.7 and 88.3%.

2.7. EFFECTS OF CHECK DAM ON WATER AND SOIL CONSERVATION IN THE WUDING RIVER WATERSHED

Check dam construction is a widely applied soil erosion control measure on the Loess Plateau of China. It plays an important role in sediment yield reduction. However, it remains unclear how these in-channel structures affect water yield and sediment load on the watershed scale. A combination of field work and modeling exercises were used to quantitatively assess the effects of check dam construction on hydrological processes in the Wuding River watershed. A large number of check dams were constructed from 1970 to 1980. Runoff and sediment yield in the watershed showed significant decreasing trends, with change points occurring in the early 1970s. Human activity contributed to 75 and 89% of runoff and sediment changes, respectively. The simulations showed that in a scenario without check dams, runoff and sediment increased by 12 and 11.7%, respectively. The combination of check dam construction had a greater impact on water yield and sediment transportation. Check dams provide short-term flood control and sediment reductions.

2.7.1. Check Dam Construction in Wuding River Watershed

The construction of check dams in the study area began in the early 1950s. By 1969, there were 160 main check dams in the channel (Figure 2.8). From 1970 to 1980, large-scale construction of check dams occurred, with 430, 49% of the total amount, being constructed. In the last 30 years, the increase in the number of check dams stabilized, with eight being constructed per year. By 2011, there were 879 main check dams in the watershed, with a large number of check dams being widely distributed throughout the hill region (Figure 2.9).

2.7.2. Long-Term Changes in Precipitation, Runoff, and Sediment in Wuding River Watershed

The variations in annual precipitation, runoff, and sediment yield are shown in Figure 2.9. Precipitation fluctuated around the 377-mm mean value. Runoff and sediment showed decreasing trends from 1963 to 2005 (Figure 2.10). The Mann–Kendall test revealed that there was no significant trend ($P > 0.05$) in the annual precipitation's variation (Table 2.11). However, both runoff and sediment in the watershed showed significant decreasing trends ($P < 0.01$), with average annual runoff and sediment reductions of 0.19×10^8 m^3a^{-1} and 0.38×10^7 t a^{-1}, respectively. The Pettitt analysis was used to examine the change points inprecipitation,

@seismicisolation

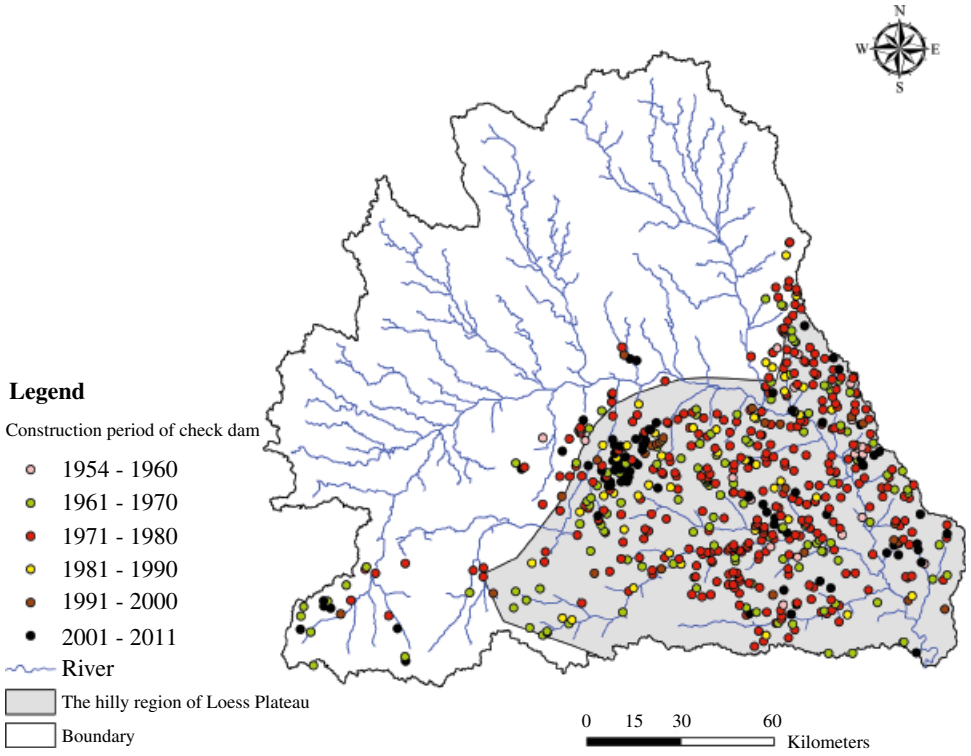

Figure 2.9 Check dam distribution in the Wuding River watershed.

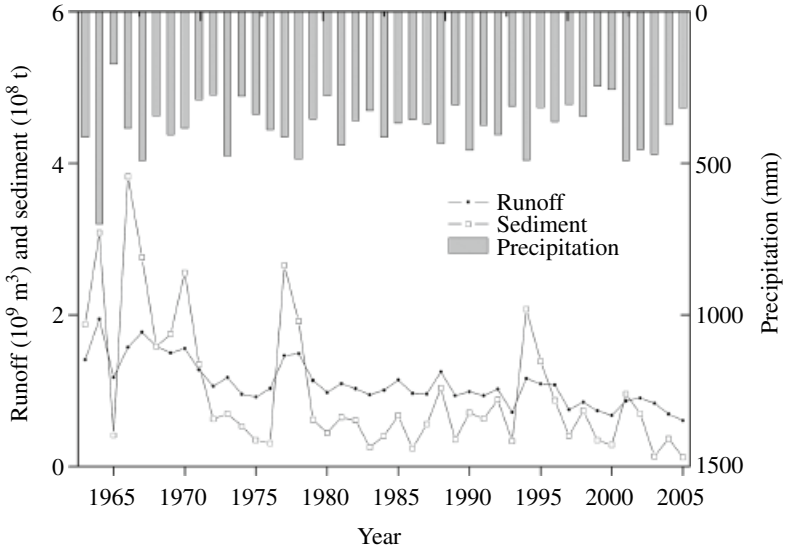

Figure 2.10 The annual precipitation, runoff, and sediment for the Wuding River from 1963 to 2005.

Table 2.11 Mann–Kendall analysis of precipitation, runoff, and sediment.

Variable	Statistic (U)	Slope (β)	Significant P	Tendency
Precipitation	−0.41	−0.60	0.521	—
Runoff	−5.68	−0.60	$P < 0.01$	Decrease
Sediment	−3.01	−81.70	$P < 0.01$	Decrease

@seismicisolation

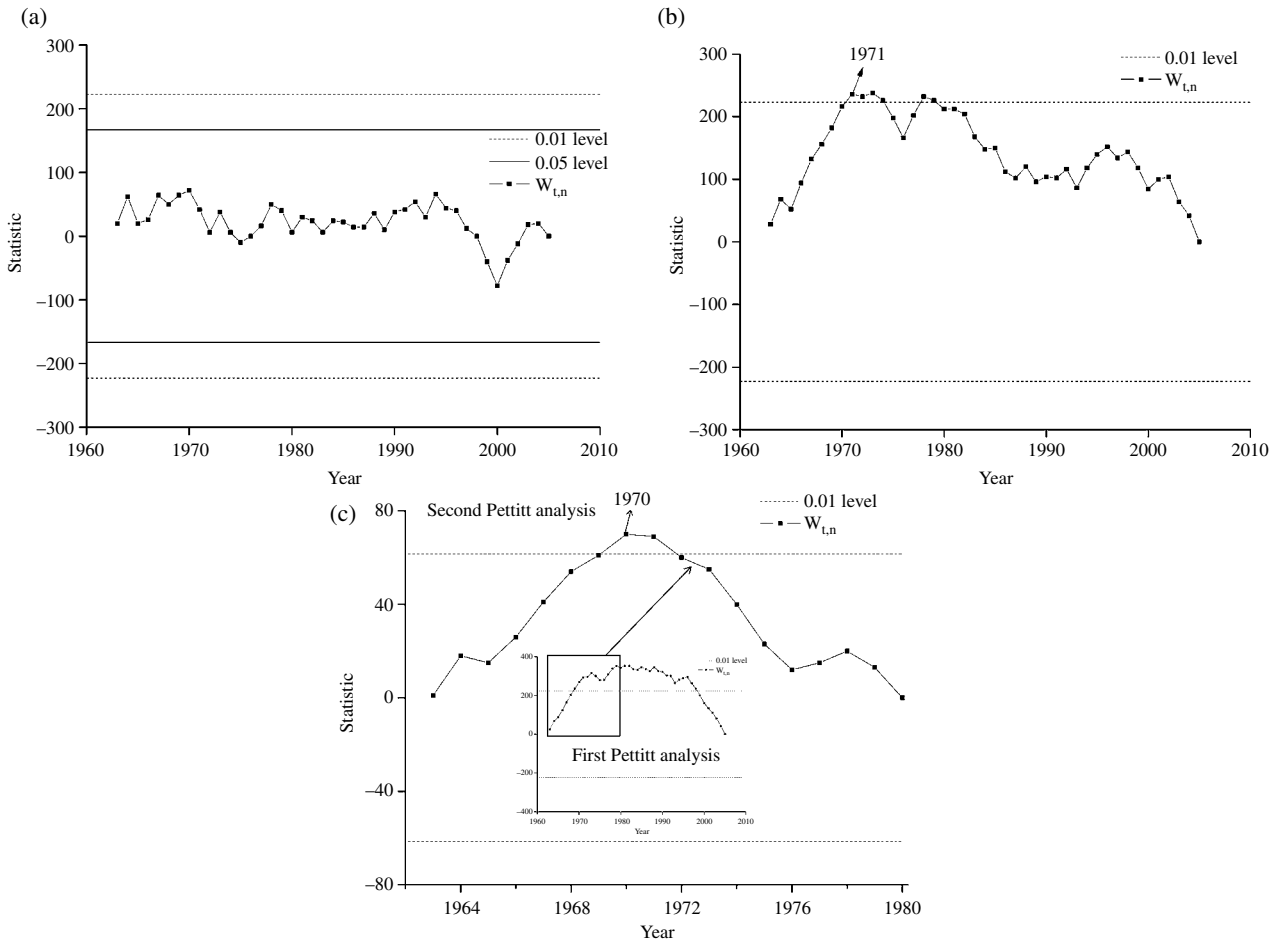

Figure 2.11 Change points in the time series of precipitation (a), sediment yield (b), and runoff (c) from 1963 to 2005 as determined by a Pettitt analysis.

runoff, and sediment from 1963 to 2005. No change point was detected in the precipitation time series (Figure 2.11a). However, the annual sediment yield showed a change point in 1971 (Figure 2.11b). The first Pettitt analysis showed transition years for runoff during 1970–1982. To accurately determine the runoff change point, a second Pettitt analysis was conducted within 1963–1982, and it revealed that 1970 and 1971 were when the significant change began (Figure 2.11c).

2.7.3. Simulation of Check Dam on Runoff and Sediment Regulation by SWAT Model

We investigated the impacts of land-use changes and check dam construction on runoff and sediment load in the Wuding River watershed using the SWAT model. The levels of runoff and sediment in the watershed have shown significant decreasing trends over the past 60 years. A change point for sediment was found in 1970, and the annual runoff showed change points in 1970 and 1971. In the early 1970s, the large-scale construction of check dams began. From 1970 to 1980, 430 check dams were constructed in the watershed, representing 49% of the total amount. Check dams play important roles in reducing runoff and sediment load. The simulation results showed that check dam construction decreased runoff and sediment by 12% and 11.7%, respectively. However, although check dams are effective for flood and sediment control, high sediment loads in the catchment result in their rapid filling. Check dam trapping may provide short-term soil erosion control benefits.

2.8. DISCUSSION

Hydrological control works, such as check dams, may substantially alter water discharge and sediment delivery [8, 22]. The in-channel structures change runoff

@seismicisolation

and sediment dynamics by interrupting the longitudinal stream flow, decreasing the velocity and peak rates, and allowing more time for infiltration and sediment trapping [23]. Flat lands are formed when check dams fill with sediment. The new land has been used for agricultural production, and high grain yields were obtained owing to humus-rich soil carried by floods and runoff. According to the monitoring data, the food production capability of dam-formed cropland is two to three times greater than that of terraced cropland and 6 to 10 times greater than that of sloped cropland [24].

Water and sediment reductions have been attributed to check dam construction, with examples documented in Spain, Japan, China, the United States, and elsewhere [25, 26]. Boix-Fayos et al. [27] applied the WaTEM-SEDEM model to scenarios with and without check dams and found that 77% of sediment was trapped behind a dam in the Rogativa catchment of Spain. Zhao et al. [15] used the sediment distributed delivery model to quantify the effects of check dams on sediment in the Huangfuchuan catchment of China, and the check dam reduced 51.9% of the sediment load in the study area. Xu et al. [28] reported that check dam construction in the Yanhe watershed had an effect on runoff and sediment. The former decreased by 15.5–28.9% in the rainy season, and the latter decreased by 79.4–85.5%. Tian et al. [29] used remote sensing to determine the numbers, controlled areas, and storage capacities of check dams and quantify their substantial trapping effects on stream flow and sediment load in a catchment. Our field surveys and simulations documented that check dams reduce surface runoff and sediment.

Check dams are intended to control soil and water erosion upstream. However, studies also indicate that check dams are temporary solutions that often fill up rapidly because of high sediment yields from the watersheds' badlands [15, 27]. Check dams may provide flood control and sediment reduction benefits for a few years. However, it is not enough to only apply sediment control measures in the channels of erodible areas. In addition, water and soil conservation measures on the sloped lands must be taken into account.

Because check dams are very effective in water and sediment reduction over the short term, and revegetation is the long-term soil erosion control measure, it is probably more efficient to combine check dam construction with adapted revegetation strategies [27]. It is likely that vegetation restoration on the slopes will reduce sediment sources and that check dams will have important long-term regulatory effects on runoff and sediment. The lack of soil moisture is an urgent problem for establishing vegetation on the Loess Plateau. More native plants should be selected for the vegetation recovery because introduced vegetation could rapidly decrease soil moisture and thus, drastically deplete local soil moisture resources [1]. The sediment-filled dams are vulnerable to large floods. For example, on 26 July 2017, more than 200 mm of rain fell in Suide and Zizhou Counties, which are located in the Wuding River watershed, resulting in a large flood that damaged 20% of the main check dams. Thus, side spillways or other infrastructures need to be constructed to withstand large floods and ensure the security of the check dams.

2.9. CONCLUSION

Check dam construction on the Loess Plateau is of great significance to prevent water and soil losses, detain floods, retain sediment, and reduce sediment flowing into the Yellow River. The mechanisms of water and soil conservation of the check dam system in the small watersheds on the Loess Plateau were studied: with the siltation of the dam land, the channel shape gradually transformed from the original V to U and the gradient was decreased; the cross-sectional area of the flow becomes larger; after the siltation, it turns into agricultural land, on which the main crop is corn, and the underlying surface of the water channel changes accordingly; the check dam serves as an obstacle of natural river channels that affects the runoff process of the basin. Flood detention and water storage effects of the check dam system were important to reduce runoff and delay the appearance of flood peaks. Check dam constructed in Wangmaogou watershed reduced runoff coefficient and sediment by 29.43 and 28.09%, respectively.

REFERENCES

1. Pal, D., Galelli, S., Tang, H., and Ran, Q. (2018). Toward improved design of check dam systems: a case study in the Loess Plateau. *China. Journal of Hydrology 1694* (18): 30128.
2. Zhao, T., Yang, M., Walling, D.E. et al. (2017). Using check dam deposits to investigate recent changes in sediment yield in the Loess Plateau, China. *Global and Planetary Change 152*: 88–98.
3. González-Romero, J., Lucas-Borja, M.E., Plaza-Álvarez, P.A. et al. (2018). Temporal effects of post-fire check dam construction on soil functionality in SE Spain. *Science of the Total Environment 642*: 117–124.

@seismicisolation

4. Cheng, Y., Li, P., Xu, G. et al. (2018). Effects of soil erosion and land use on spatial distribution of soil total phosphorus in a small watershed on the Loess Plateau, China. *Soil and Tillage Research 184*: 142–152.
5. Tian, P., Zhao, G., Mu, X. et al. (2013). Check dam identification using multisource data and their effects on streamflow and sediment load in a Chinese Loess Plateau catchment. *Journal of Applied Remote Sensing 7*: 073697.
6. Bai, L., Wang, N., Jiao, J. et al. (2020). Soil erosion and sediment interception by check dams in a watershed for an extreme rainstorm on the Loess Plateau, China. *Journal of Sediment Research 35* (4): 408–416.
7. Wen, X. and Li, Z. (2020). Soil erosion control practices in the Chinese Loess Plateau: a systematic review. *Environmental Development 34*: 1–13.
8. Li, X., Wei, X., and Wei, N. (2016). Correlating check dam sedimentation and rainstorm characteristics on the Loess Plateau, China. *Geomorphology 265*: 84–97.
9. Wei, X. and Li, X. (2016). Fractal features of soil particle size distribution in layered sediments behind two check dams: Implications for the Loess Plateau, China. *Geomorphology 266*: 133–145.
10. Xin, Z., Yu, X., and Lu, X. (2011). Factors controlling sediment yield in China's Loess Plateau. *Earth Surface Processes and Landforms 36* (6): 816–826.
11. Yang, Y., Fu, S., Liu, B. et al. (2020). Damage of check dams by extreme rainstorms on the Chinese Loess Plateau: A case study in the Chabagou watershed. *Journal of Soil and Water Conservation 75*: 746–754.
12. Li, E., Mu, X., Zhao, G. et al. (2017). Effects of check dams on runoff and sediment load in a semi-arid river basin of the Yellow River. *Stochastic Environmental Research Risk and Assessment 31*: 1791–1980.
13. Zhao, G., Klik, A., Mu, X. et al. (2015). Sediment yield estimation in a small watershed on the northern Loess Plateau, China. *Geomorphology 241*: 343–352.
14. Mishra, A., Froebrich, J., and Gassman, P.W. (2007). Evaluation of the SWAT model for assessing sediment control structures in a small watershed in India. *Transactions of the Asabe 50*: 469–477.
15. Polyakov, V.O., Nichols, M.H., McClaran, M.P., and Nearing, M.A. (2014). Effect of check dams on runoff, sediment yield, and retention on small semiarid watersheds. *Journal of Soil and Water Conservation 69*: 414–421.
16. Shi, P., Zhang, Y., Ren, Z. et al. (2019). Land-use changes and check dams reducing runoff and sediment yield on the Loess Plateau of China. *Science of the Total Environment 664*: 984–994.
17. Wang, S., Fu, B., Piao, S. et al. (2015). Reduced sediment transport in the Yellow River due to anthropogenic changes. *Nature Geoscience 9*: 38–42.
18. Zhongbao, X., Bofu, Y., and Yuguo, H. (2015). Spatiotemporal variations in annual sediment yield from the middle Yellow River, China, 1950–2010. *Journal of Hydrologic Engineering 20* (8): 04014090.
19. Xu, Y.D., Fu, B.J., and He, C.S. (2013). Assessing the hydrological effect of the check dams in the Loess Plateau, China, by model simulations. *Hydrology And Earth System Sciences 17*: 2185–2193.
20. Fu, B., Liu, Y., Lü, Y. et al. (2011). Assessing the soil erosion control service of ecosystems change in the Loess Plateau of China. *Ecological Complexity 8* (4): 284–293.
21. Tang, Q., Wang, S., Fu, B. et al. (2020b). Check dam infilling archives elucidate historical sedimentary dynamics in a semiarid landscape of the Loess Plateau, China. *Ecological Engineering 118*: 161–170.
22. Tasdighi, A., Arabi, M., and Harmel, D. (2018). A probabilistic appraisal of rainfall-runoff modeling approaches within SWAT in mixed land use watersheds. *Journal of Hydrology 564*: 476–489.
23. Fu, B., Wang, S., Liu, Y. et al. (2017). Hydrogeomorphic ecosystem responses to natural and anthropogenic changes in the Loess Plateau of China. *Earth and Planetary Sciences 45* (1): 223–243.
24. Peng, S., Yu, K., Wen, Z., and Zhang, C. (2019). Integrating potential natural vegetation and habitat suitability into revegetation programs for sustainable ecosystems under future climate change. *Agricultural and Forest Meteorology 269–270*: 270–284.
25. Mizuyama, T. (2008). Structural countermeasures for debris flow disasters. *International Journal of Erosion Control Engineering 1*: 38–43.
26. Boix-Fayos, C., de Vente, J., Martínez-Mena, M. et al. (2008). The impact of land use change and check-dams on catchment sediment yield. *Hydrological Processes 22*: 4922–4935.
27. Tang, H., Pan, H., and Ran, Q. (2020a). Impacts of filled check dams with different deployment strategies on the flood and sediment transport processes in a Loess Plateau catchment. *Water 12* (5): 1319–1341.
28. Feng, X., Fu, B., Piao, S. et al. (2016). Revegetation in China's Loess Plateau is approaching sustainable water resource limits. *Nature Climate Change 8*: 1–6.
29. Wang, Y., Fu, B., Chen, L. et al. (2011). Check dam in the Loess Plateau of China: engineering for environmental services and food security. *Environmental Science & Technology 45*: 10298–10299.

@seismicisolation

3

Regulating the Effect of a Check Dam System on Sediment Redistribution

Guoce Xu[1], Tanbao Li[2], Jibin Wang[2], Zongping Ren[1], Kunxia Yu[1], Zhanbin Li[1], Lie Xiao[1], Zhihai Wei[2], Dejun Wang[2], and Yan Zhang[3]

3.1. INTRODUCTION

Soil particle-size distribution is one of the most important physical attributes because of its great influence on soil properties related to water movement, productivity, and soil erosion [1]. In areas with high soil erosion rates attributable to water, fine particle-size fractions (accompanied by nutrients) are removed or deposited selectively during soil erosion processes [2]. Applications of fractal geometry in soil science have shown that soil exhibits fractal characteristics and is a porous medium with different particle compositions that have irregular shapes and self-similar structures [3]. Martinez-Mena et al. [4] used fractal dimension of soil aggregates (Dn) as an indicator of soil erodibility. They estimated Dn from the fractal model Rieu and Sposito [5] proposed using data collected by dry-sieving soil aggregates. The results of their study confirmed that higher Dn values were associated with lower aggregate stabilities. They also indicated that Dn can be a useful index to characterize and describe soil erodibility. Different types of land-use and vegetation types influence soil particle-size distribution largely by either enhancing or inhibiting soil erosion [2, 6–11]. Wang et al. [12] found that land use had a considerable effect on the fractal dimension of soil particle-size distribution and other soil properties. Moreover, understanding the effect of land use changes on soil properties and water resources is recognized as one of the most challenging issues in hydrology (e.g., [13]).

3.2. METHOD

Soil samples were collected using a soil sampling auger with a diameter of 5.0 cm in three locations along the middle line of the dammed farmlands in front, in the middle, and tail of the dam. There were 47 sampling points and 940 soil samples. The depth of each point was 200 cm, and soil samples were collected every 10 cm. A total of 20 layers of soil samples were collected, each with a mass of about 1.0 kg. They were taken back to the soil chemistry laboratory for analysis. A global positioning system (GPS) was used to determine sampling locations.

Soil samples were prepared for analysis by sieving to determine particle sizes ranging from 0.05 to 2.0 mm. Initially, soil samples were air dried and machine-sieved through a 2.0-mm screen to remove roots and other debris. Soil particle-size distribution was described in terms of the percentages of silt and clay (<0.05 mm), fine sand (0.05–0.25 mm), coarse sand (0.25–1.0 mm), and gravel (1.0–2.0 mm). Soil particle composition was measured by laser diffraction using a Mastersizer 2000

[1] *Institute of Water Resources and Hydro-electric Engineering, Xi'an University of Technology, Xi'an, China*

[2] *Northwest Institute of Forest Inventory, Planning and Design, National Forestry and Grassland Administration, Xi'an, China*

[3] *College of Urban and Environmental Sciences, Northwest University, Xi'an, China*

Check Dam Construction for Sustainable Watershed Management and Planning, First Edition.
Edited by Zhanbin Li, Peng Li, Yang Yu, Peng Shi, and Guillaume Piton.
© 2022 John Wiley & Sons, Inc. Published 2022 by John Wiley & Sons, Inc.

@seismicisolation

particle-size analyzer (Malvern Instruments, Malvern, England). The particle size is divided into 2–1 mm(d_1), 1–0.5 mm(d_2), 0.5–0.25 mm(d_3), 0.25–0.1 mm(d_4), 0.1–0.05 mm(d_5), 0.05–0.002 mm (d_6), and <0.002 mm (d_7).

The definition of a fractal can be given based on the relationship between number and size in a statistically self-similar system and defined by the following equation [14, 15]:

$$N\left(X > x_i\right) = kx_i^{-D} \tag{3.1}$$

where N ($X \geq x_i$) is the cumulative number of objects or fragments greater than a characteristic size x_i, k is the number of elements at a unit length scale, and D is the fractal dimension. However, the applicability of Equation (3.1) for PSD analysis is limited because complete and accurate calculations of N values are typically unavailable from conventional PSD experimental data.

In an effort to compensate for the lack of N values, Tyler and Wheatcraft [16] estimated the fractal dimension of PSD, D_m, based on the following expression:

$$M\left(r < R_i\right)/M_T = \left(R_i/R_{\max}\right)_m^{3-D} \tag{3.2}$$

where M is the cumulative mass of particles of the ith size, r less than R_i, M_T is the total mass, R_i is the mean particle diameter (mm) of the ith size class, and R_{max} is the mean diameter of the largest particle, respectively. The mean particle diameter is taken as the arithmetic mean of the upper and lower sieve sizes [3]. Taking the logarithm of both sides in Equation (3.2), we derived Equation (3.3) to solve for D_m:

$$D_m = 3 - \frac{\log M\left(r < R_i\right)/M_T}{\log\left(R_i/R_{\max}\right)} \tag{3.3}$$

3.3. PARTICLE-SIZE ANALYSIS OF SEDIMENT IN DAMS

3.3.1. Statistical Characteristics of Soil Particle Size in Dams

According to the United States soil particle standard, the mechanical composition of soil includes sand (2–0.05 mm), silt (0.05–0.002 mm), and clay (<0.002 mm). Figure 3.1 shows that there are few differences in the mechanical composition of sediment in the front, middle, and behind the dam of Wangmaogou basin.

Table 3.1 shows the descriptive statistical characteristics of soil particle-size composition in the sedimentation section of a typical check dam in Wangmaogou basin. It indicates that the silt content dominates, with a percentage that ranges from 39.64 to 85.90%, with a mean of 63.22%; the sand content is second, and its percentage ranges from 3.38 to 57.74%, with a mean of 29.94%, while the clay content is lowest, with a percentage that ranges from 2.62 to 15.26%, with a mean of 6.84%.

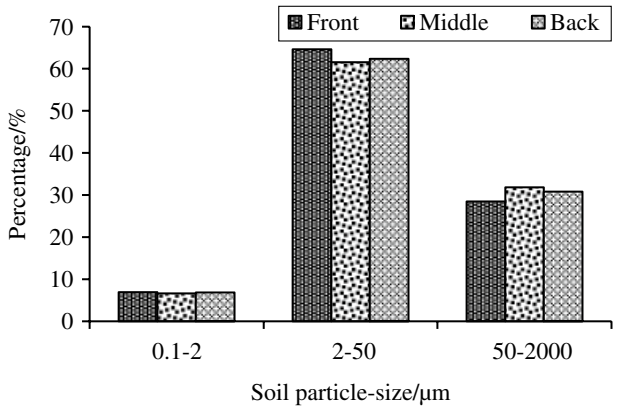

Figure 3.1 Soil particle-size distribution at different locations of dammed farmland.

Table 3.1 Statistical characteristics of soil particle size in dammed farmland.

Soil texture	Mean/%	Median/%	SD/%	CV/%	Variance
Clay	6.84	6.68	1.18	17.25	1.39
Silt	63.22	63.37	6.45	10.20	41.6
Sand	29.94	29.89	7.34	24.52	53.88

In the vertical direction, the sediment in the dam is shown in order of fine, coarse, fine, and coarse distribution from top to bottom; in the horizontal direction, the coarse sediment content in the middle of the dam > the content behind the dam > the content in front of the dam, and they are 31.47, 30.81, and 28.52%, respectively. On the whole, there is no great difference between the sediment in the middle of the dam and that behind the dam, but the coarse sediment content in front of the dam decreases significantly compared with that behind the dam, where it is coarser upstream and finer downstream.

The variation coefficient of each particle size of the dam soil in the entire profile is in the order of sand particles>clay particles > silt particles. According to Nielson and Bouma [17] classification system, when CV ≤ 10%, it has weak variability; when 10%

@seismicisolation

< CV < 100%, it has moderate variability, and when CV ≥ 100, it has high variability, indicating that the silt, clay, and sand particles in the sedimentation profile of the check dam in Wangmaogou watershed are moderately variable.

3.3.2. Texture Classification of Sediment in Dam

Figure 3.2 is a triangle diagram of the soil texture of the dam land and slope land. It shows that the dam land and slope soil can be divided into three kinds of soil textures, sandy loam, silt loam, and silt soil. The silt loam has the most soil samples, followed by sandy loam and silt soil. The soil samples on the slopes of the Wangmaogou basin are all silt loam with little clay content, and most of the soil samples in the dam are silt loam. Figure 3.2 shows that the transportation and sedimentation within the dam refines the composition of soil particles. The mean values of clay, silt, and sand content of slope soil are 0.28, 66.27, and 33.45%, respectively. Compared with the sediment in dams, the slope soil contains a large amount of sand and silt and a small amount of clay. The soil on the slope is transformed into soil in the dam through a process of sediment transport and sorting. This is primarily because clay and silt particles are more likely to be suspended and transported by runoff than sand particles in the erosion process of slope soil.

3.3.3. Coarseness of Soil Particles in Dams

Table 3.2 is a statistical table of the soil particle size and texture coarsening of the check dam in Wangmaogou basin. Table 3.2 shows that the soil particle sizes in the dam are largely 0.1–0.05 and 0.05–0.002 mm, which indicates that runoff has a certain sorting effect on the erosion of soil particles on the slope. Fine sand and silt particles can be washed down the slope by the general erosive rainfall and are transported to the check dam and deposited. The soil texture's coarseness can explain the change in soil particle composition after erosion, i.e., the ratio of the sum of gravel and sand content (>0.05 mm) to the sum of silt and clay content (<0.05 mm). (The classification of gravel, sand, silt, and clay particles in this paper is according to that in the United States.) The coarser the soil texture, the greater the proportion of coarse particles in the soil's mechanical composition; the less coarse the soil texture, the smaller the proportion of coarse particles in the soil's mechanical composition, and the greater the degree of soil erosion.

Table 3.2 illustrates that Wangmaogou's soil texture coarseness is between 0.27 and 0.58, with a mean of 0.44. The coarseness of the soil texture in front of the dam (0.40) < the coarseness behind the dam (0.45) < the coarseness in the dam (0.46). The fragmented landscape pattern of the Loess Plateau leads to a

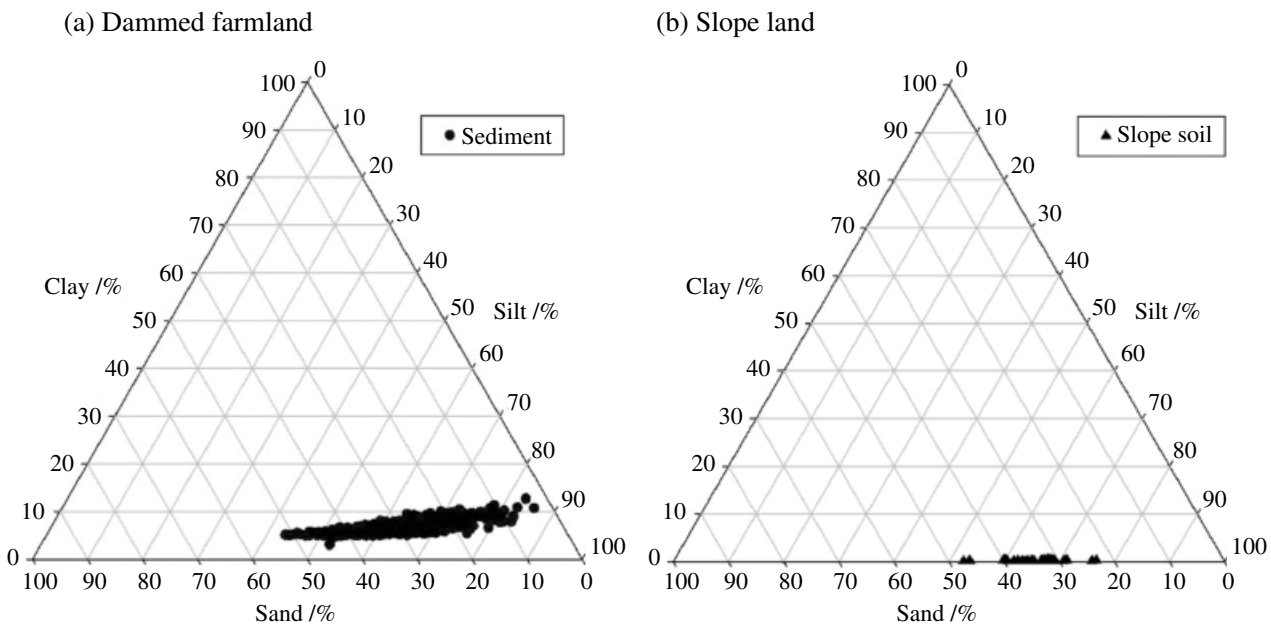

Figure 3.2 Soil texture of sediment in dammed farmland and soil in slope land.

@seismicisolation

Table 3.2 Statistical characteristics of soil particle size and texture coarsening of dammed farmland.

Sampling site	Depth/cm	Soil particle-size distribution/mm							D_{50}	Degree of soil texture coarsening degrees
		2.0–1.0	1.0–0.5	0.5–0.25	0.25–0.1	0.1–0.05	0.05–0.002	<0.002		
Front	0–10	0.00	0.04	0.25	5.50	22.48	64.56	7.17	29.81	0.39
	10–20	0.00	0.03	0.20	5.45	21.92	65.50	6.90	29.92	0.38
	20–30	0.05	0.06	0.09	5.63	22.86	64.71	6.60	31.29	0.40
	30–40	0.00	0.00	0.10	4.22	22.65	66.32	6.71	30.39	0.37
	40–50	0.00	0.00	0.14	4.55	24.04	64.72	6.55	31.52	0.40
	50–60	0.00	0.01	0.11	4.95	24.86	63.45	6.63	32.35	0.43
	60–70	0.00	0.01	0.10	4.51	23.28	65.21	6.90	30.23	0.39
	70–80	0.00	0.00	0.05	5.36	25.33	62.70	6.55	33.08	0.44
	80–90	0.00	0.03	0.21	5.86	24.34	62.88	6.67	32.45	0.44
	90–100	0.00	0.00	0.04	4.76	22.35	65.85	6.99	29.55	0.37
	100–110	0.00	0.00	0.06	4.82	23.98	64.19	6.95	31.04	0.41
	110–120	0.00	0.00	0.08	5.41	24.10	63.46	6.95	31.48	0.42
	120–130	0.00	0.00	0.02	4.96	24.18	63.98	6.85	31.31	0.41
	130–140	0.00	0.00	0.07	5.06	22.94	64.87	7.05	30.07	0.39
	140–150	0.00	0.00	0.02	4.88	24.79	63.51	6.80	31.80	0.42
	150–160	0.00	0.01	0.08	5.68	23.72	63.31	7.20	30.72	0.42
	160–170	0.00	0.00	0.04	4.59	20.91	66.95	7.51	27.67	0.34
	170–180	0.00	0.00	0.05	4.26	22.11	66.31	7.28	29.05	0.36
	180–190	0.00	0.00	0.03	4.91	22.14	65.64	7.28	28.91	0.37
	190–200	0.00	0.00	0.03	5.52	24.60	63.34	6.50	32.49	0.43
Middle	0–10	0.00	0.00	0.23	3.55	18.50	69.15	8.57	25.21	0.29
	10–20	0.00	0.00	0.17	3.39	17.73	72.20	6.53	30.41	0.27
	20–30	2.64	0.94	0.08	3.86	22.26	64.08	6.15	32.95	0.42
	30–40	3.50	0.36	0.27	6.38	25.54	58.25	5.71	37.57	0.56
	40–50	0.00	0.10	0.59	8.08	27.30	57.84	6.09	37.01	0.56
	50–60	0.00	0.00	0.04	7.48	28.01	58.21	6.26	36.54	0.55
	60–70	0.00	0.02	0.08	7.19	26.40	59.68	6.64	34.54	0.51
	70–80	0.16	0.08	0.10	5.83	23.07	63.94	6.82	31.50	0.41
	80–90	2.35	4.85	0.74	7.39	21.25	57.46	5.97	31.17	0.58
	90–100	0.00	0.00	0.06	5.18	23.69	64.20	6.87	30.87	0.41
	100–110	0.00	0.00	0.00	6.80	26.14	60.71	6.36	34.25	0.49
	110–120	0.00	0.01	0.06	5.56	24.53	63.08	6.77	31.42	0.43
	120–130	0.00	0.03	0.21	6.02	24.08	62.49	7.17	31.16	0.44
	130–140	0.00	0.00	0.11	5.75	23.49	63.47	7.17	30.70	0.42
	140–150	0.00	0.00	0.04	5.66	26.15	61.75	6.39	33.77	0.47
	150–160	0.00	0.01	0.08	6.82	28.30	58.71	6.09	36.66	0.54
	160–170	0.00	0.00	0.00	5.81	26.48	61.24	6.47	34.29	0.48
	170–180	0.00	0.00	0.00	6.65	26.04	60.46	6.85	33.50	0.49
	180–190	0.00	0.02	0.22	6.89	25.63	60.56	6.68	33.52	0.49
	190–200	0.00	0.02	0.19	6.39	25.88	61.07	6.45	33.96	0.48
Back	0–10	0.00	0.01	0.13	5.41	22.35	64.99	7.11	29.57	0.39
	10–20	0.00	0.00	0.07	5.30	23.39	64.38	6.86	30.59	0.40
	20–30	0.00	0.01	0.10	6.35	24.96	61.97	6.61	32.78	0.46
	30–40	0.00	0.01	0.11	6.61	25.11	61.44	6.71	32.87	0.47
	40–50	0.00	0.02	0.11	6.27	25.98	61.01	6.60	33.52	0.48
	50–60	0.00	0.03	0.14	6.20	25.48	61.53	6.63	32.98	0.47
	60–70	0.02	0.02	0.07	6.13	26.04	61.26	6.46	33.78	0.48
	70–80	0.00	0.04	0.25	6.23	24.92	61.94	6.62	32.89	0.46
	80–90	0.00	0.05	0.28	6.24	24.89	61.72	6.82	32.20	0.46

@seismicisolation

Table 3.2 (Continued)

Sampling site	Depth/cm	Soil particle-size distribution/mm								Degree of soil texture coarsening degrees
		2.0–1.0	1.0–0.5	0.5–0.25	0.25–0.1	0.1–0.05	0.05–0.002	<0.002	D_{50}	
	90–100	0.00	0.02	0.10	5.93	25.00	62.11	6.83	32.15	0.45
	100–110	0.00	0.01	0.10	6.10	24.62	62.31	6.85	31.96	0.45
	110–120	0.00	0.02	0.12	5.63	23.27	63.74	7.22	29.82	0.41
	120–130	0.00	0.02	0.17	5.60	23.88	63.22	7.12	30.66	0.42
	130–140	0.00	0.01	0.14	6.26	24.48	62.08	7.02	31.52	0.45
	140–150	0.00	0.00	0.04	6.08	25.44	61.77	6.67	32.98	0.46
	150–160	0.00	0.00	0.03	5.94	24.88	62.24	6.91	32.04	0.45
	160–170	0.00	0.01	0.06	5.57	23.82	63.48	7.06	30.66	0.42
	170–180	0.00	0.01	0.08	6.05	25.09	61.95	6.82	32.46	0.45
	180–190	0.00	0.02	0.12	5.84	25.16	62.02	6.84	32.36	0.45
	190–200	0.00	0.00	0.00	5.82	25.25	62.01	6.91	32.33	0.45

complex composition and distribution of sediment particles in the dam. Most of the sediment from the land between gullies is based upon a general rule: The coarser sediment particles are deposited gradually under the action of gravity, and the fine particles are deposited gradually as the water flows downstream along the channel, which is manifested in the process of gradual fining from upstream to downstream and the horizontal movement of sediment in the dam. The length of the channel or the shape of the basin affects the areas of most dams, so the sedimentation and sorting of sediment in the check dam are not particularly obvious.

3.4. SOIL PARTICLE AND FRACTAL CHARACTERISTICS IN DAMS

3.4.1. The Fractal Dimension Distribution of Soil Particles in Dams

The soil particle size determines the soil's physical, chemical, and biological properties, including the combination of soil particles, their number and geometric form, and the size of the pores, which is related closely to water and soil loss and soil degradation. Compared with the soil particle-size distribution, the fractal dimension can not only reflect the content of different particle sizes but also describe the irregular structure of the soil comprehensively. The higher the clay and silt content, the finer the soil texture, and the higher the corresponding fractal dimension; the higher the sand content, the coarser the soil texture, and the lower the corresponding fractal dimension.

The variation in the fractal dimension of soil particle volume with the depth of the soil layer throughout the Wangmaogou dam system is shown in Figure 3.3. The fractal dimension of the soil in the 0–200 cm soil layer of Wangmaogou dam was calculated, as shown in Table 3.3. The fractal dimension of the dam soil ranges from 2.651 to 2.965, and the value measured changes little. The mean and median value of the fractal dimension are 2.799 and 2.798, respectively. The similarity between the mean and median values indicates that the soil fractal dimension values are distributed relatively uniformly in the study area and are not affected by specific values. The fractal dimensions of soil particles in the front, middle, and behind the dam are 2.803, 2.783, and 2.795, respectively, i.e., the fractal dimensions of soil particles in the middle of the dam < those behind the dam < those in front of the dam, indicating that the upstream sediment is coarse and the downstream sediment is fine.

3.4.2. Relation Between the Fractal Dimension and the Composition of Soil Particles in Dams

The soil particles' fractal dimension can be used to measure the soil texture's uniformity to a certain extent. The soil particles' fractal dimension are fitted to the equations of soil sand, silt, and clay particles. The change in the fractal dimension of soil particles in the dam is used as the dependent variable, and the changes in soil sand, silt, and clay particles in the dam are used as the dependent variables. The results are as follows:

$$y = -0.0061x + 2.9817,\ R^2 = 0.9171$$

$$y = 0.0068x + 2.3711,\ R^2 = 0.8587$$

$$y = 0.0355x + 2.5557,\ R^2 = 0.7959$$

@seismicisolation

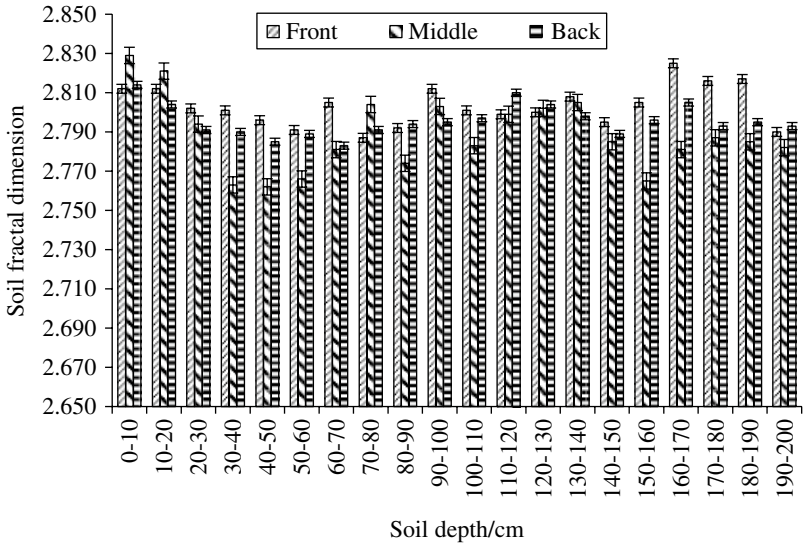

Figure 3.3 Fractal dimension of soil particles at different depths.

Table 3.3 Statistical characteristic of soil fractal dimension of dammed farmland.

Number	Min.	Max.	Mean	Median	SD	CV	Skewness	Kurtosis
940	2.651	2.965	2.799	2.798	0.046	0.016	0.141	0.548

The analysis results show that the higher the content of soil clay and silt, the higher the soil particles' fractal dimension, while the higher the content of soil sediment, the lower their fractal dimension (Figure 3.4). The fitting results above show that the effect of dam soil particles on the fractal dimension is generally as follows: sediment particles > silt particles > clay particles, indicating that sand content affects dam soil particles' fractal dimension most significantly.

3.5. RELATION BETWEEN SOIL PARTICLES' FRACTAL DIMENSION AND SOIL PROPERTIES

The correlation analysis among the soil particles' fractal dimensions, the percentage of soil particles of different sizes, and the basic properties of soil in the dam of Wangmaogou basin are shown in Table 3.4. From the calculation formula of the fractal dimension, it can be concluded that the calculation of the fractal dimension is related to the cumulative content of soil particles from large to small. The relation between the soil particles' fractal dimension and their composition can be clarified further through a correlation analysis between the soil particles' fractal dimension and the percentage of soil particles of different sizes. The analysis shows that the soil particles' fractal dimension has a highly significant positive correlation ($p < 0.01$) with the content of soil clay particles (<0.002 mm) and that of soil silt particles (0.002–0.05 mm), while the soil particles' fractal dimension has a significant negative correlation ($p < 0.01$) with the content of sand particles (>0.05 mm). The higher the clay and silt content, the larger the soil's fractal dimension, and the higher the sand content, the lower its fractal dimension.

There is no correlation between soil water content and soil organic carbon (SOC). The soil water content has a significant positive correlation with the percentage of clay and silt particles and a highly significant negative correlation with the sand volume percentage. Further, the soil water content has a significant positive correlation with the soil's fractal dimension. The higher the content of clay and silt particles, the higher the soil water content; the higher the sand content, the lower the soil water content.

The soil erodibility, K, in the dam has a highly significant positive correlation with the soil fractal dimension ($p < 0.01$), and with the clay and silt content, and a highly significant negative correlation with the sand content ($p < 0.01$). This shows that increasing the

@seismicisolation

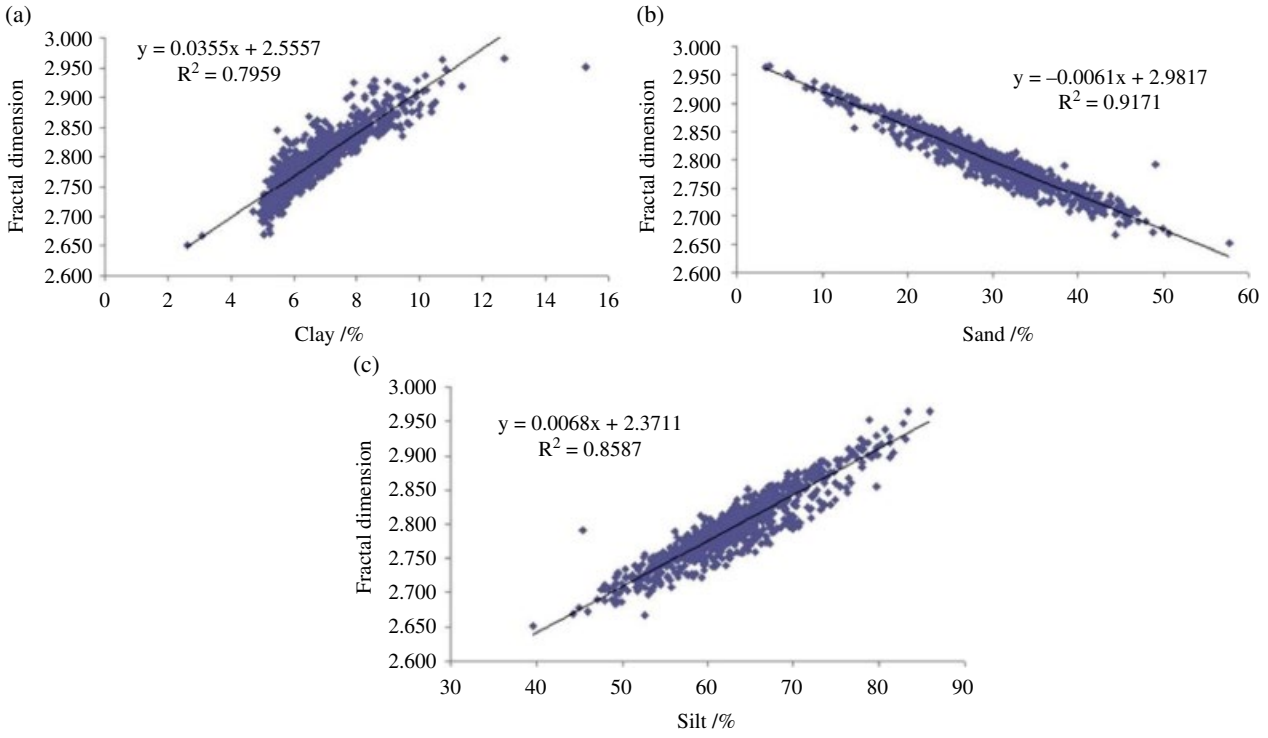

Figure 3.4 Relations among fractal dimension of soil particle and clay (a), sand (b), and silt (c).

Table 3.4 Relations between fractal dimension and soil particle-size distribution and soil properties.

Soil properties	Fractal dimension	Clay/%	Silt/%	Sand/%	SOC/(g/kg)	Soil erodibility
Fractal dimension	1					
Clay/%	0.789**	1				
Silt/%	0.920**	0.711**	1			
Sand/%	–0.938**	–0.803**	–0.990**	1		
SOC/(g/kg)	0.435	0.274*	0.555*	–0.526**	1	
Soil erodibility	0.841**	0.583**	0.800**	–0.803**	0.328	1

* Correlation is significant at $p < 0.05$
** Correlation is significant at $p < 0.01$.

sand content in the soil can improve the soil structure and reduce soil erodibility, thereby enhancing the soil's antierosion ability.

A regression analysis of the fractal dimension, D, and the content, X, of each separates is performed, and the formula obtained is shown in Table 3.5.

Taking 0.05 mm as the critical point for analysis, the mean content of particle size <0.05 mm is 69.73%, and the mean content of particle size > 0.05 mm is 30.27%. The regression analysis of the content of particle size <0.05 mm and >0.05 mm and the fractal dimension shows that the particle size <0.05 mm has a very significant positive correlation with the fractal dimension, while the particle size >0.05mm has a significant negative correlation with it. For particle size <0.05 mm, the higher the particle-size content, the greater the fractal dimension; for particle size > 0.05 mm, the higher the particle-size content, the smaller the fractal dimension.

Table 3.5 Regression analysis of soil fractal dimension and soil particle-size distribution.

Particle size (mm)	Regression equation	R^2
2.0–1.0	$D = -0.017X + 2.797$	0.25
1.0–0.5	$D = -0.025X + 2.797$	0.57
0.5–0.25	$D = -0.096X + 2.806$	0.33
0.25–0.1	$D = -0.015X + 2.881$	0.44
0.1–0.05	$D = -0.005X + 2.909$	0.19
0.05–0.002	$D = 0.006X + 2.393$	0.61
<0.002	$D = 0.036X + 2.548$	0.52

@seismicisolation

As the depth of the soil profile increases, the relation between the SOC content and the particle-size content is more complex, and there is no obvious regularity. From a statistical perspective, with 0.25 and 0.05 mm as the boundary, there is no correlation between SOC and the content of particle sizes <0.25 mm, there is a highly significant negative correlation between SOC and particle sizes $0.05 < X < 0.25$ mm, and there is a very significant positive correlation between SOC and particle sizes <0.05mm. From the surface layer to the deep layer, the relation between SOC and different particle sizes is most obvious in the particle sizes of 0.25–0.1, 0.1–0.05, 0.05–0.002, and <0.002 mm. This shows that the SOC in the dam is correlated positively with the content of silt and clay and negatively with the content of fine sand and very fine sand, which is consistent with the results of soil research in other areas of China. The particle size of the silt and clay of soil in the dam is small. They are inorganic colloid, and organic carbon is an organic colloid, and the two combine easily to form an inorganic-organic colloid. Therefore, the content of SOC in the dam is correlated positively with the content of clay and silt particles, in which the higher their content, the higher the content of organic carbon in the soil.

3.6. SEDIMENTATION CHARACTERISTICS OF DIFFERENT TYPES OF SINGLE DAMS

There are 23 check dams in the Wangmaogou basin, which are divided into two types: dams with "two facilities" and dams with "a facility." The "two facilities" include a dam body + drainage structure (shaft or horizontal pipe), and dam body + spillway. There are 5 "dam body + shaft" models, 2 "dam body + horizontal pipe" models, and 2 "dam body + spillway" models; "A facility" refers to a dam body with no drainage facilities, and is referred to also as a "check dam", of which there are 14 in total.

3.6.1. Sedimentation Characteristics of Dams with a Drainage Structure

The Wangmaogou dam system includes 7 dams with a drainage structure, Wangmaogou No. 2 dam, Guandigou No. 1 dam, Sidizui No. 1 dam, Huangbaigou No. 1 dam, Nianyangou No. 1 dam, Nianyangou No. 2 dam, and Guandigou No. 4 dam. Among them, the drainage structure of the first 5 employs shafts, and the last 2 employ horizontal pipes. The comparative analysis shows that the Wangmaogou dam system has been in operation for many years, and thus, most of the check dams are full or nearly full, so the drainage capacity of the shafts and horizontal pipes is relatively weak. Although the drainage structure has little effect on the dam's sediment particles, there is still an insignificant refinement process for the sediment through the drainage structure. In short, for the same drainage structure, the control area determines the check dam's effect in retaining the coarse sediment and discharging the fine. The effect of retaining the coarse sediment and discharging the fine of a large control area is better than that of a check dam with a small control area.

3.6.2. Sedimentation Characteristics of Dams with a Spillway

There are 2 dams with a spillway in the Wangmaogou dam system, Wangmaogou No. 1 dam and Guandigou No. 2 dam. Because Wangmaogou No. 1 dam is the first dam at the gully mouth, Guandigou No. 2 dam and Guandigou No. 1 dam downstream are used to analyze the spillway's effect on sedimentation. The Guandigou No. 2 dam is full at present. Therefore, the necessity to retain the coarse sediment and discharge the fine is relatively obvious.

3.6.3. Sedimentation Characteristics of Check Dams

There are 14 check dams in the Wangmaogou dam system. They are typical full-block and full storage check dams without a drainage structure and spillway. The variation in sediment particle size in front of and behind the 14 check dams (Table 3.6) is analyzed, and it is found that the median size before the dam is less than that behind the dam. The proportion of check dams in which the median grain size in front of the dam is smaller than that behind the dam is greater than that in which the median grain size in front of the dam is larger than that behind the dam. This indicates that there are fewer sediment particles before the dam than behind the dam. However, because most of the dams are small in area and are affected by farming, the law of sedimentation and sorting in the check dam are not particularly obvious. In short, for check dams with similar control areas, the drainage structure or spillway determines the effect of the check dam's retention of coarse sediment and discharge of the fine. The effect of retaining the coarse sediment and discharging the fine

@seismicisolation

Table 3.6 Median particle diameter at different locations in dammed farmland.

	D_{50}		
Dammed farmland	Front	Middle	Back
Wangmaogou No. 1	34.15	33.75	33.06
Huangbaigou No. 1	26.71	—	32.66
Huangbaigou No. 2	33.95	—	33.98
Kanghegou No. 1	34.80	—	37.03
Kanghegou No. 2	32.96	—	33.77
Kanghegou No. 3	35.85	—	32.46
nianyangou No. 1	26.60	—	27.02
Nianyangou No. 2	25.11	31.94	32.01
Nianyangou No. 3	29.52	—	30.58
Nianyangou No. 4	27.53	—	32.80
Wangmaogou No. 2	27.46	33.23	35.90
Sidizui No. 1	27.79	31.29	28.14
Sidizui No. 2	28.28	—	28.72
Wangtagou No. 1	36.10	—	36.63
Wangtagou No. 2	29.25	—	30.03
Guandigou No. 1	31.70	38.13	39.88
Guandigou No. 2	27.98	—	31.24
Guandigou No. 3	35.89	—	28.10
Guandigou No. 4	33.12	—	36.20
Beitagou	29.44	—	30.25
Madizui	28.86	31.38	31.52

of check dams without drainage structures or spillways is worse than that of check dams with drainage structures or spillways.

3.7. SEDIMENTATION CHARACTERISTICS OF DAM ACCORDING TO DAM SYSTEM

3.7.1. Sedimentation Characteristics of Dams Under Different Cascade Modes

The entire Wangmaogou check dam system belongs to a mixed connection mode, which is composed of partial series, parallel, and hybrid connections. The two dams in the Huangbaigou and the four dams in the Nianyangou dam system are connected in series, and the sediment changes gradually from coarse to fine from the gully head to outlet.

The three check dams in the Kanghegou dam system are also connected in series, and the sediment changes in the same way from gully head to outlet. However, each dam in the dam system changes from coarse to fine from the back to the front of the dam. This may be related to the area and different land use of the control area.

The two series dams in Wangtagou are in parallel with two series dams in Sidizui, which are in series with the Madizui dam. The Madizui dam is a hybrid model. The sediment changes gradually from coarse to fine from the gully head to the outlet of the two Wangtagou dams, while the sediment of the two Shidizui dams becomes coarser from the gully head to the outlet. In the single dam, the sediment changes from coarse to fine. Finally, after mixing into the Madizui dam, the particle size of the sediment is between that in the two branch gullies.

The Guandigou dam system is also a hybrid model. After the Guandigou No. 4 dam and Beitagou dam are connected in parallel, they are connected in series with Guandigou No. 2 dam, and then in parallel with Guandigou No. 3 dam and then in series with Guandigou No. 1 dam. From the gully head to the outlet of the longest channel, the sediment changes gradually from fine to coarse. After the branch gully merges into the main gully, the coarseness of the sand particles will be neutralized obviously.

In short, in a series dam with drainage structures, the particle size of the sediment changes gradually from coarse to fine from the gully head to the outlet; there is no obvious change in the particle size of the sediment of the check dam without a drainage structure, and sometimes it changes from fine to coarse. However, the particle size of the sediment in front of the dam in a single dam is relatively finer than that behind the dam, which is also related to the control area of the dam; after the parallel dam enters the downstream dam, the sediment particle size is neutralized.

3.7.2. Sedimentation Characteristics Under Different Channel Levels

According to the classification method of check dams, the Wangmaogou basin can be divided into three channel levels. There are 16 check dams (one small dam) in the first-level channel, 5 check dams in the secondary channel (medium dams), and 2 check dams (two major key dams) in the third channel.

Figure 3.5 shows that the fractal dimension of soil particles in the dam of the most upstream dam → gully mouth dam of the branch gully → gully mouth dam of the main gully varies from small to large, and the particle-size changes from coarse to fine, such that as the channel level increases, the sediment's particle size becomes smaller, and hence, there is less coarse and more fine sediment.

@seismicisolation

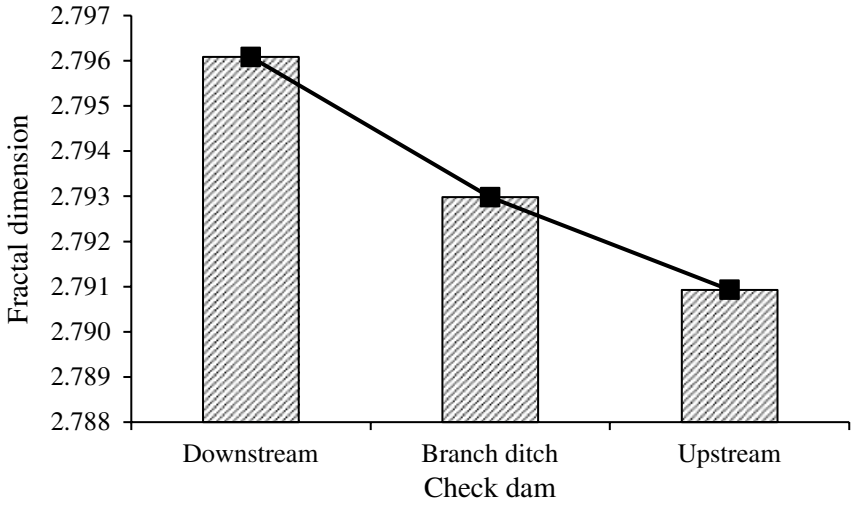

Figure 3.5 Fractal dimensions of different channel levels in Wangmaogou small watershed.

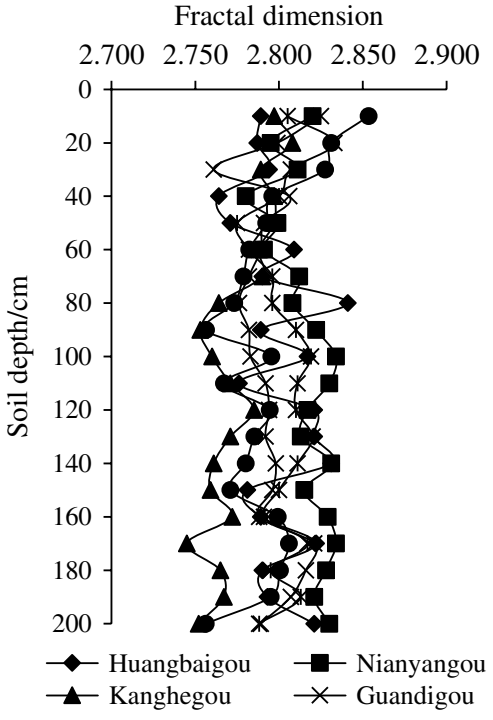

Figure 3.6 Vertical change in soil fractal dimension at different depths in different dammed farmland in Wangmaogou watershed.

3.7.3. Sedimentation Characteristics Under Different Dam Systems

Figure 3.6 indicates that the mean fractal dimension of the 6-dam system shows a wave-like change as the soil depth increases. The value of the fractal dimension of soil particles in the soil layer above 60 cm does not change drastically, while that of soil particles in the layer below 60 cm does change dramatically. The fractal dimension of soil particles in a soil layer 60 cm deep is 2.790 because the soil layer above 60cm is a cultivated layer that is affected by human activities.

The statistical characteristics of the soil's median grain size and fractal dimension under different dam systems are shown in Table 3.7. From the perspective of the entire Wangmaogou dam system, Wangmaogou No. 1 dam includes the two major check dams, as well as the dam body and the spillway, which control the Huangbaigou, Nianyangou, and Kanghegou dam systems; Wangmaogou No. 2 dam is a dam with two facilities, including the dam body and the shaft, which control the Madizui and the Guandigou dam systems. It can be considered that the runoff and sediment within the control area of Wangmaogou No. 2 dam cannot enter the Wangmaogou No. 1 dam because the shaft of Wangmaogou No. 2 dam has a small flood discharge.

The Wangmaogou dam system includes Wangmaogou No. 1 and No. 2 dams. The soil particles' fractal dimensions in the two check dams are 2.792 and 2.783, respectively. This indicates that the sediment in Wangmaogou No. 2 dam has greater sand content with a coarser texture than that in Wangmaogou No. 1 dam. The mean fractal dimension of the main gully dam system is 2.787. The mean soil particle values of the three-dam system Wangmaogou No. 1 dam controls and the 2-dam system Wangmaogou No. 2 dam controls are 2.797 and 2.799, respectively, which are higher than the fractal dimension of the control dams. This shows that the

@seismicisolation

Table 3.7 Statistical characteristics of median particle diameter and fractal dimension under different dammed farmland.

	Median-particle diameter D_{50}			Fractal dimension		
Dammed farmland	Max/%	Min/%	Mean/%	Max	Min	Mean
Guandigou	46.68	11.94	30.82	2.964	2.668	2.793
Mazuigou	50.63	11.11	32.34	2.938	2.686	2.804
Nianyangou	59.21	14.83	29.82	2.917	2.651	2.816
Kanghegou	47.27	22.26	34.66	2.858	2.667	2.774
Huangbaigou	40.44	14.74	31.65	2.925	2.740	2.780
Main channel	46.30	11.58	32.64	2.965	2.691	2.794

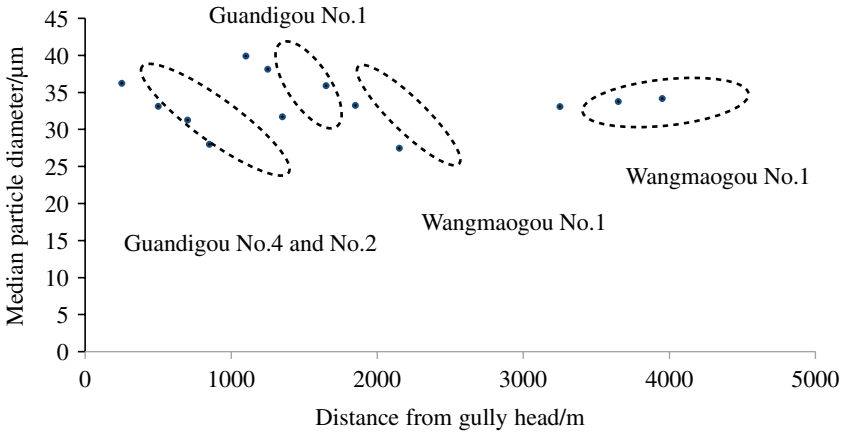

Figure 3.7 Changes in sediment along the main ditch of Wangmao watershed.

sediment particles entering Wangmaogou No. 1 and No. 2 dams become finer gradually, which further explains the effect of retaining the coarse sediment and discharging the fine.

3.8. SOIL SEDIMENTATION CHARACTERISTICS OF THE DAM SYSTEM

According to the setting of sampling points in the main gully, the variation in the median particle-size characteristics of sediment from upstream to downstream in Wangmaogou is analyzed, and the results are shown in Figure 3.7.

Figure 3.7 shows that from left to right, the d50 of sedimentation of Guandigou No. 4 and No. 2 dams show a clear downward trend from top to bottom; the d50 of sedimentation of Guandigou No. 1 dam shows a clear downward trend from top to bottom, as does the d50 of sedimentation of Wangmaogou No. 2 dam; the d50 of the sedimentation of Wangmaogou No. 1 dam shows an obvious increasing trend from top to bottom, and is a trend of phased decline. This may be caused by the control area and the different land use within the control area.

Taking Wangmaogou No. 2 dam as the boundary, the upper part of this dam belongs to the upstream, and the lower part belongs to the downstream. The fractal dimension of the downstream and upstream are 2.793 and 2.793, respectively, thus, downstream > upstream. This shows that the upstream sediment particles are coarser than the downstream sediment particles, which explains indirectly the effect of retaining the coarse sediment and discharging the fine.

3.9. CONCLUSION

The silt content is dominant in the sediment particles in dammed farmland. The mean fractal dimension shows a wave-like change as the soil depth increases in dammed farmland. In a series dam with drainage structures, the particle size of the sediment changes gradually from coarse to fine from the gully head to the outlet; there is no obvious change in the particle size of the sediment of the check dam without a drainage structure. As the channel level increases, the sediment's particle size becomes smaller, and hence, there is less coarse and more fine sediment.

@seismicisolation

REFERENCES

1. Li, J., Han, J.C., Chen, C., and Li, J.B. (2017). Effects of land use types on soil aggregate characteristics in hilly-gully region of Loess Plateau. *Journal of Soil and Water Conservation 31* (1): 248–253. +259.
2. Wang, D., Fu, B., Zhao, W. et al. (2008). Multifractal characteristics of soil particle-size distribution under different land-use types on the Loess Plateau, China. *Catena 72*: 29–36.
3. Liu, X. and Zhang, G.C. (2009). Fractal features of soil particle-size distribution as affected by plant communities in the forested region of Mountain Yimeng, China. *Geoderma 154* (1–2): 123–130.
4. Martinez-Mena, M., Deeks, L.K., and Williams, A.G. (1999). An evaluation of a fragmentation fractal dimension technique to determine soil erodibility. *Geoderma 90*: 87–98.
5. Rieu, M. and Sposito, G. (1991). Fractal fragmentation, soil porosity and soil water properties: I. theory. *J. Soil Sci. Soc. Am. J. 55*: 1231–1238.
6. Martínez-Casasnovas, J.A. and Sánchez-Bosch, I. (2000). Impact assessment of changes in land use/conservation practices on soil erosion in the Penedès–Anoia vineyard region (NE Spain). *J. Soil Tillage Res. 57*: 101–106.
7. Erskine, W.D., Mahmoudzadeh, A., and Myers, C. (2002). Land use effects on sediment yields and soil loss rates in small basins of Triassic sandstone near Sydney, NSW. *Australia. J. Catena 49*: 271–287.
8. Basic, F., Kisic, I., Mesic, M. et al. (2004). Tillage and crop management effects on soil erosion in central Croatia. *J. Soil Tillage Res. 78*: 197–206.
9. Fullen, M.A., Booth, C.A., and Brandsma, R.T. (2006). Long-term effects of grass ley set-aside on erosion rates and soil organic matter on sandy soils in east Shropshire, UK. *Soil Tillage Res 89*: 122–128.
10. Nie, M., Pendall, E., Bell, C., and Wallenstein, M.D. (2014). Soil aggregate size distribution mediates microbial climate change feedbacks. *Soil Biology & Biochemistry 68*: 357–365.
11. Fei, Q., Zhang, R., Xia, L. et al. (2018). Soil particle size distribution characteristics of different land-use types in the Funiu mountainous region. *Soil and Tillage Research 184*: 45–51.
12. Wang, X., Li, M.H., Liu, S.Z., and Liu, G.C. (2006). Fractal characteristics of soils under different land use patterns in the arid and semiarid regions of the Tibetan Plateau, China. *Geoderma 134*: 56–61.
13. Stonestrom, D.A., Scanlon, B.R., and Zhang, L. (2009). Introduction to special section on impacts of land use change on water resources. *Water Resources Research 45*: 1–3.
14. Mandelbort, B.B. (1982). *The Fractal Geometry of Nature*, 45–256. San Francisco: Freeman M.
15. Turcotte, D.L. (1986). Fractal fragmentation. *J. Geography Res. 91* (12): 1921–1926.
16. Tyler, S.W. and Wheatcraft, S.W. (1992). Fractal scaling of soil particle size distributions: analysis and limitations. *Soil Sci. Soc. Am. J. 56*: 362–369.
17. Nielsen, D.R. and Bouma, J. (1985). *Soil Spatial Variability*, 2–30. Wageningen: PUDOC.

@seismicisolation

4

An Analysis of Sediment Sources and Water–Sediment Retarding Effects of Check Dams

Guoce Xu[1], Tanbao Li[2], Jibin Wang[2], Lulu Bai[1], Kunxia Yu[1], Peng Li[1], Jingmei Sun[2], Ying Jiang[2], and Miaoxia Wen[2]

4.1. INTRODUCTION

According to statistics, since the 1950s, nearly 110 000 check dams have been built on the Loess Plateau [1]. A check dam, as an efficient measure of governing gullies, conserves soil and water and retains most of the sediment during the process of sediment transportation [2]. A large amount of natural environmental and humanistic environmental information is retained in the sediment [3]. Therefore, typical check dams in the Loess Plateau (Yuanzigou check dam in Inner Mongolia, Hengshan Zhaizimao check dam, and Nianyangou check dam) have been selected for research. Sediment samples from the check dams were collected in the whole profile, and the response relationship between erosion sediment in small basins and rainfall was analyzed according to the principle of heavy rain on large sand. Based on source-sink theory, composite fingerprinting was used to accurately calculate the distribution of erosion sediment in small basins to quantitatively study the historical change of sediment sources and the temporal and spatial distribution of erosion sediment in small basins [4].

[1] *Institute of Water Resources and Hydro-electric Engineering, Xi'an University of Technology, Xi'an, China*

[2] *Northwest Institute of Forest Inventory, Planning and Design, National Forestry and Grassland Administration, Xi'an, China*

4.2. METHOD

In mid-July 2017, the upstream slope ratio of the Yuanzigou check dam and the height difference between the top of the dam and the height of the dam were measured. Three sampling points without branches were selected along the central channel of the dam. The sediment couplet soil pillars of the dam were collected, and soil bulk density samples were collected using a stainless steel soil ring knife with a volume of 100 cm^3; samples were then weighed and recorded. In the dam-controlled basin, typical gullies and the land between gullies were divided into upper, middle, and lower points along the runoff line to take soil samples of 0–5 cm from the surfaces. The gully wall samples were obtained by scraping the wall with a shovel. After all of the samples had been sealed, numbered, and recorded, they were transferred to the soil chemistry laboratory for testing and analysis.

The soil samples in the control area of the Zhaizimao check dam were collected in July 2017. The samples were divided into two categories: (i) the dam sediment couplet soil and (ii) the soil from the sediment source area.

At a distance of 35 m from the dam's body, a drill was used to drill an original soil sample with a vertical depth of 12.02 m. Each drill was approximately 50 cm. The soil was divided into PVC pipe with a diameter of 80 cm which was fixed with tape, as shown in Figure 4.1. Soil samples in the sediment source areas were concentrated mainly on the left and right banks of the dam. When

Check Dam Construction for Sustainable Watershed Management and Planning, First Edition.
Edited by Zhanbin Li, Peng Li, Yang Yu, Peng Shi, and Guillaume Piton.
© 2022 John Wiley & Sons, Inc. Published 2022 by John Wiley & Sons, Inc.

@seismicisolation

Figure 4.1 Sampling sediment deposition in dam lands.

samples were collected, ensure that no sedimentation occurs in the sediment source area. A grid of 5.0 m × 5.0 m was selected on the long slope along the runoff line from which 10 topsoil samples with a thickness of 5 cm were randomly collected as the sloping farmland and grassland samples and then uniformly mixed. A grid of 5.0 m × 5.0 m was selected in the branch channel along the water flow direction from which 10 topsoil samples with a thickness of 5 cm were collected and mixed. The topsoil was obtained using the quarter method; it was collected from the top, middle, and bottom of the gully wall along the vertical direction and mixed evenly. A total of 36 soil samples were collected from the sediment source areas, including nine slope farmlands, nine grasslands, nine gully walls, and nine channels. All soil samples were air-dried for approximately one week, and laboratory tests were conducted in August 2017. A total of 17 geochemical indicators were determined, including Mg, Cr, Co, Fe, Ni, Mn, Cu, Zn, Rb, Cd, Pb, V, d(0,1), d(0,5), TN, TP, and TOC.

Inspired by the basic principles of tree-ring hydrology and cross-dating, the sediment couplet of each layer of the dam corresponded to one or more consecutive erosive rainfalls. For the Loess Plateau, sediment from the check dam was formed by several heavy rainstorms during the year and the flood and sand peaks were usually synchronized. Based on the correlation among the soil particle size composition of the sediment couplet layer, historical rainfall data, and the measured dam sediment couplet thickness, the sedimentation process of the check dam was inverted and the time coordinate established, as shown in Figure 4.2.

Composite fingerprinting technology accurately calculated the relative sediment contribution rate of each potential sediment source area to the sediment couplet of each layer of the dam. The quantitative calculation was divided into three steps: (i) parameter-free Kruskal–Wallis H-test statistical analysis was adopted to test and screen fingerprint identification factors that could be used to study the sediment source in the basin, (ii) multiple discriminant analysis was adopted to determine the best fingerprint factor combination, and (iii) the Collins multivariable mixed model was adopted to quantitatively calculate the sediment contribution rate of each sediment source area. The calculation formula is as follows:

$$R_{es} = \sum_{i=1}^{n} \left[\frac{C_i - \left(\sum_{s=1}^{m} C_{si} P_s \right)}{C_i} \right]^2 \tag{4.1}$$

$$\mathrm{GOF} = \left(1 - \frac{1}{n} \sum_{i=1}^{n} \frac{C_i - \sum_{s=1}^{m} P_s C_{si}}{C_i} \right) \times 100\% \tag{4.2}$$

where R_{es} is the residual sum of squares, C_i is the concentration of fingerprint factor i in sediments, P_s is the sediment contribution percentage of the sediment source S, C_{si} is the average concentration of fingerprint factor i in the sediment source S, m is the number of sediment sources, and n is the number of fingerprint factors.

It should be noted that the sediment contribution rate of all sediment sources was non-negative and their sum was 1. Under the above conditions, when the function formula took the minimum value, the sediment contribution percentage of each sediment source could be obtained. The calculation result using the Collins mixture model was believed to be accurate when the GOF was > 0.8.

@seismicisolation

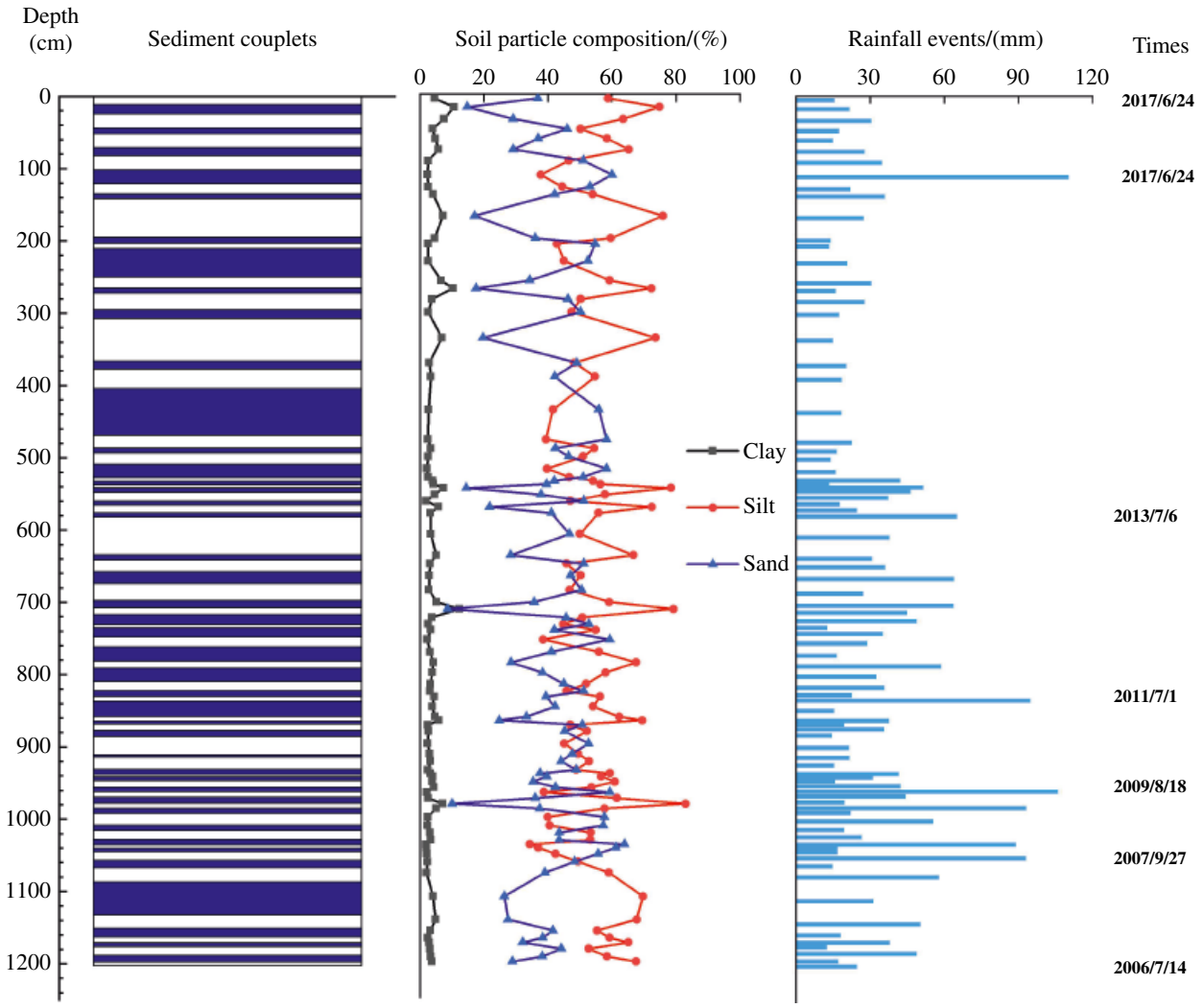

Figure 4.2 Sedimentary cycle depth, clay, silt, sand, ^{137}Cs content, precipitation, and sedimentary times of the check dam.

In June 2017, soil samples were collected from the Nianyangou watershed. Fifteen long slopes were found: four in sloping farmland, three in forest-shrub land, four in grassland, and four in terraced fields. Three long slopes were selected from each land use type. The slope farmland was mainly used for farming corn and potatoes. It was cultivated once a year with tillage, which is seriously disturbed by human beings and without fertilization. In the forest shrub land, the forest height was above 6 m, the conifer forest was planted artificially, and the planting period was over 30 years. The irrigation height was approximately 1 m, the main vegetation was Caragana, the planting period was 20 years, and there was no artificial disturbance. The grass coverage of the grassland was more than 90%, bothriochloa ischaemum was planted artificially, the planting period was 20 years, and there was no artificial disturbance. Apples and jujube trees were planted in the terraced fields, and a small amount of spray fertilizer was applied. The planting period was more than 30 years, and it was affected by artificial disturbance. In each slope landscape, ^{137}Cs soil samples of 0–5 cm were collected every 10 m, from the top to the bottom of the slope, and soil samples of 0–20, 20–40, 40–60, 60–80, and 80–100 cm were collected in layers at the origin. Three repeated samplings were carried out for each slope landscape. A total of 144 soil samples of ^{137}Cs and 780 soil samples were collected and transferred to the laboratory for indoor analysis.

Corresponding rainfall data from 1971 to 1990 with the sediment couplet of dam No. 3 of Nianyangou,

@seismicisolation

combined with the principle of heavy rain on heavy sand and rainfall data and typical rainfall events, are selected to correspond to the dam sediment couplet (August 1972, August 1987, July 1988, and July 1990).

Based on the research methods of Murray, Zhang Xinbao, Wen Anbang, and Li Shaolong, when there are differences in the nuclide content of sediments from different sources in the basin, the effect of particle sorting is not considered. The nuclides content in sediments of the basin is compared with the radionuclides content from different sources to calculate the relative sediment content of different sources. The following formula is used:

$$f_1 \cdot C_1 + f_2 \cdot C_2 + f_3 \cdot C_3 = C_d \tag{4.3}$$

$$f_1 \cdot P_1 + f_2 \cdot P_2 + f_3 \cdot P_3 = P_d \tag{4.4}$$

$$f_1 + f_2 + f_3 = 1 \tag{4.5}$$

where C_d is the content of element C in the sediment output from the basin (Bq/kg); C_1, C_2, and C_3 are the content of element C in the soil of source area types 1, 2, and 3, respectively (Bq/kg); P_d is the content of element P in the sediment output from the basin (Bq/kg); P_1, P_2, and P_3 are the content of element P in the soil of source area types 1, 2, and 3, respectively (Bq/kg); and f_1, f_2, and f_3 are the relative sediment yield of source area types 1, 2, and 3, respectively (%).

4.3. SEDIMENT SOURCE IDENTIFICATION IN TYPICAL SMALL BASINS

4.3.1. Sediment Sources in the Yuanzigou Basin of Inner Mongolia

The Huangfuchuan basin is located in the primary tributary of the right bank of the Helong Section in the middle reaches of the Yellow River and the main sandy and coarse sand areas. The basin is characterized by high elevation difference, steep bank slopes, a large area of exposed soft rock, intense rainstorm erosion, gully development, and serious soil and water loss. The Telagou basin is the first-level branch on the left bank of Nalinchuan, the main stream of the Huangfuchuan basin, with a basin area of 128.2 km^2 and is a sandy, hilly gully area, as shown in Figure 4.3. The surface material in the basin is mostly loess, sand, and soft rock, with chestnut soil distributed sporadically. The gully area in the basin accounts for approximately 25%

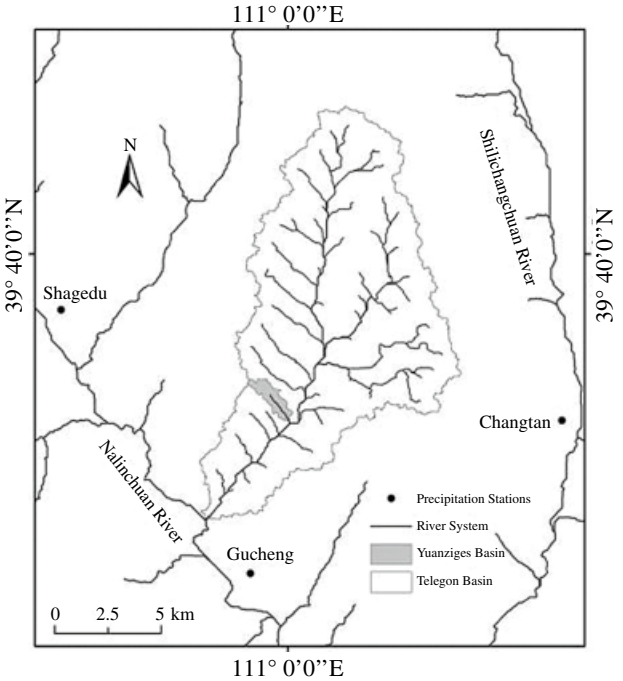

Figure 4.3 Geographic location map of the Yuanzigou basin.

of the total area. Yuanzigou check dam is located in a channel on the right bank of the main channel of Telagou, which was completed in October 2006. The dam covers an area of 1.52 km^2 and has a total storage capacity of 250 000 m^3, with a check area of 3.4 hm^2 and a dam height of 18 m. The bank slopes on both sides of the channel in the dam-controlled basin are relatively steep and the branch gully is short, deep, and narrow. The land-use type is mainly grassland, which accounts for more than 90% of the area. The Yuanzigou check dam belongs to the check dam and no crops are grown on the dam.

The sedimentation of the Yuanzigou check dam consisted mainly of sand, followed by powder, and consisted of clay the least. The sand particles making up the largest proportion of the sediment were ultrafine (0.1–0.05 mm) and fine sand (0.25–0.1 mm). The median particle size D_{50} of the sediment in the dam was analyzed in horizontal and vertical directions, results are shown in Figure 4.4. The average particle sizes of sediment near the dam, in the dam, and far from the dam were 0.055, 0.056, and 0.057 mm, respectively. The median particle size D_{50} of soil samples collected from the gully in the control area was 0.073 mm, the median particle size D_{50} of the gully wall was 0.099 mm, and the median particle size D_{50} of the gully channel was 0.119 mm. The analysis results of the median particle

@seismicisolation

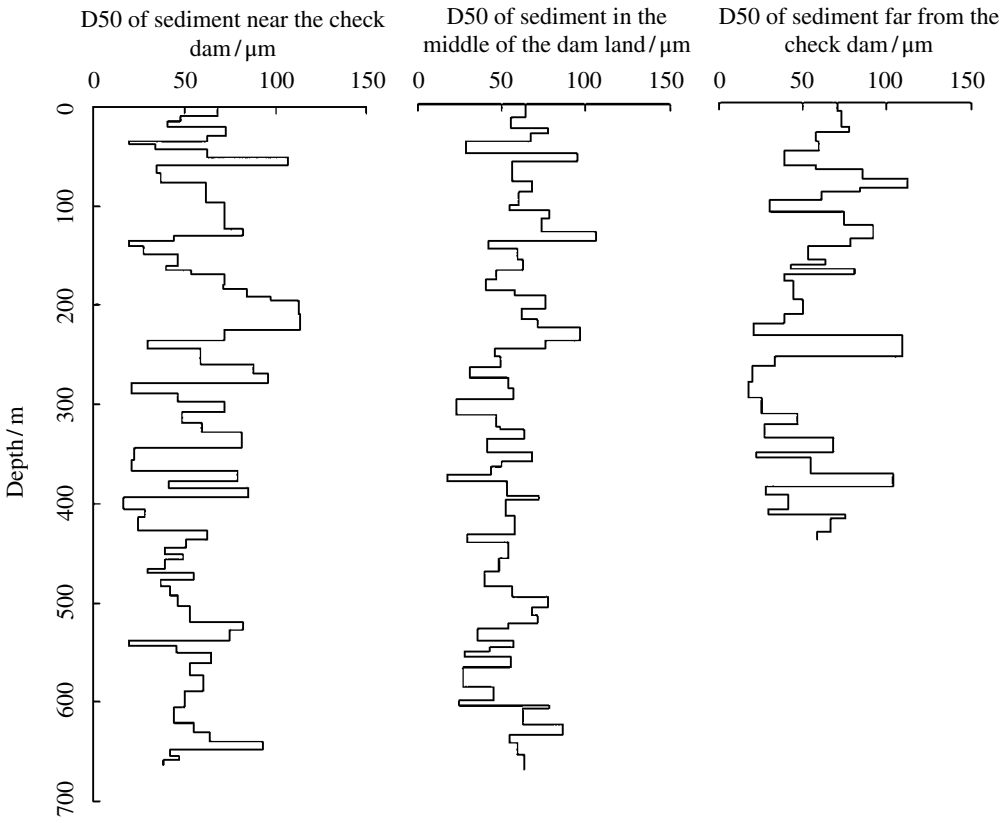

Figure 4.4 Variation of median particle size D_{50} of sediment in the sample section of the Yuanzigou check dam-controlled basin.

size of runoff sediment at the Huangfu Hydrometric Station at the exit of the Huangfuchuan basin showed that from 1990 to 1996, the average particle size D_{50} of the sediment was 0.046 mm. From this, we may derive two indications: (i) the sediment carried by the rainwater formed by the erosive rainfall subsided along the way and (ii) the short, deep, narrow gully channels narrowing the cross-section of the rainwater contributed to the gravity erosion by steep gully walls on both sides. The construction of the check dams effectively intercepted coarse sand with a particle size greater than 0.05 mm. In the vertical direction, the fluctuation of the median particle size D_{50} of the sediment near and far from the dam was larger than that in the dam. This may be because the sediment couplet collected in the dam contained more rainfall events; therefore, the sediment caused by smaller erosive rainfall may not reach the front of the dam.

The sampling section in the dam was selected for dating analysis. According to the indication of coarse sediment, the corresponding relationship between 24 erosive rainfall events and the sedimentation couplet of the dam was divided, as shown in Figure 4.5.

Figure 4.5 indicates that the sediment in the dam area was mainly the result of a few heavy rainfall events each year. The erosion rainfall events with a daily rainfall of more than 30.0 mm, accounting for 57.1% of the total rainfall events, contributed 72.4% of the total sediment in the dam. The four erosion rainfall events with a daily rainfall of more than 50.0 mm contributed 23.2% of the total sediment in the dam. The minimum daily rainfall that has been found corresponding to an erosive rainfall event in the Yuanzigou dam-controlled basin is 22.8 mm, which occurred toward the end of 2016, with a deposition ratio of 0.44. At the end of 2011, through a field survey of the key dams in the Huangfuchuan basin in the jurisdiction of Zhungeer Banner, it was found that the deposition ratio of 95.7% of the key dams built in and after 2004 was less than 0.1. The proportion of key dams with a deposition ratio of less than 0.01 was 51.1%. This shows that ecological construction such as river basin vegetation has extended the useful life of check dams.

To analyze the interannual changes in erosion and sedimentation after dams are built, the annual erosion

@seismicisolation

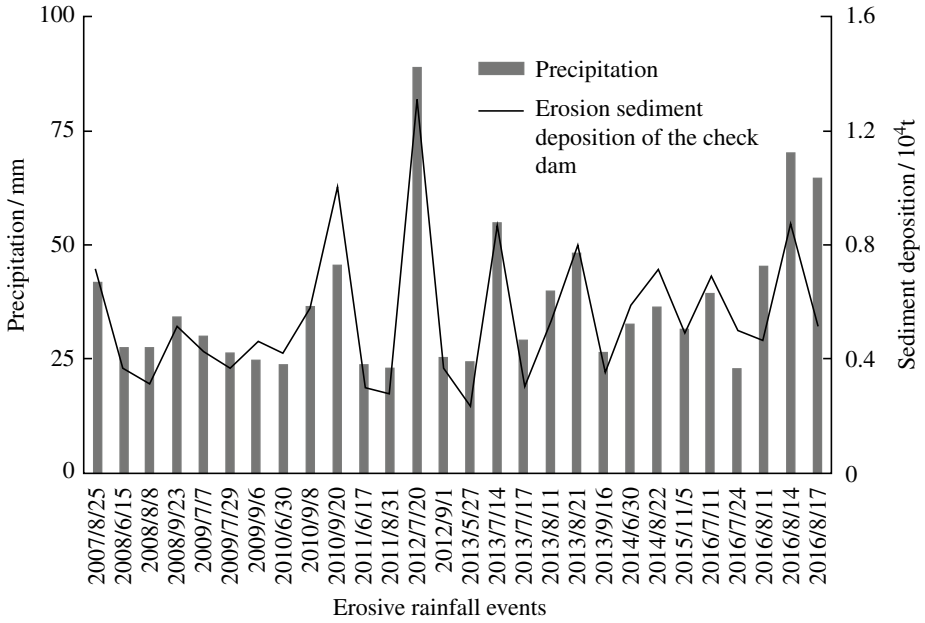

Figure 4.5 The relationship between sediment rotation and erosive rainfall events.

sediment is obtained by combining the erosion rainfall events with the year in which they occurred. Since the dams were built between 2007 and 2016, the amount of sediment in the Yuanzigou dam-controlled basin has changed greatly from year to year, with an average annual sedimentation amount of 15 000 t and an average annual erosion modulus of 10 147 t/(km^2·a). In 2011 and 2015, there were two and one erosive rainfall events in the basin, respectively, and less sediment accumulation. Moreover, no sediment transportation was detected at Bakou Station in the Telagou basin. In 2013 and 2016, there was more precipitation and heavy rainfall during the flood season, which led to a significant increase in the amount of eroded sediment. The erosion modulus of the Yuanzigou dam-controlled basin exceeded 20 000 t/(km^2·a). This shows that beneath the underlying surface of the research basin, the daily rainfall corresponding to erosive rainfall events increased to 22.8 mm. However, when daily rainfall was greater than 22.8 mm, the erosion reduction effect of the slope vegetation was relatively limited, and most of the erosion sediment in the basin was intercepted by the check dam.

The double cumulative curve of annual rainfall erosiveness and annual eroded sediment in the dam-controlled basin of Yuanzigou is shown in Figure 4.6. Figure 4.6 indicates that there was a turning point in the double cumulative curve of the annual rainfall erosiveness and eroded sediment in the dam-controlled basin of Yuanzigou, which occurred in the seventh year after the construction of the Yuanzigou check dam (2013). Thus, the construction and operation of the Yuanzigou check dam were divided into two stages: during the first stage (2007–2013), all of the eroded sediment out of the gully was intercepted by the newly built and operated check dam; in the second stage (2013–2016), a large amount of eroded sediment was deposited in the channel of the dam, which effectively raised the erosion base level of the basin, increased the cross-sectional area of the channel rainwater, and promoted the rapid settlement of sediment carried by channel runoff. The proportion of the amount of sediment directly intercepted by the check dam in the erosion sediment of the entire erosive rainfall event was significantly lower than in the first stage. According to the moisture data analysis obtained by ring knife sampling the warping layer, as the depth of the soil layer increased, the fluctuation of the water content of the dam decelerated, and the average water content was 23.8%. The increase in soil water content promoted the growth of vegetation within the dam area and further reduced the occurrence of gully erosion. Therefore, the erosion sediment reduction in the second stage was caused by the effect of raising the erosion base level and well-grown vegetation following the construction of the check dam.

The check dam at the mouth of Yuanzigou effectively intercepts the erosion sediment of various erosive rainfall events in the dam-controlled basin. The sediment in the dam can reflect the contribution rate of the potential

@seismicisolation

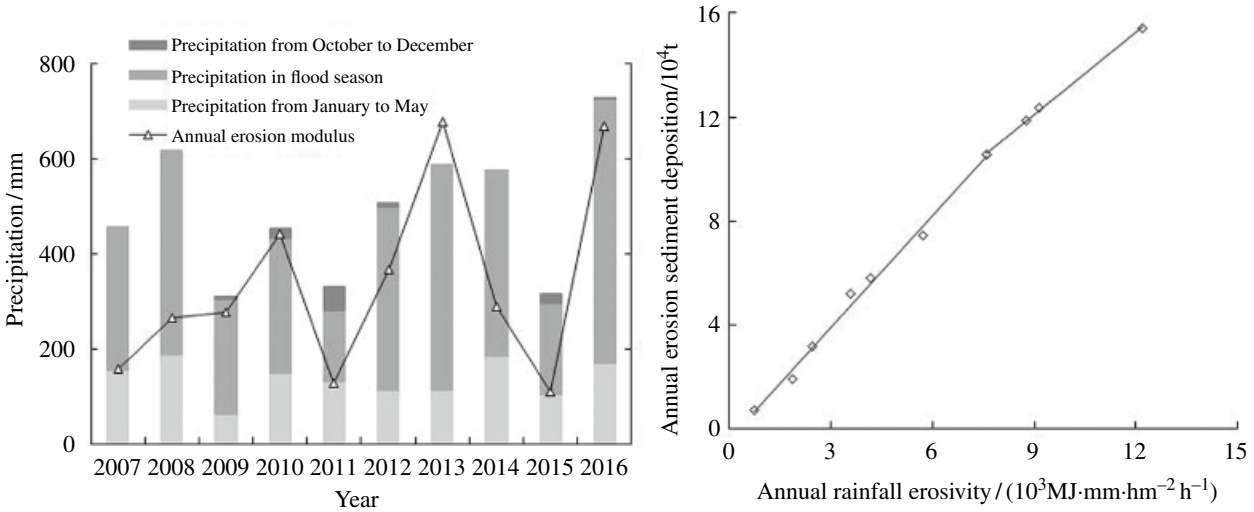

Figure 4.6 The relationship between rainfall distribution and erosion modulus; the double cumulative curve of annual rainfall erosiveness and sediment deposition.

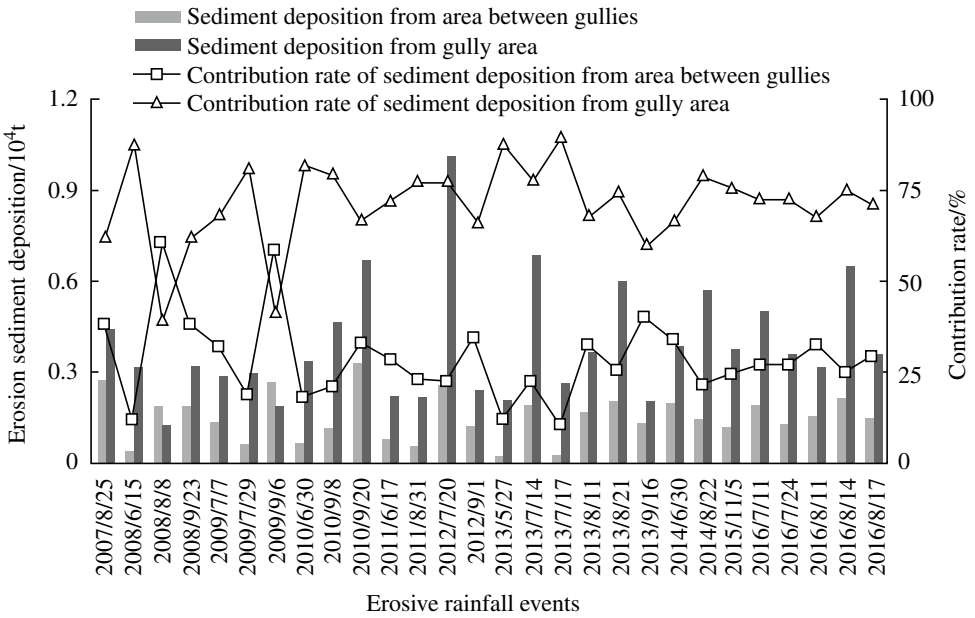

Figure 4.7 Sediment sources and changes in the Yuanzigou check dam-control basin.

sediment source to the sediment in the dam after the completion of the check dam. The potential sources of sediment in the dam-controlled basin are divided into two categories: (i) the land between gullies above the ridge line and (ii) the gullies below the ridge line and above the edge of the dam. Through the composite fingerprinting method, d0.1, d0.9, and TOC were selected as the optimal combination of fingerprint identification factors. The calculation results of the sediment source are shown in Figure 4.7; the average goodness of fit (GOF) was 81.7%.

Eroded sediment from gullies was the main source of sediment in the Yuanzigou dam, with an average proportion of 71.4%; eroded sediment from the land between gullies accounted for only 28.6%. The contribution rate of sediment in the gully and land between gullies fluctuated greatly in the first stage of the check dam's construction and operation; the change tended to be flat in the second stage. The changing trend of eroded sediment from gullies and valleys was almost equal to that of the total sediment of dams, while the eroded sediment from land between gullies fluctuated

@seismicisolation

around the average value (0.16 t). For some erosive rainfall events with small rainfall, the contribution of sediment was almost zero. In general, the eroded sediment from the land between gullies decreased steadily and slightly and the eroded sediment from the gullies increased with increases in rainfall.

4.3.2. Sediment Sources in the Yuanping Basin of Hengshan County

Yuanping basin is located in the south of Hengshan County, Yulin City, Shaanxi Province. It is approximately 10.0 km away from the county, which is a first-level branch of the Luhe, the first-level tributary of Wuding River; it has a basin area of 131.4 km^2 and a relative height difference of 369 m. It is the first subregion of the Loess' hilly and gully area. It is characterized by fragmented topography and serious water and soil loss. The soil erosion modulus is 13 000 t/(km^2·a).

The Zhaizimao check dam in Hengshan County is located in the middle reaches of the Yuanping small basin, with a control area of 3.6 km^2. The designed dam height is 20 m, the total storage capacity is 954 000 m^3, and the designed sedimentation period is 20 years. Its construction commenced on 10 November 2004 and was completed on 30 September 2005. The geographical location of the basin and the check dam is shown in Figure 4.8.

According to different sediment source areas, the samples were classified into four data classification databases of sediment source areas, and the stepwise discriminant method of "in and out" was adopted. Twelve fingerprint factors with discriminant ability were selected as variables and a Wilks statistic test was performed according to Bayesian discriminant function. If F > Fa, the discriminant ability of the factor was considered significant and assumed to affect the discriminant ability of other existing factors; otherwise, the factor was eliminated. Table 4.1 shows the K-W results. It shows that indicators such as Co, Cr, Fe, Mg, Mn, Ni, Pb, Zn, V, TN, TOC, and d(0,1) had a good subdivision ($P < 0.05$). Among them, Fe, Mg, Mn, Ni, Zn, V, TOC, and d (0,1) were significantly different ($P < 0.05$).

The initial classification was performed according to the optimal fingerprint factor combination in Table 4.2 and a sample population with an initial grouping of four was established. A total of 36 samples were collected from the sediment sources; nine samples were taken from each potential sediment source. The forecast grouping was conducted through stepwise analysis and compared with the initial grouping (see Table 11.1). The Mn element indicator was finally eliminated and the optimal factor combination obtained was Zn + Mg + Ni + d(0,1). Based on these four physicochemical properties, the accuracy rate of soil samples on the gully wall reached 100%, 66.7% for grassland,

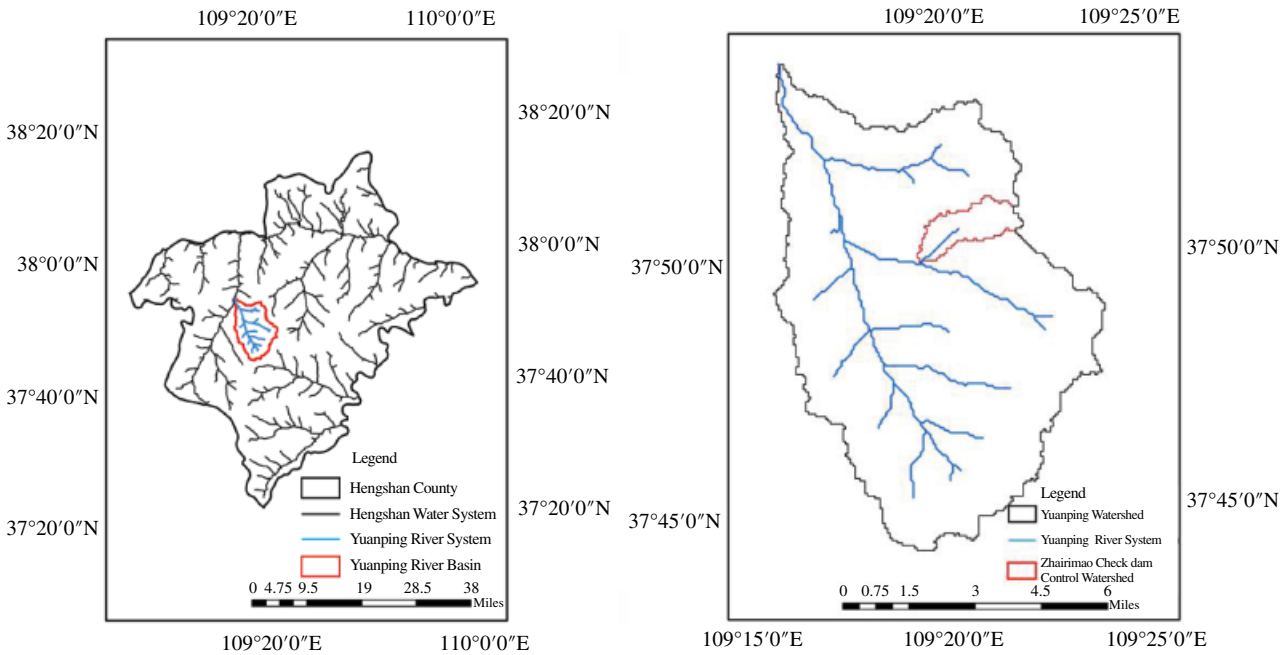

Figure 4.8 Location of the Zhaizimao check dam.

@seismicisolation

88.9% for slope farmland, and 88.9% for channels. The total accuracy rate was 86.1%.

Table 4.2 shows that in the process of classification and discrimination of the four source areas, the recognition rate of the shrubs reached 100%. However, due to human factors, some grassland was connected with sloping farmland, causing some grasslands to be identified as slope farmland or channels. The recognition rate of slope farmland, grassland, and channels was 88.9, 66.7, and 88.9%, respectively. In addition to the low recognition rate of grassland affecting the overall accuracy, other fingerprint factors had significant differences. Through calculation, the discrimination rate of optimal fingerprint factor combination met the requirements for calculating the contribution rate of different sources, exceeding 80%, and subsequent calculations could be performed.

Table 4.1 K-W test results of fingerprint factors in different sediment source areas.

Fingerprint identification factor	Chi-square	Degree of freedom	P-value
Cd mg kg-1	5.4144	3	0.143
Co mg kg-1	8.8258	3	0.031[a]
Cr mg kg-1	13.659	3	0.003[b]
Cu mg kg-1	5.1061	3	0.164
Fe mg kg-1	16.475	3	0.000[b]
Mg mg kg-1	20.558	3	0.000[b]
Mn mg kg-1	15.717	3	0.001[b]
Ni mg kg-1	19.236	3	0.000[b]
Pb mg kg-1	8.8438	3	0.031[a]
Rb mg kg-1	5.6106	3	0.132
Zn mg kg-1	21	3	0.000[b]
V mg kg-1	14.672	3	0.002[b]
TN g kg-1	7.997	3	0.046[a]
TP g kg-1	7.612	3	0.054
TOC g kg-1	12.117	3	0.006[b]
d(0,1)	28.906	3	0.000[b]
d(0,5)	2.7918	3	0.424

[a] Significant at the 0.05 level.
[b] Significant at the 0.01 level.

The best fingerprint factor combination, Mg, Zn, Ni, and d(0,1), was determined through multivariate discrimination. There was an 88.9% probability of distinguishing the sediment on the gully wall, gully slope, and slope farmland. According to the concentration of the best fingerprint factor in each sediment couplet, the relative sediment contribution rate of each sediment couplet slope farmland, grassland, gully wall, and branch channel could be calculated quantitatively using Equation (4.1). The calculation results are shown in Figure 4.9. Equation (4.2) was used to calculate the GOF of the results of each sediment couplet contribution rate; the calculated GOFs were all greater than 80%. Hence, the results are credible.

As shown in Figure 4.9, the results of the Collins hybrid model showed that during the operation period of the Zhaizimao check dam, the relative sediment contribution rates of the four different sediment source areas to the dam sediment couplet under the condition of single rainfall were markedly different. The relative sediment contribution rates were as follows: 32.96–81.08% for the gully wall, with an average value of 53.60%; 0.14–46.70% for sloping farmland, with an average value of 24.18%; 0.05–40.86% for grassland, with an average value of 19.06%; and 0.00–10.46% for gully channels, with an average value of 2.83%.

Among the four potential sediment sources in the Zhaizimao check dam control area, the gully wall contributed the largest amount of sediment, followed by slope farmland and grassland; the branch channel contributed the least. Gully wall was the main sediment source area (the mean value was 53.60%) in the

Table 4.2 Results of composite fingerprint factor identification[a].

		Predicted group information				
	Source category	Farmland	Grass	Shrubs	Trench wall	The total
The sample quantity	Farmland	8	1	0	0	9
	Grass	2	6	0	1	9
	Shrubs	0	0	9	0	9
	Trench wall	0	0	1	8	9
Distinguish rate%	Farmland	88.9	11.1	0	0	100
	Grass	22.2	66.7	0	11.1	100
	Shrubs	0	0	100	0	100
	Trench wall	0	0	11.1	88.9	100

[a] Correctly classifying 86.1% of the original four groups.

@seismicisolation

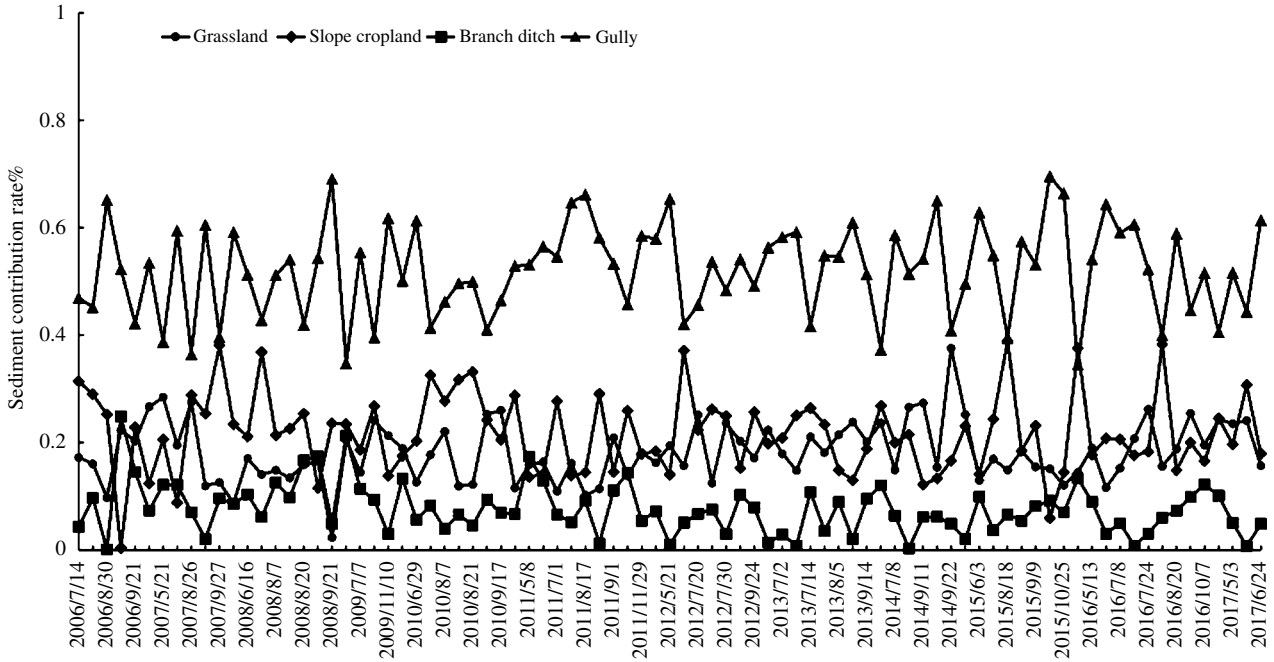

Figure 4.9 The sediment relative contribution rate results from the Collins mixing model.

Zhaizimao check dam control area. It represented the downward cutting, tracing, and collapse of gully caused by gravity erosion; part of the sediment passing through slope farmland and grassland also gathered there. The main type of land use in the Zhaizimao check dam control area was slope farmland, which was frequently plowed; thus, slope farmland was the second erosion source (the mean value was 24.18%). The grassland vegetation coverage in the Zhaizimao check dam control area was relatively large and the degree of soil erosion slightly lower than that for slope farmland (the mean value was 19.06%). The branch gully channel formed the least sediment source area (the mean value was 2.83%). Xue [5] found that the main source of erosion sediment in the Wangmaogou small basin in Suide County, Shaanxi Province was the gully wall, followed by the slope farmland and gully slope. Zhao Tianyin found that calculation results by five-source and three-source models both showed that the sediment in the Xigou small basin in Gansu Province mainly came from the gully wall, followed by farmland and gully slope. Chen Fangxin found that in the erosion sediment of the Hujiawan basin in Yanchang County, Shaanxi Province, the relative sediment contribution rate of the gully (called the gully wall in this study) accounted for 60.8%, followed by farmland (20.7%), forest land (11.3%), and grassland (7.2%), which is consistent with the results of this study for relative sediment contribution rates.

The single factor variance analysis method was used to analyze the relative sediment contribution rate of different rainfall gradients. The results show that there was no significant difference between the relative sediment contribution rate of gully walls, slope farmland, or grassland under different rainfalls ($p > 0.05$). The relative sediment contribution rate of branch gully channels was significantly different ($p < 0.05$). This shows that the sediment from the branch gully channel relates to the rainfall level. With increases in rainfall, the relative sediment contribution rate of the branch gully channel first increased and then decreased. The results of the Collins hybrid model show that under different rainfall gradients, the gully wall was the main sand area, followed by slope farmland and grassland, and the branch gully channel was the least (see Table 4.3). The proportion of relative sediment contribution rate of slope farmland and grassland was different under different amounts of rainfall; the relative sediment contribution rate of slope farmland was larger when the rainfall was 12–15, 15–20, 20–30, and 30–40 mm. The relative sediment contribution rate of grassland was greater when the rainfall was greater than 40 mm.

Figure 4.10 shows the relationship between cumulative sediment contribution rate and cumulative rainfall in the

@seismicisolation

Table 4.3 Results from the Collins mixed model with different rainfall gradients.

	Gully		Slope cropland		Grassland		Branch ditch	
Precipitation	Mean (%)	Standard	Mean (%)	Standard	Mean (%)	Standard	Mean (%)	Standard
12–15 mm	52.72	0.122	23.55	0.128	21.35	0.093	2.59	0.038
15–20 mm	50.36	0.104	28.77	0.101	19.01	0.088	2.02	0.029
20–30 mm	56.43	0.143	22.14	0.114	18.84	0.085	2.86	0.036
30–40 mm	55.17	0.094	23.65	0.114	17.05	0.078	4.30	0.045
>40 mm	54.35	0.133	18.92	0.142	23.74	0.129	3.18	0.037

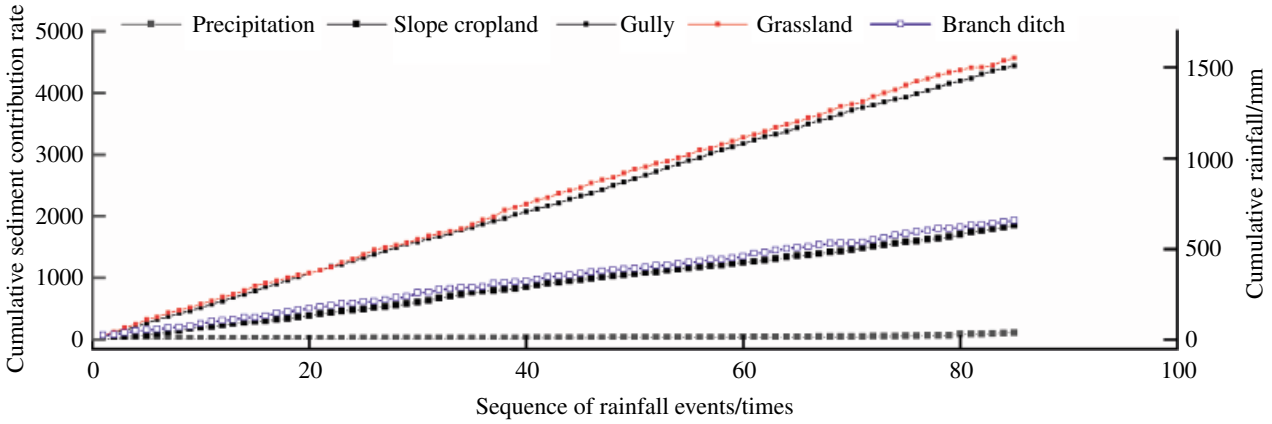

Figure 4.10 Cumulative sediment contribution rate and cumulative rainfall curve for four samples.

four potential sediment source areas of the Zhaizimao check dam control area. Figure 4.10 showed that the cumulative contribution rate of the gully wall and channels did not change. The cumulative contribution rate of slop farmland and grassland intersected at the 27th rainfall (10 August 2010). There was no obvious change in the cumulative rainfall curve. Gao et al. stated that the average deposition ratio of the failure of the key dam's sediment retention capacity was 0.77. However, during the study period, the deposition ratio of the Zhaizimao check dam was 0.41; therefore, it was in a severe erosion stage. The relative sediment contribution rate of the gully wall did not change significantly.

The change in the relative sediment contribution rate of slope farmland and grassland was mainly related to the area of their source areas. Figure 4.11 shows that slope farmland in the Zhaizimao check dam control area converted into grassland. The increase in grassland area decreased its contribution rate. The area of slope farmland also decreased. Its relative sediment contribution rate showed a weaker increasing trend as it was plowed and cultivated and the soil became loose.

4.3.3. Sediment Sources for the Nianyangou Basin in Suide County

Nianyangou is a branch of the Wangmaogou basin in Suide County, Yulin City, Shaanxi Province. It is located at 110°20′04″–110°22′ 28″ E and 37°25′ 33″–37°35′ 54″ N, with an altitude of 1027–1188 m and an average slope of 12.5°. The basin has a continental monsoon climate of medium latitude and average annual precipitation of 513 mm; 70% of the precipitation is concentrated in the rainy season.

Three check dams were built in the Nianyangou small basin. Dam Nos. 1 and 2 were equipped with drainage structures; No. 3 has no drainage structure. It was built in 1960 at the head of Nianyangou and filled in 1990. The control area is approximately 18.1 hm^2, and the area of the dam is approximately 6000 m^2 (Figure 4.12). When the check dam system was surveyed, the main land use types in the basin were found to be slope farmland, forest-shrub land, grassland, and terraced fields. In the dam-controlled area, a profile with a vertical depth of 6.59 m was drilled approximately 30 m away from the dam body,

@seismicisolation

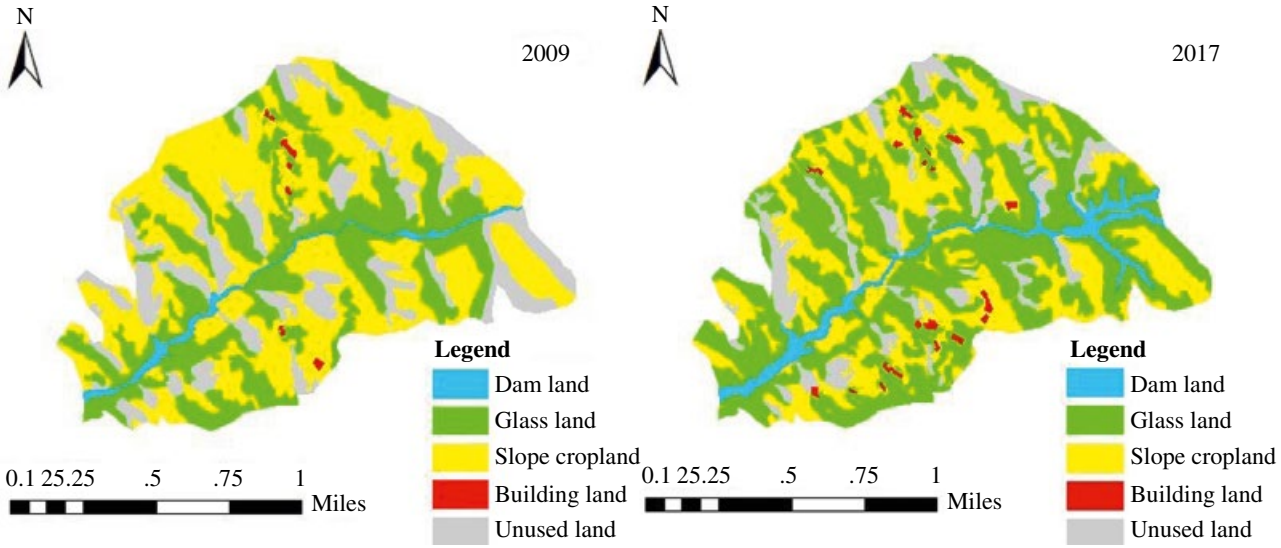

Figure 4.11 Land-use distribution map of the dam-controlled watershed in Zhaizimao from 2009 to 2017. Note: Left Figure 2009, Right Figure 2017.

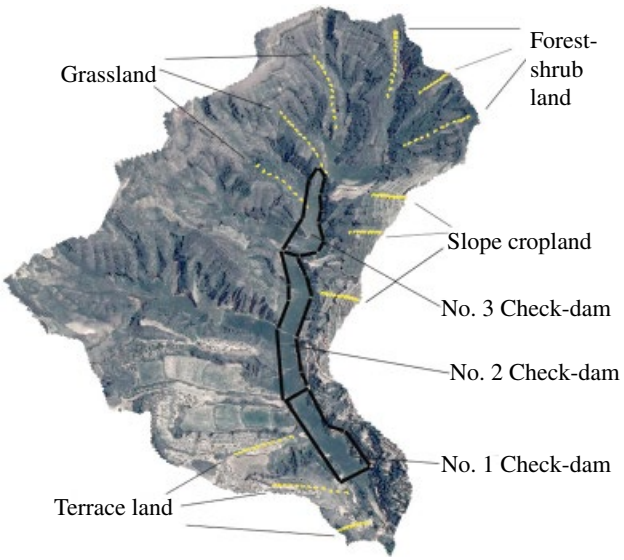

Figure 4.12 A remote sensing image of the Nianyangou watershed.

the couplet sediment thickness of each layer was measured, and soil samples were collected (Figure 4.13).

According to Table 4.4, 69% of the sediment in the Nianyangou basin came from slope farmland and the sediment from forest-shrub land, grassland, and terraced fields was relatively low, accounting for 3, 13, and 14%, respectively. The main slope landscapes in the dam control area were sloping farmland, forest-shrub land, and grassland. The sediment mainly came from sloping farmland, accounting for approximately 61% of the sediment. From the contribution rate of the sediment source of dam No. 2, the failure of dam No. 3 leads to a large amount of sediment from dam No. 3 entering dam No. 2; thus, the content of sediment provided by dam No. 3 in dam No. 2 is relatively high.

The main source of sediment in dam No. 1 is slope farmland, which provides 99% of the sediment; the sediment content provided by dam No. 2 is almost zero. Therefore, the construction of drainage structures for the check dam not only increases its service life but also avoids a large amount of sediment output. Soil and water conservation measures can effectively reduce the rate of soil erosion and the erosion sediment yield of the basin. According to the results of the "Compilation of Experimental Research Results of Soil and Water Conservation (Volume One)" of the Suide Soil and Water Conservation Scientific Experimental Station of the Yellow River Water Resources Commission of the Ministry of Water Resources, the four typical rainstorms in Jiuyuangou, and the amount of soil loss before the government over the years 1954–1964, the runoff sediment sources of various land-use types in Jiuyuangou were calculated: more than 85% of runoff sediment comes from agricultural and waste slopes in the basin and approximately 8% comes from steep cliffs. Therefore, after decades of governance, the sediment sources of the small basin have undergone considerable changes.

@seismicisolation

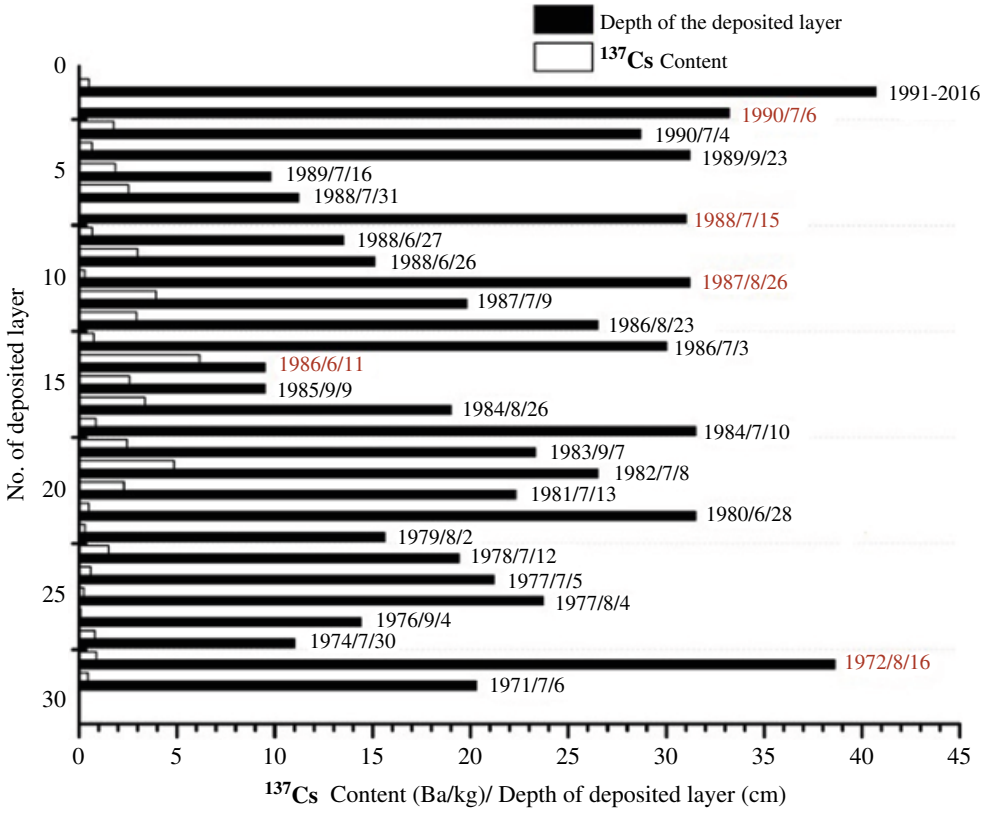

Figure 4.13 The ^{137}Cs content, depth, and deposition time of each layer of check dam no. 3 in the Nianyangou watershed.

Table 4.4 The contribution rate of the sediment sources of the check dams.

Type	Slope cropland (%)	Forest-shrub land	Grassland	Terrace land	Dam no. 2	Dam no. 3
Dam no. 1	99	—	—	0.08%	0%	—
Dam no. 2	15	35	30	—	—	20%
Dan no. 3	61	16	23	—	—	—
In total	69	3	13	14%	—	—

4.4. AN ANALYSIS OF SEDIMENT SOURCES IN A SMALL BASIN OF THE LOESS PLATEAU

The Loess Plateau is an important area for soil erosion control in China. Intense soil erosion causes soil nutrient loss, land degradation, and reduced productivity. The sediment produced by erosion flows into the river and becomes the main carrier for the migration and transformation of pollutants. As the basic unit of comprehensive management of soil and water conservation in the Loess Plateau, the basin contains a large amount of sediment erosion characteristics and erosion environment information. Since the 1950s, check dams had been constructed in many basins of the Loess Plateau; they were greatly promoted and popularized during the 1960s. Check dams recorded information on changes in the erosion environment while retaining sediment, which provides favorable conditions for scholars to study erosion sediment rate, sediment sources, and sediment delivery ratio in small basins.

Much research on the sediment sources in the Loess Plateau has been conducted in China. The study area extends from the Xiliugou Basin in Dalate Banner, Inner Mongolia in the north, the Weihe River Basin in Tianshui City, Gansu Province in the south, the Weihe River Basin near the junction of Gangu County, Gansu and Tianshui City in the west, and Sanchuan River

@seismicisolation

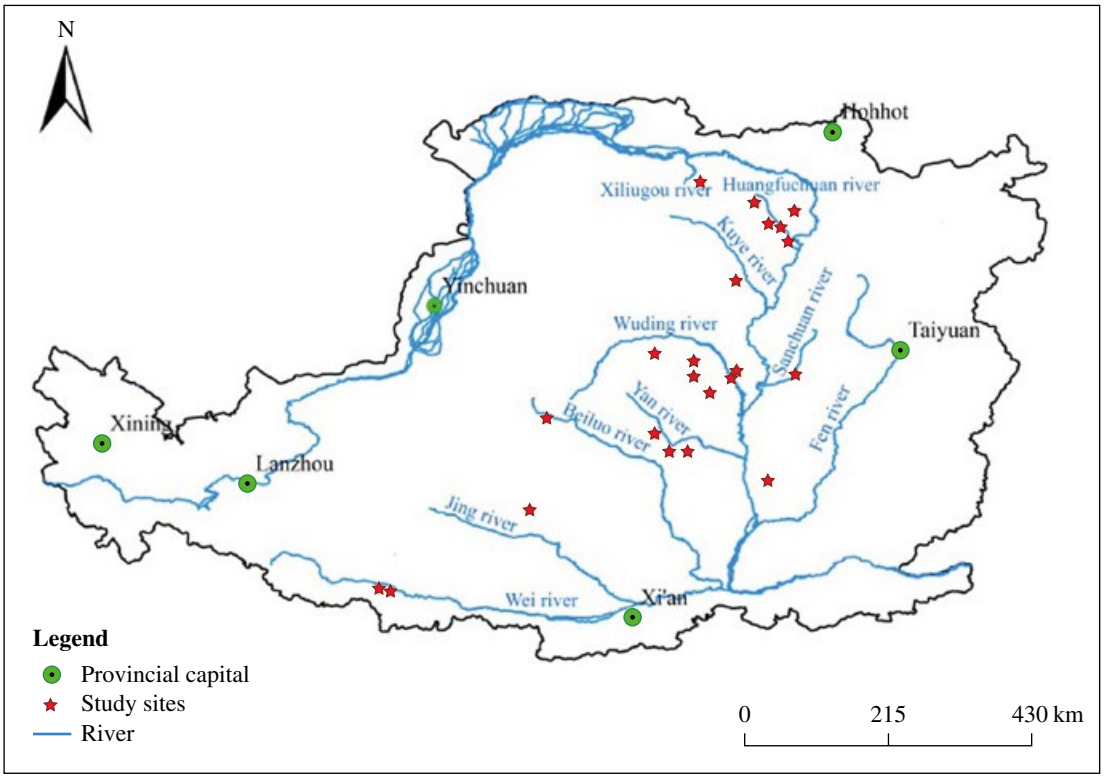

Figure 4.14 Spatial distribution map of the watershed for studying sediment sources (Loess Plateau).

Basin in Lishi City, Shanxi Province in the east (Figure 4.14). Among them, the Huangfuchuan basin in Zhungeer Banner, Inner Mongolia, the Wuding River basin in Yulin in Northern Shaanxi, and the Yanhe River basin in Yan'an City in Northern Shaanxi are the most studied.

4.4.1. The Huangfuchuan Basin

The Huangfuchuan basin is located in the transition zone between the Loess Plateau and the Ordos Plateau (Figure 4.15). It is a coarse sandy area in the upper and middle reaches of the Yellow River. The parent soil mainly consists of soft rock, loess, and sand soil. The area is characterized by deep gullies and high ridges with little terrain change. There are three types of erosion: wind, water, and gravity erosion. There is a wide distribution of arsenic in the basin. The clastic sedimentary rocks have poor diagenesis and a loose structure. Affected by dry and cold weather, there is serious mechanical weathering and peeling for the rocks. As a result, bedrock erosion sediment has become one of the main sources of sediment in the basin [6].

Table 4.5 shows the research results of some scholars on the sediment sources in the Huangfuchuan Basin. Based on detailed analysis of the sediment yield characteristics and mechanical composition of various sediment yielding strata in the Huangfuchuan basin and the mechanical composition of the suspended sediment in the control hydrological station from 1966 to 1984, Zhang established a mathematical model using the principle of equal quantity and found that the relative sediment yields of bedrock, red clay, quaternary loess, and aeolian sand in the basin were 68.49, 1.02, 30.37, and 0.12%, respectively [14]. Li selected 226Ra as a marker to study the sediment sources in Datagou, Huangfuchuan and found that the sediment yield of bedrock accounted for 55.0–76.5% of the total eroded sediment, which is consistent with the actual situation [7]. Moreover, it was concluded that the change in the amount of eroded sediment in the bedrock reflects the different effects of the flow of water at different locations in the check dam, resulting in different sedimentation conditions; thus, the composition of the sediment sources at different positions within the check dam is different. Wang used particle size analysis to calculate that 79.39–84.14% of the sediment

@seismicisolation

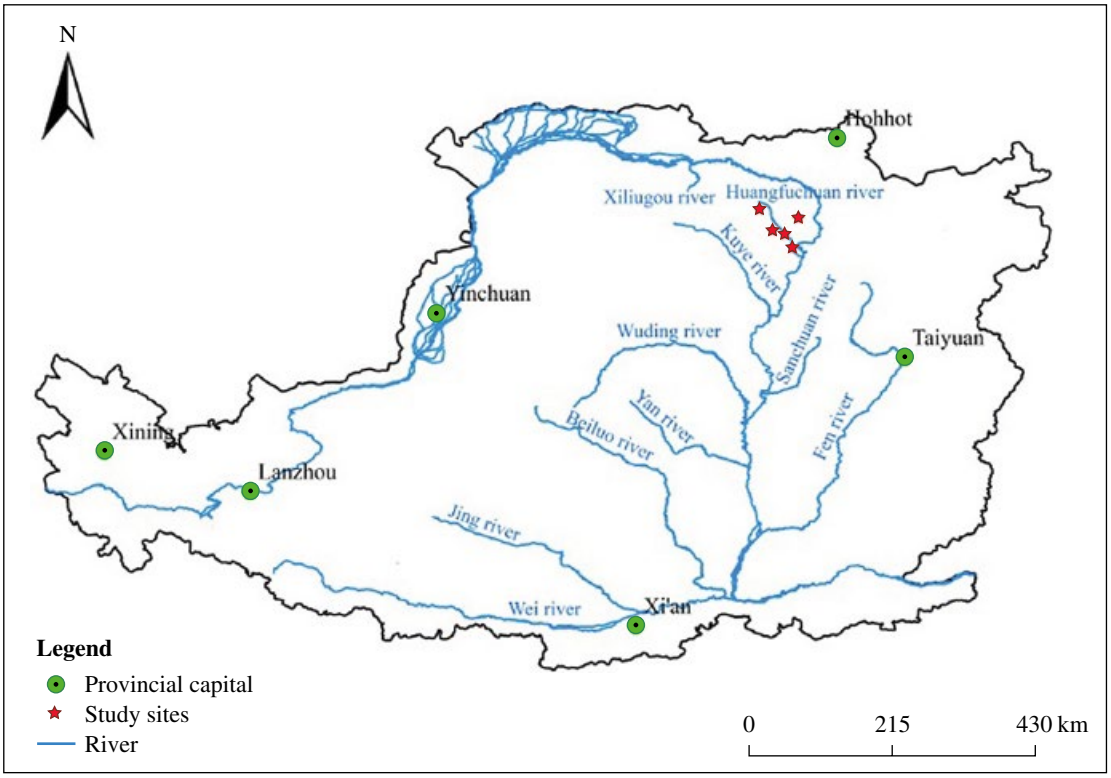

Figure 4.15 The distribution of small watersheds for the study of sediment sources in the Huangfuchuan watershed.

Table 4.5 Studies on sediment sources in the Huangfuchuan area.

Researchers	Study watershed	Contribution
Li et al. [7]	Huangfuchuan Datagou	Bedrock 55.0–76.5%
Tian et al. [8]	Huangfuchuan Huangjiagou	Weathered sandstone 74.06%, bare loess 15.67%, wasteland 10.27%
Zhao et al. [9]	Huangfuchuan Xiaoshilatagou	Weathered sandstone 61.52%, bare loess 32.54%, grassland 5.94%
	Yangjiagou	Weathered sandstone 66.8%, bare land 17.5%, grassland 15.7%
Zhao et al. [10]	Huangfuchuan Xiaoshilatagou	The sediment yield of bare weathered rock accounted for 90% of the total sediment yield
Fan [11]	Huangfuchuan Yangjiagou	Bare rock land 39.7%, slope land 36.5%, grassland 24.7%
Mi [12]	Huangfuchuan Xiaoshilatagou	Sandstone 61.7%, grassland 6.0% bare land 32.3%
An [13]	Huangfuchuan Huangjiagou	Sandstone 73.4%, farmland 15.3%, grassland 11.3%
Zhang et al. [14]	Huangfuchuan Watershed	Bedrock 68.49%, red clay of last century 1.02%, quaternary loess 30.37%, Aeolian sand formation 0.12%
Wang [15]	Heimaotugou	Gully area 82.31%, area between gullies 17.69%
	Fanpugou	Gully area 79.39%, area between gullies 20.61%
	Wufendigou	Gully area 84.14%, area between gullies 15.86%

@seismicisolation

in the three typical small basins of Heimaotugou, Fanpugou, and Wufendigou came from gullies and 15.86–20.61% came from gullies. Among them, the arsenic sandstone that was widely distributed in the gullies contributed 59.13–82.31% of the total sediment yield. Many other scholars also concluded that the sediment in the Huangfuchuan basin mainly comes from bedrock. Tian used the composite fingerprint identification factors composed of Xhf, TN, and ^{137}Cs and found that the proportions of sediment from weathered sandstone, cultivated land, and wasteland from 2001 to 2014 in the Huangjiagou basin accounted for 74.06, 15.67, and 10.27%, respectively. Zhao et al. [9] screened out Cu, Pb, P, La, W, Si, Cs, Nb, Sr, Xhf, Mo, and W as fingerprint identification factors in Yangjiagou and Xiaoshilatagou. The hybrid model was used, and it was concluded that from 2007 to 2010, 66.8% of the sediment in Yangjiagou came from weathered sandstone and the remaining 17.5 and 15.7% of sediment came from bare loess and grassland, respectively. From 1958 to 1972, 61.52% of the sediment in Xiaoshilatagou came from differentiated sandstone and 32.54 and 5.94% of the sediment came from bare loess and grassland, respectively [9]. Additionally, Zhao used the WATEM/SEDEM model to simulate the sediment in Xiaoshilatagou from 1958 to 1972 [10]. The results showed that the observed values were in good agreement with the simulated values, and it was concluded that approximately 92.8% of the sediments were from the arsenic on the gully wall and the rest from bare loess, cultivated land, and alluvial plains. Fan Lijie used composite fingerprinting to determine the source of erosion sediment in Yangjiagou from 2003 to 2008 and found that 39.75% of the sediment came from bare rock land, 35.6% from slope farmland, and 24.7% from grassland [11]. Before 2006, there was a lot of sediment from slope farmland in this area. After 2006, the area of slope farmland decreased significantly and the erosion sediment from slope farmland also decreased. Mi Zhijuan selected Nb, Sb, U, and Xfd (%) as the composite fingerprint identification factors and calculated that from 1958 to 1973, 61.7% of the sediment in Xiaoshilatagou came from sandstone, 32.3% from bare land, and 6% from grassland [12]. An Zhengfeng selected Xhf, TN, and ^{137}Cs as the optimal factor combination and found that from 2001 to 2014, the sediment in Huangjiagou mainly came from sandstone (73.4%) and the rest from farmland (15.3%) and grassland (11.3%) [13].

In short, the eroded sediment in the Huangfuchuan basin mainly came from sandstone, which was mostly located in steep gully walls below the ridges; thus, it can be determined that the sediment in the Huangfuchuan basin mainly comes from gullies.

4.4.2. Wuding River Basin

The Wuding River basin is located on the southern edge of the Maowusu Desert on the northern part of the Loess Plateau (Figure 4.16). The northwest is a sandy area. The river source area is covered by thick layers of loess and there is a hilly ridge area. The gully density is small. The surface between the valleys is relatively flat and complete, and soil erosion is dominated by gully and gravity erosion. In the southeast, there is a loess hilly and gully area with high gully density, a thick loess layer, severe soil erosion, and development of surface, gully, and gravity erosion. The basin is dominated by artificial vegetation, with strong human activities in the southeast. Most of the area is cultivated as farmland. In the northwest, the Maowusu sandy land has sparse vegetation, and the natural vegetation is mainly shrubs and herbs.

According to the observation data of the three small basins of Tuanshangou, Tuanyuangou, and Jiuyuangou, Gong and Jiang [16] concluded that the erosion of the gully accounted for 38.2–54.6% of the total erosion and that the erosion sediment of Tuanyuangou mainly came from gully [16]. The reason for the greater amount of erosion among gullies than in gully land in Tuanshangou and Juyuangou may be due to the larger proportion of cultivated land before treatment (prior to governance, the cultivated land in Jiuyuangou accounted for 66.7% of the total area). Based on the measured runoff sediment data of Jiuyuangou from 1954 to 1964, Xu Xueliang calculated the proportion of average sediment sources without government: the proportion of average sediment sources in the gully area was 69.2%, and the proportion of average sediment sources among gullies was 30.8% [17]. The research results of the Suide Water and Soil Conservation Scientific Experimental Station of the Yellow River Water Resources Commission of the Ministry of Water Resources showed that from 1982 to 2002, 38.7% of the sediment in Jiuyuangou came from hilly ridge slope, 45.8% from gully slope, and 15.5% from gullies.

Wangmaogou is a branch of Jiuyuangou and its sediment source has been studied by many scholars (Table 4.6). In 1999, based on the concept of net

@seismicisolation

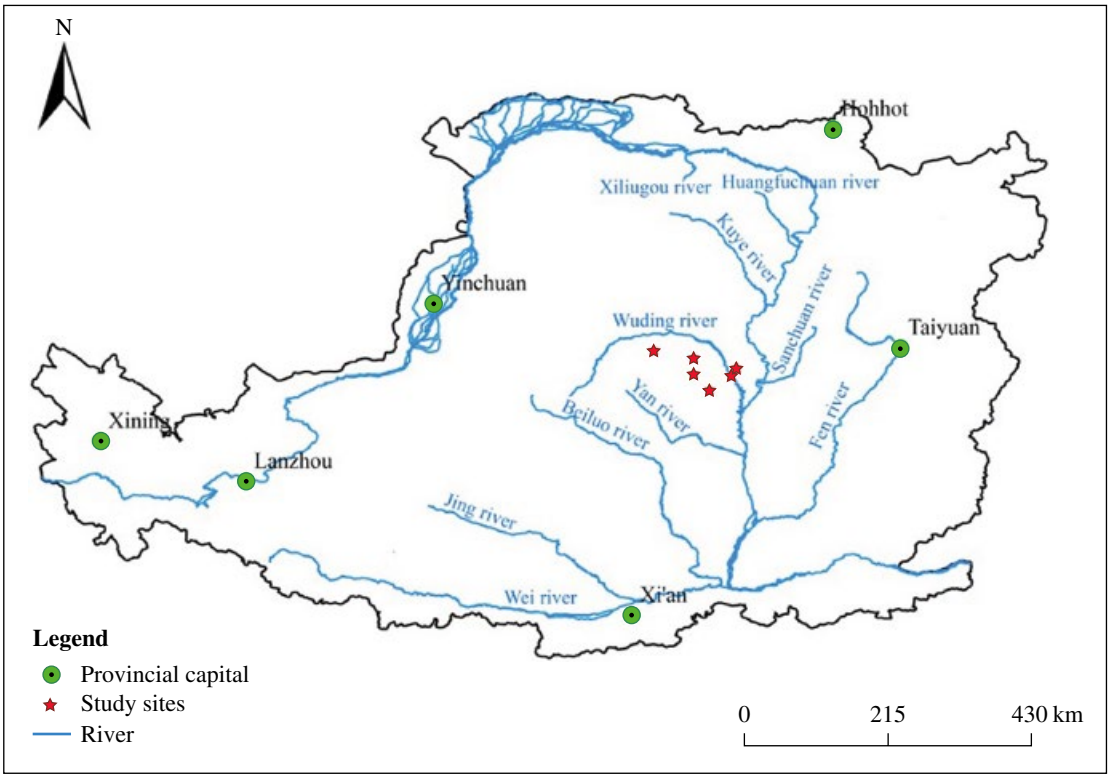

Figure 4.16 Distribution of small watersheds for the study of sediment sources in the Wuding River watershed.

Table 4.6 Studies on sediment sources in the Wudinghe area.

Researchers	Study watershed	Contribution
Zhang et al. [18]	Wangmaogou	Mainly comes from the collapse of trench wall and the expansion of trench
Chen et al. [19]	Nieyangou	Channel 45%, arable land 38.2%, steep slope 16.8%
Xue [5]	Wangmaogou	Furrow bank 68.52%, gully slope 5.03%, slope land 26.45%
Chen [20]	Nieyangou	Gully 45%, arable land 38.2%, steep slope 16.8%
Jiang et al. [21]	Jiuyuangou	The erosion dominated by sheet erosion; rill and shallow gully accounted for 28.7% of the total erosion in Liangmaopo
	Zizhoutuanshangou	Gully area 38.2%, area between gullies 61.8%
Gong and Jiang [16]	Suidetuanyuangou	Gully area 54.6%, area between gullies 43.3%
	Jiuyuangou	Gully area 43.4%, area between gullies 50.1%
Xu [17]	Jiuyuangou	Gully area 69.2%, area between gullies 30.8%
Li et al. [22]	Guandigou	Gully area 30%, area between gullies 70%
Zhang et al. [23]	Yulinmajiagou	Gully area 67%, area between gullies 33%
Li et al. [24]	Wangmaogou	Gully area 61.93%, area between gullies 38.07%
Chen [25]	Wangmaogou	Channel 21.59%, face of slope 78.41%
Zhao et al. [4]	Wangmaogou	Furrow bank 69%, plowed fields 21%, gully slope 10%
Bai [26]	Hengshanyuanping Watershed	Furrow bank 54.22%, slope land 23.56%, grassland 15.54%, branch gully channel 6.68%
Hou [27]	Guandigou no. 3	Gully area 30%, area between gullies 70%
	Guandigou no. 4	Gully area 34%, area between gullies 66%
Zhang [23]	Nieyangou	Slope land 69%, bench terrace 14%, grassland 13%, forest land 3%

@seismicisolation

increment of sediment yield as slope coming water with sediment concentration and the analysis of the sediment yield mechanism of the slope–gully erosion relationship in typical small basins in the middle reaches of the Yellow River, Chen [25] used the genesis analysis method to determine that 78.41% of the eroded sediment in the Wangmaogou basin came from the slope and 21.59% from the gully channel. Zhang studied the nutrients in the sediment of a check dam (which was silted in 1958 and back silted in 1990) in the Wangmaogou basin and concluded that the sediment mainly came from the collapse of the gully wall and channel expansion [18]. Xue screened out the best fingerprint factor combination consisting of SOM, TP, Mg, and Xfd and used a hybrid model to calculate that during the sedimentation stage of the check dam (1958–1991), the sediment from the gully wall, gully slope, and sloping land accounted for 68.52, 5.03, and 36.45% of the total sediment yield, respectively [5]. This proves that the evolution process of the channel is the main process of erosion sediment in the small basin. Zhao Tianyin used the composite fingerprinting to study and calculate the sediment sources of a check dam in the Wangmaogou basin sedimentationed from 1960 to 1990: 69% of the sediment was from the gully wall, 21% from farmland, and 10% from gully slope; there were significant changes in the amount of sediment yield in 1964–1965 and 1983–1984. These changes were caused by soil and water conservation measures for check dams and terraces that reduced slope erosion during the 1960s and 1970s and enabled large-scale reclamation of steep slopes by farmers after 1983. Li et al. studied the heavy rain on July 26 in 2017 and found that 61.93% of the erosion sediment in the Wangmaogou basin came from gullies and 38.07% from the land between gullies, showing that the vegetation restoration occurring since 1999 could effectively control the soil and water loss during heavy rainstorms (from 2000 to 2015, the vegetation coverage in the basin increased by 31%) [24].

Chen used compound fingerprint analysis to identify that from 1960 to 1990, 61.8% of sediment in the check dam of the Nianyangou basin (branch gully of Wangmaogou) came from gullies (45% from gully channel, 16.8% from steep slope) and 38.2% from land between gullies (38.2% from cultivated land) [20, 28]. Zhang used ^{137}Cs tracing technology and found that 69% of the sediment in Nianyangou from 1971 to 1990 came from sloping farmland, 14% from terraced fields, 13% from grassland, and 3% from woodland [29]. According to the "Compilation of Experimental Research Results of Soil and Water Conservation (Volume One)" of the Suide Soil and Water Conservation Scientific Experimental Station of the Yellow River Water Resources Commission of the Ministry of Water Resources, the four typical rainstorms in Jiuyuangou and the loss before the governance (1954–1964) were adopted, and it was calculated that more than 85% of the sediment in the Jiuyuangou basin came from agricultural and barren slopes and approximately 8% came from steep cliffs. In summary, after decades of governance, the sediment source in the small basin has undergone significant changes. Additionally, in other small basins, Zhang Xinbao used the ^{137}Cs tracing technique to find that the sediments in the Majiagou basin of Yulin City in 1993 were mainly from gullies (67%) [23]. Bai Lulu found that 60.9% of the sediment in the Yuanping River basin in Hengshan from 2006 to 2017 came from gullies and 39.1% from land between gullies by using a composite fingerprinting technology hybrid model [26].

Li et al. [22] used the ^{137}Cs tracer method to calculate that from 1959 to 1987, 70% of the sediment of the check dam in the Guandigou small basin came from the land between gullies and 30% from gullies. Hou [27] used the ^{137}Cs tracer technique to determine that 30% of the sediment from Guandigou dam No. 3 (which was silted from 1959 to 1984) came from gullies and 70% from land between gullies; 34% of the sediment from Guandigou dam No. 4 (which was silted from 1961 to 1987) came from gullies, and 66% from land between gullies. Comparing the above research results, it is evident that, although many studies have shown that gullies are the main source of sediment, it may be different for small basins. They indicate that the basin area, the development of the channel in the basin, and the governance of the channel all have an impact on the source of erosion sediment in the basin.

Based on the above research, most of the eroded sediment in the Wuding River basin comes from gullies. With the improvement of river basin slopes and the construction of water and soil conservation projects such as check dams, the sediment yield on the slopes has a decreasing trend.

4.4.3 Yanhe River Basin

Yanhe River basin, located in the north of Shaanxi Province, is a first-level tributary of Hekou Town-Longmen section in the middle reaches of the Yellow

@seismicisolation

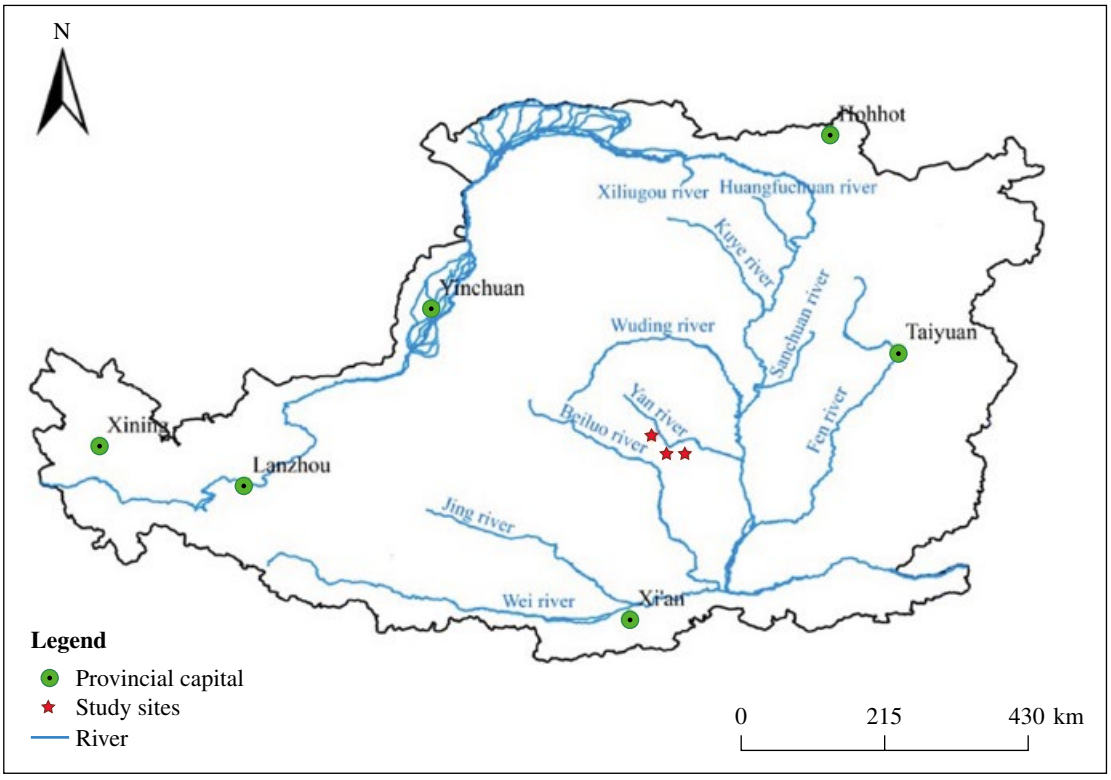

Figure 4.17 Distribution of small watersheds for the study of sediment sources in the Yan River watershed.

River (Figure 4.17). The loess hilly and gully region in the basin accounts for 90% of the total area of the basin, with densely covered gullies, staggered tributaries and branches, broken landforms, and hilly ridges. The main soil type is loose loess soil with poor erosion resistance, which is easily dispersed and transported. Soil erosion is mainly by water erosion, accompanied by a small amount of wind and gravity erosion.

Table 4.7 is the research result of some scholars on the of sediment sources in the Yanhe River basin. Chen et al. [19] screened out Mg, Y, Ti, P, Sc, Co, and Cr as fingerprint identification factors and calculated the sediment sources in the Hujiawan River basin in 30 years of early stage of returning farmland to forest (the samples were taken in 2014): 34.7% of the sediment was from the channel, 27.9% from farmland, 21.7% from woodland, 12.7% from grassland, and 3% from fallow. It was also found that as the forest land matured, the sediment yield contributed by forest land gradually decreased. In June 2014, Chen [30] re-collected sediment samples following three recent erosive rainfalls in Hujiawan and used molecular markers to perform fingerprint identification. It was found that 50.5% of the sediment came from forest land, 25.6% from cultivated land, 14.4% from grassland, and 9.5% from the channel. Forest land is not usually a potential sediment source; however, the area is covered by a large area of artificial forest (62.3%). The average slope was greater than the average slope of the basin, the surface cover was not well developed, and the low infiltration rate of the forest land lead to increased runoff when there was erosive rainfall, intensifying the erosion. Moreover, the channel connectivity in the woodland of this basin was better, which was convenient for sediment transport.

Furthermore, Chen et al. [41] collected samples following heavy rain on 12 July 2013 and combined the physical and chemical indicators of the soil and n-alkanes to form a new composite fingerprint identification factor and calculate the sediment sources: 60.8% of the sediment came from the channel, 20.7% from agricultural land, 11.3% from woodland, and 7.2% from grassland. Zhang [34] used composite fingerprinting to measure sediment sources during the operation of the check dam in the Hujiawan basin (1974–2003): 59.3% of the sediment came from the gullies and 40.7% from the land between gullies. Before returning farmland to forest (grass) in 1999, the contribution rate of erosion sediment of farmland was 29%; after 1999, it had reduced to 16%. The annual erosion

@seismicisolation

Table 4.7 Studies on sediment sources in the Yanhe area.

Researchers	Study watershed	Contribution
Chen et al. [30]	Hujiawan	Channel 34.7%, farmland 27.9%, forest land 21.7%, grassland 12.7%, fallow land 3%
Zhang and Wen [23]	Zichangzhaojiagou	Gully area 74%, area between gullies 26%
Zhang et al. [31]	Hujiawan	Bare land 44.1%, farmland 37.7%, grassland 9.0%, forest land 9.2%
Chen et al. [30]	Hujiawan	Channel 60.8%, farmland 20.7%, forest land 11.3%, grassland 7.2%
Wen et al. [32]	Zichangzhaojiagou	Gully area 76%, area between gullies 24%
Yang et al. [33]	Maidigou	Gully area 72.6%, area between gullies 27.4%
Chen et al. [30]	Huajiawan	Forest land 50.5%, arable land 25.6%, grassland 14.4, channel 9.5%
Zhang [34]	Hujiawan	Gully area 59.3%, area between gullies 40.7%
Xu [35]	Yangou(Miaogou)	Main channel furrow bank 26.4%, orchard 65.5%, arable land 4.8%, branch channel 3.3%
Yang et al. [36]	Yangou(Miaogou)	Main channel 33.7%, slope orchard 60%, slope land 3%, branch channel 3.3%
Wang et al. [37]	Washuta	Gully area 71%, area between gullies 29%
Chen et al. [30]	Hujiawan	Gully 34.7%, arable land 28.2%, forest land 21.5%, grassland 12.7%, fallow land 2.9%
Feng et al. [38]	Zhaojiagou	Gully area 77%, area between gullies 23% (in 1994) Gully area 85%, area between gullies 15% (in 1995) Gully area 94%, area between gullies 6% (in 1996)
Yang [39]	Maidigou	Gully area 72.6%, area between gullies 27.4%
Wang [40]	Washuta	Channel 65%, face of slope 35%

sediment yield of sloping farmland after the conversion was only 50% of that before returning farmland to forest. Zhang et al. [31] used composite fingerprinting to obtain the sediment sources of the Hujiawan basin during the heavy rainfall in 2013: 44.1% of the sediment came from bare land, 37.7% from farmland, 9.0% from grassland, and 9.2% from woodland.

Through the below research in the Yanhe River basin, it has been determined that the sediment in the Yanhe River basin comes mainly from gullies. Moreover, the main sediment sources before and after returning farmland to forest have changed greatly. After the conversion of farmland, the sediment yield on the slope gradually decreased, indicating that check dam construction and the implementation of converting farmland to forests and slopes to terraces play an important role in water and soil conservation in the basin.

4.4.4 Other Basins

The research on the sediment source in the Loess Plateau is mainly concentrated in the Huangfuchuan, Wuding River, and Yanhe River basins. There are few studies on other basins (Figure 4.18). Therefore, some studies on other basins are shown in Table 4.8 which shows the spatial distribution of sediment sources of small basins in other basins.

The Luoyugou basin is a primary tributary on the left bank of Jihe, a tributary of the Weihe River, and belongs to the third sub-region of the loess hilly and gully region. Zhao et al. [4] collected soil samples from the Qiaozixigou small basin in Luoyugou and flood sediment samples from eight rainfalls in 2012 (five times) and 2013 (three times) and used compound fingerprinting to determine that the average contribution of gully wall, gully slope, and farmland to sediment was 63, 13, and 24%, respectively. Liu et al. [44] used composite fingerprinting to calculate the sediment sources in the Xijiazhai basin of Luoyugou from 2002 to 2014: 29.05% of the sediment came from farmland, 12.17% from woodland, 15.39% from grassland, 21.53% from fallow land, and 21.58% from gully channels. Significant changes in land use/cover usually resulted in an initial erosion increase. Then, a new balance between vegetation and land cover was established. In the study area, since 2002, the implementation of the project of converting farmland to forests has initially increased soil and water loss [48].

Sanchuan River is located in the western part of the Luliang Mountains, most of which belong to the loess hilly and river valley regions of western Shanxi.

@seismicisolation

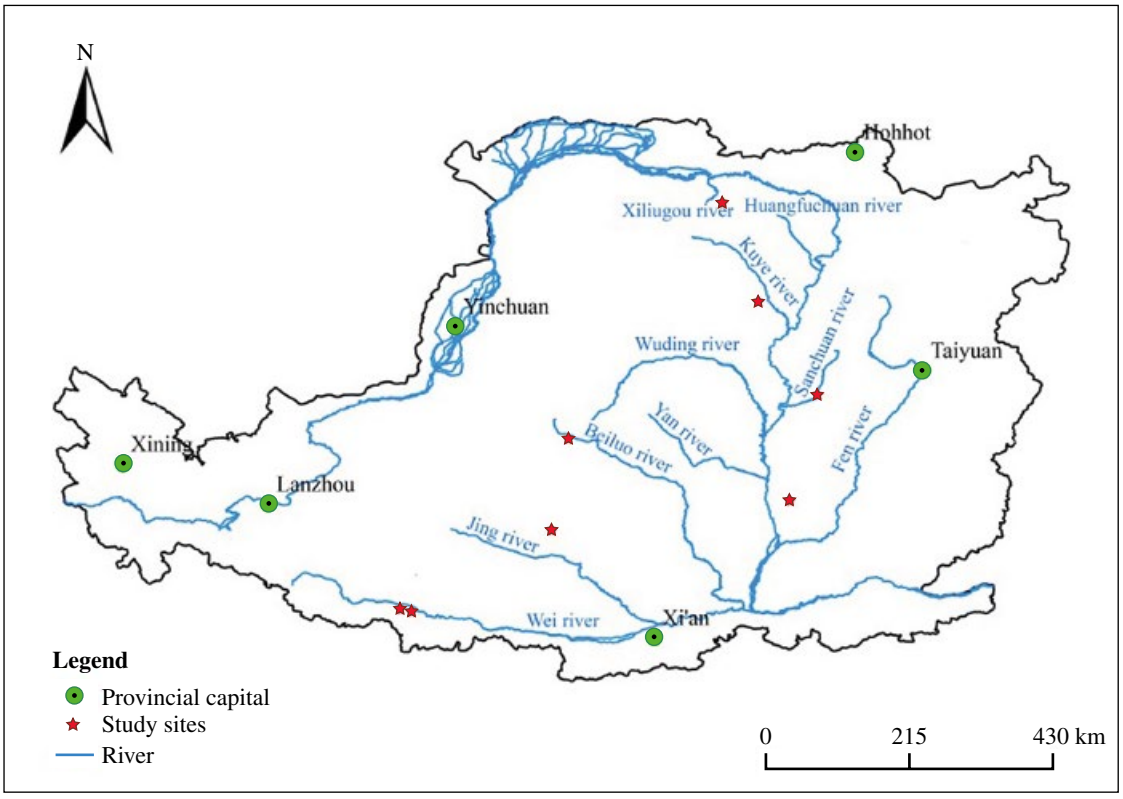

Figure 4.18 Distribution of small watersheds for the study of sediment sources in other watersheds.

Table 4.8 Studies on sediment sources in other areas.

Researchers	Watershed	Small watershed	Contribution
Zhao et al. [9]	Luoyugou	Qioazixigou	Furrow bank 63%, gully slope 13%, plowed fields 24%
Liu et al. [42]	Luoyugou	Xijiazhai	Farmland 29.05%, forest land 12.17%, grassland 15.39%, fallow land 21.53%, channel 21.58%
Gong and Jiang [16]	Sanchuanhe	Wangjiagou	Gully area 52.9%, area between gullies 47.1%
Wei [43]	Along the Yellow	Yuejiagou	Gully area >70%
Liu et al. [44]	River in Shanxi		Gully area >60%
Zhang and Wen [23]			Gully area 80%, area between gullies 20%
Qin et al. [45]	Beiluohe	Simianyaogou	Grassland is the main source, grassland > farmland > construction land > forest land
Chen [25]	Jinghe	Nanxiaohegou	Face of slope 85.23%, channel 14.77%
Wang [46]	Kuyehe	Liudaogou	Red mud furrow bank 79.7%, Sand covered area 12.9%, loess furrow bank 5.4%, abandoned farmland 2.1%
Li et al. [47]	Xiliugou	Xiliugou	Bare land 48.0%, desert 28.6%, arable land 19.3%, forest land 2.1%, grassland 2.0%

The valley is characterized by undulating mountains, continuous hilly ridges, vertical ravines, and deep slopes. The soil is loose, and soil erosion is serious. Based on the experimental observation data of the Wangjiagou small basin in Lishi, Gong Shiyang et al. concluded that the gullies' erosion accounted for 52.9% of the total erosion and the erosion of the land between gullies accounted for 47.1%. Zhang and Wen [23] used a ^{137}Cs tracer to determine that 80% of the sediment in the Yuejiagou basin of Jixian County along the Yellow River in Shanxi from 1992 to 1994 came from gullies and 20% from land between gullies. Based on the slope runoff plot data in 1993, 1998, and 1999 in the Yuejiagou basin and the measured sediment data at the

@seismicisolation

gully mouth of the small basin, Wei [43] calculated that more than 70% of the output sediment in the basin came from the gullies. In the same basin, Liu et al. [44] calculated that the sediment mainly came from gullies (gully head, gully channel, and gully slope) based on the measured data from 1993 to 2002; the erosion of gullies accounted for more than 60% of the total erosion of the basin.

Beiluo River is a primary tributary of the Weihe River, which spans the loess hilly and gully areas, Ziwuling forest area, the gully area of the Loess Plateau, and the terrace plain area from northwest to southeast. The soil types in the basin include loess soil, black loess soil, and gray cinnamon soil. The soil erosion in the small basin of Simianyaogou on the south bank of the upper reaches of Beiluo River was evaluated based on the GIS and RUSLE models by Qin et al. [45]; it was concluded that as the grassland coverage in this basin reaches 57.07%, the grassland is the main source of eroded sediment, in the order of grassland > agricultural land > construction land > forest land.

The Jinghe River basin is one of the areas with serious soil erosion in the Northwest Loess Plateau. There are two large geomorphic areas: the rocky mountainous area and the loess area. The geomorphological types are mainly composed of hills, plateaus, beams, ridges, and rivers. According to the concept of net increment of sediment yield as slope coming water with sediment concentration, based on analyzing the sediment yield mechanism of the relationship between slope and gully erosion in the typical small basin in the middle reaches of the Yellow River, Chen [25] used the genesis analysis method to determine that 85.23% of the eroded sediment in Naniaohegou of Qingyang City came from the slope and 14.77% from the channels.

The Liudaogou basin is located in Shenmu County, northern Shaanxi, in the transition zone between semi-arid grassland and desert grassland on the Loess Plateau. The main soil types include sandy loess, cotton sand, and new loess. The main erosion is water, wind, and gravity erosion.

Wang [46] screened out Cr, Mg, Na, Y, TN, and Ba as fingerprinting factors, and calculated that in the Liudaogou basin from 1978 to 2013, the Hongnigou wall contributed the most to the sediment, which reached 79.7%, followed by 12.9% of the sand-covered area, 5.4% of the loess gully wall, and 2.1% of the reclaimed land [46].

Xiliugou is one of the top ten holes that flow into the Yellow River from south to north in the Inner Mongolia Autonomous Region. The landform of the basin includes three types: loess-covered arsenic hilly and gully area, windy sand area, and alluvial plain area. It is located in an area where wind and water erosion areas overlap with severe soil erosion. The hilly and gully area is characterized by sparse vegetation, fragmented ground, and severe soil erosion, which is dominated by water and gravity erosion. It is the main sand-producing area of Xiliugou. Li et al. [47] used ^{137}Cs tracer technology to study soil samples collected in June 2011. Combined with the area of different land-use types in the basin, it was determined that the sediment yield rates of bare land, desert, cultivated land, woodland, and grassland were 48.0, 28.6, 19.3, 2.1, and 2.0%, respectively.

Based on all the above basins, it can be concluded that most of the eroded sediment on the Loess Plateau comes from gullies. With the implementation of a series of water and soil conservation measures such as converting farmland to forests and grassland, slopes-to-terraces, and constructing check dams, the sediment from the land between gullies is decreasing. Therefore, the slope management of the Loess Plateau has achieved some positive results.

4.5. FLOOD DETENTION AND SEDIMENT TRAPPING EFFECT OF CHECK DAMS FOLLOWING A TYPICAL RAINSTORM IN SUIDE ON JULY 26 IN 2017

4.5.1. The Typical Rainstorm in Suide on July 26 in 2017

From 25 to 26 July 2017, there was a sustained local heavy precipitation in parts of Suide County and Zizhou County in the lower reaches of the Dali River and the middle reaches of the Wuding River in northern Shaanxi. The precipitation process was dominated by scattered short-term heavy rain which occurred in many places. The rain intensity of 77 rainfall stations exceeded 30 mm, the rain intensity of 10 stations exceeded 50 mm/h, and the maximum reached 60.4 mm/h, with high catastrophic ability. The total precipitation was 30–100 mm, and the local precipitation exceeded 200 mm.

The rainstorm center was mainly concentrated in the Dali River basin, a tributary of the Wuding River, where the daily rainfall at Lijiatuo Station reached 218.4 mm and at Zhujiayang Bay Station reached 201.2 mm. Affected by the rainstorm, the peak discharge of Suide Station in Dali River reached 3290 m^3/s, the maximum sediment content reached 837 kg/m^{-3}, and the total sand

@seismicisolation

transporting volume was 33.73 million t. The peak discharge of the Baijiachuan Station of Wuding River reached 4480 m^3/s, the maximum sediment content reached 873 kg/m^3, and the sand transporting volume during the flood reached 77.56 million t. It was the largest flood since the two stations had been established in 1959 and 1975, respectively.

The runoff sediment observation was set up following the principle of comparison of the gully with governance and the gully without governance in Jiuyuangou (gully with governance) and Peijiamao (gully without governance). After more than 60 years of governance, a complete dam system was formed in Jiuyuangou, which is one of the governance models in the Loess Plateau that focuses on complete dam systems. There are 217 check dams, including 27 key dams, 40 medium dams, and 150 small dams. The configuration ratio is 1:1.48:5.56, and the dam density is 3.07/km^2. The Peijiamao basin has a low level of governance. Because the 307 National Road runs through the entire main channel, there is no check dam in the main channel.

Table 4.9 shows the observation results from the Jiuyuangou, Peijiamao, Wangmaogou, Qiaogou, and Xindiangou basins of the Yellow River Soil and Water Conservation and Supervision Bureau of Suide. The data in the table show that the rainfall in the Jiuyuangou and Peijiamao basins was similar. The runoff depth of Jiuyuangou basin was 18.4 mm and of Peijiamao basin was 45.5 mm, 2.47 times that of Jiuyuangou. The peak discharge modulus of Jiuyuangou basin was 0.52 $m^3/(s\ km^{-2})$ and of Peijiamao basin was 3.21 $m^3/(s\ km^{-2})$, 6.17 times that of Jiuyuangou. This shows that measures such as check dam construction played an important role in peak reduction and flood detention during the heavy rain on July 26. The maximum sand content of Jiuyuangou was 170 kg/m^3 and of Peijiamao was 382 kg/m^3. Although the rainfall continued for a long duration and the rain intensity was strong, intercepted by a check dam, the flood flow and sand content at the mouth of the Jiuyuangou basin were greatly reduced, which further proves the important role of water and soil conservation measures for blocking sand and silt.

4.5.2. Check Dam Construction in the Rainstorm Area on July 26 in Northern Shaanxi Province

4.5.2.1. Check Dam Distribution in Zizhou County and Suide County

Check dams are important engineering measures for improving gullies on the Loess Plateau, with a history of more than 400 years. According to the first national water conservancy survey, there are 5655 key dams and 52 791 small and medium dams on the Loess Plateau. Totally, 33 831 check dams have been constructed in Shaanxi Province, accounting for more than half of the total number of check dams in the Loess Plateau. The total storage capacity is 6.8 billion m^3, the accumulated mud is more than 5 billion t, there is more than 60 000 hm^2 of check dam area, and the annual grain output is 400 million kg. They have significant benefits in terms of flood cutting and storage, flood prevention and security, silt-blocking, increasing production and income, and promoting economic and social development. It is popular among local cadres and masses.

A total of 18 269 check dams have been built in Yulin City, with a total storage capacity of 4 billion m^3. The ratio of key, medium, and small dams is 1:4.2:6.7. There are 2025 check dams in Zizhou County, including 215 key dams, 864 medium dams, and 957 small dams. There are 2906 check dams in Suide County, including 138 key dams, 588 medium dams, and 2180 small dams, as shown in Table 4.10. The key dams in Zizhou County and Suide County are relatively evenly distributed, as shown in Figure 4.19.

Table 4.9 Runoff and sediment transport characteristics in the July 26 rainstorm.

Watershed	Control area/km^2	Rainfall duration	Precipitation/mm	Runoff depth/mm	Runoff coefficient	Flood peak discharge/($m^3\ s^{-1}$)	Maximum sediment concentration/($kg\ m^{-3}$)	Sediment transport modulus/($t\ km^{-2}$)
Jiuyuangou	70.11	51:20	156.1	18.39	0.12	36.14	170	1914
Peijiamao	39.30	36:30	156.7	45.50	0.29	126.10	382	7595
Wangmaogou	5.97	12:00	179.6	17.29	0.10	24.26	382	5965
Qiaogou	0.45	7:40	113.2	13.78	0.12	1.99	364	2228
Xindiangou	1.77	7:50	106.3	1.64	0.02	0.52	48	53

@seismicisolation

Table 4.10 Statistics of check dams in Shaanxi province, Yulin city, Zizhou county, and Suide county.

Region	Shaanxi province	Yulin city	Zizhou county	Suide county
Total number of check dams	33 831	18 269	2029	2910
The total capacity of check dams (10^4 m^3)	682 291	404 093	52 195	35 573
The capacity of intercepting sediment (10^4 m^3)	531 890	323 820	44 955	30 988
Siltable area (hm^2)	88 904	45 517	5537	4171
Dam control area (km^2)	33 807	21 561	1974	2052
The number of key check dams	2617	1542	215	134
The total capacity of check dams (10^4 m^3)	294 949	173 065	22 485	14 275
The capacity of intercepting sediment (10^4 m^3)	216 363	134 268	16 738	11 769
Siltable area (hm^2)	27 048	13 375	2072	973
Dam control area (km^2)	11 174	7079	862	675
The number of medium trap dams	9211	6413	864	589
The total capacity of check dams (10^4 m^3)	244 847	156 792	23 214	11 979
The capacity of intercepting sediment (10^4 m^3)	206 189	136 103	22 282	10 277
Siltable area (hm^2)	33 780	19 766	2653	1737
Dam control area (km^2)	12 218	8407	762	763
The number of small check dams	22 003	10 314	960	2183
The total capacity of check dams (10^4 m^3)	142 496	74 236	6496	9319
The capacity of intercepting sediment (10^4 m^3)	109 338	74 236	5935	8942
Siltable area (hm^2)	27 953	12 376	812	1461
Dam control area (km^2)	10 375	6075	350	614

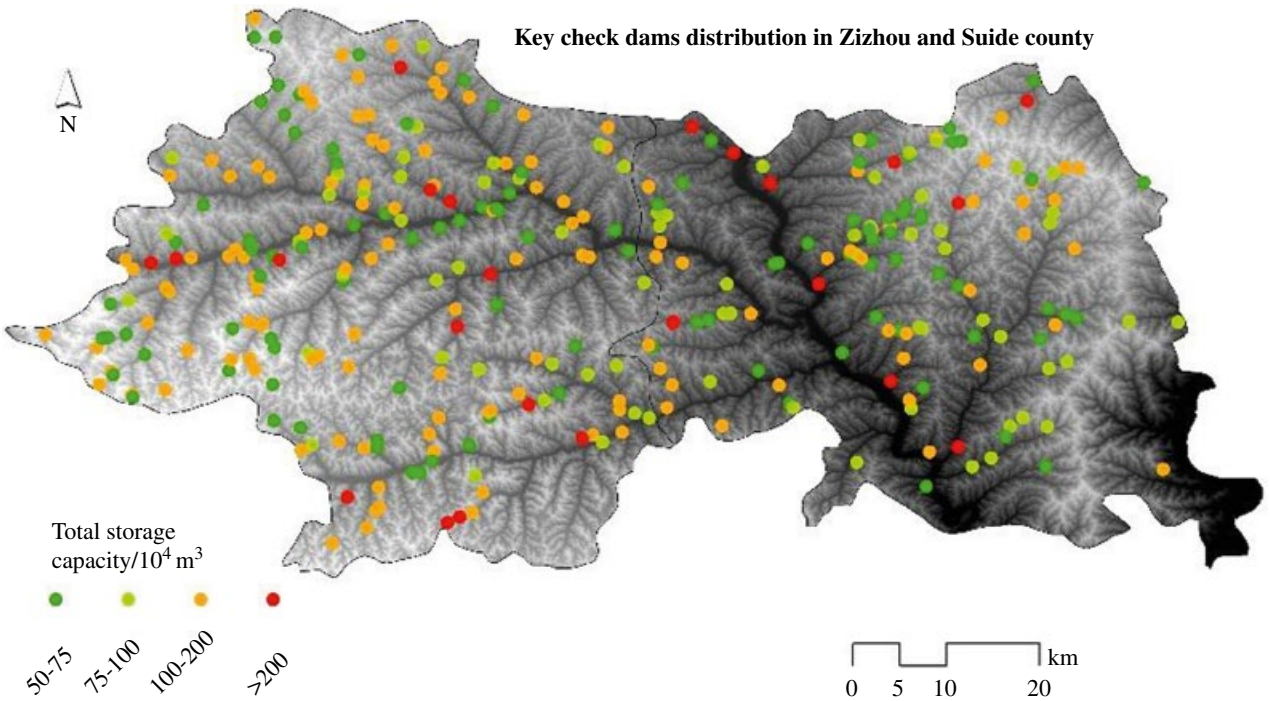

Figure 4.19 Key check dam distribution in Zizhou and Suide county.

@seismicisolation

4.5.2.2. Jiuyuangou Dam System Layout

Taking Jiuyuangou in Suide County as a typical basin, the layout characteristics of check dams in the rainstorm area were analyzed. There are 217 check dams in Jiuyuangou, including 27 key dams, 40 medium dams, and 150 small dams. The configuration ratio is 1:1.48:5.56, and the dam density is 3.07/km^2. There are nine key dams set on the main channel, accounting for 33.33%, 15 key dams set on the primary branch gully, accounting for 55.56%, and the remaining three key dams are set on the secondary branch gullies, accounting for 11.11%; therefore, the key dams are mainly distributed on the primary branch gullies and the main channel. There are two medium-sized dams set in the upstream of the main gully channel, accounting for 5%, 29 medium-sized dams set in the primary branch gully, accounting for 72.5%, and the remaining nine medium-sized dams are set in the secondary branch gully, accounting for 22.5%; therefore, the medium-sized dams are concentrated on the primary branch gullies and the small dams are mainly set on the second-level branch gullies, as shown in Figure 4.20.

According to survey statistics, the key dams in the Jiuyuangou basin are generally built with "two facilities." Among the 27 key dams, there are 10 check dams with "three facilities," accounting for 37.0%, and 15 check dams with "two major facilities," accounting for 63.0%. There is no spillway for medium dams. Among the 40 medium dams, there are seven check dams with "three facilities," accounting for 17.5%, 28 check dams with "two facilities," accounting for 70.0%, and five check dams with "one facility," accounting for 12.5%; small dams are built with "one facility." Among the 150 small dams, there are 14 check dams with "two facilities," accounting for 9.3% and 136 check dams with "one facility," accounting for 90.7% (Table 4.11).

According to the division principle of the dam system of the basin, the Jiuyuangou basin dam system is

Table 4.11 Parameters of engineering structure.

Type	Three items	Two items	One item	Total
Key check dam	10	17	0	27
Medium check dam	7	28	5	40
Small check dam	0	14	136	150
Total	17	59	141	217

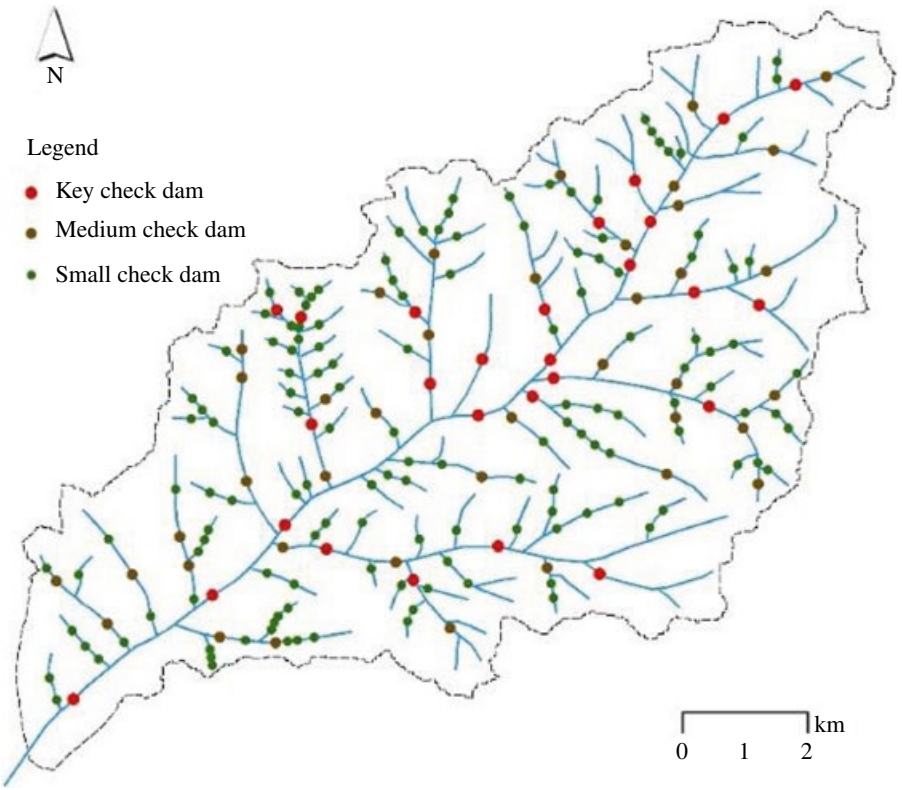

Figure 4.20 The check dam distribution in the Jiuyuangou watershed.

@seismicisolation

divided into one main gully dam system and 14 sub-dam systems. The control area of the dam system is mostly below 5 km^2, as shown in Table 4.12.

4.5.2.3. Chabagou Dam System Layout

Among the 178 check dams in Chabagou that were investigated, there were 123 small check dams, 38 medium check dams, and 17 large check dams (Table 4.13), accounting for 63.1, 27.9, and 9.0% of the total; therefore, most of them were small check dams (Figure 4.21). The average dam widths of the small, medium, and large dams were 39.4, 66.8, and 78.1 m, respectively, and the height of the silt surface from the dam crest was 2.4, 5.9, and 7.7 m, respectively.

Among the 178 dams, most of them were check dams without drainage and flood discharge facilities (101), accounting for 54.7% of the total; there were very few dams (seven) equipped with drainage (drainage tunnel) and flood discharge (spillway) facilities, accounting for only 4.5% of the total. The equipment of drainage and flood discharge facilities for different types of check dams were also different. About 65.5% of small dams had no drainage or flood discharge facilities and only 1.8% had both; 46.0% of medium dams had no drainage or flood discharge facilities and 8.0% had both; 31.3% of large dams had no drainage or flood discharge facilities and 6.3% had both. It can be concluded that the lower the level of the dam, the higher the proportion of check dams without drainage or flood discharge facilities.

Most of the dams were constructed earlier or have low design standards, resulting in very limited effective storage capacity of current check dams. The distance between the silt surface and the crest of 87 dams was less than 2 m, accounting for 48%; the distance between the silt surface and the dam crest of 53 dams was 2–6 m, accounting for 30% (Table 4.14).

Table 4.12 Statistics of basic units of dam systems in the Jiuyuangou watershed (unit/a).

Name of dam	Control watershed area/km^2	Key check dam	Medium check dam	Small check dam	Total
Dam system unit of main channel	31.70	9	7	30	46
Dam system unit of Wangjiagou	4.27	0	2	10	12
Dam system unit of Majiagou	4.37	0	2	5	7
Dam system unit of Shuiyangou	2.17	0	2	3	5
Dam system unit of Xiaqiaogou	2.60	0	1	2	3
Dam system unit of Maliangou	3.58	0	3	6	9
Dam system unit of Hejiagou	2.97	1	1	3	5
Dam system unit of Xiangtaogou	3.23	1	1	8	10
Dam system unit of Gaoshegou	7.00	3	2	20	25
Dam system unit of Xiyangou	3.10	2	1	12	15
Dam system unit of Chaijiagou	2.12	1	1	5	7
Dam system unit of Lijiazhai	10.45	2	2	5	9
Dam system unit of Wangmaogou	5.80	2	7	16	25
Dam system unit of Linjian	21.64	4	3	26	33
Dam system unit of Liushugou	5.72	2	1	3	6

Table 4.13 The quantity of three items of check dams in the Chabagou watershed.

Types of check dams	Average sink area/ha	Dam body (no.)	Dam body + Flood spillway	Dam body + Drainage tunnel	Dam body + Flood spillway + Drainage tunnel	Total
Small check dam	172.4	84	27	10	2	123
Medium check dam	224.2	11	8	15	4	38
Large check dam	321.7	6	3	7	1	17
Total		101	38	32	7	178

@seismicisolation

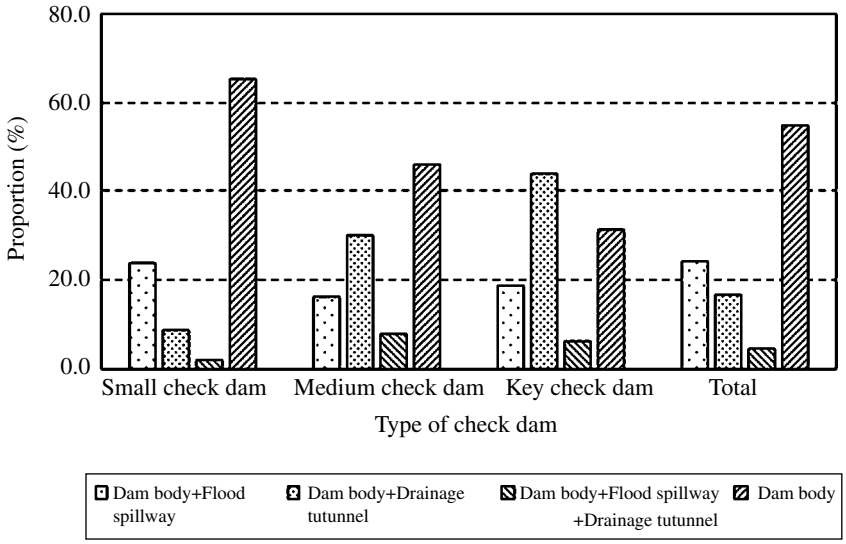

Figure 4.21 Types of check dam and their drainage and flood discharge facilities.

Table 4.14 Status check of dam deposition.

Distance from dam land surface to top of dam body	<1 m	1–2 m	2–6 m	>6 m	Total
Number	55	32	53	38	178
Proportion /%	30.90	17.98	29.78	21.35	100

Table 4.15 Sedimentation depth of check dams in the Jiuyuangou watershed

Number of surveys	Mean/cm	Median/cm	Standard deviation/cm	Min/cm	Max/cm	Percentile (P)/cm		
						25	50	75
977	20.93	13.00	22.53	0.00	135.00	5.75	13.00	30.00

4.5.3. Flood Detention and Sediment Trapping of Check Dams

4.5.3.1. Sedimentation Depth

The sedimentation depth of 977 check dams in the Jiuyuangou basin was investigated. The average sedimentation thickness was 21 cm, and the maximum sedimentation depth was 135 cm. The statistical characteristics of sedimentation depth are shown in Table 4.15. The sedimentation at the right bank of Jiuyuangou was more serious than that of the left bank, and the upstream sedimentation of most tributaries was thicker. Regarding the type, the average sedimentation depth of key dams was 42 cm, of medium dams was 27 cm, and of small dams was 14 cm.

4.5.3.2. Basin Sedimentation Amount

According to the calculation results, the entire Jiuyuangou basin had a total of 759 900 t of sediment: 346 500 t for key dams, 243 500 t for medium dams, and 169 900 t for small dams. The sedimentation amounts at key, medium, and small dams accounted for 46, 32, and 22% of the total sedimentation amount, respectively.

The ratio of the sedimentation amounts for key dams: medium dams: small dams was 1 : 0.70 : 0.49 (Table 4.16). The three branch gullies with the largest sedimentation amounts were Maliangou, Wangmaogou, and Xiyangou, with sedimentation amounts of 164 800, 111 300, and 74 800 t, respectively.

Based on the measured data at the gully mouth, the sediment retention effect of the check dams was further

@seismicisolation

analyzed. The measured sediment transport modulus of the Wangmaogou basin was 5965 t km^{-2}, the sedimentation modulus was 19 220 t/km^2, the erosion modulus was 25 185 t/km^2, and the sediment delivery ratio was 0.24. The measured sediment transport modulus in the Jiuyuangou basin was 1914 t/km^2, the sedimentation modulus was 11 045 t/km^2, the erosion modulus was 12 959 t/km^2, and the sediment delivery ratio was 0.15. This shows that the check dam is an important collector of sediment in the basin that significantly reduces the sediment delivery ratio in the basin and plays an important role in blocking sediment. The sedimentation modulus of each branch gully is shown in Table 4.17.

Table 4.16 The volume of different types of check dams (unit/t).

Type	Index	Value
Key check dam	Mean	15 066
	Median	11 185
	Standard deviation	15 359
	Min	638
	Max	66 932
	Total	346 514
Medium check dam	Mean	7160
	Median	3692
	Standard deviation	11 616
	Min	41
	Max	62 978
	Total	243 449
Small check dam	Mean	1349
	Median	666
	Standard deviation	1696
	Min	6
	Max	7807
	Total	759 878

4.5.4. Characteristics and Causes of Check Dam Damage Under Heavy Rain

4.5.4.1. Characteristics of Check Dam Damage in Zizhou County and Suide Country

In Zizhou County, 41 key dams were damaged, accounting for 19.07% of the total number of key dams; 139 medium dams were damaged, accounting for 16.09% of the total number of medium dams; and 125 small dams were damaged, and accounting for 13.02% of the total number of small dams. Sixteen key dams in Suide County were damaged, accounting for 11.94% of the total number of key dams; 142 medium dams were damaged, accounting for 24.11% of the total number of medium dams; and 143 small dams

Table 4.17 Area for siltation, deposition volume, and siltation modulus of branch gullies in Jiuyuangou.

Name	Siltation volume /t	Area/km^2	Sedimentation modulus/(t km^{-2})
Luojiagou	20 416	3.13	6514
Wujiagou	10 243	1.51	6764
Lijiazhai	67 084	5.45	12 314
Xiyangou	74 816	4.73	158 145
Zhejiagou	17 903	1.69	10 604
Gaoshegou	64 524	3.90	16 556
Hejiagou	39 088	1.90	20 603
Wangmaogou	111 295	5.79	19 220
Maliangou	164 760	3.54	46 555
Xiangtagou	25 940	1.90	13 640
Tuanyuangou	4711	0.65	7286
Linjiajiangou	31 092	12.32	2523
Majiagou	12 059	1.73	6954
Xiaqiaogou	10 183	1.70	5973
Shuiyangou	3408	1.14	2980
Wangjiagou	2105	1.73	1215
Main channel downstream of Luojiagou key check dam	33 591	4.14	8106
Main channel downstream of Zhejiagou key check dam	6272	1.72	3655
Main channel downstream of Sanjiaoping key check dam	42 782	6.11	6997
Main channel downstream of Maliangou key check dam	11 459	1.63	7031
Main channel downstream of Liujiaping key check dam	6148	2.37	2591
Total	759 878	68.80	11 045

@seismicisolation

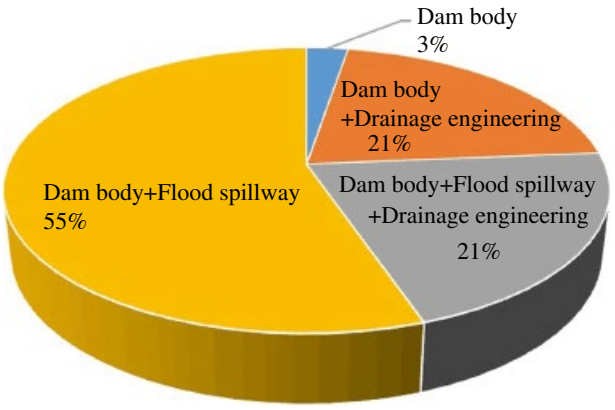

Figure 4.22 The composition of key dams damaged by the flood in Zizhou county.

were damaged, and accounting for 6.56% of the total number of small dams.

For the damaged key dams in Zizhou County, 55% of dams were equipped with a dam body and spillway, 21% of dams were equipped with a dam body and drainage structure, 21% of dams were equipped with a dam body, spillway, and drainage structure, and 3% of dams were check dams with only a dam body (Figure 4.22). Regarding the construction time of damaged key dams, 77% of the damaged key dams in this survey were built before 1980. Among the eight key dams with dam bodies and drainage buildings in Zizhou County, two drainage buildings were damaged and the dams were intact; the remaining six dam bodies and drainage buildings were all damaged. For the eight key dams with "three facilities," one dam body was damaged, two dam bodies and drainage buildings were damaged, and five drainage buildings were damaged. Among the 23 key dams with dam bodies and spillways, two dam bodies were damaged, 12 spillways were damaged, and nine spillways and dam bodies were damaged. There were 16 damaged key dams in Suide County, of which damaged dam bodies accounted for 50% of the number of damaged key dams; damaged drainage structures accounted for 6.25%. The dam body and drainage structure of 25% of dams were damaged, and the dam body and spillway of 18.75% of dams were damaged.

There were 139 medium dams damaged in Zizhou County, 28% of dams had a facility, 32% had a dam body and spillway, 38% had a dam body and drainage structure, and 2% had three facilities. Damaged dam bodies accounted for 53.02% of the damaged medium dams, the damaged drainage structures accounted for 18.14%, and the damaged spillways accounted for 8.84%. The dam body and drainage structure of 14.88% of dams were damaged, and the dam body and spillway of 5.12% of dams were damaged. There were 142 damaged medium dams in Suide County. The damaged dam bodies accounted for 24.65% of the number of damaged medium dams, the damaged drainage structures accounted for 21.83%, and the damaged spillways accounted for 19.01%. The dam body and drainage building of 16.9% of dams were damaged, and the dam body and spillway of 17.61% of dams were damaged.

4.5.4.2. Damage Characteristics of Check Dams in the Jiuyuangou Basin

The water damage of Jiuyuangou check dams was as follows: five key dams were damaged, accounting for 18.52% of the total number of key dams. Damaged dam bodies accounted for 40% of the total number of damaged key dams, the damaged spillways accounted for 40%, and damaged drainage structures accounted for 20%. Twenty-three medium dams were damaged, accounting for 57.5% of the total number of medium dams. Damaged dam bodies accounted for 69.56% of the total number of damaged medium dams, damaged spillways accounted for 4.35%, and damaged drainage structures accounted for 4.35%. The damaged dam bodies and drainage buildings of dams accounted for 17.39% and the damaged dam bodies and spillways accounted for 4.35% (Table 4.18).

4.5.4.3. Damage Characteristics of Check Dams in the Chabagou Basin

Among the 178 check dams surveyed in this paper, 29% of check dams were broken during storms: 13% of dams were damaged and 51% were intact (Table 4.19). For the broken check dams, the maximum opening width of the dam body was 45.7 m, the maximum opening depth was 22.3 m, the average opening width was 9.2 m, and the average opening depth was 5.8 m.

Among the different types of check dams, the number of broken check dams without three facilities was the largest (57) and few check dams were in good condition (32), accounting for 59% and 33% of the total number of check dams, respectively. The check dams with three facilities had fewer dam breaks (2) and many of them were in good condition (5) (Table 4.20), accounting for 25 and 63% of the total number of the check dams with three facilities. It can thus be concluded that check dams with drainage and water discharge buildings are stronger than other check dams.

@seismicisolation

Table 4.18 Damaged check dams in the Jiuyuangou watershed.

	Structural damage				
Damaged quantity/a	Damaged dam body	Damaged spillway	Damaged drainage building	Damaged dam body and discharge structures simultaneously	Damaged dam body and spillway simultaneously
Key check dam	2	2	1	0	0
Medium check dam	16	1	1	4	1

Table 4.19 Check dams damaged in the July 26 rainstorm.

	Normal	Damaged	Dam break by July 26	Dam break before July 26	Total
Number	90	23	52	13	178
Proportion /%	50.6	12.9	29.2	7.3	100.0

Table 4.20 The damage to different types of check dams.

Type	Normal	Damaged	Dam break	Total
Dam body (no)	32	8	57	97
Dam body + Flood spillway	29	11	3	43
Dam body + Drainage tunnel	24	3	3	30
Dam body + Flood spillway + Drainage tunnel	5	1	2	8
Total	90	23	65	178

Table 4.21 Damaged check dams with different sedimentation heights.

Distance from dam land surface to top of dam body	Number				Proportion		
	Normal	Damaged	Dam break	Total	Normal	Damaged	Dam break
<1 m	25	7	23	55	45.5	12.7	41.8
1–2 m	13	5	14	32	40.6	15.6	43.8
2–6 m	22	8	23	53	41.5	15.1	43.4
>6 m	30	3	5	38	78.9	7.9	13.2
Total	90	23	65	178	50.6	12.9	36.5

The sedimentation of the check dam had a relatively large impact on the flood discharge capacity. During the heavy rain, 79% of check dams with a distance of more than 6 m from the warping surface to the dam crest were in good condition and 13% of them were broken (Table 4.21). Thus, its flood resistance is better than other types of check dams.

4.6. SAND BLOCKING EFFECT OF CHECK DAMS IN THE TYPICAL RAINSTORM OF SUIDE COUNTY ON JULY 15 IN 2012

4.6.1. Rainstorm Flood in Suide on July 15

Beginning at 0:00 on 15 July 2012, continuous heavy rainfall occurred in the northeastern region of Suide County. The rainfall lasted for 2 hours and 45 minutes. The precipitation in six towns reached torrential or heavy rain. The hydrometeorological data statistics of Suide County Meteorological Bureau and Flood Control and Drought Relief Center on that day show that the rainfall in Yihe Town of Suide County was 100.5 mm and in Mantangchuan Town was 111.2 mm. The rainstorm center appeared at the rainfall station in Yanjiagou Village, Mantangchuan Town (adjacent to Jiuyuangou) and the precipitation was 111.2 mm.

According to the measured data from nine rainfall stations in the Jiuyuangou basin from the Suide Soil and Water Conservation Station of the Yellow River Water Resources Commission of the Ministry of Water Resources, the maximum precipitation in the Jiuyuangou basin was 98.4 mm. The rainfall in

@seismicisolation

Wangjiawa lasted for 2 hours and 10 minutes and the precipitation was 27.6 mm. The rainfall in Heijiawa lasted for 3 hours and 35 minutes and the precipitation was 62.2 mm. The maximum rainfall intensity occurred in the Wangmaogou basin, with a maximum precipitation of 75.7 mm in one hour. The rainfall was intense, strong, and short in duration. The heavy rainfall caused disasters such as mountain torrents, mudslides, and hail in some areas. The check dams and supporting engineering in the Jiuyuangou basin, such as flood drains, reservoirs, and artesian irrigation canals, were damaged to varying degrees during the heavy rains.

4.6.2. Sediment Retention Analysis of Check Dams During the Rainstorm in Jiuyuangou Basin on July 15

After the flood on July 15, field investigations were conducted on the flow and sediment of the check dams in the Wangmaogou small basin dam system. According to the water depth of the dam break and the thickness of sedimentation at the maximum flood level before the dam break of each dam, the total amount of flood in the dam before the dam break of each dam and the sedimentation amount in the dam after the retreat were calculated, as shown in Tables 4.22–4.24.

The results show that all the check dams controlled by Wangmaogou dam No. 2 and above were damaged by water except for the Sidizui, but all the discharge floods and sediments were blocked by Wangmaogou dam No. 2, including the upstream discharge flood of 159 405 m^3 (which only refers to the flood volume before the dam break and excludes the flood discharged from the Wangmaogou dam No. 2 through the drainage facility during rainfall), the sediment of 61 180 m^3. The sedimentation amount per unit area was 14 000 m^3/hm^2, which is 4.5 times the average sedimentation of upstream dams; therefore, almost 80% of the upstream erosion sediment was controlled by the key dam. Wangmaogou dam No. 1 retained 77 442 m^3 of flood and 15 268 m^3 of sediment. The sediment retained per unit area was 1800 m^3/hm^2.

In the entire Jiuyuangou small basin dam system, except for the Wangmaogou dam system which was seriously damaged by the rainstorm, there was no serious water damage. From the results of flood and sedimentation of dams, it was found that the entire small basin had retained a total of 2523 175 m^3 of floodwater and 455 163 m^3 of sediment, which is much smaller than the remaining storage capacity of the dam system in the entire basin and thus does not pose a serious threat to the dam system.

4.6.3 Sedimentation Characteristics of Dams During the Rainstorm Flood

According to the investigations, in the heavy rainstorm in Suide on 15 July 15 2012, the maximum water depth of Wangmaogou dam No. 2 was approximately 6 m, and the sedimentation was approximately 2 m. The flood discharge capacity of the shaft was very poor and could not meet the needs of the check dam. The sediment with a depth of 2 m was collected at different locations in layers to examine the sorting effect of the check dam on the sediment and the sedimentation law under the single rainstorm flood.

The results from the calculated fractal dimension, in the horizontal direction (Figure 4.23), revealed the fractal dimension in front of the dam > fractal dimension in the dam > fractal dimension after the dam. The soil fractal dimension in the dam gradually increased from upstream to downstream, the content of clay and powder particles increased, and the content of sand particles decreased. Thus, under the rainstorm flood, when the slope runoff reached the check dam, the sediment carried by the runoff was deposited during the movement. Under the dual action of the sand-carrying force and gravity, the coarse particles moved shortly and were deposited first and the fine particles were gradually deposited as the water flowed downstream along the channel, showing a finer and finer process from upstream to downstream and the horizontal displacement of sediment in the dam. As the control area of Wangmaogou dam No. 2 is relatively large and the distance between the front and rear of the channel is relatively long, the law of sedimentation and sorting in the check dam is particularly apparent.

In the vertical direction, as runoff was blocked by the check dam, it stopped moving. The sediment carried in the runoff was continuously deposited under the action of gravity, coarse particles were deposited first, then fine particles. From top to bottom, the sediment grew coarser, forming a sedimentation sequence dominated by sand particles–powder particles–clay particles. Figure 4.24 shows that the soil fractal dimension of Wangmaogou dam No. 2 shows a wave-shaped change with an increase of soil depth. The fractal dimension changes drastically in the range of 0–60 cm, showing an evident decreasing law. The change was relatively stable, within 60–200 cm, showing a slight wave shape. After the sediment carried by the single rainstorm runoff reached the check dam, under the influence of comprehensive factors such as topography, gravity, and sediment carrying capacity, a unique distribution pattern of sediment in the check

@seismicisolation

Table 4.22 Sediment storage in the July 15 flood in the Wangmaogou mall watershed (dam 1).

Check dam	Type	Inter-basin area/km^2	Area between dams/km^2	Sedimentation area/hm^2	Total capacity/10^4 m^3	Sedimentation capacity/10^4 m^3	Remaining storage capacity/10^4 m^3	Depth of flood/m	Flood discharge/m^3	Sediment thickness/cm	Sediment amount/t	Sediment amount per unit area/(m^3 hm^{-2})
Hejiamao Dam	Small	0.082	0.082	0.37	0.7	0.7	0	1.3	4810	8	296	800
Madizui Dam	Medium	0.605	0.257	1.45	12	12	6.5	1.35	19 575	46	6670	4600
Sidizui No. 1	Medium	0.512	0.37	2.65	24.6	24.6	6.4	1.14	30 210	48	12 720	4800
Sidizui No. 2	Small	0.142	0.142	0.41	1.2	1.2	0	0.9	3690	5	205	500
Wangtagou No. 1	Small	0.05	0.05	0.63	2	2	0	1.2	7560	42	2646	4200
Wangtagou No. 2	Small	0.298	0.298	0.97	0.3	0.3	0	1.26	12 222	6	582	600
Guandigou No. 1	Medium	1.302	0.223	2.54	40.3	19.2	21.1	1.52	38 608	42	10 668	4200
Guandigou No. 2	Small	0.12	0.12	0.43	1.4	1.4	0	1.75	7525	45	1935	4500
Guandigou No. 3	Small	0.204	0.204	0.75	1.4	1.4	0	1.42	10 650	56	4200	5600
Beitagou Dam	Small	0.186	0.186	0.75	3.2	3.2	0	1.26	9450	15	1125	1500
Guandigou No. 4	Medium	0.41	0.41	1.59	13.6	6.5	7.1	0.95	15 105	12	1908	1200
Total		3.911	2.342	12.54	100.7	72.5	41.1		159 405		42 955	
Wangmaogou No. 2	Diaphysis	3.184	0.683	4.37	105.4	41.2	64.2	2.33	101 821	140	61 180	14 000

@seismicisolation
@seismicisolation

Table 4.23 Sediment storage in the July 15 flood of the Wangmaogou system unit (Wangmaogou dam no. 2).

Check dam	Type	Inter-basin area/km^2	Area between dams/km^2	Sedimentation area/hm^2	Total capacity/10^4 m^3	Sediment modulus/(m^3 hm^{-2})	Remaining storage capacity/10^4 m^3	Depth of flood/m	Flood discharge/m^3	Sediment thickness/cm	Sediment amount/t	Sediment amount/(m^3 hm^{-2})
Huangbaigou No. 1	Small	0.188	0.188	0.39	1.4	1.4	0	1.05	4095	18	702	1800
Huangbaigou No. 2	Small	0.156	0.156	0.4	10.3	8	2.3	1.22	4880	46	1840	4600
Nianyangou No. 1	Medium	0.897	0.036	1.2	12.8	8.2	4.6	1.02	12,240	34	4080	3400
Nianyangou No. 2	Small	0.243	0.243	1.65	7.3	7.3	0	0.9	14850	13	2145	1300
Nianyangou No. 3	Small	0.227	0.227	0.89	4.2	4.2	0	1.2	10680	4	356	400
Nianyangou No. 4	Small	0.232	0.232	0.51	2.4	2.4	0	1.03	5253	31	1581	3100
Kanghegou No. 1	Small	0.058	0.058	0.47	2.9	2.9	0	1.55	7285	20	940	2000
Kanghegou No. 2	Medium	0.303	0.056	0.87	11.5	4.5	7	1.45	12615	32	2784	3200
Kanghegou No. 3	Small	0.347	0.247	0.42	2.5	2.5	0	1.32	5544	20	840	2000
Total		2.651	1.443	6.8	55.3	41.4	13.9	10.74	77,442		15268	2245
Wangmaogou No. 1	Diaphysis	2.6121	1.169	4.76	50.1	38.1	12	1.85	80,845	18	8568	1800

@seismicisolation

Table 4.24 Sediment retention in each dam system unit in the July 15 flood in the Jiuyuangou watershed.

Check dam	Inter-basin area/km^2	Area between dams/km^2	Total capacity/ 10^4 m^3	Sediment action capacity/10^4 m^3	Remaining storage capacity/10^4 m^3	Sedimentation area/hm^2	Depth of flood/m	Flood discharge/ m^3	Sediment thickness/cm	Sediment amount /10^4 m^3
Main ditch dam system	20.37	18.6	1093.89	519.43	469	88.54	0.78	690612	10	88540
Wangjiagou	4.28	3.49	83.8	23.02	50.78	6.93	0.85	58905	15	10395
Majiagou	4.37	3.05	58.99	24.5	4.49	5.86	0.66	38676	12	7032
Shuiyangou	2.18	1.12	35.38	16.9	18.48	3.64	0.72	26208	12	4368
Xiaqiaogou	2.6	1.62	38	31.2	6.8	4.81	0.66	31746	10	4810
Maliangou	3.58	2.71	194.8	120.4	74.4	15.23	0.65	98995	9	13707
Hejiagou	2.97	1.83	67.9	26.2	41.7	6.16	0.9	55440	11	6776
Xiangtagou	3.23	1.92	89.83	69.8	20.03	6.25	0.64	40000	9	5625
Gaoshegou	7	4.39	324.56	209.2	115.36	22.3	0.72	160560	10	22300
Xiyanguo	13.1	6.4	147.58	125.9	121.68	16.41	0.81	132921	8	13128
Zhejiagou	2.12	1.63	93.6	63.8	29.8	9.06	0.95	86070	16	14496
Lijiazhai	10.45	6.42	285.4	165.7	119.7	23.62	1.05	248010	19	44878
Wangmaogou	5.8	5.8	328.6	197.4	131.2	36.6	1.25	457500	34	124440
Linjian	21.65	12.91	631.66	413.6	218.06	44.36	0.67	297212	18	79848
Liushugou	5.72	3.08	301.7	139.3	162	11.4	0.88	100320	13	14820
Total	109.41	74.97	3775.69	2146.35	1578.99	293.86		2523175		455163

@seismicisolation
@seismicisolation

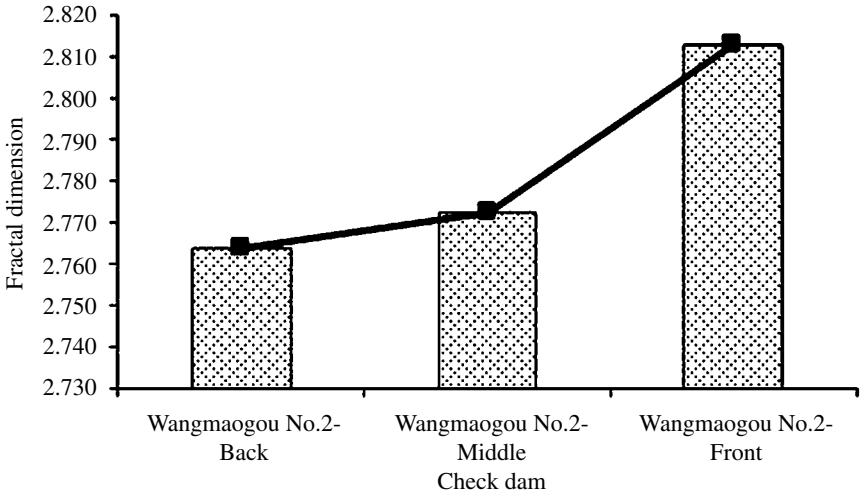

Figure 4.23 The fractal dimension at different positions of the Wangmaogou dam no. 2 on farmland.

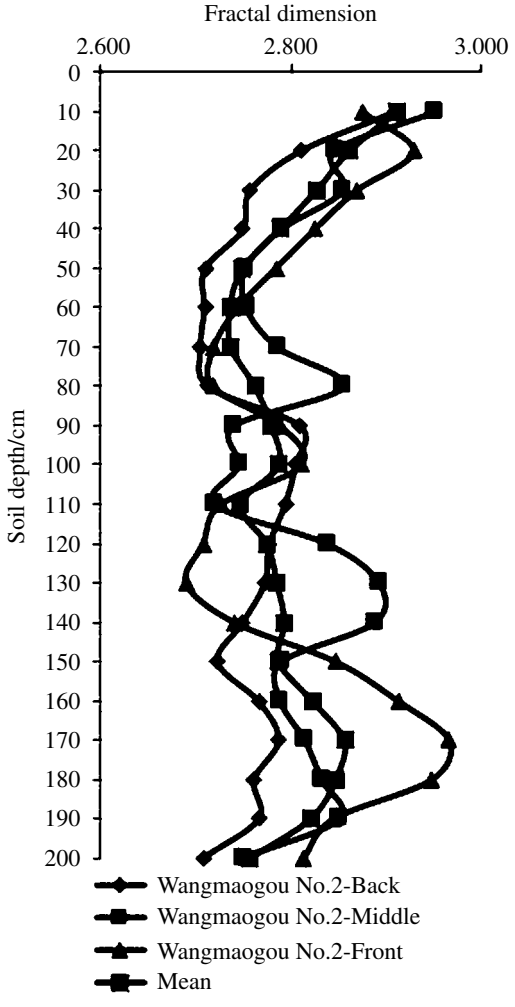

Figure 4.24 Vertical change of fractal dimension of the Wangmaogou dam no. 2 on farmland.

dam was formed in the horizontal and vertical directions. This pattern reflects the erosion sediment and changes in the erosion environment in the small basin of the control area. There is also a large amount of information stored in the erosion changes and erosion environmental changes in the small basin. Therefore, the changes in various physicochemical properties of the sediment deposited in this rainstorm are a direct manifestation of the stored information.

4.7 CONCLUSION

The sediment was mainly the result of a few heavy rainfall events each year. Eroded sediment from gullies was the main source of sediment in the Yuanzigou watershed (71.4%) and Zhaizimao watershed (53.60%). About 69% of the sediment in the Nianyangou basin came from slope farmland. The mean contributions of intergully and gully lands to the sediment deposited in dammed farmland in Huangfuchuan River Basin are 29.7 and 70.2%, respectively. The mean contributions of intergully and gully lands to the sediment deposited in dammed farmland in the Wuding River Basin are similar, each accounting for 50%. The mean contributions of intergully and gully lands to the sediment deposited in dammed farmland in the Yanhe River Basin were 38.3 and 61.7%, respectively. Under severe rainstorms or extreme rainstorms, soil erosion in the Loess Plateau is still severe. Check dam construction played an important role in peak reduction and flood detention during the heavy rain on July 26. The check dams with drainage and water discharge buildings

@seismicisolation

had fewer dam breaks and many of them were in good condition. Most upstream erosion sediment was controlled by the key dam during the rainstorm flood.

REFERENCES

1. Fu, B., Wang, S., Liu, Y. et al. (2017). Hydrogeomorphic ecosystem responses to natural and anthropogenic changes in the Loess Plateau of China. *Earth and Planetary Sciences 1*: 223–243.
2. Peng, J., Chen, S., and Dong, P. (2010). Temporal variation of sediment load in the Yellow River basin, China, and its impacts on the lower reaches and the river delta. *Catena 83*: 135–147.
3. Zhang, X.J. and Liu, B.L. (2016). Using multiple composite fingerprints to quantify fine sediment source contributions: a new direction. *Geoderma 268*: 108–118.
4. Zhao, T.Y., Yang, M.Y., Walling, D.E. et al. (2017b). Using check dam deposits to investigate recent changes in sediment yield in the Loess Plateau, China. *Global and Planetary Change 152*: 88–98.
5. Xue, K. (2011). Sediment source changes in a small watershed on the Loess Plateau. *Northwest A&F University*. (in Chinese).
6. Ni, S.X. (1992). Erosion and its harness of the pisha rock hilly region in the Shaanxi-Shanxi-inner-Mongolia border region. *Journal of Nanjing University (Natural Science) 1992* (03): 459–466. (in Chinese).
7. Li, S.L., Su, C.J., Bai, L.C. et al. (1995). ^{226}Ra analysis method of sediment source composition in a small basin. *Mountain Research 13*: 199–202. (in Chinese).
8. Tian, P., An, Z., Zhao, G. et al. (2019). Assessing sediment yield and sources using fingerprinting method in a representative catchment of the Loess Plateau, China. *Environmental Earth Sciences 78*: 261.
9. Zhao, G., Mu, X., Han, M. et al. (2017a). Sediment yield and sources in dam-controlled watersheds on the northern Loess Plateau. *Catena 149*: 110–119.
10. Zhao, G., Klik, A., Mu, X. et al. (2015). Sediment yield estimation in a small watershed on the northern Loess Plateau, China. *Geomorphology 241*: 343–352.
11. Fan, L.J. (2013). Sediment yield intensity and sediment source in a small check dam controlled watershed of Huangfuchuan. Thesis for Master's Degree. *Northwest A&F University*. (in Chinese).
12. Mi, Z.J. (2014). Sediment source and sediment yield intensity in check dam controlled watershed of loess plateau. Thesis for Master's Degree. *Northwest A&F University*. (in Chinese).
13. An, Z.F. (2017). Sources and simulation of erosion sediment yield in a small watershed of more sediment and coarse sediment region. Thesis for Master's Degree. *Northwest A&F University*. (in Chinese).
14. Zhang, P.C., Tang, K.L., and Zheng, F.L. (1990). The source and quantitative analysis of sediment of the Huangfu River watershed. *Journal of Soil and Water Conservation 4*: 29–36. (in Chinese).
15. Wang, X. (2001). Study of sediment source calculation in small watershed in pisha rock area through grain size analyze method. *Soil and Water Conservation in China 1*: 25–27. +48. (in Chinese).
16. Gong, S.C. and Jiang, D.Q. (1978). Soil and water loss and its control in small watershed of loess hilly and gully region in middle Yellow River. *China science 6*: 671–678. +707. (in Chinese).
17. Xu, X.L. (1987). A study on incoming water and sediment amounts in gully land and valley land in Jiuyuangou Watershed. *Soil and Water Conservation in China 8*: 25–28. (in Chinese).
18. Zhang, F.B., Xue, K., Yang, M.Y., and Shen, Z.Z. (2012). Variations of sediment nutrient in check dam and its implication for small catchment sediment resources. *Transactions of the Chinese Society of Agricultural Engineering 28*: 143–149. (in Chinese).
19. Chen, F.X., Zhang, F., Fang, N., and Shi, Z. (2016). Sediment source analysis using the fingerprinting method in a small catchment of the Loess Plateau, China. *Journal of Soils and Sediments 5*: 1655–1669.
20. Chen, F.X., Fang, N.F., Wang, Y.X. et al. (2017). Biomarkers in sedimentary sequences: indicators to track sediment sources over decadal timescales. *Geomorphology 278*: 1–11.
21. Jiang, D.L., Zhao, C.X., and Chen, Z.L. (1966). Analysis on the source of runoff and sediment in the small watershed in the Middle Reaches of the Yellow River. *Acta Geographica Sinica 1*: 20–36.
22. Li, M., Yang, J.F., Hou, J.C., and Shen, Z.Y. (2008). Sediment deposition process for a silt dam in a small watershed in Loess Hilly Region. *Transactions of the Chinese Society of Agricultural Engineering 2*: 64–69. (in Chinese).
23. Zhang, X.B. and Wen, A.B. (1999). Study on Cesium-137 tracer of erosion sediment in Loess Plateau. *Management of Ecological Environment in the Loess Plateau of China – Proceedings of CCAST (World Laboratory) Workshop*, 6: 123–138.
24. Li, P., Xu, G., Lu, K. et al. (2019). Runoff change and sediment source during rainstorms in an ecologically constructed watershed on the Loess Plateau, China. *Science of The Total Environment 664*: 968–974.
25. Chen, H. (1999). Sediment source on small basin in middle reaches of Yellow River. *Journal of Soil Erosion and Soil and Water Conservation 01*: 20–27. (in Chinese).
26. Bai, L.L. (2019). Sediment source analysis and comprehensive evaluation of models in typical dam control basin of Loess Plateau. Thesis for Master's Degree. *Xi'an University of Technology*. (in Chinese).

@seismicisolation

27. Hou, J.C. (2007). Study on the characteristics of soil erosion, sediment yield in small watershed in Loess Plateau hilly, gully area by using tracers. Thesis for Master's Degree. *Xi'an University of Technology*. (in Chinese).
28. Chen, F.X. (2017). Using biomarkers and the composite fingerprinting method to identify sediment sources in small catchments. Thesis for Master's Degree. *Huazhong Agricultural University*. (in Chinese).
29. Zhang, Y. (2018). The influence of water erosion on migration-deposition process of soil organic carbon under ecological construction. Thesis for Master's Degree. *Xi'an University of Technology*. (in Chinese).
30. Chen, F.X., Fang, N., and Shi, Z. (2016). Using biomarkers as fingerprint properties to identify sediment sources in a small catchment. *Science of the Total Environment 557*: 123–133.
31. Zhang, J., Yang, M., Zhang, F. et al. (2017). Fingerprinting sediment sources after an extreme rainstorm event in a small catchment on the Loess Plateau, PR China. *Land Degradation & Development 28*: 2527–2539.
32. Wen, A.B., Zhang, X.B., and Walling, D.E. (1998). A study on soil erosion rates and sediment sources using ^{137}Cs technique in a small drainage of the loess hills. *ACTA Geographica Sinica S1*: 124–133. (in Chinese).
33. Yang, M.Y., Tian, J.L., and Liu, P.L. (1999). Studying sediment sources in small watershed Using ^{137}Cs tracing. *Journal of Soil Erosion and Soil and Water Conservation 3*: 49–53. (in Chinese).
34. Zhang, W. (2015). The historical variation of soil erosion in a small watershed from past 40 years of using sediment couplets in a check dam in Loess Hilly area. *Northwest A&F University*. (in Chinese).
35. Xu, J.L. (2008). Study on the composite Fingerprinting flood suspended sediment sources in the catchment on the Loess Plateau. *Institute of Soli and Water Conservation, Northwest A&F University*.
36. Yang, M.Y. and Xu, L.J. (2010). Fingerprinting suspended sediment sources in a small catchment on the Loess Plateau. *Journal of Soil and Water Conservation 24*: 30–34. (in Chinese).
37. Wang, W., Fang, N., Shi, Z., and Lu, X. (2018). Prevalent sediment source shift after revegetation in the Loess Plateau of China: implications from sediment fingerprinting in a small catchment. *Land Degradation & Development 29*: 3963–3973.
38. Feng, M.Y., Walling, D.E., Zhang, X.B., and Wen, A.N. (2003). ^{137}Cs method for response of erosion and sediment yield in small watershed in loess hilly region to slope farmland conversion. *Chinese Science Bulletin 13*: 1452–1457. (in Chinese).
39. Yang, M.Y. (2001). Quantitative study of slope erosion process with multi-nuclides composite tracer. *Northwest A&F University*. (in Chinese).
40. Wang, W.T. (2019). Research on sediment source and particle size distribution in small catchments on the Loess Plateau. *Northwest A&F University*. (in Chinese).
41. Chen, F.X., Zhang, H.Y., Fang, N.F., and Shi, Z.H. (2016). Using two kinds of fingerprint factors to identify sediment sources in a small catchment. *Advances in Water Science 27*: 867–875. (in Chinese).
42. Liu, C., Li, Z., Chang, X. et al. (2018). Apportioning source of erosion-induced organic matter in the hilly-gully region of loess plateau in China: insight from lipid biomarker and isotopic signature analysis. *Science of the Total Environment 621*: 1310–1319.
43. Wei, T.X. (2002). Sediment sources and effects of vegetation on erosion control in the gully-hilly loess area in north China. *Journal of Beijing Forestry University Z1*: 19–24. (in Chinese).
44. Liu, H.F., Wei, T.X., Zhu, Q.K., and Yao, A.J. (2004). Sediment sources in small watersheds in western Shanxi province of the Loess Plateau. *Bulletin of Soil and Water Conservation 4*: 19–22. (in Chinese).
45. Qin, W., Zhu, Q.K., and Zhang, Y. (2009). Soil erosion assessment of small watershed in Loess Plateau based on GIS and RUSLE. *Transactions of the CSAE 25*: 157–163. +4. (in Chinese).
46. Wang, Y.J. (2017). Study on the pattern variation of soil erosion using sediment deposition behind a check dam in a small catchment of the wind-water erosion crisscross region of Chinese Loess Plateau. Thesis for Master's Degree. *Northwest A&F University*. (in Chinese).
47. Li, M., Yao, W., Shen, Z. et al. (2016). Erosion rates of different land uses and sediment sources in a watershed using the ^{137}Cs tracing method: field studies in the Loess Plateau of China. *Environmental Earth Sciences 75*: 591.
48. Kuhn, N.J., Hoffmann, T., Schwanghart, W., and Dotterweich, M. (2009). Agricultural soil erosion and global carbon cycle: controversy over? *Earth Surface Processes and Landforms 34*: 1033–1038.

@seismicisolation

5

The Regulation of Check Dam System in Erosion Dynamic Process

Tian Wang[1], Jingming Hou[1], Shuilong Yuan[1], Guoce Xu[1], Zhanbin Li[1], Dejun Wang[2], Jingmei Sun[2], Zhiqiang Min[2], Zhi Yang[3], and Zhengyan Ren[3]

5.1. INTRODUCTION

Check dams are structures commonly built for the purposes of stabilizing channels and controlling erosion in catchments [1–4]. They also influence water balance by altering the main hydrological components of a channel [1]. Check dams are constructed across a flow channel to prevent soil and water loss [5]. These structures are especially widespread throughout China [6–8], the US [9], Ethiopia [1, 10], Iran [1, 11], Italy [12, 13] and Spain [14, 15].

A growing number of scholars around the world are studying the influence of check dams on geomorphological and hydrological processes. In previous research, check dams have been shown to induce important morphological and granulometric effects in riverbeds [16], which can change the hydraulic behavior of a flow during an extreme event [17]. In fact, in one case, sediment that had accumulated raised a riverbed near a check dam, which reduced the risk of a bank collapse [18]. Bombino et al. [12] determined that the construction of check dams in the Calabrian headwater torrents greatly influences the channel shape, the sediment caliber, and the vegetation development. Their results showed the reduction of the energy gradients upstream of check dams due to the increased water retention and the accumulated sediment. In a hydrological simulation, Boix-Fayos et al. [14] applied the WaTEM/SEDEM erosion model to a region in Southeast Spain and found that about 77% of the sediment yield was retained in catchments with check dams, and land use changes did not affect it. In addition, Martín-Rosales et al. [19] used a model to estimate the groundwater recharge that check dams and gravel pits induce in a semiarid area in southeastern Spain. They found that the proportion of the check dam-infiltrated runoff varied from 3% to more than 50%. More recently, Nyssen et al. [20] investigated the hydrological response of a 200-ha catchment with check dams in North Ethiopia over the span of a year and concluded that this type of catchment management leads to a higher infiltration rate and an 81% reduction in the direct runoff volume, which positively influences the catchment water balance. In addition, gully management with check dams resulted in a significant reduction in both the runoff volume and the peak flow due to increased infiltration, groundwater recharge, and an improved base flow to streams and reservoirs during the dry season [1].

Global soil erosion severely affects the Loess Plateau in China [4, 21, 22], which has faced hundreds of years of check dam construction to prevent soil and water losses. This construction trend accelerated in the 1970s. Check dams resist the movement of floodwater and

[1] *Institute of Water Resources and Hydro-electric Engineering, Xi'an University of Technology, Xi'an, China*
[2] *Northwest Institute of Forest Inventory, Planning and Design, National Forestry and Grassland Administration, Xi'an, China*
[3] *Soil and Water Conservation Bureau of Ningxia Water Conservancy,, Yinchuan, China*

Check Dam Construction for Sustainable Watershed Management and Planning, First Edition.
Edited by Zhanbin Li, Peng Li, Yang Yu, Peng Shi, and Guillaume Piton.
© 2022 John Wiley & Sons, Inc. Published 2022 by John Wiley & Sons, Inc.

@seismicisolation

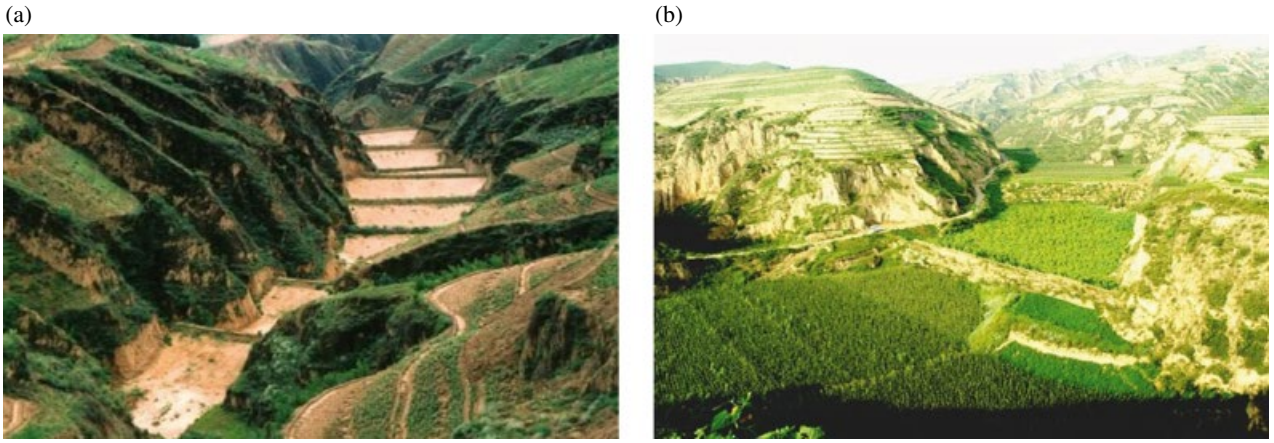

Figure 5.1 Water body storage (a) and formed check dam farmland (b) in front of check dams.

sediment, which enables water storage (Figure 5.1a) and sediment deposition. As time passes, water infiltrates, discharges, and evaporates, and the sediment fills the area in front of the check dam. After several rainfall events, the sedimentation process accumulates and may turn into check dam farmland (Figure 5.1b), which is one of the most cultivated field types in this high-production region [6, 23, 24]. By 2013, 58 446 active check dams could be found on the Loess Plateau, providing more than 10 000 m^3 of reservoir storage [25]. Several researchers in China have also reported that check dams greatly affect water and sediment transport along the gully and stream channels [26]. They generally use field measurements and mathematical models to understand the effect of check dam systems on sediment dynamics on the Loess Plateau [24, 27]. Wei et al. [27] investigated sediment accumulation by drilling 10-hole sedimentation cores combined with flood couplets. Li et al. [28] assessed check dam deposits and identified correlations between sediment layers and storm events using optimal regression models based on the peak fallout of ^{137}Cs (radioactive element). Li et al. [29] and Zhao et al. [23] also applied this method. Some studies have furthermore investigated the runoff response to the check dams. For example, Xu et al. [3] applied the Soil and Water Assessment Tool, or SWAT, model to evaluate the effect of check dams on the annual runoff and sediment transport in the Yanhe Watershed. They found that the annual runoff was reduced by less than 14.3% and that up to 85.5% of the rainy season sediment was blocked. Huang et al. [30] evaluated the effects of check dam systems on water redistribution in a small basin on the Chinese Loess Plateau using a numerical method to calculate the water volume in the year of 2006. Their results showed that the check dam system can significantly reduce surface runoff by 60%. The results also showed that the water budget of the surface runoff and groundwater inflow without the check dams was 97.3 and 2.7%, respectively, and that the water budget of the runoff, evapotranspiration, infiltration and change in the water storage was 39.1, 49.3, 11.6 and 0%, respectively, in systems with check dams.

Despite several investigations on the effects of check dams on runoff and sediment transport, the underlying hydrological processes are poorly understood and have not been systematically analyzed in the Loess Plateau. One crucial objective of a check dam system is to prevent a flood from becoming a disaster [31]. However, the few studies that have considered flood characteristics were mostly based on single rainstorm events. For example, Yuan et al. [32] applied a MIKE model (DHI) to simulate floods for a rainstorm event and found that the flood peak and flood volume were reduced by 65.3 and 58.7%, respectively, with a check dam system.

Currently, flood assessment studies do not focus on hydrological connectivity in check dam catchments. Furthermore, previous research has not yet quantified the effects of a check dam system on the flood lag time, runoff characteristics, and peak location. Therefore, assessing the impacts of check dams is of the highest importance in areas such as the Loess Plateau, and adding the quantification of the real flood characteristics can significantly improve the accuracy of the models and their predictions. With the aim of investigating and predicting how a check dam system affects the flood characteristics and processes in our study catchment, meteorological and hydrological

@seismicisolation

observations were collected for the Wangmaogou catchment. The efficient and robust graphic processing unit (GPU) accelerated surface water and transport (GAST) model, a numerical model that uses the available topography and subsurface conditions as major inputs [33], was applied for various rainfall events. For the purpose of evaluating how check dams impact runoff levels in channels, the flood response was evaluated in the case of the presence or absence of check dams. Furthermore, the relationship between longitudinal channel connectivity and flood characteristics was investigated using three hypothetical scenarios based on the number of check dams in a channel.

The slope and gully together form the gully slope system of the Loess Plateau. The complex processes of erosion and the siltation of sediment in the watershed take place in the gully system, and it is finally transported to the outlet of the watershed [34]. Wang et al. [7] divided the watershed into two systems – a slope and gully – and studied the laws of runoff and sediment movement in the two systems, respectively. They also analyzed the main mechanisms of slope erosion and sediment yield, gully slope gravity erosion, and gully runoff and sediment movement processes. The sedimentation process model was then established.

Liao et al. [35] extracted the gullies of different spatial scales of watersheds, combined with years of water and sediment observation data. They then analyzed the effects of various levels of gullies and different parts of the gullies on the erosion and sediment yield of the watershed at different timescales. Afterward, they obtained the erosion yield. When the timescale of sand is different, various levels of ravines have different effects on erosion and sediment production. Because the runoff shear force will affect the erosion capacity and sediment transport capacity of the channel flow, the sediment incipient velocity, and other hydrodynamic parameters, this paper uses a hydrodynamic model to explore the impact of silt dams on channel runoff.

Huang and Yang [36] used many laboratory flume and natural river sediment transport data to study the correlation between various flow intensity indicators and sediment transport intensity. The results showed that the current power, average velocity, and sand shear stress can be used to better predict the sediment transport rate. Parameters such as the unit current power and the Froude number can be used to better predict the sediment transport concentration, and the relationship between the unit current power and sediment transport concentration is the best.

To sum up, the objectives of this study were (i) to quantify the time delays of runoff at the basin mouths of systems with and without check dams, (ii) to quantify the differences in the peak discharge rates and the catchment runoff volumes at the outlets of systems with and without check dams, (iii) to assess the effect of a check dam on the peak location and the corresponding discharge along the main channel, (iv) to analyze the relationship between channel connectivity and flood characteristics, and (v) to regulate a check dam system in the erosion dynamic process.

5.2. METHOD AND MATERIALS

5.2.1. Governing Equations and Numerical Schemes

Shallow water equations (SWEs) are obtained by assuming the hydrostatic pressure distribution and integrating the equations of the conservation of mass and momentum. In a vector form, the conservation law of the two-dimensional SWEs can be written as follows:

$$\frac{\partial \mathbf{q}}{\partial t}+\frac{\partial \mathbf{f}}{\partial x}+\frac{\partial \mathbf{g}}{\partial y}=\mathbf{S} \tag{5.1}$$

$$\mathbf{q}=\begin{bmatrix} h \\ q_x \\ q_y \end{bmatrix},\ \mathbf{f}=\begin{bmatrix} q_x \\ uq_x+gh^2/2 \\ uq_y \end{bmatrix},\mathbf{g}=\begin{bmatrix} q_y \\ vq_x \\ vq_y+gh^2/2 \end{bmatrix}, \tag{5.2}$$

$$\mathbf{S}=S_b+S_f=\begin{bmatrix} i \\ -gh\partial z_b/\partial x-C_f u\sqrt{u^2+v^2} \\ -gh\partial z_b/\partial y-C_f v\sqrt{u^2+v^2} \end{bmatrix}$$

where t represents the time; x and y are Cartesian coordinates; $\mathbf{q}$ denotes the vectors of the conserved flow variables consisting of h, q_x, and q_y (i.e. water depth, unit-width discharges in the x and y directions, respectively); $q_x = uh$ and $q_y = vh$, u and v are depth-averaged velocities in the x and y directions; $\mathbf{f}$ and $\mathbf{g}$ are the flux vectors in the x and y directions; $\mathbf{S}$ is the source vector that may be further subdivided into slope source terms S_b and friction source terms S_f; z_b represents the bed elevation; C_f is the bed friction coefficient that is generally computed by $gn^2/h^{1/3}$, with n being the Manning coefficient; and g indicates the gravity acceleration.

It should be noted that i is the net rainfall source equal to $i_r - i_i$, where i_r is the rainfall rate, whereas i_i is the infiltration rate. In this study, the infiltration process

@seismicisolation

was computed by using the Green–Ampt model as in Wang et al. [37], Ma et al. [38], and Cuomo et al. [39].

The numerical model for solving the SWEs is within the framework of an explicit Godunov-type cell-centered structured finite volume scheme. The fluxes of mass and momentum, the slope source terms, and the friction source terms were calculated as in Hou et al. [33]. The approach presented in Hou et al. [40] was adopted to handle the problem of numerical instability stemming from wetting and drying over a complex topography. In addition, the numerical model was programmed using C++ and CUDA, which considerably accelerated the computation via GPUs [41] to release the computational burden for practical large-scale applications with relatively high resolution.

5.2.2. Overflow Weir Treatment

Drainage building in a check dam is considered in the GAST model through the inner boundary shown in red in Figure 5.2. The green boundary controls the drainage building, with the boundary representing the weir in this model [42]. The cell upstream of the weir is set up as a reservoir area with the number "1" (Figure 5.2). The cell downstream of the weir is set up as the flood evolution area with the number "2" (Figure 5.2). Water depths in the cells with the number "1" are considered to be input parameters for the weir function, which can be written as follows:

$$Q = CBH^{1.5} \tag{5.3}$$

where Q is the discharge through the inner boundary on each cell, C is the comprehensive flow coefficient, B is the size of the cell, and H is the water head on the weir. In the same step, increased water volumes in the cells with the number "1" are equal to reduced water volumes in cells with the number "2," thus fulling the mass balance equation.

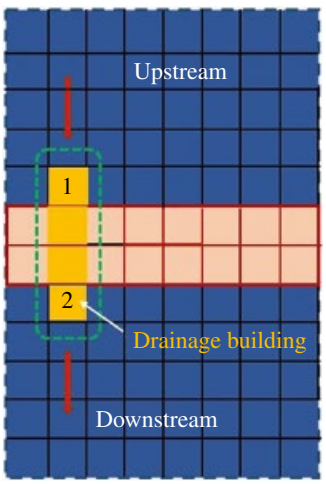

Figure 5.2 Internal boundary processing diagram.

5.2.3. Research Site and Data

The Wangmaogou catchment (110°20′26″–110°22′46″E, 37°34′13″–37°36′03″N) located in Suide County, Loess Plateau, China (Figure 5.3a and b), was chosen for this study. Here, check dams are used as a key part of the management strategy for conserving soil and water. This catchment has an area of 5.97 km^2 with a main channel length of 3.75 km and an altitude ranging from 934.55 m to 1187.75 m a.s.l. (Figure 5.3c). At the end of 2013, 17 normal check dams were in the Wangmaogou catchment, including 2 large check dams, 6 medium check dams, and 9 small check dams (Figure 5.3c). The local area is characterized by a semi-arid continental monsoon climate with an average annual precipitation of 513 mm and an average temperature of 10.2 °C. The precipitation falling between July and September generally accounts for more than 60% of the total annual precipitation. In addition, the hydrological station is located at the basin mouth.

The rainfall runoff processes were simulated using actual rain data, a digital elevation model (DEM) and land use/land cover data (LULC). A 2-m-resolution DEM for the catchment was derived from a 1:1000 scale contour map, and the domain was discretized into structured grids with 2826 630 cells. The LULC map (1:100 000) of 2010 (Figure 5.3d) was reclassified into seven categories: slope farmland, forest, grassland, transportation land, rural land, dam farmland, and terrace. A rain event characterized by 98.3 mm of precipitation within 2.5 hours and an induced runoff occurring from 0:25 am to 10:25 am of 15 July 2012 was chosen for the simulations (see Figure 5.6), without accounting for evaporation. The observed stream flow at the Wangmaogou catchment outlet was used for the model calibration and validation.

5.2.4. Scenarios Overview

For the purpose of investigating the influence of check dams on runoff characteristics, numerical calculations were performed for two scenarios: the present conditions with check dams (Scenario 1) and the original catchment without check dams (Scenario 2).

@seismicisolation

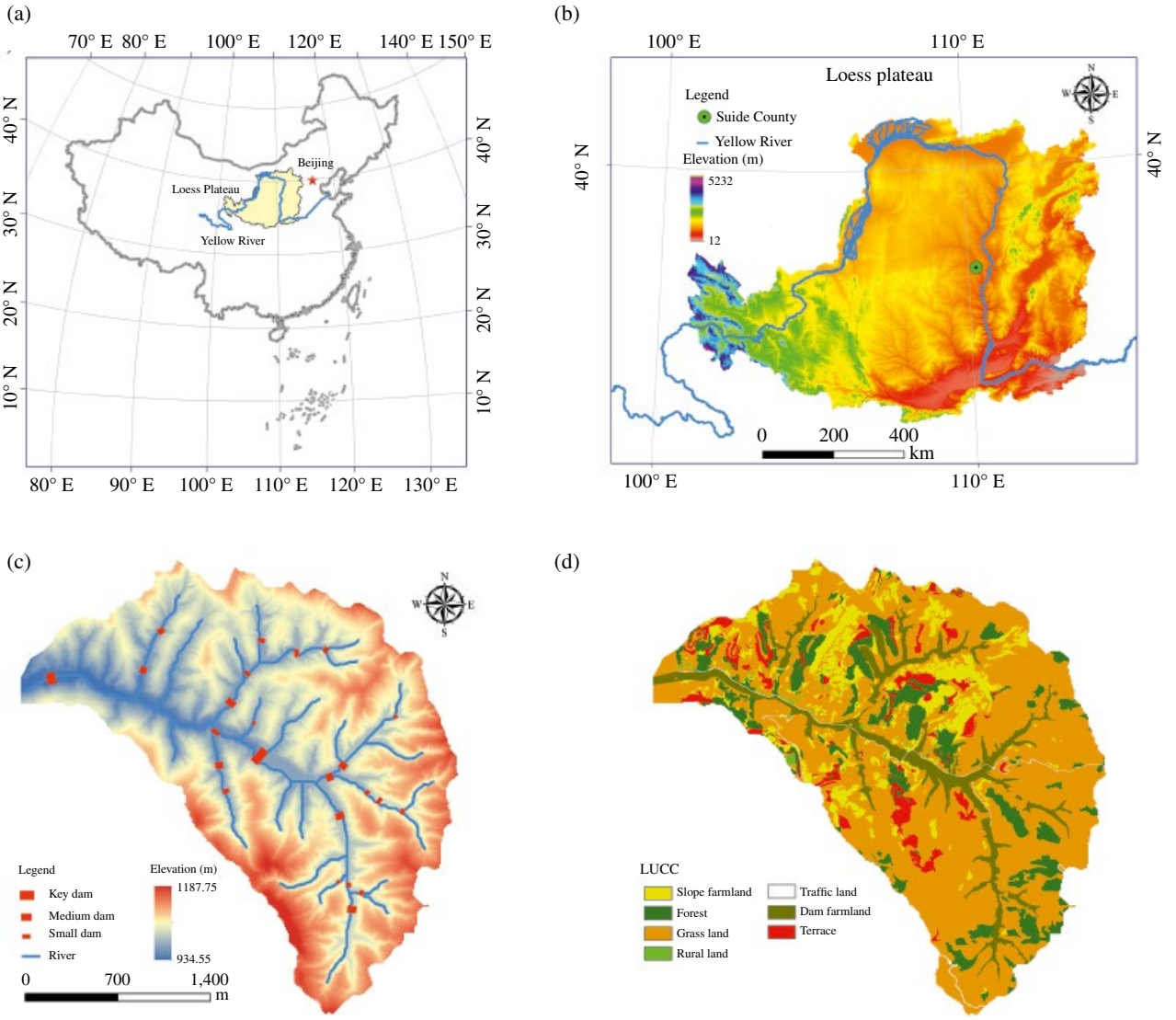

Figure 5.3 (a) Loess Plateau of China; (b) location of Wangmaogou catchment; (c) distribution and elevation of check dams; (d) distribution of the seven land use/cover types.

Original conditions without check dams were obtained by simulating the removal of check dams from the present topography. The average channel slope prior to the building of check dams across the whole domain was 2.7% [43]. Therefore, the channel elevation was corrected to this state. The removal of check dams and the correction of channel slopes were implemented using ArcGIS 10.1 software (Environmental Systems Research Institute Redlands, United states) (sample in Figure 5.4).

Furthermore, the longitudinal channel connectivity index (see Section 2.4.1) was considered to calculate the influence of the number of check dams on peak flows and discharge volumes in the catchment. For this reason, three more scenarios were designed. All five scenarios are reported in Figure 5.5.

5.2.5. Evaluation Metrics

5.2.5.1. Longitudinal Channel Connectivity

Longitudinal connectivity is defined in the context of the channel network and includes upstream–downstream and tributary–trunk stream relationships. Different sets of processes that are used at various positions in a catchment can control connectivity, meaning that fluxes may become connected (coupled) or

@seismicisolation

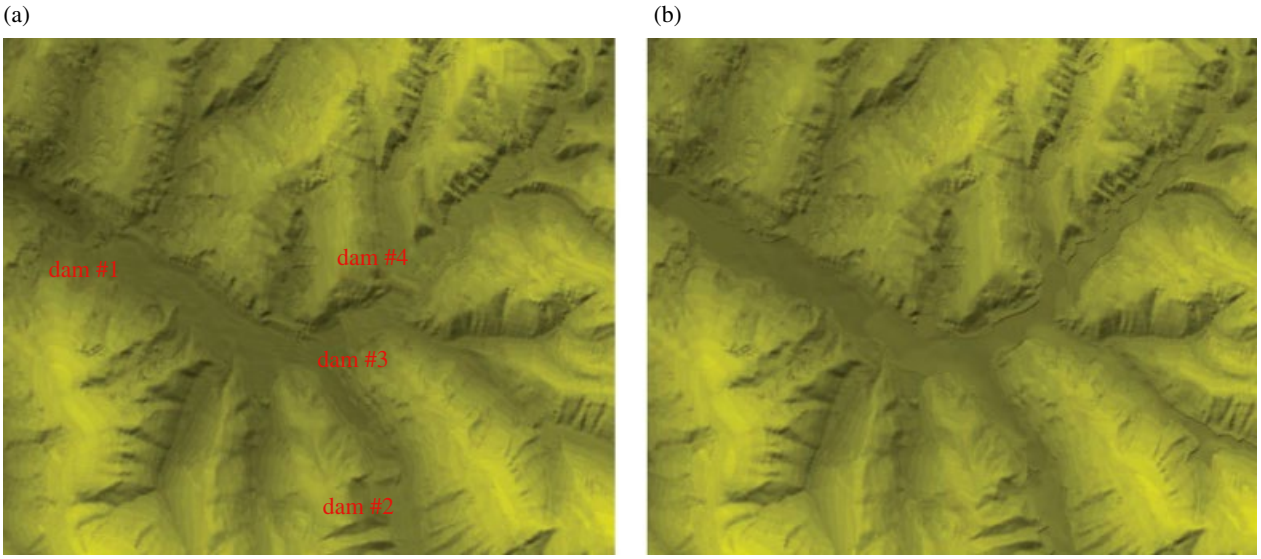

Figure 5.4 Comparison of partial terrain with check dam (a) and without check dam (b) in catchment.

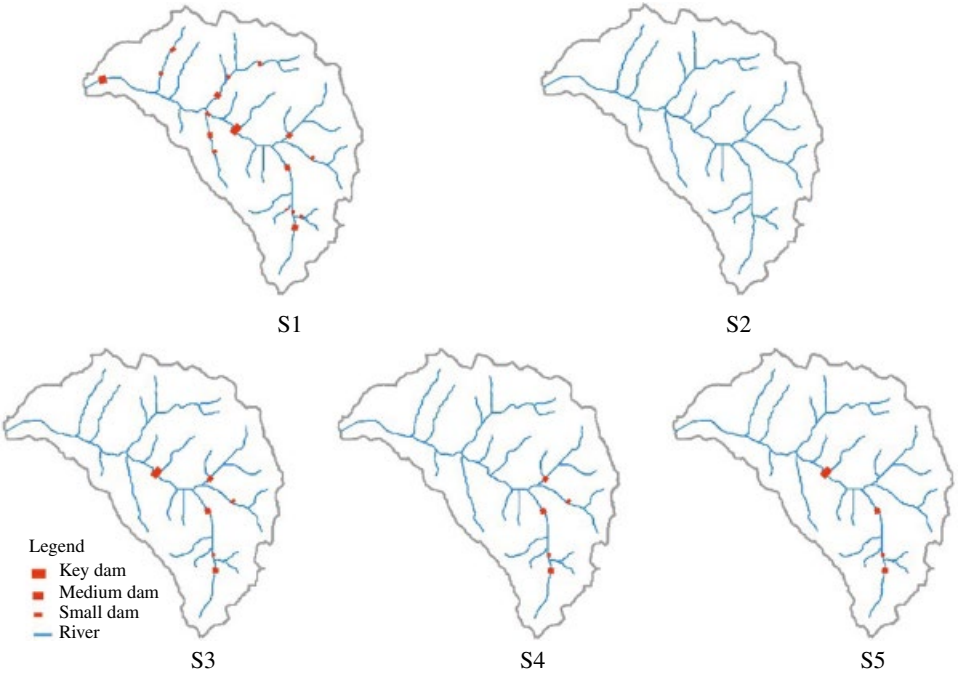

Figure 5.5 Five scenarios' designs in study catchment (S1: check dam system; S2: without check dam; S3: six check dams; S4: five check dams; S5: four check dams).

disconnected (decoupled) during different time frames [44, 45]. The longitudinal continuity index reflects the influence of obstacles, such as dams and gates, on river flow capacity, biological migration, and energy transfer processes. The longitudinal continuity index in a river is calculated using the following formula [46]:

$$C = L / (N + 1) \tag{5.4}$$

where C is the longitudinal channel connectivity, L is the total length of the channel, and N is the number of check dams.

@seismicisolation

5.2.6. Performance Metrics of Model Accuracy

The performance of the model is evaluated with three metrics: the Nash–Sutcliffe efficiency (*NSE*), the coefficient of determination (R^2), and the root mean square error (*RMSE*). *NSE* [47] is a dimensionless goodness-of-fit indicator ranging from negative infinity to 1. An *NSE* value of 1 indicates a perfect fit between observed and simulated data. *NSE* is evaluated using the following formula:

$$NSE = 1 - \frac{\sum_{i=1}^{n_d}\left(M_i - S_i\right)^2}{\sum_{i=1}^{n_d}\left(M_i - \bar{M}\right)^2} \tag{5.5}$$

where n_d is the length of the data series, M is the observed data, S is the simulated data, and $\bar{M}$ is the mean observed value. In the context of catchment hydrologic modeling, simulated results are considered to be good if the *NSE* is larger than 0.4 for daily time steps. For shorter time steps, the equivalent "goodness" threshold of *NSE* is lower [48].

Coefficient of determination R^2 reflects the degree of accuracy in the processes of simulated and observed runoff. R^2 can be calculated with:

$$R^2 = \frac{\left|\sum_{i=1}^{n_d}\left(M - \bar{M}\right)\left(S - \bar{S}\right)\right|^2}{\sum_{i=1}^{n_d}\left(M_i - \bar{M}\right)^2 \sum_{i=1}^{n_d}\left(S_i - \bar{S}\right)^2} \tag{5.6}$$

The closer the R^2 is to 1, the more the simulated runoff process is accurate.

RMSE is a frequently used measure of the differences between the values (sample or population values) that a model predicts and the values observed:

$$RMSE = \sqrt{\frac{\sum_{i=1}^{n_d}\left(M_i - S_i\right)^2}{N}} \tag{5.7}$$

An *RMSE* value of 0 indicates the perfect fit (formula indicated in Equation 5.7). If the value is less than half of the standard deviation of the observations, the model performance is considered to be good [49].

5.3. QUANTITATIVE ASSESSMENT OF CHECK DAM SYSTEM IMPACTS ON CATCHMENT FLOOD CHARACTERISTICS

5.3.1. Flood Simulation in the Wangmaogou Catchment

Parameters are required for the Manning coefficient and the infiltration rate to calibrate the numerical model. In this investigation, the infiltration rate was set to a constant value based on previous rainfall events that caused soil saturation. The range values for the Manning coefficients and infiltration rates were determined based on the land use distribution (Figure 5.3d) as well as the proposed range values from Jiang and Huang [50], Li [51], and Engman [52] (Table 5.1).

Depending on the parameter ranges values of the Manning coefficient and infiltration rate, nine calibration combinations were constructed to create a permutation of high, moderate, and low values as shown in Table 5.2. The best performance of simulated discharge

Table 5.1 Manning coefficients and infiltration rates for various land uses.

	Manning coefficient (s/m$^{1/3}$)			Infiltration rate (mm/h)		
Land use	Min.	Med.	Max.	Min.	Med.	Max.
Slope farmland	0.044	0.057	0.070	2.480	3.490	4.50
Forest	0.200	0.250	0.300	4.120	5.310	6.500
Grass land	0.059	0.105	0.150	3.250	4.125	5.00
Transportation land	0.010	0.012	0.013	0.000	0.000	0.000
Rural land	0.010	0.020	0.030	0.500	0.550	0.600
Terrace	0.180	0.260	0.340	2.600	4.050	5.500
Dam farmland	0.033	0.039	0.044	1.680	2.940	4.200

Table 5.2 Scenario permutations of the manning coefficient and infiltration rate.

Parameters	G1	G2	G3	G4	G5	G6	G7	G8	G9
Manning coefficient (s/m$^{1/3}$)	Min.	Med.	Max.	Min.	Med.	Max.	Min.	Med.	Max.
Infiltration rate (mm/h)	Min.	Min.	Min.	Med.	Med.	Med.	Max.	Max.	Max.

@seismicisolation

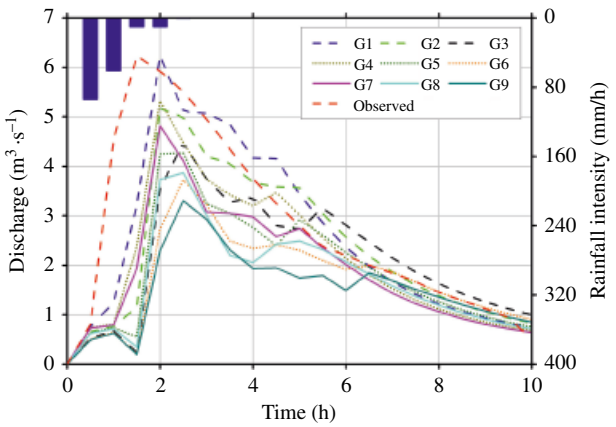

Figure 5.6 Hydrograph of observed and simulated discharge at catchment outlet during calibration.

was obtained by comparing the observed outlet discharge with the model calculations at each of the different permutations.

The observed and simulated discharges for various parameter combinations are illustrated in Figure 5.6, and the evaluation metrics of *NSE*, R^2, and *RMSE* are presented in Table 5.3; see also Jiang and Huang [50], Li [51] and Hou et al. [33]. The best performance was obtained with the combination of G1, featuring *NSE*, R^2, and *RMSE* values of 0.68, 0.70, and 1.03 m³/s, respectively.

For the peak flood processes, the peak discharge at the outlet deviated by only about 0.01% between the simulated (6.22 m³/s) and observed (6.23 m³/s) values (Figure 5.6). The simulated flood peak time was delayed by 0.5 hours (Figure 5.6) compared with the timing of the observed peak, which had a small acceptable relative error of 5%. Therefore, the G1 parameters of the model effectively represented the simulated flood event.

5.3.2. Peak Discharge and Runoff Volume

The outlet discharge reached a peak value of 6.22 m³/s with check dams and 89.05 m³/s for S1 and S2 (Figure 5.7a), which is a significant difference (about 14 times smaller). The variation in the stored surface water throughout the whole catchment during the rainfall event showed three similar states for S1 and S2: an increasing, a decreasing, and a constant stage (Figure 5.7b). In the catchment with check dams, it took two hours of rainfall to initially reach the

Table 5.3 Performance of discharge simulations over calibration processes.

Evaluation metrics	G1	G2	G3	G4	G5	G6	G7	G8	G9
NSE	0.68	0.36	0.09	0.51	0.16	0.08	0.38	0.22	0.02
R^2	0.70	0.44	0.24	0.63	0.38	0.23	0.60	0.35	0.23
RMSE (m³/s)	1.03	1.47	1.75	1.28	1.68	1.91	1.45	1.82	2.03

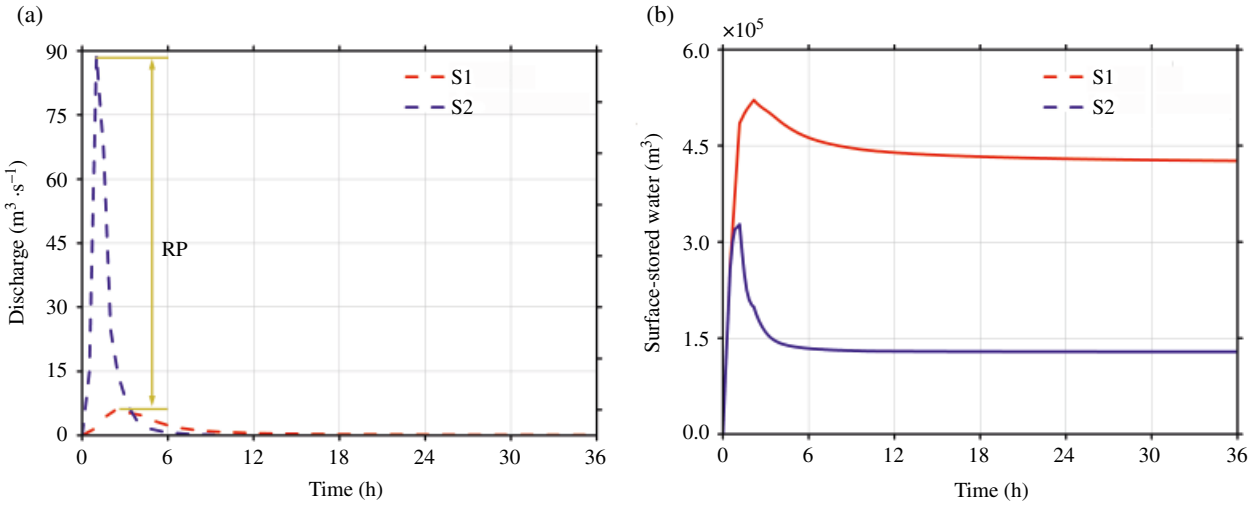

Figure 5.7 Comparison of peak discharge rates (a) and volumes of surface-stored water (b) between the catchments with and without check dams. Note: reduction peak discharge (RP).

@seismicisolation

Table 5.4 Runoff volume characteristics in catchments with and without check dams.

Runoff volumes	Check dam (m^3)	Percentage of precipitation (%)	Without check dam (m^3)	Percentage of precipitation (%)
Precipitation	569 157	/	569 157	/
Outlet discharge	114 296	20.1	428 890	75.4
Stored water	454 861	/	140 267	/
Surface-stored water	426 199	74.9	128 767	22.6
Infiltration	28 662	5.0	11 500	2.0

maximum surface-stored water volume ($5.21 \times 10^5\,m^3$) and about 22 hours to reach the constant state of full. The catchment without check dams required only one hour of rainfall to initially reach the maximum surface-stored water volume ($3.24 \times 10^5\,m^3$) and about six hours to reach the constant state of full. For this rainfall event, more than three times the surface water was stored in the catchment with check dams (42 6199 m^3) than in the catchment without them (128 767 m^3) (Table 5.4).

The amount of stored water can be calculated based on the mass conservation from the precipitation and outlet discharge (Table 5.4). The total precipitation during this rainfall was 569 157 m^3. The total outlet discharges were 114 296 and 428 890 m^3 for S1 and S2, respectively. Therefore, the stored water volumes were 454 861 and 140 267 m^3, respectively. Based on the stored water and surface-stored water volume, the infiltration volumes were calculated as 28 662 and 11 500 m^3, respectively. The average infiltration depths were 1.98 and 4.95 mm, respectively. The relative proportions of precipitation that ended up in the outlet discharge, surface-stored water, and infiltration were 20.1, 74.9, and 5.0%, respectively, in the S1, and the corresponding values for S2 were 75.4, 22.6, and 2.0%, respectively.

The peak discharge at the catchment outlet is significantly larger without check dams than with them. This can be attributed to the deposition, which slows the flow velocity and enhances the infiltration in front of the check dams. Earlier studies also documented that an inverse relationship exists between an increasing number of check dams and the peak flow discharge [53–55]. Runoff is impounded in front of the check dam and increases the detention time, which leads to an infiltration depth that is 2.5 times greater with check dams than without them (Table 5.4). The longer runoff impoundment is also a major direct factor resulting in a large difference in the catchment runoff volume. Martín-Rosales et al. [19] assessed the effect of check dams and gravel pits on groundwater recharge and found that the proportion of runoff that infiltrated the check dams varied from 3% to more than 50%. Several researchers also performed a series of field and indoor experiments to study the decrease in the runoff volume that enhanced infiltration rates [3, 20, 56–60]. Groundwater is increasingly replenished as infiltration rates in the soil profile increase [57, 61–63]. More importantly, when the flood volume is reduced and the flow has a lower velocity due to check dams, gully erosion also slows down [1, 3, 64]. At the same time, with more water infiltrated [1, 65]) and higher soil fertility [66, 67], the crop yield of the newly formed farmland can increase [65, 68].

5.3.3. Runoff Lag Times

The runoff times occurring at the outlets were compared between S1 and S2. The lag times were defined as the differences between the times at which the runoff was first generated, reached the peak, and ended. These lag times can quantify how long the check dams delayed the runoff in the catchment.

The generation runoff time was defined as the time required for the flow to reach the outlet along the channel. The generation runoff times for S1 and S2 were two minutes and six minutes, respectively (Figure 5.8). Thus, the lag time (LG) was four minutes. The outlet discharge reached the peak flow after two hours and one hour of rainfall for S1 and S2, respectively (Figure 5.8). Thus, the peak discharge lag time (LP) was one hour. The runoff ending time (LE) was defined as the time difference between when the flow first reached the outlet and when it stopped, which became close to 0 m^3/s. For the catchment systems with and without the check dams, the runoff ending times were 36 hours and 10 hours from the beginning of the rainfall, respectively. These times differed significantly as can be observed in Figure 5.6.

The results imply that check dams delay the runoff from reaching the catchment outlet. This is normal due

@seismicisolation

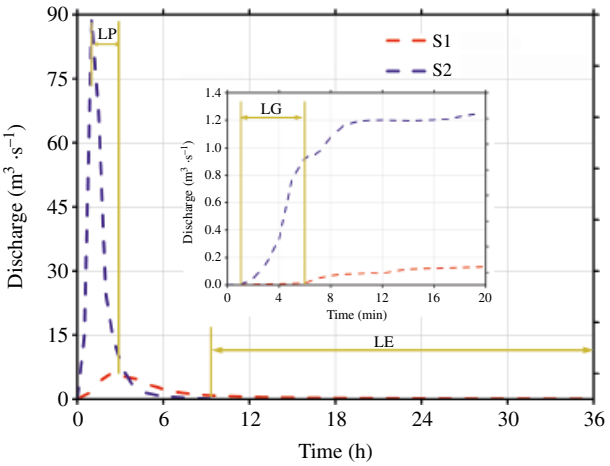

Figure 5.8 Comparison of outlet runoff times with and without check dams: the generation lag (LG), peak lag (LP), and end lag (LE).

to the sediment that accumulates at the check dams [1]. The surface slope is also responsible for slowing down runoff discharge by increasing the infiltration time and decreasing the positive velocity [1, 9, 69]. One of the main purposes of a check dam is to form check dam farmland through the sedimentation occurring in front of the check dam, as in the gullies of the Loess Plateau [7, 31, 65]. As a result, the riverbeds in the gullies in front of the check dams rise, which creates a wider and gentler gradient on the newly formed farmland and results in lower flow velocities. Researchers who evaluated the influence of check dams on channel morphology in Spain through field observations and model analysis found similar results [16, 70]. Their results showed that the check dams intercept sediments and slow the flow along the longitudinal gradient. The presence of check dams and the sediment accumulation also affect this result, as they reduce the runoff speed by increasing the channel bed roughness as several authors have described [53, 55, 71]. As a result, the runoff takes twice as long to reach the peak discharge levels with check dams than without check dams (Figure 5.8). These results are further corroborated by the research of Hood et al. [53], which showed that using check dams as a gully channel management intervention increases the amount of time it takes for the flow to peak, mainly during small and short storms, and with dry soil conditions.

Furthermore, it takes 3.6 times more time for the runoff discharge to reach the catchment outlet with check dams than the outlet without them (Figure 5.8), which can be attributed to the water impoundment within the check dams. On the one hand, the runoff discharge is intercepted in front of the check dams, so the runoff discharge decreases in front of the check dams. On the other hand, lower flow velocities in front of the check dams increase the amount of time it takes for the runoff discharge to reach the catchment outlet. Guyassa et al. [1] also discovered that it took longer for the flow to reach lower sections in a catchment with check dam gullies in Northern Ethiopia.

5.3.4. Maximum Discharge and Corresponding Location Along the Main Channel

The main channel was divided into 45 sections at even intervals of 0.05 km, and the reference section was the Wangmaogou #2 check dam, which was the key check dam on the main channel (Figure 5.9). The maximum discharges and locations of the maximum discharge were recorded at 10-minute intervals in the 45 sections along the main channel during this rainfall event. The runoff duration was considered to be 10 hours to compare the two catchment systems during the same time frame, as the catchment with check dams had a runoff ending time of 10 hours.

The maximum discharge occurred after about one hour of rainfall in the catchment with check dams (Figure 5.10a). The maximum, minimum, and mean of

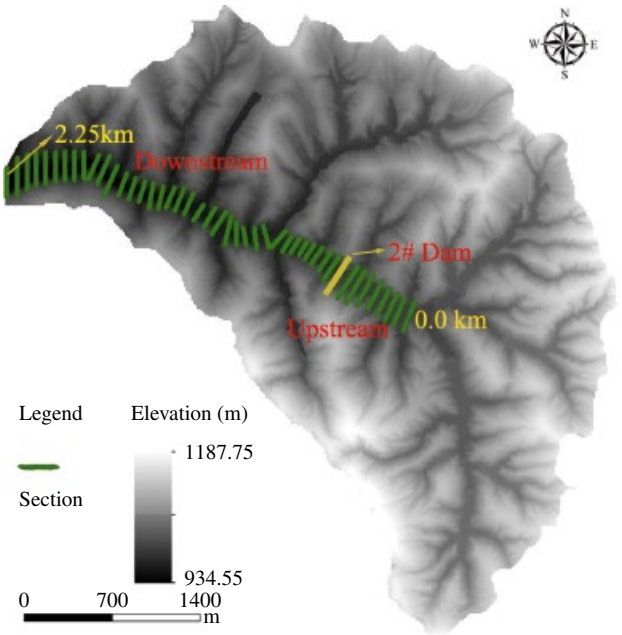

Figure 5.9 Main channel sections at Wangmaogou catchment.

@seismicisolation

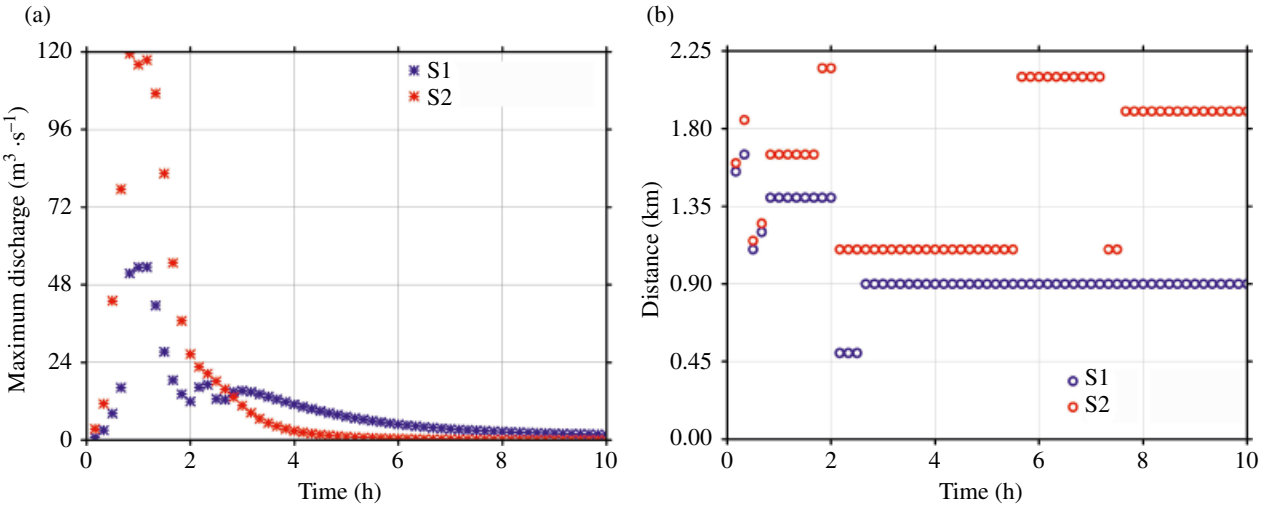

Figure 5.10 Distribution of maximum discharges and (a) the corresponding distances of occurrence (b) in catchments with and without check dams.

the maximum discharges recorded every 10 minutes during this rainfall event were 53.49, 0.91, and 10.36 m³/s, respectively. The coefficient of variation (CV) of the maximum discharge was 23.9% (Table 5.5).

The location where the maximum discharges occurred fluctuated during the initial stage of the rainfall event for the catchment with check dams (Figure 5.10b). However, the location remained constant during the middle, late, and ending periods of rainfall, occurring at 1.4, 0.5, and 0.9 km away from the upstream area, respectively (Figure 5.10a). Additionally, during this rainfall event, the maximum, minimum, and mean distances to the locations of the peak flow occurrences were 1.65, 0.5, and 0.98 km away from the upstream area, respectively (Table 5.5). The CV of the location was 117.10% (Table 5.5).

For the catchment without check dams, the maximum discharge first increased extremely and then decreased rather quickly (Figure 5.10a). The highest, lowest, and mean maximum discharges were 119.44, 0.01, and 15.79 m³/s, respectively, during this rainfall event. The CV of the maximum discharge was 26.79% (Table 5.5). For the catchment without check dams, the locations where the maximum discharges changed were less regular and did not show a clear definitive pattern. At first, the maximum discharge location also fluctuated during the initial rainfall period (Figure 5.10b). The maximum discharge location was 1.65 km downstream between 0.83 and 1.67 hours of rainfall (Figure 5.10b). Afterward, the maximum discharge shifted to 2.15 km downstream between 1.83 and 2 hours of rainfall (Figure 5.10b). Then, the maximum discharge location became 1.1 km downstream between 2.17 and 5.5 hours of rainfall, and it became 7.33 and 7.5 hours of rainfall (Figure 5.10b). The maximum discharge location was also located 2.15 km downstream between 5.67 and 7.17 hours of rainfall (Figure 5.10b). Finally, the maximum discharge location was 1.9 km downstream from 7.67 to 10 hours of rainfall (Figure 5.10b). During this rainfall event, the maximum, minimum, and mean distances of the maximum discharge locations were 2.15, 1.1, and 1.58 km away from the upstream area, respectively (Table 5.5). The CV of the maximum discharge location was 201.78%.

Table 5.5 Statistical characteristics of maximum discharge and corresponding distance downstream at occurrence for catchments with and without check dams.

	Maximum discharge (m³/s)		Maximum discharge location (km)	
Statistics	Check dam	Without check dam	Check dam	Without check dam
Highest	1.65	2.15	53.49	119.44
Lowest	0.50	1.10	0.91	0.01
Mean	0.98	1.58	10.36	15.79
CV (%)	23.90	26.79	117.10	201.78

Check dams also serve the important purpose of ensuring safety downstream by controlling or mitigating floods [31]. During the simulated rain event, the maximum discharge was larger in the S1 than the S2, although the maximum discharge became smaller during return flow processes for S1. The maximum and mean maximum discharges were 2.23 and 1.52 times

@seismicisolation

greater in the catchment without check dams than in the one with them, respectively. In addition, the CV of the maximum discharge varied more in the catchments without check dams than with check dams. The slowing of the discharge has been linked to the construction of check dams [1, 3, 65].

Second, the distance where the maximum discharge was found downstream, along with the maximum, minimum, and mean discharge locations, was larger for the catchment without the check dams than for the catchment with the check dams. This proves that the installation of check dams altered the spatial distribution of the maximum discharge locations, moving the maximum discharge locations upstream, thus contributing to greater safety downstream. In addition, a greater CV of the maximum discharge location was found for the catchment without the check dams than for the one with the check dams, which indicates that the peak flow of a catchment with check dams plays a big role in controlling flooding and thus preventing major damage. These outcomes can be attributed to mass movement processes (e.g. erosion, deposition, and side wall collapse), which affect channel morphology and sediment supply, thus resulting in a higher spatial variability of morphological features [72–76].

5.3.5. Relationship Between Channel Connectivity and Outlet Runoff Characteristics

The effect of check dams on runoff characteristics was further analyzed based on the channel connectivity index (see Section 2.4.1), where the peak discharge and the runoff volume at the catchment outlet were calculated for various scenarios (Table 5.6).

The channel connectivity index decreased with an increasing number of check dams. The connectivity index of the current catchment channel for S1 is 93.75% lower than that for the catchment for S2 under the same rainfall conditions. The peak discharge and runoff volume were found to decrease together with the channel connectivity index. The ratio of the peak discharge between S2 and S1 under the same rainfall conditions is 14.22. The flood volume is 4.64 times higher for S2 than S1 under the same rainfall conditions.

A linear relationship was found between the channel connectivity index and the peak discharge, as well as between the index and the flood volume at the catchment outlet (Figure 5.11). The regression results (Figure 5.11) showed that all of the R^2 values are high (0.98–0.99), and the correlation is significant at the 0.01 level. This suggests that the model provides a good fit between the

Table 5.6 Channel connectivity indexes, peak discharges, and runoff volumes under the conditions of various scenarios.

Scenarios	Check dams	Channel connectivity index	Outlet peak discharge (m^3/s)	Outlet runoff volume (m^3)
S1	17	0.96	6.26	151.21
S2	0	17.29	89.04	701.49
S3	7	2.47	23.16	167.76
S4	6	2.89	23.18	195.83
S5	5	3.46	25.79	201.96

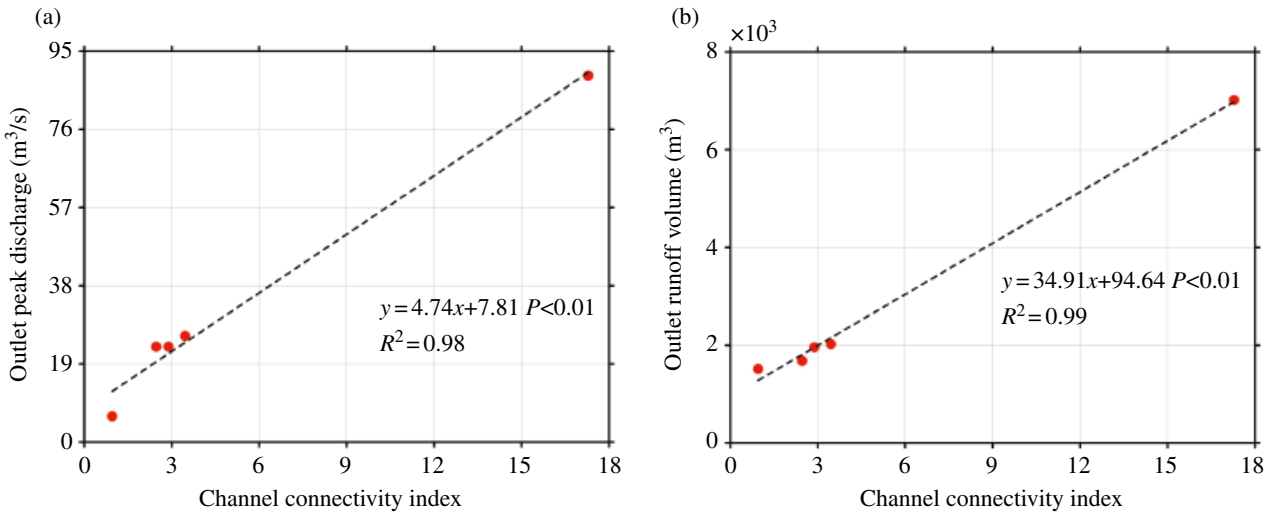

Figure 5.11 Relationship between the channel connectivity index and (a) peak discharge and (b) runoff volume at the outlet.

@seismicisolation

channel connectivity index and the peak discharge, as well as the index and the flood volume at the catchment outlet. These findings indicate that an equation based on the channel connectivity index can forecast the peak discharge and flood volume at this catchment outlet.

During the rain event, the channel connectivity was directly related to the peak discharge and flood volume at the basin mouth (Table. 5.6 and Figure 5.11). Different scenarios with increasing numbers of check dams were simulated (S3–S5) and tested to quantify how much they contributed to changes in the downstream connectivity [1, 44, 77]. The presence of discontinuities in the channel are known to obstruct the streamlines of water [78, 79] and to slow the velocity, which is the reason why check dams result in a lower peak discharge and flood volume at the basin mouth. As far as runoff is concerned, connectivity has mostly been studied at the watershed scale, with researchers investigating how well local obstructing elements can stop runoff [77, 80, 81]. These studies demonstrated that a well-connected catchment often implies a higher risk for infrastructures at the outlet (e.g. a more damaging flood). Therefore, check dam systems can both reduce disastrous flooding by cutting off the runoff channel and improve the crop yield through the accumulation of sediment in front of the check dams.

5.4. THE REGULATION OF CHECK DAM SYSTEM IN EROSION DYNAMIC PROCESS

The check dam reduces the peak value of the flood in the watershed and retains the sediment in the channel. The trapped sediment forms the flat dam land in front of the dam, thus raising the slope of the channel and changing the original hydrodynamic characteristics of the channel. The retaining effect of check dams on the runoff decreases the erosion of the downstream channel, and the retardation effect of the check dams on the runoff in front of the dam leads to a decrease in the flow velocity and sand-carrying force. The decreased channel slope can also change the flow process of the flood in the channel. By simulating the hydrodynamic process in a channel under a heavy storm in a state where Wangmaogou #2 is filled to its sediment capacity and in a state without check dams, we analyze in this chapter the velocity, shear stress, runoff power, runoff erosion power, and change process of energy in different cross sections of the channel. This is done from the viewpoints of hydrodynamics and energy to elucidate the effects of check dams on the flood process in a basin. The construction of a check dam can significantly change the flow velocity in a gully, and the trapped sediment has a significant impact on the topography and slope of the gully. In this section, we simulate the hydrodynamic process of runoff in a gully in a state where the check dams are filled to their sediment capacities and in a state without check dams. This is done to explore the effect of a check dam on the runoff along a gully. The check dam selected in this section is Wangmaogou #2, located in the main channel of the middle reaches of Wangmaogou.

5.4.1. Dynamic Parameters of Channel Erosion

The flow velocity is the most important hydraulic parameter in the analysis of runoff erosion and sediment transport. The measurement of flow velocity can be divided into direct measurement and indirect measurement. The direct measurement methods include the color tracer method, the buoy method, and the optical instrument measurement method, and each method has its own advantages and disadvantages. No unified method exists for the measurement of the flow velocity. Some scholars believe that the correction coefficient of the flow velocity is related to the flow pattern, and a different flow pattern corresponds to a different correction coefficient, that is, when the runoff is laminar, the correction coefficient value is 0.5–0.6, and when the runoff is turbulent, the correction coefficient value is 0.8. Due to the uncertainty of the measured velocity, this study first focused on obtaining the average flow rate of the study section via solving the St. Venant equation. Then, this was divided by the measured area of the cross section, and the average flow rate of the cross section was obtained:

$$\tau = \gamma RJ \tag{5.8}$$

where τ is the runoff shear force, N/m^2, γ is the bulk density of water, Kg/m^3, R is the hydraulic radius, m, and J is the hydraulic energy slope.

Bagnold referred to the concept of runoff power, which refers to the change rate of the potential energy and the kinetic energy of runoff with time per unit area. It is described as follows:

$$\omega = \gamma qs = \lambda hVJ = \tau V \tag{5.9}$$

where ω is the runoff power, N/(m·s), q is the discharge per unit width, m^3/(m·s), h is the water depth, m, and V is the average flow velocity, m/s.

@seismicisolation

When rainfall occurs in the basin, with the runoff flow going along the main channel, the potential energy of the runoff decreases gradually due to the decrease in the elevation, and the reduced potential energy is converted into kinetic energy, thus causing an increase in the runoff kinetic energy. The energy loss of the runoff in the downward movement mainly includes two aspects: first, the loss in the processes of scouring the channel and transporting sediment, and second, the blocking effect of the check dam will also reduce the energy of the runoff. This section discusses the regulation effect of Wangmaogou #2 on the runoff kinetic energy in the channel. The runoff kinetic energy is described as follows:

$$J = \frac{1}{2}mv^2 \tag{5.10}$$

where J is the runoff kinetic energy in the study section, J, and m is the mass of the flow in the study section, kg.

The runoff depth and the flood peak discharge are two important parameters reflecting the characteristics of the flood process of a single rainstorm in a watershed. The runoff depth represents the total flood volume in the basin resulting from a rainstorm, and it indirectly reflects the amount of the rainfall as well as the redistribution of the basin to the rainfall. The flood peak discharge represents the intensity of the flood, and it indirectly reflects the spatial and temporal distribution characteristics of rainfall, as well as the effect of the basin on the concentration process of the runoff. By comprehensively considering the influence of the runoff depth and flood peak flow on the sediment transport process, Lu et al. put forward the concept of the runoff erosion power of single rainstorm. They demonstrated the good correlation between the runoff erosion power and the sediment transport. The runoff erosion power is described as follows:

$$E = Q'_m H \tag{5.11}$$

where E is the runoff erosion power of a single rainstorm, $m^4/(s \cdot km^2)$, H is the average runoff depth of a single rainstorm, m, and Q'_m is the flood peak discharge modulus, $m^3/(s \cdot km^2)$, which is the ratio of the flood peak discharge of a single rainstorm and the drainage area.

5.4.2. Average Velocity of Runoff Varies Along the Channel

Figure 5.12 shows the variation in the average velocities at various sections of the channel under the state of filling and without Wangmaogou #2 check dam construction. As the variation in the flow velocity is closely related to the channel topography, the flow velocity is analyzed in combination with the longitudinal profile of the main channel in the Wangmaogou watershed (Figure 5.13). It can be seen from Figure 5.12 that the influence range of check dam construction on the channel runoff velocity is limited, and under the condition of the Wangmaogou #2 check dam being full or not being built, no difference exists in

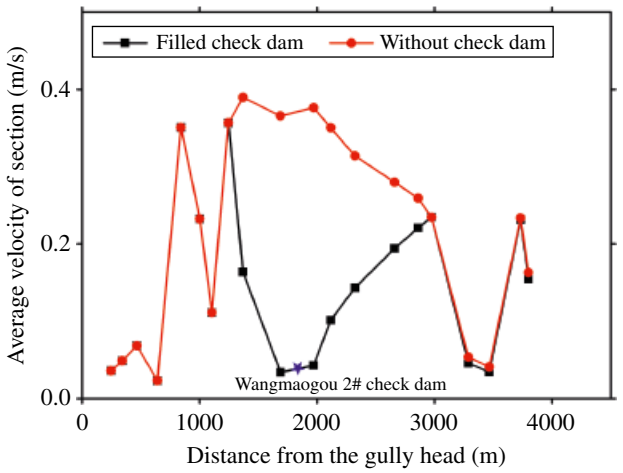

Figure 5.12 Process of average velocity changes under various conditions.

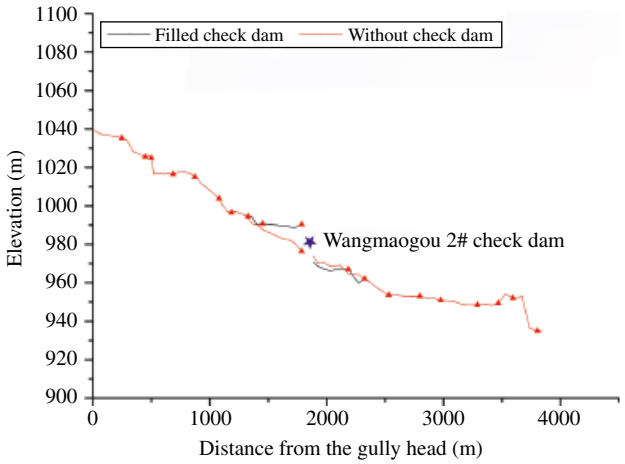

Figure 5.13 The profile of Wangmaogou main channel hypothetical cases.

@seismicisolation

the average runoff velocity of each section in the upstream channel. In the middle channel, the flow velocity in front and back of the dam site decreases rapidly under the condition of full capacity, and the shorter the distance between the section and the dam site, the more obvious the flow velocity decreases. The average runoff velocity at the outlet section is 0.16 m/s without a check dam, whereas the average flow velocity at the outlet section is 0.15 m/s under the condition that the capacity of the Wangmaogou #2 check dam is full. This is due to the water storage and sediment control of the Wangmaogou #2 check dam. The closer one is to the dam site, the smaller the flow velocity will be, thus leading to a sharp reduction in the flow-carrying capacity of this section, as well as a large amount of silt in front of the dam. The local slope of the channel decreases due to sediment deposition, and the channel in the Wangmaogou watershed falls as a whole under the condition with full capacity compared with the condition of no dam.

5.4.3. The Shear Stress of Runoff Varies Along the Channel

Figure 5.14 shows a comparison of the runoff shear stress amounts under the condition of full storage capacity and under the state of no dam. It can be seen from Figure 5.14 that the construction of the Wangmaogou #2 check dam does not affect the upstream area as much, and the runoff shear stress is the same under the condition of the full storage capacity of the check dam and the lack of dam construction. Under the state of dam construction, the smaller the distance between the section and the site of the Wangmaogou #2 check dam, the smaller the runoff shear stress of the section. The runoff shear stress of the section closest to the site of the Wangmaogou #2 check dam will be reduced to close to 0. Under the condition of no dam construction, the flood flow in the downstream channel of the Wangmaogou watershed is large, the hydraulic radius is relatively large, and the runoff shear stress is slightly larger than that under the condition of full storage capacity.

5.4.4. The Runoff Power Varies Along the Channel

Figure 5.15 shows a comparison of runoff power under the condition of full storage capacity and under the state of no dam. It can be seen from Figure 5.4 that the construction of the Wangmaogou #2 check dam does not affect the upstream areas as much, and the runoff power is the same under the condition of the full storage capacity of a check dam and the lack of dam construction. Under the state of dam construction, the smaller the distance between the section and the site of the Wangmaogou #2 check dam, the smaller the runoff power of the section. The runoff shear stress of the section closest to the site of the Wangmaogou #2 check dam will be reduced to close to 0. Under the condition of no dam being built, the runoff power of each section in the lower channel is slightly higher than that under the condition of full storage capacity. The runoff shear stress and flow velocity directly affect the runoff power according to the runoff power calculation formula. The influence range of the Wangmaogou #2 check dam is mainly

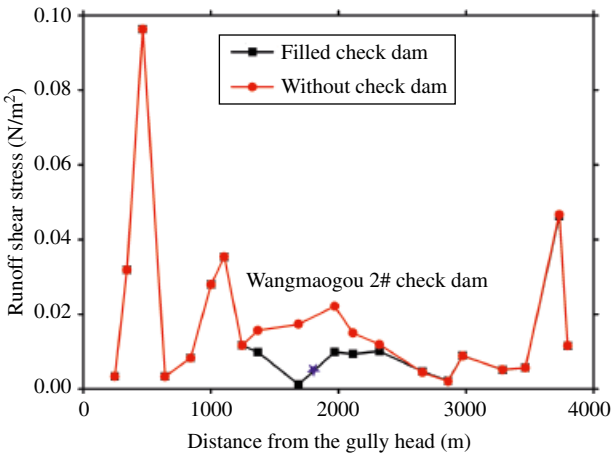

Figure 5.14 Process of runoff stress changes under the various conditions.

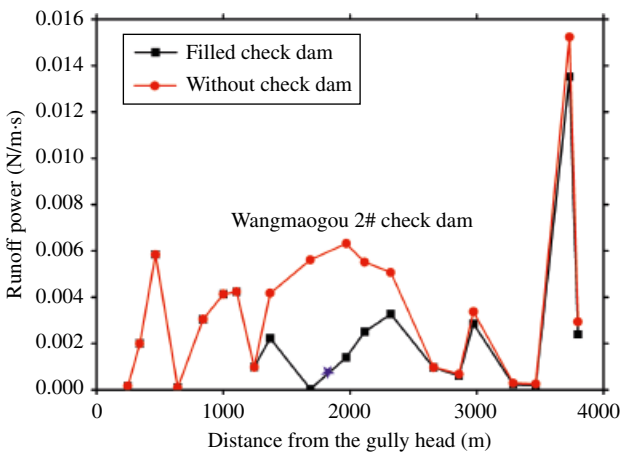

Figure 5.15 Process of runoff power changes under the various conditions.

@seismicisolation

concentrated in the middle and lower channels of the Wangmaogou watershed, so the runoff power of each section in the upstream channel is the same under the condition that the full storage capacity of check dam is full and the condition that the dam is not built. Due to the construction and silting of the Wangmaogou #2 check dam, the slope of the middle channel is changed, and the runoff shear stress is indirectly affected. The action of retaining water and sand directly affects the flow velocity in front of the dam. Therefore, a significant difference exists in the runoff power amounts among various sections in the middle channel under the condition of full storage capacity and the condition without a dam, and the runoff power under the condition without a dam is slightly larger than that under the condition of a full dam. The construction of the Wangmaogou #2 check dam obviously reduces the runoff power of each section in the middle channel and then reduces the erosion of the gully via runoff.

5.4.5. The Runoff Kinetic Energy Varies Along the Channel

Figure 5.16 shows a comparison of the runoff kinetic energy under the condition of full storage capacity and under the state of no dam. Figures 5.16 and 5.17, respectively, show the spatial distribution of runoff kinetic energy in the main channel of the Wangmaogou watershed under the above two states. As can be seen from Figure 5.16, the distribution of the runoff kinetic energy in the main channel is relatively complex, and the upstream area is not affected. Under the condition of full storage capacity of the Wangmaogou #2 check dam, the runoff kinetic energy at each section of the main channel in the upstream is basically identical. Under the condition of full storage capacity, the runoff kinetic energy at each section of the main channel in the middle and lower reaches is reduced by 60–80% compared with under the condition of no dam. The runoff kinetic energy fluctuates sharply at the section of the main channel in the middle and lower reaches of the Wangmaogou watershed. It can be seen from the kinetic energy calculation formula that the flow rate and velocity in this section directly affect the kinetic energy of the runoff. The flow velocity in front of the check dam decreases sharply due to the impoundment and sand-blocking effect of the check dam. At the same time, the amount of water stored in the check

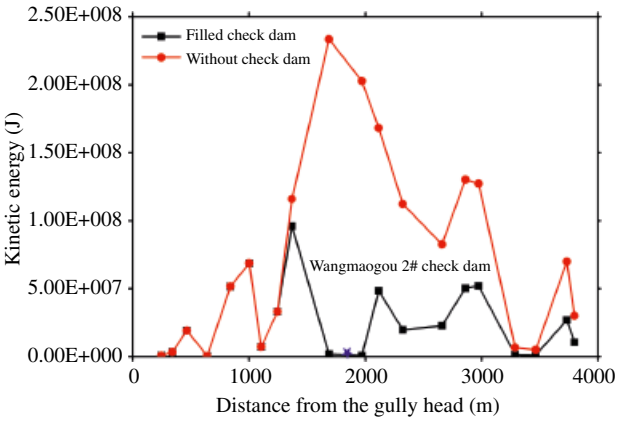

Figure 5.16 Process of kinetic energy changes under the various conditions.

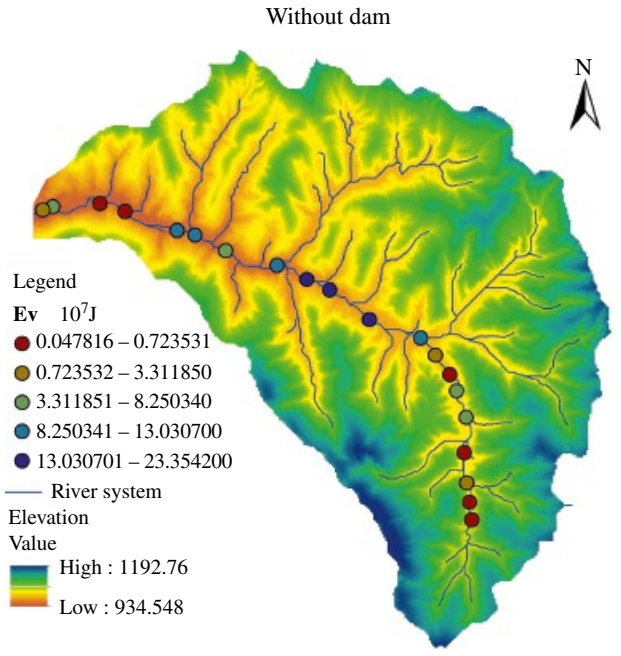

Figure 5.17 The distribution of kinetic energy under the condition of the Wangmaogou #2 check dam being filled with deposition.

dam reduces the amount of the flood in the downstream channel of the dam site, which leads to gaps between the kinetic energy of the water flow in various sections of the channel in the middle and lower reaches under the condition of full storage capacity and under the state of no dam. Therefore, the construction of the Wangmaogou #2 check dam obviously reduces the flow kinetic energy in the main channel in the middle and lower reaches of the Wangmaogou watershed (Figure 5.18).

@seismicisolation

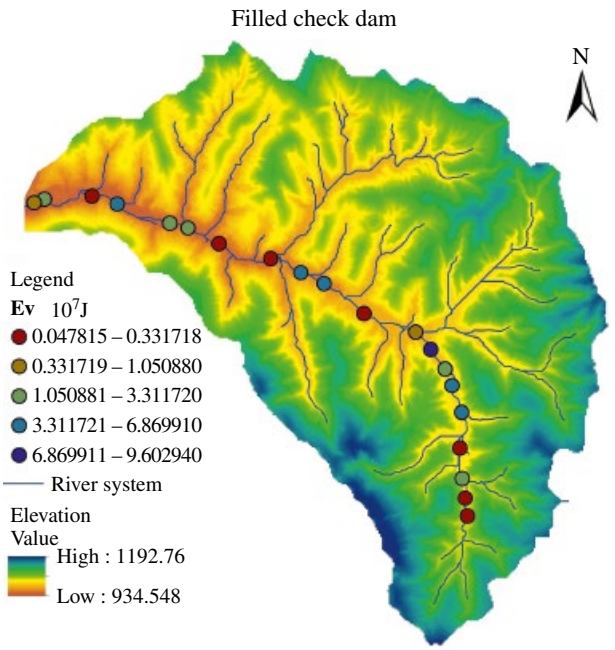

Figure 5.18 The distribution of kinetic energy under the condition of the lack of construction of the Wangmaogou #2 check dam.

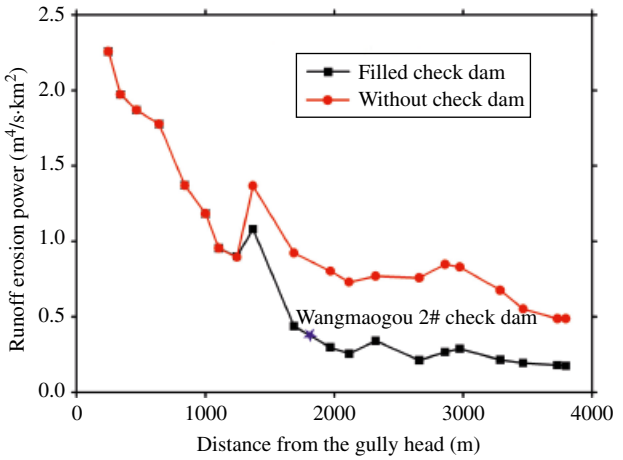

Figure 5.19 Process of runoff erosion power changes under the various conditions.

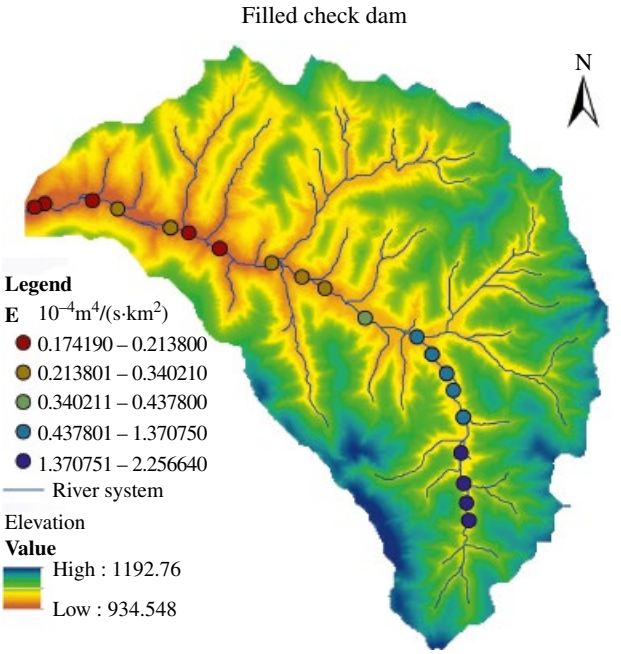

Figure 5.20 The distribution of runoff erosion power under the various conditions with filled check dam.

5.4.6. The Runoff Erosion Power Varies Along the Channel

Figure 5.19 shows a comparison of the runoff erosion power under the condition of full storage capacity and under the state of no dam. Figures 5.19 and 5.20, respectively, show the spatial distribution of the runoff erosion power in the main channel of the Wangmaogou watershed under the above two states. It can be seen from Figure 5.21 that the runoff erosion power of each section in the upstream channel is basically the same under the condition of full storage capacity and under the state of no dam. Before section 9, the erosion power of the channel runoff showed a decreasing trend. At section 9, the erosion power of the channel runoff showed a sharp increase, and then, the erosion power of the channel runoff decreased as a whole. The runoff erosion power of each section in the middle and lower channels of the Wangmaogou watershed was reduced by 50–70% compared with in the condition of no dam construction. The fluctuation of the runoff erosion power in the channel occurred in the study section with the branch channel inflow. For example, the runoff erosion power of sections 13 and 15 with a large downstream branch channel flood inflow increased by 33 and 25%, respectively, compared with the previous section. In the absence of dam construction, the runoff erosion power of sections 13 and 15 increased by only 5 and 11%, respectively, compared with the previous section. According to the topography of the watershed, the sections 1–8 selected for this study are located in the upper reaches of the Guandigou watershed. The confluence of surface floods in the upper reaches of the Wangmaogou watershed and the Wangtagou watershed before section 9 resulted in an increase in the total amount of the flood through section 9, as well as an

@seismicisolation

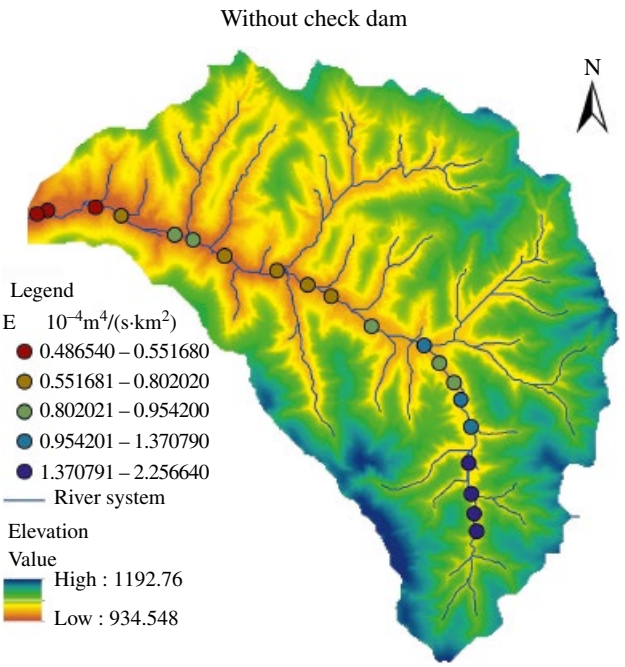

Figure 5.21 The distribution of runoff erosion power under the various conditions without check dam.

obvious increase in the peak value of the flood. Therefore, the calculation results of the runoff erosion power in section 9 were relatively large. In the middle and lower channels, the runoff erosion power also increased in sections where the branch flow flowed into the basin (such as sections 13 and 15). As a whole, under the condition of the full storage capacity of the Wangmaogou #2 check dam, the runoff was stored in accordance with the storage capacity due to the retention and retardation of the runoff via the Wangmaogou #2 check dam. The total amount of the flood in the section in front of the Wangmaogou #2 check dam decreased, and the peak value of the flood decreased. Moreover, due to the retaining water and sand, as well as the reducing flood peak, the total amount of the flood in the downstream channel of the Wangmaogou #2 check dam site decreased, and the peak value of the flood decreased, which obviously changed the runoff erosion power of the original channel.

5.5. VARIATION PROCESS OF HYDRODYNAMIC PARAMETERS BEFORE AND AFTER THE SILT DAM WITH TIME

The previous chapter studied the difference in the hydrodynamic characteristics in the Wangmaogou watershed between the silted and the unbuilt state of the Wangmaogou #2 dam. For the purpose of exploring the rapid changes in the flood process at the Wangmaogou #2 dam site, this section compares and analyzes the two dams before and after the Wangmaogou #2 dam in the silted state and the unbuilt state. The changes in the hydrodynamic parameters of each section are highlighted.

5.5.1. Variation Process of Velocity

Figure 5.22 displays the process of the velocity changes of the cross section in front of and behind the Wangmaogou #2 check dam under the various

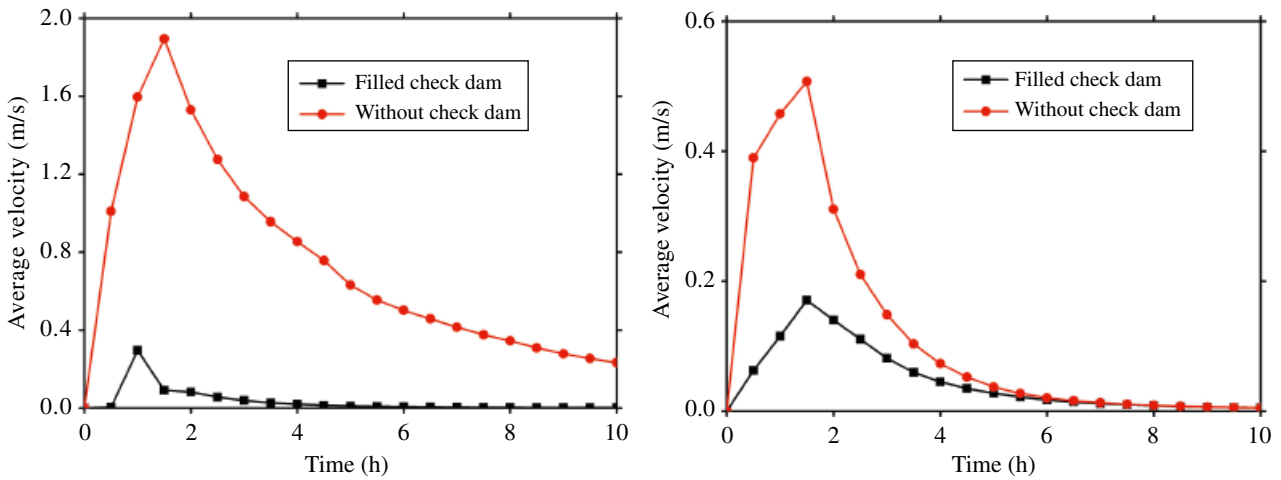

Figure 5.22 Process of velocity changes in the cross section in front of and behind the Wangmaogou #2 check dam under the various conditions.

@seismicisolation

conditions. It can be seen from Figure 5.21 that the construction of a silt dam will rapidly reduce the flow velocity in front of the dam, and the peak flow velocity in front of the dam will decrease by 85%. Compared with the state where the channel is not built, the flow velocity after the construction of the silt dam becomes smoother with time, and the peak velocity of the section behind the dam is reduced by 66%, which reduces the erosion of the channel flow to the downstream. Regardless of the front section or the rear section of the dam, the construction of the silt dam has played a significant role in reducing the flow rate of the channel flood, and it has effectively reduced the erosion of the channel via the flood.

5.5.2. Variation Process of Runoff Shear Stress

Figure 5.23 shows the change in the runoff shear stress at the front and the back with time in the silted state and the unbuilt state of the Wangmaogou #2 dam. It can be seen from Figure 5.9 that the runoff shear stress is reduced to close to 0 in front of the silted state of the Wangmaogou #2 dam. It can also be seen from the calculation formula for the runoff shear stress that the magnitude of the runoff shear stress depends on the hydraulic radius and hydraulic slope. With the sedimentation of sediment, the slope of the channel in front of the dam decreases significantly. The runoff shear stress in front of the dam is smaller than that in front of the unbuilt state. At the back section of the dam site, the runoff shear stress in the unbuilt state is 4.3 times that in the silted state of the Wangmaogou #2 dam. This is due to the interception effect of the Wangmaogou #2 dam on the gully flood, which sharply reduces the downstream flood volume. The hydraulic radius decreases accordingly and is relatively large compared with the runoff shear stress under the state of a lack of dam construction.

5.5.3. Variation Process of Runoff Power

Figure 5.24 is the process of the runoff power changes in the cross section in front of and behind the Wangmaogou #2 check dam under the various conditions. It can be seen from Figure 5.23 that the change in the trend of the runoff power over time in the study section before and after the dam site in the silted state and in the unbuilt state is basically the same as that of the runoff shear stress. The runoff power is drastically reduced in front of the Wangmaogou #2 dam when the dam is in the silted state, and the value is close to 0.

5.5.4. Variation Process of Runoff Kinetic Energy

Figure 5.25 shows the runoff kinetic energy curve of the studied section in front of and behind the silted state and the unbuilt state of the Wangmaogou #2 dam. It can be seen from Figure 5.25 that the construction of the Wangmaogou #2 dam has reduced the channel runoff velocity and the amount of water discharged, and it has a huge impact on the runoff and velocity of the cross section, greatly reducing the kinetic energy in front of and behind the dam.

After rainfall occurs in the watershed, the potential energy of the surface water flow is converted into kinetic energy during the movement process, and the

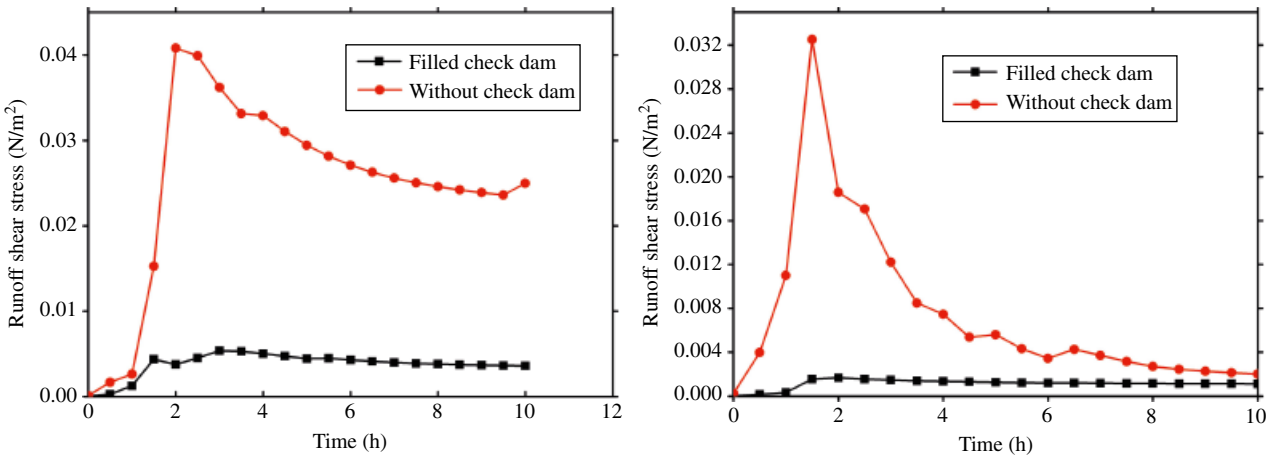

Figure 5.23 Process of runoff stress changes in the cross section in front of and behind the Wangmaogou #2 check dam under the various conditions.

@seismicisolation

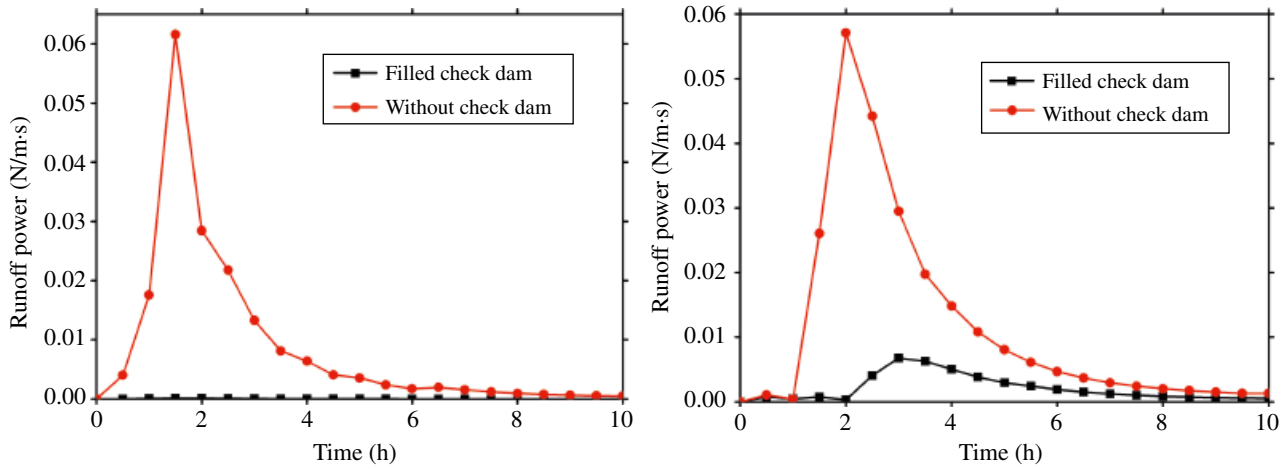

Figure 5.24 Process of runoff power changes of the cross section in front of and behind the Wangmaogou #2 check dam under the various conditions.

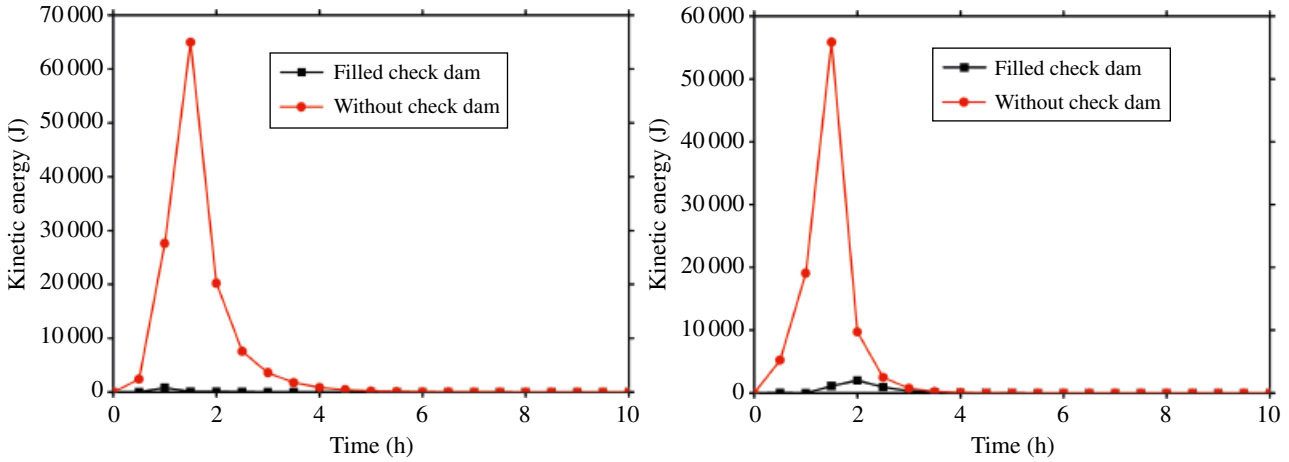

Figure 5.25 Process of kinetic energy changes in the cross section in front of and behind the Wangmaogou #2 check dam under the various conditions.

kinetic energy is continuously consumed in the processes of scouring the channel, transporting sediment and blocking the silt dam. Figure 5.26 shows the change process of the total runoff kinetic energy in each calculation grid in the Wangmaogou watershed over time during the processes of rainfall and runoff generation. The total runoff kinetic energy first increases and then decreases with time in the watershed. The peak value appears at 1.5 hours. This is related to the fact that 88% of the total rainfall in the "7.15" rainstorm occurred in the first 1.2 hours. Over time, the rainfall decreases during the time period, and the runoff in the basin confluence process is continuously discharged from the outlet of the basin. The energy of runoff during the basin flooding process decreases accordingly.

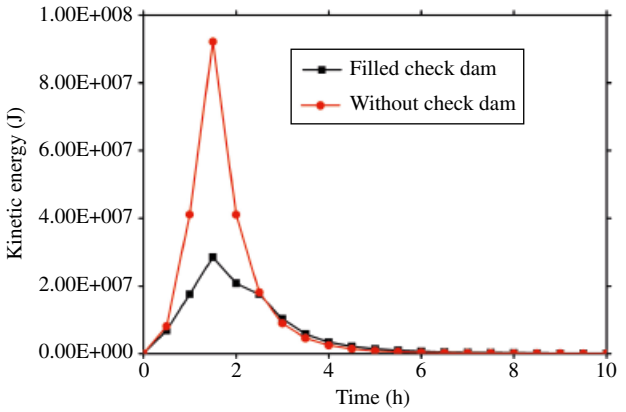

Figure 5.26 Process of total kinetic energy changes under the various conditions.

@seismicisolation

5.6. CONCLUSION

For the purpose of quantitatively evaluating the effects of check dam systems on local flood characteristics, a GAST numerical model was applied to a check dam system in the Wangmaogou catchment (Loess Plateau, China). The model was calibrated with a selected rainfall event (on 15 July 2012, about 10 hours long) using related Manning and infiltration coefficients. This GAST numerical model accurately and efficiently simulated the rainfall runoff event and captured the peak discharge as well as the flood peak time in a complex topographic domain. Numerical calculations were carried out to investigate the flood characteristics under two scenarios: Scenario 1 considered 17 check dams in the catchment, whereas Scenario 2 considered none of them. The results showed that check dams significantly increase the so-called runoff lag times (lag to generation, lag to peak, and lag to end of runoff). The check dams also lower the flood peak discharge in a significant way. The relative outlet discharge, surface-stored water, and infiltration related to precipitation were 20.1, 74.9, and 5.0%, respectively, in catchments with check dams, and they were 75.4, 22.6, and 2.0%, respectively, in catchments without check dams. The installation of the check dams changed the spatial distribution of the peak flow locations as well, moving them considerably upstream and thus enabling greater safety downstream. The maximum and mean peak discharges were 2.23 and 1.52 times greater in catchments without check dams than those with check dams, respectively. The channel connectivity was directly related to the peak discharge and discharge volume at the basin mouth.

Finally, it is worth mentioning that the northwestern part of China is a semiarid area with generally short and heavy rains during the monsoon season. Check dams are constructed there to prevent or mitigate flooding disasters by cutting off the runoff channel, as well as to improve the crop yield through the accumulation of silted sediment and the increased infiltration in front of the dams. The study outcomes confirmed the usefulness and great capacity of the check dams to prevent and mitigate flood effects.

The average thickness of the outlet section of the Wangmaogou watershed in the state of the unbuilt dam is 1.1 times that of the Wangmaogou #2 dam in the silted state. The runoff shear stress and runoff power in the downstream area and at the outlet of the basin without dam construction are, respectively, 1.1 times and 1.2 times that of the Wangmaogou #2 dam under the silted state. The runoff erosion power showed a trend of decreasing along the channel downstream. Meanwhile, the runoff erosion power in the middle and lower reaches of the silted sate was reduced by 50–70% compared with the unbuilt state.

A significant difference exists in the runoff velocity between the front and back sections of the Wangmaogou #2 dam in the silted state and in the unbuilt state. The construction of a silt dam will reduce the peak flow velocity in front of the dam by 85% and the peak flow velocity behind the dam by 66%. The runoff shear stress in front of the Wangmaogou #2 dam is reduced to close to 0 when the Wangmaogou #2 dam is fully silted. In addition, the runoff shear stress in the unbuilt state of the Wangmaogou #2 dam is 4.3 times that in the silted state. The changes in the trends of the runoff power and runoff shear stress are basically the same. In the state of dam construction, the runoff kinetic energy of the silted dams in the middle and lower reaches of the dam is reduced by 60–80% compared with the state of a lack of dam construction, and the runoff kinetic energy of the channel at the site of the Wangmaogou #2 dam is significantly reduced. The Wangmaogou #2 dam has a very obvious runoff blocking and controlling capability.

REFERENCES

1. Liao, S.Y., Cai, Q.G., Zhuo, M.N. et al. (2009). Influence of channel networks on the sediment yield under variant temporal and spatial scales: a case study of Chabagou watershed. *Progress in Geography 28* (1): 47–54.
2. Taye, G., Poesen, J., Wesemael, B.V. et al. (2013). Effects of land use, slope gradient, and soil and water conservation structures on runoff and soil loss in semi-arid Northern Ethiopia. *Physical Geography 34* (3): 236–259.
3. Zhang, Y. (1982). Practice of check dam system development in Wangmaogou watershed. *Soil and Water Conservation in China 5*: 19–23. (in Chinese).
4. Ward, J.V. (1989). The four-dimensional nature of lotic ecosystems. *Journal of the North American Benthological Society 8*: 2–8.
5. Conesa García, C., Belmonte Serrato, F., and García Lorenzo, R. (2004). Efectos de los diques de corrección hidrológico-forestal en la competencia y estabilidad de corrientes efímeras. Aplicación a la cuenca de la rambla de la Torrecilla (Murcia). In: *Territorio y medio Ambiente: Métodos cuantitativos y Técnicas de Información Geográfica* (ed. C. Conesa García and J.B. Martínez Guevara), 69–83. Murcia: Asociacion de Geógrafoś Espanoles y Universidad de Murcia. (in spanish).

@seismicisolation

6. Zhang, L., Podlasly, C., Ren, Y. et al. (2014). Separating the effects of changes in land management and climatic conditions on longterm streamflow trends analyzed for a small catchment in the Loess Plateau region, NW China. *Hydrological Processes 28* (3): 1284–1293.
7. Diaz-Ramirez (2014). *Porous Check dams on Flow Routing and Sediment Transport in Agricultural ditches: A Case Study in the Mississippi Delta*, MAFES Buletin 1213 of Mississippi Agricultural and Forestry Experiment Station. Mississippi State University.
8. CMWR (Ministry of Water Resource of P.R. China). (2014). Bulletin of first national water census for soil and water conservation. 6–8. (in Chinese).
9. Huang, C.A. and Yang, Z.D. (2003). Sediment transport and flow intensity indexes. *Journal of Hydraulic Engineering 34* (6): 1–7.
10. Zhang, Y., Li, P., Liu, X.J. et al. (2019). Effects of farmland conversion on the stoichiometry of carbon, nitrogen, and phosphorus in soil aggregates on the Loess Plateau of China. *Geoderma 351*: 188–196.
11. Yuan, S., Li, Z., Li, P. et al. (2019). Influence of check dams on flood and erosion dynamic processes of a small watershed in the Loss Plateau. *Water 11* (4): 834.
12. Engman, E.T. (1986). Roughness coefficients for routing surface runoff. *Journal of Irrigation & Drainage Engineering 112* (1): 39–53.
13. Cuomo, S., Della Sala, M., and Novità, A. (2015). Physically based modelling of soil erosion induced by rainfall in small mountain basins. *Geomorphology 243*: 106–115.
14. Helming, K., Römkens, M., and Prasad, S. (1998). Surface roughness related processes of runoff and soil loss: a flume study. *Soil Science Society of America Journal 62* (1): 243–250.
15. Li, P., Xu, G., Lu, K. et al. (2019). Runoff change and sediment source during rainstorms in an ecologically constructed watershed on the Loess Plateau, China. *Science of the Total Environment 664*: 968–974.
16. Callow, J.N. and Smettem, K.R.J. (2009). The effect of farm check dams and constructed banks on hydrologic connectivity and runoff estimation in agricultural landscapes. *Environmental Modelling & Software 24* (8): 959–968.
17. Romero-Díaz, A., Marín-Sanleandro, P., and Ortiz-Silla, R. (2012). Loss of soil fertility estimated from sediment trapped in check dams. South-eastern Spain. *Catena 99*: 42–53.
18. Huang, M. and Zhang, L. (2004). Hydrological responses to conservation practices in a catchment of the Loess Plateau, China. *Hydrological Processes 18* (10): 1885–1898.
19. Bombino, G., Gurnell, A., Tamburino, V. et al. (2009). Adjustments in channel form, sediment calibre and vegetation around check-dams in the headwater reaches of mountain torrents, Calabria, Italy. *Earth Surface Processes and Landforms 34* (7): 1011–1021.
20. Alderwish, A.M. (2010). Induced recharge at new check dam sites—Sana'a Basin, Yemen. *Arabian Journal of Geosciences 3* (3): 283–293.
21. Nyssen, J., Clymans, W., Descheemaeker, K. et al. (2010). Impact of soil and water conservation measures on catchment hydrological response - a case in north Ethiopia. *Hydrological Processes 24*: 1880–1895.
22. Shi, P., Zhang, Y., Zhang, Y. et al. (2019b). Land-use types and slope topography affect the soil labile carbon fractions in the Loess hilly-gully area of Shaanxi, China. *Archives of Agronomy and Soil Science 65*: 1–13.
23. Martín-Rosales, W., Gisbert, J., Pulido-Bosch, A. et al. (2007). Estimating groundwater recharge induced by engineering systems in a semiarid area (southeastern Spain). *Environmental Geology 52* (5): 985–995.
24. Castillo, V.M., Mosch, W.M., García, C.C. et al. (2007). Effectiveness and geomorphological impacts of check dams for soil erosion control in a semiarid Mediterranean catchment: El Cárcavo (Murcia, Spain). *Catena 70* (3): 416–427.
25. Yu, G.Q. (2010). *Study on Mechanism on Regulation Measures on Water Erosion Processes in the Slope-Gully System*, 121–126. Xi'an University of Technology.
26. Ruiz-Villanueva, V., Badoux, A., Rickenmann, D. et al. (2018). Impacts of a large flood along a mountain river basin: the importance of channel widening and estimating the large wood budget in the upper Emme River (Switzerland). *Earth Surface Dynamics 6* (4): 1115–1137.
27. Nash, J.E. and Sutcliffe, J.V. (1970). River flow forecasting through conceptual models part I—a discussion of principles. *Journal of Hydrology 10* (3): 282–290.
28. Li, X., Wei, X., and Wei, N. (2016). Correlating check dam sedimentation and rainstorm characteristics on the Loess Plateau, China. *Geomorphology 265*: 84–97.
29. Lü, Y., Sun, R., Fu, B., and Wang, Y. (2012). Carbon retention by check dams: regional scale estimation. *Ecological Engineering 44*: 139–146.
30. Hu, C.H. and Zhang, X.M. (2018). Several key questions in the researches of runoff and sediment changes and trend predictions in the Yellow River. *Journal of Hydraulic Engineering 49* (09): 1028–1039. (in Chinese).
31. Savi, S., Schneuwly-Bollschweiler, M., Bommer-Denns, B. et al. (2013). Geomorphic coupling between hillslopes and channels in the Swiss Alps. *Earth Surface Processes and Landforms 38* (9): 959–969.
32. Tebebu, T., Abiy, A., Zegeye, A. et al. (2010). Surface and subsurface flow effect on permanent gully formation and upland erosion near Lake Tana in the northern highlands of Ethiopia. *Hydrology and Earth System Sciences 14* (11): 2207–2217.
33. Jiang, D.S. and Huang, G.J. (1986). Study on the filtration rate of soils on the loess plateau of China. *Acta Pedologica Sinica 23* (4): 299–305. (in Chinese).
34. Parimala Renganayaki, S. and Elango, L. (2013). A review on managed aquifer recharge by check dams: a

@seismicisolation

case study near Chennai, India. *International Journal of Research in Engineering and Technology 2*: 416–423.

35. Thompson, C. and Croke, J. (2013). Geomorphic effects, flood power, and channel competence of a catastrophic flood in confined and unconfined reaches of the upper Lockyer valley, southeast Queensland, Australia. *Geomorphology 197*: 156–169.
36. Huang, J., Hinokidani, O., Yasuda, H. et al. (2012). Effects of the check dam system on water redistribution in the Chinese Loess Plateau. *Journal of Hydrologic Engineering 18* (8): 929–940.
37. Conesa García, C., López-Bermúdez, F., and García-Lorenzo, R. (2007). Bed stability variations after check dam construction in torrential channels (South-East Spain). *Earth Surface Processes and Landforms: The Journal of the British Geomorphological Research Group 32* (14): 2165–2184.
38. Rickenmann, D., Badoux, A., and Hunzinger, L. (2016). Significance of sediment transport processes during piedmont floods: the 2005 flood events in Switzerland. *Earth Surface Processes and Landforms 41* (2): 224–230.
39. Hou, J., Liang, Q., Simons, F., and Hinkelmann, R. (2013b). A stable 2D unstructured shallow flow model for simulations of wetting and drying over rough terrains. *Computers & Fluids 82*: 132–147.
40. Hou, J., Liang, Q., Simons, F., and Hinkelmann, R. (2013a). A 2D well-balanced shallow flow model for unstructured grids with novel slope source term treatment. *Advances in Water Resources 52*: 107–131.
41. Liang, Q. and Smith, L.S. (2015). A high-performance integrated hydrodynamic modelling system for urban flood simulations. *Journal of Hydroinformatics 17* (4): 518–533.
42. Xu, G., Cheng, S., Li, P. et al. (2018). Soil total nitrogen sources on check dammed farmland under the condition of ecological construction in a small watershed on the Loess Plateau, China. *Ecological Engineering 121*: 19–25.
43. Li, G.Y. (2007). *Comparative Study of Soil Infiltration Under Different Land Uses in Loess Hilly Regions*. Northwest A&F University. (in Chinese).
44. Gao, H.D. (2013). *Hydro-Ecological Impact of the Gully Erosion Control Works in Loess Hilly-Gully Region*, 54. Research Center of Soil and Water Conservation and Ecological Environment, Chinese Academy of Sciences and Ministry of Education.
45. Xu, X., Zhang, H., and Ouyang, Z. (2004). Development of check-check dam systems in gullies on the Loess Plateau, China. *Environmental Science and Policy 7* (2): 79–86.
46. Namadi, P.H., Saghafian, B., and Rostami, M. (2014). *The Numerical Investigation of the Effect of Subsequent Check Dams on Flood Peaks and the Time of Concentration Using the MIKE 11 Modeling System (Case Study: Golabdareh Catchment, Iran), River Flow 2014*, 1745–1750. CRC Press.
47. Singh, J., Knapp, H.V., Arnold, J.G., and Demissie, M. (2005). Hydrological modeling of the Iroquois River watershed using HSPF and SWAT. *JAWRA Journal of the American Water Resources Association 41* (2): 343–360.
48. Guyassa, E., Frankl, A., Zenebe, A. et al. (2017). Effects of check dams on runoff characteristics along gully reaches, the case of Northern Ethiopia. *Journal of Hydrology 545*: 299–309.
49. Cappelaere, B., Touma, J., and Peugeot, C. (2000). A recursive algorithm for connectivity analysis in a grid; application to 2D hydrodynamic modeling in heterogeneous soils. *Computers & Geosciences 26* (2): 121–135.
50. Wei, Y., He, Z., Li, Y. et al. (2017). Sediment yield deduction from check - dams deposition in the weathered sandstone watershed on the North Loess Plateau, China. *Land Degradation & Development 28* (1): 217–231.
51. Zhao, T.Y., Yang, M.Y., Walling, D.E. et al. (2017). Using check dam deposits to investigate recent changes in sediment yield in the Loess Plateau, China. *Global and Planetary Change 152*: 88–98.
52. Amare, T., Zegeye, A.D., Yitaferu, B. et al. (2014). Combined effect of soil bund with biological soil and water conservation measures in the northwestern Ethiopian highlands. *Ecohydrology and Hydrobiology 14* (3): 192–199.
53. Wang, T., Li, P., Ren, Z. et al. (2017). Effects of freeze-thaw on soil erosion processes and sediment selectivity under simulated rainfall. *Journal of Arid Land 9* (2): 234–243.
54. Wang, T., Li, P., Li, Z. et al. (2019). The effects of freeze–thaw process on soil water migration in dam and slope farmland on the Loess Plateau, China. *Science of the Total Environment 666*: 721–730.
55. Nyssen, J., Veyret-Picot, M., Poesen, J. et al. (2004). The effectiveness of loose rock check dams for gully control in Tigray, northern Ethiopia. *Soil Use and Management 20* (1): 55–64.
56. Wang, W.Y., Wang, Z.R., Wang, Q.J., and Zhang, J.F. (2003). Improvement and evaluation of the Green-Ampt model in loess soil. *Journal of Hydraulic Engineering 34* (5): 30–34. (in Chinese).
57. Xiang-zhou, X., Hong-wu, Z., and Ouyang, Z. (2004). Development of check-check dam systems in gullies on the Loess Plateau, China. *Environmental Science & Policy 7* (2): 79–86.
58. Shi, P., Zhang, Y., Ren, Z. et al. (2019a). Land-use changes and check dams reducing runoff and sediment yield on the Loess Plateau of China. *Science of the Total Environment 664*: 984–994.
59. Lenzi, M.A. and Comiti, F. (2003). Local scouring and morphological adjustments in steep channels with check-check dam sequences. *Geomorphology 55* (1): 97–109.

@seismicisolation

60. Hood, M.J., Clausen, J.C., and Warner, G.S. (2007). Comparison of stormwater lag times for low impact and traditional residential development. *JAWRA Journal of the American Water Resources Association 43* (4): 1036–1046.
61. Lacombe, G., Cappelaere, B., and Leduc, C. (2008). Hydrological impact of water and soil conservation works in the Merguellil catchment of central Tunisia. *Journal of Hydrology 359* (3): 210–224.
62. Lehmann, P., Hinz, C., McGrath, G. et al. (2007). Rainfall threshold for hillslope outflow: an emergent property of flow pathway connectivity. *Hydrology and Earth System Sciences 11* (2): 1047–1063.
63. Hooke, J. (2003). Coarse sediment connectivity in river channel systems: a conceptual framework and methodology. *Geomorphology 56* (1–2): 79–94.
64. Borst, L. and De Haas, S. (2006). *Hydrology of Sand Storage Check dams: A Case Study in the Kiindu Catchment, Kitui District, Kenya*. Amstercheck dam, The Netherlands: VU University Amstercheck dam.
65. Arnaud-Fassetta, G. (2013). Dyke breaching and crevasse-splay sedimentary sequences of the Rhône Delta, France, caused by extreme river-flood of December 2003. *Geografia Fisica e Dinamica Quaternaria 36* (1): 7–26.
66. Xu, M. and Wang, G. (2000). To accelerate the construction of check-check dams in the Loess Plateau. *Yellow River 22*: 26. (in Chinese).
67. Yang, D., Kanae, S., Oki, T. et al. (2003). Global potential soil erosion with reference to land use and climate changes. *Hydrological Processes 17* (14): 2913–2928.
68. Fernandez, G.P., Chescheir, G.M., Skaggs, R.W., and Amatya, D.M. (2005). Development and testing of watershed-scale models for poorly drained soils. *Transactions of ASAE 48* (2): 639–652.
69. Fang, X. (1995). Criterion and condition for the relative stability of check-check dam system. *Soil and Water Conservation in China 169*: 29–33. (in Chinese).
70. Huang, J., Hinokidani, O., Yasuda, H. et al. (2012). Effects of the check dam system on water redistribution in the Chinese Loess Plateau. *Journal of Hydrologic Engineering 18* (8): 929–940.
71. Wang, G.Q., Li, T.J., Xue, H., and He, L. (2006). Mechanism Analysis of Watershed Sediment Processes. *Journal of Basic Science and Engineering 14* (4): 455–462.
72. Ma, J.J., Sun, X.H., and Guo, X.H. (2010). Varying head infiltration moded based on Green-Ampt model and solution to its key parameters. *Journal of Hydraulic Engineering 5*: 30–33.
73. Harvey, A.M. (2002). Effective timescales of coupling within fluvial systems. *Geomorphology 44*: 175–201.
74. Bracken, L.J. and Croke, J. (2007). The concept of hydrological connectivity and its contribution to understanding runoff-dominated geomorphic systems. *Hydrological Processes 21* (13): 1749–1763.
75. Boix-Fayos, C., Barberá, G.G., López-Bermúdez, F., and Castillo, V.M. (2007). Effects of check dams, reforestation and land-use changes on river channel morphology: case study of the Rogativa catchment (Murcia, Spain). *Geomorphology 91* (1–2): 103–123.
76. Boix-Fayos, C., de Vente, J., Martínez-Mena, M. et al. (2008). The impact of land use change and check-check dams on catchment sediment yield. *Hydrological Processes: An International Journal 22* (25): 4922–4935.
77. Fryirs, K.A., Brierley, G.J., Preston, N.J., and Kasai, M. (2007). Buffers, barriers and blankets: the (dis) connectivity of catchment-scale sediment cascades. *Catena 70* (1): 49–67.
78. Hassanli, A.M., Nameghi, A.E., and Beecham, S. (2009). Evaluation of the effect of porous check dam location on fine sediment retention (a case study). *Environmental Monitoring and Assessment 152* (1–4): 319–326.
79. Hou, J., Wang, T., Li, P. et al. (2018). An implicit friction source term treatment for overland flow simulation using shallow water flow model. *Journal of Hydrology 564*: 357–366.
80. Meerkerk, A.L., van Wesemael, B., and Bellin, N. (2009). Application of connectivity theory to model the impact of terrace failure on runoff in semi-arid catchments. *Hydrological Processes 23* (19): 2792–2803.
81. Xu, Y., Fu, B., and He, C. (2013). Assessing the hydrological effect of the check dams in the Loess Plateau, China, by model simulations. *Hydrology and Earth System Sciences 17* (6): 2185–2193.

@seismicisolation

Section II
Dam Erosion Processes and Dynamics

@seismicisolation
@seismicisolation

6

The Mechanism of Erosion Reduction by Check Dam

Qihua Ran[1], Honglei Tang[1], Peng Li[2], Feng Wang[1], Tian Wang[2], Zhihai Wei[3], Jingmei Sun[3], Miaoxia Wen[3] and Zhiqiang Min[3]

6.1. RESEARCH PROBLEM AND WORKING CONDITION DESIGN

6.1.1. Problem Description

The interception effect of silt dams on runoff and sediment on the basin scale has received extensive attention and research worldwide [1–5]. For example, Shi and Wang [4] applied the Mann–Kendall test and the Pettitt turning point test in the Huangfuchuan watershed of 3264 km^2 and found that 448 silt dams in the watershed significantly reduced the annual runoff and annual sediment transport in the watershed. Norman and Niraula [6] applied the SWAT model to the Turkey Pen watershed in Arizona, United States, and found that 2000 silt dams in the watershed reduced the watershed sediment load by 50%. The above studies have shown that in arid and semi-arid watersheds, silt dams combined with a series of slope water and soil conservation measures (such as terraces, afforestation, etc.) can reduce runoff and sediment output in the watershed effectively [7]. In most studies, the silt dam is often regarded as a static system in order to simplify the calculation. Therefore, researchers often can only draw the difference between the presence and absence of silt dams from the simulation results [8, 9]. However, under actual conditions, the check dams in a watershed are often in different siltation states during the same study period, such as newly built, lightly silted, heavily silted, silted up (i.e. reaching the designed sediment holding capacity), or erosion failure, etc. Additionally, in many numerical simulations, the check dam that reaches the designed storage capacity is often regarded as a failure [10]. However, does a silt dam that has reached the designed storage capacity and siltation status really lose its ability to hold water and sediment?

As shown in Figure 6.1a, in the initial construction stage of a silt dam, the dam body mainly blocks the movement of floods and forces the sedimentation to achieve the effect of blocking water and sediment. At the same time, the deposited sediment will gradually form a silt layer (i.e. dam land) that continuously expands and rises upstream.The siltation process of the dam often extends to the tailwater area of the dam reservoir [11] and the mouth area of each connected branch [12], as shown in Figure 6.1c. The uplift and expansion of the dam will sometimes proceed quickly after single or multiple rain-flood events [2]. Throughout the process of gradual reduction in storage capacity of the silt dam, the dam land is also constantly expanding and uplifting. A silt dam should be regarded as a dynamic system when studying the control

[1] *Institute of Hydrology and Water Resources Engineering, Zhejiang University of Technology, Hangzhou, China*
[2] *Institute of Water Resources and Hydro-electric Engineering, Xi'an University of Technology, Xi'an, China*
[3] *Northwest Institute of Forest Inventory, Planning and Design, National Forestry and Grassland Administration, Xi'an, China*

Check Dam Construction for Sustainable Watershed Management and Planning, First Edition.
Edited by Zhanbin Li, Peng Li, Yang Yu, Peng Shi, and Guillaume Piton.
© 2022 John Wiley & Sons, Inc. Published 2022 by John Wiley & Sons, Inc.

@seismicisolation

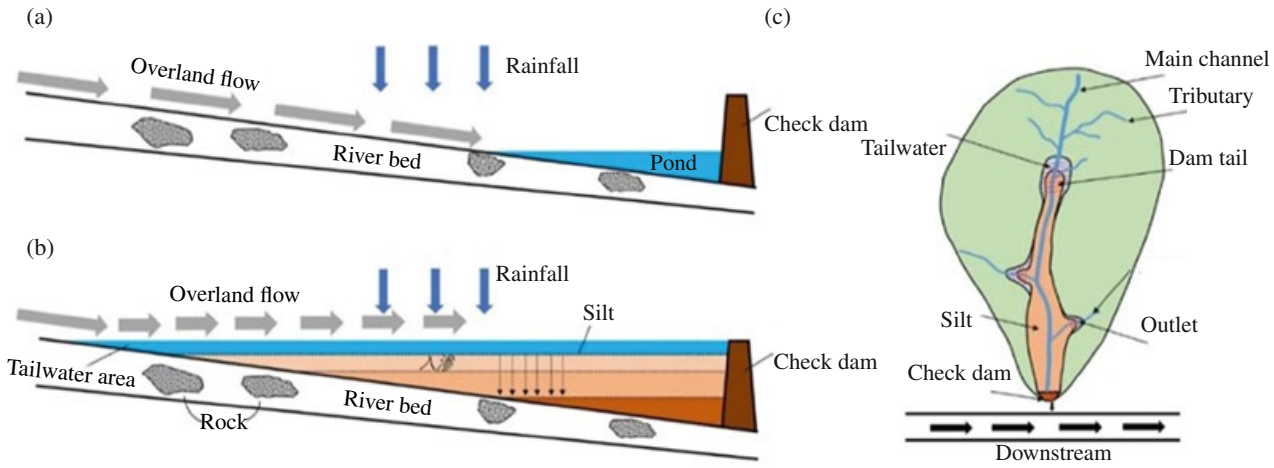

Figure 6.1 Mechanism of check dam on runoff and sediment reduction: (a) light silting stage; (b) heavy silting stage; and (c) plan view of check dam and its sedimentary land.

efficiency of the silt dam on the water and sediment in the basin. As an important part of this dynamic system, dams formed by siltation have been proven to exert an important influence on the hydrological response process of local areas such as infiltration [13], evaporation [14, 15], and groundwater recharge [16]. More importantly, during floods, due to the relatively flat slope (generally less than 2%) of the dam site, the movement of water and sediment on the dam site will be slowed down [17, 18], as shown in Figure 6.1b.

If a check dam and its dam site are regarded as a dynamic system, the impact of a check dam with a spillway on the movement of water and sediment during the life cycle of its design storage capacity has two different stages: (i) light deposition stage and (ii) heavy siltation stage [19]. In the light siltation stage, the surface runoff from upstream river channels and branch ditches enters the silt dam reservoir area and is intercepted by the dam body and sediment deposition occurs. This is the early water and sediment interception effect of the silt dam (Figure 6.1a). In the heavy sedimentation stage, as the dam elevation gradually rises to the spillway inlet elevation, surface runoff can easily leave the reservoir area through the spillway and enter the downstream after passing through the dam, so the blocking effect of the dam body on the runoff gradually weakens. However, Guyassa (2017) found through experiments that the flat land formed by siltation can slow down the movement speed of surface runoff on the dam to a certain extent and delay the peak moment of runoff. At the same time, studies have shown that the impact of tailwater from the tail of the reservoir and the mouth of the branch can also slow down the local runoff velocity [11, 20] and promote sedimentation. In the dynamic system, as the silt dam transitions from the light siltation stage to the heavy siltation stage, the dam body's water-retaining and sediment-retaining effects will gradually weaken; as a results, these effects may gradually appear and occupy a dominant position [21].

Although numerous studies have proved that silt dams are very effective water and sediment interception engineering measures, the effectiveness of silt dams in the heavy sedimentation stage has not been quantitatively evaluated. This chapter uses InHM (Integrated Hydrology Model) numerical simulation to simulate and study the water retention and sediment retention efficiency and mechanism of silt dams under different siltation conditions during the flood process and to answer the following key scientific questions:

1. Under different siltation conditions, especially heavy siltation conditions, does the silt dam still have an effective resistance to the process of water and sediment movement in the basin? If so, has its resistance and control mechanism changed?
2. What is the impact of the dam land formed by warping dams on the movement of water and sediment during the process of expansion and uplift?
3. What is the scope of influence of the silt dam system on the process of water and sediment movement?

6.1.2. Working Condition Design

In order to study the impact of check dams on runoff and sediment movement in the basin during floods under different siltation conditions, this chapter selects

@seismicisolation

a large check dam near Shejiagou and its outlet as the research object, with a series of silt storage capacity conditions constructed to represent a dynamic silt dam system.

A series of test simulation results in the early stage showed that when the siltation storage capacity of this silt dam is lower than 60% of the designed storage capacity, even under the heavy rainfall of 100 mm/hr (100-year return period), the upstream of the silt dam. The combined runoff failed to pass through the silt dam and formed a runoff response at the outlet of the basin. In this study, the working conditions of less than 60% of the siltation storage capacity can achieve complete water and sediment interception under most rainfall conditions, so a 60% siltation storage capacity was used as the dividing line between light siltation and heavy siltation of the Shejiagou silt dam. We used the silt dam and the entire watershed when it reaches 60% of the designed storage capacity as the initial working conditions for the dynamic silt storage capacity design of the silt dam. Starting from the 60% silt storage capacity condition, this simulation set a total of nine different silt storage capacity conditions at an interval of 5% of the total storage capacity (i.e. 10 300 m^3) to represent a dynamic process of silt dam development (Table 6.1 and Figure 6.2). For example, the 80% silt storage capacity condition means that 80% of the designed storage capacity of the silt dam under this condition has been consumed as silted sediment, forming a dam land of about $10.77 \times 10^4 m^2$. The biggest difference between various siltation conditions is that each silt storage capacity corresponds to a specific dam area and dam elevation. The area of the dam increased with the increase in the silt storage capacity and extended to the upstream and branch ditch, and the elevation of the dam increased correspondingly with the consumption of the storage capacity. Since the slope of the dam is very small [17, 18], a basic assumption of this simulation is that the slope of the dam is 0. This assumption simplified the topography of the dam to facilitate the construction of the simulation grid but retained the most important topographical difference (i.e. slope) between the dam and the original gully under different siltation conditions. With the increase of the silt storage capacity, a new silt layer that was higher and larger will replace the dam in the previous siltation condition. For example, from the 60% silt storage capacity condition to the 100% silt storage capacity condition, the elevation of the dam has been

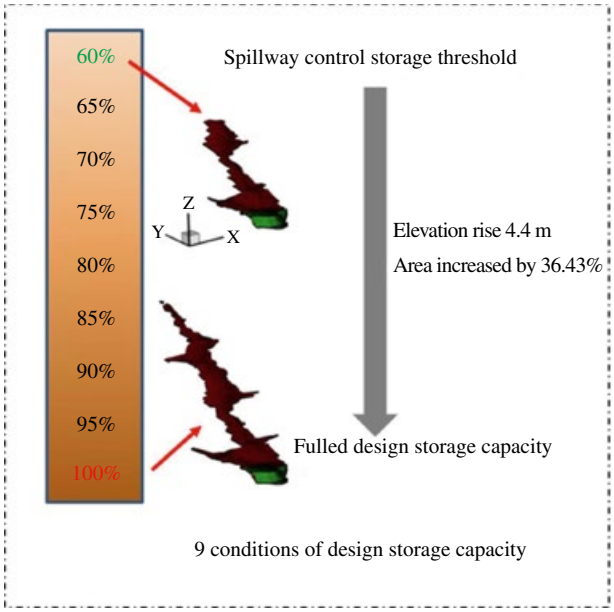

Figure 6.2 Schematic diagram of scenario design.

Table 6.1 Area and elevation of the sedimentary lands in different silting scenarios.

Simulation condition (%)	Dam land area($\times 10^4$ m^2)	Increment of dam land (%)	Elevation increment of dam land (m)	Increment of dam elevation (%)
0	0	/	0	/
60	8.95	/	14.50	/
65	9.45	5.64	15.20	4.83
70	9.89	10.49	15.80	8.97
75	10.33	15.40	16.40	13.10
80	10.77	20.36	17.00	17.24
85	11.15	24.53	17.50	20.69
90	11.52	28.74	18.00	24.14
95	11.90	33.00	18.50	27.59
100	12.21	36.43	18.90	30.34

@seismicisolation

raised by 4.4 m (30.34%) and the area has increased by 36.43% (Table 6.1).

Considering that the sediment production in this small watershed of the Loess Plateau was mainly concentrated in several rainstorm-flood events during the flood season [22, 23], five rainfall events of different intensities were selected as the input conditions of the model. In order to reduce the factors that affect the water–sand process, the difference in rain patterns was eliminated in this simulation. The rain pattern selected for the simulation was 1 hour of equal-intensity rainfall. The intensities of the five rainfall events were 55, 75, 80, 90 and 100 mm/hr, respectively, representing the medium- to high-intensity precipitation in the region.

In order to evaluate the sediment interception efficiency of the dam under different conditions, the Sediment trapping efficiency (STE) of the check dam under this silt storage capacity condition was calculated after each simulation. Brown proposed the calculation formula for the efficiency of small reservoir sediment interception in 1943, and it was used all over the world today [24, 25]:

$$STE(\%) = 100\left(1 - \frac{1}{1 + 0.0021D\dfrac{CD_{sc}}{CD_{ca}}}\right) \tag{6.1}$$

where D is the characteristic parameter describing the reservoir, and its value range is 0.046–1, CD_{sc}[L^3] is the reservoir capacity, and CD_{ca}[L^2] is the control area of the reservoir. However, this formula does not consider the change of the dam land at the same time as the storage capacity of the silt dam, and it is suitable only for a case of no spillway. Therefore, in this simulation, six observation sections are set up at the mouths of the five branch ditches connected to the dam site and the upstream river channel to monitor the runoff and sediment entering the dam site (branch sections 1–5, and upstream section 0). Based on the sediment balance, formula 6.2 calculates the sediment interception efficiency of the dam:

$$STE = \frac{\sum_{i=0}^{n} S_{input} - S_{output}}{S_{input}} \times 100\% \tag{6.2}$$

where S_{input} is the sediment flux entering the dam from the upstream branch ditch/river channel, S_{output} is the sediment flux leaving the silt dam from the spillway, and n refers to the number of each branch ditch (clockwise 1–5) and the upstream channel (0).

6.1.3. Model Building

The calculation grid used in the simulation came from the original 20 m precision digital elevation model (DEM) of the basin. First, a two-dimensional irregular triangular grid was generated based on the DEM; then, a three-dimensional numerical grid of the watershed was constructed by adding several layers of grids under the two-dimensional grid (Figure 6.3). The surface calculation grid of each simulation condition was composed of 10 062 nodes and 19 918 irregular triangular elements. The discrete steps in the horizontal direction (XY direction) of the surface grid gradually progressed from 180 m at the watershed boundary and upstream elevations to 20 m accuracy at the channel/ditch, and the accuracy of the triangular grid is enhanced near the check dam to 3–10 m. A total of 16 layers of grids representing underground spaces were added under the surface grid. Taking the elevation of 900 m as the lower boundary of the three-dimensional grid, the discrete step length between each layer of the grid in the vertical direction (Z-direction) was gradually thickened from 0.10 m (near surface) to 39.3 m (lower boundary). This discrete method not only ensured that the calculation grid had sufficient accuracy in areas where the hydrological response process is active (i.e. river channels/channels, dams, and near-surface soils) but also saves the loss of computing resources by reducing the grid accuracy in inactive places, such as watersheds and deep soils [26]. The main difference between various working conditions came from the expansion and uplift of the dam, as shown in Figure 6.3c,d.

For the three-dimensional Richards equation below the surface, the model sets the following two boundary conditions: (i) the lateral and bottom surfaces were impervious boundaries (Figure 6.3a, A-B-C-D-E and F-G-H-I-J), and (ii) at the outlet section with the lowest hydraulic gradient, the soil flow flows out from the A-B-G-F section at the outlet with a certain hydraulic gradient toward a given source and sink point (Chabagou channel) farthest downstream. The outgoing flow $Q_{b,1}$[L^3 T^{-1}] of any boundary node is calculated by formula 6.3:

$$Q_{b,1} = k_{rw}\frac{\rho_w g}{\mu_w} kA \frac{(h_1 - h_{b,pm})}{dl} \tag{6.3}$$

@seismicisolation

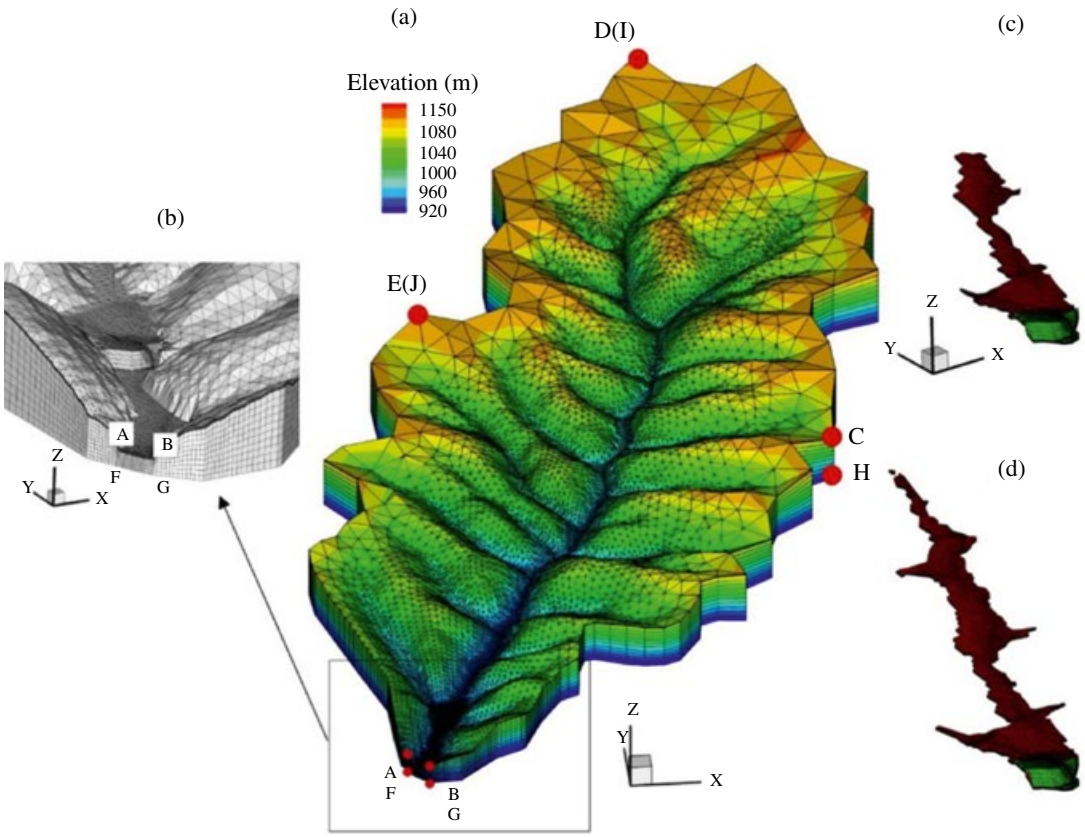

Figure 6.3 Three-dimensional mesh used in modeling: (a) the whole catchment and boundary conditions; (b) the outlet area and the outflow boundary; (c) the surface mesh representing the check dam body and its sedimentary land for the 60% silting scenario; and (d) the surface mesh representing the check dam body and its sedimentary land for the 100% silting scenario.

where k_{rw}[−] is the relative permeability of porous media soil related to saturation, ρ_w[M L^{-3}] is the density of water, g [L^{-1} T^{-2}] is the acceleration of gravity, μ_w[M L^{-1} T^{-1}] is the viscosity of water, k [L^2] is the intrinsic permeability tensor, A [L^2] is the area of the node, h_1 [L] is the total head of the source and sink, $h_{b,pm}$ [L] is the total outflow boundary point head, and dl [L] is the horizontal distance between two points. For the surface water flow equations, the two boundary conditions set by the model were the specific rainfall sequence covering the entire basin and the boundary conditions of free outflow at the outlet of the basin. In this short-duration torrential rain-flood process simulation, evaporation was not considered.

Before each formal simulation, a simulation of saturated drainage of the whole watershed lasting about one year was carried out: under no-rainfall conditions, the watershed starts to drain from a saturated state (i.e. the groundwater level is close to the surface) until the flow at the outlet of the watershed reached 0.006 m^3/s (the average base flow at the beginning of the flood season in the Shejiagou watershed). This saturated drainage process aimed to achieve an initial hydrological condition close to the actual conditions of the basin through simulation of the base flow so that the pressure head of each point inside the three-dimensional grid is continuous and approximates the actual situation [27]. The formal simulation took this condition as the initial condition and lasts for 48 hours. The rainfall process started at 3600 s and ends at 7200 s (i.e. rainfall occurs in the second hour of the simulation).

The soil of the watershed in the numerical model consisted of a layer of homogeneous near-surface (0–0.5 m) loess and another layer of homogeneous loess in the depth. This setting takes into account the differences between surface loess and deep loess and simplifies the heterogeneity of soils at different depths to a certain extent.

According to the difference of land use, the surface soil was divided into three types, namely dam silt, normal

@seismicisolation

Table 6.2 Soil parameters.

Depth (m)	Soil division	Saturated hydraulic conductivity (m s^{-1})	Porosity(–)	van Genuchten parameter		
				a(m^{-1})	n(–)	θ_r(–)
0–0.5 m	Dam silt soil	4.00×10^{-6}	0.45	0.37	1.19	0.13
	Surface loess soil	2.90×10^{-6}	0.42	1.38	1.74	0.08
	Compacted soil of dam body	4.00×10^{-10}	0.35	1.52	1.29	0.04
Under0.5 m	Loess soil in deep layer	2.70×10^{-6}	0.40	1.35	1.83	0.11
	Bedrock	1.00×10^{-9}	0.20	4.30	1.25	0.08

surface loess, and compacted soil of silt dam. Table 6.2 summarized the soil parameters used in the model to characterize soil permeability and soil water movement characteristics. Based on the measured soil water characteristic curve in the Wangmaogou watershed, the van Genuchten model was used to characterize the water movement characteristics of different soils. The formula is as follows:

$$\theta = \theta_r + \frac{(\theta_s - \theta_r)}{\left[1+(\alpha h)^n\right]^m} \tag{6.4}$$

where θ, θ_s, θ_r[L^3 L^{-3}] are soil volumetric water content, saturated volumetric water content, and residual volumetric water content, h [L] is pressure head, and α[L^{-1}] and n [−] are characteristic parameters of V-G. As mentioned earlier, the Shejiagou watershed and Wangmaogou watershed are extremely similar in topography, climate, and soil types [23, 28]. Therefore, in the absence of the Shejiagou soil sampling data, we adopted the following method to obtain the soil parameters of the Shejiagou watershed: based on the V-G parameters and saturated hydraulic conductivity of the dam soil, slope soil, and dam soil in the Wangmaogou watershed, the soil parameters of the Shejiagou watershed are obtained through model calibration.

According to the Chabagou watershed soil gradation data published by the Zizhou Runoff Experimental Station, the median diameter of the soil in the Shejiagou watershed was 0.05 mm. The simulation used this as the median diameter of the surface soil (0–0.5 m). The cohesion coefficients of the compacted soil of the dam and other soils were 0.60 and 0.30, respectively [29]. Based on the literature using soils of the same particle size [30, 31], the depth damping coefficient $c\psi$, the disturbance coefficient ξ, and the rain intensity index b that affect the kinetic energy of raindrops in the sediment module are 600 m^{-1}, 0.25, and 1.6, respectively. Table 6.3 summarized the main parameters describing surface water and sand movement in the model. The values of Manning's roughness coefficient n describing runoff movement, raindrop splash coefficient c_f describing the process of rain splash erosion and hydraulic erosion, and surface erodibility coefficient φ are determined by model calibration.

From the Shejiagou flood data, two rainfall-flood events were selected for model calibration (1964/7/14) and verification (1964/8/2). The reasons for selecting these two rain-flood events for calibration and verification are as follows: (i) the records of these two rainfall-flood events are relatively complete (rainfall process and water–sediment process) and accurate (the time step of observation and sampling is short), which is suitable for comparison between simulation and actual measurement; and (ii) the runoff and sediment yields of the selected events belong to the largest of the 31 flood events that occurred, which are typical in the simulated flood process of the Shejiagou watershed. In the calibration process, first the saturated hydraulic conductivity (*Ksat*), Manning's roughness (n), and V-G parameters are adjusted to make the simulated flow process coincide with the measured flow process; by adjusting the raindrop splash erosion coefficient (c_f) and the surface erodibility coefficient (φ), the simulated sediment transport process is consistent with the measured sediment transport process. For the simulation evaluation standard of the calibration and verification process, the Nash efficiency factor (EF) commonly used by hydrological researchers is adopted:

$$EF = \left[\sum_{i=1}^{n}\left(O_i - \bar{O}\right)^2 - \sum_{i=1}^{n}\left(S_i - O_i\right)^2\right] / \sum_{i=1}^{n}\left(O_i - \bar{O}\right)^2 \tag{6.5}$$

where O_i is the measured value, $\bar{O}$ is the average of the measured value, S_i is the analog value, and n is the number of samples used. The closer the Nash efficiency coefficient is to 1, the closer the simulated water–sediment process is to the measured water–sediment process. Generally, physics-based distributed models are used to

@seismicisolation

Table 6.3 Land surface parameters.

Land use division	Manning's roughness (–)	Runoff depth (m)	Surface micro-geomorphology height(m)	Raindrop splash coefficient $(s\ m^{-1})^{0.6}$	Surface erosion coefficient(m^{-1})
Slope	0.010	0.0015	0.0015	50.00	0.005
Channels and rivers	0.008	0.0015	0.0015	50.00	0.005
Dam land	0.008	0.0015	0.0015	0.05	0.001
Check dam	0.004	0.0015	0.0015	5.00	0.001
Source of parameters	Calibration	Document	Calibration		

simulate rainfall-flood events on a field scale. If the Nash efficiency coefficients of the runoff process and the sedimentation process are both greater than 0.65, it is an acceptable simulation effect. For example, Ni used the water and sand model (THIHMS-SW) to obtain an EF value of 0.70 in the Sanchuankou watershed of Chabagou. In this simulation, the Nash efficiency coefficients of the runoff process and the sediment transport process obtained in the calibration stage were 0.763 and 0.738, respectively; and the Nash efficiency coefficients of the runoff process and the sediment transport process obtained in the verification stage are 0.781 and 0.732, respectively. Additionally, in the calibration session, the measured and simulated sediment transport were 17 600 tons and 13 800 tons, respectively; in the verification field, the measured and simulated sediment transport were 23 000 tons and 18 800 tons, respectively. The results of the flow process line and the sediment transport process line show that the InHM model can more accurately capture the water and sand movement in the Shejiagou watershed after parameter calibration (Figure 6.4). The parameters obtained by calibration are shown in Table 6.2 and Table 6.3.

After calibration, the Manning's roughness values of the Shejiagou watershed are 0.01 $s/m^{1/3}$ (slope surface), 0.008 $s/m^{1/3}$ (main river and dam), and 0.004 $s/m^{1/3}$ (dam body). During the study period, the Shejiagou watershed was in a state of low vegetation coverage, and a large area of bare soil was the main surface cover type of the watershed [2, 32], so the Manning's roughness value obtained by calibration is small but reasonable. Similar Manning's roughness values are also used by many researchers in small watersheds with similar conditions in the Loess Plateau [23, 30, 33].

In the following content, the simulation results under different working conditions are analyzed from three aspects: the peak-shaving and detention efficiency of the silt dam, the efficiency of silt interception of the silt dam, and the erosion/siltation process on the dam.

6.2. PEAK CUTTING AND FLOOD DETENTION EFFICIENCY OF WARPING DAMS

This section will begin by outlining the changes in runoff process and sediment transport process at the outlet of the basin and will then analyze the impact of check dams on water and sediment movement under different siltation storage capacity conditions.The simulation results show that with an increase of siltation storage capacity, the control of the water and sediment process at the outlet of the basin by the silt dam system is transferred from the blocking water and sediment controlled by the dam body to the stagnant water and sediment dominated by the dam. In the heavy sedimentation stage, the silt dam system still has a certain peak cutting and flood detention efficiency.

6.2.1. Storage Capacity Threshold for Spillway Control

The simulation results showed that under a certain rainfall condition, when the siltation storage capacity of the silt dam was lower than a certain threshold (for example, under 75 mm rainfall, the threshold is 85%, as seen in Figure 6.5c), the silt dam can intercept all upstream runoff and sediment.When the siltation storage capacity falled under this threshold, the small peaks in the early stage of the water–sediment process of the same rainfall event remained consistent in different siltation conditions, for this is the hydrological response of the basin downstream of the silt dam to this rainfall event. Under a specific rainfall condition, when the siltation storage capacity of the silt dam was greater than or equal to the threshold corresponding to the rainfall, the water and sediment upstream of

@seismicisolation

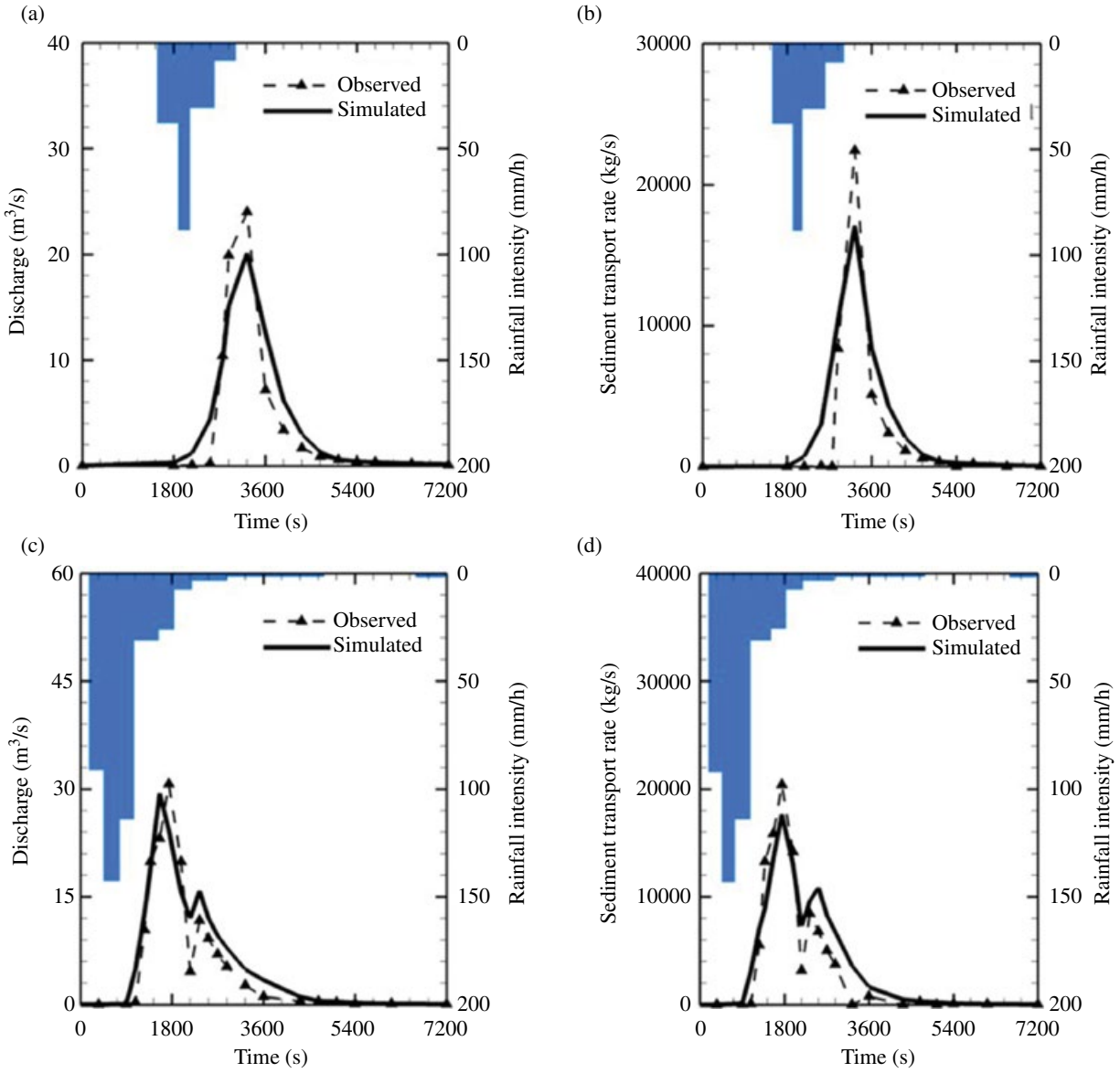

Figure 6.4 Hydrographs and sedigraphs of the model calibration and validation: (a) hydrograph of model calibration; (b) sedigraph of model calibration; (c) hydrograph of model validation; and (d) sedigraph of model validation.

the silt dam will partially enter the downstream river channel from the spillway, causing changes in the water and sediment process at the outlet of the basin. This was the second peak flow rate/sediment rate represented in Figure 6.5. The siltation storage capacity thresholds under different rainfall conditions were 100% (55 mm rainfall), 85% (75 mm rainfall), 80% (80 mm rainfall), 70% (90 mm rainfall), and 65% (100 mm rainfall). In other words, the greater the rain intensity, the faster the water- and sediment-blocking effect of the silt dam body would fail.

6.2.2. Peak Cutting and Flood Detention Efficiency of Dam Site Control

It can be seen from Figure 6.5 that under the same rainfall conditions, the water–sediment process line at the outlet of the basin was significantly different after passing through the dam under different siltation states. With the increase of the siltation storage capacity, the peak value of the water–sediment process line showed a trend of first increasing and then decreasing, and the moment of the peak also showed a trend of advance

@seismicisolation

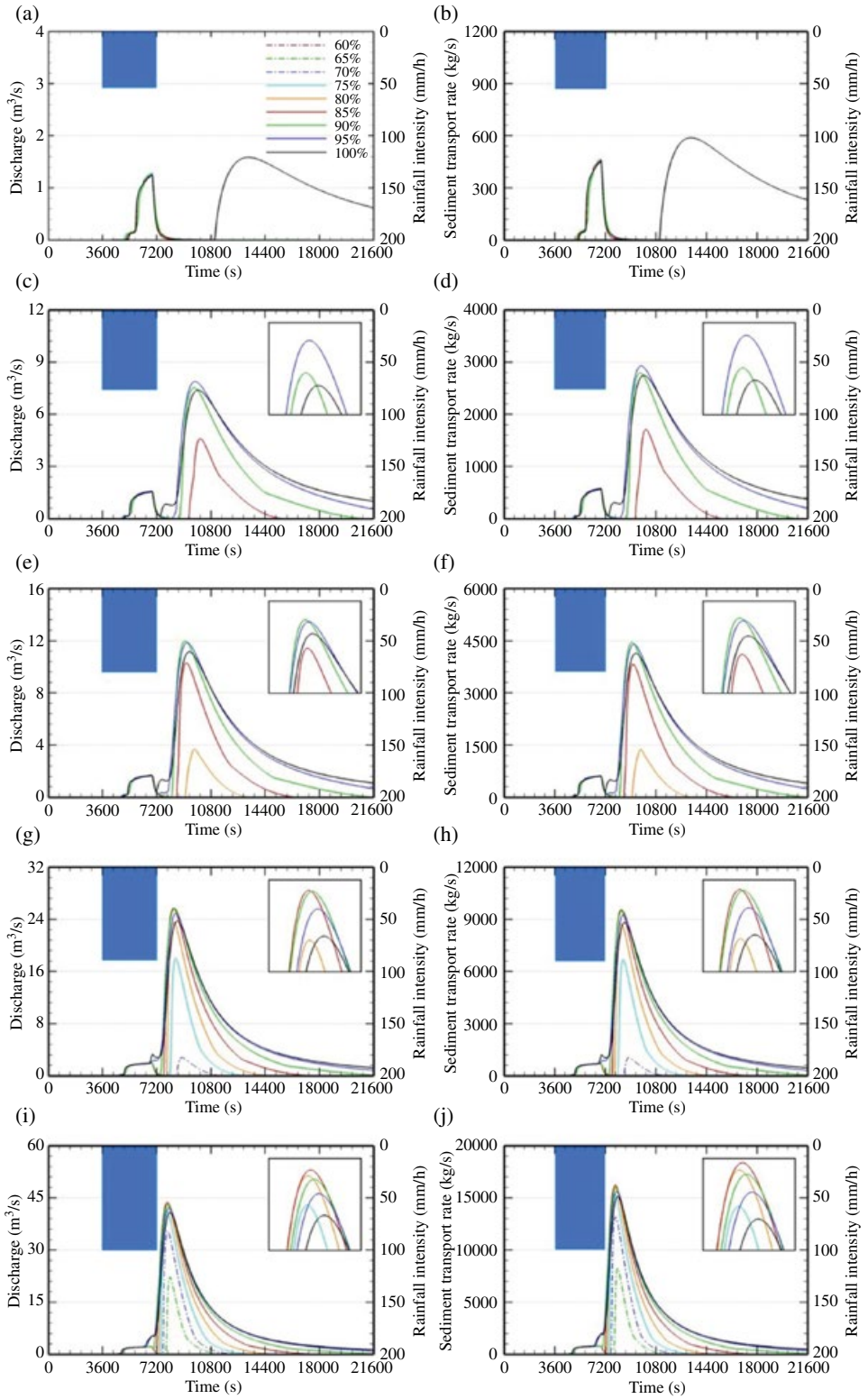

Figure 6.5 Hydrographs and sedigraphs representing the catchment outlet of the different silting scenarios under 55, 75, 80, 90, and 100 mm rainfalls. The hydrographs are in the first column, while the sedigraphs are in the second column. Different lines (colors and types) represent different silting scenarios.

@seismicisolation

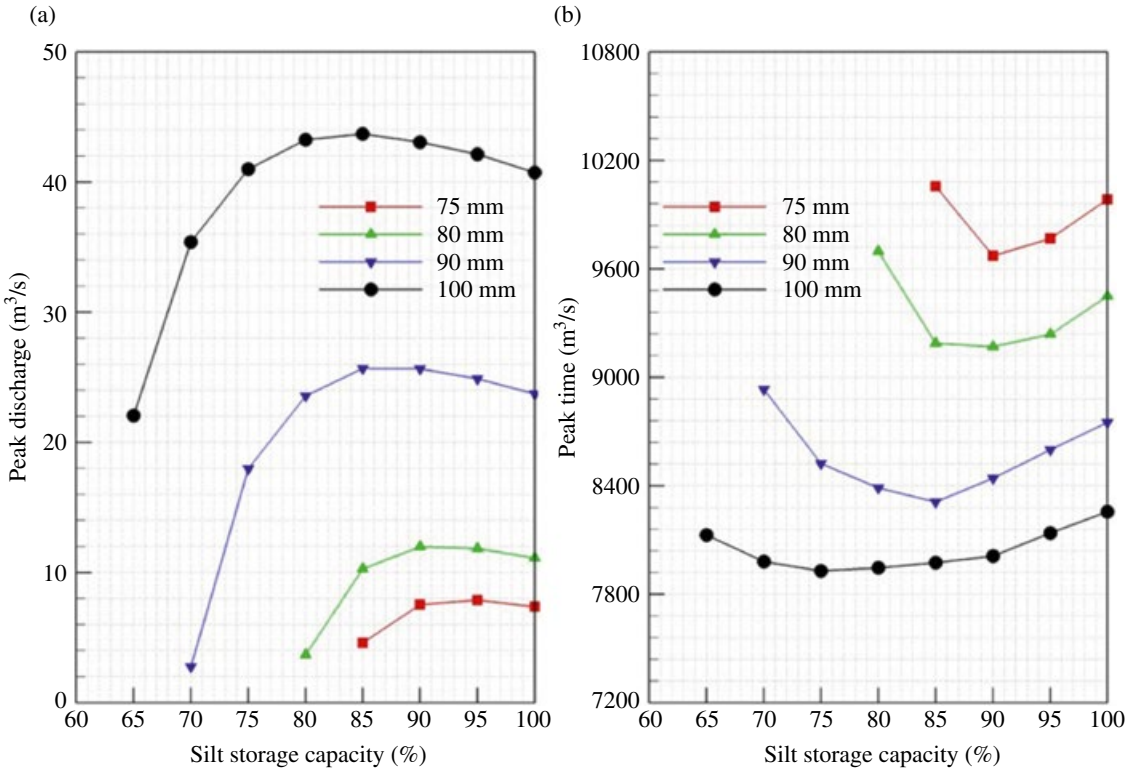

Figure 6.6 Comparison of discharge peaks for different scenarios: (a) discharge peak and (b) peak time.

and then delay. For example, under 90 mm rainfall, as the silt storage capacity increases from 70 to 85%, the peak flow rate increased from 2.76 to 25.69 m^3/s; as the silt storage capacity increased from 85 to 100%, the peak flow rate increased to 25.69 m^3/s, then was reduced to 23.75 m^3/s (Figure 6.6). Correspondingly, the occurrence time of the flow peak first advanced from 8928 s (28.8 minutes after the rain ended) to 8310 s and then was delayed from 8310 to 8748 s. Taking the 90-mm rainfall condition as an example, when the siltation storage capacity threshold controlled by the spillway (i.e. 70% siltation storage capacity) was exceeded, the hindering effect of the check dam on runoff weakens until it disappeared. This caused the peak value of runoff to increase and advance with the elevation of the dam. However, as the dam area continues to increase, the weakening effect of the dam on the runoff velocity moving on it also increased (Table 6.4) until it began to dominate (i.e. 85% siltation storage capacity). Under 90 mm rainfall, the peak-shaving and flood detention efficiency of the dam site for water and sand movement gradually appeared and continued to increase when 85% of the siltation storage capacity is reached. Compared with the maximum runoff peak at the outlet of the basin under various rainfall conditions, the peak runoff under the condition of 100% siltation storage capacity was reduced by 6.23% (75 mm rainfall), 7.27% (80 mm rainfall), 7.67% (90 mm rainfall), and 6.73% (100 mm rainfall). At the same time, under 75, 80, 90, and 100 mm rainfall, the peak runoff was delayed by 217 s (2.22%), 279 s (3.04%), 438 s (5.27%), and 283 s (3.55%), respectively. It can be seen that in a state of heavy siltation, even when the designed storage capacity

Table 6.4 Average flow velocity during peak time under a 90-mm rainfall condition.

Sedimentation conditions (%)	Average velocity at peak runoff in dam land(m/s)
60	0.31
65	0.46
70	0.87
75	0.83
80	0.59
85	0.43
90	0.40
95	0.29
100	0.24

@seismicisolation

is reached, the silt dam can play a significant role in reducing the peak of water and sand movement. When there are multiple cascading silt dams in the watershed, this inhibitory effect will be effectively amplified.

6.3. SILT INTERCEPTION EFFICIENCY OF SILT DAM

Starting from the balance of sediment on the dam, this section quantitatively analyzed the sediment interception efficiency of the silt dam system under different storage capacity conditions [34]. The simulation results showed that the sediment interception efficiency of the silt dam system was mainly divided into two parts: the direct sedimentation efficiency of the main dam site and the indirect erosion reduction efficiency of the branch trench caused by the expansion of the dam site.

6.3.1. Sediment Interception Efficiency

The simulation results showed that the sediment interception efficiency (STE) of the dam site generally decreased with the increase of the silt storage capacity, but the trend of sharp decline in STE was slowed down when the silt dam was about to reach the designed storage capacity (Figure 6.7). For example, under 90 mm rainfall, when the silt storage capacity increases from 70 to 95%, the sediment interception efficiency droped from 97.66 to 25.83%. However, as the silt storage capacity approaches a full state, the downward trend of sediment interception efficiency was weakened. In particular, under 100 mm heavy rainfall, the sediment interception efficiency (19.09%) in the state of 100% siltation storage capacity was even slightly greater than that of the 95% silt storage capacity condition (17.34%).

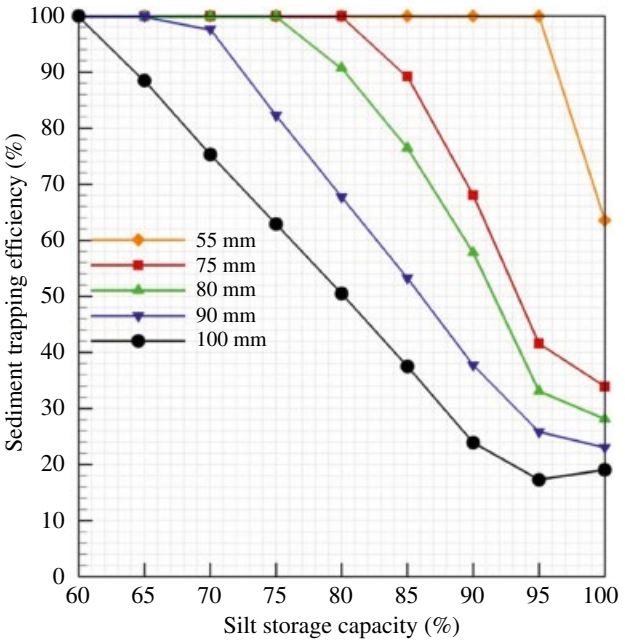

Figure 6.7 Sediment trapping efficiency (STE) at different silting scenarios under five rainfall conditions.

6.3.2. Direct Sedimentation Efficiency of the Dam

Under five different rainfall conditions, the silt interception efficiency under full siltation was 63.59, 33.94, 28.14, 23.03 and 19.09% (Figure 6.7). This showed that even if the silt dam was full under the designed storage capacity, a large amount of sediment will still be deposited in the control area of the silt dam during a flood. For example, after a runoff–sediment process caused by 90 mm rainfall, 11 700 tons of sediment (23.03%) are still left on the dam under 100% siltation conditions. In Table 6.5, the water and sediment interception efficiency of the dam under three conditions of no dam, 60% silt storage capacity, and 100% silt storage capacity are compared. Under the condition of non-silt dam, the original river channel where the dam is located will scour 5300 tons of sediment. Under the condition of 100% silt storage capacity, the dam site directly intercepts 11 700 tons of sediment and indirectly reduces the incoming sediment by 7600 tons, and the overall sediment reduction efficiency reaches 24 600 tons.

In Figure 6.8, the sand transport process at the tail section and heel section of the dam ground under the conditions of 90 mm rainfall under three storage capacity conditions (60, 80, and 100%) was compared. The following two phenomena can be summarized: (i) with the intensification of siltation, the cumulative sediment transport difference between the two sections was gradually shrinking; that is, the sediment interception capacity of the dam is weakening [10]. This phenomenon was consistent with the change trend of STE in Figure 6.7. (ii) With the intensification of siltation, the amount of sediment transported at the tail section of the reservoir droped from 49 000 tons under the 60% silt storage capacity condition to 46 000 tons under the 100% silt storage capacity condition. Phenomenon 2 showed that the expansion and uplift of the dam site reduced the amount of sediment (i.e. S_{input0}) entering the dam site from the upstream channel. It can be inferred that the dam site's influence on the water–sediment process is larger than the boundary of the dam site itself [35].

@seismicisolation

Table 6.5 Comparison of sediment and water reduction efficiency in three scenarios under a 90-mm rainfall condition.

Condition	No dam	60% storage of sedimentation	100% storage of sedimentation
Total sediment input (10^4 t)	5.84	5.67	5.08
Total sediment output (10^4 t)	6.37	0	3.91
Sediment trapping amount in dam land and river(10^4 t)	−0.53	5.67	1.17
Total inflow (mm)	34.46	31.80	29.83
Total outflow (mm)	37.50	0	24.97
Water retention in dam land and river(mm)	−3.04	31.80	4.86
Sediment trapping efficiency (STE) (%)	−9.07	100	23.03
Runoff trapping efficiency(RTE) (%)	−8.82	100	16.29

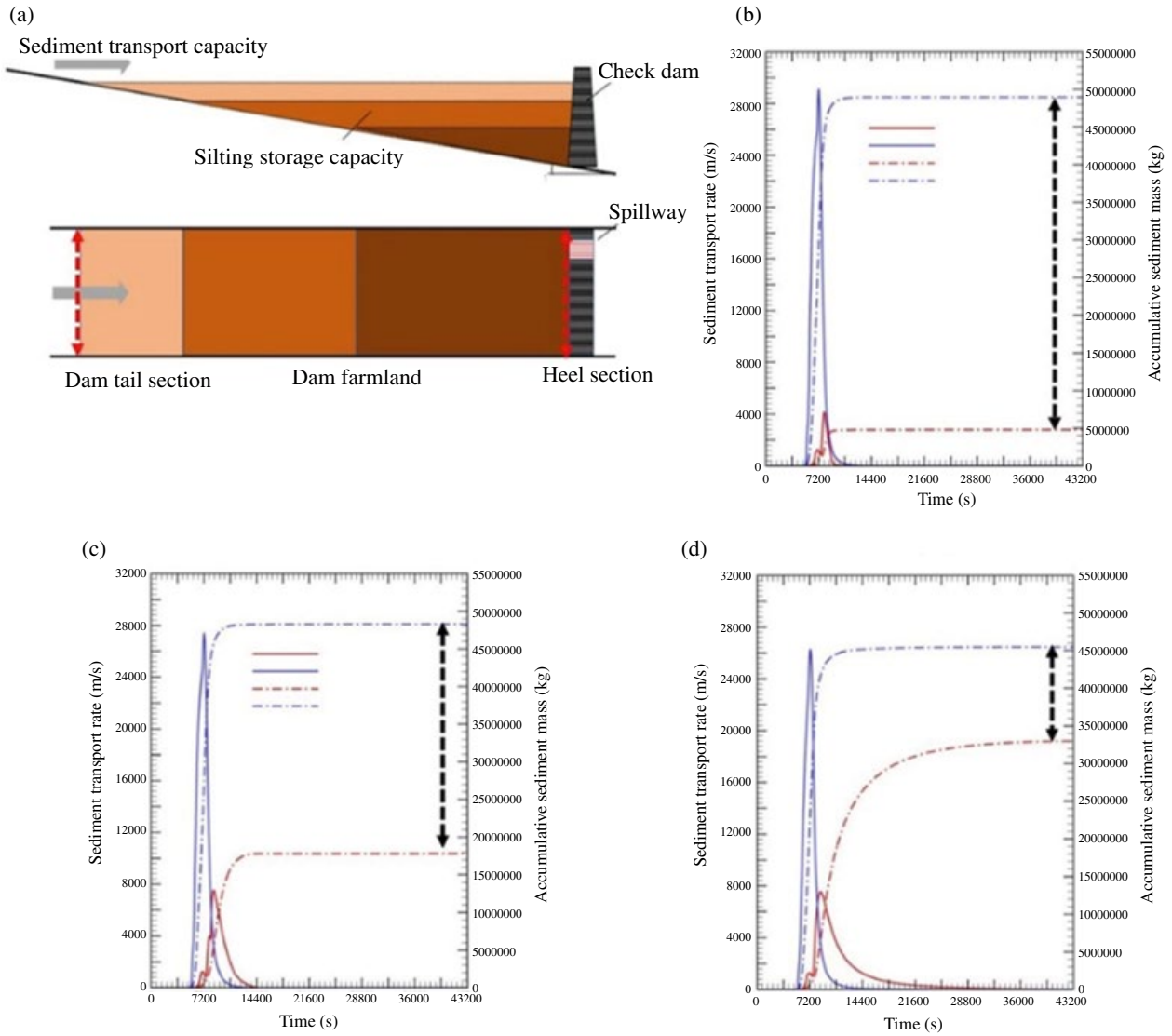

Figure 6.8 Comparison of sediment discharge and accumulative sediment mass through two observation cross sections under a 90-mm rainfall condition: (a) schematic diagram; (b) 60% silting scenario; (c) 80% silting scenario; and (d) 100% silting scenario.

@seismicisolation

Based on the sediment balance formula, the direct sedimentation efficiency of the silt dam system can be obtained from the input and output difference; the indirect erosion reduction efficiency of the silt dam system can be obtained from the change of the sediment input value. The above results showed that the silt dam system still had a very considerable direct sedimentation efficiency in the heavy sedimentation stage, and that a large number of silt dams on the Loess Plateau in the heavy sedimentation stage still had a sediment retention capacity that cannot be ignored during flood conditions.

6.3.3. Indirect Erosion Reduction Efficiency of Dam

6.3.3.1. Indirect Sediment Reduction Efficiency (ISTE)

Taking a 90-mm rainfall condition as an example, in Table 6.6, the sediment balance of the dam under different siltation conditions was compared. Table 6.7 compares the direct and indirect sediment interception efficiency under different rainfall conditions under a 100% siltation storage capacity condition. The indirect sediment interception efficiency (ISTE) is calculated as follows:

$$ISTE = \frac{\sum_{i=0}^{n} S_{input,p\%} - \sum_{i=0}^{n} S_{input,60\%}}{\sum_{i=0}^{n} S_{input,60\%}} \% \qquad (6.6)$$

where $S_{input,p\%}$ refers to the sediment flux entering the dam from the upstream branch trench/channel when the sediment storage capacity is p%, and n refers to the number of each branch trench (clockwise 1–5) and upstream channel (0). Under the same rainfall conditions, the direct sediment interception efficiency of the silt dam system decreases with the increase of sedimentation, but the indirect sediment interception efficiency gradually increases with the increase of sedimentation. In the case of full siltation, the direct sediment interception efficiency decreases with the increase of rainfall intensity, while the indirect sediment interception efficiency increases with the increase of rainfall intensity.

In fact, with the intensification of siltation, the input of sediment into the dam was continuously reduced, indicating that the impact of the silt dam on runoff and sediment would extend to the upstream river channel and branch trench [36]. On the dam site, the surface runoff velocity not only decreases when it enters the dam site but also decreases further upstream due to the influence of tailwater. The tailwater area of the silt dam reservoir area expanded with the uplift and expansion of the dam, causing runoff with a large amount of sediment to decelerate further and further upstream of the dam. Therefore, the sedimentation process in the upstream non-dam area had been locally enhanced (in other words, the erosion of the upstream non-dam area by the water flow is locally suppressed). Similar tailwater effects often occur at the ends of large reservoirs [27]

Table 6.7 Comparison of STE and ISTE in 100% silting scenario under different rainfall conditions.

Rainfall conditions (mm)	STE(%)	ISTE(%)
55	63.59	3.76
75	33.94	7.79
80	28.14	8.22
90	23.03	10.41
100	19.09	9.01

Table 6.6 Sediment budget of the sedimentary land under a 90-mm rainfall condition.

Sedimentation conditions(%)	Sediment input from upper branch S_{sum}[a]($\times 10^4$ t)	Sediment output at dam site S_{output}($\times 10^4$ t)	STE(%)	ISTE(%)
60	5.67	0	100.00	—
65	5.66	0	100.00	0.18
70	5.56	0.13	97.66	1.94
75	5.42	0.96	82.29	4.41
80	5.39	1.74	67.72	4.94
85	5.37	2.51	53.26	5.29
90	5.14	3.20	37.74	9.25
95	5.11	3.79	25.83	9.35
100	5.08	3.91	23.03	10.41

[a] S_{sum} refers to the total sediment from five branches connected with the dam and six upper observation sections along the river.

@seismicisolation

and estuary deltas [37]. However, this phenomenon was rarely involved in the evaluation of water and sediment interception efficiency of silt dams and has not been quantitatively evaluated.

6.3.3.2. Branch Test

In order to quantitatively study the impact of expansion of the warping dam on the branch ditch, we chose No. 1 branch ditch as the research object and analyzed its sediment balance under different siltation conditions under the condition of 90 mm rainfall. A branch ditch connected to the dam site was selected as the research object in order to quantitatively study the influence of the dam site tailwater effect on the channel sediment flux. In this scenario, a control section is established upstream of the selected branch trench (Figure 6.9).This control section is far enough away from the outlet of the branch ditch that its sediment flux will not change under any siltation storage capacity conditions (i.e. it will not be affected by the dam site and its tailwater).Then, an output section is set up at the junction of the branch ditch and the main dam (Figure 6.9). This output section is the branch ditch–dam junction section under the 60% siltation storage capacity condition. In addition, we set up a series of observation sections between the control section and the output section under various silt storage capacity conditions. These sections are the interface between the dam land that expands into the branch trench and the original channel under different siltation storage capacity conditions. By calculating the sediment flux through these observation sections, we quantitatively analyze the impact of dam expansion on the erosion/siltation process in the branch trench.

Simulation results showed that the sediment flux of the observation section decreases with the expansion and uplift of the dam, and that the influence range of the sediment reduction efficiency also expands upstream with the expansion of the dam. Before the dam land expanded to the observation section, the sediment flux on the observation section had already begun to decrease. This phenomenon showed that the dam's scope of influence was larger than the boundary of the dam itself. For example, taking the dam boundary under 80% siltation condition as the observation section, it can be found that the sediment flux through this observation section under different siltation storage capacity conditions is significantly different:

a. The sediment flux through the observation section under the 65% siltation condition is the same as the sediment flux through this section under the 60% siltation condition, which is 3235.70 tons. Because the sedimentation caused by the deceleration of tailwater at this time mainly occurs in the downstream of the observation section, it fails to affect the sediment flux of the observation section, as shown in Figure 6.9a.

b. The sediment flux through the observation section under 70 and 75% siltation conditions is reduced by 11.78 tons (0.36%) and 64.80 tons (2.00%), respectively, compared with 65% siltation conditions. At this time, the surface water depth at the end of the dam site is 1.95 and 1.79 m, respectively, and the tailwater flows over the dam site under the condition of 80% siltation storage capacity. Therefore, the sedimentation caused by the deceleration of tailwater has occurred in the upstream of the observation section, which slightly reduces the sediment flux of the observation section, as shown in Figure 6.9b.

c. When the silt dam expands to the location of the observation section, or even further upstream, the sedimentation process caused by tailwater becomes more intense. As shown in Figure 6.9c, the sediment flux through the same observation section under the 80% siltation storage capacity condition is only 2970.10 tons, which is 265.60 tons (8.21%) less than under the 60 and 65% siltation conditions.Under this working condition, the tailwater area extends to 25 m upstream of the observation section along with the expansion of the dam. In the tailwater boundary area, the surface runoff velocity decreases from 2.88 to 0.34 m/s, and the tailwater depth reaches 1.53 m.

With regard to the sediment balance in the branch trench, as the siltation storage capacity increases from 60 to 100%, the deceleration effect of the tailwater and the dam site increasingly reduced the sediment flux from the branch trench into the dam site. Under 60% siltation conditions, the sediment fluxes of the control section and the output section were 3207.10 tons and 3251.20 tons, respectively. That is, the runoff eroded 44.10 tons of sediment during the process of flowing through the branch ditch into the dam, leaving the branch ditch in an eroded state (Figure 6.10a). Under the condition of 100% silt storage capacity, the sediment flux of the control section and the output section were 3207.10 tons and 2490.50 tons, respectively. That is to say, the runoff not only fails to erode the soil in the branch ditch but also deposits 716.60 tons of sediment in the branch ditch, creating a silting state (Figure 6.10b). In other words, after the dam site expanded from a section of 60% siltation storage capacity to a section of

@seismicisolation
@seismicisolation

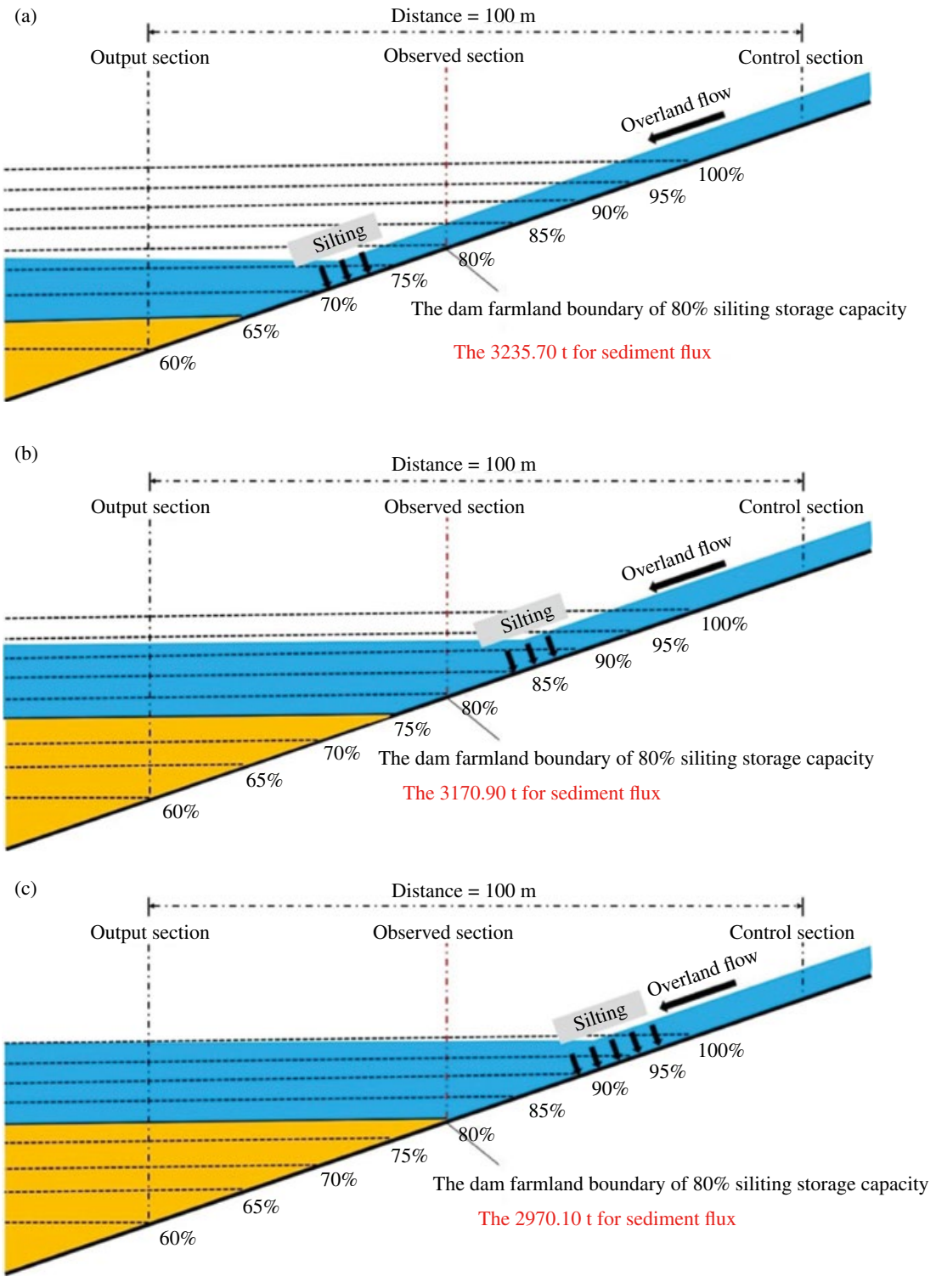

Figure 6.9 Comparison of sediment flux through the observation cross section: (a) 65% silting scenario; (b) 75% silting scenario; and (c) 80% silting scenario.

@seismicisolation

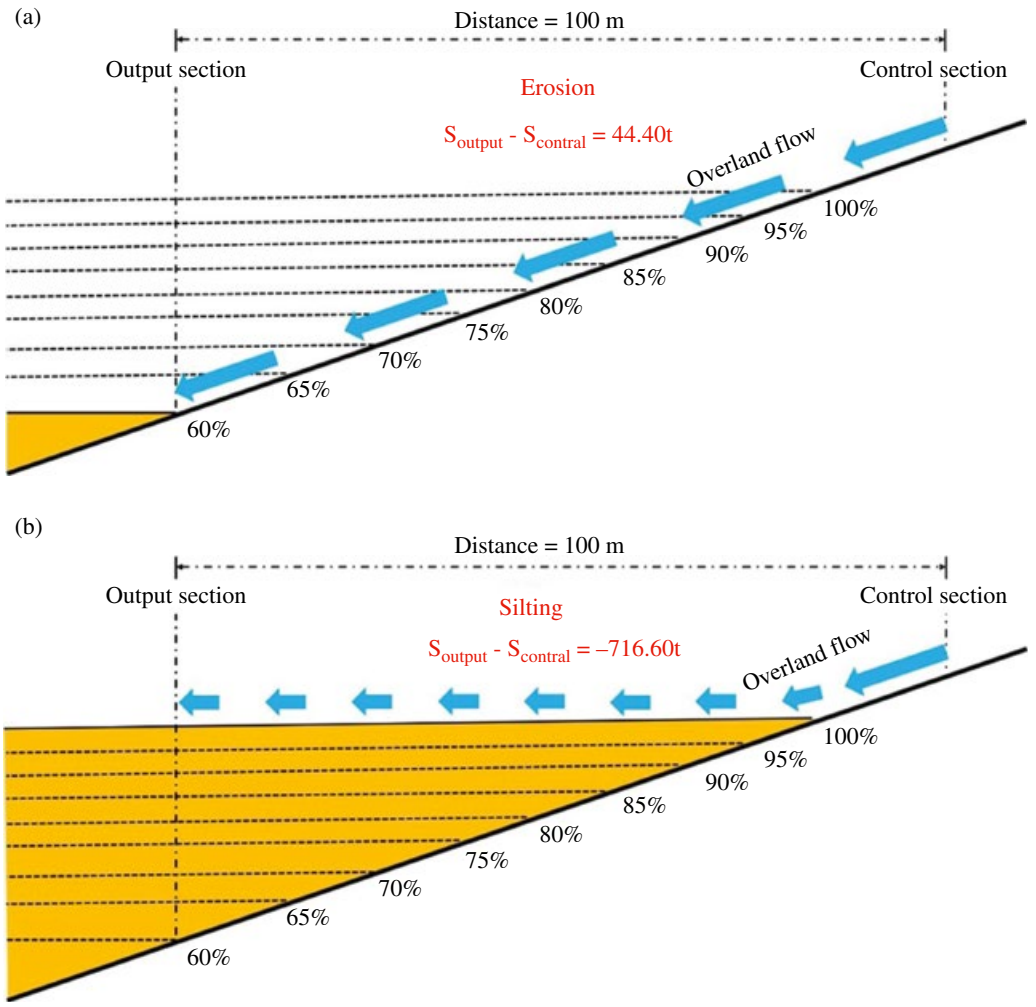

Figure 6.10 Comparison of erosion/deposition mass in the gully reach: (a) 60% silting scenario and (b) 100% silting scenario.

100% siltation storage capacity, the dam site has produced 760.70 tons of sediment reduction benefits in the branch ditch, causing the branch ditch to shift from an erosion state to a siltation state.

Based on the above simulation results, it can be determined that during the expansion and uplifting of the dam, there is a gradually increasing indirect erosion reduction effect on the branch gully. This effect mainly comes from the deceleration of runoff at the junction of the dam and the upstream channel, tailwater, and upstream runoff. With the extension and uplift of the dam, the overall slope of the channel will decrease; erosion base level rises and stagnant water occurs at the end of the dam of each channel to slow down the sedimentation. This in turn causes the overall sedimentation process in the basin to develop upstream and even changes the erosion and deposition relationship in the branch trench. Unlike the direct sedimentation efficiency of the dam, its indirect erosion reduction efficiency increases with the intensification of the sedimentation process and reaches its maximum after arriving at 100% sedimentation storage capacity. This conclusion implies that a large number of existing check dams on the Loess Plateau in the heavy sedimentation stage still play an important role in reducing branch gully erosion and enhancing channel stability.

6.4. DIFFERENCES IN SCOURING AND SILTING PATTERNS ON THE DAM

6.4.1. Erosion and Deposition Process on the Dam

Taking the 90-mm rainfall condition as an example, Figures 6.11–6.13 showed the water and sand movement process on the dam under three siltation storage

@seismicisolation

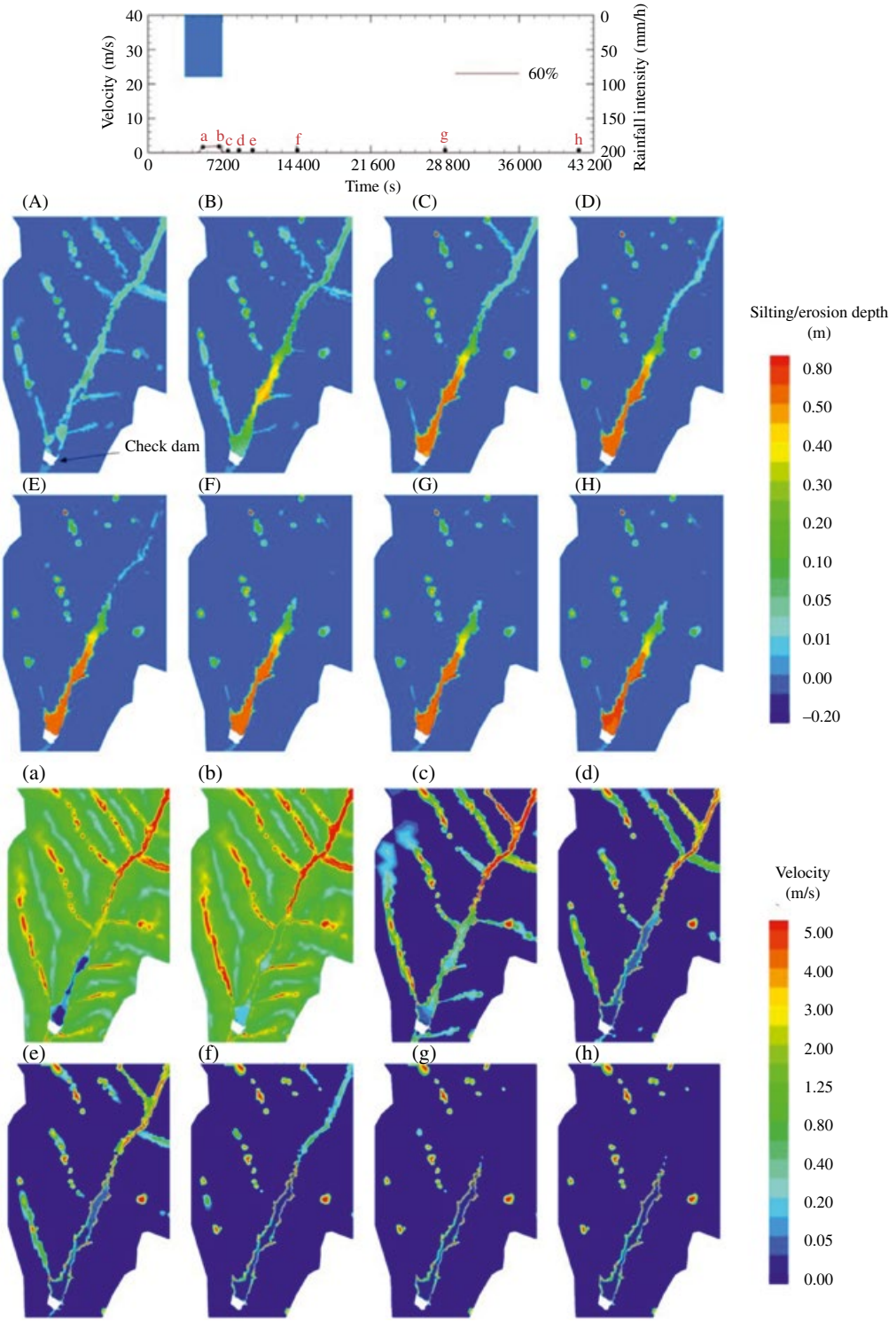

Figure 6.11 Snapshots of erosion/deposition distribution and the surface flow velocity of the 60% silting scenario under a 90-mm rainfall condition.

@seismicisolation

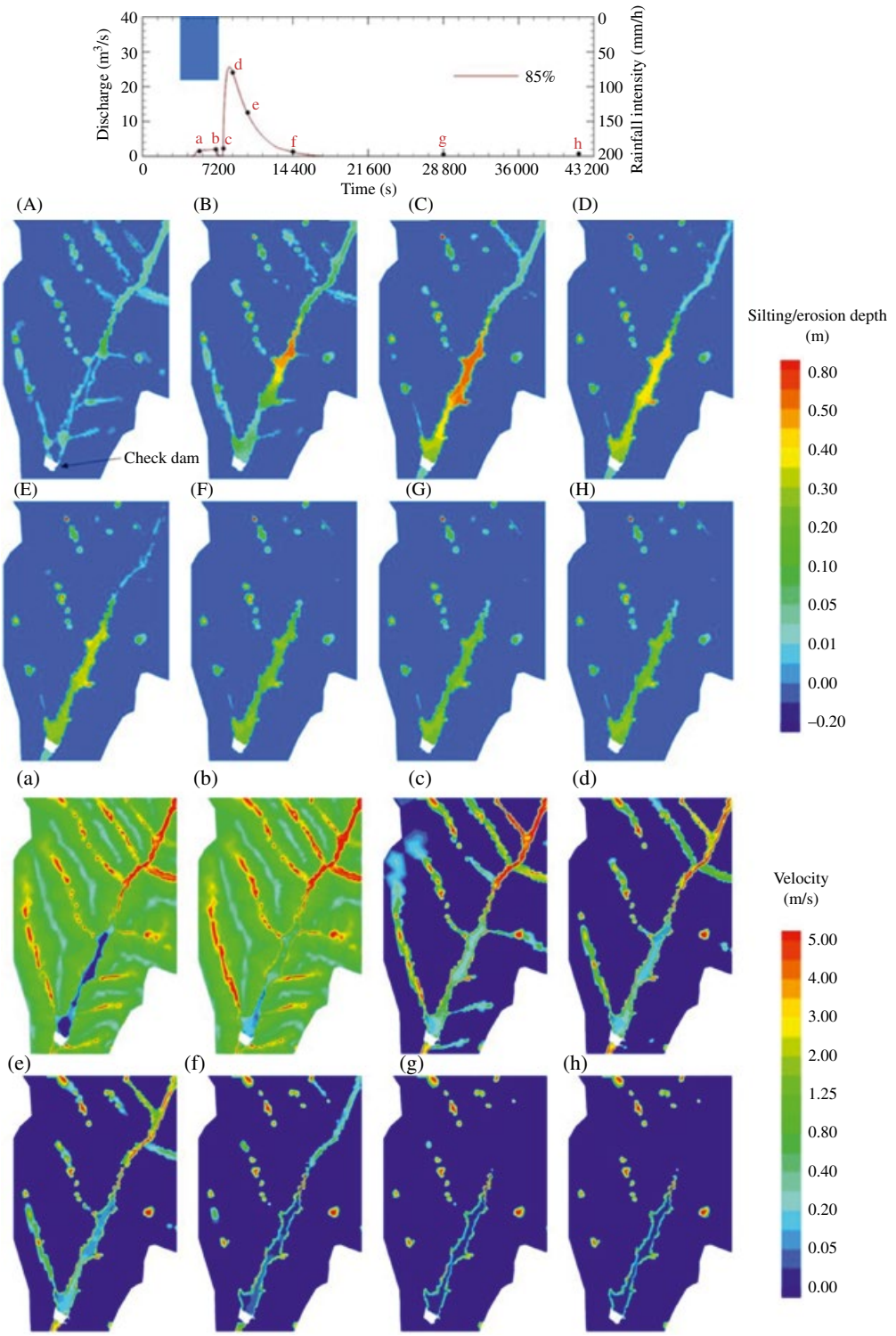

Figure 6.12 Snapshots of erosion/deposition distribution and the surface flow velocity of the 85% silting scenario under a 90-mm rainfall condition.

@seismicisolation

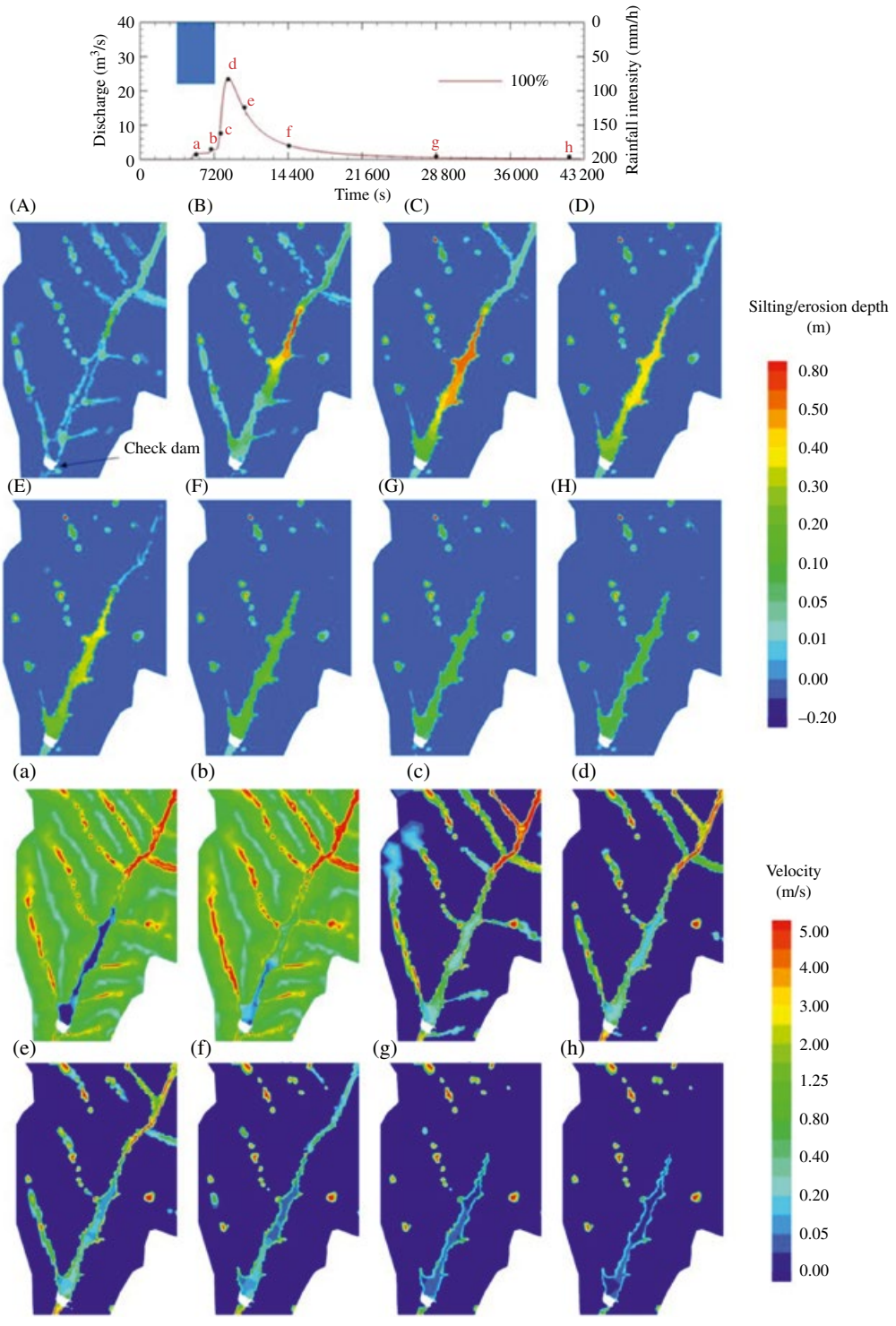

Figure 6.13 Snapshots of erosion/deposition distribution and the surface flow velocity of the 100% silting scenario under a 90-mm rainfall condition.

@seismicisolation

capacity conditions of 60, 85, and 100%. The same phenomenon is seen under all three working conditions: during the initial stage of the flood process, when the surface runoff enters the dam from the upstream channel/branch, the average flow velocity at the end of the reservoir decreases from 3.0 to 0.6 m/s; at the same time, sediment begins to deposit at the end of the reservoir (as shown in Figures 6.11 and 6.12, and periods a and b in Figure 6.13). However, there are differences in the scouring and silting process of sediment under different siltation conditions during periods of rising water and flood peaks. Under the 60% siltation condition, the sediment movement on the dam is still dominated by siltation, and an increasing amount of sediment is deposited at the front end of the dam (the area near the dam body) (Figure 6.11a–h). Under the conditions of 85 and 100% siltation, the sediment siltated in the rear area of the reservoir in the early stage will be scoured downstream during flood and peak periods. That is to say, during this period, the movement of sediment on the dam is dominated by erosion, and the originally siltated sediment has undergone "re-transportation." During the receding stage, sediment deposition occurs again.

The above results indicated that with the increase of siltation storage capacity, the process of water and sediment movement on the dam in a rainfall-flood event changed from a "sedimentation process mainly" to a "siltation-erosion-silting" process. For a silt dam system in the heavy siltation stage, the early siltation process mainly occurred in the rear area of the reservoir due to a decrease in runoff velocity after entering the dam and a weakening of the runoff's sediment-carrying capacity caused by lower flow depth. The mid-term scouring ("re-transportation") process mainly transported part of the sediment originally deposited at the tail of the silo to the downstream. This was because when the runoff that surges during flood and peak periods converged and reached the end of the dam, a phenomenon of increased sediment-carrying capacity of the local runoff was formed in the reservoir tail area. As shown in Figure 6.14, the maximum sediment-carrying capacity of the dam under the 100% siltation condition is 19.70 and 337.50 kg/m^3 at the time

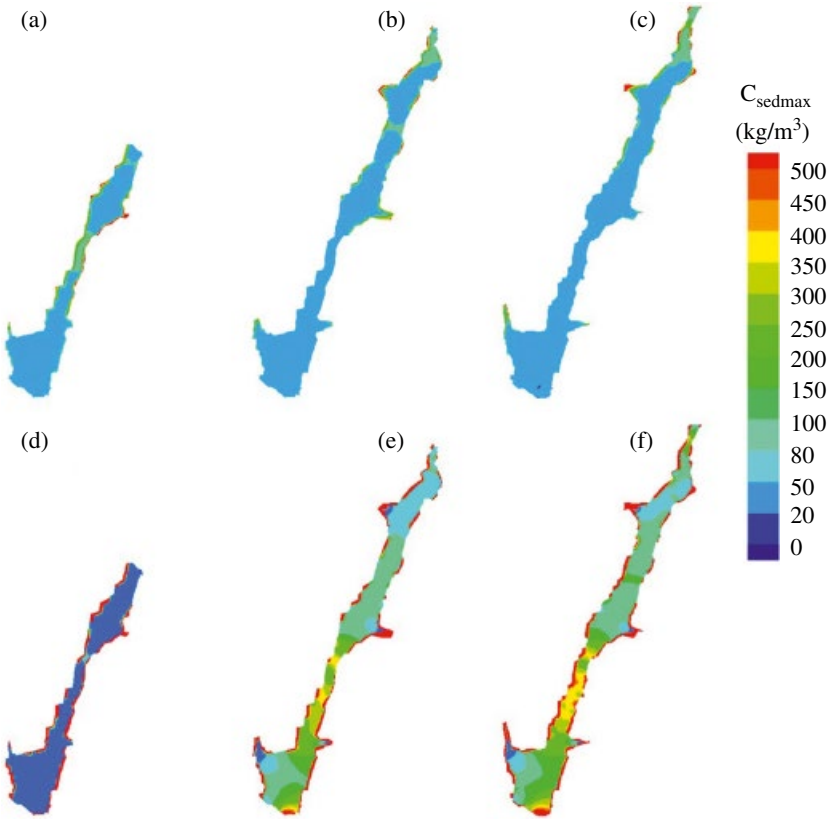

Figure 6.14 Distribution of sediment transport capacity at the start of rising limb (the first row) and peak time (the second row). The first column: 60% silting scenario; the second column: 85% silting scenario; the third column: 100% silting scenario.

@seismicisolation

of initial water rised and the peak of flow appeared, respectively. The sedimentation process in the late stage of receding water is mainly due to the sedimentation of particles caused by the decreased flow rate (decrease of flow velocity and water depth).

6.4.2. Final Distribution Law of Sediment

Figure 6.15 compared the final distribution of sediment under different siltation conditions and under 90-mm rainfall conditions. (a) (b) (c) was the distribution of erosion/siltation in the whole basin, and (d) (e) (f) was the distribution of sediment on the dam. From the perspective of the basin as a whole, erosion mainly occurred on slopes and gullies, while siltation mainly occurred on dams. Under different siltation conditions, the distribution of sediment on the dam was significantly different (Figure 6.15d–f). In the 60% siltation condition, a thick silt layer with relatively uniform distribution is formed on the dam. Under 85 and 100% siltation conditions, the thickness of the siltation layer on the dam was thin and unevenly distributed.

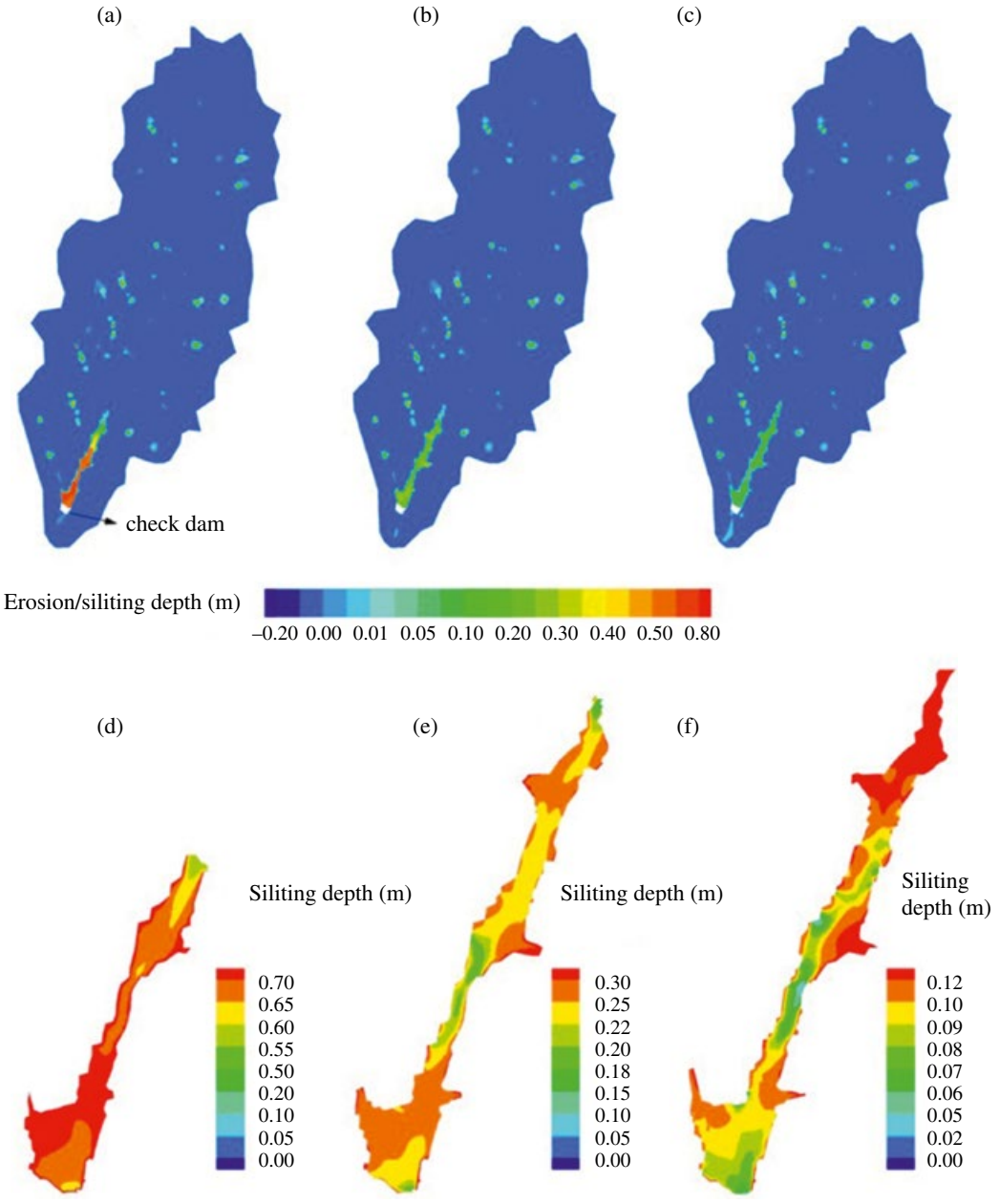

Figure 6.15 Final distribution of erosion and deposition of the catchment (a, b, c) and the sedimentary land (d, e, f) for the 60, 85, and 100% silting scenarios under a 90-mm rainfall condition.

@seismicisolation

Under the 60% siltation condition, the final sedimentation was mainly in the area close to the dam body, and the maximum siltation thickness (about 0.70 m) appeared on the boundary line between the dam and the slope (Figure 6.15d). Under the condition of 100% siltation, the final sedimentation was mainly at the end of the reservoir and the junction of the dam–branch trench, and the maximum siltation thickness also appeared here (Figure 6.15f).

Precisely describing the distribution of sediment on the dam after a flood event was of great significance to the evaluation of soil and water conservation measures. In previous studies, the silt layer, as an important feature of silt dams, was often used to reproduce the historical flood process of the river basin. Estimating the amount of erosion and the amount of carbon sequestration in the watershed under the influence of soil and water conservation measures were important methods for research hotspots.The simulation of the sedimentation process and the final distribution of the sediment on the dam will help to better guide the sediment sampling process on the dam and obtain more detailed and accurate sedimentation data in future research work.

6.5. CONCLUSION

1. The mechanism of check dam to intercept water and sediment is changed from "dam-dominated block" in light silting stage to "sedimentary-land-dominated slowing down" in heavy silting stage. The extended dam land as a buffer zone effectively reduces the flow rate of the flood. When the siltation amount reaches the designed reservoir capacity, the dam land has a significant effect of peak clipping and flood detention, which can reduce the flood peak by 7.69%, and the flood detention is about 5-8 minutes.

2. A heavy silting check dam can directly trap sediment on the dam land and indirectly attenuate erosion (or promote deposition) in tail-end area and gully-head areas. As the silting storage capacity reaching designed reservoir capacity, the indirect efficiency is increasing while the direct efficiency is decreasing but still non-negligible, making most of the sediment deposit in the tail-end area and gully-head areas. For a heavy silting check dam which reaches its designed reservoir capacity, its can still directly trap around 11 700 tons sediment and indirectly reduce 760.70 tons sediment yield for a single sub-gully in a 90-mm/hr rainfall event.

3. With the increase of siltation and the uplift and expansion of the dam land, the movement process of sediment on the dam land has changed from "mainly siltation" to "siltation-erosion-siltation." In addition, during the severe siltation stage, the sediment on the dam land is mainly distributed in the area at the end of the reservoir and the junction area between the branch and the dam land.

REFERENCES

1. Heppner, C.S. and Loague, K. (2008). A dam problem: simulated upstream impacts for a Searsville-like watershed. *Ecohydrology 1* (4): 408–424.
2. Ran, Q.H., Shi, Z.N., and Zhao, J.J. (2012a). Impact of moving rainfall on soil erosion based on crust characteristics. *Journal of Tsinghua University (Science and Technology) 52* (06): 821–829.
3. Boix-Fayos, C., Barbera, G.G., and Lopez-Bermudez, F. (2007). Effects of check dams, reforestation and land-use changes on river channel morphology: case study of the Rogativa catchment (Murcia, Spain). *Geomorphology 91* (1–2): 103–123.
4. Huang, J.B., Hinokidani, O., and Yasuda, H. (2013). Effects of the check dam system on water redistribution in the Chinese Loess Plateau. *Journal of Hydrologic Engineering 18* (8): 929–940.
5. Ran, Q.H., Loague, K., and Vanderkwaak, J.E. (2012b). Hydrologic-response-driven sediment transport at a regional scale, process-based simulation. *Hydrological Processes 26* (2): 159–167.
6. Xu, Y.D., Fu, B.J., and He, C.S. (2013). Assessing the hydrological effect of the check dams in the Loess Plateau, China, by model simulation. *Hydrology and Earth System Sciences 17* (6): 2185–2193.
7. Ran, Q.H., Shi, Z.N., and Xu, Y.P. (2013). Impacts of moving rainfall on sediment concentration of soil erosion. *Journal of Zhejiang University (Engineering Science) 47* (05): 803–811.
8. Mirus, B.B., Ebel, B.A., and Loague, K. (2007). Simulated effect of a forest road on near-surface hydrologic response: redux. *Earth Surface Processes and Landforms 32* (1): 126–142.
9. Priestley, C.H.B. and Taylor, R.J. (1972). On the assessment of surface heat flux and evaporation using large-scale parameters. *Monthly Weather Review 100* (2): 81–92.
10. Kingsford, R.T. (2000). Ecological impacts of dams, water diversions and river management on floodplain wetlands in Australia. *Austral Ecology 25* (2): 109–127.

@seismicisolation

11. Carr, A.E., Loague, K., and Vanderkwaak, J.E. (2014). Hydrologic-response simulations for the North Fork of Caspar Creek: second-growth, clear-cut, new-growth, and cumulative watershed effect scenarios. *Hydrological Processes 28* (3): 1476–1494.
12. Richards, L.A. (1931). Capillary conduction of liquids through poros mediums. *Physics 1* (5): 318–333.
13. Li, P., Mu, X., and Holden, J. (2017). Comparison of soil erosion models used to study the Chinese Loess Plateau. *Earth-Science Reviews 170*: 17–30.
14. Wang, X.Y. (2003). *Study on the Characters of Erosion Intensity Evolvement in Yangou Watershed*. Northwest Agriculture and Forestry university.
15. Penman, H.L. (1948). Natural evaporation from open water, base soil and grass. *Proceedings Of the Royal Society Of London Series a-Mathematical And Physical Sciences 193* (1032): 120.
16. Woolhiser, D.A.S., Goodrich, D.C., and Kineros, A. (1990). *Kinematic Runoff and Erosion Model: Documentation and User Manual, ARS-77*. Fort Collins, Colorado: USDA Agricultural Research Service.
17. Yuan, S.L. (2017). *Study on the Regulation Effect and Simulation of Check Dam System on the Dynamic Process of Water and Sediment in Basin*. Xi'an University Technology.
18. Lemzi, M.A. and Comiti, F. (2003). Local scouring and morphological adjustments in steep channels with check-dam sequences. *Geomorphology 55* (1–4): 97–109.
19. Comiti, F., Cadol, D., and Wohl, E. (2009). Flow regimes, bed morphology, and flow resistance in self-formed step-pool channels. *Water Resources Research 45* (4): 18.
20. Xu, X.X., Zhang, B.Y., and Ju, T.J. (2005). The Spatial-temporal distribution of rainfall, runoff, and soil water in small watershed and its utilization. *Ecology and Environment 6*: 890–893.
21. Loague, K., Heppner, C.S., and Abrams, R.H. (2005). Further testing of the Integrated Hydrology Model (InHM): event-based simulations for a small rangeland catchment located near Chickasha, Oklahoma. *Hydrological Processes 19* (7): 1373–1398.
22. Ran, Q. (2006). *Regional Scale Landscape Evolution: Physics-Based Simulation of Hydrologically- Driven Surface Erosion, in Geological and Environmental Science*. Stanford, California: United States: Stanford University.
23. Ran, Q.H., Heppmer, C.S., and Vaderkwaak, J.E. (2007a). Further testing of the integrated hydrotogy modet (InHM): multipte-species sediment transport. *Hydrological Processes 21* (11): 1522–1531.
24. Ran, Q.H., Hong, Y.Y., and Li, W. (2018). A modelling study of rainfall-induced shallow landslide mechanisms under different rainfall characteristics. *Journal of Hydrology 563*: 790–801.
25. Richardson, C.P. and Parr, A.D. (1991). Friction and free-surface flow over porous media. *Journal of Hydraulic Engineering 117* (11): 1496–1512.
26. Gao, H.D. (2013). *Hydro-Ecological Impact of the Gully Erosion Control Works in Loess Hilly-Gully Region*. Chinese Academy of Sciences and Ministry of Education (Research Center of Soil and Water Conservation and Ecological Environment).
27. Ran, D.C., Luo, Q.H., and Zhou, Z.H. (2008). Sediment retention by check dams in the Hekouzhen-Longmen section of the Yellow River. *International Journal of Sediment Research 23* (2): 159–166.
28. Yuan, S., Li, Z., and Li, P. (2019). Influence of check dams on flood and erosion dynamic processes of a small watershed in the Loss Plateau. *Water 11* (4): 834.
29. Guyassa, E., Frankl, A., Zenebe, A., Poesen, J., and Nyssen, J. (2017). Effects of check dams on runoff characteristics along gully reaches, the case of Northern Ethiopia[J]. *Journal of Hydrology 545*: 299–309.
30. Mirus, B.B. and Loague, K. (2013). How runoff begins (and ends): characterizing hydrologic response at the catchment scale. *Water Resources Research 49* (5): 2987–3006.
31. Zhang, L., Li, Z., and Wang, H. (2016). Influence of intra-event-based flood regime on sediment flow behavior from a typical agro-catchment of the Chinese Loess Plateau. *Journal of Hydrology 538*: 71–81.
32. Zhi, Z.X. (2018). *Study on Regulation of Check Dam on Channel Flow*. Xi'an University Technology.
33. Zhang, L.T. (2016). *Spatial Scale Effects on Erosive Energy Based Water Flow Driven Sediment Delivery on the Hilly Loess Region of the Chinese Loess Plateau*. Chinese Academy of Sciences and Ministry of Education (Research Center of Soil and Water Conservation and Ecological Environment).
34. Ran, Q., Li, W., Liao, Q. et al. (2016). Application of an automated LSPIV system in a mountainous stream for continuous flood flow measurements. *Hydrological Processes 30* (17): 3014–3029.
35. Norman, L.M. and Niraula, R. (2016). Model analysis of check dam impacts on long-term sediment and water budgets in Southeast Arizona, USA. *Ecohydrology & Hydrobiology 16*: 125–137.
36. Heppmer, C.S., Ran, Q.H., and Vaderkwaak, J.E. (2006). Adding sediment transport to the integrated hydrology model (InHM): development and testing. *Advances in Water Resources 29* (6): 930–943.
37. Shi, H.Y. and Wang, G.Q. (2015). Impacts of climate change and hydraulic structures on runoff and sediment discharge in the middle Yellow River. *Hydrological Processes 29* (14): 3236–3246.

@seismicisolation

7

The Mechanism of Water Damage of Check Dam

Wen Wang[1], Guoqiang Yu[1], Shengdong Cheng[1], Mengjing Guo[1], Tanbao Li[2], Jibin Wang[2], and Dejun Wang[2]

7.1. INTRODUCTION

The check dam built in the channel of small watershed in the soil erosion area of Loess Plateau is one of the important soil and water conservation measures to reduce the sediment into the Yellow River and improve the local planting conditions, which plays the role of flood detention and silt retention and check land for farmland [1]. In this paper, an approach including consistency handling and regional formulae for statistical parameters was proposed to solve the problem encountered in calculation of design flood in no data regions influenced by check dam projects. Analysis showed that the calculation results of such an approach are close to the actual situations and the approach has flexibility [2]. Restricted by economic and technical conditions, the design and construction standards of check dams in the past were not high, the quality control was not strict, the operation mode was special, and the emergency rescue was difficult. In rainstorm years, check dams are often destroyed or even burst, which causes many scholars to pay attention to the causes of erosion and the effect of sediment retention, and they worry about whether silt retention by check dam will be "zero deposit and lump sum," and the relative stability of the dam system and the structural form of the dam body are studied. According to the storage capacity, check dams can be divided into three categories: large, medium, and small, which are 500,000–5 million m^3, 100,000–500,000 m^3, and 10,000–100,000 m^3, respectively. Large check dams are also called backbone dams [3]. Based on the variation law of dam area and guaranteed yield of check dams with different engineering composition with years, the determination method of initial proportion of dam land is put forward, and then the calculation formula for predicting the economic benefit of check dams in the economic calculation period is deduced according to the dynamic economic analysis method [4]. The over-topping collapse of earth rockfill dam often produces huge flood disaster in its downstream. The study of dam collapse and flood routing is the need of disaster prevention and reduction. This paper summarizes the research progress on the phenomenon, mechanism, and simulation of over-topping collapse process of earth rock dams. The scale design of physical model test is discussed, and the research results of dam break test with different scales, types, and conditions are summarized [5]. A numerical simulation method which can correctly reflect the seepage failure and collapse mechanism of earth rock dams and reasonably describe the whole process of dam collapse and over-topping collapse from the seepage channel is proposed. By analyzing the stress of soil particles in the seepage channel, the critical starting velocity when seepage failure occurs is

[1] *Institute of Water Resources and Hydro-electric Engineering, Xi'an University of Technology, Xi'an, China*

[2] *Northwest Institute of Forest Inventory, Planning and Design, National Forestry and Grassland Administration, Xi'an, China*

Check Dam Construction for Sustainable Watershed Management and Planning, First Edition.
Edited by Zhanbin Li, Peng Li, Yang Yu, Peng Shi, and Guillaume Piton.
© 2022 John Wiley & Sons, Inc. Published 2022 by John Wiley & Sons, Inc.

@seismicisolation

obtained. The formulas for calculating the dam body impact in the development process of the overflow break after the overflow break of the dam with the expansion of the seepage channel are proposed, which can reasonably reflect the impact of the particle gradation, density, strength, the inclination of the seepage channel, the dam slope, the friction velocity, and the water velocity on the impulse [6]. This paper discusses the real-time risk assessment method of earth rock dam and uses the point estimation method to analyze the real-time probability of earth rock dam failure [7]. A numerical model and the numerical calculation method for describing the whole process of seepage failure of earth rock dam are proposed, and its rationality is verified by using the investigation data of seepage failure of Xiaohaizi reservoir in Gansu Province. Using this model, the influence of the initial seepage channel elevation on the seepage failure process of earth rock dam is compared and analyzed. The results show that the elevation of the initial seepage channel has an important influence on the development process of the breach, the flood flow process of the breach, and the maximum discharge. The lower the elevation of the initial seepage channel, the later the pipeline flow into weir flow caused by the collapse of the dam body at the upper part of the channel, the stronger the erosion at the bottom of the breach, and the larger the final breach width. The lower the elevation of the initial infiltration channel, the smaller the peak flow of the breach, the more flat and fat the flow process curve of the breach, and the maximum discharge [8] Due to the wide project scope, large quantity and low design standard, and most of the early check dams were built spontaneously by the masses, the project quality is poor, and over-topping dam break is easy to occur in case of rainstorm. Especially in the check dam system, when the layout of the dam system is unreasonable, the failure of a single dam is easy to cause the chain dam failure of the whole dam system. Super standard rainstorm flood is the main factor inducing the dam failure of medium and small check dams. However, in some dam systems, due to the lack of a certain number of backbone dams, or the unreasonable layout design of backbone dams and the lack of necessary discharge structures, the flood control capacity of the whole dam system is low, and one dam breaks, causing chain dam failure. The flood damage events of large-scale check dams in the 1970s and 1990s are mostly related to the lack of flood resistance capacity of the dam system as a whole. Therefore, it is of great significance for the safe operation of check dam system to simulate the dam break process of check dam system under rainstorm and flood conditions, analyze the causes of chain break, and put forward improvement measures to improve the flood control capacity of check dam system. The process of check dam collapse includes the evolution process of check dam breach, the change process of flood peak discharge at the breach, and the downstream flood evolution process after the breach. The process of check dam system collapse is the simulation of all check dams in the whole basin on the basis of considering the adjacent relationship between the whole basin water system and check dams.

7.1.1. Water Loss Characteristics and Cause Analysis of Check Dams in Loess Plateau

Check dam is an important engineering measure of soil and water conservation in the soil erosion area of the Loess Plateau. It is an effective means to raise the erosion base level, ensure that the sediment does not go out of the ditch, and build high-yield farmland in mountainous areas. It is also an important measure to reduce the sediment into the Yellow River and ensure the safety of the lower Yellow River. By 2008, more than 90,000 check dams had been built on the Loess Plateau, controlling soil erosion of more than 20000 square kilometers and intercepting more than 21 billion tons of sediment, effectively reducing sediment into the Yellow River. However, we should also see that there are still many potential safety hazards in check dams. The flood control standard of the project itself is low, and the ability to resist risks is weak. In recent years, the frequency of extreme climate has increased. If the safety production management of check dams is not effective, and sudden heavy rainfall is encountered, it is very likely that serious consequences such as dam collapse or even dam burst will occur. Once such a situation occurs, it will be very dangerous. It will bring serious negative effects to the construction of check dams and restrict the healthy development of soil and Water Conservation Ecological Construction in the Loess Plateau.

7.1.2. Analysis on the Forms and Causes of Check Dam Break

7.1.2.1. Causes of Check Dam Failure in the Early 1980s

According to the data of field investigation and the analysis of the causes of dam break in history, it is concluded that the causes of dam break in Some Random

@seismicisolation

Place Somewhere area are flood over-topping, seepage damage, structural damage, unreasonable operation and management, and other reasons. Over-topping dam failure, seepage damage, and structural damage are the main reasons for the break of check dams.

(1) Meteorological cause: Heavy rains and flooding exceeded design standards

The over-standard flood is the primary reason for the failure of the check dam in this stage. Based on the analysis of the causes of dam failure of check dams in the 1970s, it is found that most of the dam failures occurred in the form of over-topping the design flood standard. It is difficult to resist the over-standard flood for the reason that the silt dam is not completed or the silting reservoir capacity has been reached. Over-standard flood is the main cause of dam collapse in this period.

(2) Planning imbalance: Lack of backbone projects and low flood control standards of the dam system.

After a rainstorm in 1977, the Yellow River Commission investigated 19 channel and dam dystems in Shanbei and western Shanxi. The results showed that none of the main flood control projects failed to break the dams. Zhifang Gully in Suide County, Yangjiagou in Mizhi County, Sigou in Zizhou County, and other river basins are all caused by the chain reaction of the dam and reservoir floods. However, other check dams in the basin have also been damaged to varying degrees.

(3) Self-limiting factors of check dam.

1. Over-topping dam break.

There are many reasons that lead to the over-topping of the dam, and these reasons combine to cause the over-topping of the flood. The main reasons are summarized as follows: the operation time of the check dam is too long, the operation time of the check dam has already exceeded the operation time, the storage capacity of flood detention is insufficient, and there is no water discharge structure, or the water discharge structure has been damaged, resulting in the flood in the reservoir area cannot be discharged downstream.

2. The former check dam has not been designed systematically or is not fully considered in the design, and the present dam crest height may be lower than the design dam crest height after a long period of settlement.

3. Long-term rainfall has resulted in soil saturation, soil strength reduction, landslide soil clogging the discharge structure, or upstream floating debris clogging the discharge structure.

4. Seepage failure.

Seepage failure is one of the common causes of check dam failure. Because of the uneven settlement of the dam body, there are cracks running up and down the river; small animals such as rats and ants build burrows; the parts between the dam body and the discharge structure are not properly handled, and the flood seepage velocity in the dam area is relatively high, scour and carry nearby soil downstream through the discharge structure, gradually developed into piping, when piping cannot be controlled, the formation of a dam break. Another common form of seepage failure is that the high flood water level in the reservoir area leads to the uplift of the invasion line, the large area of soil behind the dam is invaded by water, the strength is reduced, the stability of the dam body is decreased, and finally the dam is broken.

5. Structural failure.

There are two forms of structural failure, the cracks caused by dam instability and deformation, and the damage of the discharge structure. Cracks occur in almost every check dam, the key is whether these cracks will continue to develop, and ultimately affect the check dam safety. Rainfall in flood season will form seepage in cracks and accelerate the development of cracks. If it is a longitudinal crack, it will affect the overall safety of the check dam, and it is also a sign of the overall failure. Combined with previous investigations and studies, the water damage of silt dams caused by over-topping of dams due to accumulation of water is a rare phenomenon, and the water damage caused by discharge structures may be the main cause; meanwhile, the spillway accident will directly endanger the safety of the dam.

(4) Poor construction quality and inadequate management measures.

A survey of silt dams in Yulin area found that 7 of the 57 medium-sized water dams invested by the state were destroyed, accounting for 12% of the total number of projects; two of them were "half-pull sub-projects" under construction, and one was an unfinished spillway, one is caused by the over-topping of the flood due to the blockage of the spillway, and the other three are caused by the bad connection between the dam body and the spillway tunnel and the poor masonry quality of the culvert. Earth dams, such as Zhaojiajian in Suide County, Liujiawa and Wangjiamao in Fugu County, and Fengjiachagou in Zizhou County, collapsed due to the failure of the connection between the Spillway Tunnel and the dam body. Zhaojiaping and Linjiajian

@seismicisolation

No. 2 Dams in Suide County, Hongshimomaogou No. 3 Dams in Zichang County, and Shengtiangou and Zhangjiacha dams in Qingjian County all failed to reach the spillway in time before the rain, resulting in flood over-topping the dams. Therefore, the poor quality of the project and the poor management and protection are also one of the important reasons for the dam collapse.

In the implementation of the rural land policy, the dam land was given to the people as farmland, but the responsibility and obligation for the protection of the Some Random Place Somewhere were not clearly defined. Some people expand the area of cultivation in the dam body, then the dam body gradually become thinner and eventually leading to a dam failure. On the other hand, leading cadres in rural areas have been formed. The purpose of inspectating check dam is to prevent a small problem becoming a big problem and check if dam maintenance is still dependent on the local water department funding.

(5) Poor slope management increases the flood threat of channel engineering.

Investigation data show that most of the gully with serious dam break is poor slope management, and the small watershed with good slope management has less loss due to water damage. Under the condition of 130-mm rainfall in Hongshimao Gully of Zichang County, Shaanxi Province, 39 tributary dams and 38% of the silting dams in the basin were destroyed due to poor slope management (6%). For the similar Dantougou, there are only 17 dams broken by branch ditches and 24% of dams and reservoirs are broken by branch ditches because of good management (16.3%). This shows that the slope management is an effective guarantee for the safe utilization of the gully dam system in the basin.

7.1.2.2. Reasons for Check Dam Failure in 1990s

(1) Over-standard storm flood is the main cause of water damage.

The survey shows that in July–August 1994, many places were hit by regional storm floods that happened once in a century or more, which greatly exceeded the flood control standards of the existing silt dams. From August 3 to 5, the area with rainfall of more than 50 mm was 35,000 km^2 from north to south and more than 10,000 km^2 from 100 mm in Shaanxi. The Storm Center of Suide County received 63 mm of rainfall in 0.5 h, 44.2 mm in 6 h, 41 mm in 0.5 h in Wubao County, and 48 mm in 1 h in Liulin County, Shanxi Province. After the storm, 798 dams were destroyed in Suide County, accounting for 21.2% of the total of 3,769 dams in the county. On August 10, Yangfujing, Dingbian County, at the junction of Shaanxi and Ningxia, received 178 mm of rainfall in 12 hours. Flash floods caused two floods in Dingbian County. A total of 272 check dams were destroyed by water, accounting for 76.6% of the total number of 355 dams. On August 30 ~ 31, a regional heavy rain occurred in Wuqi County, Zhidan, and Huan County at the junction of Shaanxi and Gansu provinces. The rainfall in 6 hours was 214 mm, of which the area larger than 100 mm was 1966 km^2, the area of 90–100 mm was 4900 km^2, and the area of 50–90 mm was 4250 km^2, and 65 check dams were destroyed by water, accounting for 23.6% of the total number of 275 dams in the county. The three heavy rainstorms are characterized by heavy rainfall, high intensity, wide area, and 50%–60% more precipitation than the same period of previous years.

(2) The effective storage capacity of most check dams is full, and the flood retention capacity is insufficient.

The vast majority of silt dams in the Yellow River Basin were built from the 1960s to 1970s. After long-term operation, the reservoir capacity is basically filled up and the flood retention capacity is sharply reduced. Most silt dams are not equipped with flood discharging facilities, and in the event of a heavy storm flood, it will cause an earth dam to fail. According to the statistics of Shanbei at that time, there were 26,233 silting dams, accounting for 82% of the total. Among them, 22,772 were small silting dams, accounting for 90% of the total number of small silting dams. After the rainstorm, 493 "bottle-neck" dams have been filled with water, which can only be discharged by evaporation and leakage. If no remedial action is taken, there is always the possibility of a breakdown.

(3) In many parts of the check dams, the discharge capacity is insufficient and the building quality is not high.

The investigation found that due to lack of funds, buried rubber pipes or small-caliber ceramic pipes were used as drainage facilities in some places during the construction of the dam, or earth spillways were used to discharge flood water, resulting in silting of culvert pipes in operation, or the bottom of the spillway is pulled deeper and deeper by the flood, the longer and longer the scour, the continuous extension and expansion of the gullies, resulting in water damage to the dam.

(4) Can't keep up with the maintenance.

A small number of dam land use rights are not fixed, and some local grassroots village cadres change

@seismicisolation

frequently, which leads to the predatory management of farmers in production. They only care about farming land regardless of maintenance, and the system of responsibility for maintenance is virtually nonexistent, and the engineering problems cannot be found and handled in a timely manner.

7.1.2.3. Analysis on the Cause of Check Dam Water Damage

Washout surveys indicate that the main causes of dam failure include

1. The dam broke because of excessive rainfall.

The times of dam collapse in small watershed are all under the condition of heavy rainstorm, such as 1977, 1978, 1994, and so on. On 27 July 1978, in the Ningzhaizi River Basin of Qingjian County, the average rainfall was 283.3 mm and the maximum rainfall was 350 mm. The design standard of the two silt dams in the basin was 20 years, and there was no check. The measured peak flow reached 3.75 times of the designed value, the measured flood volume is 2.6 times of the design value, and finally overflows the dam.

2. Lack of backbone projects and low flood control standards of the dam system.

The lack of flood control capacity of the river basin dam system resulted in dam collapse. Before the 1980s, there were five large-scale silt dams in the main gully, but most of them were filled up and had no flood control capacity. Heavy rains occurred in 1977 and 1978 destroyed the upstream dams, and the downstream dams were all washed away in succession. The same problem existed in the Zhifanggou watershed of Suide County before the 1980s, when the lack of key engineering controls caused "chain dam failure." In 1973, 144 silt storage dams in Nianzhuanggou Valley of Yan 'an were destroyed by water, which was caused by the failure of the upstream silt storage dams and the lack of backbone projects in the downstream. In Wuqi County, Jingbian, some river basins because of the construction of large-scale flood control backbone, in the case of the same heavy rain, almost have no dam collapse.

3. The backbones engineering facilities do not match and the drainage is not smooth causes the dam to collapse.

The main function of the backbone project is flood retention and mitigation, and it is the main body of the dam system project for flood control. However, in the course of the construction of the project, the necessary facilities for discharging and draining water are not set up, resulting in serious silting and damage to the storage capacity of the backbone project and insufficient flood control capacity, eventually, the dam will collapse. In 1969, there were four silting dams in the main gully of the Wangjiagou valley, with a total control area of 5.53 km^2 and a total storage capacity of 1.3 million m^3. However, due to the fact that most of the projects were "silting Hulu dams" which could not be drained, all four silting dams were washed down by a rainstorm (87.6 mm) on 26 July 1969, and in 1974, only two key dams were built in the main gully, and silos and spillways were set up, with a total storage capacity of 1.22 million m^3 and a total controlled area of 5.53 km^2. On 5 July 1977, rainfall of 79.5mm was recorded, and the project is still intact.

4. Poor slope management reduces the function of dam system engineering.

According to the survey data, where the dam collapse is serious, most of the slope governance is poor watershed; on the contrary, the better the slope governance of the small watershed, the loss of water damage is much less. For example, some small branches of Ershilipu in Qingjian County and Dabiangou in Yan'an have better vegetation, so the sediment concentration of the flood is small, and the confluence time is retarded, the flood peak is reduced, and the flood volume is reduced. Therefore, the check dam in the channel can operate safely under the same rainstorm conditions.

Rainfall in Hongshishaigou of Zichang County is up to 130 mm in the condition of basin area. The rainfall conditions, topography, and landforms are different. The degree of governance of the Hongshichi basin is relatively poor. Governance area only accounted for 6% of the basin area. 39 branch dam collapsed in 1977 and 1978, and the main channel projects were all washed out, and water damage projects accounted for 38% of the total basin; this indicates that the higher the degree of slope management, the higher the safety factor of river basin dam system.

According to the experimental data of Suide Water Conservation Station from 1957 to 1962, with the improvement of slope management, the amount of sediment storage of silting dam project decreased gradually with the pass of time, while the benefits of forest and grass measures and agricultural tillage measures increased gradually with the pass of time.

From 4 August to 5 August, 1994, the flood damaged 901 silting dams of 3574 in Suide, among which 22 were large dams, accounting for 25.2%, 163 were medium-

@seismicisolation

sized dams, accounting for 37.5%, 716 were small dams, accounting for 23.1%, losing much, and in this heavy rainstorm, the Jiuyuangou basin near the center of rainstorm, 202 silting dam projects were safe, and this is not only associated with the dam system planning of river basin but also related to the degree in 64.8% of the slope administration [9].

5. Poor construction quality

According to the results of investigation and historical data, a considerable part of warp dam projects is caused by the construction quality problems. The Xiaoruzi Dam in Baode County, Shanxi Province, reported by the Administration of the Upper and Middle Reaching of the Yellow River, collapsed in the flood season in 1991 due to the substandard masonry construction of the water discharge project. The flood first destroyed the water discharge project and then made the dam burst open. And in 1977, flood washed out dams in Suide Zhaojiajian, Fugu Liujiawa, Wang Jiashi, typical small watershed in Jiuyuan Valley watershed of Xiaqiaogou No.2, Kanghegou watershed small project water damage, and so on are caused by construction quality that is not up to the standard. Dam collapse events in the 60s and 70s and there are quite a few events were due to the upstream engineering construction quality is not high, string holes in certain parts of the dam caused check dam and then downstream engineering chain collapse, such as Jiucaiyuan basin happened chain dam collapse in 1977, Hongqi reservoir earth rock dam abutment string hole in combining site, is one of the direct causes of the dam failure. The chain dam collapse that occurred in 1973 in the Nianzhuanggou watershed was also closely related to the construction quality.

6. The management system is not reliable and management measures cannot be maintained

The main reason for the outburst of Hongqi Reservoir in Jiuyuangou watershed on 5 August 1977 was that the soil spillway of the reservoir had not been dug and could not be discharged. The water impoundment of the previous rainfall and the flood discharge of the upstream dams caused by the current rainfall caused the Hongqi Reservoir to burst under the condition of poor discharge, which led to the chain collapse of the downstream Maliangou Dam.

The unsound management system and inadequate management measures are an important factor affecting the safety of small watershed dam system. At present, most of the small- and medium-sized projects are operating under the condition of exceeding the designed sedimentation period, and the dam body is not raised, the water discharge buildings are not maintained, and the dam slope is not protected, which have caused great hidden dangers to the safe operation of the dam system. In recent years, due to the occurrence of fewer floods, there are a lot of projects of the spillway idle, local cadres and the masses thought paralysis, spillway clogged but no one pays attention, and even the phenomenon of stealing dismantled stone.

7.1.3. Development History of Check Dams on the Loess Plateau

Check dams in China have a long history of more than 400 years. The original check dams were formed naturally. The history of manual construction of check dams began in the Wanli period of the Ming Dynasty. In 1945, the Yellow River Water Conservancy Commission built the first check dam in jingyugou basin of the Loess Plateau. After the founding of new China, through the summary, demonstration, and promotion of water conservancy and soil conservation departments, the construction of check dam has achieved rapid development, which has roughly experienced three stages.

Spontaneous construction stage: Before 1986, the construction of check dams was mainly carried out in combination with agricultural production and basic farmland construction. Most of the check dams built during this period were small- and medium-sized check dams spontaneously built by the masses. Due to the lack of unified planning and scientific design and low standards, most of them have been silted up and failed at present.

Normative construction stage: From 1986 to 2003, by summing up the experience and lessons of the first-stage check dam construction, the Ministry of Water Resources successively issued technical specifications and standards such as Interim Provisions on design and construction of water falling dam (SD 124-84), interim technical specifications for key ditch control projects of water and soil conservation (SD 175-86), and technical specifications for water and soil conservation (SD 238-87). The construction level of check dams has been greatly improved. In 1986, the State Development Planning Commission listed the "key project of soil and water conservation and ditch control in the sandy and coarse sand area in the middle reaches of the Yellow River" as a special investment. The construction of check dams accelerated and entered the stage of standardized development.

Scale development stage: After 2003, in order to further ensure the operation safety of check dams and

@seismicisolation

Figure 7.1 Typical dam break process of earth rock dam.

improve the overall defense capacity of the basin, on the basis of comprehensively summarizing the construction experience of check dams, after repeated scientific experiments and research, it is scientifically summarized "taking tributaries as the framework, small flow area dam system as the unit, large dam control, and reasonable allocation and joint application of small- and medium-sized check dams." In 2003, the Ministry of Water Resources took the construction of check dam as one of the three "highlight projects," and the construction of check dam achieved large-scale development.

In recent years, heavy rainfall has occurred from time to time in some areas of the Loess Plateau, and extreme weather has increased. Especially after the debris flow disaster in Zhouqu, Gansu Province in 2008, the safe operation of check dam has attracted great attention of the government and all sectors of society (Figure 7.1). The Ministry of Water Resources timely issued opinions on further strengthening of the construction of check dams and other water and soil conservation retaining projects. The Ministry of Water Resources launched the danger removal and reinforcement project of medium-sized and dangerous check dams, focusing on danger removal and reinforcement.

7.2. EXPERIMENT ON DAM DAMAGE MECHANISM CAUSED BY CAVITATION EROSION OF WATER DISCHARGE STRUCTURE

7.2.1. Overview of the Experiment

Trapping and combination of the Loess Plateau typical check dam project, the impact of the water flow under different inlet shape on the tower wall and floor is studied. The structure of the borehole energy dissipation is in siloed shape. The hydraulic characteristics are studied by combining theoretical analysis and experimental methods. The shape of stilling well is optimized, and the reasonable size of baffle hole is put forward.

The shape of the upper inlet hole has been changed in three ways. There are four series changes in the size of energy dissipation well. Under the condition of not changing the pressure slope ratio, three kinds of changes are made to the outlet height of the pressure slope section. Through a series of comparative experimental studies, some results rich in innovation and engineering practical application value have been obtained. No matter from the breadth or from the depth, this research has certain exploratory and pioneering.

The experiment is divided into clear water experiment and muddy water experiment. The clear water experiment adopts the pressure distribution along the drainage capacity of the drainage building, the vertical shaft, the water cushion pond, the pressure slope section, and the backwater tunnel under the non-discharge flow rate (full pipe and unsatisfied pipe). Flow velocity and flow pattern were observed. The cavitation along the spillway under various working conditions is analyzed. In view of the design of different structure and size of the water outlet of the shaft, the structure design of the optimal water passage section is sought and verified by experiments. According to the test results, the optimization scheme of the shape of the shaft, the water cushion pond, the sloping section, the depth of the water cushion pond, and the size of the steps are put forward and verified by experiments.

In the muddy water test, using the muddy water mixing device, according to the field investigation and access to the data, the particle accumulation during the flood process is analyzed, and the pressure distribution along the drainage capacity of the drainage building, the vertical shaft, the water cushion pond, the pressure slope section, and the backwater tunnel is analyzed under different sediment flow. The flow velocity and flow pattern were observed. The cavitation along the spillway under various working conditions is analyzed. Compared with the clean water experiment under the same flow rate, and aiming at the design of different drainage structure and size of the shaft, the structure design of the optimal water crossing section is sought and verified by experiments.

All models are made of plexiglass, and flow is measured by triangular weir. The water discharge test of vertical shaft is supplied by 1 # tank. According to the model test conception, the model is designed according

@seismicisolation

Table 7.1 Scale tables of various physical quantities in model test.

Name of physical quantity	Geometric scale	The velocity scale	Flow scale	Stress scale	The time scale	The roughness scale
Scale relations	λ_L	$\lambda_V = \lambda_L^{0.5}$	$\lambda_Q = \lambda_L^{2.5}$	$\lambda_{\frac{P}{\gamma}} = \lambda_L$	$\lambda_t = \lambda_L^{0.5}$	$\lambda_n = \lambda_L^{1/6}$
Scale numerical	10	3.16	316.23	10	3.16	1.47

to the gravity similarity criterion, and the model size should not be too small. The geometric scale is 1:10, and the corresponding other physical scale is shown in Table 7.1.

Considering that the main force of the water movement of the prototype and model is gravity and both are turbulent, the secondary influence is omitted, the model is designed according to the gravity similarity criterion, that is, the original model requires the same Froude number.

The model adopts plexiglass design, and the roughness of plexiglass plate (tube) is between n=0.0085 and n=0.009, which is basically similar to that of PVC pipe, while the roughness of horizontal tube model is slightly smaller. However, because the flow of horizontal tube is limited below the small flow of open flow, there is no impact of roughness on the flow. Therefore, the roughness of the experimental model is basically similar to that of the original model.

In accordance with the principle of geometric similarity, the structural size of the drainage building laid out in this experiment is the inner diameter R=10 *cm*, the size of the drainage hole is a square hole with a side length of 2 *cm*, the length and width are a rectangle with a length of 4 *cm* and 2 *cm*, and the other is a circular hole with the same area and an area of $4cm^2$.

Different structural forms of spillway tunnel lead to different energy dissipation rate. The optimized flow field structure can reduce the water flow energy and reduce downstream scouring. The optimal structure of spillway tunnel can be obtained through physical model experiments.

7.2.2. Results Analysis

7.2.2.1. Flow Pattern Change Analysis

The flow regime in the drainage building has been the concern for the design personnel. The good or bad of the flow regime directly affects discharge capacity of the building, the building itself, and the safety of the downstream. The flow can be qualitatively studied through experimental observation and analysis of flow pattern, so as to provide the basis for optimization of the building body shape. In this paper, the critical hydraulic conditions when the divergent state of each part changes are obtained by observing and analyzing the flow state of each part, such as the water intake, energy dissipation well and water discharge tunnel, and the factors affecting the flow state change are analyzed.

(1) Water flow pattern at the upper intake

The flow pattern at the entrance is basically similar, because water is within the reservoir water depth range of inlet together; therefore, the import water shrinkage is more fully than those of the flat brake orifice discharge, but the water from the tongue under gravity can be drained freely, and its thickness decreases.

When the water head is low, the inlet water drops freely into the energy dissipation well at the bottom of the tower. With the increase of the water head, the water begins to impact the tower wall, and the position of the impact point increases with the increase of the water head. Because the water inlet is a square inlet, the water flow and the side wall of the water inlet are separated. Water due to the constraints of the tower wall at the part before and after the tower wall reflection diffusion involved in a lot of air and then mixed with the original water tongue, with the original fluid movement, the observation shows that with the increase of water level, water flows to the impact of the tower wall increases gradually, the tower body vibration, upper inlet flow is shown in Figure 7.2.

As can be seen from the figure, when the head at the bottom of the inlet is H/R > 2.5, a circular hydro jump occurs at the inlet, and the reflected water begins to

@seismicisolation

Figure 7.2 Schematic diagram of upper inlet flow pattern.

flood the inlet, and the reflected water completely floods the inlet. At this time, the jet flow velocity is high, and the reflected water rolls violently around the inlet, and there is a milky water and air mixture around the inlet.

(2) Flow pattern of the bottom hole

For the outflow of gate hole on the horizontal bottom, it is generally believed that when the hydraulic jump position behind the gate hole goes up over the contracted section, the gate hole is the submerged outflow, and the following method is used for quantitative determination. Suppose the water depth of the shrinking section is h_c and the flow velocity is v_c. When critical water jump happens, the water depth before the jump is h_c and the corresponding water depth after the jump is h_c'', then the submerge discrimination standard is

when $h_c \le h_c''$, for free flow

when $h_c > h_c''$, for submerge the outflow flow

h_c'' is calculated according to the formula:

$$h_c'' = \frac{h_c}{2}\left(\sqrt{1+8\frac{v_c^2}{gh_c}}-1\right) \tag{7.1}$$

However, for a drainage structure, the water jumps into a ring because of the rapid diffusion of the water in the vertical direction after the water passes through the inlet and the binding effect of the tower wall, and the flow pattern is obviously different from that of the gate outlet on the horizontal bottom, so the above discriminant formula is not applicable.

It is found through experimental observation that when the angle between the bottom hole and the inlet axis is 0° and 90°, respectively, the flow pattern at the inlet has obvious difference. When the angle between the bottom hole and the outlet is zero, the discharge increases with the increase of the reservoir water level, but the water level in the tower basically does not change and is always lower than the upper edge of the inlet. The inlet is always in a state of free outflow, and a small number of water fins are generated at the upper inlet of the drainage tunnel. The flow pattern at the inlet is shown in Figure 7.3. The water level in the tower increases gradually with the increase in the reservoir water level, and the water intake is submerged, thus forming the submerged outflow.

(3) Analysis of water flow pattern in the discharge tower

Water from the upper inlet into the water tower, when the low water head, imported water free fell to the bottom can well, with the increase of water head, the water began to impact the tower wall, the location of the impact point H '/R changing with the water inlet bottom R/H camp head as shown in Figure 7.4, when the inlet end of camp head H/R > 2.5, the location of the impact point began to stabilize, and the position of the impact point and inlet was basically the same height.

It can be seen from the experimental observation that at H/R > 2.5, the water falls into the energy dissipation well of the water cushion pond at the bottom of the tower after impinging the wall of the tower. At the same time, a large amount of air is brought in to make the

@seismicisolation

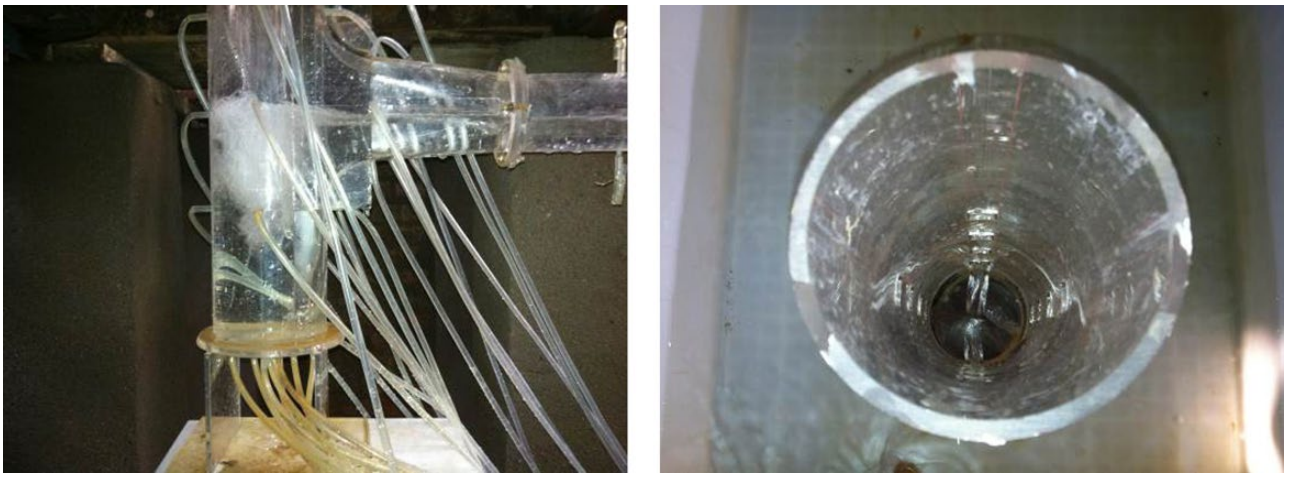

Figure 7.3 Flow pattern of inlet water at bottom hole.

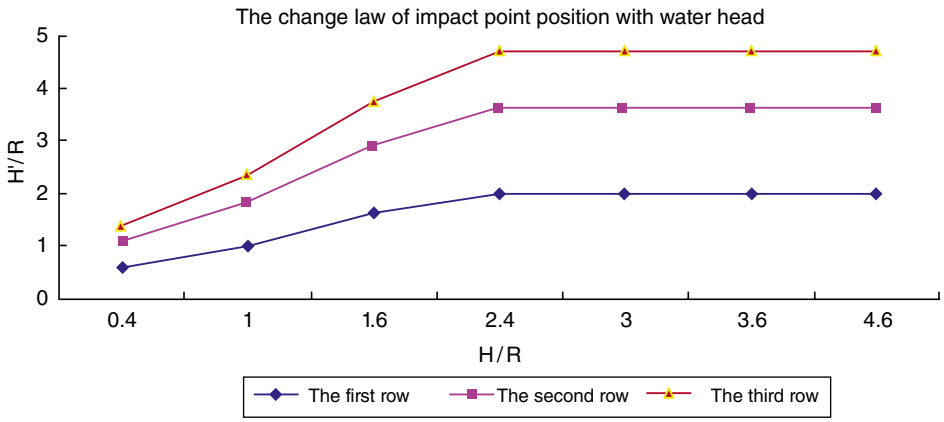

Figure 7.4 Variation rule of impact point position with water head.

water flow of the energy dissipation well of the water cushion pond in the tower fully aerated and expanded in volume. The speed of water mixture in the process of falling accelerated and fell into energy dissipation well after water from bottom hole reflection along the wall back up, and the falling water collide with each other, leading to the dramatic consumption of energy. Most of the mixed gas enters the water cushion pond of the tongue before falling, and then, combining with moisture into the mixture. The cavitation erosion in the water cushion pond will not occur, and this is because the cycle running at low speed around the tower wall can be for the aeration of air and at the same time, the bottom air can rise. Air is pumped along the wall of the tower so that cavitation does not occur. Figure 7.5 shows the flow pattern of the tower body.

The water flow pattern in the energy dissipation well was observed when the angle between the upper inlet and outlet axis was 0° and 90°, respectively, and the water flow pattern in the energy dissipation well was mainly observed when the angle between the first row of holes, the third row of holes, and the fifth row of holes and the outlet axis was 0° and 90°, respectively. After the water and gas mixture falls into the energy dissipation well from the upper inlet, it is reflected from the bottom of the well and then rises up along the well wall, forming a water pad in the energy dissipation well, colliding with the falling water flow. The aeration and turbulence of the water flow in the well are more sufficient, and the energy is consumed sharply. Because import since the aeration characteristics of water flow put at the bottom of the water tower water aeration concentration is higher, the water white foam flow pattern, the energy dissipation at the bottom of the well, better than the formation water cushion, the water in the aeration concentration decreases, through the bottom of the white foam well trajectory energy dissipation can be clearly observed in large-scale vortex

@seismicisolation

Figure 7.5 Flow pattern of tower body.

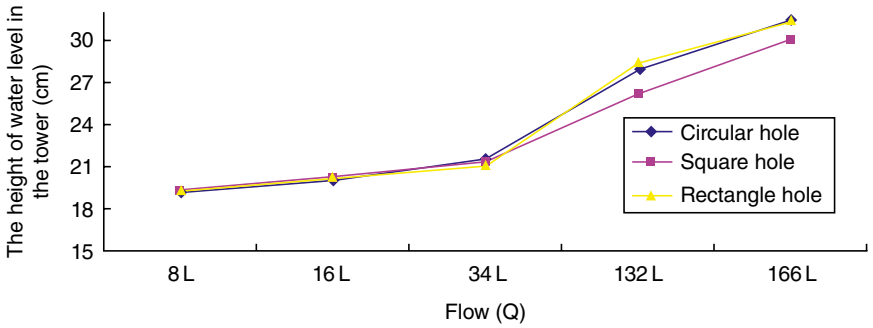

Figure 7.6 Variation of water level with water head in a tower at flow from 8 to 166 L.

motion. The experimental observation shows that the change of angle has little influence on the flow pattern in the energy dissipation well. Although the angle is different, the water level in the tower changes with the water head at the bottom of the inlet basically the same rule, as shown in Figures 7.6 and 7.7. As can be seen from the figure, when the flow rate is small, there is little difference between the water level in the rectangular square hole and the circular hole tower. With the increase of the flow rate, the water level in the tower with the circular hole rises greatly.

Tower water level in the same water head, different angles are basically the same, this is largely because, due to the higher inlet position, regardless of the number of inlet and outlet axis angle to flow into the inlet is toward the tower wall first, after well by the outlet flow out, then fell to energy dissipation angle changes have little impact on the water level of the tower (Figure 7.8).

The experiment also focuses on the observation of the flow pattern in energy dissipation wells when the angle between the bottom hole and the outlet axis is 0° and 90°, respectively. It is found in the test that the flow pattern in energy dissipation wells has obvious difference when the angle is different. When the angle between the bottom hole and the outlet axis is 0°, the water level in the tower almost does not change with the increase of the water head, the fluctuation of the water surface gradually increases, the aeration concentration of the bottom hole water flow is low, and the water fins appear at the upper part of the inlet of the drainage tunnel. When the angle between the bottom hole and the axis of the outlet is 90°, the water will rotate counterclockwise after entering the inlet, and the water level in the tower will rise with the rise of the water head, and a counterclockwise vortex will be generated on the water surface, and almost no bubbles will be generated in the energy dissipation well.

@seismicisolation

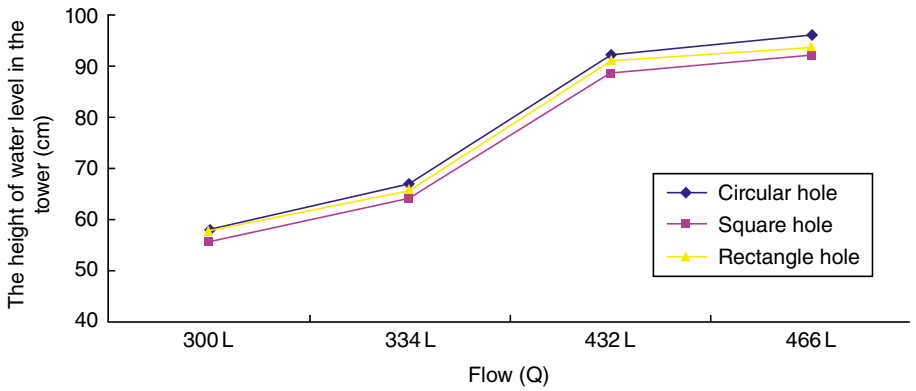

Figure 7.7 Variation of water level with water head in a tower at flow from 300 to 466 L.

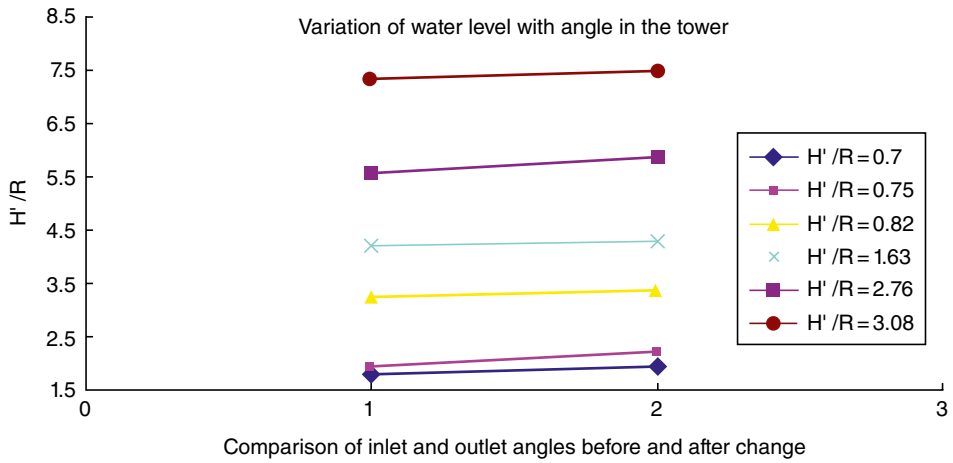

Figure 7.8 Variation of water level with angle in the tower.

Taking the third row of wells as an example, the influence of the change of well depth on the flow pattern in the energy dissipation well was observed in the test. It can be observed that when the well depth is larger, the water in the energy dissipation well is relatively stable with only occasional bubbles mixing, while when the well depth is smaller, the water and gas mixing in the energy dissipation well is obvious and the water body is tumbling violently. When the water flows into the shaft from the third row of holes, the change of well depth is opposite to the fluctuation of water surface in the energy dissipation well. It can be seen that when the well depth is H_0/D_0 and the water head is $H/R < 3.2$, the fluctuation value of water surface increases rapidly with the water head H/R. When the water head is $H/R > 3.2$, the fluctuation of water surface gradually decreases with the increase of the water head H/R. At the same water head H/R, with the increase of well depth H_0/D_0, the fluctuation value of the water surface in the energy dissipation well shows a decreasing trend. This is because with the increase of well depth, the energy dissipation volume increases, the water cushion depth in the energy dissipation well also increases, and the impact degree of the drainage water on the bottom plate of the water discharge tower decreases. The impact degree of the drainage water on the bottom floor of the drainage tower is reduced, which leads to the decrease of the turbulence degree of the water flow in the well, and this makes the energy dissipation well the internal fluctuations to slow down below. But in general, because of the small water head, the change of well depth has little influence on the flow pattern in energy dissipation well.

Test more than two holes, for example, observed the energy dissipation can well caliper change cancelation borehole flow pattern, the influence of water flow by 3-hole inflow, energy dissipation borehole water vapor mixture violently, for the same flow rate under different baffle well depth (H_0) and the relationship between the shaft diameter (R) changes, baffle well within the flow

@seismicisolation

regime is also changing. When H_0/R = 1.67, energy dissipation of the borehole flow is shown in Figure 7.9. When H_0/R = 2.5, flow regime of the energy dissipation well is shown in Figure 7.10. It can be seen from Figure 7.11, when the diameter is same, energy dissipation of the borehole water wave showed a trend of increase with the increase of RH/head. Under the same water head, the energy dissipation from the turbulence of borehole water is relatively lower, owing to less borehole water fluctuation.

(4) Water flow pattern in the drainage tunnel

After the water is fully dissipated in the energy dissipation well, the milky water and gas mixture enter the drainage tunnel through the pressure slope section, and the fluctuation of the water surface in the cave increases with the increase of water head. It was observed in the test that the aeration concentration of the water flow into the water discharge tunnel was larger, the water depth was smaller, and the velocity was larger. After a

Figure 7.9 Flow pattern in energy dissipation wells (H_0/R = 1.6).

Figure 7.10 Flow pattern in energy dissipation wells (H_0/R = 2.5).

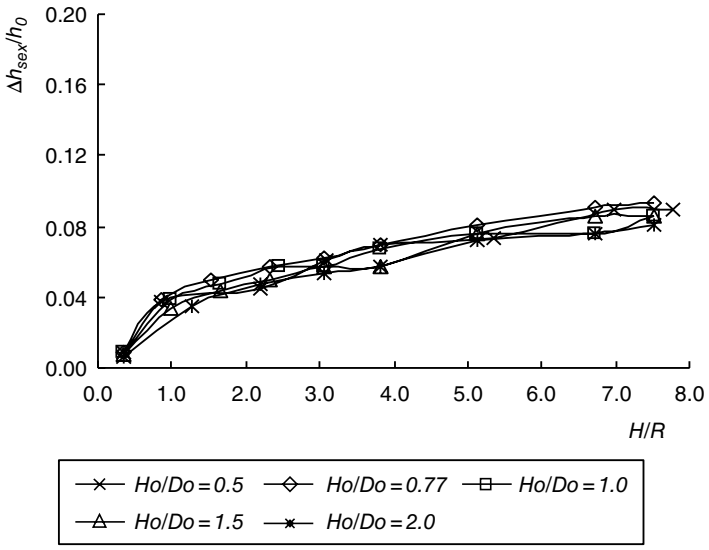

Figure 7.11 Influence of well depth change on in-well water surface fluctuation.

@seismicisolation

considerable distance, a large number of bubbles flowed out, water and gas separated, the water flow in the water discharge tunnel was gradually stable, and the water depth was gradually increased.

The angle between the inlet and outlet axis is 0°: when the water flows from the bottom hole, the water depth in the drainage tunnel increases with the increase of the water head H/R. When $H/R = 3.2$, the water depth in the drainage tunnel reaches the maximum, and then the water depth in the drainage tunnel gradually decreases, and the flow rate increases. The drainage tunnel is a clear flow, and there is no alternate flow pattern of clear full flow within the test range. When the water flows from the upper inlet, the water surface in the cave fluctuates greatly. When $H/R > 3.2$, the water will hit the roof of the cave. Within the test range, the water discharge tunnel is open flow. The flow pattern in the drainage tunnel is shown in Figures 7.12 and 7.13.

Axis of the inlet and outlet angle is 90°: water from bottom hole inflow, water level increase with the increase of head tower H/R, water inlet for flood discharge, and energy dissipation borehole is relatively smooth, the water flow aeration concentration is low, the water, combining with steady flow, when $2.4 \leq H/R \leq 5.5$, appear alternately bright full flow phenomenon, when $H/R > 5.5$, in almost a full flow, hole filled inside the tunnel flow pattern as shown in Figure 7.14. When the water flows from the upper inlet, the water surface in the drainage tunnel fluctuates violently. At $H/R > 3.2$, the alternating flow pattern of bright and full flow appears. With the increase of the water head, the alternating frequency of bright and full flow increases.

The axis angle between the inlet channel and the outlet channel is 90°. When the flow direction of the water changes, a large amount of gas will be mixed into the flat hole, resulting in the phenomenon of water and gas mixing. When the size of the pressure slope section in the upstream section of the flat tunnel is small, it will cause poor drainage.

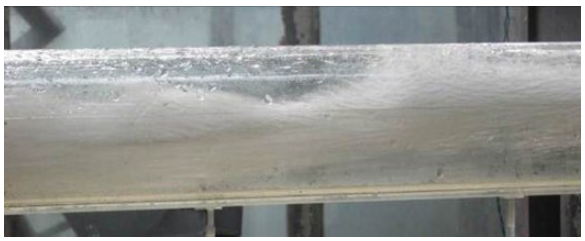

Figure 7.12 Flow pattern in water discharge tunnel.

Figure 7.13 Water flow pattern in the drainage tunnel at full flow.

7.2.2.2. Analysis of Energy Dissipation Mechanism in Energy Dissipation Well

The water flow enters the shaft from the water inlet, hits the tower wall, and then falls into the energy dissipating well. A water cushion is formed in the energy dissipating well. Similar to the flow pattern of a plunge pool, it is a complex turbulent submerged jet with a more complicated flow pattern. Regarding the law of water flow in the energy dissipation well, most of the existing research results are still based on the basic theory of binary submerged free jet. In fact, the water flow in energy dissipation wells is far more complicated than dual submerged free jets. This is mainly reflected in the following four aspects: first, the cross-sectional shape of the incident water tongue is complicated, and the flow pattern is obviously a ternary flow; second, a large amount of air is mixed into the water when the jet enters the water, which is a water–gas two-phase flow; third, the jet diffusion is limited by the solid wall boundary of the energy dissipation well. It belongs to the restricted jet flow in a limited space; fourth, the turbulence intensity of the water flow is particularly large. For such a complicated flow, there are few researches at present, which has certain research significance.

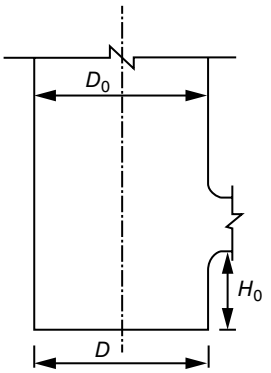

Figure 7.14 Energy dissipation well structure diagram.

@seismicisolation

(1) Characteristics of flow pattern evolution in energy dissipation wells

The characteristics of the flow pattern and its evolution in the energy dissipation well are related to factors such as the depth of the water cushion, the single width of the water inlet, the angle of the water, and the thickness of the water. With the difference of the depth of the water cushion and the change of the water inlet angle, the flow pattern in the energy dissipating well may present three flow patterns: free impinging jet, submerged impinging jet, and surface flow.

When the depth of the water cushion in the energy dissipation well with a small water head is very shallow, the energy dissipation well will appear as an oblique free impinging jet flow state. At this time, the jet water tongue is completely exposed to the air, directly hitting the bottom of the well, and in the jet impact area a free water jump is formed nearby. In the case of large water head and large flow rate, because the impact pressure of this fluid jet on the bottom plate is too large, and the flow pattern in the energy dissipation well changes sharply and unstable, it is easy to cause cavitation damage. In energy problems, this flow pattern must be avoided.

As the water head increases, the depth of the water cushion in the energy dissipation well increases and the water cushion plays a role in supporting the incident flow. At this time, the jet hits the wall first and then falls into the energy dissipation well. The energy dissipation well shows a mixed flow state of submerged impinging jet and submerged hydraulic jump. After the water flow falls into the energy dissipating well, the main flow turns and the streamline is bent, the flow velocity decreases rapidly, and the pressure increases sharply, which generates huge impact pressure on the bottom of the energy dissipater, which can easily cause instability and damage of the bottom.

With the further increase of the depth of the water cushion, or when the jet inflow angle is not large, the jet water will rise from the bottom of the energy dissipation well to near the water surface, forming a surface flow state. Surface flow is divided into three types: surface wave breaking, surface wave current, and surface jet. According to the flow characteristics of the water flow in the water discharge tower, it is easy to form a surface wave breaking flow pattern in the energy dissipation well. When a surface flow pattern appears in the energy dissipation well, the high-speed main flow rises from the bottom to the surface layer of the water surface. The water surface fluctuates violently, which can easily cause damage to buildings.

(2) Energy dissipation mechanism of energy dissipater in energy dissipation well

From the perspective of energy dissipation, the energy dissipation mechanism of energy dissipation well is basically the same as that of a plunge pool. The process of energy transfer, redistribution, and dissipation in the process of flow changes along the way. The time-averaged kinetic energy of the mainstream continuously transfers energy through strong turbulent shearing and diffusion. At the same time, the energy transfer and redistribution are accompanied by viscous dissipation caused by shearing. For the impingement jet in the energy dissipation well, due to the space limitation of the energy dissipation well, the jet in the energy dissipation well and the rising water flow along the wall collide with each other to dissipate the energy, which further increases the turbulence degree of the water flow in the well.

The pulsating energy of the turbulent flow is mainly provided by the time-averaged motion of the jet in the strong shear layer (interface area), and through the splitting, stretching, and breaking of the turbulent vortex, the energy is gradually transferred by the large-scale vortex. For the small-scale vortex bodies, up to a certain level of small-scale vortex bodies, the transmitted energy is dissipated through viscosity. Generally speaking, in the process of transfer, redistribution and dissipation of jet energy, the energy extracted by turbulence pulsation is the most, followed by the energy absorbed by the main vortex region around the jet region, and the energy consumed by time-averaged shear is the least.

(3) Parameter design of energy dissipation well in this experiment

This test conducted a series of optimization studies on the shape of the energy dissipation well. Through a series of changes in the depth of the energy dissipation well, we observed the changes of various hydraulic parameters when the depth of the energy dissipation well changed and sought a reasonable depth of the energy dissipation well. Diameter design plan, this test has made five changes to the energy dissipation well depth and three changes to the diameter. The test conditions are shown in Table 7.2. At the same time, in order to study the changes of the time-averaged

Table 7.2 Structure size of energy dissipation well.

Changes in well depth	D (cm)	10	10	10	10
	H_0(cm)	10	15	17	25

@seismicisolation

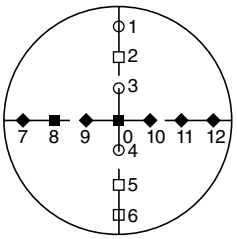

Figure 7.15 Layout of pressure measurement points on the floor of the energy dissipation well.

pressure and fluctuating pressure of the bottom plate when the size of the energy dissipating well is changed, the test respectively arranged pressure measurements on the bottom plate of the energy dissipation well along the axis of the discharge tunnel (X direction) and perpendicular to the axis (Y direction). A series of pressure measurement points are arranged at the points. The structure of the energy dissipation well and the floor pressure layout of the energy dissipation well are shown in Figures 7.14 and 7.15.

7.2.2.3. Wall Pressure Distribution Law

The wall pressure distribution is an important hydraulic parameter for studying whether the shape of the discharge structure is reasonable. It can directly reflect whether there are bad hydraulic phenomena such as cavitation and cavitation in the discharge structure. It is important for the design and application of actual projects. There are often cavitation erosion, cavitation, and other phenomena in vertical drainage structures, which bring serious hidden dangers to engineering safety. Therefore, this paper studies the distribution law of pressure on the wall of the drainage tower.

(1) Time-averaged wall pressure distribution law

For a free jet on a smooth surface, it can generally be divided into three subregions with different properties. Namely: I – a free jet zone, the flow characteristics are similar to the free jet; II – an impact zone, the main flow is deflected by the wall, the streamline bends, the main flow turns, the flow velocity decreases rapidly, and the pressure increases sharply; III – a wall jet zone, the main flow sticks wall jets have flow characteristics completely similar to wall jets.

The water flows into the tower from the inlet of the water discharge tower, and as the water head rises, the water hits the tower wall, forming an impingement jet, which easily causes problems such as erosion damage to the tower wall and building vibration. Therefore, it is

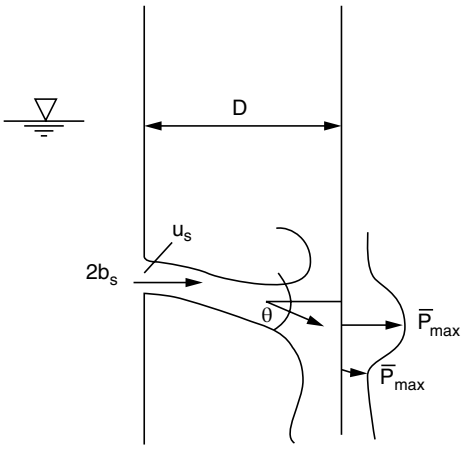

Figure 7.16 Schematic diagram of hourly average pressure.

of great practical significance to study the impact pressure distribution of water flow on the tower wall.

For the characteristics of the impact pressure of the impinging jet, the dimensionless number of the maximum impact pressure converted into the flow velocity can be expressed by the formula $u_m/u_0 = K(b_0/s)^m$, where $u_m = \sqrt{2gH}$, H is the maximum impact pressure head of the bottom plate, u_0 is the jet exit velocity, K is the coefficient, and different scholars give different values, The range of impact pressure is 2.28 ~ 2.81, and most scholars suggest that the index m should be 0.5; the distribution of impact pressure on the floor has good self-modeling, which is close to normal distribution; the range of impact zone is $-2.4 \le y/b_{1/2} \le 2.4$, where y is the distance from the maximum pressure equalization point, and $b_{1/2}$ is the half width, that is, $b_{1/2} = y/\overline{p} = 0.5\overline{p}_m$.

The experiment researched the change rule of impact pressure when the angle between the water inlet and outlet axis is 0° and 90°, respectively. The time-averaged pressure diagram is shown in Figure 7.16. For a free jet, its internal pressure is the same as that of the surrounding fluid, and there is no pressure gradient. The flow velocity distribution of the section approximately conforms to the Gaussian distribution. The free jet zone in the impinging jet has this property, while the impinging zone affected by the wall, the flow rate decreases, and the flow rate gradient turns into a pressure gradient. Convert the measured maximum impact pressure $\overline{p}_{\max}$ into a converted flow velocity according to the relationship of $u_m = \sqrt{2g\overline{p}_{\max}}$, and draw the relationship curve of $u_m \sim u_0$, as shown in Figure 7.17. It can be seen from the

@seismicisolation

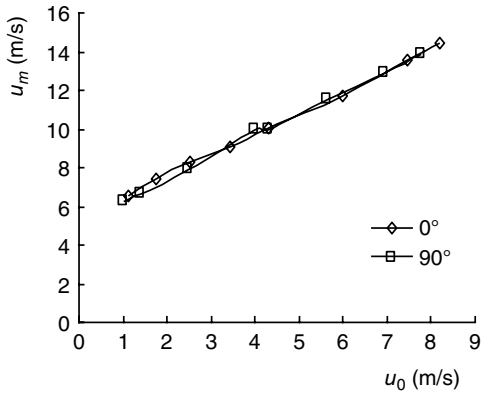

Figure 7.17 u_m~u_0 Relationship diagram.

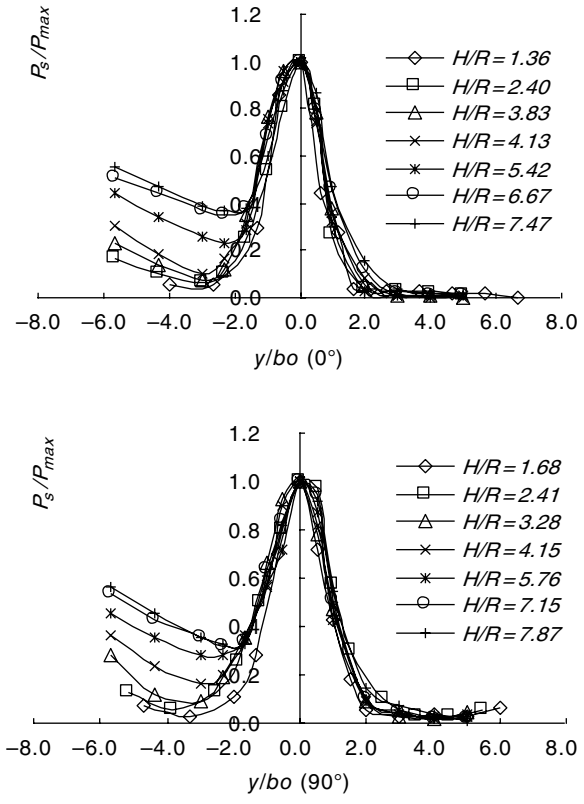

Figure 7.18 Time-averaged pressure distribution at each measuring point on the longitudinal axis.

figure that u_m increases linearly and regularly with the increase of u_0.

Using y/b_0 as the abscissa, the time-averaged impact pressure distribution curve of each measuring point on the vertical axis is obtained, as shown in Figure 7.18. From the figure, it can be found that when $y/b_0 \geq -1.8$, the time-averaged impact pressure distribution of different measuring points is very similar. The properties (self-modeling and self-protecting) are similar to the normal distribution; when $y/b_0 < -1.8$, with the change of the water head, the p_s/p_{max} of each measuring point is different and basically increases gradually with the increase of the water head. This is due to increasing the water level in the tower increases, and the water level in the tower gradually affects the pressure of each measuring point of $y/b_0 \leq -1.8$. The pressure of each measuring point of $y/b_0 < -1.8$ is caused by the water cushion in the tower and the wall jet water.

(2) Distribution law of pressure at the bottom of shaft

In this test, the flow rates are 8, 16, 34, 132, 166, 300, 344, 432, 466L/min, and different water inlets. Under the shape, the pressure change at the bottom of the shaft is studied (Figure 7.19). When the flow rate is small, the bottom pressure of various shapes does not change much. With the increase of the flow rate, the pressure on the bottom of the square hole is greater than that of the circular hole and the rectangular hole. It can be seen from the figure above that for the same flow rate, the pressure distribution law of different water inlet holes on the bottom of the shaft is square hole>circular hole>rectangular hole.

When the test flow rate was greater than 300 L/min, the bottom pressure distribution of different water inlets under the same flow rate and small flow changed somewhat. The bottom pressure division rule is circular hole>square hole>rectangular hole.

Through the analysis of water head changes under different flow rates, it can be seen from the above figure that under the same flow rate, the water level in the tower is round hole>square hole>rectangular hole. For the same flow rate, different shapes of drain holes have different discharge capacities. It can be seen from the figure that for the same flow rate, the water tank height change law is square hole>rectangular hole>circular hole.

Combining the height of the reservoir water level in the water tank, the height of the water level in the tower in the shaft, and the changes in the pressure at the bottom of the shaft, a comprehensive comparison can be made, and it can be analyzed that at the same flow rate, the order of the discharge holes of the shaft is circular hole>square hole>rectangular hole.

(3) Time-averaged pressure distribution at the bottom of the culvert

The test also studied the variation law of the time-averaged pressure along the center of the discharge tunnel floor under various working conditions. For small flows, the overall pressure distribution of the discharge culvert floor has little change. The pressure dis-

@seismicisolation

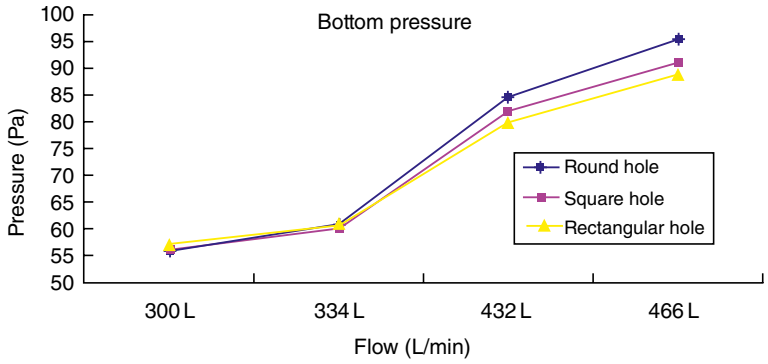

Figure 7.19 The distribution of pressure at the bottom of the shaft under different flow rates.

tribution increases slightly along the way; when the flow rate is greater than 132L/min, the pressure distribution of the culvert floor shows a decreasing trend along the way; this experiment is also aimed at the same flow rate and different discharge hole shapes, square, rectangular, and round holes. The study on the distribution law of pressure along the bottom of the spillway culvert shows that the pressure distribution law of the bottom of the spillway is square hole>circular hole>rectangular hole under the discharge conditions corresponding to different inlet holes; in addition, through the test, it is concluded that with the increase of the flow, the pressure on the bottom of the spillway culvert also increases correspondingly, and the discharge flow and the pressure of the bottom of the spillway have a positive correlation. It can be found from the figure: 1) when the flow rate is less than 34L/min, there is open flow in the discharge tunnel, and the time-averaged pressure in the center of the plate gradually increases along the way. The change of the water head has little effect on the pressure, and the pressure distribution is more uniform; 2) when the flow is more than 34 L/min but less than 334 L/min, when the water flows into the discharge tower from the bottom hole, the water level in the tower rises rapidly, and there is an alternating flow pattern of open and full flow in the discharge tunnel, and the time-averaged pressure at the center of the tunnel bottom is along the way. With the increase of water head, the pressure of the bottom of the hole gradually increases. When the water flows from the fifth row of holes, the pressure change of the bottom of the hole is similar to that of the bottom hole, but when it flows from the fourth row of holes and the third row of holes, the pressure of the bottom of the cave gradually increases along the way, and the change of water head has little effect on the pressure.

(4) The pressure of each part of the energy dissipation well

In this experiment, the pressure distribution on the walls of the energy dissipation well and the shaft was studied, using 8, 16, 34, 132, 166, 300, 344, and 432 L/min. Under nine flow rates of 466 L/min, the depth of the energy dissipation well is H=17cm, and the diameter of the shaft is 10 cm, and the pressure distribution of the energy dissipation well and the four walls of the shaft corresponding to the different water inlet shapes at the same flow rate is shown in Figure 7.20.

It can be seen from the figure that when the flow rate is 8 and 16 L/min, the regular area of the pressure distribution on the four walls of the shaft is constant, basically at a horizontal line, and the pressure slope section appears to decrease at the No. 5 measuring point. The performance response the water flows from the water inlet of the vertical well, and as the water head rises, the water hits the tower wall, forming an impinging jet, which easily causes problems such as erosion damage to the tower wall and building vibration. Therefore, the distribution law of the impact pressure of the water flow on the tower wall is studied. It has important practical significance.

When the flow rate is 34L/min, negative pressure appears at No. 6, 7, 8, and 9 measuring points. These four measuring points are mainly distributed in the compression section. After the water hole enters the shaft, when the water head is small and the depth of the water cushion in the energy dissipation well is very shallow, the energy dissipation well will appear as a diagonal free impinging jet flow state. At this time, the jet water tongue is completely exposed to the air and goes straight to the bottom of the well and forms a free hydraulic jump near the jet impact area. In the case of large water head and large flow, due to the excessive

@seismicisolation

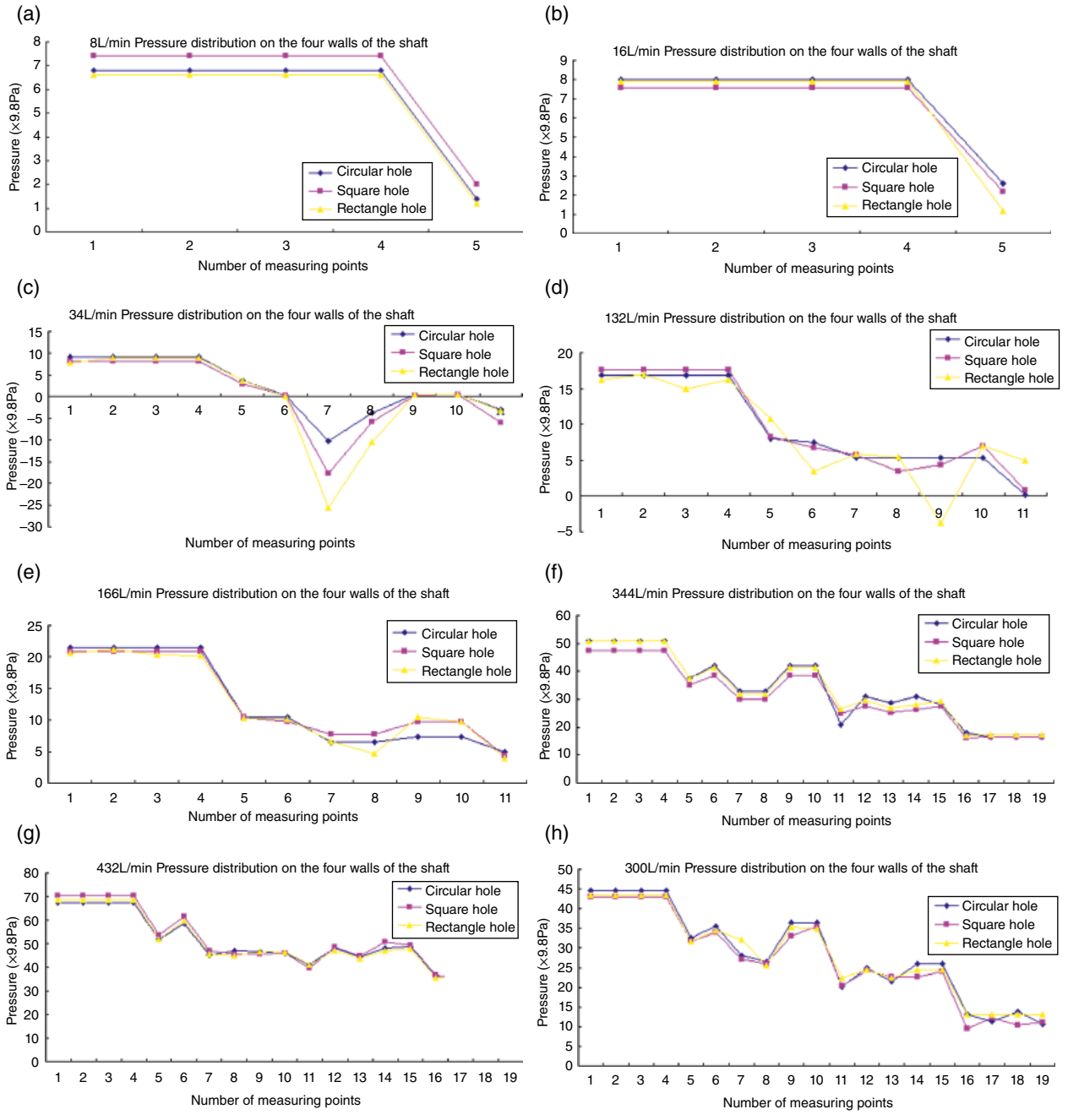

Figure 7.20 Pressure distributions under different inlet hole shapes.

impact pressure of this fluid jet on the bottom plate, and the rapid and unstable fluid changes in the energy dissipation well, it is easy to cause cavitation damage. It is found through experiments that the location of the compression section A negative pressure zone appeared due to the hydraulic jump. With the increase of flow, the discharge culvert changes from open channel flow to open and full alternate, and then into pressure flow. At this time, the bottom section of the shaft is completely submerged by the water flow, and the pressure on the walls of the shaft also increases with the increase of the flow rate. Through this experiment, it is concluded that there will be a negative pressure zone in the compression section. The next experiment is to eliminate the negative pressure by optimizing the shaft structure.

@seismicisolation

In this experiment, the energy dissipation rate was studied in different depth energy dissipation wells, and the influence of the inlet angle on the energy dissipation effect was evaluated. Experiments show that with the increase of well depth, the energy dissipation rate increases, and the pressure of each measuring point also increases with the increase of the upstream water level. The negative pressure at the top of the flat hole outlet also increases with the increase of the discharge flow. The uniformity of the pressure distribution has increased; when the water head is small, the change in well depth has little effect on the pressure change at each point, and the effect is gradually obvious with the increase of the water head, and the pressure at each measurement point increases with the increase in well depth.

7.2.2.4. The Distribution Law of Water Depth and Velocity Along The Discharge Structure

The water depth and velocity distribution along the discharge culvert with different inlet shapes were measured. The water surface profiles of nine discharge tunnels were measured, including 8, 16, 34, 132, 166, 300, 344, 432, and 466L/min. The measured values of water surface profile along the flood discharge tunnel are shown in the Table 7.12, or the stable pressure flow pattern, without water surface profile. When the test flow is small, the flow along the discharge structure is open channel flow. With the increase of the test flow, when the test flow is 334L/min, the measured flow changes into open full alternate flow. When the test flow was more than 432L/min, the flow changed into pressurized flow.

In this test, according to different inlet hole shapes, three types of inlet holes with the same area and different shapes, round hole, square hole, and rectangular hole, were tested, and different inlet holes corresponding to different flow rates were measured, respectively. The water depth along the way is measured and the corresponding flow velocity is measured and calculated, and the water depth distribution law and flow velocity distribution law of different water inlet and discharge structures along the way are studied.

In this test, the water depth of the discharge structure was measured under different flow conditions, and the water depth along the way showed a decreasing trend. When the flow rate reaches 432 L/min, the discharge structure reaches full pipe operation, changing from full to pressurized flow. At the same flow rate, the flow rate of the discharge structure is inversely proportional to the water depth. As the distance from the outlet increases, the water flow rate increases, while the water depth is the opposite. See the measured data in Tables 7.3–7.6 for details.

From the velocity calculation results, it is known that when the floods discharge tunnel is Q=466L/min, the maximum velocity of the flood discharge tunnel is 2.75m/s. From the above tests, it is estimated that the maximum velocity of the flood discharge tunnel is 2.75m/s, which does not belong to the range of high-speed flow. As long as we pay attention to control the construction unevenness, we can ensure that the cavitation flow problem does not occur in the flood discharge tunnel.

7.2.2.5. Analysis of Cavitation Number of The Flow Along Flood Discharge Tunnel

In hydraulics, the flow cavitation number σ is commonly used to measure the cavitation characteristics of each point in each part of the discharge structure and

Table 7.3 Water depth distribution law of discharge buildings under different flow rates of circular holes (unit: L/min).

Number	8	16	34	132	166	300	334	432	466
1	2.10	2.50	4.10	5.80	6.00	6.20	6.40	6.50	6.50
2	1.90	2.40	3.40	5.70	5.70	6.10	6.40	6.50	6.50
3	1.70	2.10	3.20	5.60	5.60	6.00	6.40	6.50	6.50
4	1.80	2.10	2.80	5.60	5.50	5.90	6.40	6.50	6.50
5	1.70	2.00	2.70	5.30	5.30	5.70	6.30	6.50	6.50
6	1.60	1.80	2.40	4.90	5.00	5.70	6.30	6.50	6.50
7	1.50	1.80	2.40	4.80	4.60	5.60	6.30	6.50	6.50
8	1.50	1.70	2.00	4.60	4.50	5.60	6.30	6.50	6.50
9	1.40	1.60	2.20	4.60	4.40	5.50	6.20	6.50	6.50
10	1.20	1.50	2.00	4.30	4.30	5.50	6.20	6.50	6.50

@seismicisolation

Table 7.4 Flow velocity distribution law of discharge culvert under different flow rates of circular holes (unit: L/min).

Number	8	16	34	132	166	300	334	432	466
1	0.22	0.32	0.32	0.83	1.02	1.80	1.98	2.55	2.75
2	0.27	0.35	0.42	0.85	1.06	1.82	1.98	2.55	2.75
3	0.33	0.44	0.46	0.86	1.08	1.84	1.98	2.55	2.75
4	0.30	0.44	0.57	0.86	1.10	1.87	1.98	2.55	2.75
5	0.33	0.48	0.60	0.91	1.14	1.92	1.99	2.55	2.75
6	0.38	0.59	0.74	0.99	1.22	1.92	1.99	2.55	2.75
7	0.43	0.59	0.74	1.01	1.34	1.95	1.99	2.55	2.75
8	0.43	0.66	1.03	1.07	1.38	1.95	1.99	2.55	2.75
9	0.50	0.75	0.86	1.07	1.42	1.99	2.01	2.55	2.75
10	0.72	0.86	1.03	1.17	1.47	1.99	2.01	2.55	2.75

Table 7.5 Water depth distribution law of sluice culvert under different flow rate of square hole (unit: L/min).

Number	8	16	34	132	166	300	334	432	466
1	2.20	2.90	3.50	5.80	6.40	6.50	6.5	6.5	6.50
2	2.00	2.80	3.20	5.70	6.10	6.40	6.5	6.5	6.50
3	1.80	2.50	3.60	5.60	5.90	6.30	6.5	6.5	6.50
4	1.90	2.50	3.40	5.60	5.80	6.30	6.5	6.5	6.50
5	1.60	1.90	3.00	5.30	5.40	6.30	6.4	6.5	6.50
6	1.50	1.80	2.60	4.90	5.10	6.20	6.4	6.5	6.50
7	1.50	1.70	2.70	4.80	5.00	6.10	6.4	6.5	6.50
8	1.40	1.60	2.60	4.60	4.90	6.10	6.4	6.5	6.50
9	1.40	1.50	2.30	4.60	4.80	6.00	6.4	6.5	6.50
10	1.35	1.35	1.90	4.30	4.80	6.00	6.4	6.5	6.50

Table 7.6 Flow velocity distribution law of discharge culvert under different flow rates of square holes (unit: L/min).

Number	8	16	34	132	166	300	334	432	466
1	0.20	0.25	0.40	0.83	0.98	1.77	1.97	2.55	2.75
2	0.24	0.27	0.46	0.85	1.01	1.77	1.97	2.55	2.75
3	0.30	0.32	0.38	0.86	1.03	1.79	1.97	2.55	2.75
4	0.27	0.32	0.42	0.86	1.05	1.79	1.97	2.55	2.75
5	0.38	0.53	0.51	0.91	1.12	1.79	1.98	2.55	2.75
6	0.43	0.59	0.64	0.99	1.19	1.80	1.98	2.55	2.75
7	0.43	0.66	0.60	1.01	1.22	1.82	1.98	2.55	2.75
8	0.50	0.75	0.64	1.07	1.25	1.82	1.98	2.55	2.75
9	0.50	0.86	0.79	1.07	1.28	1.84	1.98	2.55	2.75
10	0.54	1.09	1.13	1.17	1.28	1.84	1.98	2.55	2.75

as an index to judge the possibility of cavitation erosion on the nearby side wall:

$$\sigma = \frac{h_0 + h_a - h_v}{\frac{v_0^2}{2g}} \tag{7.2}$$

where h_0 indicates the average hydrodynamic pressure head when calculating the side wall of the cross section, that is, the pressure tube head, m; $\frac{v_0^2}{2g}$ represents the velocity head for calculating the average velocity of the section, m; h_v indicates the vaporization pressure head of the water, and the water temperature of this

@seismicisolation

test is 15 °C. Take h_v=0.174 m; h_a represents the atmospheric pressure head, which can be estimated by the following formula based on the calculated point elevation ∇z:

$$h_a = 10.33 - \frac{\nabla z}{900} - 0.39 = 9.94 - \frac{\nabla z}{900} \tag{7.3}$$

where 10.33 represents the standard atmospheric pressure water column, m; 0.39 is the maximum pressure drop considering meteorological factors, m; ∇z is the altitude of the calculation point (generally every 900 m increase, the atmospheric pressure head decreases by 1 m), m.

In this experiment, the parameter measurement of the relevant cavitation coefficient is carried out for the shaft discharge structure, and the flow cavitation coefficient along the discharge structure is obtained by calculation (Tables 7.7 and 7.8). It can be seen from Table 7.9 that when the discharge is 8 L/min, the minimum flow cavitation number along the retreat

Table 7.7 The distribution law of water depth of discharge culvert under different flow rates of long holes (unit: L/min).

Number	8	16	34L/min	132	166	300	432	466
1	2.00	2.30	3.20	5.80	6.20	6.20	6.50	6.50
2	1.70	2.10	3.00	5.50	6.00	6.10	6.50	6.50
3	1.50	1.90	2.90	5.40	5.50	6.10	6.50	6.50
4	1.40	2.00	2.90	5.40	5.20	6.00	6.50	6.50
5	1.40	1.70	2.50	4.80	5.00	5.90	6.50	6.50
6	1.20	1.50	2.30	4.40	4.90	5.90	6.50	6.50
7	1.30	1.50	2.20	4.30	4.80	5.90	6.50	6.50
8	1.30	1.40	2.00	4.30	4.70	5.90	6.50	6.50
9	1.30	1.40	2.00	4.30	4.60	5.90	6.50	6.50
10	1.10	1.50	2.00	4.10	4.50	5.90	6.50	6.50

Table 7.8 Flow velocity distribution law of discharge culvert under different flow rates of rectangular holes (unit: L/min).

Number	8	16	34	132	166	300	432	466
1	0.24	0.37	0.46	0.83	1.00	1.80	2.55	2.75
2	0.33	0.44	0.51	0.87	1.02	1.01	2.55	2.75
3	0.43	0.53	0.54	0.89	1.10	1.01	2.55	2.75
4	0.50	0.48	0.54	0.89	1.16	1.02	2.55	2.75
5	0.50	0.66	0.69	1.01	1.22	1.03	2.55	2.75
6	0.72	0.86	0.79	1.13	1.25	1.03	2.55	2.75
7	0.59	0.86	0.86	1.17	1.28	1.03	2.55	2.75
8	0.59	1.00	1.03	1.17	1.31	1.03	2.55	2.75
9	0.59	1.00	1.03	1.17	1.34	1.03	2.55	2.75
10	0.91	0.86	1.03	1.24	1.38	1.03	2.55	2.75

Table 7.9 Estimation of cavitation number of water flow along the discharge structure (unit: L/min).

Serial number	8	16	34	132	166	300	334
1	27.42	24.70	10.46	5.17	3.30	1.83	1.58
2	18.52	15.09	8.48	4.24	3.30	1.70	1.51
3	11.10	10.75	5.99	3.85	3.51	1.76	1.44
4	14.33	14.09	4.81	4.01	3.37	1.67	1.48
5	9.25	7.07	4.03	4.01	3.29	1.53	1.56
6	5.09	4.18	3.75	3.01	3.21	1.55	1.45
7	4.63	3.91	2.24	2.38	3.05	1.54	1.44
8	4.09	3.71	2.36	2.29	2.19	1.56	1.45
9	3.53	2.76	2.00	2.05	1.99	1.53	1.42

@seismicisolation

tunnel is 3.53, and when the discharge is 16 L/min, the minimum flow cavitation number along the retreat tunnel is 2.76. When the discharge is 34 L/min, the minimum cavitation number is 2.00; when the discharge is 132 L/min, the minimum cavitation number is 2.05; when the discharge is 166 L/min, the minimum cavitation number is 1.99; when the discharge is 300 L/min, the minimum cavitation number is 1.53. When the discharge rate is 334 L/min, the minimum cavitation number of water flow along the retreat tunnel is 1.42.

From the estimated results, it is known that the flow cavitation number of the retreat tunnel under all working conditions is large under non-overflow conditions, and the measured minimum flow cavitation number is 1.42, which is much larger than the flow cavitation number required by the code, so the cavitation flow problem will not occur in the retreat tunnel. Cavitation damage can be eliminated as long as the construction unevenness is controlled.

7.3. SAFETY STABILITY ANALYSIS OF CHECK DAM

7.3.1. Explanation of the Theoretical Model

This section takes three check dams in the Wangmaogou small watershed on the left bank of Jiuyuangou in northern Shaanxi as an example, after analyzing the factors affecting the stability of the dam, the static stability analysis of the dam is carried out by using the GeoSlope software based on the limit equilibrium method (Figure 7.21). The safety factor of check dam under the condition of rainstorm stagnant water in different return period and the safety factor and the most dangerous sliding surface of rainstorm check dam on 15 July 2012 are obtained.

7.3.1.1. Description of Dam Body Characteristics of Check Dam

After field investigation, the measured geometric characteristic parameters of check dam are shown in Table 7.10.

7.3.1.2. Calculation Principle and Method

At present, the widely used methods for slope stability assessment and landslide and collapse disaster investigation are field investigation method, qualitative analysis method, multivariate analysis method, stability classification method based on slope, lithology and geological structure, and traditional method and finite element method based on limit equilibrium. Limit equilibrium method (such as Swedish arc method, Bishop method, and Janbu method) is the most commonly used method in slope stability analysis. It calculates the degree of slope stability under the action of itself and external load by analyzing the balance between the external force and the resistance provided by the internal strength of the slope under the condition of near failure. The general limit equilibrium equation (GLE method) is based on two safety factor equations and allows the shear force and normal force of the interstrip force to change in a certain range. One equation is the safety factor (Fm), about the moment balance and the other is the safety factor (Ff) about the horizontal force balance.

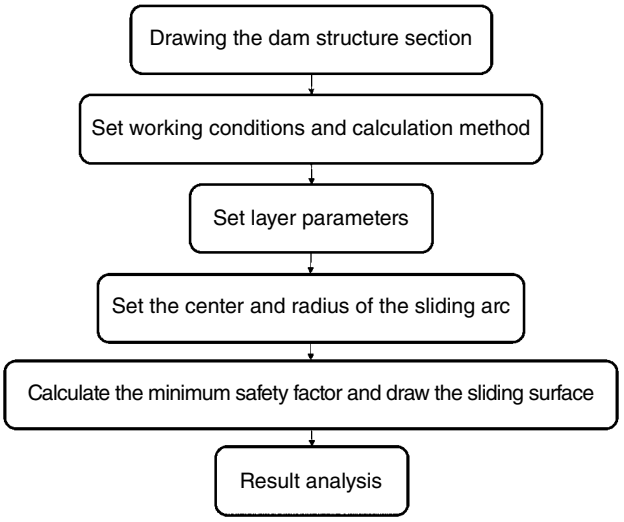

Figure 7.21 Block diagram of stability analysis and calculation of check dam.

Table 7.10 Geometric characteristic parameters of check dams.

Dam name	Dam crest width (m)	Dam crest length (m)	Upstream slope length of dam (m)	Downstream slope length of dam (m)	Upstream slope angle of dam (°)	Downstream slope angle of dam(°)
Nianyangou No.1	5	72	28	28	30	30
Nianyangou No.2	4	60	21	20	35	40
Guandigou No. 1	4	58	53	42	27	35

@seismicisolation

The shear force between strips in GLE method can be expressed by an equation:

$$X = E\lambda f(x) \tag{7.4}$$

where $f(x)$ represents a function;

λ λ represents the percentage used by the function (decimal form);

E is the normal force between bars (kPa);

X is the shear force between strips (N).

GLE method torque balance safety factor equation:

$$Fm = \frac{\sum\left[c'\beta R + (N - \mu\beta) R \tan\phi'\right]}{\sum Wx - \sum Nf \pm \sum Dd} \tag{7.5}$$

The horizontal static balance safety factor equation:

$$Ff = \frac{\sum\left(c'\beta\cos\alpha + (N - \mu\beta)\tan\phi'\cos\alpha\right)}{\sum N\sin\alpha - \sum D\cos\omega} \tag{7.6}$$

where c′ is the effective cohesion (kPa);

ϕ' is the effective friction angle (°);

μ is the pore water pressure (N);

N is the normal force at the bottom of the soil strip (kPa);

W is the weight of the soil strip (kN);

D is the concentrated point load (kN);

β(m)、R(m)、x(m)、d(m)、ω(°) are geometric parameters;

α is the inclination of the soil strip bottom surface (°).

7.3.1.3. Selection and Determination of Parameters

According to the principle of GLE method for seepage calculation and stability calculation, the following parameters need to be determined, such as seepage coefficient, soil water characteristic curve, soil water content, cohesion, internal friction angle, and weight. In this study, the check dam body and the dam land adjacent to the dam body are selected, and the specific material characteristic parameters of the check dam body are shown in the following Table 7.11.

Table 7.11 Material characteristic parameters of check dam.

Name of check dam	Water content (%)	Cohesion (kPa)	Internal friction angle (°)	Heavy weight (kN/m³)
Nianyangou No.1	10.89	42.33	28.80	13.90
Nianyangou No.2	11.35	41.60	30.5	15.4
Guandigou No. 1	10.92	43.33	28.92	15.5

7.3.1.4. Establishment of Calculation Model of Slope Stability

The calculation uses slope/w, a module of the geotechnical analysis software Geo-Slope developed by Geostudio Company of Canada, to calculate the slope stability. Its principle adopts limit equilibrium method, including Swedish slice method, Bishop method, Jiangbu method, Morgenstern-Price method, etc., which can calculate the slope stability considering pore water pressure. At present, it has been used in many large-scale hydropower projects in China, such as the reservoir slope of Jinping cascade power station, the slope of the three Gorges reservoir area, some hydropower slopes of Dadu River, etc., and the reliability has been fully verified. The effect is good. In this paper, it is applied to the stability analysis and calculation of check dam structure. The block diagram of the program calculation process is shown in Figure 7.22.

The stability calculation model is established in Geo-Slope software, and the steps are as follows:

1. According to the measured data and boundary characteristics, the geometric model of check dam is drawn in Geo-Slope software.
2. The calculation method of seepage model is set, the height of water level in front of the dam in different recurrence periods is set, and the seepage calculation is carried out.
3. The calculation method is set and the GLE method is adopted.
4. The material of the model is assigned according to the parameters, and the assigned values are weight, angle of internal friction, and cohesion.
5. The range of slide-in and out-of-face is specified.
6. The model test is carried out.

7.3.2. Results of Numerical Simulation Calculation

According to the above calculation model, the influence of seepage should be considered in calculating the overall stability of the check dam under stagnant water conditions. The seepage infiltration line of the check dam under different working conditions is calculated by using the SEEP/W module of the

@seismicisolation

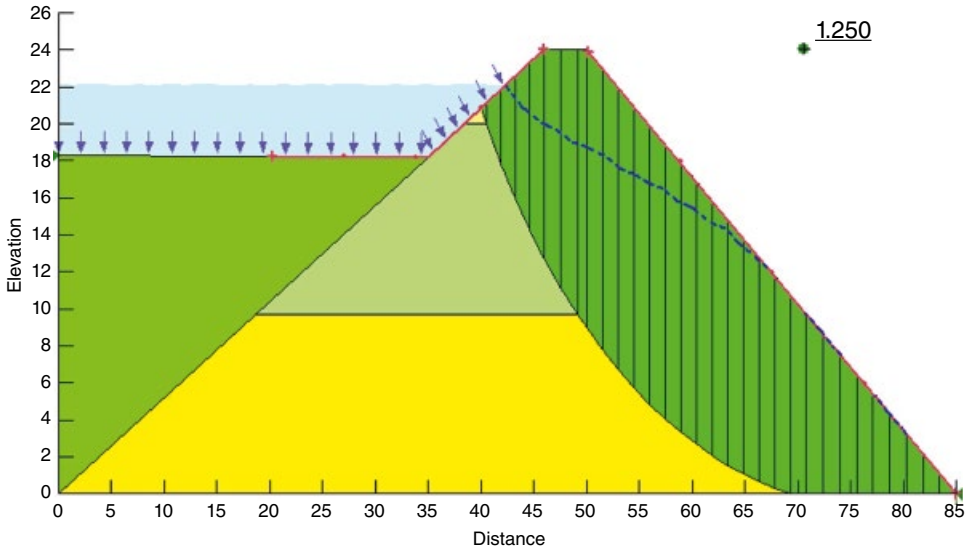

Figure 7.22 The minimum safety factor and most dangerous slip surface in the case of "7.15" rainstorm flood in Guandigou1# Dam.

Table 7.12 Statistical table of water level process and maximum water level in front of check dam under the condition of "7.15" rainstorm flood.

Guandigou 1#	T0	T1	T2	T3	T4	T5	T6	T7	Highest water level(m)
Time (h)	0.00	1.00	1.19	1.30	1.56	2.88	6.30	12.60	3.71
Water level (m)	0.00	0.06	0.11	0.24	0.63	1.22	3.71	3.41	
Nianyangou2#	T0	T1	T2	T3	T4	T5	T6	T7	Highest water level(m)
Time (h)	0.00	1.00	1.13	1.22	1.40	2.34	6.22	12.43	0.61
Water level (m)	0.00	0.03	0.05	0.10	0.22	0.41	0.61	0.58	

Geo-Slope software and then imported into the SLOPE/W module. The overall stability is calculated according to the limit equilibrium theory GLE method, that is, the safety factor and the most dangerous sliding surface.

(1) Safety analysis and calculation of check dam under the condition of "7.15" rainstorm

According to the results of the water level height in front of the dam calculated by the 7.15 rainstorm caused by the 7.15 rainstorm calculated in Section 3.3.2, the safety and stability calculation is carried out by introducing the model. Among them, in the case of "7.15" rainstorm, the water level process and the highest water level in front of the Qianyangou dam in Guandigou are shown in Table 7.12.

The highest water level in front of Guandigou1# dam and Nianyangou2# dam is brought into the SEEP/W seepage model established above, and the seepage calculation is carried out. The calculated results are then introduced into the SLOPE/W stability model, and the minimum safety stability coefficient and the most dangerous sliding surface of check dam are calculated. Figures 7.22 and 7.23 are shown, respectively.

The analysis results show that under the condition of "7.15" rainstorm, the safety factor of Guandigou1# dam is 1.25 when the water depth reaches 3.71 m, which is greater than 1.20 stipulated in the Code for Design of rolled Earth-rockfill Dam (SL274-2001) issued by the state in 2007, and the check dam is in a stable state (Figure 7.24). Under the "7.15" rainstorm water accumulation condition, the safety factor of the check dam body is 2.396 when the stagnant water depth reaches 0.61 m, which is larger than 1.20 stipulated in the Code for Design of rolled Earth-rockfill Dam (SL274-2001) issued by the state in 2007. The check dam is in a stable state.

@seismicisolation

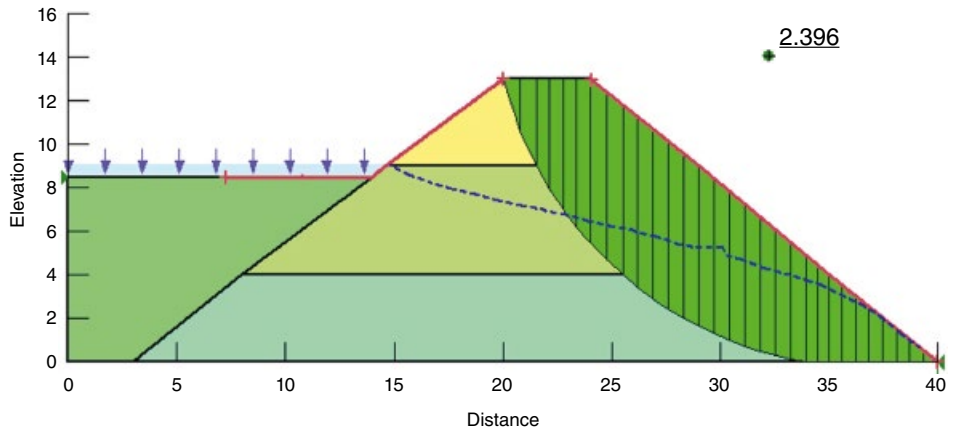

Figure 7.23 The minimum safety factor and most dangerous slip surface in the case of "7.15" rainstorm flood in Nianyangou2# dam.

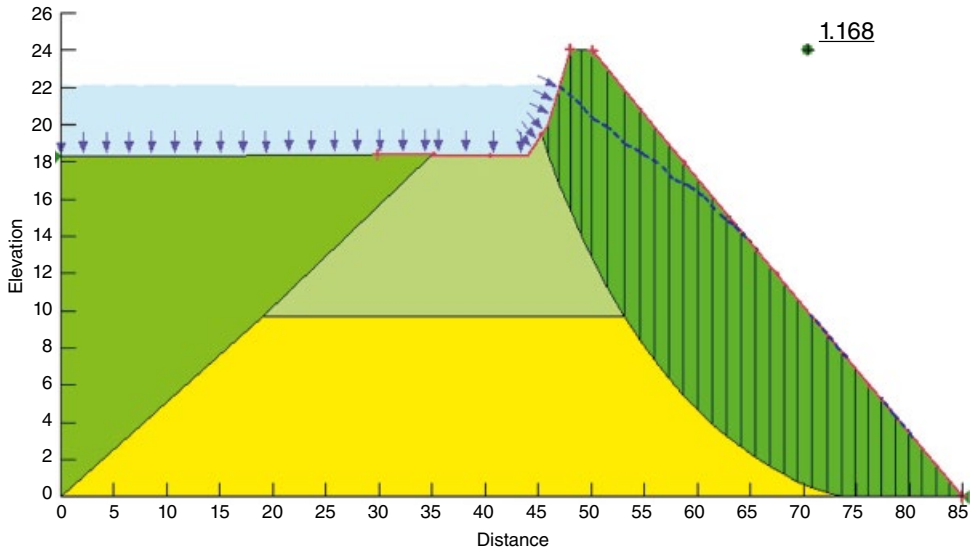

Figure 7.24 The minimum safety factor and the most dangerous sliding surface under the 7.15 storm flood after the partial reduction of Guandigou1# dam.

However, in the actual situation of "7.15" rainstorm, both Guandigou1# dam and Nianyangou2# dam broke (Figure 7.25). It is found that before the "7.15" rainstorm flood, the check dam body has been damaged to varying degrees due to the previous rainstorm flood, which is specifically manifested by the collapse of the shaft in front of the Guandigou1# dam to a certain extent. It is equivalent to the reduction of the dam body at the shaft in front of the dam. After the "7.15" rainstorm, the Guandigou1# dam was connected back and forth at the shaft, resulting in dam break. Before the "7.15" rainstorm flood of the Nianyangou2# dam, the lying pipe and culvert had seriously collapsed, and the surroundings of the lying pipe had been washed away and separated from the surrounding soil. After the "7.15" rainstorm, the tunnel jumped from the culvert and eventually caused the dam to break. Therefore, the reduction of the check dam body caused by the flood is assumed here, the dam body in front of the silt dam in the model is partially reduced, and then the seepage stability of the dam body is simulated. The specific results are shown in Figures 7.26 and 7.28.

The analysis results show that under the condition of "7.15" rainstorm, the safety factor of Guandigou1# dam is 1.168 when the water depth reaches 3.71 m, which is less than 1.20 stipulated in the Code for Design of rolled Earth-rockfill Dam (SL274-2001) issued by the state in 2007, and the check dam is in an unstable state. Under

@seismicisolation

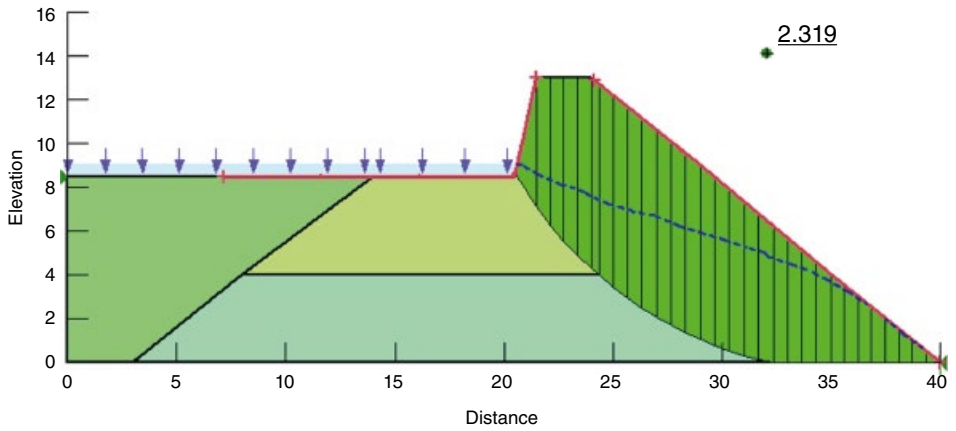

Figure 7.25 The minimum safety factor and the most dangerous sliding surface under the 7.15 storm flood after partial reduction of the Nianyangou2# dam.

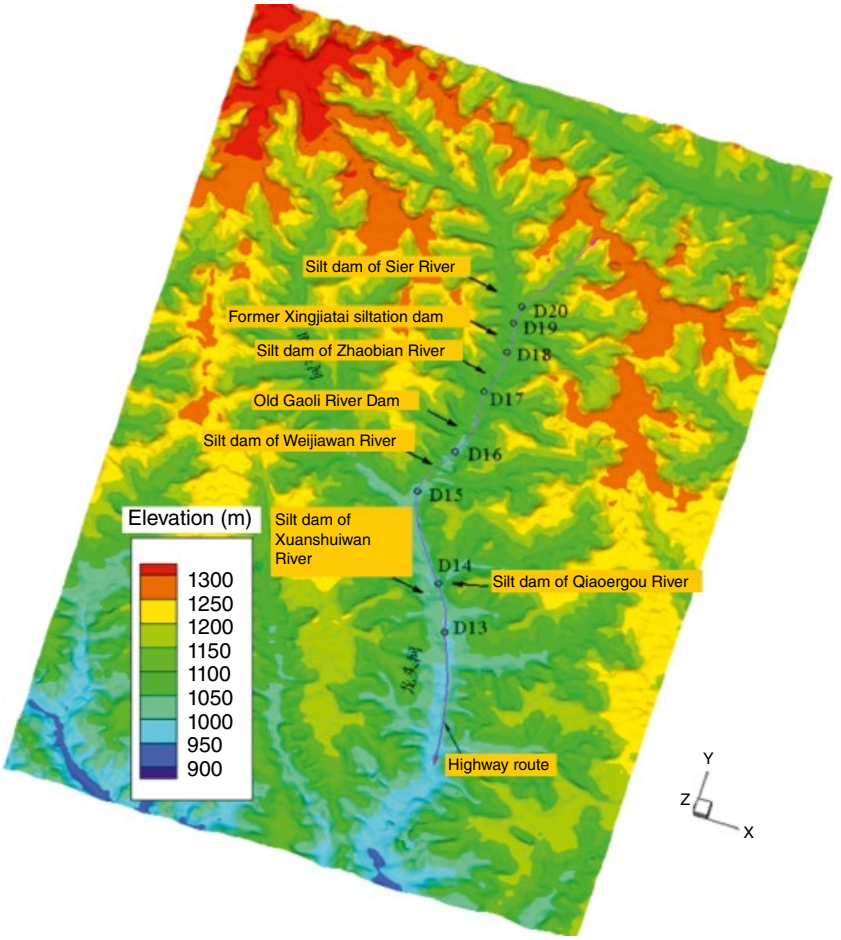

Figure 7.26 Topographic map of calculation area of check dam in Longtou River basin.

the "7.15" rainstorm water accumulation condition, the safety factor of the check dam body is 2.319 when the stagnant water depth reaches 0.61 m, which is larger than 1.20 stipulated in the Code for Design of rolled Earth-rockfill Dam (SL274-2001) issued by the state in 2007. The check dam is in a stable state.

After the hypothetical reduction of the dam body, the Guandigou1# dam is in a state of instability and

@seismicisolation

dam break occurs, which is consistent with the results of the investigation. However, the Nianyangou2# dam is still stable, which is not consistent with the actual investigation, which may be due to the separation of the soil around the rain at the lying pipe and the culvert, and there may have been a small seepage hole or perforation inside the dam, resulting in the case of "7.15" rainstorm flood. It is easy to break the dam. Therefore, it is suggested that in the follow-up risk assessment of check dam, in the analysis of the factors of dam break caused by discharge structure, priority should be given to the damage of horizontal pipe culvert and its occurrence in the case of soil separation, followed by the collapse factor caused by the shaft in front of the dam, and the spillway at the end.

(2) Safety analysis and calculation of check dams under different recurrence periods

According to the rainstorm flood analysis and calculation of this study, this section is divided into three parts to study the safety and stability of check dams in Wangmaogou basin under rainstorm water accumulation conditions in different return periods.

1) Safety and stability of dam under rainstorm water accumulation in different return periods under current conditions

According to the results of the water level height in front of the dam calculated by the flood caused by rainstorm in different return periods calculated in Section 3.3.4, the safety and stability calculation is carried out by introducing the model. Under the condition of rainstorm in different return periods, the calculation table of safety factor of Guandigou1# Dam and Nianyangou2# Dam under the condition of rainstorm stagnant water is shown in Table 7.13.

2) Safety and stability of dam under rainstorm water accumulation in different return periods under the condition of returning farmland

According to the results of the water level height in front of the dam calculated by the flood caused by rainstorm in different return periods calculated in Section 3.3.4, the safety and stability calculation is carried out by introducing the model. Under the condition of rainstorm in different return periods, the calculation table of safety factor of Guandigou1# Dam and Nianyangou2# Dam under the condition of rainstorm stagnant water is shown in Table 7.14.

3) Safety and stability of dam under rainstorm water accumulation in different return periods under the condition of soil and water conservation measures capacity

According to the results of the water level height in front of the dam calculated by the flood caused by rainstorm in different return periods calculated in Section 3.3.4, the safety and stability calculation is carried out by introducing the model. Under the condition of the capacity of soil and water conservation measures, under the condition of rainstorm in different return periods, the calculation table of safety factor under the condition of rainstorm stagnant water in Guandigou1# Dam and Nianyangou2# Dam is shown in Table 7.15.

Table 7.13 Calculation table of safety factor under rainstorm stagnant water conditions in different return periods.

Different return periods	Guandigou1# Dam	Nianyangou2# Dam
$T = 10$	1.377	2.482
$T = 20$	1.363	2.421
$T = 30$	1.353	2.417
$T = 50$	1.342	2.412
$T = 100$	1.331	2.401
$T = 200$	1.315	2.386
$T = 300$	1.305	2.381

Table 7.14 Calculation table of safety factor under rainstorm stagnant water conditions in different return periods.

Different return periods	Guandigou1# Dam	Nianyangou2# Dam
$T = 10$	1.383	2.428
$T = 20$	1.367	2.422
$T = 30$	1.367	2.418
$T = 50$	1.348	2.413
$T = 100$	1.336	2.402
$T = 200$	1.324	2.387
$T = 300$	1.317	2.382

Table 7.15 Calculation table of safety factor under rainstorm stagnant water conditions in different return periods.

Different return periods	Guandigou1# Dam	Nianyangou2# Dam
$T = 10$	1.383	2.428
$T = 20$	1.369	2.423
$T = 30$	1.363	2.419
$T = 50$	1.352	2.414
$T = 100$	1.343	2.404
$T = 200$	1.332	2.397
$T = 300$	1.328	2.387

@seismicisolation

From the safety factors of Guandigou1# dam and Nianyangou2# dam in different return periods in Wangmaogou small watershed under the above three scenarios, they are in line with the 1.20 stipulated in the Code for Design of rolled Earth-rockfill Dam (SL274-2001) issued by the state in 2007, and the check dam is in a stable state.

On the whole, the safety factor of check dam in Wangmaogou small watershed is greater than the safety factor stipulated in the code, which meets the stability requirements. When stagnant water is caused by sudden rainstorm or other reasons, the safety factor is downloaded sharply, and there is a hidden danger in check dam at this time. Attention should be paid to preventive measures to avoid dam collapse or dam break, resulting in losses. However, according to the actual investigation, the dam break occurred on the right side of the dam body of the Nianyangou2# dam, which may be mainly due to the lack of close contact between the culvert of the check dam discharge structure and the dam body, which leads to scouring in the case of heavy rainstorm, thus causing the dam break. However, in terms of seepage stability analysis of the dam itself, the dam is safe.

7.4. SIMULATION OF CHECK DAM BREAK

7.4.1. Description of Model

The two-dimensional flood evolution numerical model of the research group of Xi'an University of Technology was used to analyze the dam break. The model is based on digital elevation model (DEM) topographic data and the finite volume method is used to solve the hydrodynamic equation of two-dimensional mean water depth distribution. The upwind conservation scheme and The Harten–Lax–van Leer (HLL) approximate Riemann scheme are used to solve the flood wave problem, which can effectively avoid the numerical oscillation and capture the flood wave movement, and has good reliability, conservation, and stability. The model adopts a two-step explicit solution to the governing equation, and the dry and wet points in the calculation domain are judged according to the water depth, so the calculation efficiency is high. In addition, various conditions such as instantaneous total dam break, instantaneous local dam break, dam break, gradual total dam break, and multistage dam break in the basin can be considered. Erosion and sediment transport during flood can also be considered.

(1) Explanation of model calculation

The preliminary flood risk analysis is aimed at the most unfavorable situation when the check dam on Fucunchuan and Longtou River overflows and breaks instantaneously. In Longtou River basin, the multi-dam chain break of seven check DAMS was considered, that is the check dam in the upper reaches of Siergou occurred dam break at the beginning, and Xingjiatai check dam caused dam break before flood impact downstream, and so on, the check dam in the lower reaches occurred break in turn under flood impact. Since Qiaoergou is on the tributary of Longtou River in order to consider the influence of the most unfavorable dam break condition, it is set that the dam will also break when the flood reaches XuanShuiWan check dam.

The dam break calculation adopts two-dimensional flood evolution numerical simulation that can consider multi-dam break, and the topographic data adopt 30m×30m DEM elevation data provided by NASA. The terrain of the calculation area of check dam in Longtou River basin is shown in Figure 7.26.

7.4.2. Result Analysis

Figure 7.27 shows the variation curve of maximum water depth at each control point in the calculation of check dam break in Longtou River basin. Figure 7.28 shows the distribution diagram of maximum water depth calculated for dam break of check dam in Longtou River basin, and Figure 7.29 shows the distribution diagram of velocity and flow line.

As can be seen from the figure, when multistage dam break occurs, the flood develops rapidly due to the gradual exhaustion of the flood. After the check dam

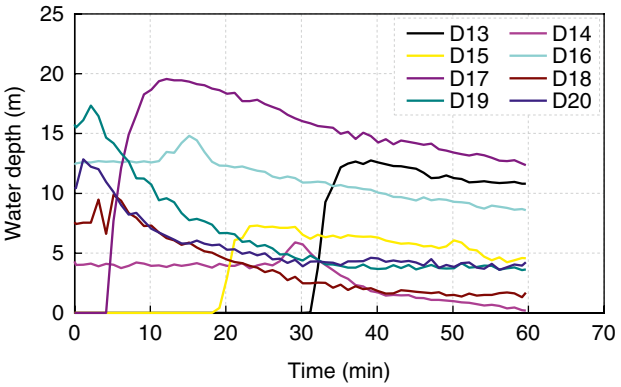

Figure 7.27 Water depth change curve of check dam break calculation at each control point in Longtou River basin.

@seismicisolation

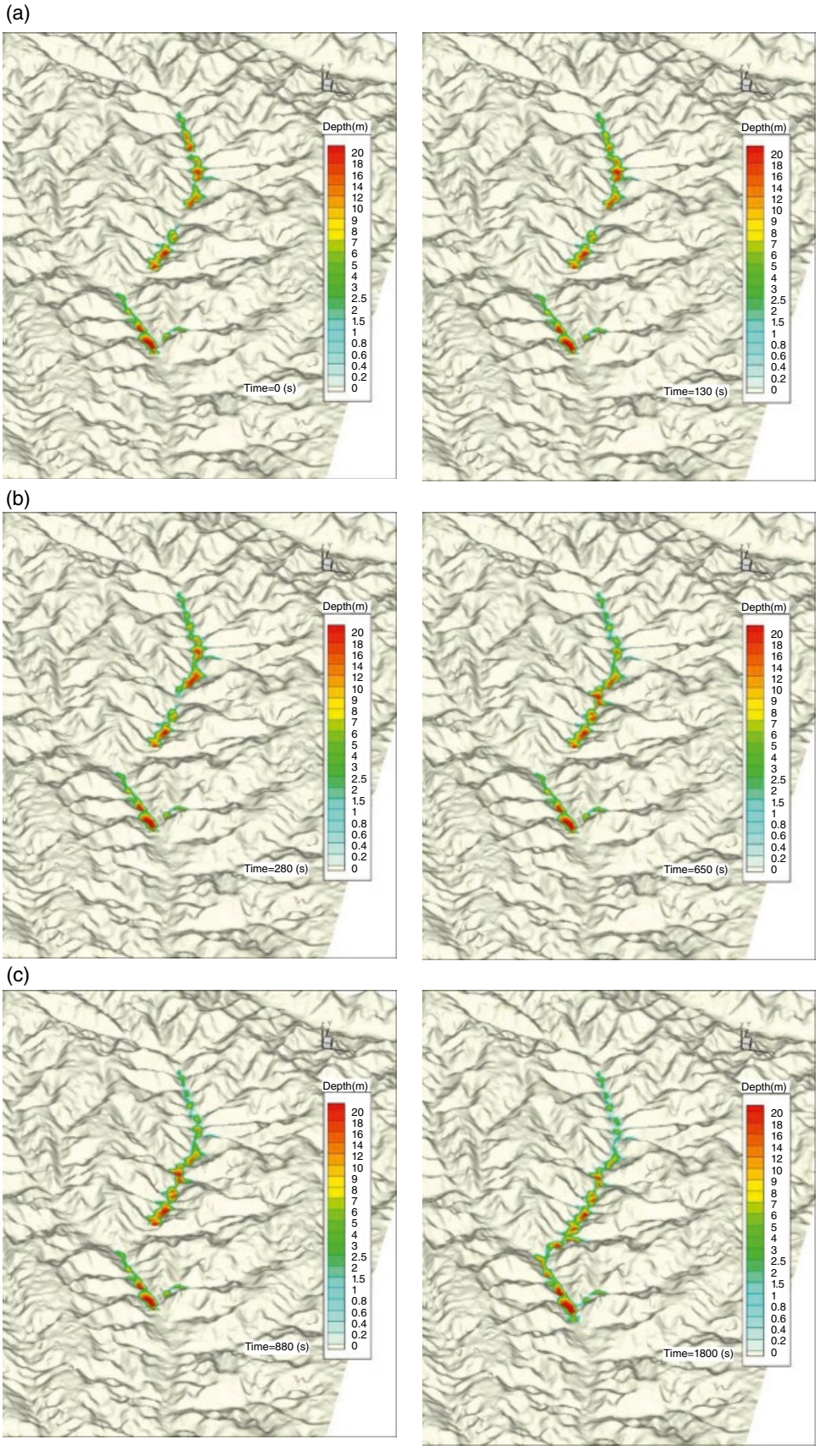

Figure 7.28 (a) Water depth distribution of check dam break calculation in Longtou River basin. (b) Water depth distribution of check dam break calculation in Longtou River basin. (c) Water depth distribution of check dam break calculation in Longtou River basin.

@seismicisolation

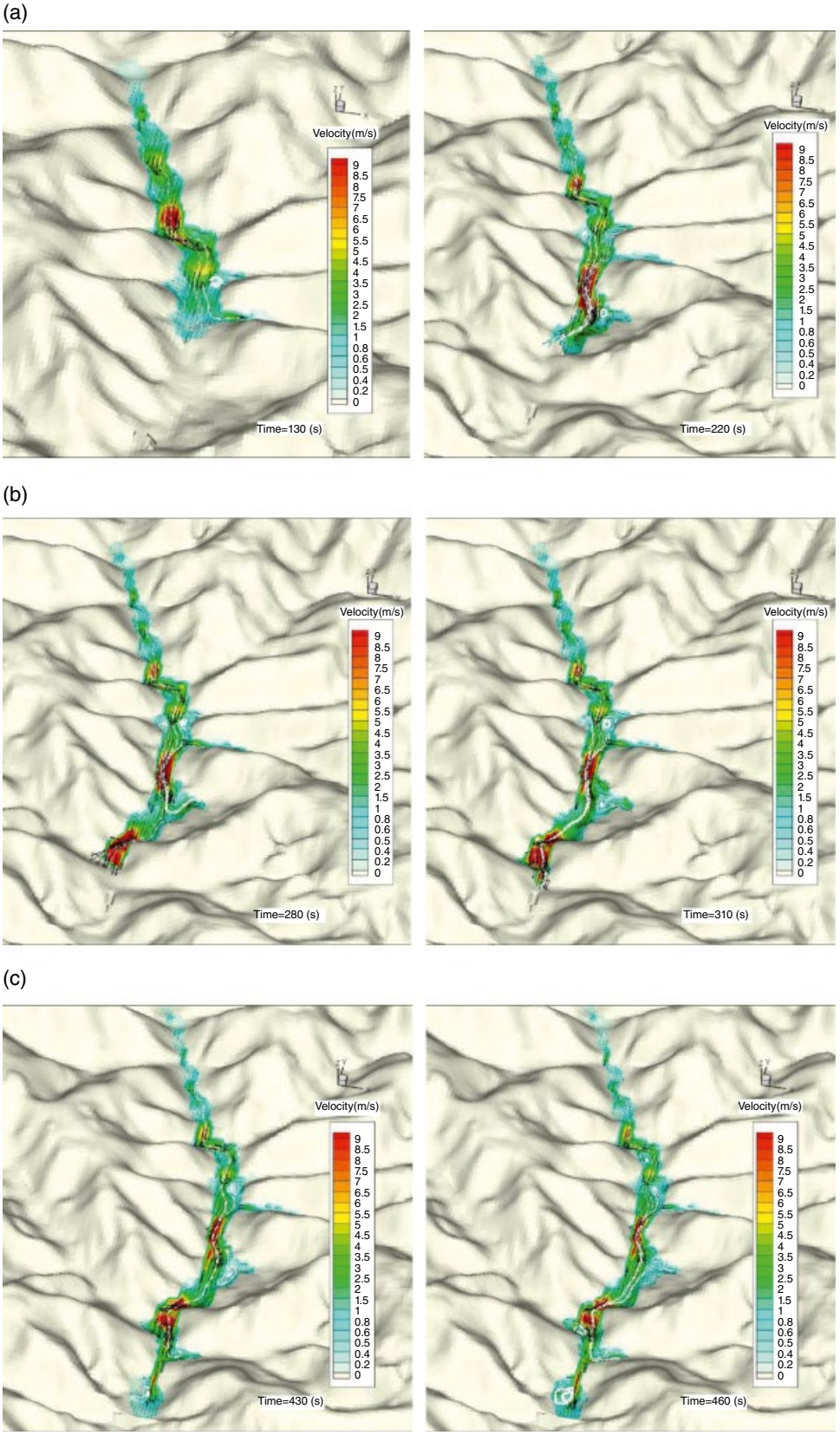

Figure 7.29 (a) Schematic diagram of velocity and streamline distribution at 130s. (b) Schematic diagram of velocity and streamline distribution at 280s. (c) Schematic diagram of velocity and streamline distribution at 430s. (d) Schematic diagram of velocity and streamline distribution at 640s. (e) Schematic diagram of velocity and streamline distribution at 880s. (f) Schematic diagram of velocity and streamline distribution at 1600s. (g) Schematic diagram of velocity and streamline distribution at 1810s–1960s.

@seismicisolation

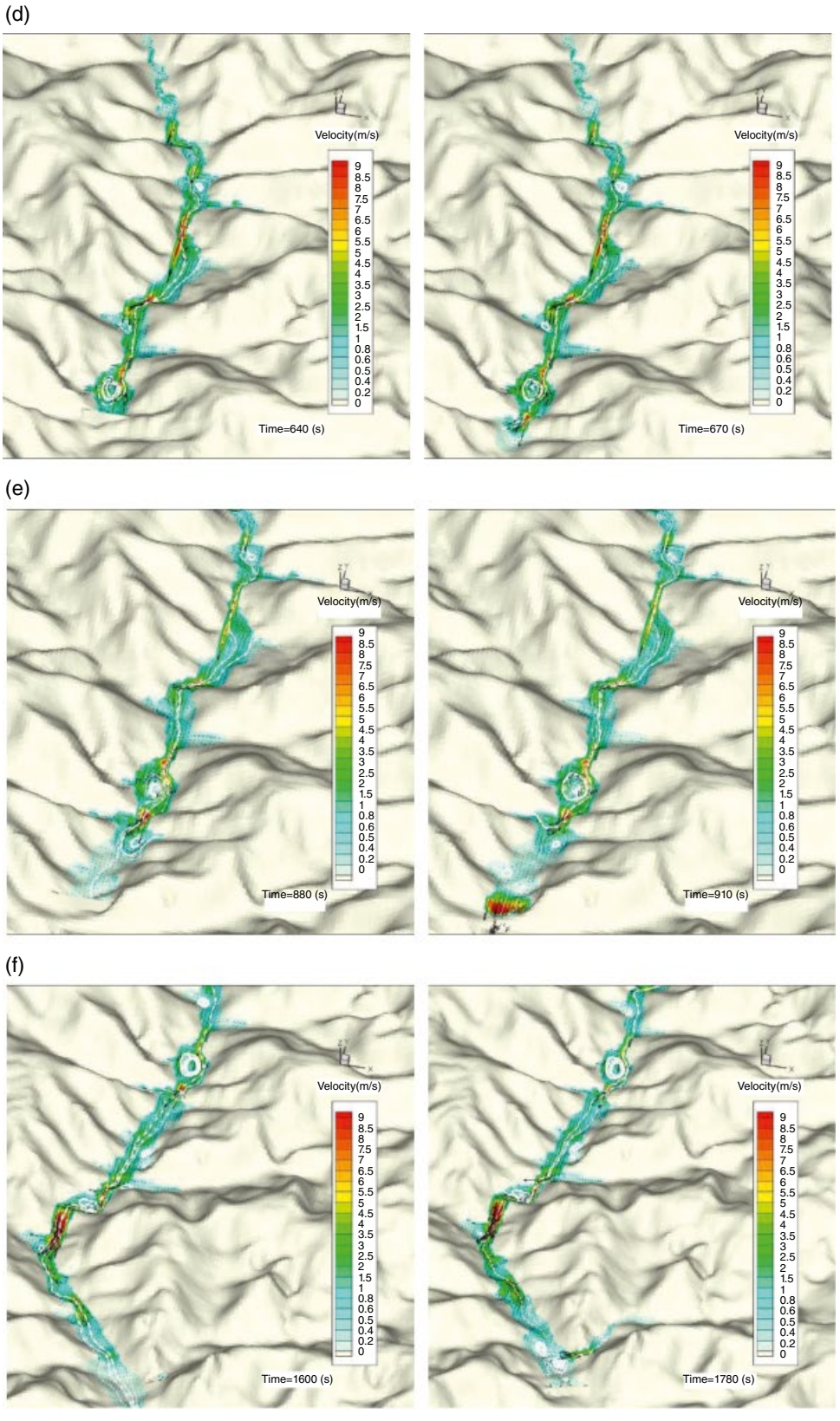

Figure 7.29 (Continued)

@seismicisolation

(g)

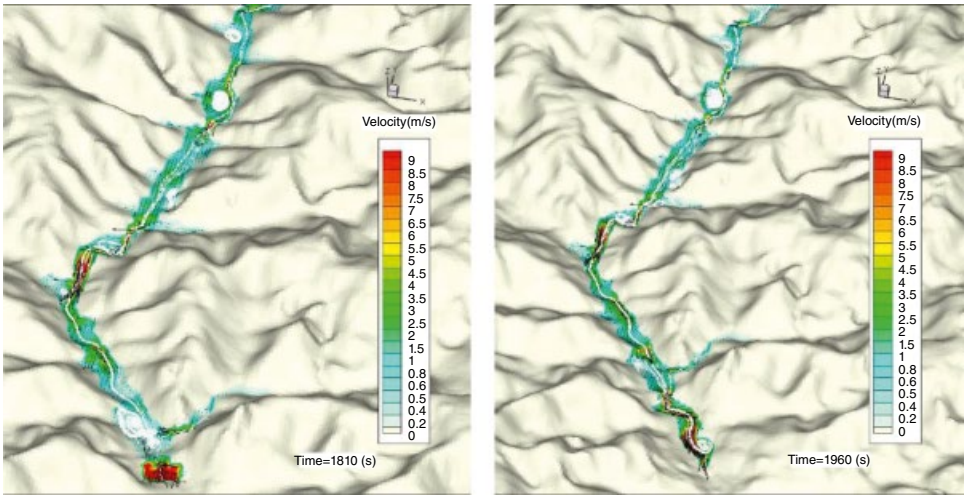

Figure 7.29 (Continued)

of Sier River in the most upstream occurs, the flood will wash out the check dams along the way one by one in about 30 minutes, leading to the break of XuanShuiWan check dam in the most downstream. In the process of dam break, the upstream channel is narrow and the flow velocity is large. The flow velocity of most mainstream is about 3 m/s, and some areas are close to 10 m/s. The impact of flood is highly destructive. The downstream channel is relatively open with a relatively small flow rate, and the mainstream flow rate is about 1.5 m/s. During the whole process, the turbulence of the flood is severe, and large eddies appear, which will cause serious scour to the river channel. When the cascade dam break occurs, when the upstream flood reaches the current check dam, strong flood wave reflection will be formed due to the obstruction of the dam body, so it may cause problems such as landslides.

7.4.2.1. Study on the Method of Check Dam Break

(1) The morphology of the break was confirmed

Dam break is the gap formed when check dam breaks, and the shape of break is mainly related to dam type and dam building material. At present, the actual mechanism of dam break is still not very clear, so the shape of the break is mainly determined by approximate assumption. It is generally assumed that the burst begins at a certain point on the crest of the dam and develops in a linear proportion during the break duration until the final width is formed. The final width of dam burst was calculated by referring to Lu Jikang's empirical formula (7.7) of China Institute of Water Resources and Hydropower Research:

$$B_m = 0.1803 k V_r^{0.32} H_b^{0.19} \tag{7.7}$$

where H_b is the water depth of burst (water level at the moment of reservoir burst – average base elevation of dam site section) (m), V_r is the effective downdraft storage capacity (m^3), B_m is the average width of the final burst (m) (referring to the average width of the upper and lower trapezoidal burst), K is the correction factor, and k=1 for dam break caused by over-topping.

(2) Calculation of burst time

In principle, the dam break is expanded at the current rate, and the development time of the dam break is determined as follows:

$$T_f = 0.00245 k V_r^{0.53} H_b^{(-0.09)} \tag{7.8}$$

where T_f is the development time of the break, and other symbols have the same meanings as the formula (7.7).

(3) Calculation of maximum break flow

Combined with the actual situation of check dam in WangMaoGou small watershed, Rouse formula is finally selected to calculate the maximum break flow:

$$Q_m = \frac{8}{27}\sqrt{g}\left(\frac{B}{b_m}\right)^{\frac{1}{4}} b_m H^{\frac{3}{2}} \tag{7.9}$$

@seismicisolation

where Q_m is the maximum flow rate of break (m^3/s), g is the acceleration of gravity (m/s^2), B is the dam length (m), b_m is the final burst width (m), and H is burst depth (m).

(4) Dam break flow process line

Assuming that the base flow is 0, the calculation formula of dam break flood process line at time t is as follows, based on the obtained peak discharge of the burst flood, total flood volume W and flood duration T_n:

$$Q = Q_{\max}\left(\frac{Q_{\max}}{5W}t - 1\right)^4 \tag{7.10}$$

According to the above formula, the parameters of check dam break can be calculated. For the check dam with flood over-topping in Wangmaogou small watershed in the case of rainstorm and flood once every 100 years, the relevant parameters of each dam with dam break calculated by the above formula are shown in Table 7.16.

7.4.2.2. Analysis of the Result of Check Dam Break

It can be seen from Table 7.16 that when a check dam breaks, the time for the maximum flow rate $Q_{\max}$ of the dam site to reach from 0 is very short, with the shortest and longest flow rate only 23 s and 116 s. Flood duration refers to the time taken for the discharge of the dam site to $Q_{\max}$ return to 0 again. It can be seen from the table that this period of time is also very short. For check dam, when the dam break occurs, the dam break will be formed in a very short time, and the break flow is very large, and the stock flood will be empty-drained in a very short time. The time from the occurrence of dam break to the termination of dam break is very short, and there is no warning time at all in the downstream, which causes serious damage to the downstream villages and vegetation after the break of the check dam, and the flood of the reservoir of the check dam in the downstream will suddenly increase, and the water level will rise accordingly, increasing the risk of dam break in the downstream.

7.5. CONCLUSION

For the purpose of quantitatively describing the mechanism of water damage of check dam, three main research methods, field investigation, experiment. and numerical simulation, are adopted. According to the data of field work, it is reported that over-topping dam failure, seepage damage, and structural damage are the main reasons for the break of check dams in the early 1980s. Four main causes of water damage, also including the over-standard storm flood, are concluded in the 1990s. In conclusion, the main causes of dam failure are listed as: (1) the dam broke because of excessive rainfall; (2) lack of backbone projects, low flood control standards of the dam system; (3) the backbones engineering facilities that do not match and the drainage that is not smooth cause the dam to collapse; (4) poor slope management reduces the function of dam system engineering; (5) poor construction quality; and (6) the management system is not reliable, and management measures cannot be maintained.

The dam damage mechanism caused by cavitation erosion of water discharge structure is investigated by the experiment. The results show that with the increase of the water head, the water begins to impact the tower wall, and the position of the impact point increases with the increase of the water head. The experimental observation shows that the change of angle between the upper inlet and outlet axis has little influence on the flow pattern in the energy dissipation well. Additionally, cavitation damage can be eliminated as long as the construction unevenness is controlled.

Furthermore, the static stability analysis of the dam is carried out by using the Geo-Slope software based on

Table 7.16 The main parameters of dam break flood calculation scheme.

Dam	Dam length (m)	Burst depth (m)	Effective drainage capacity (m)	The final width of the burst (m)	The development time of the burst(s)	Maximum burst flow (m^3/s)	Flood duration(s)
Hejiamao	48.00	5.20	104.10	1.09	23.46	30.89	15.63
Wangtagou 2 #	42.00	3.40	1040.00	2.10	116.46	25.83	187.74
Huangbaigou 2# Dam	30.00	15.10	4748.40	4.53	68.07	395.78	62.51
Guandigou3#Dam	40.00	20.10	3673.45	4.41	45.93	639.69	27.88
Kanghegou 1#Dam	55.00	10.90	2775.90	3.59	68.67	237.04	56.30

@seismicisolation

the limit equilibrium method under the condition of "7.15" rainstorm. It is summarized that in the analysis of the factors of dam break caused by discharge structure, priority should be given to the damage of horizontal pipe culvert and its occurrence in the case of soil separation, followed by the collapse factor caused by the shaft in front of the dam, and the spillway at the end.

A two-dimensional flood evolution numerical model was utilized to analyze the dam break. The results demonstrate that after the check dam of Sier River in the most upstream occurs, the flood will wash out the check dams along the way one by one in about 30 minutes, leading to the break of XuanShuiWan check dam in the most downstream, which develops rapidly. The time for the maximum flow rate of the dam site to reach from 0 is very short, with the shortest and longest flow rate of 23 s and 116 s, respectively.

REFERENCES

1. Geng, S., Fan, B., Liu, S., and Li, S. (2020). *Soil and Water Conservation in China 10*: 30–31.
2. Yi, Q., Qi, Q., and Ke, L. (2015). *Calculation of design flood for regions with no data but influencedby warping dam projects 368*: 281–286.
3. Zhang, X. and Chen, Z. (2019). Analysis of burst flood of warp dam system in small watershed. *Chinese Journal of Geotechnical Engineering 41*: 1845–1853.
4. Wang, Y., Wang, Y., and Wang, Y. (1995). Investigation on the Flood Warping Dam in the Middle Yellow River in 1994. In: *Soil and Water Conservation in China*, 8.
5. Zhou,J., Yao,S., Wang,M., Zhu,Y., Chen,D. (2020). Research progress on overtopping collapse and flood routing of earth rockfill dams. *Progress in water science*, 2020,*31* (02),287–301
6. Chen, S., Zhong, Q., and Cao, W. (2012). Seepage failure mechanism and numerical simulation of earth rock dams. *Chinese Science: Technical Science 42* (06): 697–703.
7. Cai, Y., Wang, Z., Zhu, S., and Ding, J. (2018). Real time risk assessment and comprehensive early warning model of earth rock dam. *Progress in Water Resources and Hydropower Science and Technology 38* (04): 57–63.
8. Cao, W., Zhong, Q., and Chen, S. (2013). An analysis method of seepage failure process of earth rock dams. *Journal of Disaster Prevention and Reduction Engineering 33* (01): 47–52.
9. Li, Z. (2019). Analysis of seepage and slope stability of earth-rock dam based on GEO-Studio. *Northeast Water Resources and Hydropower 37*: 3–5+71.

@seismicisolation

8

Flood Control Risk Assessment on Warping Dam Systems

Shengdong Cheng[1], Tanbao Li[2], Jibin Wang[2], Zhihai Wei[2], Ying Jiang[2], Kunxia Yu[1], Binhua Zhao[1], Wen Wang[1], Penglei Hang[1], and Ganggang Ke[1]

8.1 INTRODUCTION

Warping dams have changed since they were first constructed in the 1950s, mostly due to frequent washouts caused by sudden heavy rainfall [1]. In the early stages, due to the lack of complete theoretical system guidance for design, and due to the failure to repair dangerous dams in a timely manner, inadequate management measures, and excessive rainstorms, the benefits of a warping dam system were yet to be fully utilized [2]. In recent years, however, investment in warping dam construction is increasing, and more and more warping dam systems have been constructed. However, to our best knowledge, studies remain limited on the relationship between the mechanisms of dam breach and rainfall frequency as well as assessment of flood control safety of basin warping dam systems [3].

The progress of warping dam risk assessment is as follows: Qin et al. established a backbone dam structure optimization model, analyzing the proportion of the number of dams of different scales in small watersheds [4, 5]; Wen and Zhang [6] discussed the height of warping dams, spillway design, and check flow from the perspective of flood control and ensuring harvest; Gao et al. [7] studied the flood control standards of warping dams and proposed countermeasures for warping dams that do not meet the standards; Lin et al. [8] established a nonlinear optimization planning model for the warping dam system [8]; Wu [9] studied the optimal construction time of the key dam system and the calculation method of the actual silting date; Jiang [10] used the model of analyzing the overtopping failure risk of dikes to evaluate river section safety; Liu [11] established a variable fuzzy pattern recognition model to evaluate flood control risks of the warping dam system. The existing flood control risk assessment technology for warping dams cannot meet the basic requirements of regional ecological engineering construction, social and economic development, and people's living standards [3]. In the flood control risk assessment of the warping dam system, starting from internal and external causes, the risk factors are identified, a warping dam risk assessment index system is constructed, and the fuzzy analytic hierarchy is used to calculate the weight of each index and analyze and calculate the warping dam risk. Then, the warping dam system risk is analyzed and evaluated. The risk assessment analysis of the Jiuyuangou warping dam system reveals the influence of different rainfall frequencies on the different risk values of the warping dam system [12]. In practice, the critical value of rainfall on warping dam systems can be used to guide later management and operation of warping dam systems and early warning and emergency avoidance during a flood, which can effectively reduce risks during the operation of a warping dam [13].

[1] *State Key Laboratory of Eco-hydraulics in Northwest Arid Region, Institute of Water Resources and Hydro-electric Engineering, Xi'an University of Technology, Xi'an, China*

[2] *Northwest Institute of Forest Inventory, Planning and Design, National Forestry and Grassland Administration, Xi'an, China*

Check Dam Construction for Sustainable Watershed Management and Planning, First Edition.
Edited by Zhanbin Li, Peng Li, Yang Yu, Peng Shi, and Guillaume Piton.
© 2022 John Wiley & Sons, Inc. Published 2022 by John Wiley & Sons, Inc.

@seismicisolation

8.2 COMPOSITION AND DETERMINATION OF FLOOD CONTROL RISK ASSESSMENT SYSTEM FOR WARPING DAMS

8.2.1 Construction of Risk Assessment Index System for Warping Dams

According to the warping dam burst data, related literature analysis, and the relevant principles of constructing an index system, the warping dam risk index system is divided into a single-dam operation risk evaluation system with 4 levels and a total of 12 indicators [14]. The specific structure system is shown in Table 8.1.

8.2.2 Assessment Index Calculation and Standardization

Based on the above classification of the risk assessment system of warping dams, the flood control risk assessment of warping dams is mainly analyzed from four aspects, i.e. engineering risk, management risk, economic risk, and environmental risk.

8.2.2.1 Engineering Risk (R_a)

Engineering risk mainly covers three indexes: warping dam design criterion, dam damage, and flood-carrying capacity. Based these indexes, the concept introduction, standardization, and calculation of indexes are performed.

1. Design criterion

The risk brought by the warping dam design is affected by flood storage, silted storage, and flood design frequency. Therefore, the design risk of the warping dam is defined as:

$$R_{a1} = \frac{T_1}{kT_2}, k = \frac{V_2 - V_3}{V_2}, \tag{8.1}$$

where R_{a1} is the design risk index of the warping dam. The larger the R_{a1}, the more dangerous it is. Its maximum is 1; T_2 is design of warping dams that can intercept once-in-T_2-year floods; T_1 is the biggest flood in T_1 years; V_2 is flood storage for warping dam, 10 000 m^3; V_3 is the current silted storage of warping dam, 10 000 m^3; k is the conversion factor for the flood control capacity of the warping dam.

2. Dam damage

Cracks, gullies, breaches, and collapse of a dam are typically caused by sudden heavy rainstorms, construction quality, or failure to repair in a timely manner. The damage risk value of the warping dam is expressed as follows:

$$R_{a2} = \begin{cases} k & \text{Crack} \\ \dfrac{dh}{DH} & \text{Gullu} \\ 1 & \text{Breach} \end{cases}. \tag{8.2}$$

where R_{a2} is the risk index of warping dam damage. The larger the R_{a2} value, the more dangerous it is. Its maximum is 1; d is the transverse depth of the crack along the width of the dam, m; h is the longitudinal depth of the crack along the height of the dam, m; D is the average width of the warping dam, m; H is the remaining height of the flood dam, which is the height difference between the mud surface and the top of the dam, m.

3. Drainage facility damage

The drainage facility damage is related to the rainfall duration, the control area of the warping dam, the average rainfall depth per unit, the runoff coefficient, the waste discharge per unit time of the discharge facility, and the remaining storage. Its risk value is expressed as follows:

Table 8.1 Flood control risk assessment index system for warping dams.

Target layer (a)	Criterion layer (b)	Index layer (c)
Flood control risk assessment index of warping dam (a)	Engineering risk (b)	Design criterion (c)
		Dam damage (c)
		Drainage facility damage (c)
	Management risk (b)	Management system (c)
		Emergency warning (c)
		Personnel on duty (c)
	Economic risk (b)	Ecological environment (c)
		Social economy (c)
		Loss of life (c)
	Environment risk (b)	Earthquake disaster (c)
		Extreme rainstorm (c)
		Excess flood (c)

@seismicisolation

$$R_{a3} = \frac{\frac{itAs}{1000} + qt}{V}, \tag{8.3}$$

where R_{a3} is the risk index for the discharge facility defect of a warping dam. The larger the R_{a3} value, the more dangerous it is. Its maximum value is 1; i is the average rainfall depth per unit time, mm/h; is the rainfall time, h; A is the control area of the warping dam, km^2; s is the runoff coefficient, which refers to the ratio of runoff depth to rainfall depth per unit time; q is the flood discharge capacity of the warping dam, which refers to the average flood discharge capacity of the flood discharge facility per unit time, m^3/h; V is the remaining storage of the warping dam, m^3.

8.2.2.2 Management Risk (R_b)

Operation and management risks of warping dams mainly include personnel performance, emergency warning capabilities, and management systems. Because there are no indicators that can be directly quantified and measured for management risks, based on the improvement of the local warping dam operation and management system and the implementation of relevant measures, onsite investigations are conducted; further, the management risk of a warping dam is quantified hierarchically in multiple dimensions by using back-to-back independent scoring. Specific quantitative indicators are shown in Table 8.2.

8.2.2.3 Environment Risk (R_c)

Environmental risk refers to the risks caused by the external natural environment, such as extreme rainstorms, excessive floods, and earthquake disasters, to the operation of warping dams. In particular, rainfall runoff is the most direct cause of warping dam failure.

1. Extreme rainstorm

It is believed that warping dam overtopping is the warping dam failure discussed in this paper, and the risk is greatest at this time. An extreme rainstorm risk is calculated as:

$$R_{c1} = \frac{\sum_{t=0}^{T} \left(i_t AS/1000 - qt\right)\Delta t}{V}, \tag{8.4}$$

where R_{c1} is the extreme rainstorm risk index for warping dams. The larger the R_{c1}, the more dangerous it is. Its maximum value is 1; T is the rainfall duration, h; Δt is the length of the unit rainfall period, h; i_t is the unit rainfall depth in the period t, mm; A is the control area of the warping dam, km^2; S is the runoff coefficient, which refers to the ratio of runoff depth to rainfall depth per unit time; q_t is the flood discharge capacity of the warping dam in t period, which refers to the average flood discharge of the flood discharge facility per unit time, m^3/h; and V is the remaining storage of the warping dam, m^3.

2. Excess flood

The excess flood risk index is related to flood process, flood duration, discharge facilities, and flood storage. The excess flood risk is calculated as follows:

$$R_{c2} = \frac{\sum_{t=0}^{T} \left(r_t - qt\right)\Delta t}{V}, \tag{8.5}$$

where R_{c2} is the excess flood risk index of a warping dam. The larger the R_{c2}, the more dangerous it is. Its maximum value is 1; T is the flood duration, h; Δt is the length of the unit period, s; Δt is the flow in time period t, m^3/s; q_t is the flood discharge capacity of the warping dam in time t, which refers to the average flood discharge capacity of the flood discharge facility per unit

Table 8.2 Assessment of project management risk level of warping dam.

Indicator component	Project management risk level of warping dam				
	Primary level/0	Secondary level/0.2	Third level/0.5	Fourth level /0.8	Fifth level /1.0
Personnel performance R_{b1}	Every warping dam is supervised and maintained regularly	Most warping dams are supervised and maintained regularly	The warping dams are checked thoroughly only before the annual flood	There is almost no person checking the warping dam	The operation of warping dams is not regulated
Emergency warning capabilities R_{b2}	Quick warning, timely evacuation	Quick warning, and people are not evacuated in time	Slow warning, and people are not evacuated in time	No emergency warning, and people evacuate spontaneously	No emergency warning, lack of crisis awareness
Management system R_{b3}	Perfect system	Relatively complete system	Relatively backward system	Backward system	No relevant policies

@seismicisolation

time, m^3/s; and V is the remaining storage capacity of the warping dam, m^3.

3. Earthquake disaster risk

The seismic intensity indicates the strength of the earthquake's impact on the ground and engineering buildings, taking the average earthquake damage index in the China seismic intensity scale as the earthquake disaster index value of the warping dam (Table 8.3). Based on this, the earthquake disaster index and magnitude of the warping dam established are calculated as follows:

$$R_{c3} = \begin{cases} 0 & x < 4.5 \\ ax^3 + bx^2 + cx + d & 4.5 \le x \le 8, \\ 1 & x > 8 \end{cases} \tag{8.6}$$

where R_{c3} is the earthquake disaster risk index. The larger the R_{c3}, the more dangerous it is. Its maximum value is 1; x is earthquake magnitude; and a, b, c, and d are earthquake disaster risk coefficients of a warping dam; their values are $a = -0.0214$, $b = 0.4115$, $c = -2.2853$, and $d = 3.8883$.

4. Economic risk (R_d)

The economic risk of the warping dam is calculated before and after the collapse of the dam and includes downstream economic loss, ecological damage, and loss of life and property caused by flood sweeping away farmland, houses, roads, living areas, industrial areas, and ecological areas.

5. Downstream economic losses

Collapse of a warping dam causes flooding of farmland, houses, roads, living areas, and industrial areas, leading to social and economic losses. The downstream economic loss risk is calculated as:

$$R_{d1} = \frac{S_G}{G}, \tag{8.7}$$

where R_{d1} is the social and economic loss risk index of a warping dam. The larger the R_{d1}, the more dangerous it is. Its maximum value is 1; S_G is the social and economic loss, 10 000 yuan; G are the local funds available for flood relief, 10 000 yuan.

6. Ecological environment risk

The ecological environment risk can be measured by the funds needed to restore the ecological environment and the funds available for the construction of the ecological environment in the local area. The risk value can be expressed as:

$$R_{d2} = \frac{S_u}{U}, \tag{8.8}$$

Table 8.3 China seismic intensity scale.

Intensity	Magnitude	Average earthquake damage index	Earthquake damage phenomena
I	1.90	0	Only be recorded by instrument
II	2.50	0	Sensitive people can feel in complete stillness
III	3.10	0	A few people indoor can feel in stillness, hanging objects swing slightly
IV	3.70	0	Most people indoors, a few people outdoors can feel it, hanging objects swing, unstable utensils make noise
V	4.30	0	Most people outside can feel it, livestock is restless, doors and windows rustle, wall surface cracks
VI	4.90	0–0.1	People cannot keep standing, livestock flee, utensils fall over, shanties are damaged, there is landslide
VII	5.50	0.11–0.3	The house is slightly damaged, decorate archways, and chimneys are damaged; there are cracks on the ground, and sand and water start to blow on the ground
VII	6.10	0.31–0.5	Most houses are destroyed, a few are damaged, roadbed collapses, underground pipes are broken
IX	6.70	0.51–0.7	Most houses are destroyed, a few are damaged; decorate archways, and chimneys are collapsed; the track is curving
X	7.30	0.71–0.9	Houses are collapsed, roads are destroyed, rocks collapse, and big waves buffets the shore
XI	7.90	0.91–1.0	A large number of houses are collapsed, roadbeds and embankments are collapsed, the ground is changed greatly
XII	8.50	1.00	All buildings are destroyed, and animals and plants are destroyed by drastic changes in terrain

@seismicisolation

where R_{d2} is social and economic loss risk index of a warping dam. The larger the R_{d2}, the more dangerous it is. Its maximum value is 1; S_U is the ecological environment loss, 10 000 yuan; U are funds available for the local construction of the ecological environment, 10 000 yuan.

7. Loss of life

The RESCDAM method is a simplified method for estimating the loss of life of the dam breach proposed by Peter Reitr, which takes into account factors such as the dam breach warning time, population at risk, and flood severity. Its risk index is calculated as:

$$R_{d3} = PAR \times f \times i \times c, \tag{8.9}$$

where R_{d3} is the loss-of-life risk index. The larger the R_{d3}, the more dangerous it is. Its maximum value is 1; PAR is the population at risk; f is the risk mortality; i is the flood severity; c is the correction factor for life loss of warping dam, which mainly considers the impact of early warning and rescue on life loss. The F-value is selected according to the Graham method. See Tables 8.4 and 8.5 for the F-value.

In Table 8.5, $DV = \left(Q_{df} - \bar{Q}\right) / W_{df}$ represents the ratio of the peak flood flow of the dam break to the maximum water surface width at the characteristic section; Q_{df} is the peak flow of dam break for calculating section; $\bar{Q}$ is the average annual flow for calculating sections, and its value can be approximated to 0; and W_{df} is the maximum water surface width caused by the flood of the dam break.

Table 8.4 Flood severity.

Flood severity	DV	Flood severity description
Low	DV ≤ 4.6 m²/s	Building foundations are not washed away by floods
Moderate	4.6 < DV ≤ 12 m²/s	Houses are destroyed by floods, but trees or damaged houses can still provide refuge for people
High	DV > 12 m²/s	The flood washes away everything in the flooded area

8.2.3 Indicator Weight Determination Based on Fuzzy Analytic Hierarchy Process

The fuzzy analytic hierarchy process (FAHP) combines qualitative and quantitative research. It is believed that human subjective factors interfere with the selection of indicators and weights, which have a certain impact on risk assessment results. Therefore, the fuzzy theory is combined with the analytic hierarchy process, and FAHP is used to determine the flood disaster risk index weight of a warping dam system.

(1) Fuzzy consistent judgment matrix R represents the comparison of relative importance between this level and related elements for an element of the upper level. Assuming that the element C of the upper level is related to the elements a_1, a_2, ⋯, a_n of

Table 8.5 Suggested casualty rate.

Flood severity	Warning time/h	Understanding of flood severity	Casualty rate	
			S suggested value	Value range
High	No warning		0.75	0.3–1.0
	0.25–1.0	Vague		
		Clear		
	>1.0	Vague		
		Clear		
Moderate	No warning		0.15	0.03–0.35
	0.25–1.0	Vague	0.04	0.01–0.08
		Clear	0.02	0.005–0.04
	>1.0	Vague	0.03	0.005–0.06
		Clear	0.01	0.002–0.02
Low	No warning		0.01	0–0.02
	0.25–1.0	Vague	0.007	0–0.15
		Clear	0.002	0–0.004
	>1.0	Vague	0.0003	0–0.0006
		Clear	0.0002	0–0.0004

@seismicisolation

the next level, the fuzzy consistent judgment matrix can be expressed as:

C	a_1	a_2	. . .	a_n
a_1	r_{11}	r_{12}	. . .	r_{1n}
a_2	r_{21}	r_{22}	. . .	r_{2n}
. . .	. . .	. . .	. . .	. . .
a_n	r_{n1}	r_{n2}	. . .	r_{nn}

The element r_{ij} has the following practical meaning: r_{ij} represents that, when a_i and a_j are compared with the element C, there is a fuzzy relationship between a_i and a_j in that the degree of membership is "more important than. . .." In order to quantitatively describe the relative importance of any two schemes with respect to a criterion, the following 0.1–0.9 scale can be used to obtain a quantitative scale (Table 8.6).

Table 8.6 Importance scale.

Scale	Definition	Note
0.5	Equally important	Comparing the two elements, they are equally important
0.6	Slightly more important	Comparing two elements, one element is slightly more important than the other
0.7	Obviously more important	Comparing two elements, one element is obviously more important than the other
0.8	Much more important	Comparing two elements, one element is much more important than the other
0.9	Extremely more important	Comparing two elements, one element is extremely more important than the other
0.1–0.4	Anti-comparison	If the element *ai* is compared with the element j to get the judgment *rij*, the judgment obtained by comparing element *aj* with element *ai* is *rji* = 1 − *rij*

Table 8.8 Secondary-level fuzzy consistent judgment matrix of engineering risk.

Indicator type	Low design standard	Dam damage	Drainage facilities failure
Low design standard	0.5	0.3	0.4
Dam damage	0.7	0.5	0.6
Drainage facilities failure	0.6	0.4	0.5

Table 8.9 Secondary-level fuzzy consistent judgment matrix of management risk.

Indicator type	Personnel on duty	Emergency warning	Management system
Personnel on duty	0.5	0.2	0.3
Emergency warning	0.8	0.5	0.6
Management system	0.7	0.4	0.5

When the numerical scale above is established, the elements $a_1, a_2, \cdots, a_n$ are compared with the element C of the upper level. Based on this, five fuzzy judgment matrices can be obtained (Table 8.7, 8.8, 8.9, 8.10 and 8.11).

(2) Indicator weight obtained from the fuzzy consistent judgment matrix

Suppose that the fuzzy consistency matrix obtained by pair comparison of the importance of the elements $a_1, a_2, \cdots, a_n$ is $R = (r_{ij})_{n\times n}$, and the weights value of elements $a_1, a_2, \cdots, a_n$ are $w_1, w_2, \cdots, w_n$, respectively. Thus, there are the following relations:

$$r_{ij} = 0.5 + a\left(w_i - w_j\right)\left(i, j = 1, 2, \ldots, n\right) \tag{8.10}$$

$0 < a < 0.5$, where a is a measure of the difference degree among perceived objects and is related to the number of

Table 8.7 Primary-level fuzzy consistent judgment matrix.

Indicator type	Engineering risk	Management risk	Environment risk	Economic risk
Engineering risk	0.5	0.7	0.6	0.4
Management risk	0.3	0.5	0.4	0.2
Environment risk	0.4	0.6	0.5	0.3
Economic risk	0.6	0.8	0.7	0.5

@seismicisolation

Table 8.10 Secondary-level fuzzy consistent judgment matrix of environmental risk.

Indicator type	Extreme rainstorm	Excess flood	Earthquake disaster
Extreme rainstorm	0.5	0.4	0.7
Excess flood	0.6	0.5	0.8
Earthquake disaster	0.3	0.2	0.5

Table 8.11 Second-level fuzzy consistent judgment matrix of economic risk.

Indicator type	Downstream economic loss	Ecological environment loss	Loss of life
Downstream economic loss	0.5	0.6	0.3
Ecological environment loss	0.4	0.5	0.2
Loss of life	0.7	0.8	0.5

evaluation objects and the degree of difference. When the fuzzy judgment matrix R is not consistent, the equal sign of Eq. (8.11) is not strictly true. The least squares can be used to find the weight vector $W = [w_1, w_2, \ldots w_n]^T$, in which s is used to solve the constrained programming of the following formula of Eq. (8.12):

$$\begin{cases} \min z = \sum_{i=1}^{n}\sum_{j=1}^{n}\left(0.5 + a\left(w_i - w_j\right) - r_{ij}\right)^2 \\ st\sum_{i=1}^{n} w_i = 1, w_i \geq 0\left(1 \leq i \leq n\right) \end{cases}. \tag{8.11}$$

According to the Lagrange multiplier, the above-mentioned constrained programming problem (Eq. 8.12) is equivalent to Eq. (8.13), and there is no constrained programming:

$$\begin{aligned} \min L\left(w\lambda\right) = &\sum_{i=1}^{n}\sum_{j=i}^{n}\left(0.5 + a\left(w_i - w_j\right) - r_{ij}\right)^2 \\ &+ 2\lambda\left(\sum_{i=1}^{n} w_i - 1\right). \end{aligned} \tag{8.12}$$

where λ is Lagrange multiplier.

Take the derivative of Eq. (8.13) min L ($w\lambda$) with respect to w_i and set it to zero, and the following equation holds

$$\begin{aligned} &a\sum_{j=1}^{n}\left(0.5 + a\left(w_i - w_j\right) - r_{ij}\right) \\ &- a\sum_{k=1}^{n}\left(0.5 + a\left(w_k - w_i\right) - r_{ki}\right) \\ &+ \lambda = 0\left(i = 1, 2, \ldots, n\right), \end{aligned} \tag{8.13}$$

$$\sum_{i=1}^{n}\left(2a^2\left(w_i - w_j\right) + a\left(r_{ji} - r_{ij}\right) - r_{ij}\right) + \lambda = 0\left(i = 1, 2, \ldots, n\right), \tag{8.14}$$

In summary, the following equations can be obtained:

$$\begin{cases} 2a^2\left(n-1\right)w_1 - 2a^2 w_2 - \cdots - 2a^2 w_n + \lambda = a\sum_{j=1}^{n}\left(r_{1j} - r_{j1}\right) \\ -2a^2 w_1 - 2a^2\left(n-1\right)w_2 - \cdots - 2a^2 w_n + \lambda = a\sum_{j=1}^{n}\left(r_{2j} - r_{j2}\right) \\ \cdots\cdots\cdots\cdots\cdots\cdots\cdots\cdots = \cdots \\ -2a^2 w_1 - 2a^2 w_2 - \cdots - 2a^2\left(n-1\right)w_n + \lambda = a\sum_{j=1}^{n}\left(r_{nj} - r_{jn}\right) \\ w_1 + w_2 + \cdots + w_n = 1 \end{cases}. \tag{8.15}$$

The risk weight value of each part can be obtained by solving Eq. (8.15) $W = [w_1, w_2, \ldots, w_n]^T$, and the summary is shown in Table 8.12.

8.3 FLOOD CONTROL RISK ASSESSMENT OF WARPING DAM SYSTEM IN JIUYUANGOU WATERSHED

8.3.1 Risk Calculation and Risk-Level Standard Classification

8.3.1.1 Risk Calculation

The flood disaster risk of warping dams is divided into three levels, i.e. comprehensive risk, primary risk, and secondary risk. Comprehensive risk is the weighted average of primary risks; primary risk is the weighted average of corresponding secondary

@seismicisolation

Table 8.12 Weights of risk indicators for flood breach of warping dams.

Target layer	First-level indicator weight	Second-level indicator weight	
Flood risk indicator of warping dam system (R)	Engineering risk $W(R_a) = 0.28$	Low design standard	$W(R_{a1}) = 0.26$
		Dam damage	$W(R_{a2}) = 0.39$
		Drainage facilities failure	$W(R_{a3}) = 0.35$
	Management risk $W(R_b) = 0.17$	Personnel in duty	$W(R_{b1}) = 0.16$
		Emergency warning	$W(R_{b2}) = 0.63$
		Management system	$W(R_{b3}) = 0.21$
	Environment risk $W(R_c) = 0.33$	Extreme rainstorm	$W(R_{c1}) = 0.34$
		Excess flood	$W(R_{c2}) = 0.40$
		Earthquake disaster	$W(R_{c3}) = 0.26$
	Economic risk $W(R_d) = 0.22$	Downstream economic loss	$W(R_{d1}) = 0.33$
		Ecological environment loss	$W(R_{d2}) = 0.24$
		Loss of life	$W(R_{d3}) = 0.43$

risks. Risk value can be expressed by the following formula:

$$R^k = \frac{1}{n}\sum_{i=1}^{n} w_i R_i^{k-1}, \tag{8.16}$$

where R^k is a certain risk value corresponding to the k level, n is the number of subitems corresponding to a certain level of risk, and w_i is the weight value of the ith subitem.

8.3.1.2 Risk-Level Standard Classification of Warping Dam System in Jiuyuangou Watershed

The ultimate goal of the flood control risk assessment system for warping dams in small watersheds is to determine the possibility of flood control risks from warping dams in small watersheds so that decision-makers can understand the flood control risks of warping dam systems in small watersheds, which provides theoretical guidance for investments and the later operation and management of the warping dam system Risk-level standards formulated based on relevant literature and actual conditions are shown in Table 8.13. The greater the value, the greater the risk of dam breach.

Table 8.13 Flood control risk assessment classification of warping dams in small watersheds.

Primary risk	Degree of risk	Value range
Primary risk	Severe dangerous	[0.7,1]
Secondary risk	Moderate dangerous	[0.5,0.7)
Third level	Mild dangerous	[0.3,0.5)
Fourth level	Safe	[0.1,0.3)
Fifth level	Very safe	[0,0.1)

8.3.2 Flood Control Risk Analysis and Assessment of Warping Dam

According to the measurement and assignment methods of each evaluation index in the flood control risk assessment index system of warping dams in a small watershed, combined with the onsite survey of each warping dam in the Jiuyuangou watershed, the relationship between the various indicators of the warping dam system risk assessment and different rainfall frequencies is as shown in Table 8.14. The analysis results show that, with the increase of rainfall frequency, the flood disaster risk of the warping dam system gradually increases, and the environmental risk increases the most; engineering and management risks are only related to the warping dam project, which do not change with the increase of rainfall frequency; further, there is a small increase in economic risks. The Jiuyuangou warping dam system is at the third level of risk under different rainfall frequencies, and the warping dam project itself is in a mildly dangerous state (Figure 8.1); the management system is in a moderately dangerous state; environmental risks change from mild to moderately dangerous as the rainfall frequency increases; the economic risk changes from a basic safe state to a mildly dangerous state with the increase of rainfall frequency. The flood control risk assessment of the Jiuyuangou warping dam system

@seismicisolation

Table 8.14 Risk assessment indicators of warping dams under different rainfall frequencies.

Recurrence interval/year	5	10	20	50	100	200	500
Engineering risk	0.3	0.3	0.3	0.3	0.3	0.3	0.3
Low design standard	0.47	0.47	0.47	0.47	0.47	0.47	0.47
Dam damage	0.42	0.42	0.42	0.42	0.42	0.42	0.42
Drainage facilities failure	0.03	0.03	0.03	0.03	0.03	0.03	0.03
Management risk	0.55	0.55	0.55	0.55	0.55	0.55	0.55
Personnel performance	0.8	0.8	0.8	0.8	0.8	0.8	0.8
Emergency warning capacity	0.5	0.5	0.5	0.5	0.5	0.5	0.5
Management system	0.5	0.5	0.5	0.5	0.5	0.5	0.5
Environment risk	0.34	0.48	0.54	0.58	0.58	0.61	0.64
Extreme rainstorm	0.53	0.72	0.81	0.86	0.86	0.87	0.91
Excess flood	0.41	0.59	0.67	0.71	0.73	0.79	0.83
Earthquake disaster	0	0	0	0	0	0	0
Economic risk	0.25	0.27	0.31	0.34	0.34	0.34	0.36
Downstream economic loss	0.62	0.65	0.7	0.74	0.74	0.74	0.75
Ecological environment loss	0.17	0.24	0.33	0.4	0.4	0.41	0.44
Loss of life	0	0	0	0	0	0	0.01
Comprehensive level	0.34	0.39	0.42	0.44	0.44	0.45	0.47
Risk level	III	III	III	III	III	III	III

reveals that the influence of rainfall on the flood risk of the Jiuyuangou warping dam system is sensitive. Therefore, the existing warping dam design should be strengthened, and the operation and management system of the warping dam should be improved quickly and make full use of the increasing critical risk value of the warping dam when there is a sudden change in rainfall frequency. Good dynamic emergency management and early warning mode can fully reduce the risk damage and avoidable economic loss caused by the warping dam system in the event of flood with the combination of hydrological forecasting.

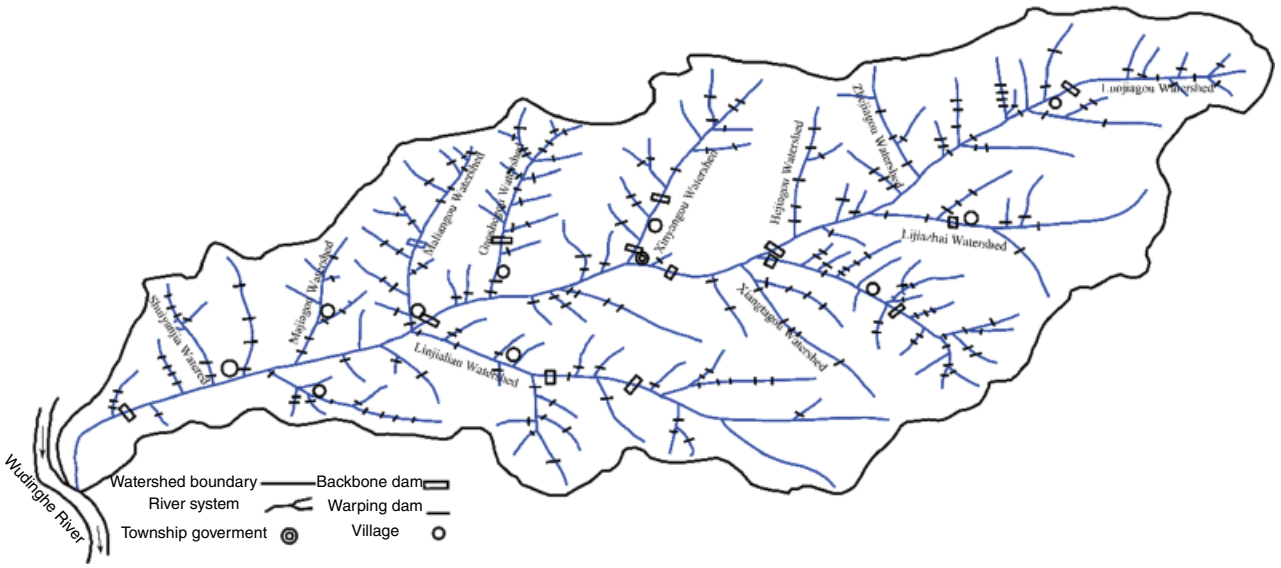

Figure 8.1 Location distribution of the warping dams in Jiuyuangou.

@seismicisolation

The flood risk of the warping dams in the Jiuyuangou watershed under different rainfall frequencies is averaged. The statistical analysis shows 18 warping dams in a moderately dangerous state, 53 warping dams in a mildly dangerous state, and 2 warping dams basically safe, accounting for 24.7, 72.6, and 2.7%, respectively. The results show that most of comprehensive risks of the warping dams in the Jiuyuangou are in mild danger, a quarter of the comprehensive risks of warping dams are in a moderately dangerous state, and only a few of warping dams are basically safe. Warping dam projects in a very safe state account for 29%, warping dam projects in basic safe state account for 25%, warping dam projects in mild risk state accounts for 22%, and warping dam projects in moderate dangerous state accounts for 25%.

Further, management risks of warping dam projects are all in a moderately dangerous state; environmental risks of warping dams in basic safe state account for 7%; environmental risks of warping dams in mildly dangerous account for 7%; environmental risks of warping dams in moderately dangerous state account for 44%; and environmental risks of warping dams in severely dangerous state account for 42%.

Moreover, the loss risk of warping dams in very safe state accounts for 14%; the loss risk of warping dams in basic safe state account for 29%; the loss risk of warping dams in mildly dangerous state accounts for 45%; and the loss risk of warping dams in a moderately dangerous state accounts for 12%. From the evaluation results, engineering risks are relatively evenly distributed, environmental risks are generally high, loss risks are relatively concentrated, and management risks are more serious. In the subsequent reinforcement of warping dams and construction of new warping dams, attention should be given to the management of warping dams, strengthening the emergency warning capabilities of warping dam systems and speeding up the improvement of warping dam management systems. In addition, high-risk warping dams should be heightened to increase flood storage capacity to cope with natural risks; meanwhile, if there are safer or stronger flood arresting dams downstream, additional discharge facilities can be installed, or the flood discharge capacity of the discharge facilities can be improved to transfer the risk of the warping dam; for downstream warping dams with greater risk and local warping dams with lower risks, the flood discharge capacity of local warping dams can be reduced, thereby sharing part of the risks of downstream warping dams; for warping dams with a greater risk of loss, the upstream and downstream dams should be reinforced to prevent floods, especially in densely populated areas, and effective measures should be taken to ensure the safety of people's lives and property.

8.4 CONCLUSION

Check dam is a widely and effective structure of soil and water conservation in the world. In the past few hundred years, people have increasingly recognized the expected advantages of check dams, such as land development, ecological environment improvement, increasing agricultural production, raising gully erosion base level, improving slope stability, and peak cutting flood detention. However, with the lack of management measures in the application of check dam, the early check dam construction lacks complete system guidance, and the dangerous dam brings potential operation risks. The risk identification of check dam is extremely important for the healthy development of check dam.

Through the actual investigation of the current operation of check dams in Jiuyuangou basin, starting from the internal and external causes of check dam failure, the risk factors are identified, the risk evaluation index system of check dams is comprehensively constructed, and the operation risk of check dams is comprehensively evaluated. The evaluation shows that most of the comprehensive risks of check dams in Jiuyuangou basin are mild, 25% of the comprehensive risks of check dams are moderate, and only a small number of check dams are basically safe. The risk of check dam project is very safe, accounting for 29%, basic safety 25%, mild risk 22%, and medium risk 25%; all management risks are in a medium dangerous state; the check dams with basically safe environmental risks are 7%, 7% of mild risks, 44% of moderate risks, and 42% of severe risks; among the loss risks, 14% are very safe check dams, 29% are basically safe, 45% are slightly dangerous, and 12% are moderately dangerous. From the evaluation results, the project risks are evenly distributed, the environmental risks are generally large, the loss risks are concentrated, and the management risks are generally serious.

Through the risk assessment of Jiuyuangou check dam system, in the subsequent risk removal and reinforcement of check dam and new check dam, we should pay attention to the operation management of check dam, strengthen the risk emergency early warning ability of check dam, and further accelerate the improvement of healthy check dam management system. Similarly, when dealing with natural risks, the

@seismicisolation

resistance and control effect of high-risk check dams and backbone dams on extreme floods should be strengthened. The local government shall establish a complete emergency risk plan for check dams to minimize the risk loss rate in case of high-risk events.

REFERENCES

1. Wu, Y. (1992). Dynamic economic analysis and optimal value calculation of silt retention capacity of silt Dam. *Chinese Journal of Soil and Water Conservation 4*: 49–53.
2. Liu, D.F. (2010). Study on risk identification of dam break in small reservoirs. *Heilongjiang Water Conservancy 8*: 138–141. (in Chinese).
3. Qin, H., Jia, S., and Fu, M. (2004). Research on dam system construction in small watershed on Loess Plateau. *People's Yellow River 26*: 33–36.
4. Wen, J. and Zhang, J. (1996). Discussion on the design of backbone warping Dam from the perspective of flood control and collection. *Soil and Water Conservation in China 1*: 18–20.
5. Jiang, B. (2010). *Study on Dike Safety Evaluation and Countermeasures Based on Flood Numerical Simulation*. Dalian University of Technology.
6. Ma, L. (2007). *Benefit Value Analysis of Several Soil and Water Conservation Measures on the Loess Plateau*. Xi'an University of Technology.
7. Wang, D., Ha, Y., and Li, Z. (2017). Operational risk assessment of warping dam system in ningxia typical River basin. *Science of Soil and Water Conservation in China 15*: 17–25.
8. Chen, Z., Li, Z., and Wang, Z. (2020). Reflections on strategic positioning of silt Dam construction on the Loess Plateau. *Soil and Water Conservation in China 9*: 32–38.
9. Li, L. (2006). *Dam Risk Assessment and Risk Management*. China Water Resources and Hydropower Press.
10. Li, Z.B. (2015). Flood control risk assessment technology of check dam system in small watershed(M). *People's Yangtze River 41*: 92–95.
11. Gao, J., Cao, W., and Wang, X. (2003). Discussion on some technical problems in planning and design of warping dam in the new era. *Journal of Chinese Academy of Water Resources and Hydropower Research 1*: 9–16.
12. Lin, M., Zhu, M., and Bai, F. (1995). Optimization planning model for small watershed DAMS and its application. *People's Yellow River 11*: 29–33.
13. Qin, X. and Zheng, X. (1994). Research on optimal planning model of Jiagou Backbone Dam system in small Watershed. *Soil and Water Conservation in China 1*: 18–22.
14. Zhang, J. (2000). Fuzzy analytic hierarchy process (FAHP). *Fuzzy Systems and Mathematics 2*: 80–88.

@seismicisolation

9

Development and Utilization Model of a Check Dam System

Peng Shi[1], Peng Li[1], Shengdong Cheng[1], Lulu Bai[1], Laizhang Zhang[2], Daxiang Wang[2], Anli Ma[2], and Yan Zhang[3]

9.1. INTRODUCTION

Soil erosion and drought are the two restrictive factors for crop planting on the Loess Plateau [1–3]. Common measures for coping with these constraints include construction of water conservancy, planting drought-tolerant crops, and adoption of drought-resistant and moisture-preserving farming techniques [4, 5]. In response to soil erosion, the local people of the Loess Plateau historically created numerous water and soil conservation ways to conserve water and soil, for example, terraces, check dams, water cellars, and waterlogging ponds [6, 7]. Inspired by the naturally formed ponds, the local people turned harm into profit by making full use of the soil and water resources lost on the Loess Plateau, and constructing dams in the channels to retain water and soil [8, 9]. The siltation and sedimentation of this lost water and soil leads to the formation of flat arable land [10, 11]. Check dams are constructed on this kind of land (called dam land by the locals) [12]. Check dams, an important engineering measure for soil erosion control on the Loess Plateau, are capable of silting and reclaiming land [13, 14]. It is a unique land use method based on local conditions, and its origin can be traced back to the Wanli period of the Ming Dynasty.

The construction of check dams is vital to the ecological protection and high-quality development of the Loess Plateau [15, 16]. In order to change the current serious soil erosion on the Loess Plateau [17, 18], the Chinese government formulated a strategy to vigorously promote the construction of check dams in accordance with the natural environmental characteristics of the Loess Plateau [19, 20]. In the beginning, check dams were generally used to block sediment and silt to create land [21, 22]. At the same time, check dams also played a role in flood control and could reduce the impact of flood disasters on the local area. With the further development of check dams, there are now more utilization modes, for example, (i) combined use of water resources in reservoirs, dams, and cellars; (ii) water diversion irrigation from a check dam; and (iii) fish farming in a check dam. This paper focuses on the development process and existing utilization modes of check dams on the Loess Plateau.

[1] *Institute of Water Resources and Hydro-electric Engineering, Xi'an University of Technology, Xi'an, China*
[2] *Upper and Middle Yellow River Bureau, YRCC, Xi'an, China*
[3] *College of Urban and Environmental Sciences, Northwest University, Xi'an, China*

Check Dam Construction for Sustainable Watershed Management and Planning, First Edition.
Edited by Zhanbin Li, Peng Li, Yang Yu, Peng Shi, and Guillaume Piton.
© 2022 John Wiley & Sons, Inc. Published 2022 by John Wiley & Sons, Inc.

@seismicisolation

9.2. DEVELOPMENT OF CHECK DAMS ON THE LOESS PLATEAU

9.2.1. Distribution Characteristics of Check Dams on the Loess Plateau

9.2.1.1. Number and Regional Distribution of Check Dams

The number of check dams from first national water conservancy census data in 2011 plus the quantitative changes caused by the newly built check dams and by functional shift from 2012 to 2018 gives total dams as of November 2019. There are a total of 58 776 check dams on the Loess Plateau: 5905 large ones, 12 169 medium ones, and 40 702 small ones, as shown in Figure 9.1, each accounting for 10.05, 20.70, and 69.25% of the total, respectively, as shown in Figure 9.2.

The number of check dams over three periods/stages – spontaneous construction (before 1986), standardized construction (1986–2003), and scale development (after 2003) – are 32 055, 13 876, and 12 845, respectively, accounting for 54.54, 23.61, and 21.85% of the total, respectively. As shown in Table 9.1, before 1986, constructed check dams were mainly small- and medium-sized, accounting for 94.98% of the total number of check dams at this stage; large dams only accounted for 5.02%. From 1986 to 2003, the construction of large dams began to accelerate, and the proportion of newly built large dams doubled compared with the previous period. After 2003, the construction of check dams trended toward large and medium dams, and their proportions were about twice those in the previous period. The number of newly constructed small-scale dams declined significantly.

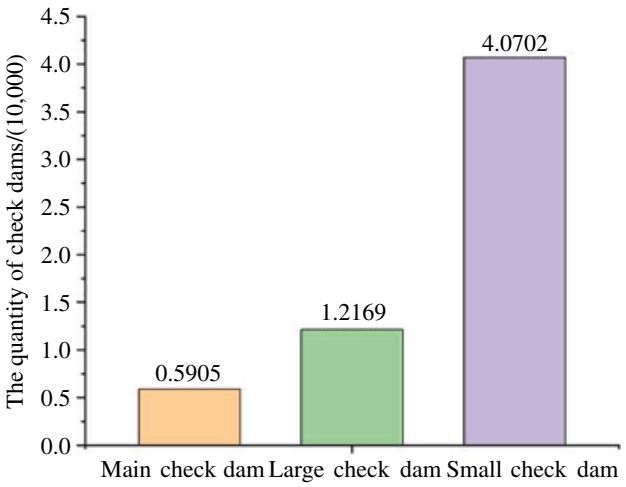

Figure 9.1 Different types of check dams on the Loess Plateau

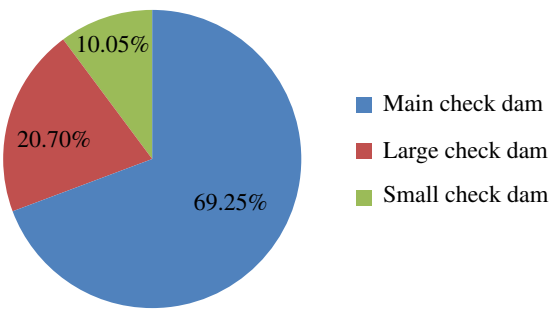

Figure 9.2 Proportions of different types of check dams on the Loess Plateau

9.2.1.2. Provincial (Regional) Distribution of Check Dams

As shown in Table 9.2, Shaanxi and Shanxi provinces (regions) have the greatest number of check dams, accounting for 57.99 and 30.89% of the total check dams on the Loess Plateau, respectively.

9.2.1.3. Distribution of Check Dams in Major Areas of Soil Erosion

Rich sediment areas, rich and coarse sediment areas, and coarse sediment areas are the key areas of soil erosion on the Loess Plateau. The number of check dams in these three regions is 52 241, 40 876, and 12 072, respectively, accounting for 88.88, 69.55, and 20.54%, respectively, of the total check dams on the Loess Plateau, as shown in Table 9.3 and Figure 9.3.

The distribution densities of check dams in rich sediment areas, rich and coarse sediment areas, and coarse sediment areas are 0.25, 0.52, and 0.64 dam/km^2, respectively, significantly higher than the average value of 0.09 dam/km^2 on the Loess Plateau. The distribution of different types of check dams in key areas of soil erosion is illustrated in Figures 9.4 and 9.5.

Table 9.1 Check dams on the Loess Plateau in three different periods (unit: dam).

	Type			
Period	Medium check dams	Large check dams	Small check dams	Total
Before 1986	1609	7090	23 356	32 055
1986–2003	1579	1602	10 695	13 876
After 2003	2717	3477	6 651	12 845
Total	5905	12169	40 702	58 776

@seismicisolation

Table 9.2 Distribution of check dams on the Loess Plateau (unit: dam).

	Province							
Type	Qinhai	Gansu	Ningxia	Inner Mongolia	Shaanxi	Shanxi	Henan	Total
Medium	173	559	329	877	2651	1191	125	5905
Large	128	451	373	702	9483	844	188	12 169
Small	373	590	400	698	21953	16 126	562	40 702
Total	674	1600	1102	2277	34087	18 161	875	58 776

Table 9.3 Check dams in soil erosion areas on the Loess Plateau (unit: dam).

	Type				
Area	Medium check dam	Large check dam	Small check dam	Total	Percentage
Coarse sediment area	1104	3680	7288	12 072	20.54
Rich and coarse sediment area	3174	9652	28 050	40 876	69.55
Rich sediment area	4930	11 269	36 042	52 241	88.88
Loess Plateau	5905	12 169	40 702	58 776	100

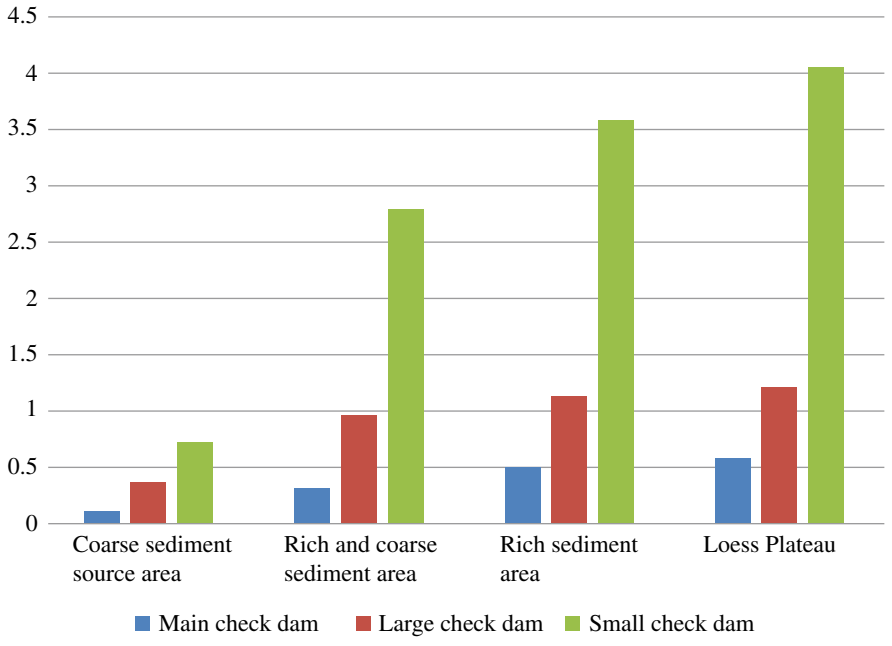

Figure 9.3 Distribution of check dams in major soil erosion areas

9.2.1.4. Distribution of Check Dams in Main Tributaries

The region of Helong Interval is the most serious area of soil erosion on the Loess Plateau and is the main source of the Yellow River's coarse sediment. The check dams in this region account for 80.47% of the total on the Loess Plateau. Most of them are distributed in Wuding River, Qingjian River, Yanhe River, Jialu River, Kuye River, Huangfuchuan River, and Tuwei River, accounting for 59.22% of the total, of which Wuding River accounts for 30.57%; Jinghe River, Luo River, Wei River, and Fen River account for 10.13%; and other regions account for 9.40% (Table 9.4).

The above analysis on the temporal and spatial distribution of check dams can be used to explain why, along with the increasing awareness of the safe

@seismicisolation

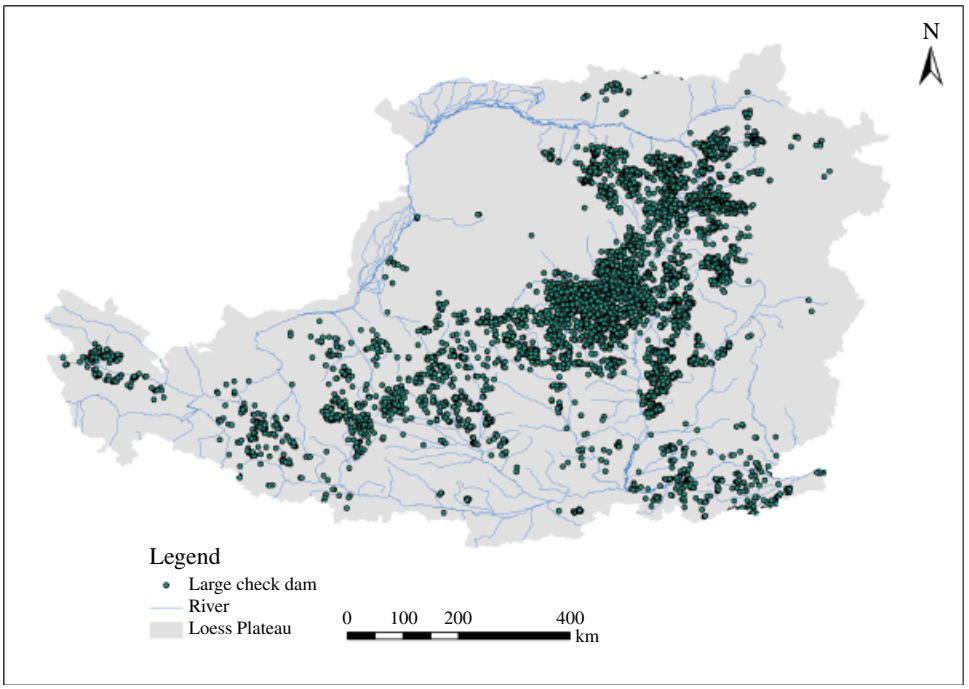

Figure 9.4 Distribution of large check dams in major areas of soil erosion on the Loess Plateau

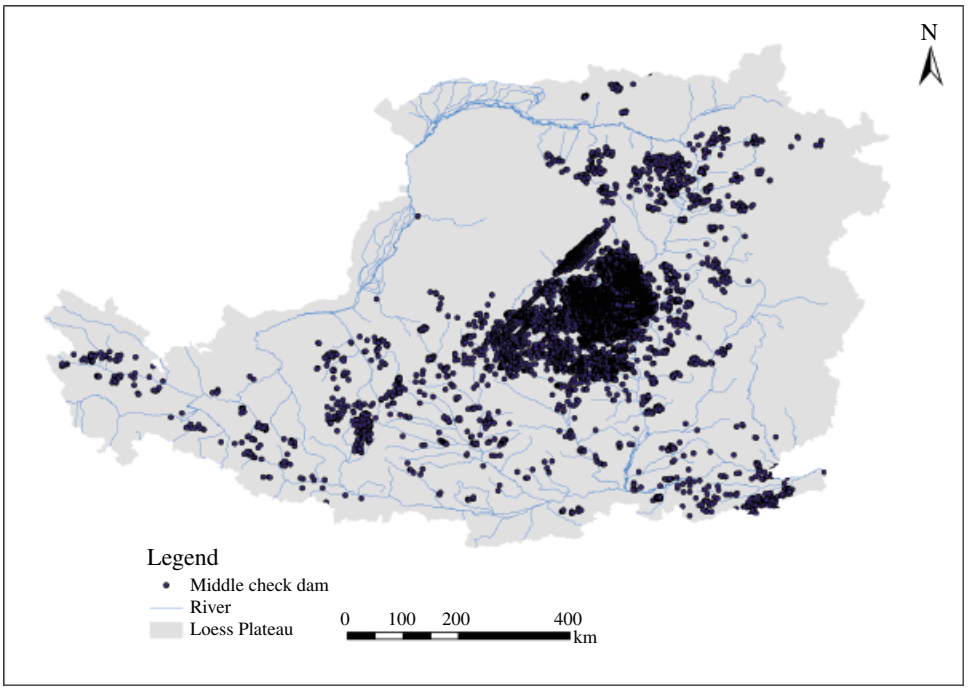

Figure 9.5 Distribution of medium check dams in major areas of soil erosion on the Loess Plateau

operation of check dams as well as advancements in dam-building techniques, the construction of check dams has gradually shifted from small and medium dams to large dams. Moreover, the construction standards for check dams have gradually improved, and their prevention and control capabilities have been enhanced. The analysis also found that different types of check dams show similar spatial patterns distribution. They are concentrated in sandy areas with developed gullies, strong channel erosion, and urgent

@seismicisolation

Table 9.4 Check dams in main tributaries on the Loess Plateau (unit: dam).

Drainage basin		Medium check dams	Large check dams	Small check dam	Total
Hekouzhen–Longmen reach	Huangfuchuan	296	427	1429	2152
	Qingshuichuan	45	113	377	535
	Gushanchuan	58	97	326	481
	Kuye River	301	543	1817	2661
	Tuwei River	93	426	1426	1945
	Jialu River	95	665	2223	2983
	Wuding River	1021	3902	13047	17970
Hekouzhen–Longmen reach	Qingjian River	181	902	3015	4098
	Yan River	112	664	2220	2996
	Yuanyan River	0	65	217	282
	Shiwangchuan	5	13	44	62
	Hun River	178	92	309	579
	Yangjiachuan	44	23	79	146
	Pianguan River	38	36	119	193
	Xianchuan River	182	25	84	291
	Zhujiachuan	90	66	221	377
	Lanyi River	30	28	95	153
	Weifen River	14	11	37	62
	Qiushui River	50	187	625	862
	Sanchuan River	70	64	214	348
	Quchan River	16	14	47	77
	Qingshui River	207	80	268	555
	Not centralization	468	1616	5405	7489
	Subtotal	3594	10059	33644	47297
Jing Luo Wei Fen	Jing River	549	296	992	1837
	Beiluo River	140	351	1172	1663
	Wei River	408	289	967	1664
	Fen River	184	153	456	793
	Subtotal	1281	1089	3587	5957
Average		1030	1021	3471	5522
Total		5905	12169	40702	58776

demand for basic farmland, especially in tributaries such as the Wuding River, Qingjian River, Yanhe River, Jialu River, Kuye River, and Huangfuchuan in the hilly loess area.

9.2.2. Development History of Check Dams on the Loess Plateau

The history of check dam development on the Loess Plateau can be divided into three separate stages: spontaneous construction, standardized construction, and scale development.

9.2.2.1. Spontaneous Construction

Before 1986, the construction of check dams was mainly carried out in conjunction with agricultural production or basic farmland construction. During this period, check dams were mostly small and medium dams built spontaneously by local people. Due to the lack of unified planning and scientific design, as well as the low construction standards, most check dams have been fully silted up and abandoned.

9.2.2.2. Standardized Construction

From 1986 to 2003, by learning from the experience and lessons of the first stage of check dam construction, the Ministry of Water Resources successively issued the *Provisional Regulations of Design and Construction of Sluicing-siltation Earth Dam* (SD 124-84), the *Technical Code of Key Dam for Soil and Water Conservation* (SD 175-86), the *Technical Standards for Soil and Water Conservation* (SD 238-87), and other technical

@seismicisolation

standards, which greatly improved the construction level of check dams. In 1986, the State Development Planning Commission listed the "Key Project for Water and Soil Conservation and Gully Control in the Sand and Coarse Sand Area of the Middle Yellow River" as a special investment project. The construction of check dams accelerated thereafter and entered a standardized development stage.

9.2.2.3. Scale Development

After 2003, in order to further ensure the safe operation of check dams and improve the overall defensive capacity of the basin, based on comprehensive experience of check dam construction, the following technical route for the construction of a dam system was proposed after repeated scientific experiments and research: the tributaries are regarded as the framework and the small-watershed dam system as the units; the large dams dominate, and small and medium check dams supplement. In 2003, the Ministry of Water Resources included the construction of check dams as one of three "highlight projects." Since then, the construction of check dams has achieved large-scale development.

In recent years, the Loess Plateau has experienced occasional heavy rainfall and an increase in extreme weather. Especially after the debris flow disaster in Zhouqu, Gansu, in 2008, the safe use of check dams has attracted much attention from the government and all sectors of society. In response, the Ministry of Water Resources issued an opinion on further strengthening the construction of water and soil conservation blocking projects such as check dams. Furthermore, the Ministry of Water Resources also launched a project to reinforce damaged check dams of medium-scale and larger to eliminate potential risks. Focus changed from construction of new check dams to risk elimination and reinforcement of existing check dams.

9.3. SILTATION SITUATION OF CHECK DAMS

The main functions of check dams are to block sediment, silt land, weaken flood peaks, and retain floodwater. Thus, the analysis of the siltation situation of check dams is conducive to ascertaining the operation status of check dams, thereby providing technical support and decision-making basis for their planning, design, risk prevention, operation management, and benefit evaluation.

Primary data for this analysis of individual dams through 2019 are obtained from 2019 province reports on the investigation of check dams, dam information from first (2011) national water conservancy census data, and the 2008 large-scale safety inspection of check dams. Subsequently, these primary data are updated, checked, and supplemented by data from 2011 to 2019 statistical annual report, survey of various provinces, special survey, and monitoring. Incomplete data are calculated and supplemented by the available siltation data of the same type of dam in the same period.

Based on this, the overall silting situation of various types of check dams in each period, siltation situation of check dams in provinces (key areas of soil and water loss), and the distribution of fully silted check dams are analyzed.

9.3.1. Analysis of Overall Siltation Situation

The siltation analysis of various types of check dams in different periods is helpful to explore the operation rule of check dams, understand the siltation situation of different types of check dams, and provide data support for check dam construction, operation management, benefit assessment, and risk warning. The siltation rate is thus introduced to help discover the current situations of check dams and scientifically analyze the operation status of check dams.

The siltation rate is the percentage of the siltation amount to the total storage capacity. It is a physical quantity that indicates the siltation degree of the check dam and can be divided into the designed siltation rate, the actual siltation rate, and the siltation loss rate. Specifically, the designed siltation rate refers to the ratio of the design silt storage capacity to the total storage capacity and is the threshold for judging whether one check dam is full. The actual siltation rate refers to the percentage of the actual siltation volume to the total storage capacity. The siltation loss rate refers to the siltation rate when a check dam is incapable of retention and is usually a constant for different types of check dams. When the actual siltation rate exceeds or equals the designed siltation rate, the check dam is determined to be fully silted up. Based on this, it is judged and analyzed whether the check dam is full in different periods. As shown in Table 9.5, the check dams on the Loess Plateau area have a total designed storage capacity of 11.033 billion m^3 and a siltation storage capacity of 7.75 billion m^3. At present, they

@seismicisolation

Table 9.5 Siltation situation of check dams on the Loess Plateau.

	Project period			
Storage	Before 1986	1986–2003	After 2003	Total
Total storage (100 million m^3)	52.9	23.81	33.62	110.33
Design silting storage capacity (100 million m^3)	41.31	15.35	20.84	77.5
Silted-up storage capacity (100 million m^3)	38.39	10.35	6.3	55.04
Remaining capacity (100 million m^3)	2.92	5	14.54	22.46
Deposition rate (%)	72.57	43.47	18.74	49.89

Table 9.6 Silted check dams in different periods on the Loess Plateau (unit: dam).

Project period	Full sedimentation	Not full sedimentation	Totality	Full sedimentation (%)
Before 1986	28 198	3857	32055	87.97
1986–2003	8624	5252	13876	62.15
After 2003	4186	8659	12845	32.59
Total	41 008	17768	58776	69.77

Table 9.7 Siltation situation of large check dams on the Loess Plateau.

	Project period			
Storage	Before 1986	1986–2003	After 2003	Total
Total storage (100 million m^3)	18.26	15.16	24.52	57.94
Design silting storage capacity (100 million m^3)	13.71	9.33	14.98	38.02
Silted-up storage capacity (100 million m^3)	12.54	5.98	3.84	22.36
Remaining capacity (100 million m^3)	1.17	3.35	11.14	15.66
Deposition rate (%)	68.67	39.45	15.66	38.59

have accumulated 5.504 billion m^3 of silt, remaining a siltation storage capacity of 2.246 billion m^3. The siltation rate is 49.89%. The siltation rates of check dams built before 1986, 1986–2003, and after 2003 are 72.57, 43.47, and 18.74%, respectively.

According to the statistics, 41 008 check dams on the Loess Plateau area have been silted up, accounting for 69.77% of the total of 58 776. The number of fully silted dams built before 1986, 1986–2003, and after 2003 are 28 198, 8624, and 4186, respectively, accounting for 87.97, 62.15, and 32.59%, respectively, of the total, as shown in Table 9.6.

9.3.1.1. Large Check Dams

The large dams on the Loess Plateau have a designed storage capacity of 5.794 billion m^3 in total and a siltation storage capacity of 3.802 billion m^3. At present, they have accumulated 2.236 billion m^3 of silt, and the remaining siltation storage capacity is 1.566 billion m^3, with a siltation rate of 38.59%. The siltation rates of large dams constructed before 1986, 1986–2003, and after 2003 are 68.67, 39.45, and 15.66%, respectively, as shown in Table 9.7.

There are 5905 large dams on the Loess Plateau, of which 1390 have been fully silted, accounting for 23.54%. The number of large dams built before 1986, 1986–2003, and after 2003 are 1042, 252, and 96, respectively, accounting for 64.76, 15.96, and 3.53%, respectively, of the total large dams, as listed in Table 9.8.

9.3.1.2. Medium Check Dams

The medium check dams on the Loess Plateau have a designed total storage capacity of 2.731 billion m^3 and a siltation storage capacity of 2.132 billion m^3. At present, they have retained 1.658 billion m^3 of silt, and the remaining silt storage capacity is 474 million m^3, with a siltation rate of 60.71%. The siltation rates of medium

@seismicisolation

Table 9.8 Fully silted large check dams on the Loess Plateau in three different periods (unit: dam).

Project period	Full sedimentation	Not full sedimentation	Total	Full sedimentation (%)
Before 1986	1042	567	1609	64.76
1986–2003	252	1327	1579	15.96
After 2003	96	2621	2717	3.53
Total	1390	4515	5905	23.54

Table 9.9 Siltation situation of medium check dams on the Loess Plateau.

	Project period			
Storage	Before 1986	1986–2003	After 2003	Total
Total storage (100 million m^3)	18.77	2.86	5.68	27.31
Design silting storage capacity (100 million m^3)	15.52	2.13	3.67	21.32
Silted-up storage capacity (100 million m^3)	14.02	1.41	1.15	16.58
Remaining capacity (100 million m^3)	1.5	0.72	2.52	4.74
Deposition rate (%)	74.69	49.3	20.25	60.71

Table 9.10 Fully silted medium check dams on the Loess Plateau in three different periods (unit: dam).

Project period	Full sedimentation	Not full sedimentation	Total	Full sedimentation (%)
Before 1986	5484	1606	7090	77.35
1986–2003	314	1288	1602	19.6
After 2003	117	3360	3477	3.36
Total	5915	6254	12 169	48.61

Table 9.11 Siltation situation of small check dams on the Loess Plateau.

	Project period			
Storage	Before 1986	1986–2003	After 2003	Total
Total storage (100 million m^3)	15.87	5.79	3.42	25.08
Design silting storage capacity (100 million m^3)	12.08	3.89	2.19	18.16
Silted-up storage capacity (100 million m^3)	11.83	2.96	1.31	16.1
Remaining capacity (100 million m^3)	0.25	0.93	0.88	2.06
Deposition rate (%)	74.54	51.12	38.3	64.19

dams constructed before 1986, 1986–2003, and after 2003 are 74.69, 49.30, and 20.25%, respectively, as shown in Table 9.9.

There are 12 169 medium dams on the Loess Plateau, of which 5915 have been fully silted, accounting for 48.61%. The number of medium check dams built before 1986, 1986–2003, and after 2003 are 5484, 314, and 117, respectively, accounting for 77.35, 19.60, and 3.36%, respectively, of the total medium dams, as shown in Table 9.10.

9.3.1.3. Small Check Dams

The small check dams on the Loess Plateau have a total designed storage capacity of 2.508 billion m^3 and a siltation storage capacity of 1.816 billion m^3. They have retained 1.610 billion m^3 of silt, and the remaining siltation capacity is 206 million m^3, and the deposit rate is 64.19%. As shown in Table 9.11, the siltation rates of small dams built before 1986, 1986–2003, and after 2003 are 74.54, 51.12, and 38.30%, respectively.

There are 40 702 small dams on the Loess Plateau, of which 33 703 have been fully silted, accounting for 82.8%. As presented in Table 9.12, the number of small dams built before 1986, 1986–2003, and after 2003 are 21 672, 8058, and 3973, respectively, accounting for 92.79, 75.34, and 59.74%, respectively, of the total.

The above analysis of the siltation conditions of various types of check dams in different periods shows

@seismicisolation

Table 9.12 Fully silted small check dams on the Loess Plateau in three different periods (unit: dam).

Project period	Full sedimentation	Not full sedimentation	Total	Full sedimentation (%)
Before 1986	21 672	1684	23 356	92.79
1986–2003	8058	2637	10 695	75.34
After 2003	3973	2678	6651	59.74
Total	33 703	6999	40 702	82.8

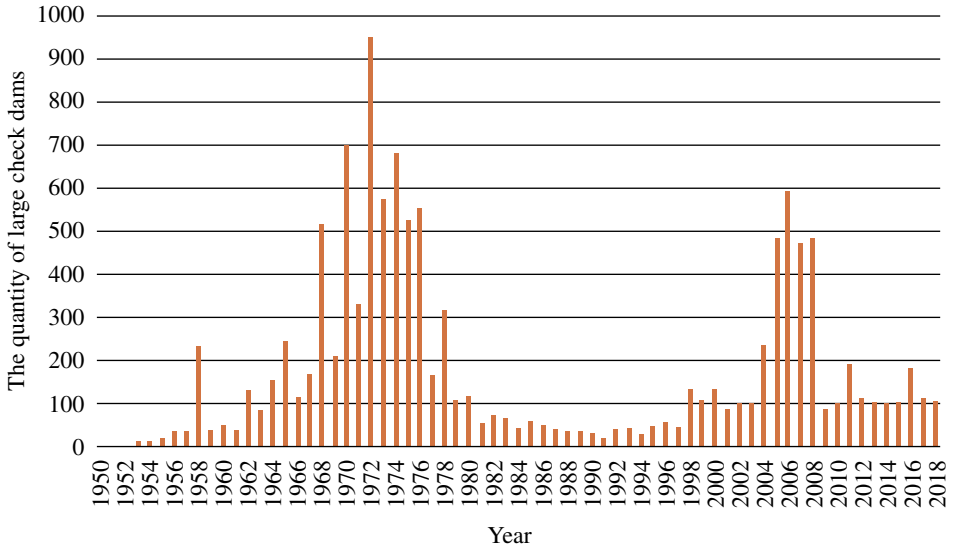

Figure 9.6 Medium dams constructed annually on the Loess Plateau

that those check dams exhibit the same siltation law in the time dimension: the earlier the dam is built, the higher the degree of siltation. From the perspective of design standards, the higher the design standard, the lower the degree of siltation. That is, the siltation degree of large dams built during the same period is lower than that of medium dams, which is lower than of small dams.

9.3.2. Analysis of Regional Siltation Situation

Analyzing the siltation situation of check dams by region is helpful to grasp the operation status and siltation rates of check dams in different provinces, key areas of water and soil loss, and areas with representative types of soil erosion, and to provide a basis for the layout and configuration of check dams (Figures 9.6 and 9.7).

9.3.2.1. Analysis of Siltation Situation in Provinces

According to the analysis of statistics, the fully silted check dams on the Loess Plateau are mostly distributed in Shaanxi and Shanxi provinces, accounting for 60.99% and 34.63%, respectively, of the total fully silted, as shown in Table 9.13. Figures 9.8 and 9.9 present the distribution of different types of fully silted check dams in provinces.

9.3.2.2. Analysis of Siltation Situation in Key Areas of Water and Soil Loss

The number of large and medium check dams that have been fully silted in the three key areas of water and soil loss – rich sediment areas, rich and coarse sediment areas, coarse sediment areas – are 6975, 6668, and 3287, respectively, accounting for 43.06, 51.99, and 68.71%, respectively, of the total number of large and medium dams in the corresponding area. They are all higher than the average percentage on the Loess Plateau, as shown in Table 9.14 illustrate the distribution of different types of fully silted dams in the key areas of soil erosion.

9.4. MODE OF COMBINED USE OF WATER RESOURCES IN RESERVOIRS, DAMS, AND CELLARS

The mode of combined use of water resources in reservoirs, dams, and cellars is comprehensive technology to combine water retention projects, for example, small

@seismicisolation

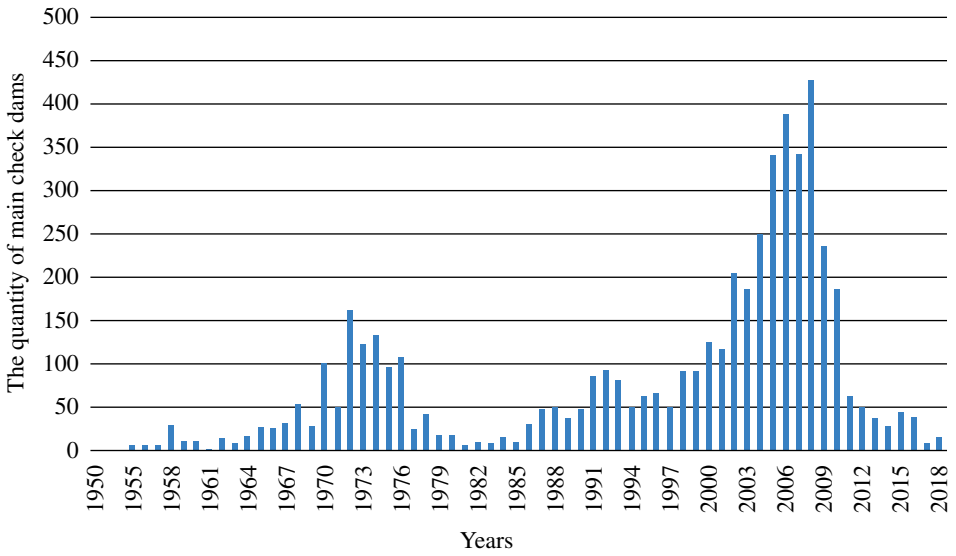

Figure 9.7 Large dams constructed annually on the Loess Plateau

Table 9.13 Fully silted check dams in provinces on the Loess Plateau.

		Province							
Type		Qinhai	Gansu	Ningxia	Inner Mongolia	Shaanxi	Shanxi	Henan	Total
Medium check dam	Full sedimentation	9	81	15	39	1148	88	10	1390
	Amount	173	559	329	877	2651	1191	125	5905
	Proportion of full sedimentation (%)	5.2	14.49	4.56	4.45	43.3	7.39	8	23.54
Large check dam	Full sedimentation	0	40	72	53	5689	33	28	5915
	Amount	128	451	373	702	9483	844	188	12 169
	Proportion of full sedimentation (%)	0	8.87	19.3	7.55	59.99	3.91	14.89	48.61
Small check dam	Full sedimentation	197	317	248	365	18 172	14 078	326	33 703
	Amount	373	590	400	698	21 953	16 126	562	40 702
	Proportion of full sedimentation (%)	52.82	53.73	62	52.29	82.78	87.3	58.01	82.8
Total	Full sedimentation	206	438	335	457	25009	14199	364	41008
	Amount	674	1600	1102	2277	34 087	18 161	875	58 776
	Proportion of full sedimentation (%)	30.56	27.38	30.4	20.07	73.37	78.18	41.6	69.77

reservoirs, soil and water conservation projects, and check dams, with water storage projects like pools and water cellars, to make efficient use of water resources. That is, through primary or secondary pumping, the water retained by the dam is transported to the cellars in the surrounding highlands to adjust the time and space for water resource utilization. In this way, the irrigation area is expanded, and water-saving irrigation techniques can be adopted to develop high-efficiency agriculture.

9.4.1. Details of the Mode of Combined Use of Water Resources in Reservoirs, Dams, and Cellars

Through the reasonable layout and operation of water regulation and storage projects, the mode of combined use of water resources in reservoirs, dams, and cellars adjusts the utilization time and space of the water resources previously intercepted by the water conservation projects so that the rainfall runoff in lower places can be transported to higher ones and the

@seismicisolation

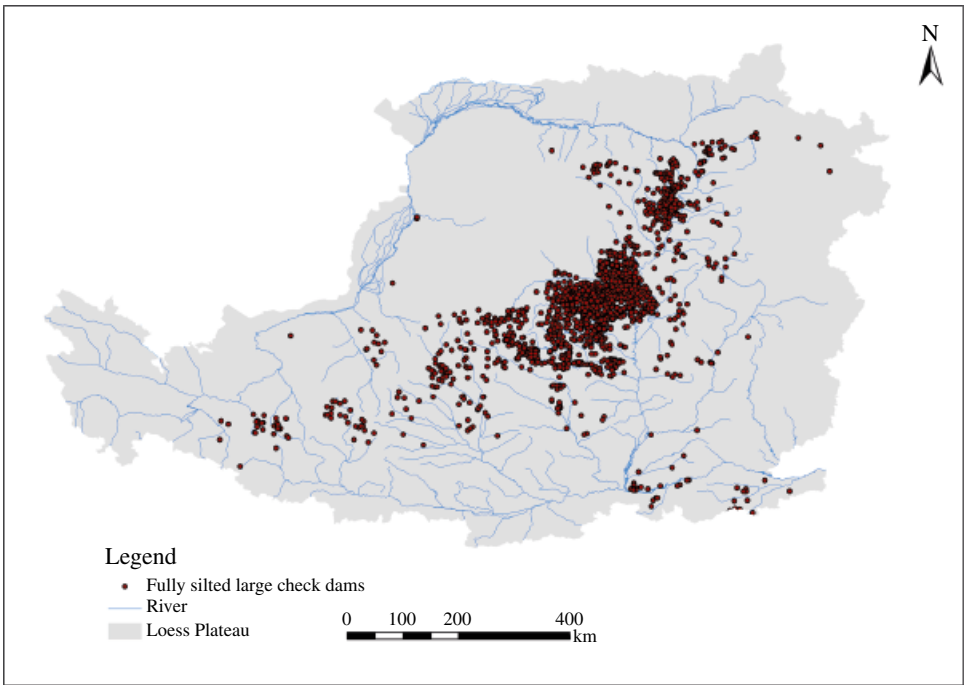

Figure 9.8 Provincial (regional) distribution of fully silted large check dams on the Loess Plateau

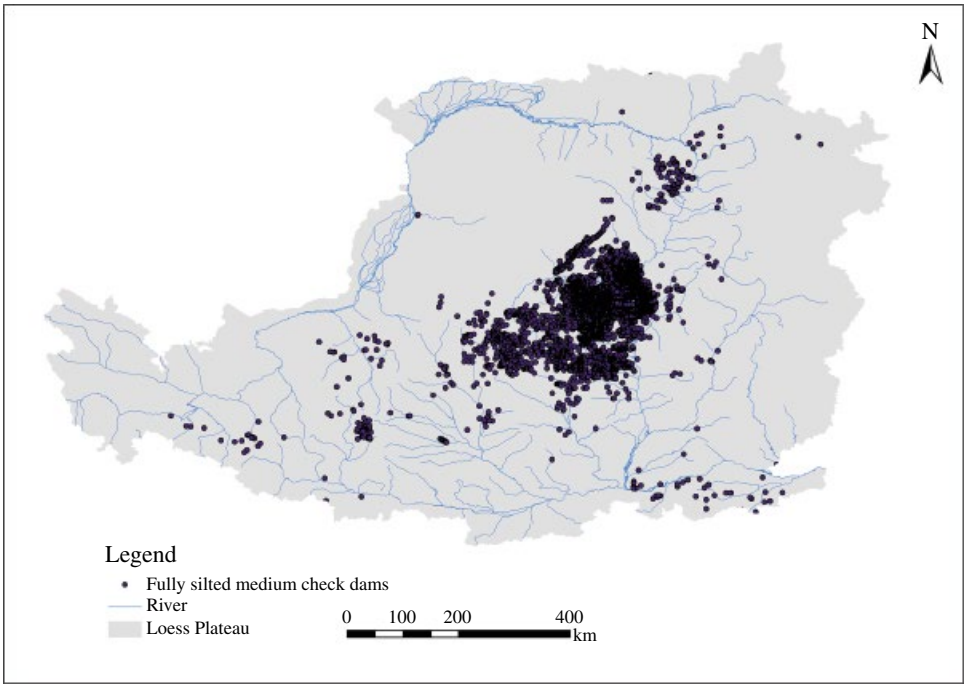

Figure 9.9 Provincial (regional) distribution of fully silted medium check dams on the Loess Plateau

water stored in autumn can also be utilized in spring. The efficient use of water resources via water-saving irrigation techniques is aimed at reasonably and economically regulating and utilizing water resources to increase the income of local people. The mode of combined use of water resources in reservoirs, dams, and cellars in the Niejia River Basin is mainly suitable for the dispatch of water resources in small-scale reservoirs, key gully control projects, check dams, ponds, waterlogging ponds, and other water storage and soil

@seismicisolation

Table 9.14 Siltation situation of large and medium check dams in key areas of soil erosion on the Loess Plateau.

Type		Partition			
		Coarse sediment source area	Rich and coarse sediment area	Rich sediment area	Loess Plateau
Medium check dam	Full sedimentation	709	1257	1348	1390
	Amount	1104	3174	4930	5905
	Proportion of full sedimentation (%)	64.22	39.6	27.34	20.68
Large check dam	Full sedimentation	2578	5411	5627	5915
	Amount	3680	9652	11 269	12 169
	Proportion of full sedimentation (%)	0.7005	0.5606	0.4993	0.4861
Total	Full sedimentation	3287	6668	6975	7305
	Amount	4784	12 826	16 199	58 776
	Proportion of full sedimentation (%)	0.6871	0.5199	0.4306	0.1243

conservation projects, as well as the supplementary irrigation of surrounding farmland. It consists of four parts: water source projects, water lifting facilities, water regulation and storage projects, and water-saving irrigation.

The principles for water resource utilization in the mode of combined use of water resources in reservoirs, dams, and cellars are as follows. (i) The land development scale is determined by the water situation. That is, the suitable scale of supplementary irrigation land is determined according to the situation of water retained in the water conservation and storage projects, as well as the water-saving irrigation technology. The efficient use of water resources is therefore realized. (ii) Under the premise that water resources are guaranteed, the suitable scale and topographical conditions of the supplementary irrigation land are used to determine the layout, scale, and equipment parameters of the water storage and transfer projects. (iii) The primary purpose of this technology is to guarantee the irrigation requirements of crops during the spring dry period. Therefore, it mainly regulates water resources in time and space.

In the mode of combined use of water resources in reservoirs, dams, and cellars, water pumping is one of the main technical links, and it is also the most costly link in the entire water resources dispatching project. Different water lifting heights require different water lifting technologies and equipment, and different irrigation scales require different water storage capacities, water lifting technologies, and equipment. Therefore, according to the characteristics of local water resources and topography, it is determined that the water pumping facilities are mainly small- and medium-sized. According to the technical performance analysis of current small- and medium-sized water lifting equipment, a water lifting height of 40 m is the most reasonable and economical. Therefore, according to the height of the water lifted (pumped up), the combined use of water resources in reservoirs, dams, and cellars can be divided into high-efficiency use of water resources in primary reservoirs, dams, ponds, and cellars and high-efficiency use of water resources in secondary reservoirs, dams, and cellars. Their water lifting heights are within 40 m and 80 m, respectively. For areas where the water lifting height exceeds 80 m, due to the insufficient performance of small- and medium-sized water lifting facilities, the large water lifting (lifting) height and high cost, it is recommended not to use this technology.

9.4.1.1. Mode of High-Efficiency Use of Water Resources in Primary Reservoirs, Dams, and Cellars

In this mode, a water-lifting pump station is built near the water source (dam), a reservoir is built in a relatively flat area in the middle of the slope about 40 m above the water surface, and a water cellar is built on the farmland between the reservoir and the water source. Generally, in the rainy season, the water is first delivered to the reservoir through the pumping station for storage and adjustment and then transported to the water cellar under self-pressure for storage or the water is directly delivered to the water cellar for storage through the pumping station. The unit mode controls a water-saving irrigation area of 50–100 mu.

@seismicisolation

9.4.1.2. Mode of High-Efficiency Use of Water Resources in Secondary Reservoirs, Dams, and Cellars

In this mode, a water-lifting pump station is built near the water source (dam), a primary reservoir is constructed in a relatively plat area in the middle of the slope about 40 m above the water surface, and a secondary reservoir is constructed in a relatively flat area in the upper part of the slope about 80 m above the water surface; water cellars are built respectively on the farmland between the water source and the primary reservoir, and between the primary reservoir and the secondary reservoir. Generally, in the rainy season, the water is first delivered to the primary reservoir through a pumping station for storage and regulation and then transported under self-pressure to the water cellar between the water source, and the primary reservoir for storage or the water is directly delivered to the cellar for storage through the pumping station. Meanwhile, a mobile pumping station is built at the primary reservoir. The water resource in the primary reservoir is transported to the secondary reservoir through this mobile station and then transported to the cellar between the primary reservoir and the secondary reservoir through self-pressure for storage or the water is directly transferred from the primary reservoir to the cellar for storage through the pumping station. In this mode, the water in the primary reservoir is mainly used to directly irrigate the agricultural land between the primary reservoir and the water source and to supply water to the secondary reservoir, whereas the water in the secondary reservoir is mainly used to directly irrigate the farmland between the secondary reservoir and the primary reservoir and to supply water to the cellar between the secondary reservoir and the primary reservoir. The unit mode controls a water-saving irrigation area of 100–300 mu.

Due to the limited amount of water resources and the high cost of regulating water resources, the water stored in the cellars of these two modes is mainly used in the critical period of crop water use in the following spring, and water-saving irrigation must be implemented. Handlances, small electric submersible pumps, and manual or siphon water lifting, as well as techniques such as point irrigation, hole irrigation, furrow irrigation, microspray irrigation, and small tube irrigation are adopted to irrigate the surrounding high-efficiency crops. The main purpose of the model is to realize the spring use of autumn water and the efficient use of water resources through the joint dispatch of reservoirs, dams, and cellars, so as to ensure crop growth.

9.4.2. Application Conditions and Technical Features

9.4.2.1. Application Conditions

The application of the mode of combined use of water resources in reservoirs, dams, and cellars should comprehensively consider the amount of water in the water source project, the water lifting height between the farmland and the water source, the area of farmland that can be irrigated, and the topographical conditions. The general applicable conditions are as follows: first, there must be a small reservoir and a water and soil conservation interception project; second, there must be a stable water source in the interception project, and a certain area of farmland that can be built into horizontal terraces and is close to local residential areas; third, there must be topographic and geological conditions suitable for the construction of water regulation and storage projects.

The mode of high-efficiency use of water resources in primary reservoirs, dams, and cellars is mainly suitable for agricultural areas where the water pumping height is less than 40 m. Considering the overall economic benefits, each water resource regulation project needs to develop at least 50 acres of supplementary irrigation planting area; that is, at least 50 acres of farmland can be developed for water-saving irrigation planting. According to the current water-saving irrigation technology, the annual supplementary irrigation quota for main crops is generally 10–40 m^3/mu. Calculated by this irrigation quota, to ensure that the amount of water resources in the water source project is enough for the supplementary irrigation of the irrigated area, the amount of water resources in the water source project must be about 500–2000 m^3. In addition, the terrain and geological conditions must meet the requirements of the construction of pumping stations, reservoirs, water cellars, and other water regulation and storage projects

The mode of high-efficiency use of water resources in secondary reservoirs, dams, and cellars is mainly suitable for agricultural areas where the water pumping height is less than 80 m. Each water resource regulation project needs to develop at least 100 acres of supplementary irrigation area; that is, at least 100 acres of farmland can be developed for water-saving irrigation planting. The amount of water resources of the water source project must be able to meet the supplementary irrigation requirements of the farmland in the irrigation area. According to the current water-saving irrigation technology and the annual

@seismicisolation

supplementary irrigation quota for main crops, the amount of water resources in the water source project must be about 1000–4000 m^3. Meanwhile, terrain and geological conditions must meet the requirements of the construction of pumping stations, reservoirs, water cellars and other water regulation and storage projects.

9.4.2.2. Technical Features

The major technical characteristics of high-efficiency use of water resources in secondary reservoirs, dams, and cellars are as follows:

1. It can make full use of the constructed small reservoirs and water and soil conservation projects, with low cost and a wide application range.
2. The joint dispatch of water resources by reservoirs, dams, and cellars adjusts the temporal and spatial distribution of water resources, so the water resources are able to meet the demands of crops on supplementary irrigation water during water shortage period.
3. It saves the cost of water cellar construction and water cellar dredging, further lowering the technical costs.
4. Through the timely joint dispatch of water resources of reservoirs, dams, and cellars, the leakage and evaporation losses of water resources are reduced. Meanwhile, the dam is emptied, which increases the water storage capacity and reduces the flood control pressure of the water and soil conservation project during the flood season, and further enhance the safety factor of the project.
5. This technology cannot only be used for the supplementary irrigation of crops directly in the irrigation season but also can be used for water resources regulation, supplementary irrigation of crops during the critical growth period, thereby increasing the planting area of supplementary irrigation crops.
6. Compared with the small high pumping irrigation technology, this technology uses the water regulation and storage project to realize the temporal and spatial adjustment of water resources and solves the contradiction between the concentrated precipitation period and the critical period of crop water demand. At the same time, water-saving irrigation techniques are adopted to improve the utilization efficiency of water resources as well as the economic benefits.
7. Compared with traditional dry farming, this technology adopts water-saving irrigation techniques so that the agricultural production is guaranteed partly, and the grain output is more stable and higher.

9.5. MODE OF WATER DIVERSION IRRIGATION FROM CHECK DAMS

9.5.1. Significance of Water Diversion Irrigation from Check Dams

The constructed check dams have successfully retained the sediment but performed poorly in water blocking and are still insufficient in the use of floodwater. Thus, it is very difficult to achieve sustainable and scientific development of agriculture and forestry in arid areas. As for the check dams built in the 1960s and 1970s, after they are fully silted, they no longer have the ability to retain soil, let alone water. Some of them had been damaged by floods, resulting in a waste of resources and even out of control of soil erosion. The reasons for the above phenomena are the factors of emphasizing construction and neglecting management, but the more important reason is the lack of water, and local people cannot get their due benefits from the check dam (the growth of crops is restricted by water shortage). In fact, for local people in arid mountainous areas with more land and less water, the increase or decrease in dry land will make little difference, but the increase in water resources will have direct benefits to them. Therefore, while conserving the soil, it is necessary to conserve the water resources. Only when the water is preserved can the land be truly preserved, and local people's continuous income from the check dam can be guaranteed; thus, the check dams can be preserved. It is, thus, more important to conserve water in arid mountainous areas than soil. In the arid areas of the Loess Plateau, the annual precipitation is around 400 mm or less, over 60% of which is concentrated in the form of torrential rain in the three months of July, August, and September, when the growth of crops or economic woods and grasses requires the most water. Nevertheless, more than 60% of the heavy rains cause floods due to their high intensity and short duration, and these floods will carry a large amount of mud and sand while discharging. Consequently, the crops, woods, and grasses on the slope will suffer yield reduction or even wither for the lack of timely irrigation; meanwhile, the discharged floods will destroy the upstream farmland, roads, and villages, and silt up the river channel and raise the river bed in the downstream, inducing great losses. The retention and utilization of floodwater can not only effectively prevent soil erosion but also increase the amount of water

@seismicisolation

resources available in arid areas, thereby greatly promoting the economic and social development of dry areas. With the increasing efforts of the state to conserve the ecological environment, there are more and more gully treatment projects in arid mountainous areas. For example, a large number of dam system projects on the Loess Plateau, mostly check dams, have changed the previous state of the channel without protective measures, slowed the flow of floods, and extended the duration of floods. These projects intercepted most or all of the floodwater in the channel collected from the slope surface, and the intercepted floods are no longer destructive, creating conditions for further development and utilization. The blocked floodwater can be useful as long as corresponding measures are taken to store it. Water resources in the gully areas of the Loess Plateau are extremely limited. The channel floodwater is partly blocked by check dams and then stored in reservoirs and cellars, by which means the utilization of flood resources can be increased. According to the geographical characteristics of the areas (rocky mountainous area or earth-rocky mountainous area and loess area) where the check dam is located, different cellar layouts are designed. Vertical wells or horizontal pipes for water diversion and storage, as well as water outlets that can discharge sand by themselves, are adopted in these areas. If these measures are implemented, the problem that the check dam can only silt land but cannot store water can be solved. They are of great significance to alleviate the shortage of water resources in the gully areas of the Loess Plateau, improve the ecological environment, and promote the construction of a new socialist countryside.

9.5.2. Purposes of Water Diversion Irrigation from Check Dams

9.5.2.1. Increasing the Utilization Rate of Water and Soil Resources in the Dam System

In this mode, the dam can be used for storing water for irrigation, afforestation, grass planting, and fish culture during the siltation process rather than for planting alone after the siltation. The simultaneous development of various industries bring forward the dam's available period. By making full use of the water and soil resources of the dam, the optimal utilization of channel, check dam, and dam land is realized, and the utilization rate of the water and soil resources of the dam system is enhanced.

9.5.2.2. Increasing Economic Benefits

Water diversion irrigation from check dams provides water resources stored in the check dams in small watersheds on the Loess Plateau to help promote agricultural production, farmers' income, and rural economy. Local people can use the dam land to store water right after the completion of the check dam, and divert water for irrigation, thereby increasing income and economic benefit. The original method of using the dam land after it is fully silted is changed, which shortens the utilization time of the dam land, and brings economic benefits in advance.

9.5.2.3. Eliminating the Shortage of Drinking Water

The gully areas of the Loess Plateau have long been suffering from water shortage. Drinking water for both humans and livestock is insufficient. The development and utilization of dam storage projects can, to a certain extent, solve the problem of drinking water shortage in the watershed and bring into play the social benefits of dam storage projects.

9.5.2.4. Providing Ecological Water

The water stored in dam land can be delivered to irrigate the soil conservation plants in the basin to promote plant diversity, improve the ecological environment of the watershed, and produce ecological benefits.

9.5.3. Technical Approaches of Water Diversion Irrigation from Dam Land

9.5.3.1. Dam-Cellar Water Storage Project

The dam-cellar storage project combines check dams and water cellars organically. It uses a check dam to retain the floodwater and then builds a water cellar or reservoir in or around the check dam area to store the water, in which way the floodwater can be used.

The arrangement of the dam-cellar water storage project is as follows. Gully control projects to prevent and control soil erosion are constructed in the gully area of the Loess Plateau, mostly in check dams. Due to the high location, simple structure, low flood resistance, and design standards of a check dam, its water storage functions are generally not considered. In the early stage of dam operation, the check dam, however, has a certain storage capacity and can store a certain amount of floodwater in a short period. Water storage facilities such as cellars or reservoirs are constructed in or around the check dam area, realizing the reasonable

@seismicisolation

combination of water storage facilities and check dam. Water cellars or reservoirs are used to store water so that floodwater that cannot be used or is difficult to use can be utilized. The combined storage method of dam and cellar can refer to the following two schemes.

First, if the check dam is located in a rocky or rocky mountainous area with good geological conditions, it is suitable to build water storage facilities in the dam area (Figure 9.10). Due to the good geological conditions in this area, the cellar can be built directly within the reservoir area according to the topographical conditions, and the irrigation water is delivered through the drainage pipe connected to the higher cellar under the gravity (Figure 9.11).

Second, if the check dam is situated in loess or other soil mountainous areas, the geological conditions of the dam area are bad. Thus, after the soil is infiltrated by water, it is easy to damage the foundation of the water cellar, causing the water cellar to rupture or tilt. In this case, the second scheme should be adopted. Water cellars or reservoirs are generally built in the downstream area of the dam, which has a stable foundation and is not susceptible to water infiltration. The water in the dam is diverted to a downstream cellar or reservoir through horizontal pipes. Compared with the first scheme, this scheme has the following advantages: first, the water is delivered through horizontal pipes, which is easy and safe; second, the foundation of the water cellar is not in direct contact with water, which increases the safety and stability of the water cellar or reservoir. Since most of the water and soil loss occurs in such areas, the second scheme is recommended. The project layout of the second scheme is shown in Figures 9.12 and 9.13.

The layout of water storage facilities should meet the needs of water storage, while following the principles of safety, low investment, and easy construction. It should be determined according to factors such as channel gradient, soil quality, and channel shape

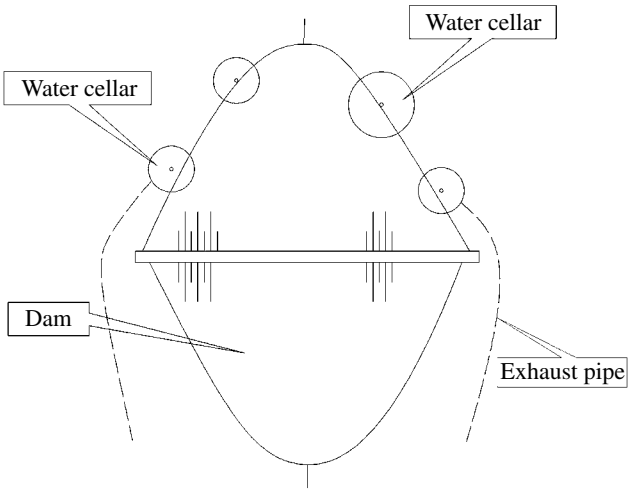

Figure 9.10 Layout cross section of water storage facilities of a check dam in an area with good geological conditions

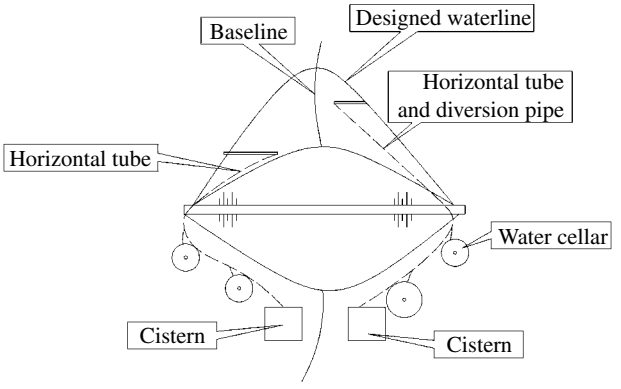

Figure 9.12 Layout cross section of water storage facilities of a check dam in an area with bad geological conditions

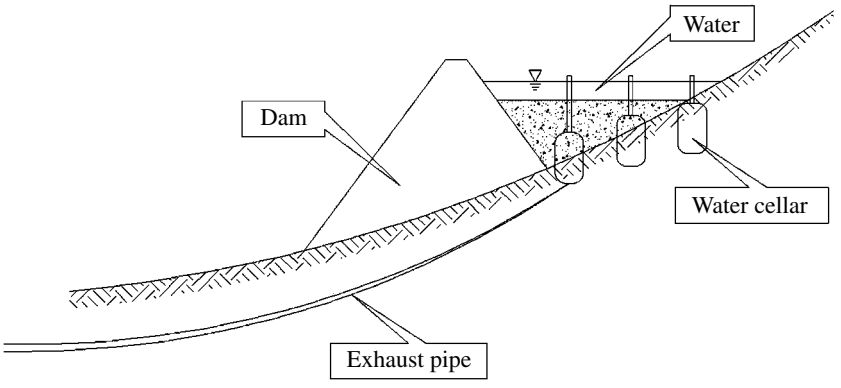

Figure 9.11 Layout profile of water storage facilities in an area with good geological conditions

@seismicisolation

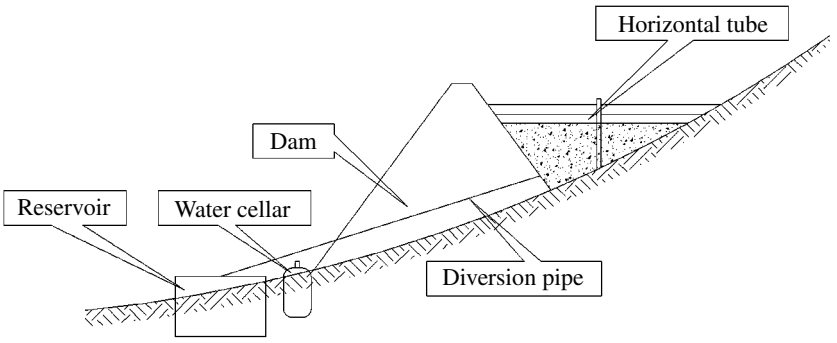

Figure 9.13 Layout profile of water storage facilities of a check dam an area with bad geological conditions

(a wide and shallow U shape or a narrow and deep V shape). Generally, for wide, shallow channels that are easy to construct and have good foundation conditions, reservoirs with a large capacity are selected; while for narrow, deep channels that are difficult for construction or foundation treatment, it is suggested to choose a water cellar with a small floor area – a small amount of construction. For the channels in the rocky mountainous area, a tetrahedral reservoir can also be a choice, and the reservoir is built directly in the channel.

9.5.3.2. One-dam-and-one-pond Project

1. Design principle

The design of the project should fully adjust to local conditions, be scientifically planned, and give top priority to benefits while emphasizing economic feasibility.

2. Design mechanism

The one-dam-and-one-pond water source project is to develop irrigated land by retaining rainwater, replenishing groundwater, and utilizing pond water. The basic method is to build an earth dam in the channel to block runoff and then excavate a pond at a distance of 15–20 m from the foot of the dam downstream. The runoff retained in the dam penetrates through the coarse sediment layer at the bottom of the dam to replenish the pond downstream, which not only intercepts the runoff but also the underflow, increases the water amount, and expands the irrigated land. The design process is as follows: firstly, the optimal position of the one-dam-and-one-pond water source project is determined according to the location of the land resources to be developed; subsequently, based on the water retention capacity of the project, the area of irrigated land that can be developed, the water demand of crops, the irrigation interval, and the opening diameter and volume of the pond are determined.

3. Design features

First, each pond is protected by one dam to prevent the pond from being destroyed by floods and sediment. Compared with simple underflow interception projects, the pond has a long service life and a high safety factor. Second, each dam replenishes one pond. Since the dam-building material is sandy loam, the sand layer above the channel bedrock has large porosity and good permeability. The runoff intercepted by the dam can continuously replenish the pond, ensuring the demand for irrigation. Third, the pond improves the economic benefits of the dam, so that the check dams, or other runoff blocking projects not only have the long-term benefits of retaining sediment and silting land but also serve as a water conservation project with significant short-term benefits. Due to the protection of the dam, the opening diameter of the pond can be excavated according to the width of the channel. It is tens of meters, more than 10 times that of the general underflow interception project. Therefore, the pond can store a large amount of water, and the irrigated area increases substantially. With sufficient water sources, the riverside platform and hillside sloping farmland can be built into terraces. Submersible pumps with a certain lift are used to transport the water in the channel to the land on the hillside through deep-buried low-pressure plastic pipes built for water-saving irrigation. Every 0.67–1.0 hm^2 of land has one water outlet for irrigation.

4. Design form

The one-dam-and-one-pond water source project controls an area of 0.5–3 km^2. The pond is usually rectangular with a depth of 3–5 m (from the bottom of the pond to the bedrock). According to site conditions, there are three specific forms of a one-dam-and-one-pond project. The first is the typical form of one dam with one pond, that is, there is only one pond downstream of one dam. The second form is one dam with

@seismicisolation

multiple ponds, that is, there are two or three ponds at certain intervals in the downstream of the dam. The third form is two dams share one pond, each of which has a small control area. In this form, one dam is built in each of the two adjacent branch channels, and a pond is excavated at the junction of the channels.

5. Supporting measures

The one-dam-and-one-pond water source project is mainly used for water storage and flood control. Due to serious water loss, large soil erosion, high sediment content in floods, and rapid sedimentation in the dam, the comprehensive management of soil and water conservation on the slope of the dam area should be strengthened to extend the service life of the dam. Horizontal ditches and fish-scale pits are excavated on slopes to plant Pinus tabuliformis and sea buckthorn to reduce soil erosion. The slope surface covered with gravel has little soil erosion, so sea buckthorn forests are planted. When the water supply of the water source project is insufficient, a clay or concrete cutoff wall can be built 2–4 m downstream of the pond. The wall is excavated to the bedrock and crosses the river bed and, thus, can prevent the underground water from leaking downstream.

9.6. MODE OF FISH FARMING IN CHECK DAMS

9.6.1. Significance of Fish Farming in Check Dams

The check dams constructed effectively control soil erosion and have a large water surface before they are silted up. Due to the high design standards, the newly built check dams generally have spillways, so the safety factor for fish culture is relatively large. Implementation of the Beautiful Mountains and Rivers Project coupled with the year-by-year decrease in soil erosion increases the time available for fish culture. These provide a reliable resource guarantee for the development of large-scale fishery production and greatly increase the water surface for fishery. Furthermore, check dam aquaculture also has the advantages of small investment and fast return, thus, opening up new areas for the further development of aquaculture.

Fish farming in check dams is carried out in accordance with pond-intensive culture and is characterized by multi-species and multi-specification fry stocking, as well as catching and stocking in rotation. In combination with the characteristics of check dams, an integrated ecological farming model of fish, poultry, livestock, and recreational fishing is developed. At the same time, emphasis should also be placed on water quality control and comprehensive prevention and control of aquatic animal diseases, etc. Full control of the aquaculture environment and production process is implemented to improve the quality of aquatic products and their market competitiveness and, thus, increase fishery economic benefits.

9.6.2. Technical Approaches of Fish Farming in Check Dams

9.6.2.1. An Integrated Ecological Model of Fish Farming, Poultry Farming, Livestock Breeding, and Recreational Fishing

This mode should be adopted for newly built check dams with many ravines, uneven substrate, narrow and long terrain, poor ventilation and illumination, inconvenient transportation, and average economic foundation and management level. It is a diversified ecological breeding mode in which the farming of filter-feeding fish species like spotted-silver carp and silver carp is supplemented by the raising of hogs and chickens. The stocking density of fry ranges 200–400 fish/mu, and the size of the fry should be large, most with a specification of more than 50 g/fish. Hogs are raised safely at low cost by using the dam area to grow forage feed, with supplementary full-price feed. Chickens are raised in a natural way – they are authentic free-ranging chickens with high prices and good economic benefits. And the chicken and hog manure can be utilized as fertilizer after fully fermented, which can promote fish growth and increase the economic benefits of fish farming. In this mode, fish farming, livestock breeding, poultry farming, and recreational fishing can promote each other, forming a virtuous economic cycle.

9.6.2.2. A Grass-Feed Combined Culture Mode with Grass Carp as the Major Species

This model can is appropriate for check dams with a large open dam area available for planting grass. The land resources in the dam area are made full use of by planting a large number of high-quality and high-yield forage grasses. In terms of varieties, forage grasses such as alfalfa, sudangrass, and ryegrass suitable for the growth in the Loess Plateau soil are mainly adopted. In addition to the dominant fish species, grass carp, there are some filter-feeding fish species, carp, and crucian. The major fish species accounts for over 60%. The general stocking density ranges

@seismicisolation

300–600 fish/mu, and the specification of grass carp is above 100 g/fish. Under the premise of sufficient forage grass and effective disease prevention measures, the fish are mainly fed by grass, supplemented by pellet feed. When forage grass becomes fibrous in autumn, the amount of grass is moderately reduced and the amount of pellet feed is increased. If grass carp fingerlings of different specifications are stocked, rotation can be implemented to catch only the large fish while leaving the small ones. In this fishing farming mode, special attention must be paid to the prevention of fish diseases.

9.6.2.3. An Intensive Pellet Feed-Based Culture Mode with Carp as the Major Species

This mode requires that the check dam has convenient transportation, sufficient water resources, good ventilation and illumination, a flat substrate, easy fishing conditions, and that the farmers possess a good economic foundation and certain management experience. This farming mode is suitable for areas where fish prices are high and fish is in short supply. It is required that the water source is easily available and drainage of the check dam is convenient, and that the farmers have good fish farming techniques and relatively abundant funds. The adoption of this mode can greatly increase the production and improve the economic benefits. This mode is implemented with reference to pond-intensive culture and is characterized by multi-species and multi-specification polyculture, and stocking and fishing in the same year. The fry stocking density ranges 500–1000 fish/mu, and the fish species specification is above 50 g/fish. The major fish species is carp, accounting for 65% of the total. In addition to carp, there are some other fish species. The feed is mainly high-quality pellets.

9.6.2.4. A Recreational Fishery-Oriented Comprehensive Development Mode

With the rapid development of regional economy and an increasing number of immigrant populations, the comprehensive development of recreation, fishing, catering, and entertainment is an effective way to improve the benefit of check dams. In check dams with convenient transportation and proximity to the city, fish farming can be combined with the entire dam area development, forming a diversified integrating development mode of breeding, recreation, entertainment, fishing, and catering, thereby achieving better economic and social benefits.

9.6.3. Main Measures of Fish Farming in Check Da

1. Medicine is applied once a month to prevent fish diseases. During the peak season of fish growth, the medicine is administered once every 7–10 days depending on the practical situation of the dam. It can be sprinkled throughout the dam or placed in hanging baskets or fed with baits. The stocked fry is better if large in size and strong, and fish of the same species have the same specification. In addition, the fry must be disinfected before stocking. Generally, they are soaked in 2–5% salt water or 20–40 ppm potassium permanganate solution for 5–10 minutes.
2. Fish blocking facilities are built. Management is strengthened, especially the daily management during flood control.
3. Technical training and onsite training are carried out to improve the theoretical and practical levels of the check dam contractors. It is recommended to fish in the same year of stocking rather than every few years. The advanced management experience of particular check dams is summarized and popularized to give a comprehensive effect in all check dams.
4. Patrolling of check dams in the morning and evening is required. A registration system is established, and the four key aspects of fishery medicine, feed, fertilizer, and water quality are under particular control.
5. Water quality and inputs such as feed and fishery drugs strictly comply with the following standards: NY/T5051-2001 Non-polluted Food: Water Quality for Freshwater Aquaculture, NY/T5072-2002 Non-polluted Food: Safety Limits of Compound Feed for Fishing, and NY/T5071-2002 Non-polluted Food: Guidelines for the Use of Fishery Drugs. The aquatic products produced are in accordance with relevant pollution-free food standards such as NY/T5070-2002 Non-polluted Food: Limits of Residues of Fishery Medicines in Aquatic Products.

9.7. CONCLUSION

Check dam development on the Loess Plateau can be divided into stages of spontaneous construction, standardized construction, and scale development. According to statistic, there were a total of 58 776 check dams on the Loess Plateau in 2019. By making full use of the water and soil resources of the dam, the optimal utilization of channel, check dam, and dam land is realized, and the utilization rate of the water and soil resources of the dam system is enhanced.

@seismicisolation

Technical approaches of water diversion irrigation from dam land included dam-cellar water storage project and one-dam-and-one-pond project. Significance and technical approaches of fish farming in check dams were suggested in the study.

REFERENCES

1. Chen, L., Wei, W., Fu, B., and Lü, Y. (2007). Soil and water conservation on the Loess Plateau in China: review and perspective. *Progress in Physical Gepgraphy 31*: 389–403.
2. Fu, B., Wang, S., Liu, Y. et al. (2017). Hydrogeomorphic ecosystem responses to natural and anthropogenic changes in the Loess Plateau of China. *Earth and Planetary Sciences 45*: 223–243.
3. Zhao, G., Mu, X., Wen, Z. et al. (2013). Soil erosion, conservation, and eco-environment changes in the Loess Plateau of China. *Land Degradation and Development 24*: 499–510.
4. Jiao, J., Tzanopoulos, J., Panteleimon, X. et al. (2007). Can the study of natural vegetation succession assist in the control of soil erosion on abandoned croplands on the Loess Plateau, China? *Restoration Ecology 3*: 391–399.
5. Shi, P., Zhang, Y., Ren, Z. et al. (2019). Land-use changes and check dams reducing runoff and sediment yield on the Loess Plateau of China. *Science of the Total Environment 664*: 984–994.
6. Fu, B., Zhao, W., Chen, L. et al. (2005). Assessment of soil erosion at large watershed scale using RUSLE and GIS: a case study in the Loess Plateau of China. *Land Degradation and Development 16*: 73–85.
7. Li, J., Liu, Q., Feng, X. et al. (2019). The synergistic effects of afforestation and the construction of check-dams on sediment trapping: four decades of evolution on the Loess Plateau. *Land Degradation and Development 30* (6): 622–635.
8. Liang, W., Bai, D., Wang, F. et al. (2015). Quantifying the impacts of climate change and ecological restoration on streamflow changes based on a Budyko hydrological model in China's Loess Plateau. *Water Resources Research 51*: 6500–6519.
9. Wen, X. and Zhen, L. (2020). Soil erosion control practices in the Chinese Loess Plateau: a systematic review. *Environmental Development 19*: 30220–30229.
10. Xu, X., Zhang, H., Wang, G. et al. (2009). An experimental method to verify soil conservation by check dams on the Loess Plateau, China. *Environmental Monitoringand Assessment 159*: 293–309.
11. Yang, T., Zhang, Q., Chen, Y. et al. (2008). A spatial assessment of hydrologic alteration caused by dam construction in the middle and lower Yellow River, China. *Hydrological Processes 22*: 3829–3843.
12. Tang, H., Pan, H., and Ran, Q. (2020). Impacts of filled check dams with different deployment strategies on the flood and sediment transport processes in a loess plateau catchment. *Water 12* (5): 1319–1341.
13. Feng, X., Fu, B., Piao, S. et al. (2016). Revegetation in China's Loess Plateau is approaching sustainable water resource limits. *Nature Climate Change 31*: 3547–3554.
14. Jiang, C., Zhang, H., Wang, X. et al. (2019). Challenging the land degradation in China's Loess Plateau: Benefits, limitations, sustainability, and adaptive strategies of soil and water conservation. *Ecological Engineering 127*: 135–150.
15. Liu, Y. and Fu, B. (2016). Assessing sedimentological connectivity using WATEM/SEDEM model in a hilly and gully watershed of the Loess Plateau, China. *Ecological Indicators 66*: 259–268.
16. Pal, D., Galelli, S., Tang, H., and Ran, Q. (2018). Toward improved design of check dam systems: a case study in the Loess Plateau. *China. Journal of Hydrology 1694*: 30128.
17. Peng, J., Chen, S., and Dong, P. (2010). Temporal variation of sediment load in the Yellow River basin, China, and its impacts on the lower reaches and the river delta. *Catena 83*: 135–147.
18. Wu, B., Wang, G., Xia, J. et al. (2008). Response of bankfull discharge to discharge and sediment load in the Lower Yellow River. *Geomorphology 100*: 366–376.
19. Xin, Z., Yu, X., and Lu, X. (2011). Factors controlling sediment yield in China's Loess Plateau. *Earth Surface Process Landforms 36*: 816–826.
20. Fu, B., Liu, Y., Lü, Y. et al. (2011). Assessing the soil erosion control service of ecosystems change in the Loess Plateau of China. *Ecological Complexity 8*: 284–293.
21. Shao, M., Wang, Y., Xia, Y., and Jia, X. (2018). Soil drought and water carrying capacity for vegetation in the critical zone of the Loess Plateau: a review. *Vadose Zone Journal 17*: 1–8.
22. Shen, H., Wang, D., Wen, L. et al. (2020). Soil erosion and typical soil and water conservation measures on hillslopes in the Chinese mollisol region. *Eurasian Soil Science 53*: 1509–1519.

@seismicisolation

10

The Safety Distribution of Check Dam System and Potential of Check Dam Construction

Peng Li[1], Zhanbin Li[1], Laizhang Zhang[2], Binhua Zhao[1], Shuilong Yuan[1], Peng Shi[1], Daxiang Wang[2], Anli Ma[2], Ying Jiang[3], Miaoxia Wen[3], Zhiqiang Min[3], and Yan Zhang[4]

10.1. COMPOSITION AND DETERMINATION OF FLOOD CONTROL RISK EVALUATION INDEX SYSTEM FOR CHECK DAMS

10.1.1. Determination of Evaluation Index System

According to the existing literature data, survey data from the Suide Soil and Water Conservation Station [1], and the relevant principles of establishing an index system, nine flood control risk evaluation indices for check dams are selected. Based on the purpose and principles of establishing the flood control risk evaluation index system, the flood control risk evaluation index system of the warping dam system in the Wangmaogou watershed is divided into three layers: target layer, criterion layer, and index layer [2].

1. Target layer: it indicates the risk of check dams in the Loess Plateau, providing a theoretical basis for comprehensively evaluating the investment, construction, and management of check dams and dam systems in small watersheds.

2. Criterion layer: major indices included in the flood control risk evaluation of check dams in the watershed. Based on the existing literature and research results from experts, the flood control risk evaluation of check dams is divided into three categories: flood risk, management risk, and economic risk.

3. Index layer: indices belonging to the criterion layer that can reflect a specific flood risk event. The nine specific indices selected in this paper are shown in Table 10.1.

10.1.2. Evaluation Index Calculation and Standardization

According to the flood control risk evaluation index system for warping dams determined above, the flood risk, management risk, and economic risk of the warping dam are analyzed in the flood control risk evaluation [3].

10.1.2.1. Flood Risk

The flood risk layer primarily includes four indices: instability coefficient, hazard coefficient, risk of flood storage, and flood discharge risk. The calculation and standardization of these four indices are explained specifically [4].

1. Instability coefficient

The instability coefficient is defined as:

$$U = 1 - \frac{I}{0.04} \tag{10.1}$$

[1] *Institute of Water Resources and Hydro-electric Engineering, Xi'an University of Technology, Xi'an, China*
[2] *Upper and Middle Yellow River Bureau, YRCC, Xi'an, China*
[3] *Northwest Institute of Forest Inventory, Planning and Design, National Forestry and Grassland Administration, Xi'an, China*
[4] *College of Urban and Environmental Sciences, Northwest University, Xi'an, China*

Check Dam Construction for Sustainable Watershed Management and Planning, First Edition.
Edited by Zhanbin Li, Peng Li, Yang Yu, Peng Shi, and Guillaume Piton.
© 2022 John Wiley & Sons, Inc. Published 2022 by John Wiley & Sons, Inc.

@seismicisolation

Table 10.1 Flood control risk evaluation index system for check dams.

Target layer(a)	Criterion layer (b)	Index layer (c)
Flood control risk evaluation index system for check dams (a)	Flood risk (b1)	Instability coefficient (c1)
		Hazard coefficient (c2)
		Flood detention risk (c3)
		Flood discharging risk (c4)
	Management risk (b2)	Daily management risk (c5)
		Emergency risk (c6)
		Monitoring facility (c7)
	Economic risk (b3)	Downstream economic risk (c8)
		Yield ensuring risk (c9)

where U is the instability coefficient. If the value of U is less than 0, $U = 0$, then I is a relatively stable index.

The relative stability index I in formula (10.1) is calculated as follows:

$$I = \frac{S}{F} \tag{10.2}$$

where S is the dam area (km^2) and F is the control area (km^2).

2. Hazard coefficient

The hazard coefficient is defined as:

$$W_d = 1 - \frac{1}{I_P} \tag{10.3}$$

where W_d is the hazard coefficient. If the value of W_d is less than 0, $W_d = 0$, then I_p is the safety factor of the warping dam.

The safety factor I_p of a warping dam in formula (10.1) is calculated as follows:

$$I_P = \frac{W_p}{A(h + h_c)} \tag{10.4}$$

where I_p is the safety factor of land, W_p is the flood volume with design frequency p (10 000 m^3), A is the actual area of the dam (hm^2), h is the average permissible flooding depth of the dam (m), and h_c is the average thickness of sediment deposition in the flood (m).

3. Flood storage risk coefficient

The flood storage risk coefficient is the ratio of detention storage capacity to the sum of remaining storage capacity and discharge flow [4].

4. Flood storage coefficient

The flood storage coefficient is defined as:

$$X_d = 1 - X_a \tag{10.5}$$

Where X_d is the flood discharging risk coefficient and X_a is the flood discharge capacity coefficient of the warping dam spillway and drainage structure.

The discharge capacity X_a in formula (14.5) is calculated as:

$$X_a = X_p / L_p \tag{10.6}$$

where X_p is the flood discharge of dam spillway and drainage structure and L_p is the flood volume of the warping dam.

10.1.2.2. Management Risk

The management risk layer primarily includes three indices: daily management risk, emergency risk, and monitoring risk [2]. The calculation and standardization of these three indices are explained in detail below.

After the warping dam starts running, the rainstorms, floods, and burrowing by animals cause varying degrees of damage to the dam. Therefore, it is necessary to manage and monitor the warping dam during its operation period in order to prevent it from breaking. In addition, a corresponding emergency plan should be established to prevent the failure of the warping dam caused by sudden floods due to rainstorms [5]. However, there are very few daily management strategies, emergency plans, and monitoring facilities in the actual operation of check dams, which are also important factors that cause dam breaks. Therefore, it is necessary to evaluate the management risk of the warping dam in order to provide a basis for the flood control risk evaluation of the warping dam.

According to the influence of management factors on the potential risk of warping dam failure, the risk value of each management factor is determined as follows:

1. Daily management risk

Daily management risk is scored according to the local Ministry of Water Resources or the management and maintenance of the warping dam by local residents.

@seismicisolation

If there exists well-placed daily management and maintenance for the warping dam, the daily management risk value is 0; otherwise, it is 1.

2. Emergency risk

If the emergency measures for the flood control risk of the warping dam are formulated, the value of emergency risk is 0; otherwise, it is 1.

3. Monitoring risk

If there are monitoring facilities and various supporting facilities in place, the monitoring risk value is 0; otherwise, it is 1.

10.1.2.3. Economic Risk

The economic risk layer primarily includes downstream economic risk and yield ensuring risk. The calculation and standardization of these two indices are explained in detail below.

1. Downstream economic risk

The downstream economic risk indices are determined according to whether there are houses, production bases, roads, etc., downstream of the warping dam within a certain scale. If there are important residential buildings and production plants downstream of the key dam, the downstream economic risk index is 1. The downstream economic risk index of the warping dam at the exit of each branch is 0.8, and the downstream economic risk index of the second warping dam is 0.6 from the gully mouth along the channel to the gully head. By analogy, the downstream economic risk index of each warping dam in the watershed is assigned.

2. Yield ensuring risk

According to research by Xin et al. [6], the yield ensuring rate depends on the flood detention depth of the warping dam. If the detention water depth of the dam is less than the allowable submerged water depth for crop growth, the crops are harvested; otherwise, the crops are considered to have failed. Based on this, the yield ensuring rate of the dam is calculated as follows:

$$P = 1 - 1/N \tag{10.7}$$

where P is the yield ensuring rate of dam and N is the flood return period corresponding to the flood detention depth of the dam (year).

The yield ensuring risk is calculated based on the following formula:

$$\mathrm{Bd} = 1 - P \tag{10.8}$$

where B_d is the yield ensuring risk.

10.1.3. Flood Control Risk Evaluation Index Weights of the Warping Dam

The flood control risk evaluation of check dams is quite complicated, so the reasonable weight determination of the flood control risk evaluation index is the key to obtaining scientific and reasonable evaluation results [7].

The weight value of the evaluation index of the flood control risk evaluation of the warping dam reflects the importance of the evaluation index in the flood control risk evaluation of the watershed. In order to reasonably and accurately determine the weight of each index in the evaluation system, the relevant research experts and technicians of the check dams are organized in order to independently provide the weight of each index back to back. According to the results, the AHP is used in order to calculate the final weight of each evaluation index. Tables 10.2–10.5 show the obtained judgment matrix

Table 10.2 Expert-assigned flood risk index and comparative judgment matrix.

Index	Instability coefficient	Hazard coefficient	Food detention risk	Flood discharge risk	Weight value
Instability coefficient	1.00	0.67	0.57	0.70	0.21
Hazard coefficient	1.50	1.00	0.85	1.05	0.26
Flood detention risk	1.77	1.18	1.00	1.24	0.28
Flood discharge risk	1.42	0.95	0.80	1.00	0.25

Table 10.3 Expert-assigned management risk index and comparative judgment matrix.

Index	Daily management risk	Emergency risk	Monitoring risk	Weight value
Daily management risk	1.00	0.65	0.86	0.31
Emergency risk	1.55	1.00	1.33	0.37
Monitoring risk	1.16	0.75	1.00	0.32

@seismicisolation

Table 10.4 Expert-assigned economic risk index and comparative judgment matrix.

Index	Downstream economic risk	Yield ensuring risk	Weight value
Downstream economic risk	1.00	0.86	0.49
Yield ensuring risk	1.16	1.00	0.51

Table 10.5 Expert-assigned flood control risk evaluation index of the warping dam and comparative judgment matrix.

Index	Flood risk	Management risk	Economic risk	Weight value
Flood risk	1.00	1.30	1.86	0.38
Management risk	0.77	1.00	1.43	0.33
Economic risk	0.54	0.70	1.00	0.29

Table 10.6 Weight of each evaluation index in the flood control risk evaluation index system of check dams.

Target layer (a)	Criterion layer (b)	Weight value (q)	Index layer (c)	Weight value (w)
Flood control risk evaluation index for warping dam (a)	Flood risk (b1)	0.38	Instability coefficient (c1)	0.21
			Hazard coefficient (c2)	0.26
			Flood detention risk (c3)	0.28
			Flood discharge risk (c4)	0.25
	Management risk (b2)	0.33	Daily management risk (c5)	0.31
			Emergency risk (c6)	0.37
			Monitoring risk (c7)	0.32
	Economic risk (b3)	0.33	Downstream economic risk (c8)	0.49
			Yield ensuring risk (c9)	0.51

and weight of the flood control risk evaluation index system of the warping dam.

Based on the results in Tables 10.2–10.5, the calculated weight results of each evaluation index in the flood control risk evaluation index system of small watershed check dams are shown in Table 10.6.

10.2. FLOOD CONTROL RISK EVALUATION OF WARPING DAM SYSTEM IN WANGMAOGOU WATERSHED

10.2.1. Risk Score Calculation and Risk-Level Division

10.2.1.1. Risk Score Calculation

1. Flood control risk index calculation in the criterion layer of check dams [5]. The flood control risk index of the criterion layer of the flood control risk evaluation index system of the small watershed warping dam is calculated based on the following formula:

$$B = \sum_{i=1}^{3} C_i W_i \tag{10.9}$$

where B_i is the flood control risk index value of warping dam, C_i is the value of each evaluation index in the index layer, and W_i is the weight of each evaluation index in the index layer.

2. Flood control risk score calculation of warping dam

In order to comprehensively, systematically, and accurately reflect the flood control risk of a warping dam in a small watershed, the calculation formula of flood control risk score of a warping dam in a small watershed is

$$A = B_1^{q_1} B_2^{q_2} B_3^{q_3} \tag{10.10}$$

where A is the flood control risk score of warping dam, B_i is the each flood control risk index score of the criterion layer, B_1 is the flood risk score of the warping dam, B_2 is the management risk score of the warping dam, B_3 is the economic risk score of the warping dam, and q_i is the weight corresponding to the three indices in the index layer.

10.2.1.2. Risk-Level Division

The ultimate goal of the flood control risk evaluation system of check dams in small watersheds is to determine the possibility of flood risks of check dams so that

@seismicisolation

Table 10.7 Flood control risk evaluation classification of check dams in small watersheds.

Risk level	Flood control risk value range
Extremely dangerous	[0.8, 1.0]
Dangerous	[0.6, 0.8)
Less dangerous	[0.4, 0.6)
Safe	[0.2, 0.4)
Safer	[0, 0.2)

decision-makers can understand the flood control risks of check dams in small watersheds, which provides theoretical guidance for decision-makers investment and the subsequent management of check dams. With reference to relevant materials and the existing literature, combined with actual conditions [8], the final flood control risk evaluation standards for check dams in small watersheds are formulated in Table 10.7.

10.2.2. Flood Control Risk Evaluation Index for Warping Dam in Wangmaogou Watershed

According to the measurement standards and assignment methods of each evaluation index in the flood control risk evaluation index system of check dams in small watersheds, combined with the onsite investigation of each warping dam in the Wangmaogou small watershed, the calculated scores of each evaluation index in the flood control risk evaluation system of the warping dam in Wangmaogou watershed under the once-in-30-year and once-in-100-year storm flood are shown in Tables 10.8 and 10.9.

Based on the safety evaluation index system of the warping dam in the small watershed established in this section, combined with the evaluation index score in Tables 10.8 and 10.9, as well as the weight value of each evaluation index in Table 10.6, the formula (10.9) and formula (10.10) are adopted in order to calculate the flood control risk evaluation results of a warping dam in the Wangmaogou watershed under the once-in-30-year and once-in-100-year rainstorm floods, as shown in Tables 10.10 and 10.11.

The flood control risk evaluation results in Tables 10.10 and 10.11 comprehensively reflect the flood control risk of each warping dam in the Wangmaogou small watershed. Judging from the evaluation results, most of the check dams in the Wangmaogou small watershed are in either a dangerous state or a less dangerous state for flood control, and only Wangmaogou No.1 dam and Wangmaogou No. 2 dam are in a safe state.

From the perspective of the various layers of the flood control risk evaluation index system, the flood risk scores of the check dams in the Wangmaogou small watershed are in a dangerous state, while some are in a less dangerous state, and some are in an extremely dangerous state. For these warping dams, it is necessary to increase the height of the corresponding warping dam in order to expand the capacity of the flood detention or to increase the discharge capacity by dredging or repairing the discharge structure to reduce the flood control risk of the warping dam.

Due to early construction, a low flood control design standard, and a small flood control capacity of most of the check dams in the Wangmaogou small watershed, smaller rainstorm floods can lead to a greater detention depth on the warping dam, causing the crops to be submerged or damaged. Furthermore, most of the houses, production bases, and roads in the Wangmaogou small watershed are located either in the main channel of the watershed or near the warping dam. They are easily affected by dam breaks caused by rainstorm floods, and the economic risks are high [9].

Some management measures are taken for two key dams. Other check dams in the Wangmaogou small watershed are neglected, and their management risk values are 1, which is extremely dangerous. A high management risk value leads to a higher score of the final flood control risk evaluation result of the warping dam. Thus, it is urgent for relevant departments to formulate management regulations in order to strengthen the daily management and monitoring of check dams in the Wangmaogou small watershed. For those check dams with ineffective management, the daily management must be strengthened, and for check dams lacking management measures due to their remote locations and blocked roads, corresponding daily management should be added. Scientific research institutions and government departments should deploy monitoring equipment in a timely manner and organize relevant personnel to conduct regular investigations and monitoring in order to obtain true, detailed, and accurate first-hand information about the check dams. Different measures are taken for different check dams to strengthen the dam's defense against rainstorm floods to protect people's lives as well as for wealth security.

10.2.3. Flood Control Risk Evaluation of the Warping Dam System in the Wangmaogou Watershed

Based on the flood control risk evaluation index system of the warping dam in the small watershed established above, in this section, the warping dam

@seismicisolation

Table 10.8 Flood control risk evaluation index for check dams in the Wangmaogou watershed under rain flood over 30 years.

	Evaluation index								
Name of check dams	Instability coefficient	Hazard coefficient	Flood detention risk	Flood discharge risk	Daily management risk	Emergency risk	Monitoring risk	Downstream economic risk	Yield ensuring risk
Guandigou No. 4 Dam	0.00	0.00	0.18	0.68	1.00	1.00	1.00	0.20	0.03
Beitagou Dam	0.60	0.56	0.38	1.00	1.00	1.00	1.00	0.00	1.00
Guandigou No. 2 Dam	0.76	0.40	0.27	0.00	1.00	1.00	1.00	0.60	0.00
Guandigou No. 3 Dam	0.00	0.40	1.00	1.00	1.00	1.00	1.00	0.40	1.00
Guandigou No. 1 Dam	0.46	0.00	0.07	0.79	1.00	1.00	1.00	0.80	1.00
Sidizui No.1 Dam	0.00	0.13	0.48	0.51	1.00	1.00	1.00	0.60	1.00
Wangtagou No.1 Dam	0.28	0.33	0.33	1.00	1.00	1.00	1.00	0.60	1.00
Wangmaogou No. 2 Dam	0.79	0.21	0.05	0.70	0.10	0.00	0.10	1.00	0.05
Kanghegou No.3 Dam	0.00	0.00	0.20	1.00	1.00	1.00	1.00	0.40	0.03
Kanghegou No.2 Dam	0.12	0.00	0.14	1.00	1.00	1.00	1.00	0.60	0.01
Kanghegou No.1 Dam	0.00	0.00	0.82	1.00	1.00	1.00	1.00	0.80	0.00
Nianyangou No.3 Dam	0.47	0.39	0.39	1.00	1.00	1.00	1.00	0.40	1.00
Nianyangou No.2 Dam	0.00	0.00	0.05	1.00	1.00	1.00	1.00	0.60	0.00
Nianyangou No.1 Dam	0.65	0.00	0.05	1.00	1.00	1.00	1.00	0.80	0.01
Huangbaigou No. 2 Dam	0.00	0.00	1.00	1.00	1.00	1.00	1.00	0.60	0.00
Huangbaigou No. 1 Dam	0.35	0.00	0.17	0.29	1.00	1.00	1.00	0.80	0.01
Wangmaogou No.1 Dam	0.58	0.23	0.53	0.00	0.10	0.00	0.10	1.00	0.00

@seismicisolation
@seismicisolation

Table 10.9 Flood control risk evaluation index for check dams in the Wangmaogou watershed under rain flood once in 100 years.

	Evaluation index								
Name of check dams	Instability coefficient	Hazard coefficient	Food detention risk	Flood discharge risk	Daily management risk	Emergency risk	Monitoring risk	Downstream economic risk	Yield ensuring risk
Guandigou No.4 Dam	0.00	0.26	0.28	0.66	1.00	1.00	1.00	0.20	1.00
Beitagou	0.60	0.66	0.62	1.00	1.00	1.00	1.00	0.20	1.00
Guandigou No.2 Dam	0.76	0.55	0.35	0.26	1.00	1.00	1.00	0.60	0.00
Guandigou No.3 Dam	0.00	0.51	1.00	1.00	1.00	1.00	1.00	0.40	1.00
Guandigou No.1 Dam	0.46	0.19	0.11	0.73	1.00	1.00	1.00	0.80	1.00
Sidizui No.1 Dam	0.00	0.38	0.68	0.48	1.00	1.00	1.00	0.60	1.00
Wangtagou No.1 Dam	0.28	0.51	0.53	1.00	1.00	1.00	1.00	0.60	1.00
Wangmaogou No.2 Dam	0.79	0.44	0.09	0.65	0.10	0.00	0.10	1.00	1.00
Kanghegou No.3 Dam	0.00	0.25	0.32	1.00	1.00	1.00	1.00	0.40	1.00
Kanghegou No.2 Dam	0.12	0.00	0.23	1.00	1.00	1.00	1.00	0.60	0.01
Kanghegou No.1Dam	0.00	0.00	1.00	1.00	1.00	1.00	1.00	0.80	0.00
Nianyangou No.3 Dam	0.47	0.53	0.64	1.00	1.00	1.00	1.00	0.40	1.00
Nianyangou No.2 Dam	0.00	0.00	0.09	1.00	1.00	1.00	1.00	0.60	0.00
Nianyangou No.1 Dam	0.65	0.00	0.08	0.06	1.00	1.00	1.00	0.80	0.01
Huangbaigou No.2 Dam	0.00	0.00	1.00	1.00	1.00	1.00	1.00	0.60	0.00
Huangbaigou No.1 Dam	0.35	0.19	0.25	0.21	1.00	1.00	1.00	0.80	0.01
Wangmaogou No.1 Dam	0.58	0.45	0.63	0.00	0.10	0.00	0.10	1.00	0.00

@seismicisolation
@seismicisolation

Table 10.10 Flood control risk evaluation of check dams in the Wangmaogou watershed under rainstorm floods for once in 30 years.

	Risk type			
Name of warping dam	Flood risk	Management risk	Economic risk	Flood control risk evaluation
Guandigou No. 4 Dam	0.57	1.00	0.54	0.30
Beitagou Dam	0.84	1.00	0.82	0.69
Guandigou No.2 Dam	0.66	1.00	0.70	0.47
Guandigou No.3 Dam	0.84	1.00	0.90	0.76
Guandigou No.1 Dam	0.65	1.00	0.97	0.63
Sidizui No.1 Dam	0.64	1.00	0.94	0.60
Wangtagou No. 1 Dam	0.76	1.00	0.94	0.72
Wangmaogou No.2 Dam	0.71	0.40	0.83	0.23
Kanghegou No.3 Dam	0.64	1.00	0.64	0.41
Kanghegou No.2 Dam	0.65	1.00	0.70	0.46
Kanghegou No.1 Dam	0.76	1.00	0.76	0.58
Nianyangou No.3 Dam	0.80	1.00	0.90	0.73
Nianyangou No.2 Dam	0.61	1.00	0.70	0.43
Nianyangou No.1 Dam	0.71	1.00	0.77	0.54
Huangbaigou No.2 Dam	0.79	1.00	0.70	0.56
Huangbaigou No.1 Dam	0.54	1.00	0.77	0.41
Wangmaogou No.1 Dam	0.66	0.40	0.81	0.21

Table 10.11 Flood control risk evaluation of check dams in the Wangmaogou watershed under rainstorm floods for once in 100 years.

	Risk type			
Name of warping dam	Flood risk	Management risk	Economic risk	Flood control risk evaluation
Guandigou No.4 Dam	0.64	1.00	0.87	0.56
Beitagou	0.89	1.00	0.87	0.77
Guandigou No.2 Dam	0.75	1.00	0.70	0.53
Guandigou No.3 Dam	0.86	1.00	0.90	0.78
Guandigou No.1 Dam	0.68	1.00	0.97	0.66
Sidizui No.1 Dam	0.72	1.00	0.94	0.67
Wangtagou No.1 Dam	0.82	1.00	0.94	0.77
Wangmaogou No.2 Dam	0.75	0.40	1.00	0.30
Kanghegou No.3 Dam	0.71	1.00	0.90	0.64
Kanghegou No.2 Dam	0.67	1.00	0.70	0.47
Kanghegou No.1 Dam	0.79	1.00	0.76	0.60
Nianyangou No.3 Dam	0.86	1.00	0.90	0.78
Nianyangou No.2 Dam	0.62	1.00	0.70	0.43
Nianyangou No.1 Dam	0.51	1.00	0.77	0.39
Huangbaigou No.2 Dam	0.79	1.00	0.70	0.56
Huangbaigou No.1 Dam	0.59	1.00	0.77	0.45
Wangmaogou No.1 Dam	0.72	0.40	0.81	0.23

system of the Wangmaogou small watershed and the dam system layout, as well as the flood control risk of the dam system, are evaluated. Because the rationality of the warping dam system layout plays an important role in the flood control risk of the warping dam system in the watershed, a new index is added based on the existing flood risk indices, namely the dam system layout risk index.

@seismicisolation

10.2.3.1. Dam System Layout Evaluation

1. The dam system layout evaluation index definition

Proportion of large dams: The proportion of large dams refers to the ratio of the storage capacity of large- and medium-sized dams to the total storage capacity of the warping dam system in the watershed. Because the flood control standards of the entire watershed depend on the regulation and storage of the entire warping dam system, especially the key dams, the larger the proportion of large dams, the greater the regulating effect of the basin dam system to floods, and thus the stronger the defending flood ability of the watershed.

Series rate: The series rate refers to the maximum number of check dams connected in series in the channel per unit length in a watershed. In the limited length of the drainage channel, the more the check dams connected in series, the higher the risk of chain dam failure when there is excessive rainstorm flooding. Therefore, the lower the series rate, the more reasonable the dam system layout.

Capacity equilibrium degree: The capacity equilibrium degree refers to the ratio of the range of the storage capacity of a single dam to the control area of the warping dam system in watershed, which is used to measure the distribution of the storage of the warping dam system in the watershed. The smaller the capacity equilibrium degree, the more even the storage capacity distribution of the warping dam system in the watershed will be.

Silt area design: The silt area design refers to the silt land area of the warping dam system. The designed silt land area affects the relative stability of the warping dam system and the economic benefits of the watershed. The stability and economy of the warping dam system are also important content in terms of evaluating the warping dam system layout.

Erosion modulus: The erosion modulus refers to the amount of soil erosion eroded and displaced per unit area and unit time, and this is used to measure the total soil erosion degree. The construction of the warping dam system in the watershed can to a certain extent intercept the sediment generated on the upstream slope and change the erosion form of the watershed. Erosion modulus is one of the indices for judging the reasonability of the warping dam system layout.

2. Standardization of evaluation index elements for the dam system layout

Proportion of large dams: Quantitative assignments are made based on the flood regulation capacity of large dams. When the storage capacity control rate of a large dam reaches or exceeds 50%, the total proportion of large dams is assigned as 1; for every 10% decrease in the storage capacity control rate of a large dam, the value is correspondingly reduced by 0.2.

Series rate: Quantitative assignments are made according to the threat to downstream projects. When the series rate is 0, the value is 1; every time the series rate increases by 1, the value decreases by 0.2.

Capacity equilibrium degree: Quantitative assignments are made according to the equilibrium of the storage capacity distribution. When the capacity equilibrium degree is 0, the value is 1; each time the equilibrium degree increases by 50 000 m^3/km^2, the value is reduced by 0.1.

Silt area design: Quantitative assignments are made according to the contribution to the relative stability of the watershed. When the designed silt area is 0, its value is 0; for every 10 hm^2 increase in the area of designed silt land, the value increases by 0.2.

Erosion modulus: Quantitative assignments are made according to the soil erosion control. When the erosion modulus is less than or equal to 5000 t/(km2.a), the assigned value is 1; for every 1000 t/(km2.a) increase in the erosion modulus, the assigned value is reduced by 0.2.

3. Weight determination of the system layout evaluation index

In order to more accurately and reasonably determine the weight of each evaluation index in the dam system layout evaluation system, according to relevant data, existing literature, and the field survey data, the relevant research experts and technicians of check dams are first organized to provide the relative importance of each evaluation index in a back-to-back manner, and each evaluation index is scored on this basis. Then, the AHP is used to process the evaluation results, and the reasonable weight results of the evaluation indices of each dam system layout are obtained. Table 10.12 shows the judgment matrix of the dam system layout evaluation index system and the weight results of each evaluation index.

4. Evaluation criteria for dam system layout rationality

The evaluation criterion for dam system layout rationality is shown in Table 10.13.

5. Warping dam system layout evaluation result in the Wangmaogou small watershed

The above calculation method is used to calculate and assign the five evaluation indices of different

@seismicisolation

Table 10.12 Expert-assigned dam system layout evaluation index and comparison judgment matrix.

Index	Erosion modulus	Capacity equilibrium degree	Proportion of large dams	Series rate	Silt area design	Weight value
Erosion modulus	1.00	0.17	0.14	0.33	0.50	0.0559
Capacity equilibrium degree	5.99	1.00	0.50	2.00	5.00	0.2750
Proportion of large dams	6.99	2.00	1.00	5.00	6.00	0.4009
Series rate	3.03	0.50	0.20	1.00	4.00	0.1739
Silt area design	2.00	0.20	0.17	0.25	1.00	0.0943
Consistency test	λmax=5.312, CI=0.078, RI=1.12, CR=0.070< 0.10, Satisfaction consistency					

Table 10.13 Valuation for dam system layout rationality evaluation

Dam system layout rationality	Value range
Reasonable	(1, 0.65)
Basically reasonable	(0.65, 0.4)
Unreasonable	(0.4, 0)

Table 10.14 Evaluation index for warping dam system layout rationality in the Wangmaogou small watershed.

	Evaluation index				
Dam system name	Proportion of large dams/%	Capacity equilibrium degree/10 000 m^3/km^2	Series rate/ one/km^2	Silt area design/hm^2	Erosion modulus/ t/(km^2.a)
Guandigou	0.00	20.58	1.94	7.28	9356.64
Wangtagou	0.00	24.37	3.30	14.19	7809.74
Wangmaogou No. 2 Dam	53.07	35.39	1.94	29.50	8845.90
Nianyanggou	0.00	5.73	3.24	5.60	6071.58
Kanghegou	0.00	14.29	18.18	1.01	9221.47
Huangbaigou	0.00	17.12	1.84	0.71	6422.89
Wangmaogou watershed	51.56	17.94	1.33	31.73	7960.67

Table 10.15 Score table of dam system layout rationality evaluation index in the Wangmaogou small watershed.

	Evaluation index				
Dam system name	Proportion of large dams	Capacity equilibrium degree	Series rate	Silt area design	Erosion modulus
Guandigou	0.00	0.59	0.61	0.15	0.13
Wangtagou	0.00	0.51	0.34	0.28	0.44
Wangmaogou No.2 Dam	1.00	0.29	0.61	0.59	0.23
Nianyangou	0.00	0.89	0.35	0.11	0.79
Kanghegou	0.00	0.71	0.00	0.02	0.16
Huangbaigou	0.00	0.66	0.63	0.01	0.72
Wangmaogou watershed	1.00	0.64	0.73	0.63	0.41

warping dam systems in the Wangmaogou small watershed, and the calculation results are shown in Tables 10.14 and 10.15. The dam system layout evaluation index elements are standardized on this basis. The rationality of the dam system layout of warping dam system in the Wangmaogou watershed is evaluated based on the related results in Tables 10.11 and 10.13, and the evaluation results are shown in Table 10.16.

@seismicisolation

10.2.3.2. Flood Control Risk Evaluation of the Dam System

According to the flood control risk evaluation of check dams in Section 10.2.2, the flood control risk evaluation results of the warping dam system unit and warping dam system in the Wangmaogou small watershed under the once-in-30-year and once-in-100-year rainstorm flood are calculated. Table 10.17 shows the recalculation results of flood risk index weights; Tables 10.18 and 10.19 show the index assignment results; and other weights remain unchanged.

The flood control risk evaluation results of the warping dam system in the Wangmaogou small watershed under the once-in-30-year and once-in-100-year rainstorm floods are shown in Tables 10.20 and 10.21.

Tables 10.20 and 10.21 show that the overall flood control risk evaluation risk value of the warping dam system in the Wangmaogou small watershed is higher, showing a higher flood control risk value of the dam system of only medium and small check dams, and a lower flood control risk value of the dam system in Wangmaogou No. 2 dam with key dam and the dam system in the Wangmaogou watershed. The main reasons for this may be due to the low construction standards of small and medium check dams, small storage capacity, and a lack of daily management, emergency plans, and monitoring measures for check dams, resulting in higher flood risk and management risk, and also causing a higher flood control risk evaluation value of the warping system and higher flood control risk of the dam system. On the contrary, with the high construction standards of key dams, large flood detention storage capacity, total storage capacity, well-placed management, and relatively reasonable dam system layout, the flood control risk of the dam systems of key dams is relatively low.

It can be seen from Table 10.20 that when a once-in-30-year rainstorm flood occurs, the flood control risk values of each warping dam system in the Wangmaogou small watershed are as follows: dam system of Wangmaogou watershed < Wangmaogou No.2 dam system < Huangbaigou unit dam system < Nianyangou unit dam system < Guandigou unit dam system < Kanghegou unit dam system < Wangtagou unit dam system.

It can be seen from Table 10.21 that when a once-in-100-year rainstorm flood occurs, the flood control risk values of the warping dam system in the Wangmaogou small watershed are as follows: dam system of Wangmaogou watershed < Wangmaogou No.22 dam system < Kanghegou unit dam system < Huangbaigou unit dam system < Nianyangou unit dam system < Guandigou unit dam system < Wangtagou unit dam system.

Table 10.16 Evaluation result of dam system layout rationality in the Wangmaogou small watershed.

Dam system name	Dam system layout score	Evaluation result
Guandigou	0.29	Unreasonable
Wangtagou	0.25	Unreasonable
Wangmaogou No.2 Dam	0.66	Reasonable
Nianyangou	0.36	Unreasonable
Kanghegou	0.21	Unreasonable
Huangbaigou	0.33	Unreasonable
Wangmaogou watershed	0.79	Reasonable

10.3. ANALYSIS OF CONSTRUCTION SCALE SUITABLE FOR A WARPING DAM SYSTEM ON LOESS PLATEAU UNDER A CHANGING SITUATION

10.3.1. Guiding Ideology of Warping Dam Construction in the New Period

The Loess Plateau has the most serious soil erosion in the world, and severe soil erosion threatens flood control safety in the lower reaches of the Yellow River, deteriorating the ecological environment and restricting the sustainable development of the economy and society as a whole [10]. Meanwhile, the Yellow River Basin is located in both arid and semi-arid areas [11].

Table 10.17 Flood risk index weight.

Index	Instability coefficient	Hazard coefficient	Flood detention risk	Flood discharge risk	Dam system layout risk	Weight value
Instability coefficient	1.00	0.67	0.57	0.70	0.58	0.16
Hazard coefficient	1.50	1.00	0.85	1.05	0.87	0.21
Flood detention risk	1.77	1.18	1.00	1.24	1.02	0.23
Flood discharge risk	1.42	0.95	0.80	1.00	0.82	0.20
Dam system layout risk	0.95	1.15	0.98	1.22	1.00	0.20

@seismicisolation

Table 10.18 Flood control risk index score of the warping dam system in the Wangmaogou small watershed under the once-in-30-year rainstorm flooding.

Dam system	Instability coefficient	Hazard coefficient	Flood detention risk	Flood discharge risk	Dam system layout risk	Daily management risk	Accident emergency	Monitoring facility	Downstream economic risk	Yield ensuring risk
Guandigou	0.30	0.00	0.12	0.39	0.71	1.00	1.00	1.00	0.80	0.50
Wangtagou	0.07	0.13	0.41	1.00	0.75	1.00	1.00	1.00	0.80	1.00
Wangmaogou No.2 Dam	0.51	0.07	0.12	0.19	0.34	0.10	0.00	0.10	1.00	0.79
Kanghegou	0.00	0.00	0.20	1.00	0.79	1.00	1.00	1.00	0.80	0.01
Nianyangou	0.23	0.00	0.10	1.00	0.64	1.00	1.00	1.00	0.80	0.32
Huangbaigou	0.00	0.00	0.37	0.29	0.67	1.00	1.00	1.00	0.80	0.01
The whole watershed	0.40	0.00	0.15	0.00	0.21	0.10	0.00	0.10	1.00	0.54

Table 10.19 Flood control risk index score of the warping dam system in the Wangmaogou small watershed under the once-in-100-year rainstorm flooding.

Dam system	Instability coefficient	Hazard coefficient	Flood detention risk	Flood discharge risk	Dam system layout risk	Daily management risk	Accident emergency	Monitoring facility	Downstream economic risk	Yield ensuring risk
Guandigou	0.30	0.19	0.19	0.56	0.71	1.00	1.00	1.00	0.80	0.97
Wangtagou	0.07	0.41	0.76	0.66	0.75	1.00	1.00	1.00	0.80	1.00
Wangmaogou No.2 Dam	0.51	0.38	0.19	0.08	0.34	0.10	0.00	0.10	1.00	0.98
Kanghegou	0.00	0.00	0.32	1.00	0.79	1.00	1.00	1.00	0.80	0.33
Nianyangou	0.23	0.05	0.17	0.06	0.64	1.00	1.00	1.00	0.80	0.32
Huangbaigou	0.00	0.00	0.66	0.21	0.67	1.00	1.00	1.00	0.80	0.01
The whole watershed	0.40	0.24	0.25	0.00	0.21	0.10	0.00	0.10	1.00	0.68

@seismicisolation
@seismicisolation

Table 10.20 The flood control risk evaluation results of the warping dam system in the Wangmaogou small watershed under the once-in-30-year rainstorm.

Dam system	Risk category			Flood control risk evaluation result
	Flood risk	Management risk	Economic risk	
Guandigou	0.64	1.00	0.88	0.56
Wangtagou	0.76	1.00	0.97	0.74
Wangmaogou No.2 Dam	0.58	0.40	0.97	0.22
Kanghegou	0.71	1.00	0.77	0.55
Nianyangou	0.70	1.00	0.84	0.59
Huangbaigou	0.62	1.00	0.77	0.47
The whole watershed	0.48	0.40	0.93	0.18

Table 10.21 The flood control risk evaluation results of the warping dam system in the Wangmaogou small watershed under the once-in-100-year rainstorm.

Dam system	Risk category			Flood control risk evaluation result
	Flood risk	Management risk	Economic risk	
Guandigou	0.70	1.00	0.97	0.68
Wangtagou	0.80	1.00	0.97	0.78
Wangmaogou No.2 Dam	0.63	0.40	1.00	0.25
Kanghegou	0.73	1.00	0.85	0.62
Niannyangou	0.57	1.00	0.84	0.48
Huangbaigou	0.66	1.00	0.77	0.50
The whole watershed	0.56	0.40	0.95	0.21

With the development of industrial and agricultural production, the contradiction between the supply and demand of the Yellow River's water resources has become increasingly prominent [1]. How can the water-saving potential from various links be tapped, such as increasing recourse and reducing water flow? Establishing a water-saving society is an urgent task. Therefore, in order to construct a warping dam on a large scale in the new period, we must adhere to the principle of "unity of ecological benefits, economic benefits, and social benefits," take the river basin as the system, fully reflect the overall point of view, take into account the interests of local and downstream areas, and scientifically and effectively realize sand retaining, water retaining, and silting, which can increase local agricultural production and farmers' incomes, promote rural economic development, consolidate the achievement of returning farmland to forests, and improve the ecological environment, effectively reducing the sediment flowing into the Yellow River and ensuring the safety of the Yellow River, as well as building a well-off society in an all-round way.

In order to plan, design, and construct check dams scientifically and rationally, as well as to ensure their safe operation and engineering benefits, the guidelines for the planning and construction of check dams in the Loess Plateau that meet the requirements of ecology, water-saving, safety, and sustainable development are proposed as follows:

10.3.1.1. Ecology – Ecological Soundness

Warping dam construction should focus on reducing soil erosion and blocking sediment in order to create land with stable and high-yield fields, as well as to closely integrate with the ecological construction of the Loess Plateau to promote the conversion of sloping farmland into forests and grasslands. Based on the local climate, topography, soil, and water resources and other conditions, forest and grass construction should be carried out combined with local conditions. Full play should be given to the ecological self-rehabilitation in order to form a strong eco-morphology under similar climate, terrain, and soil conditions. In terms of dam land utilization, fertilizers and pesticides should be used rationally, and natural fertilizers and biological pest control should be adopted as often as possible. The soil residues of fertilizers and pesticides and the parts discharged with water should meet the relevant national standards.

@seismicisolation

For some unfavorable changes in the process of ecosystem restoration, such as massive damage to saplings caused by the massive breeding of rabbits in some locations, appropriate manual interventions should be taken on the basis of scientific demonstration.

During the construction of check dams, the relevant standards of the Soil and Water Conservation Law of the People's Republic of China should be strictly observed.

10.3.1.2. Water Saving – Save and Utilize Water Resources Efficiently

Based on the actual situation of the Loess Plateau and the demand for the efficient utilization of water and soil resources in the basin, complete drainage facilities are required in the construction of check dams in order to achieve successful sediment blocking and drainage. The check dams should provide drinking water for both people and animals, and all of the water after the annual flood should be drained to reduce ineffective evaporation. The newly silted dam must form an effective drainage system to prevent secondary soil salinization and swamping. Dry farming should be adopted as much as possible for agriculture stock production on the dam land and to promote the water-saving irrigation. Taking the basin controlled by the warping dam system as the calculation unit, the development and utilization rates of local water resources should be controlled within an appropriate range.

10.3.1.3. Safety – Ensure Flood Control

Ensuring the flood control safety of the warping dam system is a prerequisite for the sustainable use of water and sediment resources in the dam-controlled basin, and this should be planned in a unified way, designed according to particular specifications. Combined with the specific conditions of the dam-controlled basin, flood control safety should be measured and the dam system layout and structure of the warping dam should be determined through scientific demonstration. For the existing warping dam systems short of flood control capabilities, the reinforcement project of the dam system is required in order to improve the flood control standards of the warping dam systems and to ensure flood control and production safety.

10.3.1.4. Sustainable Development – Good Management, Rolling Development, and Increasing Farmers' Incomes

A warping dam construction plan with a rational layout that is scientifically proven is created in order to promote the effective implementation of the returning farmland to the forests and grasslands and the local economic and social development plans. The check dams should be constructed with scientific and reasonable design, effective cost-down, good construction quality, and fast construction speed [9]. The use efficiency of check dams is higher, which is 6–10 times that of the general slope land. It is important to establish a reasonable fundraising and investment mechanism with appropriate investment proportions of the state, localities, and farmers. The user participation management mechanism, the silt dam (including supporting facilities), and property rights and use rights of the dam land are clear, and the management system is sound as well. Some of the proceeds from the warping dam should be used for the management and protection of the warping dam system, and the proceeds from the key dams invested entirely by the state should be used in an appropriate proportion for the maintenance of the check dams already built, as well as the rolling construction of new ones. Relevant measures should be taken to ensure that the integrity rate of the utilization rate of the dam is greater than 95%. Through the efficient use of the dam land, the planting and breeding structure are adjusted and optimized by the farmers, and the processing of agricultural and sideline products is also developed. Thus, their income will increase year by year. In addition, the water supply for both people and animals in the construction area should be resolved through reasonable means.

10.3.2. Construction Scale of Warping Dam on the Loess Plateau

10.3.2.1. Planning Target

There are two important indices in the planning target of the warping dam. One is the area of the siltable land after the warping dam is constructed, and the other is the reduced sediment into the Yellow River. Other indices can then be determined accordingly.

1. Silt area

Long-term practices have proven that the 0.067 hm^2 of per capita dam land in the sandy and coarse areas of the Yellow River Basin can guarantee the grain supply for the rural population and feed. Planting economic forests and cash crops on gentle slopes less than 15° can not only increase farmers' incomes but also promote the return of farmland to forests and grasses, guaranteeing the comprehensive construction of a well-off society. Therefore, the plan states that by 2020, the per capita

@seismicisolation

dam land in key areas such as the sandy and coarse and areas of the Yellow River Basin should reach about 0.067 hm^2. There is more basic farmland in other areas, and the per capita dam land can reach about 0.033 hm^2. By 2020, the total area of newly added dams on the Loess Plateau should reach 500 000 hm^2.

2. Reduce sediment into the Yellow River

The "Recent Development Plan for the Yellow River" approved by the State Council in 2002 proposed that by the middle of the twenty-first century, through water and soil conservation, an average annual reduction of 800 million tons of sediment into the Yellow River will be required. The average annual sediment into the Yellow River can be reduced by 500 million tons, and this goal connects the control of soil erosion in the Yellow River Basin with the goal of building a well-off society in an all-round way, conforming to the natural law of governance. Therefore, by 2020, the reduced sediment into the Yellow River by check dams can be approximately 700 million tons.

3. Planning target

By 2010, 60 000 check dams were built in the Loess Plateau, and a relatively complete channel dam system focusing on 25 tributaries in the sandy and coarse sand area was initially completed. The comprehensive control of soil erosion in the project implementation area reaches 60%. Rural land use and industrial structures tend to be more reasonable, and farmers' incomes increase steadily. The severe soil erosion in the Loess Plateau is basically controlled, and the ecological environment is significantly improved. Combined with the implementation of other water and soil conservation measures, the annual sediment into the Yellow River can be reduced by 500 million tons. After the project creates these benefits, the intercepted sediment amount reaches 14 billion tons; the dam area with high yield and stable yield will be 180 000 hm^2; the promoted farmland conversion area will be 800 000 hm^2; and the enclosure protection area will be 1.333 million hm^2.

By 2020, 163 000 check dams were built, and a relatively complete channel dam system was basically completed in the main tributaries into the Yellow River of the Loess Plateau. The comprehensive control of water and soil erosion in the project implementation area reaches 80%; the basic farmland, primarily dam land, increases significantly, and the sustainable development capacity of rural areas is significantly improved. The annual sediment into the Yellow River reaches 700 million tons. The goal of "planting forests and grasses in the mountains and rice in gully among ricers" is realized, contributing to the realization of the long-term stability of the Yellow River, the sustainable development of the regional economy and society, and the comprehensive construction of a well-off society. After these benefits are created, the intercepted sediment amount will reach 40 billion tons. There is a 500 000 hm^2 dam area with a high and stable yield, 2.2 million hm^2 of the promoted farmland conversion area, and 4 million hm^2 of the enclosure protection area.

10.3.2.2. Construction Scale

1. Analytical method

The typical investigation is combined with a comprehensive analysis and a demonstration. First, detailed investigations are carried out on small watersheds with well-constructed warping dam systems in different types of areas, as well as areas with different erosion intensity, and the warp dam system for untreated small watersheds is planned to summarize the governance model of dam systems in a small watershed; second, by analyzing and demonstrating the construction potential and construction demand of the warping dam, the construction scale and construction layout of the warping dam are determined; finally, according to the national and Yellow River Basin water and soil conservation ecological construction, the implementation plan for the construction of check dams in the Loess Plateau of the Yellow River Basin is drawn up. The plan makes full use of advanced technology such as computer simulation technology, "3S" technical achievements, the latest remote sensing survey results, and dam system optimization design schemes.

2. Construction potential analysis

a. The multi-year average annual erosion

According to each erosion area and the multi-year average erosion modulus, the multi-year average erosion amount of each erosion area is calculated, and the total multi-year average erosion is determined to be 2.5 billion tons.

b. Calculating the total erosion within the design life of the warping dam

According to the technical specifications, the design period of check dams is 20 years. Based on this, the erosion amount of each erosion area in 20 years is calculated, and the total erosion amount over 20 years is determined to be 50.1 billion tons.

c. Determining the control area of key dams and the silt storage capacity of single dams

According to current survey results of 111 small and medium-sized check dams in different erosion areas,

@seismicisolation

the average single-dam silt storage capacity of check dams ranges from 130 000 to 170 000 tons, and the average of 150 000 tons is taken after analysis.

The planning of warping dam systems in 35 small watersheds are surveyed in order to analyze the distribution density of key dams in different erosion intensity areas, as well as the allocation ratio of key dams and small and medium-sized check dams. The single-dam control area of the key dam in severe, extreme strong, strong, and mild erosion areas are 3–3.5, 3.5–5, 4–7, and 6–9 km^2, respectively. The allocation ratios of key dams and small and medium-sized check dams in the corresponding erosion areas are 1:6.4–1:8.3, 1:3.7–1:5.5, 1:3–1:5, and 1:2.8–1:4.1, respectively.

d. Determining the total amount of constructed warping dam

According to the requirements of constructing the dam system, the main function of the key dam is to retain the sediment and protect the land,which requires the key dam to maintain a large remaining storage capacity in order to meet the requirements of retaining the sediment and protecting the land during the design period of the check dams. When the upstream dam is not collapsed, the sediment amount in the small check dams between the key dam and the control area within 20 years is considered. The sediment reduction of key dams in 20 years is calculated according to the sediment reduction capacity of small and medium-sized check dams.

According to the erosion over 20 years of each erosion area and the average single-dam silt storage capacity of small and medium-sized check dams, the number of check dams (including key dams) that should be installed in each erosion area is calculated, and the construction potential of the warping dam is determined to be 334 000 check dams. Among these, 98 000 check dams should be constructed in areas with severe erosion, 77 000 check dams should be constructed in areas with extreme erosion, 57 000 check dams should be constructed in areas with severe erosion, and 102 000 check dams should be constructed in areas with moderate and mild erosion.

e. Determining the number of key dams and small and medium-sized check dams

According to the number of check dams in each erosion area and the average allocation ratio of key dams and small and medium-sized check dams, the number of small and medium-sized check dams and the number of key dams in each erosion area are calculated. It is determined that the number of key dams is 62 000, and the number of medium-sized and small check dams is 272 000, which is to say that the construction potential of check dams in the Loess Plateau is 334 000.

3. The required construction scale with the goal of reducing sediment

a. The total erosion of the 337 000 km^2 of the soil erosion area is 2.5 billion tons, and the sediment into the Yellow River is approximately 1.6 billion tons. It is necessary to store 1.1 billion tons of erosion in order to reduce sediment by 700 million tons.

b. According to the dam construction conditions of each erosion area, as well as the need to reduce sediment, the ratio of the intercepted erosion required by each erosion area to the total intercepted erosion of is determined to be 1.1 billion tons. The erosion required to be intercepted by each erosion area is also calculated. The erosion modulus of areas with severe erosion and extreme erosion is high, which is primarily in sandy and coarse sandy areas. The potential for dam construction in these areas is large. 40% and 30% of the total erosion needed to be intercepted are determined, respectively, to be 440 million tons and 330 million tons of erosion that must be intercepted in the areas with severe erosion and the extreme erosion. The erosion modulus of areas with severe erosion and moderate and mild erosion is low, and the potential for dam construction is small. 20% and 10% of the total erosion that should be intercepted, respectively, are 220 million tons and 110 million tons in areas with severe erosion and moderate and mild erosion, respectively. Thus, the annual erosion to be intercepted in the soil erosion area of the Loess Plateau is 1.1 billion tons.

c. In accordance with the same method as the analysis of warping dam potential, the number of check dams (including key dams) that should be constructed in each area is calculated according to the erosion that needs to be intercepted in each erosion area over 20 years, as well as the average single-dam storage capacity of small and medium-sized check dams. It is concluded that a total of 147 000 check dams need to be built. Among these, 59 000 are required in severely eroded areas, 44 000 are required in extremely eroded areas, 29 000 are required in eroded areas, and 15 000 are required in moderately and mildly eroded areas.

d. Based on the multi-year average erosion modulus of each erosion area and the average single-dam control area of the key dam, the erosion over 20 years of the average single-dam control area of the key dam is calculated, and the construction scale of the key dam

@seismicisolation

in each area is also calculated accordingly; according to the total number of check dams in each area, the scale of small and medium-sized check dams is calculated, and the number of key dams and small and medium-sized dams is determined to be 24 800 and 122 200, respectively.

According to the above analysis and the calculation results, in order to reduce the sediment into the Yellow River, a total of 147 000 check dams need to be built in the Loess Plateau, including 24 800 key dams and 122 200 small and medium-sized dams.

4. The warping dam scale required with the goal of silting land

An analysis is conducted primarily in the sandy and coarse sandy areas of the Loess Plateau in order to determine the construction scale required by the silting land.

a. The scale of dam construction in the sandy and coarse sand area

First, through an investigation and analysis of the current status of the sandy and coarse sand areas and related indices of the warping dam, it has been found that by 2000, the total population was 6.1 million, including a 5.2 million agricultural population; there were 379 200 hm^2 of terraced fields, 50 170 hm^2 of dam land, and 65 900 hm^2 of water land; and the per capita dam land was 0.01 hm^2 and per capita water land was 0.013 hm^2. According to the survey results of dam systems in typical small watersheds in areas with coarse sand, the per capita dam area is 0.053–0.067hm^2, and the per capita income is about 2000 yuan. According to the survey results of small watersheds where the dam systems are built in the sandy and coarse sand areas, the number of key dams accounted for 14% of the total number of check dams, and the number of medium-sized and small dams accounted for 86% of the total number of check dams. The silted land area by average single dam is 3 hm^2, and the ratio of key dams to small and medium-sized dams is 1:6.1.

Second, the number of agricultural population in the sandy and coarse sand areas in 2020 is predicted; according to the per capita area of dam land from the typical investigation, the total dam area in each area is also calculated. By 2020, the per capita dam area of 0.067 hm^2 in sandy and coarse sand areas can be realized; a total of 427 300 hm^2 of dam land is needed, and a total of 376 700 hm^2 of dam land needs to be added.

Third, the number of key dams and small and medium-sized check dams can be obtained based on the area of siltable dams by a single dam and the proportion of key dams and small and medium-sized check dams in the total number of dams. According to typical investigation results, the silting land of an average single dam is approximately 3hm^2. By 2020, 376 700 hm^2 of new dams will be added, and a total of 126 000 check dams should be set in sandy and coarse sand areas. Based on the proportion of the key dams and small and medium-sized dams to the total number of check dams, it is found that there are 18 000 key dams and 108 000 small and medium-sized dams.

b. Scale of dam construction in the Loess Plateau

In areas other than sandy and coarse sand areas, there exists is a large amount of basic farmland. According to the planning target, the silting land capacity was increased by 500 000 hm^2 in 2020. Except for the newly added dam land area of 376 700 hm^2 in the sandy and coarse sand area, in areas other than the sandy and coarse sand area, 123 300 hm^2 of dam land will be built. Combined with other measures, the regional food security requirement can be met. According to the survey results of the status of check dams in this area, the proportion of large and medium-sized check dams is relatively large, and the silt area of the average single dam is approximately 3.33hm^2. Therefore, 37 000 check dams are required.

In the area of check dams built in the Loess Plateau, the annual average soil erosion is 2 billion tons, and the total sediment yield is 40 billion tons within the 20-year period. According to calculations, it takes approximately 75 000 t of sediment to silt into 10 000 hm^2 dams, and it takes approximately 37.5 billion tons of sediment to silt into 500 000 hm^2 dams. Therefore, the sediment in this area meets the siltation requirements of the dam.

5. Total construction scale

Through the demonstration of construction potential, demand analysis for sediment reduction, and silt land targets, the overall construction scale of the warping dam in the Loess Plateau is shown in Table 10.22.

According to the requirements of dam system construction, some of the existing small and medium-sized silt dams should be converted into key dams. It is included in the key dam construction plan due to the large amount of reconstruction work and the high technical requirements. According to the survey of dam systems in typical small watersheds, approximately 3% of the existing small and medium-sized check dams need to be converted into key dams, which means that 3000 key dams should be rebuilt.

Based on the above analysis and the demonstration results in all aspects, the construction potential of check dams can meet the needs of sediment reduction and silt land.

@seismicisolation

Table 10.22 Analysis and demonstration of warping dam construction potential, sediment reduction, and silt land target.

Index	Key dams/10 000	Small and medium-sized dam/10 000	Total/10 000
Construction potential	6.2	27.2	33.4
Goal of reduction	2.5	12.2	14.7
Goal of silted land	2.4	13.9	16.3

Combined with factors such as topography, landform, population, and cultivated land distribution characteristics, dam construction conditions, current silt dams in areas with different erosion intensity, the adjustment of local rural industrial structure, the requirements of returning farmland to forests and grasslands, sustainable agricultural development, and the reconstruction of old dams, it has been determined that the overall scale of warping dam construction in the Loess Plateau is 163 000, including 30 000 key dams and 133 000 small and medium-sized check dams.

10.3.3. Construction Scale of Check Dams in Typical Regions Using Yan′an City as an Example

The construction scale and dam construction potential of the warping dam in Yan'an are analyzed from the perspective of erosion control and sediment reduction control by collecting and sorting out the situation of warping dam construction in different river basins in Yan'an.

10.3.3.1. Overview of the Research Area

Yan'an City is located between 107°40′110°31′ E and 35°31′37°30′ N, with a width of approximately 198 km from east to west, a length of about 212 km from north to south, and a total area of 36712km^2. The area of soil erosion is 28 773 km^2, and the average amount of sediment into the Yellow River for many years is 258 million tons. The area has among the most serious soil erosion in the middle reaches of the Yellow River. Yan'an is part of the Ordos platform of the North China Platform, and it belongs to the Mesozoic sedimentary rock series. The rocks are getting newer and newer from east to west, mostly in the northwest direction. The northern part of the landform is dominated by hilly and gully areas with a gully density greater than 46 km/km^2; the south is dominated by plateau gully areas with a gully density of 24 km/km^2.

The annual average soil erosion modulus in Yan'an City is 9800 t/(km^2·a). The average annual precipitation for many years has been 390–700mm, and the precipitation is unevenly distributed throughout the year, decreasing from south to north. The precipitation from June to September accounts for approximately 75% of the total annual precipitation; the annual average temperature is 7.8°C–10.6°C, the frost-free period is 150–209 days, and the annual average water surface evaporation is 1400–1700 mm.

The vegetation in Yan'an is poor, and its spatial distribution is extremely uneven. The deciduous broad-leaved forests of Huanglong Mountain, Lao Mountain, Qiaoshan Mountain, and Ziwuling Mountain in the southern part of Yan'an City have a forest coverage rate of approximately 50%, which represents the well-preserved zonal vegetation in this city. There are no concentrated contiguous deciduous broad-leaved forests in the northern part of Yan'an City, only a few poplar forests, birch forests, duli forests, and mountain apricot forests. The herbaceous shrubs are distributed throughout a large area of barren hills.

10.3.3.2. Analysis Method of Dam Construction Scale Potential

Erosion control dam construction potential analysis is based on the investigation and analysis of the dam ratio and dam density of typical small watersheds in different erosion and erosion intensity areas in Yan'an, and the dam ratio and density in the corresponding areas are proposed. The erosion control dam construction potential in Yan'an is analyzed as well.

Through a comprehensive survey of small watersheds in Yan'an City where silt dams have been built, the basic conditions of the dam system layout, siltation status, operating status, and the ratio of key dams and small and medium-sized dams in each small watershed are determined. Twenty typical dam systems with different types and different erosion intensity areas are selected from 13 counties and districts in Yan'an City, and the dam density and the ratio of key dams to small and medium-sized dams in different erosion intensity areas are analyzed and determined. The investigation and analysis results of check dams in typical small watersheds in Yan'an are shown in Table 10.23.

@seismicisolation

Table 10.23 Investigation of dam density and dam system allocation ratio in typical small watersheds in Yan'an.

Erosion type		Watershed	Country	Watershed area /km²	Erosion modulus /t/(km²·a)	Key dam	Key dam density/ km²/	Medium dam	Small dam	Adopted value: Key dam: medium dam: small dam	Adopted value: Dam density /km²/
Extremely eroded areas	Hilly region	Goucah	Zichang	63.1	16 000	16	3.94	52	117	1:3:8	4.02
		Guanzhuang	Yanchuan	83.0	15 000	21	3.95	67	166		
		Bajiahe	Ansai	25.2	15 000	6	4.20	17	51		
		Wolanggou	Wuqi	44.0	16 000	11	4.00	28	95		
Severely eroded areas	Hilly region	Zhangjiahe	Zichang	53.7	14 600	11	4.88	23	63	1:2:6	5.02
		Zhouwan	Wuqi	48.6	12 000	10	4.86	21	60		
		Songchayu	Yanchuan	37.2	10 000	7	5.31	15	40		
Strongly eroded areas	The hilly region	Zhnegdong	Ynachang	36.6	7000	5	7.32	9	17	1:2:3	6.73
		Ynagbiangou	Zhidan	45.0	8000	7	6.43	15	22		
		Wuzhuanggou	Baota	51.6	8000	8	6.45	15	23		
	The plateau region	Fanyaoke	Yichuan	30.1	7000	3	10.03	6	13	1:2:4	11.69
		Jizixian	Fuxian	58.7	7000	5	11.74	11	19		
		Yucha	Ganquan	53.2	6000	4	13.30	7	16		
Moderately and mildly eroded areas	The hilly region	Zhaizigou	Ganquan	38.9	4500	3	12.97	7	9	1:2:3	14.86
		Yingwang	Yichuan	32.6	4500	2	16.30	4	5		
		Dingzhuang	Baota	61.2	5000	4	15.30	7	14		
	The plateau region	Zaozigou	Luochuan	47.4	3000	3	15.80	5	6	1:2:2	17.84
		Dadonggou	Huangling	44.3	3000	2	22.15	4	5		
		Getai	Huanglong	63.9	2500	4	15.98	8	9		
		Rentai	Fuxian	52.3	2500	3	17.43	5	6		

@seismicisolation
@seismicisolation

It can be seen from Table 15.47 that the density of key dams in the severe erosion area is 3.94–4.20 km²/seat, and the allocation ratio of key dams and medium-sized and small check dams is around 1:3:8; the dam density of key dams in the extreme erosion area is 4.86–5.31 km², and the allocation ratio of key dams and medium-sized and small check dams is around 1:2:6; the dam density of key dams in the strongly eroded hilly area is 6.43–7.32 km², and the allocation ratio of key dams and medium-sized and small silt dams is around 1:2:3; the dam density of key dams in the high plateau area with strong erosion is 10.03–13.30 km², and the allocation ratio of key and medium-sized and small check dams is around 1:2:4; the dam density of the key dams in the moderately and mildly eroded hilly area is 12.97–15.30 km², and the allocation ratio of key dams and medium-sized and small check dams is around 1:2:3; and finally, the dam density of key dams in the moderately to mildly eroded high plateau area is 15.80–22.15 km², and the allocation ratio of key dams and medium-sized and small check dams is around 1:2:2.

According to the control area of key dams that can be built in different erosion types, the technical indices of each single dam, and the allocation ratio of key dams and small and medium-sized dams, the construction potential of key dams and small and medium-sized dams is calculated by formula 10.11:

$$N = \sum_{i=1\sim5}\left[\sum_{j=1\sim2}\left(\sum_{k=1\sim3} d_i a_j r_k\right)\right] \qquad (10.11)$$

where N is the potential number of check dams that can be built, and d_i is the dam density for the i-th erosion intensity zone (km²). The value varies with different erosion intensity levels; i is the erosion intensity code, where 1 represents the mildly eroded area, 2 represents the moderately eroded area, 3 represents the eroded area, 4 represents the extremely eroded area, and 5 represents the severely eroded area; a_j is j-th erosion type area; j is the code of the erosion type area, where 1 represents the hilly area and 2 represents the high plateau area; r_k is the allocation ratio of the k-th dam type; and k is the dam type number, where 1 represents the key dam, 2 represents the medium dam, and 3 represents the small dam.

10.3.3.3. Determining the Number of Check Dams That Can Be Built

The total land area of Yan'an is 36 712 km², of which the water and soil erosion area is 28 773km², the average soil erosion modulus annually is 9800t/(km²·a), and the gully density is 4.87km/km². In theory, the water and soil erosion area can be used as a dam construction area, but the hilly area, with an area of 20 724 km², is the key area for the construction of check dams in Yan'an. The plateau gully area, with an area of 8049 km², has relatively light erosion intensity, and the number of check dams should not be excessive. The number of check dams that can be built is calculated by formula according to the key dam density and the area of dams that can be built in different erosion type areas and different erosion intensity areas. According to the calculated number of check dams that can be built, as well as the ratio of key dams to small and medium-sized dams in the different erosion type areas, the number of key dams, medium-sized, and small-scale check dams can be calculated.

According to the above principles, the total number of check dams that can be built in Yan'an is 40 377, including 4460 key dams, 10 449 medium-sized dams, and 25 468 small-scale dams. Divided by geomorphic areas, there are 37 661 dams that can be built in the Loess hilly and gully area, including 3975 key dams, 9512 medium-sized dams, and 24 173 small dams. The number of dams that can be built in plateau and gully areas is small, with a total of 2716, among which 485 are key dams, 937 are medium-sized dams, and 1295 are small dams. The number of key dams, medium-sized dams, and small dams that can be built in different erosion type areas and different erosion intensity areas in Yan'an is shown in Table 10.24.

According to the results of analysis of dam construction potential, the total number of check dams that can be built in the water and soil erosion area in Yan'an is 40 377. And according to statistics from the Yan'an Water Resources and Soil Conservation Bureau, by the end of 2010, 11 998 check dams had been built in Yan'an. Therefore, the actual number of check dams that can be built in Yan'an is 28 379.

10.3.3.4. Scale Analysis of the Dam Construction Required for Sediment Reduction

According to the requirements of the overall plan for the construction of soil and water conservation and ecological environment in Yan'an, the expected sediment reduction is as follows: by 2020, the reduction amount of the sediment inflow into the Yellow River will account for approximately 65% of the total annual erosion in Yan'an. The scale of warping dam construction required to achieve the goal of sediment

@seismicisolation

Table 10.24 Number of check dams that can be built in different geomorphological areas in Yan′an.

Landform type	Erosion intensity	Key dam	Medium-sized dam	Small dam	Subtotal
Hilly and gully area	Moderately and mildly eroded	86	172	259	517
	Eroded	821	1560	2545	4926
	Extremely eroded	1583	3325	9340	14 248
	Severely eroded	1485	4455	12029	17 970
Gully area in plateau	Moderately and mildly eroded	65	130	259	454
	Eroded	405	769	931	2105
	Extremely eroded	8	17	49	74
	Severely eroded	7	21	56	83
Total		4460	10449	25468	40377

reduction is estimated based on the relationship between the amount of soil erosion and the amount of sediment transport.

1. Determining the amount of erosion reduction by zone

The average annual soil erosion amount is calculated based on the average erosion modulus and the erosion area. The water and soil erosion area in Yan'an is 28 773 km^2, the average annual erosion modulus is 9800t/(km^2·a), and the total amount of average annual erosion is 282 million tons. Among these, the Loess hilly and gully area covers an area of 20 724 km^2, and the average annual soil erosion modulus is 12 300 t/(km^2·a), which means that the total amount of average annual soil erosion is 255 million tons. The plateau and gully area covers 8049 km^2, and the average annual soil erosion modulus is 3363 t/(km^2·a), which means that the total amount of average annual soil erosion is 27 million tons.

According to the ratio of the average annual sediment inflow into the Yellow River to the total amount of annual average erosion in Yan'an, it is estimated that the sediment transport ratio in Yan'an is 0.91. Therefore, it is necessary to reduce the erosion amount of 183 million tons to reduce the sediment inflow into the Yellow River by 167 million tons.

In order to achieve this requirement, the erosion reduction rates of different erosion intensity areas are determined as follows, according to the soil erosion characteristics and dam construction conditions of different water and soil erosion areas in Yan'an, the erosion reduction rate of moderate and mild erosion areas is 15%, the erosion reduction rate of severe erosion areas is 35%, the erosion reduction rate of extremely intense erosion areas is 75%, and the erosion reduction rate of severe erosion areas is 80%.

Based the above-identified indices, the planned sediment reduction results of different erosion intensity areas in Yan'an are calculated as shown in Table 10.25.

According to the different erosion intensities and the corresponding erosion areas, the amount of erosion required to be reduced in the different erosion areas in Yan'an is calculated. From this, the annual reduction of sediment inflow into the Yellow River in the Loess hilly and gully area is 161 million tons, and the erosion sediment needs to be reduced by 177 million tons; for the Loess plateau and gully area, the sediment inflow into the Yellow River needs to be reduced by 0.06 billion tons per year, and the erosion sediment needs to be reduced by 0.07 billion tons.

2. Determining the sediment retention capacity

According to the survey and long-term practical experience of the construction status of silt dams in typical small watersheds, the single-dam sediment retention capacity of backbone dams in the Loess hilly and gully region of Yan'an is approximately 58.63 million m^3, 25.27 million m^3 for medium-sized dams, and approximately 40 000m^3 for small-scale dams; the single-dam sediment retention capacity of the backbone dams in the Loess plateau and gully area is approximately 48.53 million m^3, approximately 20.22 million m^3 for medium-sized dams, and approximately 30 000 m^{3}for small-scale dams. The survey values and actual adopted values of the storage capacity of backbone dams, small- and medium-scale dams, and sediment retention capacity in Yan'an are shown in Table 10.26.

3. Determination of the number of dams to be built for sediment reduction

According to the dam system allocation ratio and dam densities calculated in Table 10.23, the sediment retention capacity of key dams, medium-sized dams,

@seismicisolation

Table 10.25 Distribution of planned annual erosion reduction in different erosion intensity areas in Yan′an.

Category	Different erosion area	Mild erosion	Moderate erosion	Strong erosion	Extreme erosion	Severe erosion
Annual erosion (10 000 t)	Loess hilly and gully area	112.88	313.18	4147.70	10555.30	10342.46
	Gully area in Loess plateau	757.73	1504.16	568.89	55.01	47.94
	Total	870.61	1817.34	4716.59	10 610.31	10 390.40
Annual erosion reduction (10 000 t)	Loess hilly and gully area	16.93	46.98	1451.70	7916.48	8273.97
	Gully area in Loess plateau	113.66	225.62	199.11	41.26	38.35
	Total	130.59	272.60	1650.81	7957.73	8312.32

Table 10.26 Main technical indices of typical check dams built in Yan′an.

				Total storage capacity/10 000 m³		Sediment retaining storage capacity/ 10 000 m³	
Different erosion area	Dam type	Country	River system	Actual value	Adopted value	Actual value	Adopted value
Loess hilly and gully area	Key dam	Yanchuan	Qingianhe	104.0	100.0	63.0	60.0
		Wuqi	Beiluohe	98.0		58.8	
		Baota	Yanhe	98.0		62.4	
	Medium dam	Zichang	Qingjianhe	44.0	40.0	26.5	27.0
		Zichang	Wudinghe	39.0		27.0	
		Baota	Yanhe	36.0		25.0	
	Small dam	Wuqi	Beiluohe	7.0	8.0	4.0	4.0
		Yanchang	Yanhe	8.0		4.0	
Gully area in Loess Plateau	Key dam	Luochuan	Beiluohe	87.0	95.0	52.7	50.0
		Fuxian	Beiluohe	97.0		48.4	
	Medium dam	Yichuan	Shiwanghe	38.0	35.0	22.0	20.0
		Fuxian	Beiluohe	34.9		20.4	
		Ganquan	Beiluohe	9.0		3.5	
	Small dam	Fuxian	Beiluohe	8.0	9.0	3.2	3.0

and small dams calculated in Table 10.26, and the total amount of sediment reduction during its design period (30 years), the number of key dams, medium-sized dams, and small dams required for different types and different erosion intensity areas in Yan'an can be calculated. The calculation results are shown in Table 10.27.

Table 10.27 shows that in order to achieve the goal of sediment reduction, a total of 2847 key dams are required in Yan'an City, of which 2705 and 142 key dams need to be built in the Loess hilly and gully area and the gully area in the Loess Plateau, respectively; a total of 27 705 check dams should be built in Yan'an City, including 2847 key dams, 6804 medium-sized dams, and 18 054 small dams.

10.3.3.5. The Scale of the Proposed Warping Dam in Yan′an

In summary, from the perspective of erosion control, 28 379 check dams can be built in Yan'an City; from the perspective of the demand for sediment reduction, 27 705 check dams need to be built. Considering the topography, population distribution characteristics, dam construction conditions, dam construction status, dam system layout, and the reconstruction and reinforcement of dangerous check dams in areas with different erosion intensities, combined with the adjustment of local rural industrial structure, the conversion of farmland to forests, the requirements for grass restoration and sustainable agricultural development,

@seismicisolation

Table 10.27 Statistics of construction scale of check dams in different types of areas in Yan′an.

Different erosion area	Dam type	Areas with different erosion intensity					Total
		Moderately eroded	Mildly eroded	Strongly eroded	Extremely eroded	Severely eroded	
Loess hilly and gully area	Key dam	3	9	266	13 245	1103	2705
	Medium-sized dam	6	17	532	2648	3311	6514
	Small dam	10	26	7975	7942	8830	17605
	Subtotal	19	52	1595	11 914	13 244	26824
Gully area in Loess plateau	Key dam	27	54	45	9	7	142
	Medium-sized dam	55	108	89	18	20	290
	Small dam	55	109	181	52	52	449
	Subtotal	137	271	315	79	79	881
Total		156	323	1910	11 993	13 323	27705

and the demand for sediment reduction in Yan'an, it is determined that the total scale of the proposed check dams in Yan'an is 27 705, including 2847 key dams, 6804 medium-sized dams, and 18 054 small dams.

10.4. CONCLUSION

In this chapter, by selecting nine indicators for the evaluation of the flood risk in check dams, an indicators system for the evaluation of the flood risk of check dams is constructed. Based on that, indicators for flood risk of dam systems were constructed by adding check dam system layout into the indicator system. After evaluating the flood risk of the typical dam system in Wangmaogou, the results showed that the overall flood risk evaluation risk value in the Wangmaogou watershed is high. It is mainly because that the flood control risk of the dam system in the small and medium-sized check dam is high, while the risk of Wangmaogou 2 # dam system is lower as there is key dam in the watershed. By proposing the concept of ecological, water-saving, safe and sustainable development for dam construction, the construction potential of check dams in the Yan'an area is assessed and the dam number for different needs is determined.

REFERENCES

1. Wang, D., Li, Z., Gao, H. et al. (2016). Evaluation of overall distribution of check dam system in the Jiuyuangou watershed. *Research of Soil and Water Conservation 23* (5): 49–55.
2. Ali, R., Kuriqi, A., and Kisi, O. (2020). Human–environment natural disasters interconnection in China: a review. *Climate 8* (4): 48.
3. Zhao, B. (2015). *Breaking Mechanism and Flood Control Risk Assessment of Check Dam System*. Xi'an University of Technology.
4. Yuan, S. (2017). *Study on the Regulating Effect and Simulation of Check Dam System on the Dynamic Process if Runoff and Sediment in Basin*. Xi'an University of Technology.
5. Li, H., Zhang, Q., Singh, V.P. et al. (2017). Hydrological effects of cropland and climatic changes in arid and semi-arid river basins: a case study from the Yellow River basin, China. *Journal of Hydrology 549*: 547–557.
6. Cai, X. and Rosegrant, M.W. (2004). Optional water development strategies for the Yellow River Basin: balancing agricultural and ecological water demands. *Water Resources Research 40* (8): W08S04.
7. Hu, G., Wu, Y., Liu, B. et al. (2009). The characteristics of gully erosion over rolling hilly black soil areas of Northeast China. *Journal of Geographical Sciences 19* (3): 309–320.
8. Wang, D., Ha, Y., Li, Z. et al. (2017). Evaluation on the operation risk of dam system in the typical watersheds of Ningxia. *Science of Soil and Water Conservation 15* (3): 17–25.
9. Saaty, T.L. (2008). Decision making with the analytic hierarchy process. *International Journal of Services Sciences 1* (1): 83–98.
10. Li, Z.B. (2016). *Flood Risk Assessment Techniques for Small Basin Silt Dam Systems*. Beijing: Science Press.
11. Xin, Q., Sha, J., and Zhu, L. (1995). Benefit prediction of soil saving dam land. *Journal of Soil and Water Conservation 9* (2): 45–51.

@seismicisolation

Section III
Check Dams and Open Check Dams in Debris-flows and Debris-flood Catchements

@seismicisolation
@seismicisolation

11

Design of Torrential Barriers: An Austrian Perspective

Johannes Hübl[1], Jürgen Suda[2], and Georg Nagl[1]

11.1. INTRODUCTION AND HISTORICAL BACKGROUND

There is a long tradition in mitigating natural disasters by forestal and technical measures in Alpine regions due to numerous catastrophic natural hazards. Especially in the second half of the nineteenth century, disastrous torrential events occurred in the Austrian Alps causing substantial damage. These catastrophes may be traced back to non-sustainable land-use management and inadequate alpine pasture farming. This fact led to forests in a poor condition, enormous denuded areas, and steep incised channels. Starting with an analysis of these disasters, political decisions were taken to implement mitigations measures, combining forestal, agricultural, and technical measures. In addition, the interest of persons exploring the alpine region and their threatening hazards increased the knowledge of the alpine environment. One of the first scientific investigations of glacial lake outburst was discussed in the eighteenth century by Joseph Walcher (1719–1830). The Austrian Jesuit, physicist and mathematician, worked on the topic of hydraulics and glacial lakes. In his publication "*Nachrichten von den Eisbergen in Tyrol*" [1], he investigated the Vernagt glacier, Gurgler glacier, and especially the lake caused by the Rofner glacier, which threatened the Ötz valley by repeated glacial lake outburst floods (Figure 11.1). These outburst floods had catastrophic consequences for the state of Tyrol in the years 1600, 1678, 1680, and 1845. In the year 1788, an edict promulgated by Wenzel Graf von Sauer promoted working groups to establish mitigation measures [2]. Franz Seraphin von Zallinger zum Thurn (1743–1828), priest and physicist, worked on this edict and addressed the issue of inundation in Tyrol in his work "*Abhandlung von den Überschwemmungen in Tyrol*" in the year 1779 [3].

One of the first technical drawings can be found in this publication. In France, Jean Antoine Fabre (1748–1834) was involved in the topic of mitigation measures in Alpine regions and published his "Essai sur la théorie des torrens et des rivières" [4]. In the next decades, the topic gained interest, but most work remained theoretical [5–7]. It was the work of Josef Duile (1776–1863) that demonstrated practical implementation of mitigation measures [8]. He was an engineer, primarily in the field of hydraulics and road construction with a keen interest in torrent control. Due to his leading role in this field, he was called to Switzerland and applied his knowledge there too. He can be considered as the father of the European structural torrent control (Figure 11.2). In this time, two technical domains characterized the progression of systematic torrent control: one part was hydraulic engineering and the other part was forest engineering.

[1] *Institute of Mountain Risk Engineering, Department of Civil Engineering and Natural Hazards, University of Natural Resources and Life Sciences, Vienna, Austria*

[2] *Alpinfra engineering + consulting GmbH, Vienna, Austria*

Check Dam Construction for Sustainable Watershed Management and Planning, First Edition.
Edited by Zhanbin Li, Peng Li, Yang Yu, Peng Shi, and Guillaume Piton.
© 2022 John Wiley & Sons, Inc. Published 2022 by John Wiley & Sons, Inc.

@seismicisolation

(a) (b)

Figure 11.1 Glacier lakes illustration of Walcher [1]; (a) Rofner glacier lake; (b) Passyer lake. *Source:* Joseph Walcher/Wikimedia Commons/Public Domain.

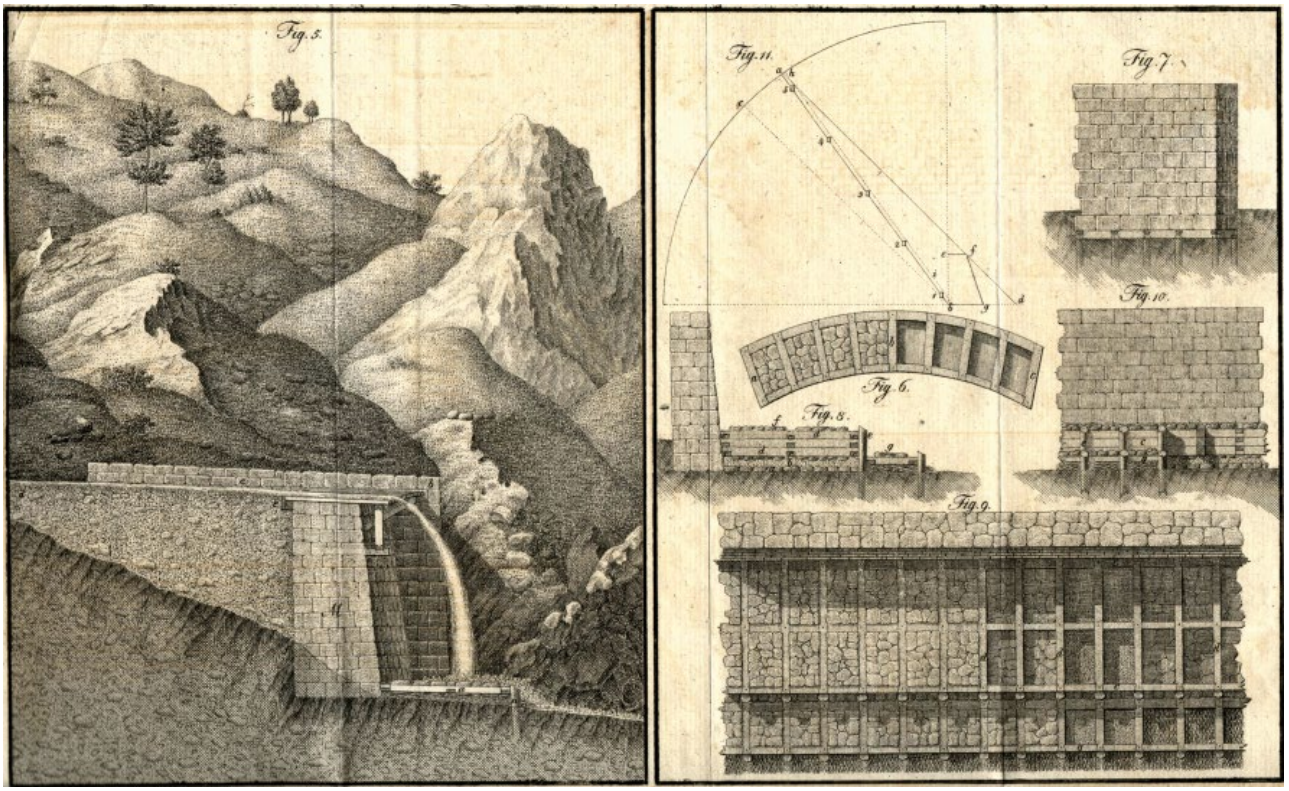

Figure 11.2 Technical illustration of mitigation measures [8]. *Source:* Duile, J. 1826/J.F. Wagner/Public Domain.

Within the so-called perimeter hydraulic engineering was mainly applied to the lower part of the torrent, while forest engineering addressed the headwaters. The political question who should further be responsible for torrent control works in Austria led to a controversy between Arthur Freiherrn von Seckendorff as forest engineer and Weber von Ebenhof as hydraulic engineer [9]. To overcome this problem, Seckendorff started to study the methods developed in France, especially the works of Demontzey [10], which were implemented in France since 1863. Seckendorff translated Demontzey's book about reafforestation of mountain

@seismicisolation

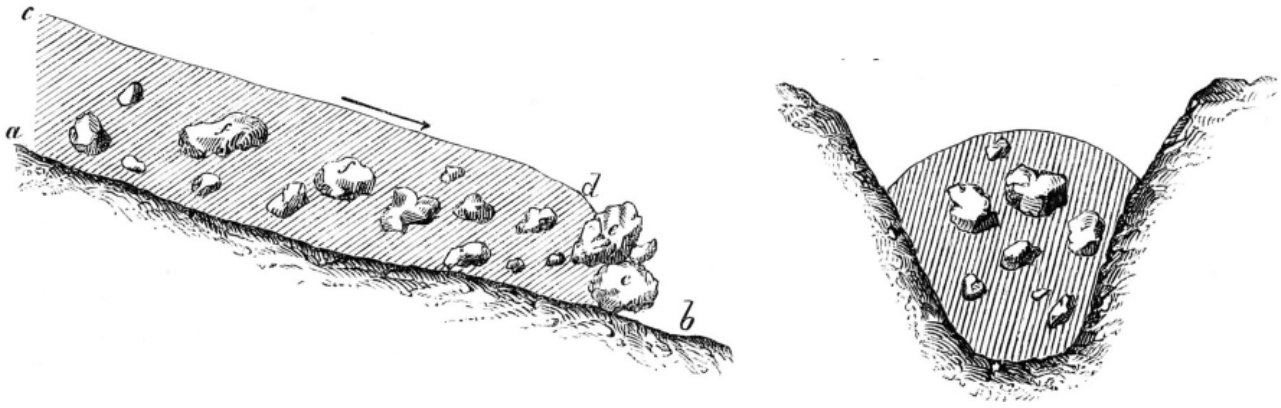

Figure 11.3 These drawing originate from a report of an eyewitness (forester) of a debris flow near the Faucon torrent (Barcelonette, France) in [10]. The longitudinal section shows the accumulation of coarse boulders at the debris flow front and the right picture displays the debris flow cross section during the passage of the front.

regions to German (1880), which in turn provided the basis of the Austrian type of torrent control. In this book, not only torrential countermeasures were specified, but also the first detailed description of debris flows with their typical features were characterized (Figure 11.3).

The large floods in Tyrol and Carinthia in the year 1882 initiated, similar to France, a political demand to prevent such disasters. Therefore, Seckendorff organized in the year 1883 an excursion to France to show the responsible Austrian Minister of Agriculture the methods already established in France and to convince him to implement similar measures and to constitute an equal organization in Austria [11]. Already in 1884, the emperor of the Austrian-Hungarian monarchy passed the torrent control act (this act is still valid), stating that torrent control works have to be executed on a national level, with public funding and with a systematic approach. The government implemented a legal basis for financing and organizing the Forest Technical Service of Torrent Control to ensure further development. Educational courses were established in Vienna at the University of Natural Resources and Life Sciences (BOKU) for students and the staff of the new established service. Even technicians from Japan were interested by this topic and started to study in Vienna, providing the basis of SABO works in Japan.

11.2. EMPIRICAL DESIGN APPROACHES

The construction materials used in the early years consisted of the locally available construction material near the torrents, mainly stones, timber, and living vegetation [11]. Wooden crib walls and dry stone masonry were used for structural measures (Figure 11.4). Progress was achieved through dissemination of experience and not by research because no research facilities existed at the time. In the first half of the twentieth century, cement mortar structure became the best available technology leading to new designs and possibilities in sediment management.

Nonetheless, first innovative experimental structures were raised, for example:

- First barrier with a self-cleaning function (called dosing) was installed in the Fischbach, Tyrol (1924–1928) (Figure 11.5)
- Prefabricated construction of a barrier of reinforced concrete in the Winklergraben, Upper Austria (1929–1933) (Figure 11.6)

The design load was calculated either as earth or as hydrostatic water pressure, independent of the assumed torrential process.

Due to the improvement of materials and mechanization on building sites, new methods were established for structural torrent control. Increasing usage of cableways and heavy machinery even in the steep regions enhanced construction efficiency.

Depending on the two main types of structures, the arch dam and the gravity wall, different formulas were used for design [12]. The focus of the gravity wall laid on external stability (safety against tilting, sliding, and bearing capacity failure) and was controlled by the bottom width of the structure in relation to the dam height. Arch dams reduce the construction volumes by using the arching effect for stability. Hampel [13] designed an arch dam in the Finsingbach to verify the

@seismicisolation

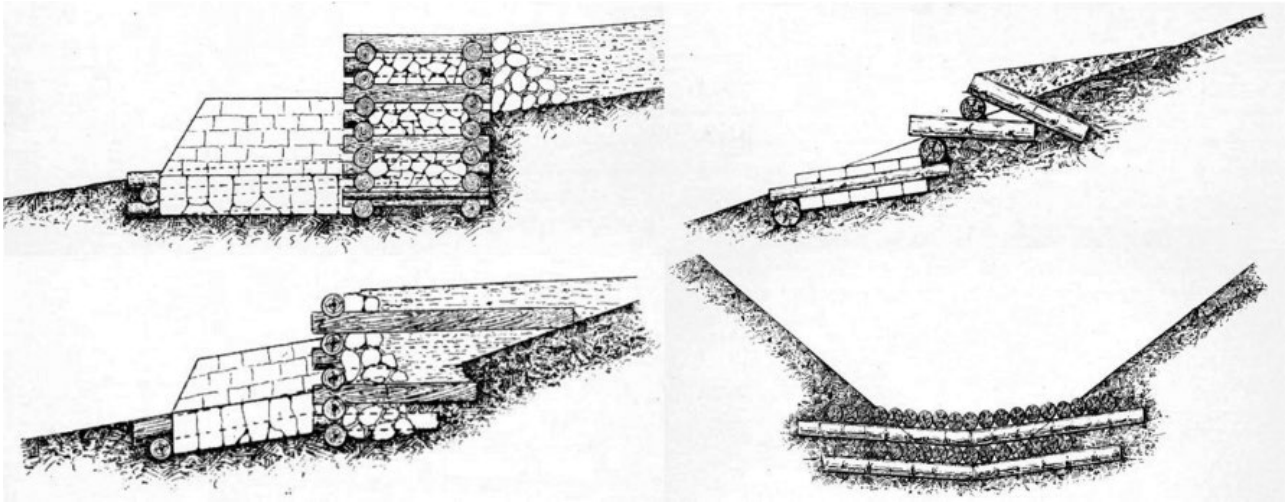

Figure 11.4 Examples of technical structures [11].

Figure 11.5 Barrier with a self-cleaning function (1928); Fischbach, Längenfeld, Tyrol. *Source:* IAN-Archive.

design method and the properties of the construction material. This cement mortar arch dam was built in the years 1951/52, especially to study the failing condition of this construction type. The experiment showed that the so-called ring tension formula is valid, but the material properties and the load distribution had to be adapted [14].

Due to the improvement of concrete technology and the need to improve sediment connectivity, the openings in the structures grew larger. It was the doctoral thesis of Leys [15] that summarizes practical experience with different types of check dams and established large-slot dams and open check dams. These new structural types with the function of dosing sediment were named large-slot, slit, beam, rake, and grid dams. They should facilitate the sedimentation of gravel and large wood during a torrential event and afterward the self-cleaning of the sediment retention basin to provide the full storage capacity again for the next torrential event.

In 1972, the Austrian Centre for Forest Research (BFW) held an international colloquium on check dams in Vienna, where Lichtenhahn presented his load model for design [16]. He proposed an empirical multiplier k to increase the hydrostatic pressure p_{st} to include the load of debris flow pressure. In practice, this

@seismicisolation

Figure 11.6 Barrier made out of prefabricated elements of reinforced concrete (1933); Winklergraben, Ebensee, Upper Austria *Source:* IAN-Archive.

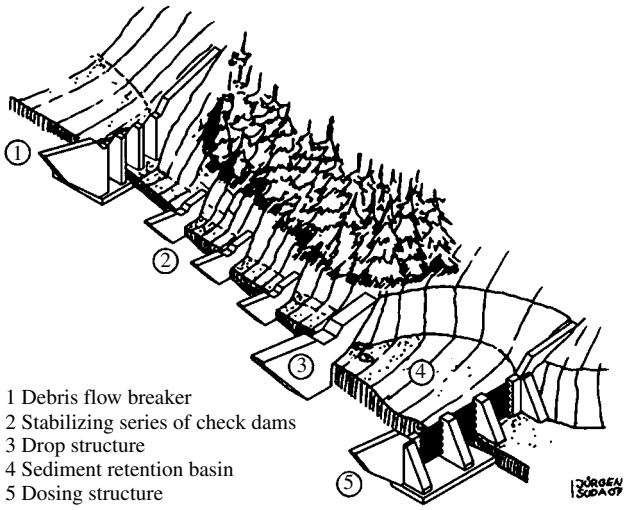

Figure 11.7 Sketch of a functional chain of check dams. *Source:* Bergmeister et al. [18].

multiplier ranges significantly and led to different structural designs of check dams:

$$p_{st} = k \cdot \rho \cdot g \cdot h \tag{11.1}$$

Additionally, a concept of sediment management by "sorting" and "dosing" was introduced [17]. To fulfill these functions, different types of check dams were developed. The effectivity in sediment management was further increased by the combination of dams with different functions (Figure 11.7). This approach was called a functional chain of check dams [19]. Usually, the uppermost structure is designed as a debris flow breaker, followed by a series of open check dams with a dosing or filtering function. Between these structures, channel stabilizing dams were installed.

11.3. ACTIVE AND PASSIVE MITIGATION MEASURES

Nowadays, two types of mitigation measures can be distinguished [20]: active measures and passive measures.

@seismicisolation

Active mitigation measures may affect the initiation, transport, or deposition of torrential flows and can therefore modify its magnitude and frequency characteristics. This can be achieved either by changing the probability of occurrence (disposition management) or by manipulating the flow process itself (event management). Passive mitigation measures are used to reduce the potential losses by, for example, altering the spatial and temporal character of either the damage produced by the torrential process or the associated vulnerability [21].

Active mitigation measures comprise forest management and soil bioengineering activities, catchment care, and structural measures. The latter can be classified by their fulfillment of defined requirements within the protection strategy, the so-called functions [22].

In case of disposition management:

• Stabilization

Stabilization of the horizontal and vertical position of the channel and the embankment to minimize debris mobilization along the channel. The design channel slope should match with the transport capacity, assessed with sediment transport equations. Stabilization is usually realized by a combination of longitudinal and transverse structures (e.g. trench, channel adjustment).

• Consolidation

Lowering the probability of slope failures close to the channel by a considerable raise of the channel bed by a series of check dams to get a toe counterweight of the adjacent hillslope and bank. Thereby the channel gradient is decreased, leading to less erosion within the channel. Consolidation can be supported by soil bioengineering techniques.

• Diversion

Creating a bypass from the original channel to avoid excessive sediment mobilization along specific channel reaches (tunnel, rock channel).

In case of event management:

• Retention

Regulation of the flow rate for water-dominated processes (flood) during an event by dampening the peak discharge in the downstream section. The temporarily stored water is released after the flood has subsided.

• Deposition

Permanent deposition of sediment upstream of a structure. Until the deposition basin is filled, it completely interrupts bedload transport and can lead to excessive erosion downstream. When the basin is filled, the deposition angle of the retained material strongly depends on the volumetric sediment concentration of the flow. A dosing function might be obtained when the falling limb of the hydrograph or subsequent flows with lower sediment concentration erode sediment from the basin.

• Filtration

Separation and deposition of grain sizes exceeding a defined diameter or of large woody debris at the structure that may clog downstream reaches. This can be reached by an open structure with a rake or grill situated upstream. In case the filter element is blocked by coarse material or woody debris, it behaves like a structure with a deposition/dosing function. There is no natural remobilization of the deposited material, and the basin must be excavated mechanically.

• Buffering

Temporary deposition of sediments by creating backwater in a bottleneck (e.g. open check dam) or by changing channel geometry, e.g. slope reduction or channel widening. Some of the deposited material may be later eroded by subsequent flows deficient of sediment.

• Transformation

Slowing and depositing of the surge front of a debris flow to ensure lower dynamic impact in the downstream reaches. In an array of different mitigation structures, a structure with this function is always in the most upstream position and should retain at least the volume of a debris flow surge. The commonly used term is debris flow breaker for a structure with this function.

Within the group of structural measures, two functions do not modify magnitude or frequency but just influence the flow direction of the torrential process on the fan:

• Conveyance

Enlargement and strengthening of the channel to assure the passing of the design flow without inundation of a potentially endangered area (e.g. trench, channel adjustment).

• Deflection

Directing the flow toward areas of non-developed areas (e.g. agricultural or forested areas) in the deposition area with dikes or deflection walls. Deflection is commonly utilized as the last element of a systematic torrent control to diminish any remaining risk.

In contrast to the former alpine method of channel stabilization by quite a lot of smaller check dams to

@seismicisolation

prevent erosion (disposition management), the newer concepts led to a concentration of a few bigger structures nearby the fan apex (event management). This positioning has the big advantage of an easier access for maintenance and for mechanical excavation of the basins.

11.4. ADAPTATION TO EUROCODE CONCEPT

Due to this long tradition in torrent control works in the Austrian Alps, numerous types of protection works were designed (Figure 11.8). To harmonize these different approaches and to include life circle assessment, a working group within the Austrian Standardization Committee was established in the year 2006. The design of technical structures should be based on the EUROCODE concept that specifies how structural design should be conducted within the European Union (EU).

Based on this, the ONR technical standards Series 248xx was established, encompassing torrential processes, snow avalanches, and rock fall. The interdisciplinary working group (ONK-256) developed new standards for the load models, design, construction, and life cycle assessment of torrent control works. The following standards have been developed:

ONR 24800: 2009 02 15 [23], protection works for torrent control – terms, definitions, and classification; contains the terminology and classifications of torrent control works including the terms concerning the design and function of torrential barriers. An important classification is the definition of functional barrier types.

ONR 24801: 2013 08 15 [24], protection works for torrent control – impacts on structures; stresses on torrential barriers result from water (hydrostatic, dynamic), earth, and debris flow impacts. In special cases, effects from avalanches, falling rocks, and earthquakes must also be considered.

ONR 24802: 2011 01 01 [25], protection works for torrent control – design of structures; for the design of torrential barriers, the Ultimate Limit States (ULS) and the Serviceability Limit States (SLS) must be considered. The concept gives specific design rules (e.g. stress combinations) for torrential barriers.

ONR 24803, 2008 02 01 [26], protection works for torrent control – operation, monitoring, maintenance; a fundamental requirement to guarantee a minimum

Figure 11.8 Development of barrier types within one century. *Source:* IAN-Archive.

@seismicisolation

safety level of the protection works is periodic monitoring of their condition and effectiveness. The monitoring concept in this ONR is divided into two parts, first the inspection and second the intervention part.

By these technical standards, the "traditional" assessment and construction concepts for torrent control structures were adapted to the EUROCODE standards. The working group was able to achieve remarkable progress. These documents are based on and interact with EN 1990 (basic of structural design), EN 1992-1-1 (design of concrete structures), EN 1997-7 (geotechnical design), and the related documents for the Austrian national specifications. A revised version, based on the gained experience with the ONR series within the last years, is now combined in one national standard ÖNORM B4800.

11.5. THE REVISION OF ONR SERIES AND THE DEVELOPMENT TO ÖNORM B4800 STANDARD

The national standard ÖNORM B4800 enables practitioners to design torrential countermeasures with the restriction that usually only little data are available. The standard delivers a holistic approach, starting with

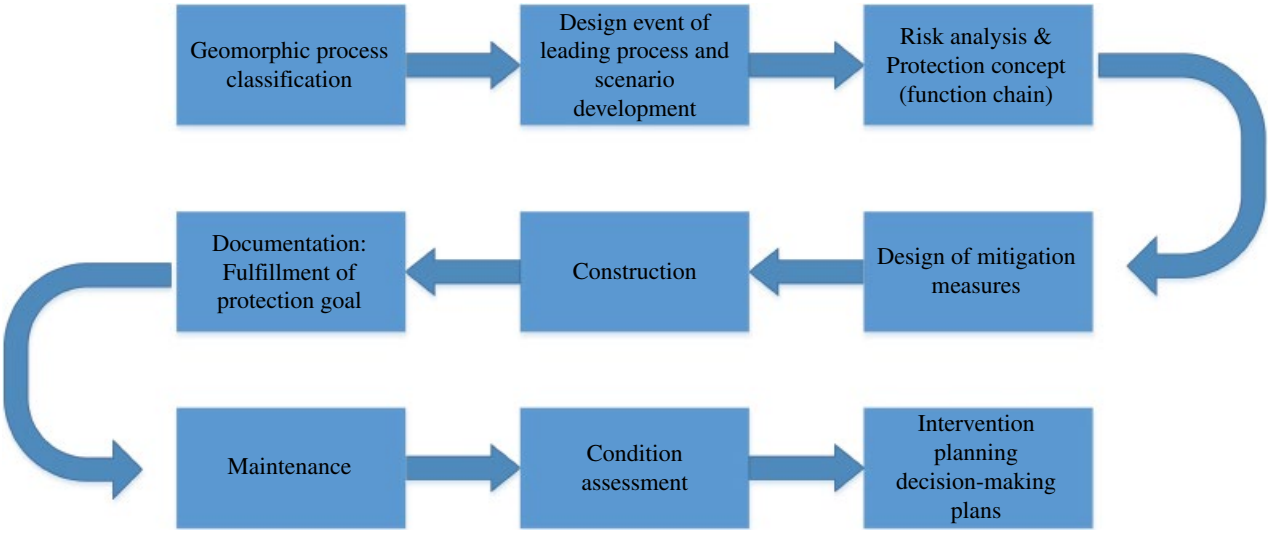

Figure 11.9 Road map of the Austrian standard ÖNORM B4800 torrent control.

Figure 11.10 Recently completed debris flow barrier with the sediment retention basin (Schallerbach, Tyrol), designed according to the ONR National Guidelines.

@seismicisolation

a geomorphic classification [22], definition of design situations, implementing the partial safety factor concept, condition assessment, and intervention planning (Figure 11.9).

The ÖNORM B4800 provides a standardized model for the design of structural measures in torrents [27], which has been developed from field and small-scale experiments and from comparative calculations of common engineering practice in torrent control.

11.6. CONCLUSION

Each torrent shows its unique behavior and needs a customized protection concept in order to reduce the risk to an accepted level. Therefore, it was necessary to harmonize different design approaches, taking already existing structures and the need to construct new ones or to replace older ones into account. The challenge in developing national guidelines was to connect the experience of the practitioners with scientific research results and to derive a state of the art, starting with terminology, definitions, construction rules, and design procedures. The published guidelines should on the one hand provide a standardized method for the design of torrent control structures, and on the other hand should leave a degree of freedom to adjust the design according to the peculiarity of the torrent (Figure 11.10).

REFERENCES

1. Walcher, J. (1773). Nachrichten von den Eisbergen in Tyrol, Kurzböck.
2. Graf von Sauer, W. (1788). Gubernialverordnung.
3. Zallinger, F. (1779). *Abhandlung von den Ueberschwemmungen in Tyrol: gedruckt allda in der kais. königl.* Innsbruck: Hofbuchdruckerey.
4. Fabre, J.A. (1797). Essai sur la théorie des torrens et des rivières: chez Bidault, Libraire, An VI 1797, p. 284. http://dx.doi.org/10.3931/e-rara-44675.
5. Aretin, G. (1808). Über Bergfälle und die Mittel, denselben vorzubeugen oder wenigstens ihre Schädlichkeit zu vermindern, Innsbruck.
6. Müller, F. (1857). *Die Gebirgs-Bäche und ihre Verheerungen wie die Mittel zur Abwendung der Letzteren*, 44. Krüll'sche Universitäts-Buchhandlung.
7. Streffleur, V.R.V. (1852). Über die Natur und die Wirkung der Wildbäche. Sitzungsberichte der Akademie der Wissenschaften mathematisch-naturwissenschaftliche Klasse 08 1852, pp. 248–261.
8. Duile, J. (1826). *Ueber Verbauung der Wildbäche in Gebirgs-Ländern, Zum Gebrauche für Bau- und Forstbeamte, Obrigkeiten, Seelsorger und Gemeinds-Vorstände*, 179. Innsbruck: Wagner http://doi.org/10.3931/e-rara-19671.
9. Länger, E. (2003) Der forsttechnische Dienst für Wildbach- und Lawinenverbauung in Österreich und seine Tätigkeit seit der Gründung im Jahre 1884. Doctoral Thesis. University of Natural Resources and Life Sciences (BOKU) Vienna.
10. Demontzey, P. (1880). *Studien über die Arbeiten der Wiederbewaldung und Berasung der Gebirge*. [translated by Seckendorff-Gudent, A.]. A Vienna: C. Gerold's sohn.
11. Wang, F. (1901). *Grundriss der Wildbachverbauung*. Leipzig: S. Hirzel.
12. Leys, E. (1968). Zum Bau von Gewölbesperren in der Wildbachverbauung. In: *Oesterreichische Wasserwirtschaft*, vol. *20*. Jahrgang (ed. J. Kar), 243–249. Wien, New York: Springer.
13. Hampel, R. (1952). Bruchversuche an einer Bogensperre, p. 42, unpublished.
14. Hampel, R. (1960). Bruchversuch an einer Bogensperre der Wildbachverbauung. In: *Österreichische Wasserwirtschaft* (ed. J. Kar), 187–193. Wien, NY: Springer.
15. Leys, E. (1969). Die technischen und wirtschaftlichen Grundlagen der großdoligen und kronenoffenen Bauweise in der Wildbachverbauung. Doctoral Thesis. University of Natural Resources and Life Sciences (BOKU) Vienna.
16. Lichtenhahn, C. (1972). Berechnung von Sperren in Beton und Eisenbeton. In: *Forstlichen Bundesversuchsanstalt in Wien*, Kolloquium über Wildbachsperren, vol. *1*, 91–118. Wien: Österreichischer Agrarverlag.
17. Üblagger, G. (1973). Retendieren, Dosieren und Sortieren, Mitteilungen der Forstlichen Bundesversuchsanstalt, 102, pp. 335–372.
18. Bergmeister, K., Suda, J., Hübl, J., and Rudolf-Miklau, F. (2008). Schutzbauwerke gegen Wildbachgefahren. In: *Betonkalender 2008 Bd. 1 II* (ed. K. Bergmeister and J.-D. Wörner), 89–289. Berlin: Ernst & Sohn Verlag; ISBN 978-3-433-01839-2.
19. Kettl, W. (1984). Vom Verbauungsziel zur Bautypenentwicklung: Wildbachverbauung im Umbruch, Wildbach- und Lawinenverbau, 48. Jahrgang, Sonderheft, pp. 61–98
20. Zollinger, F. (1985). Debris detention basins in the European Alps. Int. Symp. on Erosion, Debris Flow and Disaster Prevention, Tsukuba, Japan, pp. 433–438.
21. Hübl, J. and Fiebiger, G. (2005). Debris-flow mitigation measures. In: *Debris-Flow Hazards and Related Phenomena*, Praxis Books in Geophysical Sciences (ed. M. Jakob and O. Hungr), 445–487. Berlin, Heidelberg, New York: Springer.
22. Hübl, J. (2018). Conceptual framework for sediment management in torrents. *Water 10* (12): 1718, p.13, https://doi.org/10.3390/w10121718.

@seismicisolation

23. Austrian Standards (2009). Protection works for torrent control - Terms and their definitions as well as classification, (ONR 24800: 2009 02 15).
24. Austrian Standards (2013). Protection works for torrent control - Static and dynamic actions on structures, (ONR 24801: 2013 08 15).
25. Austrian Standards (2011). Protection works for torrent control - Design of structures, (ONR 24802: 2011 01 01).
26. Austrian Standards (2008). Protection works for torrent control - Operation, monitoring, maintenance, (ONR 24803: 2008 02 01).
27. Hübl, J., Nagl, G., Suda, J., Rudolf-Miklau, F.2017, Standardized stress model for design of torrential barriers under impact by debris flows (accordimg to the Austrian Standard Regulation 24801), *International Journal of Erosion Control Engineering*, Vol. *10*, Nr.1, pp. 47–55

@seismicisolation
@seismicisolation

12

Effect of Check Dams on Sediment Connectivity

Tomáš Galia, Václav Škarpich, and Ivan Smažák

12.1. INTRODUCTION

Mountain catchments are important sources of water, sediment, and nutrients for the fluvial network. In this sense, bedload transport belongs to crucial processes that shape the morphology and dynamics of mountain streams [1]. However, frequency, volume, and grain-size character of bedload transported material in steep channels do not necessarily correspond to the flow competence (i.e. peak discharge and flood duration), and these characteristics are often in direct relation with the incoming sediments from individual inputs [2]. Therefore, it is convenient to manage these streams from the whole catchment-scale perspective including past and recent activity of available sediment sources and intensity of hillslope-channel coupling instead of focusing on the time- and space-limited observations in a single channel reach.

To complexly describe fluxes of coarse sediments in bedload transport mode in these catchments, the concept of sediment (dis)connectivity can be involved [3–5]. This concept identifies vertical, lateral, and longitudinal dimensions of possible sediment movement with regard to the stream channel. The vertical (dis)connectivity is represented mainly by the exchange between surface and subsurface sediment layers and release of bed sediments for downstream transport during high-flow events. In the context of mountain streams, the lateral (dis)connectivity can be understood as the activity of hillslope-channel coupling processes and thus, direct supply of material to the channels from individual sediment inputs allocated along the stream longitudinal profiles. Finally, the longitudinal (dis)connectivity describes downstream transport of sediments in the channels, which usually has a pulse character corresponding to the frequency and magnitude of individual flood events. Indeed, all these three dimensions of sediment (dis)connectivity can be altered by human interventions. For example, large dams act as non-permeable "barriers" in the longitudinal dimension, whereas artificial bank stabilizations are effective "buffers" for sediment transfer between the channel and adjacent hillslopes or out-of-channel alluvial deposits [6]. Finally, the long-term stabilization of the profile associated with check dam series helps the bed surface armor and its "blanket" effect to survive extreme floods [7].

The spatial and temporal scales of the basic interactions between channel control works including several types of check dams and sediment (dis)connectivity were briefly summarized by Marchi et al. [6]. The main aim of this chapter is to describe impacts of individual full-body retention check dams and whole sequences of consolidation check dams on longitudinal, lateral, and vertical dimensions of sediment (dis)connectivity, when these alterations in (bedload) sediment fluxes are frequently accompanied by notable changes in channel

Department of Physical Geography and Geoecology, University of Ostrava, Ostrava, Czechia

Check Dam Construction for Sustainable Watershed Management and Planning, First Edition.
Edited by Zhanbin Li, Peng Li, Yang Yu, Peng Shi, and Guillaume Piton.
© 2022 John Wiley & Sons, Inc. Published 2022 by John Wiley & Sons, Inc.

@seismicisolation

morphology and geometry. High retention check dams are often constructed in the steepest parts of confined valleys where bed material comes both from upstream fluvial (torrential) transport and from hillslope processes (landslides, rock fall, avalanches, and debris flows). Therefore, their main aim is to decrease bedload transport rates in downstream reaches. On the other hand, the main purpose of lower consolidation check dams presented on alluvial fans and more generally in alluvial unconfined reaches is to decrease overall stream morphodynamics by complete stabilization of the longitudinal profile.

12.2. DEPOSITION AND EROSION PROCESSES RELATED TO INDIVIDUAL CHECK DAMS

Indeed, the construction of retention check dams (i.e. a full-body check dam designed to effectively trap sediment transported from upstream) in steep confined valley disrupts longitudinal fluxes of coarse sediments, although the connectivity can be to some extend restored after complete filling of the retention space [6, 8]. In any case, a sedimentary wedge consisted of trapped sediments starts to develop upstream a check dam body after its construction or the dredging of its retention basin. The length of the channel influenced by forced sediment deposition is dependent on the final equilibrium bed slope, which in turn reflects the original bed slope, the height of a check dam, hydrologic regime, and characteristics (volumes and grain sizes) of incoming sediments [9–11]. Surface bed layers of sedimentary wedges often indicate grain-size fining in downstream direction from the beginning of sedimentary wedge, which corresponds to gradual downstream decline of shear stresses by decreasing bed slope and increasing channel width (i.e. hydraulically controlled deposition) (Figure 12.1). Establishment of specific vegetation guilds was documented owing to these site-specific soil properties and hydrologic regime in the sedimentary wedges when compared to unaffected channel reaches [11, 12]. In addition, sedimentary wedges are quite efficient in trapping of transported large wood due to local decrease of flow velocity and flow depth [13].

Scour holes are developed immediately downstream the check dam body as the result of the diffusing jet if bed material can be entrained and removed by the flow [14]. Except some specific hydraulic parameters as drop height or jet inclination, the final geometry of scour holes is dependent on sediment supply from upstream [10, 15]. In general, low sediment-supply conditions can lead to origin of deeper scour holes, whereas even entire check dam bodies can be buried in sediments under extraordinary high sediment supply or debris flow character of the hydrogeomorphic event [16]. This way, the final scour depth can be relevant for the effectivity of flow energy dissipation, except when shallow scours filled by sediments no longer act as important hydraulic roughness elements affecting downstream transport of coarse sediments.

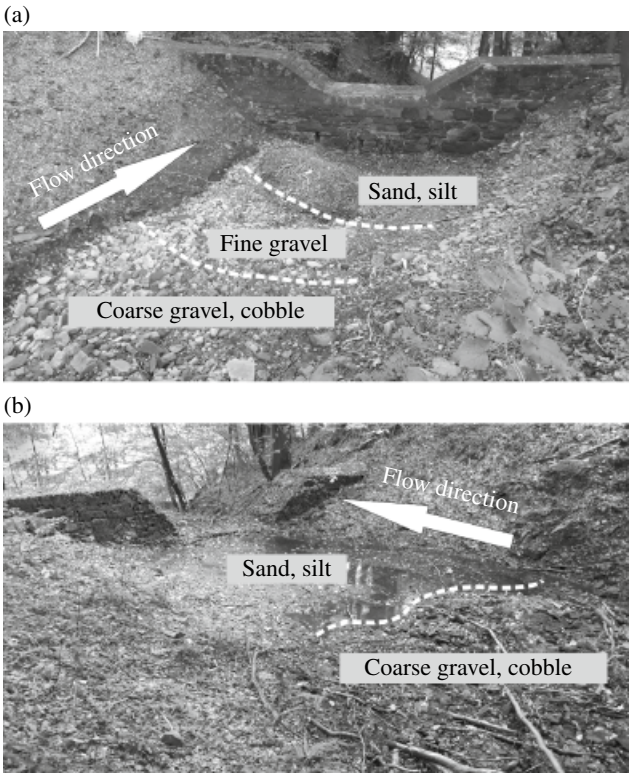

Figure 12.1 Examples of downstream surface bed sediment fining in the sedimentary wedges of retention check dams: (a) half-filled retention space in the Tosenovsky, Western Carpathians, (b) almost completely filled retention space in the Psarky, Western Carpathians.

Nevertheless, erosion processes are very often propagated up to 100 m downstream individual check dams, which results into narrower and deeper channels in these sites when compared to channel reaches completely without check dams [17–20]. This channel degradation can be triggered by "hungry water effect" due to lower volume of incoming sediments, yet trapped by upstream structures [21]. Indeed, development of sedimentary wedges, scour holes, and channel degradation downstream is significant also for the case of individual consolidation check dams within their

@seismicisolation

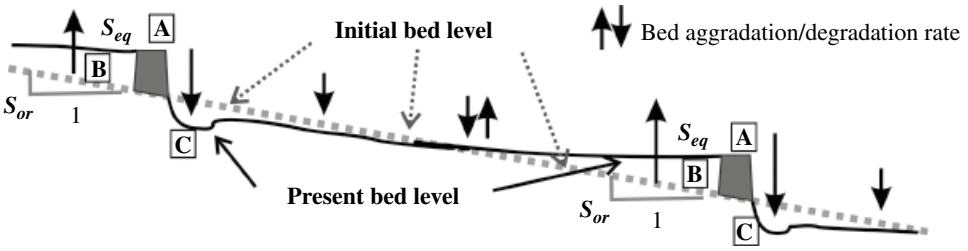

Figure 12.2 Schematization of erosional and depositional processes in relation to individual check dams. (A) – check dam crest, (B) – sedimentary wedge, (C) – scour hole, S_{eq} – equilibrium bed level, S_{or} – initial bed slope.

sequences in straightened mountain and unconfined foothill streams, although the dimensions of the wedges and scours are usually smaller due to lower heights and steeper initial slope compared to depositions slope inducing more frequent spacing of these grade control structures. Despite overall tendency of the channel degradation in these managed streams, the propagated erosion downstream of individual structures and aggradation upstream of check dam bodies may lead to anticlockwise rotation of longitudinal profile between individual structures [22]. This implies long-term inverse bed-level changes from its original level upstream and downstream of particular check dam (Figure 12.2).

12.3. SIGNS OF THE SEDIMENT (DIS)CONNECTIVITY IN STREAMS MANAGED BY CHECK DAMS

The alterations in channel geometry triggered by individual retention check dams in steep reaches or whole sequences of consolidation check dams in unconfined reaches suggest some complex adjustments of sediment fluxes at the catchment scale, which are represented by all the three dimensions of sediment (dis)connectivity. Indeed, other alterations on the sediment (dis)connectivity can be referred to additional artificial interventions that occur in check-dam-managed streams as channel straightening, bank reinforcements, hillslope consolidation, or removal of flow obstructions (immobile boulders and large wood). As the consequence, a variety of forced changes of bed sediment grain-size characteristics along these longitudinal profiles of managed streams are expected.

These assumptions somehow contradict to laboratory experiments, which documented practically no changes in long-term bedload-transported volumes after complete filling of retention spaces of check dams and establishment of final equilibrium slopes upstream individual check dams. However, reduced volumes for a single-transport event were measured pointing on the "buffer effect" of a check dam sequences [7]. Similar field observations for fine grain-size fractions were documented in the case of semi-arid Spanish catchment, where an unaltered longitudinal connectivity of fine grain-size fractions was reported after the complete silting of check dams [17]. Moreover, only a small penalty to consolidation grade control structures (e.g. sequences of consolidation check dams) in terms of the longitudinal sediment connectivity was assigned in the complex hydromorphologic assessment of Italian fluvial systems [23].

Nevertheless, our field observations from the flysch-based medium-high mountain landscape show some tendencies for downstream coarsening of bed sediments (or lacks of grain-size response on notably decreasing shear stresses) along the channelized streams stabilized by sequences of consolidation check dams. Downstream coarsening of D_{95} grain-size percentile was observed in the sedimentary wedges of consolidation check dams at various stage of their destruction in ca. 2.5 km long reach of the Mohelnice, Western Carpathians, Czechia. These grade control structures were built in this relatively steep (S ~ 1–2%) and 15–20 m wide river in the 1950s and 1960s to control bed slopes and decrease sediment transport rates produced by local flysch lithology [21]. Their gradual destruction accompanied by lowering of the elevation of their crests led to increase of bed equilibrium slopes between subsequent check dams and thus, some degree of restoration of the longitudinal coarse sediment connectivity is expected. This example also demonstrated limited temporal scale for the proper functioning of check dams as barriers for coarse sediment transport owing to their insufficient maintenance for several decades. Further research in the narrower (bankfull width 4–5 m) but a little steeper (S ~ 1.5–4%) foothill unconfined stream of the same region was focused on sediment response on the

@seismicisolation

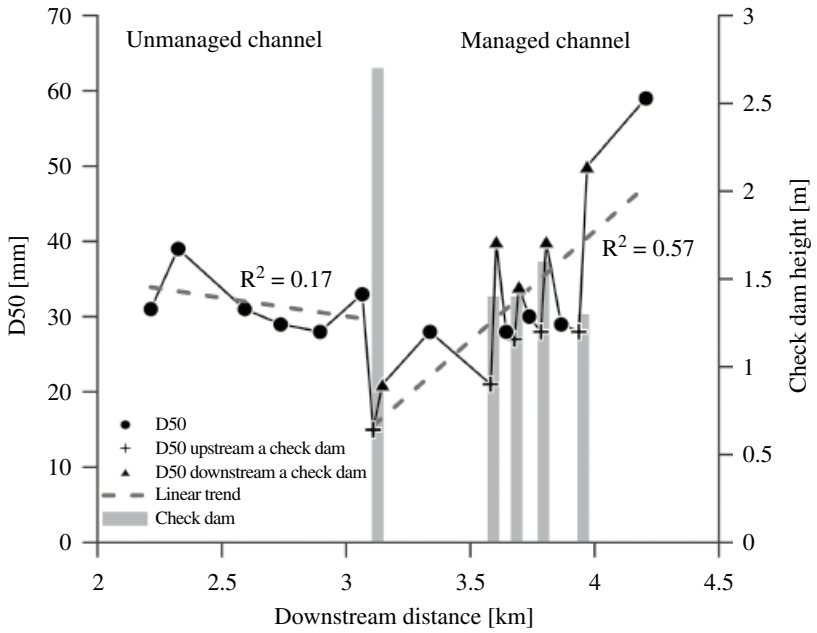

Figure 12.3 Downstream variations in D_{50} in the Velka Hanzluvka, Czech Carpathians.

presence of consolidation check dams along 2.7-km-long reach. Together with additional interventions (channel straightening and bank stabilizations), sediment caliber of the deposits did not produce any systematic downstream fining and thus, the grain sizes did not correlate with a significantly downstream decreasing bankfull shear stresses or bed slopes [24]. Recent tracking experiment in this stream also pointed on the acceleration of downstream transport of the tagged particles as the response of the intensive torrent control works. In this specific case, longer travel distances of the tagged particles were recorded during high-flow events in comparison with those in the neighburing untreated pool-riffle stream with the same catchment-scale characteristics and unconfined valley settings [25]. The results of this monitoring demonstrated that even increased longitudinal sediment connectivity can be expected in unconfined streams managed by consolidation check dams. Marchi et al. [6] consistently recall that if check dams intend to reduce connectivity near sources and in gorges, on alluvial fans they should rather facilitate sediment transfer and are often built along with dykes and bank protection.

The presence of notably coarser bed sediments downstream of check dams when compared to grain-size characteristics of sedimentary wedges or intermediate reaches between subsequent check dams was previously reported from a set of steep Calabrian streams (southern Italy) [18]. The pebble counts along the reach managed by check dams and unmanaged reach in a steep but rather unconfined Carpathian stream also pointed on the different pattern of sediment adjustment on the presence or absence of check dams. Figure 12.3 displays rather smooth variations in the median bed grain size in the confined unmanaged reach, whereas the complex response was observed in the managed reach in relation to the prevailing process (aggradation or degradation) upstream and downstream of the particular check dam together with the general downstream sediment coarsening [26]. These variations suggest (i) effective trapping of sediments upstream individual check dams and, on the other hand, (ii) the general downstream sediment coarsening in the managed reach produced by increased flow competence (and possible acceleration of sediment transport). Note also higher degree of fining in the sedimentary wedge of the highest (2.5 m) retention check dam in comparison with substantially lower (1.5 m) consolidation check dams in the downstream sections (3.5–4.0 km).

The detailed analysis of channel heterogeneity proved different response of bed sediments on the presence of check dams between high-gradient (S ~ 10%) confined streams and less steep unconfined streams (S ~ 1–2%). Whereas signs of decreased bed sediment heterogeneity (e.g. presence of well-sorted sediments) were observed in the high-gradient stream when compared to unmanaged stream with similar bed slope characteristics, no change was detected for bed grain sizes in the case of unconfined stream despite its

@seismicisolation

forced transformation of bed morphology from pool-riffles to rather uniform plane beds [27]. This decreased sediment heterogeneity in the managed high-gradient stream likely resulted from the trapping efficiency of (relatively high) check dams, especially for coarse sediments and the scour of fine particles in the intermediate reaches together with potential removal of some large boulders during the historical construction of these torrential works. This suggests decreased longitudinal connectivity for coarser sediment fractions in the managed high-gradient streams, when finer grains may still freely pass the series of check dams. On the other hand, usually lower consolidation check dams designed primarily to control lower bed slopes in the unconfined stream were not so much efficient in coarse sediment trapping and instead, the accelerated longitudinal connectivity may exist here as the consequence of the channel straightening and loss of original bed morphology (pool-riffle transformed into low-roughness plane bed). This proposed pattern for unconfined and less steep streams managed by consolidation check dams can be supported not only by previously mentioned acceleration of the downstream transport of the tagged particles but also by observations of the significant differences between the grain sizes of surface and subsurface bed layers. Analysis of surface and subsurface composition of sediments revealed that the presence of consolidation check dam sequence triggered strong bed armoring processes [25]. The observed bed armoring likely made vertical exchange between the individual bed sediment layers difficult and thus, vertical sediment connectivity can be very limited, at least during flows that are not competent to disrupt the armor layer. Therefore, we can expect boosted longitudinal sediment connectivity in these managed unconfined streams, but lateral and vertical dimensions of sediment (dis)connectivity can be variously altered by the presence or absence of additional bank stabilizations preventing from lateral erosion and strength of armoring processes acting on the channel bed (Figure 12.4). Note that the effectiveness of torrent control works toward all three dimensions of sediment (dis)connectivity is likely dependent not only on the present management (e.g. height and spacing of check dams, presence/absence of bank stabilizations) but also external boundary conditions related to the characteristics of supplied sediments, hydrological regime, local topography, channel confinement, and channel material type (alluvium or colluvium with poorly mobile boulder supplied by hillslope processes) are important as well.

12.4. CONSEQUENCES FOR SUSTAINABLE CATCHMENT-SCALE MANAGEMENT

The importance of the sediment connectivity within the fluvial system is emphasized in the EU's Water Framework Directive 2000/60/EC. Moreover, alterations of channel geometry and sediment properties in relation to individual check dams further shift fluvial processes and consequent development of fluvial forms far from the natural state of the channel despite possible origin of some unique habitats in sedimentary wedges [20]. Therefore, it is convenient to allow maximal possible degree of sediment connectivity at the catchment scale not only to sustain good hydromorphologic state of mountain channels but also to enable sediment transfer to downstream gravel-bed rivers, which are often treated by intensive channel degradation. However, any removal or non-maintenance of check dams and other torrential works should be carefully justified with regard to risk mitigation [28]. Possible ecologically more friendly solution can be installation of open (or filter) check dams, which are designed for selective sediment retention. Although the stopping of incoming sediment (and thus, the disruption of longitudinal sediment connectivity) is often more substantial than the designers aimed to, they usually allow some degree of connectivity at least for finer sediment fractions when compared to traditional closed retention check dams [6, 29]. Nevertheless, design of safe complex torrent control works which sustain acceptable level of hydromorphologic state in the mountain fluvial network is still a challenging task under land use and climate changes. One should also take into consideration some delays between these processes and morphological response in mountain catchments [30].

The downstream coarsening of bed sediments together with the forced channel transformation to uniform plane bed morphology in the unconfined streams managed by series of consolidation check dams may degrade frequency and size of suitable habitats (riffles, pools, and bars) for local aquatic and semi-terrestrial biota. Addition of (stable) large wood and large boulders can be helpful to increase habitat heterogeneity and trapping efficiency for finer sediment fractions in the intermediate sub-reaches between subsequent check dams. Without these roughness elements, the intensive bed armoring processes decrease potential to compose incoming sediments from upstream during transport events into channel bed, which produces "flushing" of bedload to adjacent downstream reaches. This

@seismicisolation

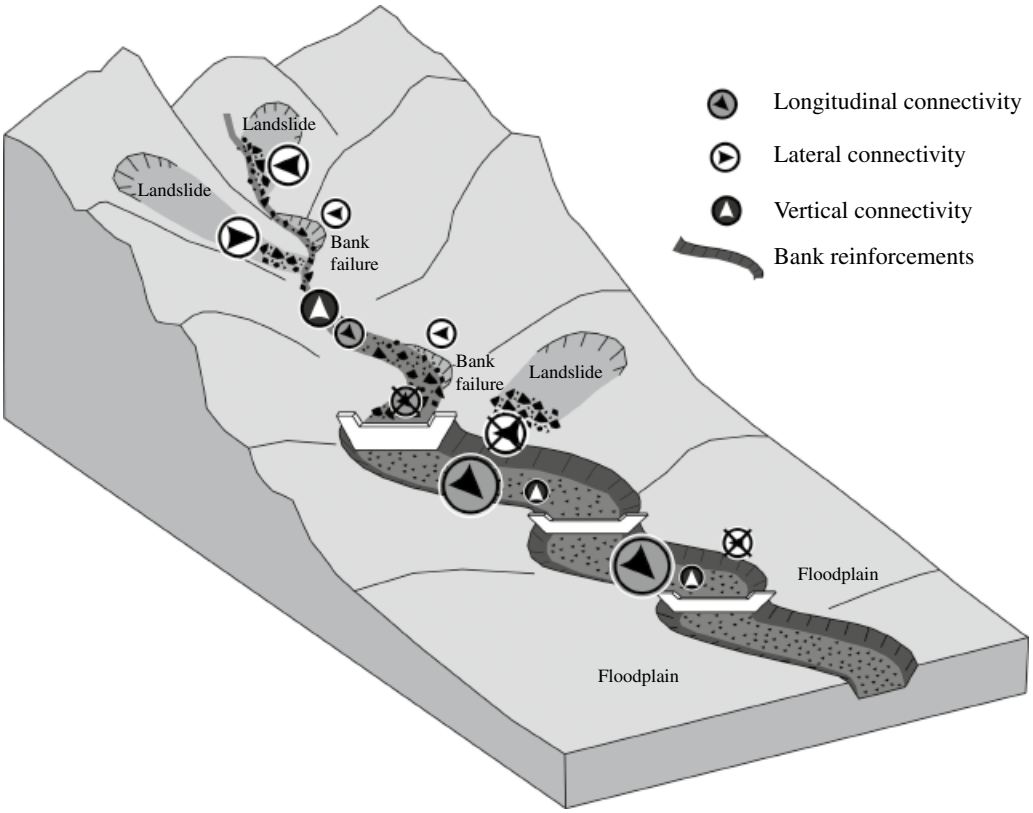

Figure 12.4 Conceptual model of the impact of torrent control works on the longitudinal, lateral, and vertical dimensions of coarse sediment (dis)connectivity. The random steep channel is managed by the retention check dam and the sequence of consolidation check dams accompanied by bank reinforcements. Symbol size is proportional to the impact when compared to the upstream completely unmanaged reach and a cross out symbol means blocking of coarse sediment transfer.

pavement of the channel bed may significantly degrade spawning habitats for salmonid fish species [31]. Moreover, the strong bed armoring and lacks of lateral sediments sources in artificially stabilized streams has some consequences for calculations of bedload transport, when the grain-size distribution of paved surface bed layer likely does not much fit to the grain size of bedload-transported particles incoming from upstream. Thus, the computation strategy should be considered with regard to traveling sediment production within the catchment instead of present composition of bed between subsequent check dams [2].

12.5. FINAL REMARKS

Check dams as typical representatives of torrent control works influence downstream transport rates of coarse sediments as well as release of individual grains for transport by lateral erosion or bed morphodynamics. Indeed, the set of protection measures may have different and sometimes contradictory impacts on all three dimensions of sediment connectivity. Whereas large sediment volumes can be trapped by high retention structures in the confined stream reaches, straightened unconfined channels stabilized by series of consolidation check dams may accelerate downstream movement of sediment coming from adjacent upstream reaches. Both effects can be of interest for stream managers because each catchment is unique and its suitable masterplan must be tailored to the catchment peculiarities. One should also take into account the temporal scale, when e.g. complete filling of sedimentary wedges or gradual destruction of old torrential works may lead (at least to some extent) to restoration of coarse sediment connectivity. Optimal planning, design, and maintenance of torrent control works to reduce their impact on longitudinal sediment connectivity still remains a challenging task under spatio-temporal variations of land use and climate changes.

@seismicisolation

REFERENCES

1. Rainato R, Mao L, Picco L. 2020. The effects of low-magnitude flow conditions on bedload mobility in a steep mountain stream. *Geomorphology 367*: 107345. DOI: https://doi.org/10.1016/j.geomorph.2020.107345.
2. Piton G, Recking A. 2017b. The concept of travelling bedload and its consequences for bedload computation in mountain streams. *Earth Surface Processes and Landforms 42*: 1505–1519. DOI: https://doi.org/10.1002/esp.4105.
3. Fryirs K A., Brierley GJ, Preston NJ, Kasai M. 2007. Buffers, barriers and blankets: the (dis)connectivity of catchment-scale sediment cascades. *Catena 70*: 49–67. DOI: https://doi.org/10.1016/j.catena.2006.07.007.
4. Poeppl RE, Fryirs KA, Tunnicliffe J, Brierley GJ. 2020. Managing sediment (dis)connectivity in fluvial systems. *Science of the Total Environment 736*: 139627. DOI: https://doi.org/10.1016/j.scitotenv.2020.139627.
5. Wohl E Brierley G, Cadol D et al. 2019. Connectivity as an emergent property of geomorphic systems. *Earth Surface Processes and Landforms 44*: 4–26. DOI: https://doi.org/10.1002/esp.4434.
6. Marchi L, Comiti F, Crema S, Cavalli M. 2019. Channel control works and sediment connectivity in the European Alps. *Science of the Total Environment 668*: 389–399. DOI: https://doi.org/10.1016/j.scitotenv.2019.02.416.
7. Piton G, Recking A. 2017a. Effects of check dams on bed-load transport and steep-slope stream morphodynamics. *Geomorphology 291*: 94–105. DOI: https://doi.org/10.1016/j.geomorph.2016.03.001.
8. Cucchiaro S, Cazorzi F, Marchi L, Crema S, Beinat A, Cavalli M. 2019. Multi-temporal analysis of the role of check dams in a debris-flow channel: Linking structural and functional connectivity. *Geomorphology 345*: 106844. DOI: https://doi.org/10.1016/j.geomorph.2019.106844
9. Ferro V, Porto P. 2011. Predicting the equilibrium bed slope in natural streams using a stochastic model for incipient sediment motion. *Earth Surface Processes and Landforms 36*: 1007–1022. DOI: https://doi.org/10.1002/esp.2128
10. Lenzi MA, Comiti F. 2003. Local scouring and morphological adjustments in steep channels with check-dam sequences. *Geomorphology 55*: 97–109. DOI: https://doi.org/10.1016/S0169-555X(03)00134-X.
11. Lucas-Borja ME, Zema DA, Hinojosa Guzman MD, Yang Y, Hernández AC, Xiangzhou X, Carrà BG, Nichols M, Cerdá A. 2018. Exploring the influence of vegetation cover, sediment storage capacity and channel dimensions on stone check dam conditions and effectiveness in a large regulated river in México. *Ecological Engineering 122*: 39–47. DOI: https://doi.org/10.1016/j.ecoleng.2018.07.025.
12. Bombino G, Boix-Fayos C, Gurnell AM, Tamburino V, Zema DA, Zimbone SM. 2014. Check dam influence on vegetation species diversity in mountain torrents of the Mediterranean environment. *Ecohydrology 7*: 678–691. DOI: https://doi.org/10.1002/eco.1389.
13. Galia T, Tichavský R, Škarpich V, Šilhán K. 2018. Characteristics of large wood in a headwater channel after an extraordinary event: the roles of transport agents and check dams. *CATENA 165*: 537–550. DOI: https://doi.org/10.1016/j.catena.2018.03.010.
14. Comiti F, Andreoli A, Lenzi MA. 2005. Morphological effects of local scouring in step-pool streams. *Earth Surface Processes and Landforms 30*: 1567–1581. DOI: https://doi.org/10.1002/esp.1217
15. Marion A, Tregnaghi M, Tait S. 2006. Sediment supply and local scouring at bed sills in high-gradient streams. *Water Resources Research 42*: 1–11. DOI: https://doi.org/10.1029/2005WR004124.
16. Marchi L, Cavalli M, Cucchiaro S, Beinat A, Crema S, Cazorzi F, Llena M, Vericat D. 2018. Geomorphic effectiveness of check dams in a debris-flow catchment using multi-temporal topographic surveys. *Catena 174*: 73–83. DOI: https://doi.org/10.1016/j.catena.2018.11.004.
17. Boix-Fayos C, Barberá GG, López-Bermúdez F, Castillo VM. 2007. Effects of check dams, reforestation and land-use changes on river channel morphology: case study of the Rogativa catchment (Murcia, Spain). *Geomorphology 91*: 103–123. DOI: https://doi.org/10.1016/j.geomorph.2007.02.003.
18. Bombino G, Gurnell AM, Tamburino V, Zema DA, Zimbone SM. 2009. Adjustments in channel form, sediment calibre and vegetation around check-dams in the headwater reaches of mountain torrents, Calabria, Italy. *Earth Surface Processes and Landforms 34*: 1011–1021. DOI: https://doi.org/10.1002/esp.1791
19. Fortugno D, Boix-Fayos C, Bombino G, Denisi P, Quiñonero Rubio JM, Tamburino V, Zema DA. 2017. Adjustments in channel morphology due to land-use changes and check dam installation in mountain torrents of Calabria (southern Italy). *Earth Surface Processes and Landforms 42*: 2469–2483. DOI: https://doi.org/10.1002/esp.4197
20. Zema DA, Bombino G, Denisi P, Lucas-Borja ME, Zimbone SM. 2018. Evaluating the effects of check dams on channel geometry, bed sediment size and riparian vegetation in Mediterranean mountain torrents. *Science of the Total Environment 642*: 327–340. DOI: https://doi.org/10.1016/j.scitotenv.2018.06.035.
21. Galia T, Škarpich V, Hradecký J, Přibyla Z. 2016. Effect of grade-control structures at various stages of their destruction on bed sediments and local channel parameters. *Geomorphology 253*: 305–317. DOI: https://doi.org/10.1016/j.geomorph.2015.10.033.
22. Martín-Vide JP, Andreatta A. 2009. Channel degradation and slope adjustment in steep streams controlled through bed sills. *Earth Surface Processes and Landforms 34*: 38–47. DOI: https://doi.org/10.1002/esp.1687.

@seismicisolation

23. Rinaldi M, Surian N, Comiti F, Bussettini M. 2013. A method for the assessment and analysis of the hydromorphological condition of Italian streams: the Morphological Quality Index (MQI). *Geomorphology 180–181*: 96–108. DOI: https://doi.org/10.1016/j.geomorph.2012.09.009.
24. Galia T, Škarpich V. 2017. Response of bed sediments on the grade-control structure management of a small piedmont stream. *River Research and Applications 33*: 483–494. DOI: https://doi.org/10.1002/rra.3111.
25. Galia T, Škarpich V, Ruman S. 2021. Impact of check dam series on coarse sediment connectivity. *Geomorphology 377:* 107595.DOI:https://doi.org/10.1016/j.geomorph.2021.107595.
26. Smažák I. 2017. Grain-size analysis of bed sediments of the Velká Hanzlůvka Stream. Bachelor thesis. University of Ostrava, Czechia.
27. Galia T, Škarpich V, Ruman S, Macurová T. 2019. Check dams decrease the channel complexity of intermediate reaches in the Western Carpathians (Czech Republic). *Science of The Total Environment 662*: 881–894. DOI: https://doi.org/10.1016/j.scitotenv.2019.01.305.
28. Piton G, Carladous S, Recking A, Tacnet JM, Liébault F, Kuss D, Quefféléan Y, Marco O. 2017. Why do we build check dams in Alpine streams? An historical perspective from the French experience. *Earth Surface Processes and Landforms 42*: 91–108. DOI: https://doi.org/10.1002/esp.3967.
29. Piton G, Recking A. 2015. Design of sediment traps with open check dams. I: hydraulic and deposition processes. *Journal of Hydraulic Engineering 142*: 04015045. DOI: https://doi.org/10.1061/(asce)hy.1943-7900.0001048.
30. Liébault F, Gomez B, Page M, Marden M, Peacock D, Richard D, Trotter CM. 2005. Land-use change, sediment production and channel response in upland regions. *River Research and Applications 21*: 739–756. DOI: https://doi.org/10.1002/rra.880.
31. Škarpich, V., Kubín, M., Galia, T., et al. (2018). Impacts of gravel-bed rivers transformation on fluvial ecosystems and human society: Examples from the Czech flysch Carpathians. Paquier A and Rivière N (eds). E3S Web of Conferences *40*: 02005. DOI: https://doi.org/10.1051/e3sconf/20184002005.

@seismicisolation

13

French Experience With Open Check Dams: Inventory and Lessons Learnt Through Adaptive Management

Simon Carladous[1], Guillaume Piton[2], Damien Kuss[1], Gilles Charvet[3], Romain Paulhe[3], Maxime Morel[2], and Yann Quefféléan[1]

13.1. INTRODUCTION

Within a torrential watershed, several complementary facilities can protect people, housing, networks, and facilities against floods and debris flows. Classical closed-type check dams completed with reforestation and soil conservation bioengineering are very common in headwaters to prevent erosion near the source and stabilize streambeds and hillslopes [1–3]. Closer from assets are found dykes, bank protection, and open check dams interacting with solid transport, i.e. boulders, gravel, and wood, before it reaches elements-at-risk [4].

Open check dams, also called sediment traps, open sabo dams, torrential barriers, or debris basins, are widely used protection structures across Europe and Asia [5–7]. Historically, from the end of the nineteenth century onward, some "places de dépôt" (deposition zones) were set up in European torrents but remained confined to limited volumes because they should be manually dredged [8, 9]. Mechanically dredged structures emerged just after World War II. However, in France, most open check dams were built during the 1980s and 1990s by the French torrent control service (ONF-RTM). The number of new construction decreased in France since the 2000s [10]. We started this analysis notably to understand why. The first hypothesis is a reduction in the financial resources allocated for building this type of structure, either directly by the State in State-owned lands or by subsidies for municipality projects. Second hypothesis is that maintenance experience sheds light on several problems such as downstream incision and excessive dredging costs. Third hypothesis is that design is not so easy in practice. A field general inventory and a second step of focus on structures on which lessons could be learnt and share were thus undertaken.

The used method of research involved four main steps. (i) A GIS general inventory of French open check dams, whose methodology is detailed in Section 13.3.1, enabled to sort them according to storage capacity and main functions. (ii) A more detailed inventory was implemented by field ONF-RTM officers for "large" open check dams, i.e. with retention capacity > 1000 m^3. As explained in detail in Section 13.4.1, data were gathered on design context, type of processes experienced, elements-at-risk, structural components, maintenance history, and malfunctions. (iii) In-depth surveys on a dozen of selected structures involved a watershed analysis, description of local peculiarities, redefinition of structure objectives, and functional and structural analysis. By exchanging with several specialists on the same site, this analysis of existing structures enabled to identify the adaptations performed during the

[1] *ONF, Département Risques Naturels, Grenoble, France*
[2] *Univ. Grenoble Alpes, INRAE, ETNA, Grenoble, France*
[3] *ONF-RTM, Agence Alpes du Nord, Service de Savoie, Chambéry, France*

Check Dam Construction for Sustainable Watershed Management and Planning, First Edition.
Edited by Zhanbin Li, Peng Li, Yang Yu, Peng Shi, and Guillaume Piton.
© 2022 John Wiley & Sons, Inc. Published 2022 by John Wiley & Sons, Inc.

@seismicisolation

structure life so far but also those that would be necessary to improve its functioning, in view of the malfunctions observed or to be feared. Examples are provided in Section 13.5. (iv) Finally, the confrontation of this experience feedback with the recent development of scientific knowledge has made it possible to establish an approach not only for the design of new structures but also for the diagnosis of existing structures. This point is discussed in Section 13.6.2.

Reanalyzing failures through case studies [11–13] and malfunctioning of existing structures [14–20] help better designing new structures and anticipating suitable adaptation of similar existing ones. This chapter provides for the first time a perspective on the French experience in designing and maintaining open check dams. To the best of our knowledge, the only existing similar analysis at country scale is the report published by Hübl et al. [21] in German on Austrian structures. Obviously, many uncertainties remain at each stage of this approach, but we hope that sharing our past mistakes and the lessons we learnt will prevent their potential reproduction elsewhere. The chapter first recalls what are the main functions and type of open check dams. It secondly provides an overview of the French inventory and the main malfunctions identified. It thirdly focuses on three examples of structure adaptations and finally discusses the main lessons learnt and our new design and diagnosis protocol.

13.2. BASIC FEATURES OF OPEN CHECK DAMS

13.2.1. Structure Functions and Control of Deposition

Open check dams and sediment traps intend to control solid transport (boulders, cobbles, gravel, and large wood) with the main goal of protecting downstream elements-at-risk as buildings and roads. To be more precise, four main functions can actually be achieved by open check dams [22]: (i) "sediment retention," i.e. trapping of a given sediment *volume* before dredging (long-term retention closed check dams are different structures, see discussion of [23]); (ii) "solid transport dosing," i.e. sediment *discharge* buffering; (iii) "boulder trap," also called debris flow breaker because they break *debris flow fronts* and store big *boulders* that would likely clog downstream narrow section; and (iv) "large wood traps" to store *logs* that would have a similar obstruction adverse effect.

Understanding of the processes leading to deposition is crucial to achieve such selective trapping. Zollinger [7] highlighted that four mechanisms interact and eventually lead to deposition (Figure 13.1a). The first two mechanisms are driven by basin geometry. (i) An eventual slope break at the basin entrance results in a loss of flow energy and thus a decrease in transport capacity. (ii) The flow spreads if the basin is widened, dropping shear stresses and thus decreasing transport

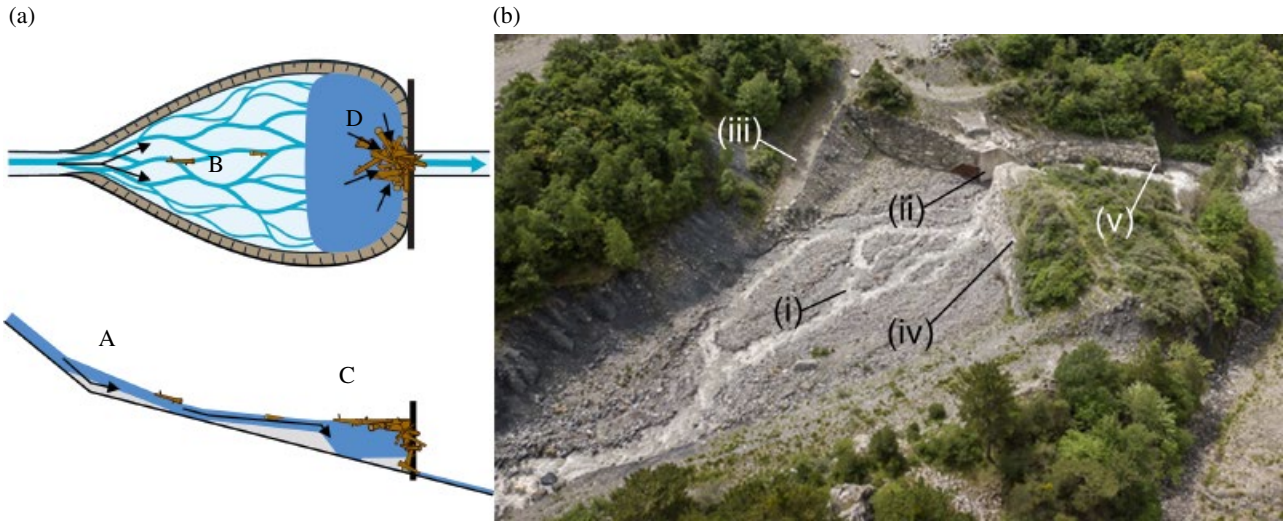

Figure 13.1 (a) Schematic top view and side view of bedload depositing in a basin due to (A) slope break, (B) flow spreading, (C) flow velocity drop in the barrier backwater, and (D) mechanical blockage at the barrier, and (b) drone view of the Saint-Martin torrent upper sediment trap (Saint-Martin-la-Porte, France) with (i) deposition basin, (ii) slit barrier, (iii) access track, (iv) side dikes, and (v) scouring protection. A natural slope break and upstream armored bed makes an inlet structure unnecessary. *Source:* Picture courtesy of Alban Pernet.

@seismicisolation

capacity too. The two other mechanisms are driven by the barrier. (iii) "Hydraulic control" refers to a delta-like deposition in the water accumulating upstream of the barrier during the event. (iv) "Mechanical control" refers to the blocking of elements that are too large to pass through the openings, especially boulders and large wood. Depending on the barrier and basin geometry and the type of torrential phenomenon, combination of these mechanisms may facilitate (or not) deposition.

13.2.2. Structure Components

Natural slope breaks and/or widening of the streambed are consequently best-suited location for open check dams because sediment deposition naturally occurs in such areas. An open check dam merely increases the thickness and volume of the deposit [24]. In addition to the basin and barrier, a sediment trap is made up of several components (Figure 13.1b), each having a specific function to achieve, as detailed in the French guideline of Deymier et al. [25] inspired by Zollinger [7]:

- The basin (or deposition area) is where material will be stored, and its trapping capacity may be modified by widening and/or reducing the bottom slope;
- The outlet barrier filters the solid discharge: its shape drives the main structure function (see §13.6.1);
- An upstream inlet structure eventually guides flows at the basin entrance and stabilizes the upstream streambed profile against headwards erosion if the basin is dredged too deeply;
- A scour protection prevents the scouring of foundations (at inlet foot, at barrier foot, and eventually along certain portions of the side dikes);
- The lateral dikes confine and guide flows to the downstream outlet barrier and prevent its outflanking;
- An access track facilitates access to engines for maintenance operations.

Not all components are systematically encountered on every open check dam, especially on sites with natural channel confinement and/or bedrock outcrops. The basic features of any open check dams are a deposition basin, an access track, and a barrier.

13.2.3. Design Events

The previously mentioned trapping mechanisms vary with flood features as discharge and grain sizes. These parameters should be estimated for the whole range of events that the structure may eventually experience to design the various structure components:

- The "routine" events do not cause damage. Full transfer of water and solid discharge must be sought for these events to minimize maintenance. Barrier bottom opening and basin guiding channel are designed using routine event features;
- The "project" (or "design") event is used to design the trapping capacity and central part of the barrier in order to achieve one or more functions with freeboard;
- The "safety-check" events are used to design side dikes preventing lateral overflowing and a spillway preventing barrier outflanking which must be above and wider than the openings (5 m-wide slits cannot be considered spillways and are regularly obstructed by boulders up to the crest, e.g. [26]). Safety-check events correspond to the range of events more intense than project events for which the structure should not failed;
- The "danger" event is used to raise awareness that above a certain magnitude, the structure stability is no longer guaranteed, and failure is likely to occur (but not sure). It is most of the time associated with barrier outflanking (zero freeboard on spillway wings) or barrier scouring excess.

It should be noted that this design process based on differentiating these different levels of events is very recent and inspired by standards on flood retention dams [27]. There was a lack of specifications in technical guidelines available at the time of construction of most of French open check dams (the only known reference was [7]). In practice, the volume design was mainly guided by the last known event of high magnitude and the room available on the chosen site, without necessarily specifying a design event with a known return period. Concerned by chronic deposits, the designers tailored solutions empirically to limit material trapping during the routine events as e.g. guiding channel in basins (see Manival torrent below or e.g. Figure 7 of [10]), bottom outlet (see Saint-Martin and Claret torrents below). In many cases, such adaptations were initially planned but not built due to lack of available funding.

13.3. OVERVIEW OF THE FRENCH EXISTING OPEN CHECK DAMS

13.3.1. Selection of Structures to Be Inventoried

Solid transport deposition and management also take place out of open check dams. The advent of earth-moving machines has favored regular clean-up

@seismicisolation

operations in other areas: directly in steep reaches or at deposition areas (natural or upstream of closed dams). As this inventory aims at providing feedback on open check dams, dredged sites without outlet barriers were considered as "solid transport regulation areas" and were excluded of the inventory. Some open check dams are no longer dredged: these sediment traps became solid transport regulation areas. Their barrier now acts as classical closed check dams merely generating bed-load transport regulation by transient deposit during high solid concentration event and latter spontaneous re-erosion [28]. This operational adaptation usually resulted from excessive maintenance cost and/or chronic downstream incision, while residual risk was considered reasonable. Finally, structures of more than 1000 m^3 and less than 1000 m^3 were differentiated: a detailed feedback was requested for the firsts, while only information on the location was collected for the latter.

Out of 394 structures located in French mountain areas (Northern and Southern Alps, Pyrénées), 330 were included in the inventory, excluding 28 solid transport regulation zones, 17 sediment traps transformed into solid transport regulation zones, and 19 structures that have been removed from the inventory after field visit and checking of data availability.

13.3.2. Structure Number: Regional and Temporal Trends

About 50% of the 330 sediment traps inventoried have a retention volume < 1000 m^3, 22% are between 1000 m^3 and 5000 m^3, 26% are between 5000 and 50 000 m^3, and 2% are > 50 000 m^3. The Northern Alps host 79% of the total number and 73% of the structures larger than 1000 m^3 (Figure 13.2a). They are several reasons to this higher concentration of structures in this region, among them a higher density of elements at risks, stronger influence of the past glaciation on valley geomorphologies inducing more frequent disconnections in alluvial systems, and associated chronic sediment deposition issues [1, 29]. For these same 330 sediment traps, 20% are located in public forests having the specific status of Restoration of Mountain Land (RTM) and are maintained by the French State. All other sediment traps are under the responsibility of the local authorities.

The construction date is known for 311 of the 330 selected structures. Figure 13.2b highlights the clear growth of structure number during the 1980s and 1990s, but also the decrease in their construction rate from the 2000s onward. This slowdown is likely due to

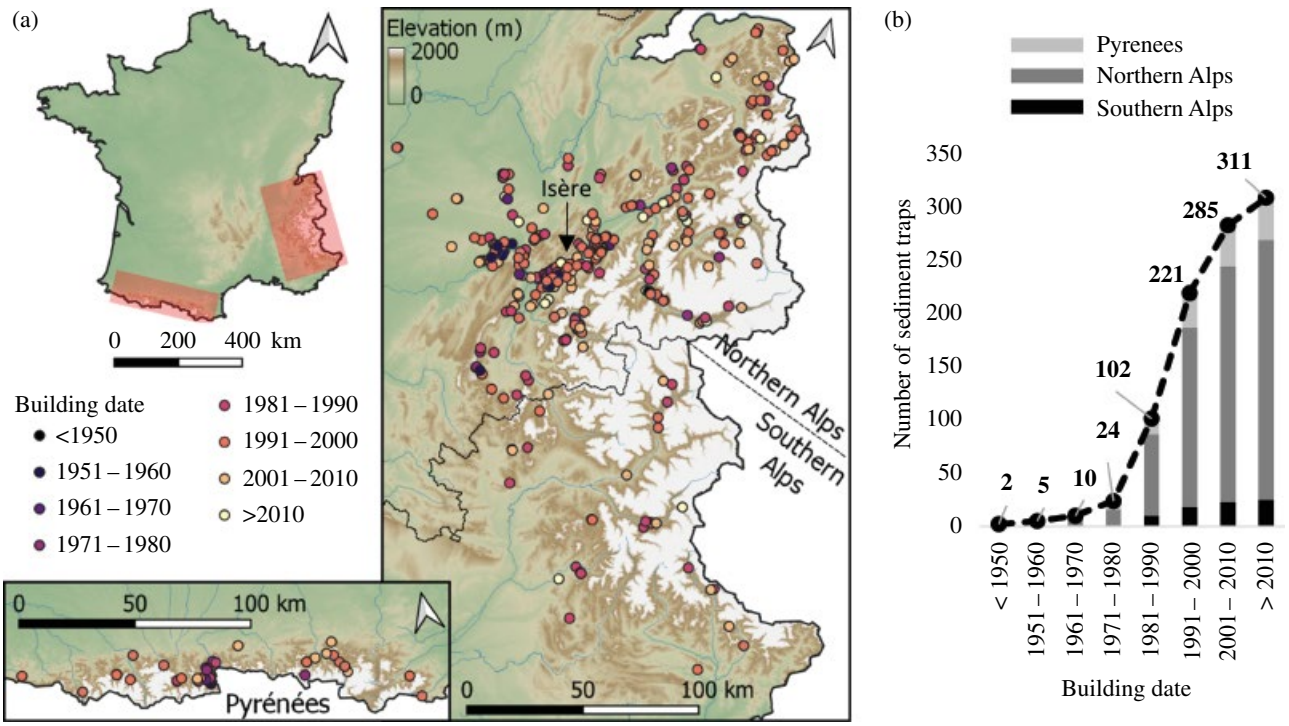

Figure 13.2 (a) Location of structures inventoried and (b) cumulative evolution over time of open check dam construction in France (all volumes combined).

@seismicisolation

several reasons: the investment cost was too high in relation to the available financial resources; the maintenance efforts proved to be higher than expected on existing structures (see next section); the difficulties in real estate acquisition to build these structures, as well as increases in regulatory constraints both on land development (the rule used in France is not to allow new urban development even though open check dams or other protection measures were built, in fear of their failure – see [30]) and environment: in line with the EU Water Framework Directive and the concept of sediment river continuity [31] wherever it is possible, dredged sediment must now be replenished downstream, which is also more expensive. Note that for alluvial fans disconnected from downstream rivers, whether naturally due to river migration or artificially because of river embankment, sediment connectivity is lost and chronic deposition with higher torrential hazard is the rule [32]. In such cases, trapping sediment and stabilizing sediment sources is the only solution to protect elements-at-risk located on the fan. The biggest cluster of structures that can be seen on Figure 13.2a is for instance located in the wide Isère alluvial plain where many torrents flow in drainage ditches with slope so gentle that it cannot accommodate any bedload transport. The only other option would be to abandon these sites and to let the whole alluvial fan grow again until sediment connectivity is recovered.

13.3.3. Type of Structures

Barriers can be equipped with basal or full opening (one or several slits or slots), partially or totally closed by grills (Figure 13.3).

Among the 164 sediment traps larger than 1000 m^3, 60% are equipped with bars in the barrier openings, the most common configuration being horizontal bars. 70% of the barriers are slit dams, most of them being single slit. Finally, 11% are slot barriers, horizontal slots (i.e. width > height) being almost not used. Some techniques are found only in certain regions: arch dams with bottom openings (nozzles and small gutters) for instance in the Luchon's valley (Pyrenees) where ONF-RTM officers were inspired by flood retention dams.

Rudolf-Miklau and Suda [33, 34] suggest now in Austrian standards to use series of open check dams on torrents; each structure having a specific function tailored to the site peculiarities: e.g. trapping boulder and large wood first and secondly a retention structure (e.g. [35]). This is not the choice that has been made so far in France because of budget limitations.

The function of 95% of the inventoried structures is sediment transport retention. It highlights that the practice in France was conservatively to seek trapping most of solid volume transported by floods. Lacking comprehensive design criteria, designers selected conservative options: it was thought better to trap too much sediment than too little. However, after several years of operation, chronic and regular deposition was observed on most structures (see §13.4.3). This led to the two main undesirable side effects [16, 36]. (i) Sediment starving downstream of structures triggered rapid incision, scouring of banks and of bridges and weirs, requiring to build series of new check dams and/or a flow channel with a solid apron downstream of the sediment trap to stabilize the streambed and avoid its incision. (ii) Often immediately after complement, high frequency of dredging and its cost often called into question the fact of allowing more sediment to pass through, which was considered uncertain, potentially dangerous due to insufficient understanding of the processes at work, and thus rarely done until recently (see §13.5). It should be stressed that French open check dams were built before the publication of most scientific works dedicated to this topic. Consequently, in most French sites, a single structure is often intended to perform several functions, e.g. a large retention

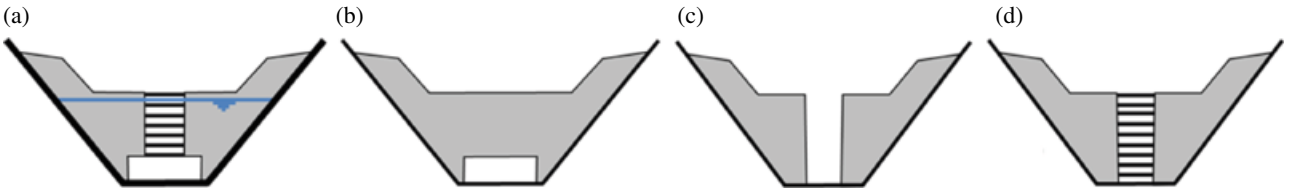

Figure 13.3 Elementary types of opening in barriers: (a) slit dam with horizontal bars and a basal slot; (b) slot dam; (c) slit dam; (d) slit dam with horizontal bars. *Source:* Adapted from Piton and Recking [10].

@seismicisolation

structure will also trap boulders, cobbles, gravel, and large wood with poor control of the interaction that may emerge (see e.g. [37]).

Only three structures inventoried were designed with the specific function of boulder trap and three other aims at dozing solid transport. Ten large wood traps were inventoried, but a complementary inventory would be necessary because many other of these structures are also located on small rivers, upstream of small hydraulic structures (culverts, pipes).

13.4. MAINTENANCE FEEDBACK

13.4.1. Template Form for Structure Inventory

In order to conduct a general appraisal on works, a template form was drawn up and divided into seven sections:

1. *General:* geographical location (department and watershed name), construction administrative elements (year of construction, project managers, and designer), and precise location (altitude and GIS coordinates).

2. *Natural phenomena:* upstream catchment features (geomorphological parameters, vegetation cover, geology, and type of most common torrential phenomena), natural phenomena (main event that led to the creation of the sediment trap, design events), and grain sizes of the supplied material (mean diameter and range of diameter of boulders).

3. *Elements-at-risk:* protected elements (housing and networks) that may be affected by torrential phenomena in the absence of the structure.

4. *Existing complementary torrent control structures:* general description of complementary works located both upstream and downstream (drainage, diversion, check dam series, dykes, and other sediment trap); detailed description of the structure itself (assigned function, initial and current retention capacity, barrier outlet features and, if present, upstream inlet structure and side dikes).

5. *Management and maintenance of the sediment trap:* history of past dredging (years of completion, cost, supply stored in the sediment trap during each flood, volumes of material dredged and their destinations); list of maintenance or modification/improvement works.

6. *Malfunctions:* list of the major malfunctions observed or foreseeable during future events and/or in the long term. The adaptations implemented or to come on the structure are also described.

7. *References:* main existing studies, officer and date of filling, availability of pictures, plans and topographical data.

Parts 1–4 are a simplified, but factual, description of the structure environment, the torrential hazards it is supposed to act on and the functional characteristics, particularly of the barrier. Parts 4–6 identify malfunctions that occurred or are expected. Adaptations are most often proofs of malfunctions, ill design, or misunderstanding during the design. It must be stressed that malfunctions observed or foreseeable can affect both the sediment trap and its side effects, for instance on the downstream channel. For instance, if one of the downstream structures was implemented after the sediment trap, it may indicate a malfunction of the latter. Excessive dredging costs can also be seen as a malfunction, sometimes leading to an operational failure. The capacity of the structure to meet the expected objective was also reported in order to identify any malfunctioning of the entire structure rather than of its components. With the available time and data, inventory sheets were completed by the ONF-RTM services for 115 out of the 164 structures with a retention capacity > 1000 m^3.

13.4.2. A Good Opportunity to Appraise Costs of Dredging

Dredging cost can be a large share of the structure total cost at the life cycle timescale. The inventory was a good opportunity to gather data on the cost of cleaning and dredging open check dams. Only dredging operation with volume bigger than 1000 m^3 are considered: for smaller volume, costs are more driven by the flat rate costs related to bring the earth-moving machinery on the site than by the actual volume to dredge.

Figure 13.4 shows that what is made of the material, i.e. its destination, plays a key role on dredging costs. The most expensive (median value of 14 €/m^3) is to replenish sediment in the downstream river system in order to maintain river quality status, though we only have five data. Conversely, whenever the trapped sediment is of sufficiently good quality to be reused for construction purpose, it is much cheaper (median value of 3 €/m^3). It can be done for free or even against payment for extremely good material (such cases were considered exceptional and not considered). Evacuation, partial replenishment, or storage on site are in between these two extreme cases. Note that large data samples are available only for material that was

@seismicisolation

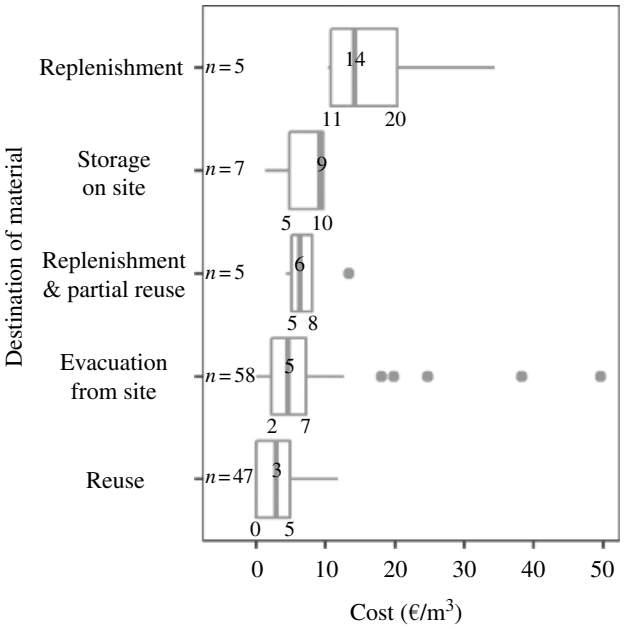

Figure 13.4 Variability of dredging costs depending on destination of the excavated material for n = 122 dredging operations in several open check dams from the Alps with volume dredged > 1000 m³. The central mark and black number in the boxplot indicate the median, and the left and right edges and gray numbers indicate the 25th and 75th percentiles, respectively.

reused or evacuated. The variability in dredging cost can be explained by e.g. exceptionally high cost to bring the earth-moving machinery on remote sites, variable ease of dredging the material (granular material is easier than muddy), and distance on which material must be transported on access tracks of very variable quality or necessity to open new access tracks on rarely dredged sites.

13.4.3. Most Frequent Malfunctions Identified

Of the 115 detailed inventory sheets completed, no malfunction was noted for 67 (58%) of them. This can be explained by (i) the good functioning of these structures, but also (ii) by the fact that some malfunctions could be considered as minor and did not deserve to be noted or (iii) by the absence of stresses on these structures, for instance if no event of major or moderate magnitude occurred since their construction. Table 13.1 summarizes the malfunctions reported on the 48 other structures. It differentiates the malfunctions, their potential causes, and related consequences. Malfunctions called differently but actually similar were grouped together. Overall, about 20 types of malfunctions (observed or foreseeable) were extracted and can be clustered into seven main types (hereafter noted as "MF"). Note that some structures experienced several malfunctions. The consequences identified are the direct consequences without an analysis of the real consequences on downstream elements-at-risk (residual risk analysis including the occurrence of the malfunction) having been carried out: this would be an improvement to be made.

According to Table 13.1, the main malfunctions identified are 38 cases, i.e. one-third of structures, of excess in trapping, especially during routine events, leading to a chronic decrease in the retention capacity (MF#1, Figure 13.5a) or to stop dredging because this maintenance is too expensive (MF#6, Figure 13.5b); 21 cases (18% of structures) of barrier outflanking (MF#1, Figure 13.5d); and height cases (7% of structures) of unsuitable location resulting in incision downstream (MF#3, Figure 13.5c). Conversely, only seven cases of barrier structural damage were reported, although it attracts much of the current research effort. Operational or functional failures are actually much more frequent.

13.5. THREE CASES OF ADAPTIVE MANAGEMENT

As shown in Table 13.1, the most reported malfunction is the excess of trapping, especially during routine events. It usually results in significant dredging costs and in bed incision downstream [16, 36]. Adaptation as functional modifications were then made to some structures to cope with this issue (e.g. [38], p. 53). We provide hereafter three detailed examples.

13.5.1. Where Not to Put Grill in Slit Dams

The Saint-Martin torrent experiences a debris flows event on average every seven years ([39], p. 38; [26]). The downstream fan channel is located near residential areas and crosses several local roads and the France–Italy highway on a canal bridge. The risk is mainly due to eventual channel obstruction by boulders of diameter 3–6 m. Such boulders can be found on channel banks and spread across the entire fan [40]. The current protection strategy mainly relies on two sediment traps and an artificial channel on the alluvial fan to transfer debris flows to the Arc River. The upper sediment trap, with a retention volume of 10 000 m³, was built by the State in 1986–1987. Figure 13.6 reports the structure's

@seismicisolation

Table 13.1 List of identified malfunctions, the associated causes, the consequences, and the number (*n*) and frequency (freq) of case reported among all detailed inventory sheets.

Malfunctions	Causes	Consequences	*n* (freq)
MF#1 Trapping excess: stopping of materials and filling for routine event (Figure 13.5a)	• Undersized slot • Vertical bars or slots down to the apron • Openings/channel section too small • Opening/side channel clogged by cobbles or large wood • Not steep enough • Oversized/too large basin • Poor location on the longitudinal profile	• Incision downstream (Figure 13.5c) • Maintenance too expensive (cf MF#6) • Decrease in retention capacity prior to an upcoming project event	38 (33%)
MF#2 Outflanking of the barrier (Figure 13.5d)	• The height of the deposit near the inlet is too high compared to the height of the lateral dikes • Lateral avulsion upstream of the inlet • Access track built to low in the dikes • Wing slopes and dyke crests too low • Dynamic side overflow • Barrier spillway too small	• Trapping failure or partial (cf MF#5)	21 (18%)
MF#3 Location too far upstream of element at risks	• Land constraints • Easier realization (land, financial) on State land (RTM policy) than on municipality or private land	• Incision downstream • Bypassing the structure because the deposit is too steep • Hazard can be due to downstream material recovery (cf MF#7)	8 (7%)
MF#4 Structural damage on the open check dam	• Steel bars damages/destroyed by impacts of boulders • Material wear • Soil compaction • Lateral dike erosion	• Lower structure stability and/or durability	7 (6%)
MF#5 Insufficient storage capacity	• Unsuitable location on the longitudinal profile • Deposition slope lower than the design slope for the design event • Reduction of the capacity by frequent bedload transport • Available space limited by land constraints • Limited construction budget • Lack of knowledge of the design event volume	• Deposit in the downstream channel • Formation of a plug at the confluence with the main river downstream	6 (5%)
MF#6 Lack of maintenance: no more dredging or a long period without dredging after an event (Figure 13.5b)	• Access difficulties, no access • Location too far from elements-at-risk upstream • Materials of poor quality, nonreusable • Storage space limitation • Very costly transfer • Systematic deposit leading to very costly dredging	• Systematic reduction of actual structure retention capacity	4 (3%)
MF#7 Transfer of debris flows downstream of the structure	• Location too far upstream from elements-at-risk and re-erosion of the intermediate reach	• Ineffective protection	1 (1%)

@seismicisolation

Figure 13.5 Illustration of main malfunctions identified for sediment traps: (a) decrease in the retention capacity due to wood logs frequent clogging in the Lavanchon torrent (Saint-Paul-de-Varces, France); (b) no more too costly dredging in the Clavaux torrent (Barcelonnette, France); (c) location too far from elements-at-risk upstream and stopping of materials and filling for frequent floods resulting in downstream bed incision in the Manival torrent, (Saint-Ismier, France); (d) bypass of the open check dam by right side in the Castelvieil ravine (Luchon, France).

history: building, adaptations, and events. The building by the highway manager of the second lower sediment trap in 1995 can be seen as an adaptation to increase the capacity of the global protection system. It is also an example of the easier realization on State land than on municipality land (Table 13.1, MF#3): the initial project for the implementation of the first structure, located in State land, was at the location of the second one (municipality land).

After the two successive debris flows of 1993, the most important adaptation was to decide not to replace the grill in the slit: the former grill dam became a single slit dam (see Adaptation #2 and description of 1993 events in Figure 13.6). This experience led local practitioners to consider slit dams as relevant solutions in debris flows prone watersheds where flooding and damages are not due to the debris flow overall volume that can be damped by the confluence; in these sites, problems rather occur (i) if huge boulders may stop in the channel and obstruct it, for instance at bridges (in this case, the slit dam can trap boulders), or (ii) if the instantaneous flow discharge is much higher than the fan channel capacity (in this case, the slit dam can dose, i.e. buffer the discharge). The protection system

@seismicisolation

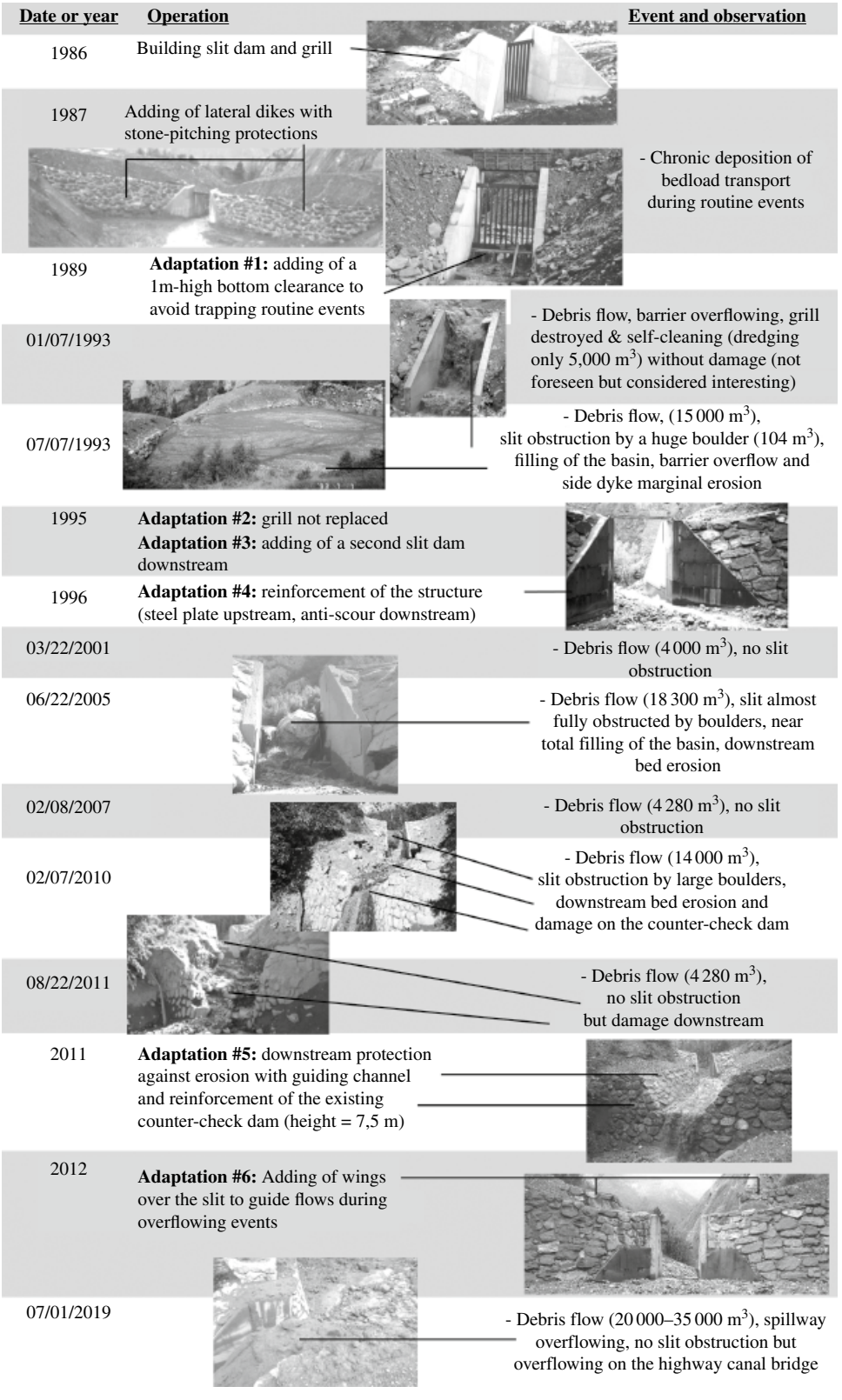

Figure 13.6 Historical design, technical adaptations, and events experienced by the upper sediment trap of the Saint-Martin torrent (Saint-Martin-La-Porte, France). See Figure 13.1b for a general view.

@seismicisolation

functioning was considered satisfying for the five debris flows observed since this adaptation. Slit obstruction sometimes occurs, but events without blockage, are more frequent (Figure 13.6). In addition to the previous functional adaptation, damage was observed on the slit apron and on the barrier downstream face during overflowing. This led to several structural reinforcements with stone pitching and steel plates.

Moreover, it is worth stressing that field observations after five different debris flow events brought evidences of the solid transport dosing function in the second downstream slit dam (Adaptation #3 in Figure 13.6). This structure was designed as a 5-m-wide slit dam from the start, i.e. same width than the upstream barrier. Since its construction in 1995, much lower dredging is required than in the upper dam (only 10 000 m^3 in 2011). One could believe that the dam was never filled but mud marks were observed, sometimes showing slight spillway overflowing, indicating temporary storage during surges. It is however reckoned that the choice of a slit width identical to that of the upstream open check dam does not offer any additional safety with regard to the risk of transit of large boulders, a smaller opening than the upstream one would be better.

13.5.2. Cutting a Slit in a Slot Dam

The Claret torrent experiences a debris flows event on average every two to three years [41, 42]. This tributary of the Arc River crosses and threatens several strategic infrastructures: a doubled-culvert passing below a large canal supplying a hydro-electricity power plant, a departmental road bridge, a canal bridge over the France–Italy highway, the France–Italy railway bridge, and another departmental road bridge before the confluence. A factory is additionally located right in front of the torrent mouth, on the left bank of the confluence and was several times flooded when debris flows dammed the river. Here also, problems on the fan channel occur mostly when large boulders obstruct any of the many crossing structures. Conversely, near the confluence, flooding and damage occur if the debris flow volume exceeds the confluence buffering capacity, dams the Arc River, and eventually triggers channel backfilling in the river and torrent beds.

The current protection strategy mostly relies on an artificial channel conveying debris flows to the Arc River, and on a sediment trap built by the State in 1991, after a significant debris flows in 1987 that caused the obstruction of the doubled-culvert under the hydro-electricity canal and a beginning of overflowing in it. Its retention volume is estimated to be 25 000 m^3, which is actually only about a 10-year return period event, i.e. closer from routine events than from a project design event with return period of a century or more.

The barrier was initially equipped with a 1 m × 5 m bottom outlet and an intermediate 1.5 m × 3 m slot (Figure 13.7a). Facing excessively high dredging costs (on average 17 000 €/year for 6000 m^3 dredged/year between 1991 and 2018) and following the lesson learnt on the Saint-Martin torrent (§13.5.1), the ONF-RTM service proposed, yet in 1995 and again in 2001, to increase the barrier opening into a large slit dam. The managers of the downstream elements-at-risk refused the adaptation but agreed to provide financial support to the dredging operations.

During the major flood of 2008, the Arc River experienced significant incision, thus increasing the confluence buffering capacity. A third study by Koulinski [43] recommended again to increase the barrier opening sufficiently to allow routine event (partial) transfer. The slit should however still trap the large boulders prone to obstruct the downstream structures. After much negotiation and administrative procedure, the work was completed in 2018 (Figure 13.7b). Two criteria were finally used to define the 4-m width slit: (i) it was sufficiently narrow to trap boulders with diameter bigger than 2–4 m (mechanical blockage criterion), and (ii) the total slit section was about the same than each of the doubled-culvert located downstream (hydraulic blockage criterion). Thus, what passes the slit should normally pass the whole fan channel.

Since the cutting, the structure experienced two debris flows on 17 June 2019 (very low magnitude) and on 1 July 2019 (10 000–20 000 m^3). During the latter, only a few large boulders (2–5 m^3) and a limited volume of material (1000–2000 m^3) remained in the basin. Nearly, the whole debris flow was transferred to the confluence with the Arc River without damage. The deposit was reworked by earth-moving machinery to ease its recruitment by the river flows, but at a much lower cost than dredging the sediment trap. The whole system thus functioned as expected. The open check dam is equipped with a monitoring system including a camera and we hope to gather useful data during the next events and compare them with the former functioning [44].

@seismicisolation

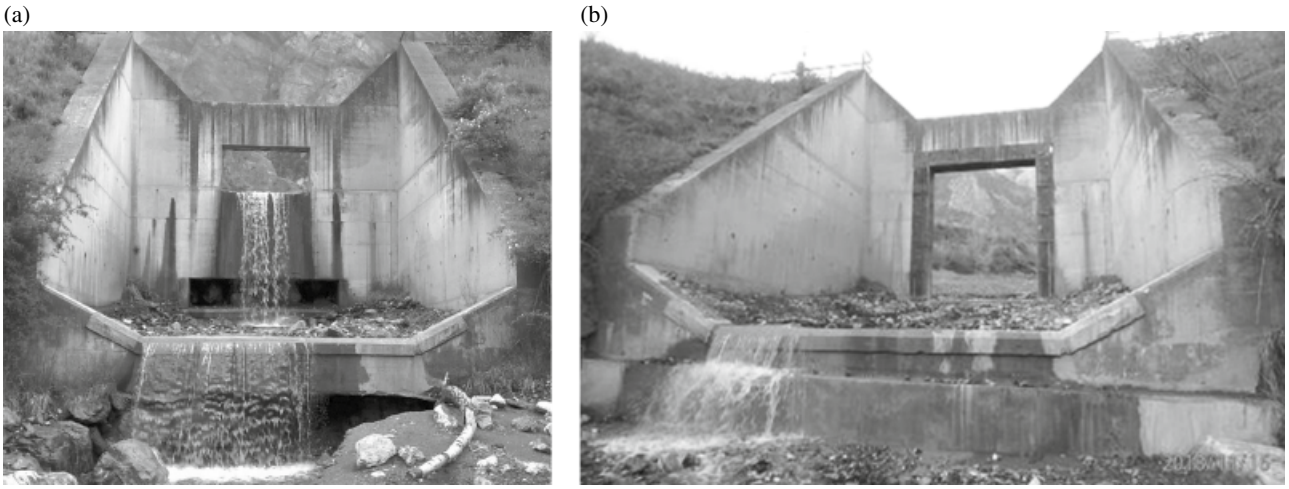

Figure 13.7 Recent adaptation of the open check dams in the Claret torrent (Saint-Julien-Montdenis, France): downstream views in 2018 (a) before (initial design) and (b) after modification.

13.5.3. Adapting Basin Shape and Slope: Adding a Guiding Channel with a Steeper Slope

The adaptation made on the sediment trap of the Manival torrent (Saint-Ismier, France) rather concerns the basin geometry. It is a good example of creating a guiding channel in the basin to promote routine event transfer, knowing that this idea had already guided the initial design of the Saint-Ours torrent's sediment trap (Val d'Oronaye, Alpes-de-Haute-Provence).

More than 10 000 peoples live on the Manival alluvial fan. The State has been building and maintaining a huge protection system in this catchment since the nineteenth century [45]. It is a kind of textbook case of the French torrent control approaches: longitudinal dikes on the alluvial fan (1830–1870); dozens of check dams to stabilize headwaters (1890–1940); two "V"-shape dikes built in 1926 to confine flows in a natural deposition zone (Figure 13.8i and ii); an open check dam, with five vertical slots, created in 1992 to increase the trapping capacity of the basin confined by the V-shape dikes (Figure 13.8vi).

A downstream bed incision was quickly observed (Figure 13.5c and Figure 13.9) due to routine bedload transport fully trapped by the structure [44]: (i) the slope break (Figure 13.1aA) was too important after the dredging operations which promoted the upstream material deposition during the most frequent events; (ii) for less frequent events (without being at the level of the design event), the reaching of the barrier with too narrow slots, in addition to a too wide basin, promotes mechanical blockage at the barrier (Figure 13.1aD). Given this downstream incision, dozens of check dams had to be built downstream in 1999–2000 and later reinforced to stabilize the profile [16]. If we consider the protection objective, the retention capacity of the sediment trap is 15 000 m^3 compared to a retention requirement of 15 000 m^3 for events with a return period of about 100 years and 30 000 m^3 for rarer events, to avoid downstream damage by overflowing [45].

The study undertaken by ONF-RTM 38 [45] proposed the first stage of adaptations, initiated in 2017, with too main goals: (i) upstream the sediment trap, to increase the overall retention volume to 30 000 m^3 for the design event (in this case, rarer than the 100 years return period) by storing 15 000 m^3 of additional material through a promoted lateral overflowing toward an area without any elements-at-risk (forested zone upstream of the basin in Figure 13.8a); (ii) on the sediment trap, to promote routine event transfer while ensuring deposition for less frequent events. In essence, the latter adaptation transformed the basin into a so-called "parallel trap" or "derivation trap" on which the basin can be excavated deeply because it is located on the side of a guiding channel (see e.g. [46]). An inlet structure was added to be obstructed by big boulders and thus divert design events toward the side basin (Figure 13.8iv), a dike was built to form a guiding channel confining routine events (Figure 13.8v), and the basin was excavated deeper than before to maintain the former storage capacity (Figure 13.8vi). Since 2017, the sediment trap is monitored [44] to get feedback on the new functioning of the basin. If

@seismicisolation

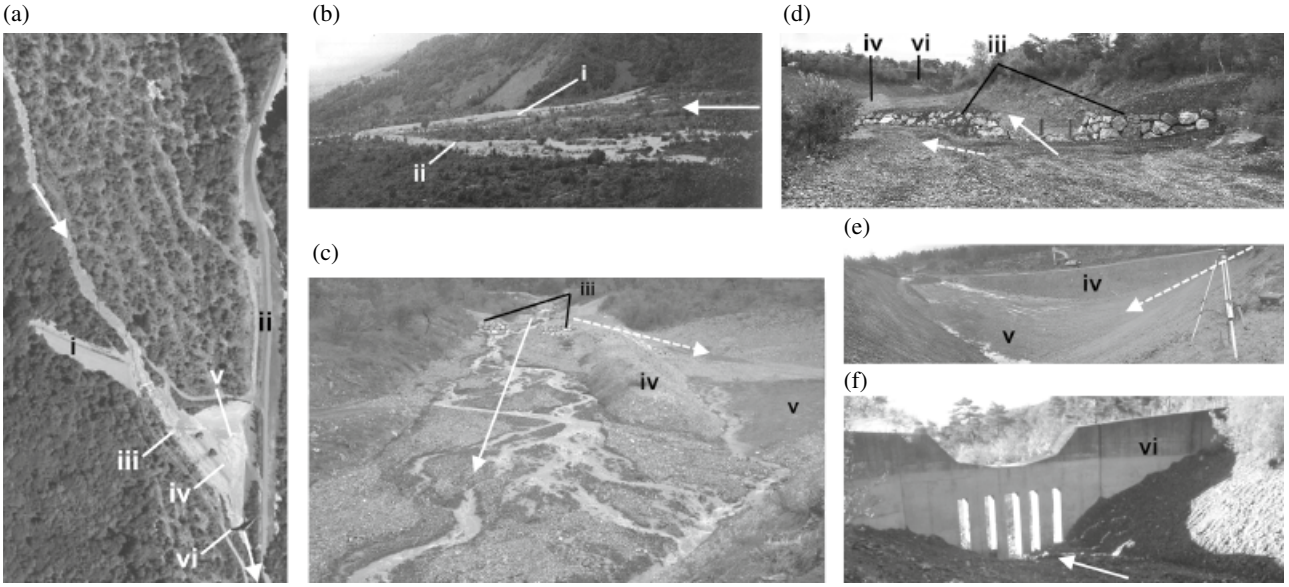

Figure 13.8 Recent adaptations of the sediment trap basin in the Manival torrent (Saint-Ismier, France): (a) aerial view for localization of all the components of the sediment trap with (i) the right bank dike, (ii) the left bank dike, (iii) the flow deflecting inlet structure, (iv) the guiding channel left bank, (v) the excavated lateral basin, and (vi) the downstream slot barrier; (b) far side view of the V-shape dikes in 1929, (c) view from the barrier toward the basin during a routine event with white arrow showing flow trajectory for routine event (continuous line) and design event (dotted line), (d) upstream view of the deflecting inlet structure, e) side view of the basin and guiding channel outer flank (photo during works in 2017), and (f) the outlet slot barrier built in 1992.

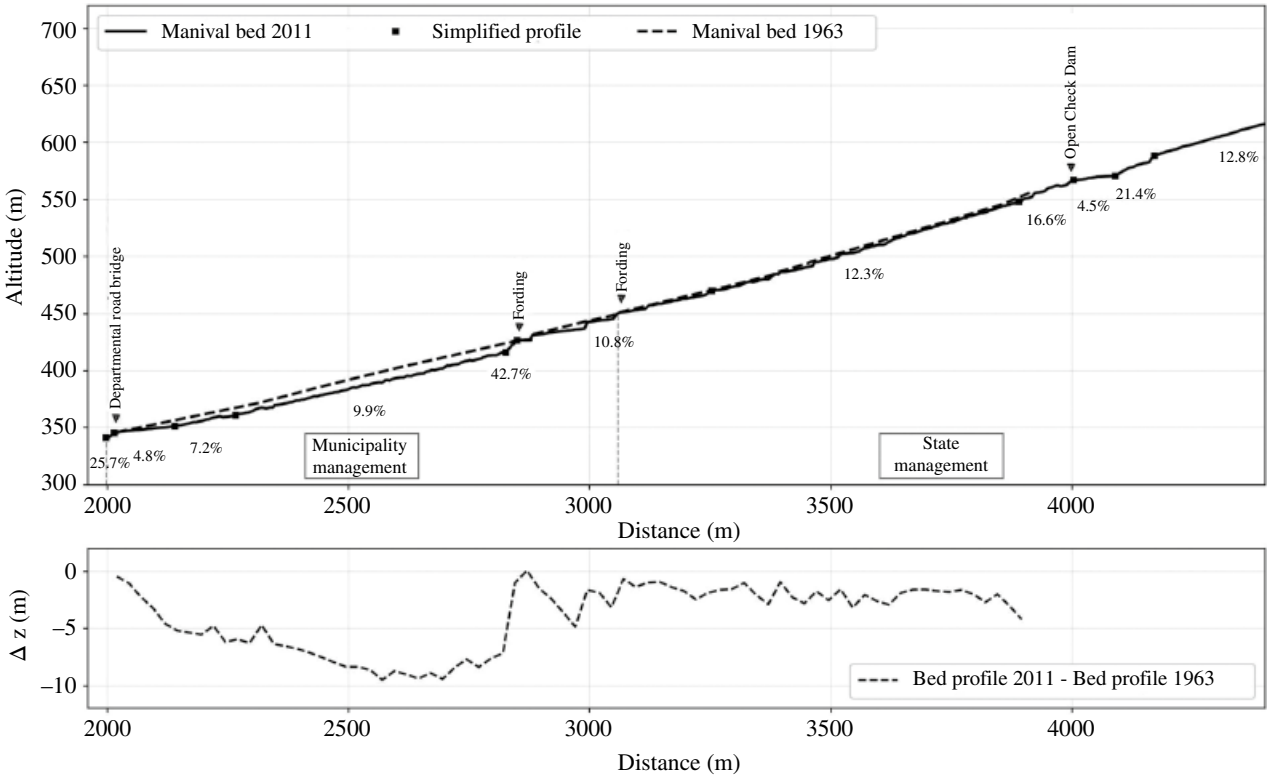

Figure 13.9 Longitudinal profile of the Manival bed downstream of the sediment trap in 1963 and 2011 (upper panel) and change in bed level **Δ**Z between the two dates (lower panel): incision reach up to 10 m. *Source:* Adapted from ONF-RTM 38 [45].

@seismicisolation

additional increase in sediment transfer is desirable, the second stage of adaptation could be to widen the barrier slots, as in the case of the Saint-Martin and Claret torrents.

13.6. DISCUSSION

13.6.1. Selection of Opening Size Adapted to Structure Function

As reported throughout this entire chapter, selecting the suitable function to a structure and the proper associated opening size is crucial when designing open check dams. According to field and laboratory works, the quantile 95%, noted D_{95}, is a relevant proxy of the diameter used for the design [47, 48]. Actually, selecting the opening size is both a matter of choosing which material should be trapped, but also which material should not be trapped. We thus recommend appraising:

- The size of *boulders that could not pass the downstream channel and bridges* (hereafter D_{dw}): if the torrent seems able to recruit and supply such boulders, the barrier openings should be small enough to ensure their trapping;
- The size of cobble, gravel, and small wood *typically transported down to the downstream river system for routine events* (hereafter D_{freq}): openings should be designed to allow D_{freq} to pass, otherwise chronic deposition will occur with many costly side effects.

Table 13.2 is an attempt to associate criteria for the barrier and basin design according to open check dam functions.

We think important to stress that designer must take into account both sediment *and large wood* in their design. Even though most open check dams were not built first to trap large wood, wood pieces are regularly supplied by active torrent [49], interact with barriers [15, 35, 37], and too often disrupt sediment transport during routing events (Figure 13.5a). According to the guidelines of Table 13.2, in typical cases, retention structure should trap 0.2–0.5 m cobbles, thus and opening should be 0.3–0.75 m wide if one considers 1.5 times the grain diameter. Such narrow widths are easily clogged by branches and logs, even during quite low flows transporting small pebbles. To allow routine flow to pass, the best option it to add a well-designed bottom outlet under grids with vertical bars, under vertical slots or under the first bar of grids with horizontal bars [47, 50] or to add an upstream small structure dedicated to large wood and boulder trapping [35].

For sediment transport dozing structures, openings must be designed so that they are not blocked by large wood [51]. To achieve this, possible solutions include (i) setting an inclined grid upstream the structure: water pressure causes the logs to rise along the structure, allowing sediment to pass underneath [15, 35, 52] or (ii) a protective crested siphon or net immediately upstream of the structure [15, 53].

13.6.2. Design and Diagnosis General Recommendations

Given the main malfunctions observed, an approach was created to guide the design or adaptation of structures (Table 13.3, adapted from [10]). The first step of analysis is carried out at the catchment scale to determine the protection objectives, the usefulness of creating a sediment trap, and its possible location on the longitudinal profile (steps #1–#6). The design is then detailed at the scale of components (steps #7–#14). The last step (#15) consists in a cross control of the project feasibility and consistency (spillway, dike height, and closure check dam height): if some inconsistency are found, one must iterate with another design option or a revised the objective (function or magnitude of the design event).

Table 13.3 gives the design general steps without technical and calculation details: a comprehensive review can be found in Piton and Recking [10, 51] for functional design, in Bergmeister et al. [22]; Rudolf-Miklau and Suda [34], and Hubl et al. [55] for structural design, as well as in new publications regularly improving these guidelines. We wish to highlight here the logic of the approach: if it seems theoretically obvious, it is not so obvious to implement in practice. Indeed, many land, environmental, and cost constraints drive project designs. There are for example sediment traps located too far upstream due to land constraints (step #4), and barriers with too small openings because of overconservative choice unsuitable to the upstream supply and downstream channel (step #2). The non-differentiation between routine and project event scenarios (step #1) for the dimensioning of the opening (steps #8 and #9) trigger problems in one-third of structures. An insufficient longitudinal slope of the dikes (step #12) in relation to the height and slope of potential deposition (step #7) trigger outflanking of several barriers. Finally, compensatory measures for long-term side effects are sometimes lacking (step #14)

@seismicisolation

Table 13.2 Potential functions of sediment traps and associated barrier and basin features and design criteria.

		Barrier opening(s)		Basin		
Structure type	Function description	Type	Design criteria	Slope break	Volume	Criteria
Sediment retention	Stopping and temporary storage of transported materials until dredging	Grid or slots, or even slit(s)	Small enough to be clogged by the transported materials ≈ max spacing of typically 1.5–2 times D_{freq}	Marked	Large	Volume of material to be stored before artificial dredging
Solid transport dosing	Reduction of the peak flow rate of transported material and spreading of the solid volume transit over time	Slit(s) or even slot(s)	As large as required and possible: total spacing driven by instantaneous flow rate, each opening being narrower than 1–1.5 times D_{dw}	Limited	Large	Volume of materials to be stored before recovery and self-cleaning
Boulder trapping	Stopping and storage of large boulders only	One or several slits (preferably several)	Very large, typically opening width ≈ D_{dw}	None	Limited	Volume of boulders to be stopped before evacuation by excavators
Large wood trapping	Stopping and storage of large wood that may obstruct downstream sections (size adapted to downstream capacity)	Vertical bars or inclined grid dam or net	Large enough to allow gravel to pass (i.e. $>>D_{freq}$) but narrower than 1/3 times large wood length	Variable		Volume of driftwood and upstream material to be stored before artificial dredging

@seismicisolation

Table 13.3 Main steps for the design of a sediment trap with a filtering closure check dam.

N°	Step	Objective	Description
1	Study of the torrential watershed	Identification of the type of torrential phenomenon (only bedload transport, mainly bedload transport with limited driftwoods, bedload transport, and driftwoods, mainly driftwood transport, debris flows) and flood scenarios (routine, project, safety-check, and danger)	Historical, geomorphological, hydrological, hydro-sedimentary studies
2	Study of downstream flow conditions and assets to be protected	Definition of potential channel malfunction to be prevented	Obstruction by boulders or large wood, insufficient discharge capacity, and probable high aggradation [54]
3	Comparison of several options of protection strategies	Determining the most appropriate protection strategies	Description, investment cost including the strengthening of the channel downstream if necessary, maintenance cost (annual maintenance and dredging)
4	Analysis and comparison of criteria	Identification of the implantation site	Land, topography, accessibility, possibility of evacuating, and storing the dredged material
5	Definition of the objectives assigned to the sediment trap	Assignment of the function(s), definition of its capacity, and choice of the type of barrier	See §13.2.1; §13.3.3, and §13.6.1
6	Structure number and side basin option	Choice according to objectives, finance, and available space	In series, in derivation or several in series
7	Definition of the shape and size of the basin	Determination of its width, length, shape, eventual guiding channel, bottom slope as well as the probable deposition slope to estimate the height of the deposit	Field measurements, archive analysis, and solid transport options available
8	Design of the barrier bottom outlet	Dimensioning of its openings in line with the structure function	According to discharge and D_{95} of routine and design events
9	Compliance with the type of trapping mechanism desired	Checks for consistency between the desired function and (i) the mechanical controls (boulders and driftwood), (ii) the hydraulic control (including eventual head loss associated with large wood)	Cf paragraph §13.2.3, for the project event
10	Design of the barrier spillway	Estimation of the total height, dimensioning of the overflow section and side wings	For the safety-check event.
11	Structural design of the barrier	Choice of the structure type (gravity, cantilever, and frame) and verification of its external and internal stability	Local standard, e.g. Eurocodes (European civil engineering design standards)
12	Design of side dikes	Estimating their height including freeboard, crest slope in accordance with deposition slope, length, cross section wide enough for structural strength, and foot reinforcement	For the safety-check event.
13	Design of the inlet structure	Functional design and structural dimensioning	Transfer of project and safety-check scenarios without lateral overflow
14	Prevention of long-term side effects (bed incision downstream)	Design of scour protection downstream of inlet and outlet structures	Accounting for jet scouring during overflow by safety-check event
15	Final verification of the overall project by cross control	The structure footprint must fit within the available real estate	Ensure that the estimated heights of the side dikes and barrier remain correct and not excessive, otherwise iterate

@seismicisolation

due to an excessively high project investment cost (step #3).

All these observations on existing sediment traps have finally led to the formalization of this approach also applicable to existing structures. It is based on a resumption of a design approach, from the catchment analysis, the identification of the problems to be solved at the level of the elements-at-risk, and thus of the functional objectives given to the sediment trap, to the dimensioning of the various components [3]. Managers must deal with old structures built in a different context. Former constraints regarding land availability, environment, or costs explained design choices on location, shape, or size, which nowadays would be different. Undertaking a detailed diagnosis of existing structures, with a particular focus on past malfunctions and adaptations, is the first step to eventually adapt structures in a world where everything changes: climate, process understanding, finance, societal expectation, and risk perception.

13.7. CONCLUSION

An inventory of the French sediment traps, located in the Alps and Pyrenees, was undertaken. A three-step approach was followed: all known open check dams were first located in a database; detailed inventory sheets were secondly filled to describe 115 structures with retention capacity > 1000 m^3; and finally in-depth reanalysis was performed on a small panel of structures with interesting and rich histories. Among the 330 sediment traps first inventoried, most are in the Northern Alps. Almost all French structures have a main function of sediment transport retention and half of them have retention capacity > 1000 m^3. During the second step, no malfunctions were reported for 60% of 115 structure surveyed. For the other 40%, main identified functional malfunctions were (i) excess in trapping leading to basin too frequently filled and downstream sediment starving, (ii) lateral bypasses of the structure, (iii) structures located too upstream along the channel, and (iv) a lack of regular dredging. During the third step, a methodology with standardized forms was developed and tested allowing clustering and disentangling several failure modes of open check dams. This approach helps to exchange between specialists and field practitioners, to gather information and to improve design and maintenance processes. The comparison of new scientific knowledge with the elements resulting from this field reanalysis provides a wealth of recommendations for the design of new structures and the analysis of potential failures of existing structures.

With improved design and maintenance guidelines and innovative solutions to allow routine events to pass in compliance with the EU Water Framework Directive, it might turn out that a new generation of sediment trap will be implemented in number. For example, the choice of derivation trapping structure is a tried and tested solution both for the design of new structures and for the adaptation of existing structures (e.g. adaptation of the Manival sediment trap). It should also be noted that models can help with these innovative design: the numerical tools are a potential contribution [56, 57], provided that the fields of application and limits are mastered; physical models have already been used to help the design of certain sediment traps [58], especially closure open check dams (Verdarel torrent in Saint-Chaffrey; Combe de Lancey torrent in Villard-Bonnot – [50]), and are a very interesting way, but raise the question of the increase in the cost of study and therefore the investment cost.

Obviously, as usual in torrent control, risk assessment and structure design are and will be done in a context of major uncertainties (poor knowledge of torrential phenomena, surprising effects of structures and unexpected feedback loop or new process) and high constraints (land, environment, and finance). We nonetheless hope that the experience gained for more than 50 years by the French ONF-RTM officers, and partially gathered in this chapter, can be an aid for others and followers.

ACKNOWLEDGMENTS

The work of S.C., D.K., G.C., R.P., and Y.Q. was funded by the Ministry of Agriculture, owner of the RTM public forests, and the Ministry of the Environment, in charge of French risk prevention policy. The work of M.M. and G.P. was performed within the HydroDemo research project funded by the French State through the FNADT-CIMA funds and the European Union through the FEDER-POIA funds (Grant agreement PA0020551). The European Union is committed to the Alpine massif with the European Regional Development Fund (FEDER). The authors would like to thank Christian DEYMIER (ONF-RTM 04) who participated in the preparation of the detailed inventory sheets and all the staff of the ONF-RTM services who completed the detailed inventory sheets and

@seismicisolation

participated in the in-depth feedback on some case studies, as well as Mélanie BRACHET for the internship she carried out on the subject.

REFERENCES

1. Carladous, S., Piton, G., Tacnet, J.M., et al. (2016b). From the restoration of French mountainous areas to their global management: historical overview of the Water and Forestry Administration actions in public forests. *13th INTERPRAEVENT Conf. Proc. Klagenfurt (Austria): International Research Society INTERPRAEVENT*, 34–42. http://www.interpraevent.at/palm-cms/upload_files/Publikationen/Tagungsbeitraege/2016_1_34.pdf.
2. Evette, A, Labonne, S, Rey, F, Liebault, F, Jancke, O and Girel, J (2009) History of bioengineering techniques for erosion control in rivers in western europe. *Environmental Management43*(6): 972–984: DOI: https://doi.org/10.1007/s00267-009-9275-y.
3. Piton, G, Carladous, S, Recking, A, Liebault, F, Tacnet, J, Kuss, D, et al. (2017) Why do we build check dams in Alpine streams? An historical perspective from the French experience. *Earth Surface Processes and Landforms 42* (1): 91–108: DOI: https://doi.org/10.1002/esp.3967.
4. Hübl, J and Fiebiger, G (2005) Chap. 18 - Debris-flow mitigation measures. In: Jakob, M and Hungr, O (eds) *Debris-Flow Hazards and Related Phenomena*. Berlin, Heidelberg: Springer, 445–487: DOI: https://doi.org/10.1007/3-540-27129-5_18.
5. Ikeya, H. (1989). Debris flow and its countermeasures in Japan. *Bulletin - International Association of Engineering Geology 40* (1): 15–33.
6. VanDine, D.F. (1996). Debris Flow Control Structures for Forest Engineering. Res. Br., B.C. Min. For.
7. Zollinger, F. (1985). Debris detention basins in the European Alps. *International symposium on Erosion, Debris Flow and Disaster Prevention*. Tsukuba, Japan: Japan Erosion Control Engineering Society, 433–438.
8. Eaux et Forêts (1911). *Restauration et conservation des terrains en montagne. Première partie, Renseignements généraux*. Imprimerie Nationale http://gallica.bnf.fr/ark:/12148/bpt6k6365750f.
9. Vischer, D.L. (2003). *Histoire de la protection contre les crues en Suisse, Des origines jusqu au 19e siècle*. Série Eaux: OFEG https://www.bafu.admin.ch/dam/bafu/fr/dokumente/wasser/uw-umwelt-wissen/die_geschichte_deshochwasserschutzesinderschweizvondenanfaengenb.pdf.download.pdf/histoire_de_la_protectioncontrelescruesensuissedesoriginesjusqu.pdf.
10. Piton, G and Recking, A (2016a) Design of sediment traps with open check dams. I: hydraulic and deposition processes. *Journal of Hydraulic Engineering 142*(2): 1–23: DOI: https://doi.org/10.1061/(ASCE)HY.1943-7900.0001048.
11. Benito G, Grodek T and Enzel Y (1998) The geomorphic and hydrologic impacts of the catastrophic failure of flood-control-dams during the 1996-Biescas flood (Central Pyrenees, Spain). *Zeitschrift fur Geomorphologie*. *42*(4): 417–437: DOI: https://doi.org/10.1127/zfg/42/1998/417.
12. Horiguchi, T. and Richefeu, V. (2020). Post-analysis simulation of the collapse of an open sabo dam of steel pipes subjected to boulder laden debris flow. *International Journal of Sediment Research 35*(6): 621–635: DOI: https://doi.org/10.1016/j.ijsrc.2020.05.002.
13. Wang, GL (2013) Lessons learned from protective measures associated with the 2010 Zhouqu debris flow disaster in China. *Natural Hazards 69*(3): 1835–1847: DOI: https://doi.org/10.1007/s11069-013-0772-1.
14. Bezzola, G.R. (2008). Unexpected processes in a sediment retention basin - the "stiglisbrücke" basin on the schächen torrent during the flood of august 2005. *INTERPRAEVENT Conference Proceedings*, Dornbirn, Vorarlberg, Austria (May 2008), 271–282. http://www.interpraevent.at/palm-cms/upload_files/Publikationen/Tagungsbeitraege/2008_1_271.pdf.
15. Bezzola, G.R., Sigg, H., and Lange, D. (2004). Driftwood retention works in Switzerland [Schwemmholzrückhalt in der Schweiz]. *INTERPRAEVENT Conference Proceedings*, Riva del Garda, Italy (May 2004), 29–40. http://www.interpraevent.at/palm-cms/upload_files/Publikationen/Tagungsbeitraege/2004_3_VII-29.pdf.
16. Brochot, S., Duclos, P., and Bouzit, M. (2003). L'évaluation économique des risques torrentiels: intérêts et limites pour les choix collectifs de prévention. Ingénieries Numéro Spécial: 53–68. http://www.set-revue.fr/sites/default/files/articles-eat/pdf/GR2003-PUB00011910.pdf.
17. Chen, J, Chen, X, Wang, T, Zou, Y and Zhong, W (2014) Types and causes of debris flow damage to drainage channels in the Wenchuan earthquake area. *Journal of Mountain Science*. Springer *11*(6): 1406–1419: DOI: https://doi.org/10.1007/s11629-014-3045-x.
18. Mihalache, A.L., Marin, M., Davidescu, S¸.O. et al. (2020). Physical status of torrent control structures in Romania. *Environmental Engineering & Management Journal (EEMJ) 19* (5): 861–872.
19. Wang, H-W and Kondolf, GM (2014) Upstream sediment-control dams: five decades of experience in the rapidly eroding dahan river basin, Taiwan. *Journal of the American Water Resources Association*. Blackwell Publishing Inc. *50*(3): 735–747: DOI: https://doi.org/10.1111/jawr.12141.
20. Yang, Y, Fu, S, Liu, B, Sun, B, Liu, C, Wang, Z, et al. (2020) Damage of check dams by extreme rainstorms on the Chinese Loess Plateau: a case study in the Chabagou watershed. *Journal of Soil and Water Conservation 75*(6): 746–754: DOI: https://doi.org/10.2489/jswc.2020.00138.

@seismicisolation

21. Hübl, J., Holub, M., Ganahl, E. et al. (2005). *Checkdam: Evaluierung offener Wildbachsperren unter Lastannahme*. Wien, AUT: BOKU - Institut für Alpine Naturgefahren - Department Bautechnik & Naturgefahren https://boku.ac.at/fileadmin/data/H03000/H87000/H87100/DAN_IAN_Reports/Rep069_-_CHECKDAM_Evaluierung_offener_Wilbachsperren_unter_Lastenannahme.pdf.
22. Bergmeister K, Suda J, Hübl J and Rudolf-Miklau F (2009) *Schutzbauwerke gegen Wildbachgefahren: Grundlagen, Entwurf und Bemessung, Beispiele*. Ernst & Sohn: DOI: https://doi.org/10.1002/9783433600283.
23. Piton, G, Carladous, S, Marco, O, Richard, D, Liebault, F, Recking, A, et al. (2019a) Usage des ouvrages de correction torrentielle et plages de dépôt : origine, état des lieux, perspectives. *La Houille Blanche* (*1*): 57–67: DOI: https://doi.org/10.1051/lhb/2019008.
24. Van Effenterre, C. (1982). Les barrage perméables de sédimentation. *Revue Forestière Française 5*: 87–93. http://documents.irevues.inist.fr/bitstream/handle/2042/21614/RFF_1982_5_87.pdf.
25. Deymier, C., Tacnet, J.M., and Mathys, N. (1995). *Conception et calcul de barrages de correction torrentielle*. Cemagref Grenoble Pegr.
26. Piton, G., Charvet, G., Kuss, D., and Carladous, S. (2020a). Putting a grill (or not) in slit dams aiming at trapping debris flows? lessons learnt from France. *AGHP Technical Notes*. The Association of Geohazard Professionals *1*: 1–5. Available at: https://hal.archives-ouvertes.fr/hal-02701076.
27. Royet, P., Degoutte, G., Peyras, L., et al. (2010) Cotes et crues de protection, de sûreté et de danger de rupture. La Houille Blanche. *EDP Sciences* (*2*):51–57: DOI: https://doi.org/10.1051/lhb/2010018.
28. Piton, G and Recking, A (2016b) Effects of check dams on bed-load transport and steep slope stream morphodynamics. *Geomorphology 291*(Sediment dynamics in alpine basins): 94–105: DOI: https://doi.org/10.1016/j.geomorph.2016.03.001.
29. Carladous, S., Piton, G., Recking, A., et al. (2016a). Towards a better understanding of the today French torrents management policy through a historical perspective. *E3S Web Conf*., Lyon, France (October 2016), 1–11: DOI: https://doi.org/10.1051/e3sconf/20160712011.
30. Philippe, F., Carladous, S., Tacnet, J.-M., and Bouvet, P. (2016). Taking into account protective works in land-use planning for mountain torrential floods: state of the art of present French practices. *E3S Web of Conferences. EDP Sciences* 7: 12003. DOI: https://doi.org/10.1051/e3sconf/20160712003.
31. Habersack, H, Liébault, F and Comiti, F (2017) Sediment dynamics in Alpine basins. *Geomorphology 291*: 1–3. https://linkinghub.elsevier.com/retrieve/pii/S0169555X17302301 DOI: https://doi.org/10.1016/j.geomorph.2017.05.014.
32. Harvey, AM (2012) The coupling status of alluvial fans and debris cones: a review and synthesis. *Earth Surface Processes and Landforms 37*(1): 64–76: DOI: https://doi.org/10.1002/esp.2213.
33. Rudolf-Miklau, F and Suda, J (2011) Technical standards for debris flow barriers and breakers. *Italian Journal of Engineering Geology and Environment*. Università LaSapienza (201103): 1083–1091: DOI: https://doi.org/10.4408/IJEGE.2011-03.B-117.
34. Rudolf-Miklau, F and Suda, J (2013) Chap. 26-Design criteria for torrential barriers. In: Schneuwly-Bollschweiler, M, Stoffel, M and Rudolf-Miklau, F (eds) *Dating Torrential Processes on Fans and Cones*. Springer Netherlands, 375–389: DOI: https://doi.org/10.1007/978-94-007-4336-6_26.
35. Cerato M and Coali R (1997) Open check dams in the Italian alps. *Structural Engineering International 7*(2): 89–91: DOI: https://doi.org/10.2749/101686697780495157.
36. Gruffaz, F. (1996). *Etude de description et analyse des plages de dépôt torrentilles réalisées dans les Alpes et Pyrénées Françaises*. ONF-RTM (Office National des Forêts -Service de Restauration des Terrains en Montagne).
37. Piton, G, Horiguchi, T, Marchal, L and Lambert, S (2020b) Open check dams and large wood: head losses and release conditions. *Natural Hazards and Earth System Sciences 20*(12): 3293–3314: DOI: https://doi.org/10.5194/nhess-20-3293-2020.
38. Piton, G. (2016). Sediment transport control by check dams and open check dams in Alpine torrents. PhD Thesis. Univ. Grenoble Alpes. https://tel.archives-ouvertes.fr/tel-01420209.
39. ONF-RTM 73 (2013a). *Torrent du Saint Martin - Etude de bassin versant*. Office National des Forêts - Service de Restauration des Terrains en Montagne de la Savoie.
40. Hugerot, T. (2020). Trajectoires socio-environnementales des cônes de déjection torrentiels en vallée de Maurienne depuis la fin du Petit Âge Glaciaire. PhD Thesis. Univ. Savoie Mont Blanc. https://tel.archives-ouvertes.fr/tel-03204526
41. Hugerot, T, Astrade, L, Ployon, E and Gauchon, C (2017) Reconstituer les trajectoires paysagères par photo-interprétation semi-automatisée et télédétection : géohistoire d'un cône de déjection torrentiel en vallée de Maurienne (Savoie). *VertigO 17*(2). http://journals.openedition.org/vertigo/18620: DOI: https://doi.org/10.4000/ertigo.18620.
42. ONF-RTM 73 (2013b). *Torrent du Claret - Etude de bassin versant*. Office National des Forêts - Service de Restauration des Terrains en Montagne de la Savoie.
43. Koulinski, V. (2011). *Proposition d'aménagement de la Plage de dépôt du Claret - Rapport technique*. ETRM for Office National des Forêts - Service de Restauration des Terrains en Montagne de la Savoie.
44. Piton, G, Fontaine, F, Bellot, H, Liébault, F, Bel, C, Recking, A, et al. (2018a) Direct field observations of massive bedload and debris flow depositions in open

@seismicisolation

check dams. In: Paquier A and N. Riviere (eds) *E3S Web of Conferences*. paper presented at the RiverFlow 2018. EDP Sciences, 1–8: DOI: https://doi.org/10.1051/e3sconf/20184003003.

45. ONF-RTM 38 (2016). *Forêt domaniale du Saint-Eynard. Etude de Bassin de Risques*. Division domaniale RTM du Manival. Office National des Forêts - Service de Restauration des Terrains en Montagne de l'Isère.
46. Ghilardi, T., Boillat, J.L. Schleiss, A., et al. (2012) Gestion du risque d\' inondation sur l'Avançon par rétention de sediments - optimisation sur modèle physique [Flood risk management of the Avançon river by means of sediment retention-physical model based study]. *INTERPRAEVENT Conference Proceedings*, Grenoble, France (April 2012), 687–698. http://www.interpraevent.at/palm-cms/upload_files/Publikationen/Tagungsbeitraege/2012_2_687.pdf.
47. Moldenhauer-Roth, A, Piton, G, Schwindt, S, Jafarnejad, M and Schleiss, AJ (2021) Design of sediment detention basins: Scaled model experiments and application. *International Journal of Sediment Research 36*(1): 136–150: DOI: https://doi.org/10.1016/j.ijsrc.2020.07.007.
48. Shima, J, Moriyama, H, Kokuryo, H, Ishikawa, N and Mizuyama, T (2016) Prevention and mitigation of debris flow hazards by using steel open-type sabo dams. *International Journal of Erosion Control Engineering*. Japan Society of Erosion Control Engineering *9*(3): 135–144: DOI: https://doi.org/10.13101/ijece.9.135.
49. Ruiz-Villanueva, V, Mazzorana, B, Bladé, E, Bürkli, L, Iribarren-Anacona, P, Mao, L, et al. (2019) Characterization of wood-laden flows in rivers. *Earth Surface Processes and Landforms*. Wiley *44*(9): 1694–1709: DOI: https://doi.org/10.1002/esp.4603.
50. Piton, G, Mano, V, Richard, D, Evin, G, Laigle, D, Tacnet, JM, et al. (2019b) Design of a debris retention basin enabling sediment continuity for small events: the Combe de Lancey case study (France). *Proc. 7th Int. Conf. on Debris-Flow Hazards Mitigation*. paper presented at the International Conference on Debris-Flow Hazards Mitigation: Mechanics, Prediction, and Assessment. Golden, Colorado, USA, 1019–1026: DOI: https://doi.org/10.25676/11124/173113.
51. Piton, G and Recking, A (2016c) Design of sediment traps with open check dams. II: woody debris. *Journal of Hydraulic Engineering 142*(2): 1–17: DOI: https://doi.org/10.1061/(ASCE)HY.1943-7900.0001049.
52. D'Agostino, V., Degetto, M., and Righetti, M. (2000). Experimental investigation on open check dam for coarse woody debris control. *Dynamics of water and sediments in mountain basins*. Bios, 201–212. http://intra.tesaf.unipd.it/people/dagostino/Pubblicazioni/P43_2000.pdf.
53. Lange, D., and Bezzola, G. (2006). Schwemmholz - Probleme und Lösungsansätze [Driftwood - Problems and solutions]. Versuchsanstalt für Wasserbau Hydrologie und Glaziologie der Eidgenössischen Technischen Hochschule (VAW) Zürich. https://ethz.ch/content/dam/ethz/special-interest/baug/vaw/vaw-dam/documents/das-institut/mitteilungen/2000-2009/188.pdf.
54. Piton, G., Recking, A., and Tacnet, J.M. (2018b). An attempt to classify malfunctions of steep channel flows justifying building of open check dams or other torrent control works. *Proc. of the 5th IAHR Europe Congress*. paper presented at the New Challenges in Hydraulic Research and Engineering, 377–378: DOI:https://doi.org/10.3850/978-981-11-2731-1_230-cd.
55. Hubl, J, Nagl, G, Suda, J and Rudolf-Miklau, F (2017) Standardized stress model for design of torrential barriers under impact by debris flow (according to Austrian Standard Regulation 24801). *International Journal of Erosion Control Engineering 10*(1): 47–55: DOI: https://doi.org/10.13101/ijece.10.47.
56. Gonzales de Linares, M., Mano, V., Piton, G., and Recking, A. (2020). Modelling of massive bedload deposition in a debris basin: cross comparison between numerical and small scale modelling. *River Flow 2020: Proceedings of the 10th Conference on Fluvial Hydraulics*, Delft, Netherlands, 7–10 July 2020), 282–289. https://hal.archives-ouvertes.fr/hal-02935173.
57. Kaitna, R, Chiari, M, Kerschbaumer, M, Kapeller, H, Zlatic-Jugovic, J, Hengl, M, et al. (2011) Physical and numerical modelling of a bedload deposition area for an Alpine torrent. *Natural Hazards and Earth System Science 11*(6): 1589–1597: DOI:https://doi.org/10.5194/nhess-11-1589-2011.
58. Couvert, B and Lefebvre, B (1994) Contribution de modèles physiques à l'étude du charriage torrentiel. *La Houille Blanche 3*(3): 81–90: DOI: https://doi.org/10.1051/lhb/1994046.

@seismicisolation

14

Design of Open Check Dams and Their Application in the Wenchuan Earthquake Area

Jiangang Chen[1,2], Huayong Chen[1,2], Xi′an Wang[1,2], and Xiaoqing Chen[1,2]

14.1. DEBRIS FLOW MAGNITUDE AMPLIFICATION AND SECONDARY DISASTERS

The Wenchuan earthquake-affected area exceeded 100 000 km^2 and was concentrated along the Longmen Mountains fault in western Sichuan, China. The main shock attained an intensity of XI at the epicenter, and the number of landslides and rock avalanches was generally estimated to be between 15 000 and 20 000, although certain estimates exceeded 50 000 [1]. Based on remote sensing image data, collapses and landslides produced approximately $2.6 \times 10^9 m^3$ of material [2], providing abundant sources for potential debris flow formation. In particular, debris flow events have been expected to increase in frequency for 10–15 years following the earthquake [3]. A group of debris flows occurred in the Longmen Mountains area after the earthquake. On 24 September 2008, a debris flow triggered by heavy rainfall caused 42 deaths and infrastructure damage in Beichuan County [4]. On 20 August 2019, a strong rainstorm struck Wenchuan County, and a total of 15 debris flows were triggered by this rainfall.

Mitigation engineering in certain catchments failed to regulate the debris flow peak discharge, density, and particle size. The structures were destroyed by large-scale debris flows with a total volume larger than $1.0 \times 10^6 m^3$. Meanwhile, the destruction of these engineering projects amplified the debris flow magnitudes. Detailed cases are described below.

One case was the debris flow in the Wenjia Gully, a tributary gully on the left bank of the Mianyuan River, Qingping town, Sichuan Province, which was strongly affected by the Wenchuan earthquake. The catchment area of the Wenjia Gully is 7.7 km^2, and the length of the main channel is 4.5 km. The average longitudinal gradient of the main gully is 33.8%. There were no debris flow events during the 100 years before the earthquake. The Wenchuan earthquake triggered a large landslide upstream of the gully. The volume of loose deposits reached $50 \times 10^6 m^3$, and the deposits accumulated primarily in the lower part of the channel [5]. At the beginning of 2010, 19 check dams with 5-m heights, 41 bed sills, one 8-m-high check dam, and a 225-m-long drainage channel were constructed at the gully outlet [6] with the design standard of a 20-year return period. On 13 August 2010, 227 mm of rainfall fell during 10 hours in the Wenjia Gully. An extremely large-scale debris flow occurred, and $4.3 \times 10^6 m^3$ of solid material was carried out in the gully [7].

A field survey provided an explanation for the larger scale of the debris flow in the Wenjia Gully in 2010 than in 2008. The results indicated that there were no mitigation measures in Wenjia gully before 2010 and that the debris flow was formed by the convergence of

[1] *CAS Key Laboratory of Mountain Hazards and Earth Surface Process, Institute of Mountain Hazards and Environment, Chinese Academy of Sciences (CAS), Chengdu, China*

[2] *University of Chinese Academy Sciences, Beijing, China*

Check Dam Construction for Sustainable Watershed Management and Planning, First Edition.
Edited by Zhanbin Li, Peng Li, Yang Yu, Peng Shi, and Guillaume Piton.
© 2022 John Wiley & Sons, Inc. Published 2022 by John Wiley & Sons, Inc.

@seismicisolation

upstream water, causing a large-scale mountain torrent that scoured the loose materials on the gully bed and induced an erosional debris flow. Furthermore, the slope stability was greatly reduced by rainfall infiltration and the consequent fluidized debris flow. The superposition of the two types of debris flows increased the magnitude of the event, creating a very large-scale debris flow. Certain mitigation projects had been constructed within the channel; if these mitigation measures had withstood the impact of the debris flow and the destruction caused by downward erosion, the check dams would not have outbreaks, and the debris flow volume would not have been amplified [8]. According to Liu [9], the volume of 2010 debris flow in Wenjia gully was 7.6 times that in 2008 without mitigation engineering. The peak discharge at the gully outlet reached approximately 1100 m^3/s [10]. Due to the successive destruction of the check dams in the midstream of Wenjia Gully (Figure 14.1a), the slide mass was eroded by the debris flow, and a 10- to 100-m-wide, 40- to 60-m-deep incision was scoured (Figure 14.1b).

Another case was the debris flow disaster in Zhouqu County, Gansu Province. This county is located at the fan of Sanyanyu Gully and is a tributary on the left bank of the Bailongjiang River. Its drainage area is 21.8 km^2, and the length of the main gully is 10.4 km. The elevation at the highest point is 3825 m; the elevation at the gully mouth is 1317 m, so the maximum relative height difference is 2508 m; thus, the gradient ratio of the main gully is 19.6%. The terrain is generally low in the south and high in the north, forming a typical alpine canyon landscape. Eleven large-scale debris flows have occurred in the Sanyanyu Gully in the past [11]. Very large-scale debris flows induced by rainstorms at the Sanyanyu and Luojiayu gullies on 8 August 2010 caused 1765 deaths and disappearances, destroyed 4321 houses and 21 office buildings, and left 22 667 people homeless [12]. This was the most serious debris flow event in China.

To keep the county safe, debris flow control works have been constructed in the gully. Six check dams were built from 1997 to 1998, and three check dams and two retaining walls were built in 2009. However, the nine check dams were all destroyed by the very large-scale debris flow on 8 August 2010; the No. 2 dam were completely destroyed (Figure 14.2), and the remainder dams were partly destroyed. The peak discharge of this debris flow was 1830 m^3/s, the maximum debris flow velocity was 9.2 m/s, the total volume of material rushed out was 1.52×10^6 m^3, and the maximum boulder size on the debris flow fan was 11.2 m [13].

The main reasons for the destruction of control structures in the Sanyanyu Gully were as follows: (i) outburst of collapsed accumulation due to prior earthquakes enlarged the scale of the debris flow and imparted a very strong destructive capacity and (ii) the masonry dams in the middle and lower reaches were weak in resisting the impact of the flow, and their breakages increased the debris flow velocity by approximately 3.6 times.

Debris flows that block rivers can result in the raising of the upstream streambed and considerable siltation, which endanger the natural environment and infrastructure along the rivers. This secondary disaster should be considered in the design of mitigation engineering. The debris flow that occurred in the Hongchun Gully on 14 August 2010 entered and

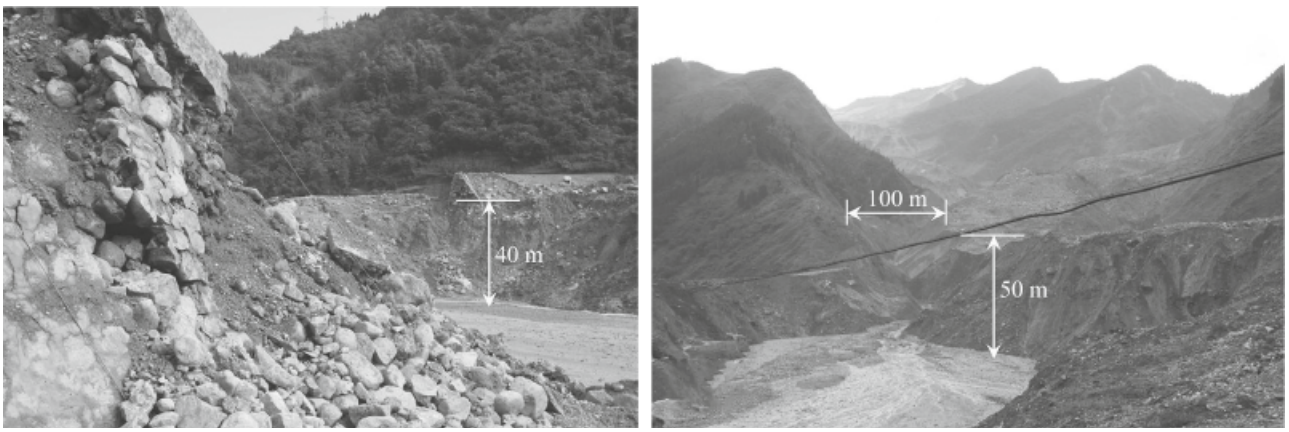

Figure 14.1 The destroyed check dam and deep incision in the landslide deposit.

@seismicisolation

Figure 14.2 The check dam before and after the disaster. *Source:* Photographs by Chen X.Q.

Figure 14.3 Debris flow blocking the river (left: the Hongchun Gully; right: the Wenjia Gully).

blocked the Minjiang River. The dam led to flooding in Yingxiu town, causing 13 deaths and 59 disappearances [14]. The debris flow that occurred in the Wenjia Gully on 13 August 2010 rushed into the Mianyuan River to form a 1650-m-long, 420-m-wide dam (Figure 14.3). The upstream roads and houses were submerged. The debris flow also caused five deaths and one disappearance [7].

14.2. DIFFICULTIES FOR DEBRIS FLOW HAZARD MITIGATION

Based on the characteristics of debris flows in the Wenchuan earthquake area, the difficulties of mitigation measures are summarized as follows:

1. Timing of mitigation engineering construction: Many rock avalanches and landslides were triggered by the Wenchuan earthquake in the Longmen Mountains area, providing abundant loose materials for debris flow formation and dramatically changing the conditions of debris flow formation. It is difficult to predict the effects of debris flow control structures if they are built immediately after an earthquake. Thus, the timing of the construction of debris flow mitigation structures should vary from one earthquake-affected area to the next.

2. Design standards of the control measures: Large amounts of loose solid materials that were induced by landslides and collapses triggered by earthquakes greatly reduce the threshold for debris flow formation. Thus, the design standard of mitigation engineering based on pre-earthquake criteria may not satisfy the needs of debris flow disaster prevention and mitigation after an earthquake. Thus, the design standards of mitigation engineering should improve according to the protection target.

3. Systematic planning of mitigation engineering: The engineered debris flow control system in place before the Wenchuan earthquake did not take into account the transport capacity of the main river. The transport capacity should be incorporated in the design of engineered control measures after an earthquake to prevent debris flows from blocking rivers and causing secondary disasters.

4. New technologies for mitigation and control measures: Most of the debris flow control measures built before the earthquake consisted of masonry structures. However, these structures had difficulty resisting impacts from boulders with diameters larger than 0.5 m in debris flows. Therefore, new structures must be developed that require a relatively low investment but have the capability of withstanding such impacts. Additionally, the construction period for debris flow

@seismicisolation

control measures should be considered, as they are typically constructed during the dry season. Because debris flows primarily occur in mountainous areas where land for development is limited, competing land demands for debris flow control measures and normal development must be weighed.

14.3. PLANNING METHOD OF DEBRIS FLOW HAZARD MITIGATION

14.3.1. Design Method of Mitigation Engineering

The peak discharge and total volume of the debris flow are the key parameters in designing these mitigation measures. To date, engineering mitigation systems have primarily been based on protected objects [15] and have lacked clear parameters to allocate certain sizes of debris flows to various types of mitigation structures. The planning of engineered mitigation systems is based largely on the experience of the designers. Thus, it is difficult to meet the mitigation requirements of post-earthquake debris flows with previous planning methods. Due to the terrain limitation of the high mountain valley area in Southwest China, there is not enough room to deposit debris flows, and they are usually directly discharged into the main river. Therefore, the sediment carrying capacity of the river becomes a key factor in whether the river is blocked.

The new design principles for debris flow mitigation engineering consider the sediment transport capacity of a river, as the post-earthquake debris flow frequently blocks the river (Figure 14.4), as proposed by Chen et al. [8]. The total volume of the debris flow can be allocated to open or closed check dams located along the gully channel (hereafter denoted as "blocking structures"), and the debris flow volume that exceeds the check dam capacity can be deposited in a deposition basin or directly discharged into the main river. The peak discharge of the debris flow volume that is neither blocked by check dams nor deposited in deposition basins must be conveyed by drainage channels in the main gully or diverted toward side gullies. Based on this layout of mitigation measures, the peak discharge of the debris flow can be decreased, and the movement of the debris flow can be well regulated.

The primary steps in designing a mitigation system are as follows (Figure 14.4):

- First step: the peak discharge Q_{Total} and total volume V_{Total} of the debris flow are determined based on the design standard.
- Second step: based on the transport capacity of the main river, the critical peak discharge of the debris flow $Q_{Drainage,}$ is defined.
- Third step: when $Q_{Total} \leq Q_{Drainage}$, only a drainage channel is required to conduct the debris flow to the main river; when $Q_{Total} > Q_{Drainage}$, such drainage measures should be combined with diverting or blocking or deposit-stopping measures.
- Fourth step: if neighboring gullies would be suitable to divert part or all of the debris flow using an intake structure (side weir, bottom grill) and a diversion channel, this capacity $Q_{By\text{-}pass}$ is assessed. If $Q_{Total} \leq Q_{Drainage} + Q_{By\text{-}pass,}$ the protection strategy can simply rely on drainage in the gully and the diversion structure. Conversely, $Q_{Total} > Q_{Drainage} + Q_{By\text{-}pass}$, it is necessary to reduce the discharge of the debris flow by blocking or deposition structures.
- Fifth step: if various types of check dams and drainage measures are selected for mitigating and regulating the debris flow, then the debris flow discharge that can be blocked by the check dams Q_{Block} is determined by summing the individual capacities of the dams. If the deposit-stopping and drainage measures are selected, then the proper peak discharge $Q_{Deposit}$ of the debris flow that can be accommodated by the deposit-stopping measures is calculated.
- Sixth step: drainage, diverting, and blocking measures are adopted when $Q_{Total} \leq Q_{Drainage} + Q_{By\text{-}pass} + Q_{Block}$; drainage, diverting, blocking, and deposit-stopping measures are adopted when $Q_{Total} > Q_{Drainage} + Q_{By\text{-}pass} + Q_{Block}$.
- Seventh step: the peak discharge $Q_{Deposit}$ entering the deposit-stopping measures is determined using $Q^*_{Deposit} = Q_{Total} - Q_{Drainage} - \mathrm{Q}_{By\text{-}pass}\text{-}Q_{Block}\ \mathrm{Q}$.

Figure 14.4 shows only one case of this design method. According to the specific project, the priority of diverting, blocking and deposit-stopping needs to be adjusted. If only drainage measures are used for debris flow control, then the value of the drainage measures discharge is $Q^*_{Drainage} = Q_{Total}$. When only drainage and blocking measures are adopted, the value of the peak discharge in the drainage measures is $Q^*_{Drainage} = Q_{Drainage}$, and the reduced value of peak discharge produced by the blocking measures is $Q^*_{Block} = Q_{Total} - Q_{Drainage}$. When only drainage and deposit-stopping measures are adopted, the value of the peak discharge in the drainage measures is $Q^*_{Drainage}$

@seismicisolation

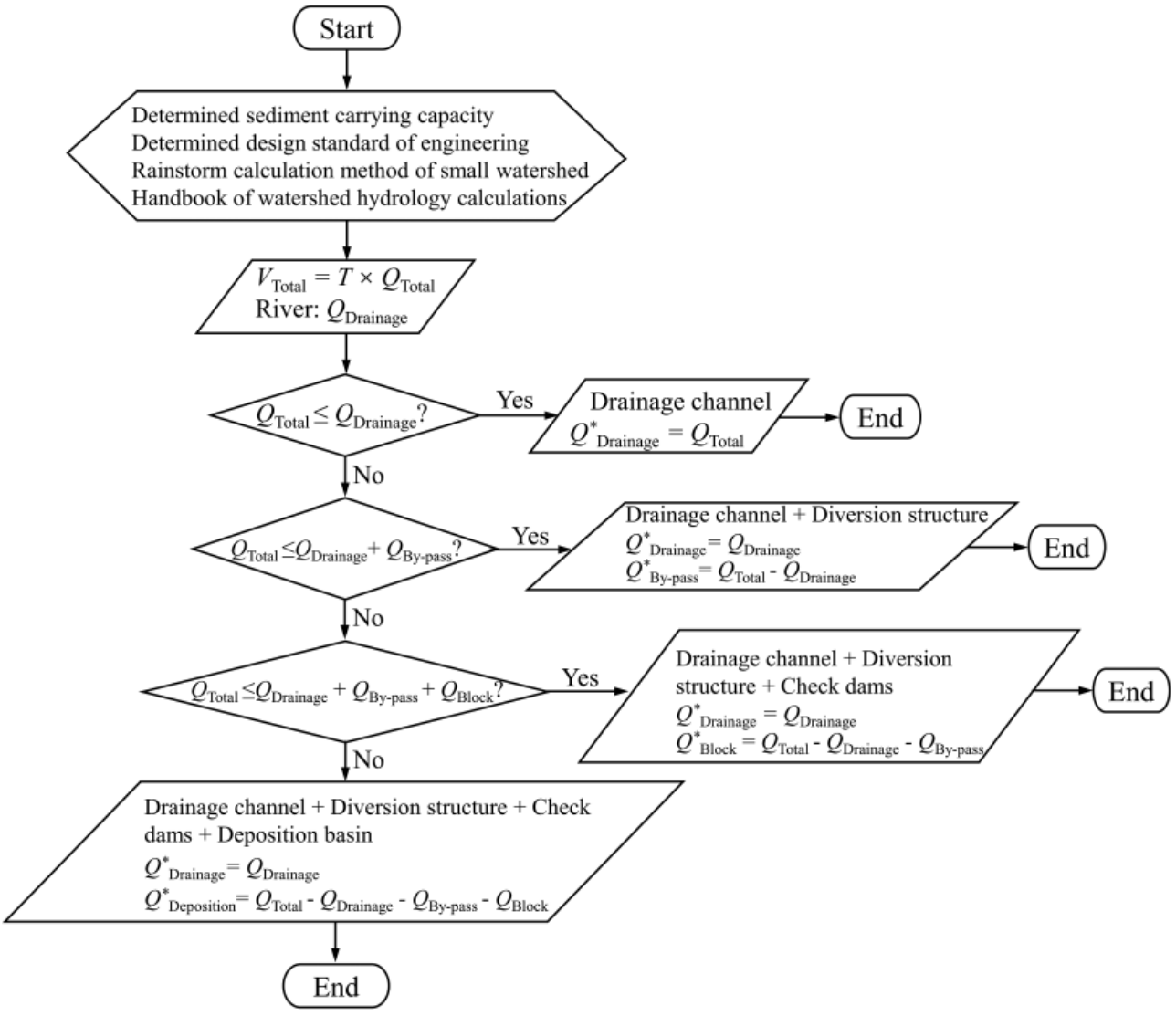

Figure 14.4 Planning method for debris flow hazard mitigation.

$= Q_{Drainage}$, and the portion of the peak discharge of the debris flow accepted by the deposit-stopping measures is $Q^*_{Deposit} = Q_{Total} - Q_{Drainage}$.

The key design method is determined by the sediment transport capacity of the main river. The main river can be either partially or completely blocked by a debris flow. Based on flume experiments with a length of 15 m, width of 0.3 m, and depth of 0.65 m, He [16] proposed an equation for calculating the peak discharge $Q_{Drainage}$ when the main river is completely blocked by a debris flow:

$$Q_{Drainage} = \frac{bQ_M}{B\exp\left(0.883(1-\cos\theta)^2 + 2.587\gamma_c/\gamma_w - 8.572\right)}$$

where Q_M is the peak discharge of the main river based on the design standard, B is the width of the main river, θ is the included angle between the debris flow drainage channel and the main river, γ_c is the density of the debris flow, γ_w is the density of the main river, $Q_{Drainage}$ is the peak discharge of the debris flow that drains into the main river via the debris flow drainage channel and b is the width of the drainage channel. This equation may be applied under the following conditions: (i) the riverbed gradient is approximately 0.5%; (ii) the angle between the alignments of the debris flow gully and the main river ranges from 30° to 90°; (iii) the density of the debris flow exceeds 1500 kg/m³; (iv) the debris flow contains primarily small particles; and (v) the river blockage is caused by a one-time debris flow event.

@seismicisolation

14.3.2. Successive Blocking Measures

A group of small check dams has been applied in many debris flow control engineering systems. In the debris flow formation area, small check dams with heights < 5 m were used to stabilize the loose soil. Their main functions are blocking sediment, raising the erosion benchmark of the gully bed and lowering the channel-bed gradient of the siltation segment. Therefore, the downcutting erosion of the gully bed can be controlled, soils in the gully bed can be prevented from being involved in debris flow activities, and silting soil can press the slope foot upstream, thereby inhibiting slope collapses and landslides.

In the movement area, to control damage from large boulders carried by debris flows to downstream buildings, a group of check dams with various opening sizes is used to block stones by mechanical trapping (Figure 14.5).

The mean particle size gradually decreases further downstream, thereby decreasing the impact forces of large boulders. Such structures can achieve a uniform distribution of debris flow materials along the gully. As such, this method makes use of both the siltation and hazard mitigation functions of check dams. Cascade check dams have completely prevented debris flows [17]. Since cascade check dams have the advantage of reducing debris flow particles with sequentially decreasing orifice sizes and regulating the debris flow peak discharge, this method is expected to have major impacts on the mitigation of debris flows.

14.4. CASE STUDY

14.4.1. Overview of the Xiaogangjian Gully (XGJ)

The catchment area of the XGJ Gully measures approximately 1.36 km^2. The main channel of the gully is 2590 m long, and the longitudinal gradient is 41.2%. The elevation of the catchment ranges from 810 to 1987 m, representing an elevation difference of 1177 m. The XGJ basin is elongated in shape, and the terrain is steep. The area with slope gradients equal to or greater than 25° measures 1.16 km^2 [18]. The slopes in this catchment are mostly steep with large longitudinal gradients, favoring the concentration of storm runoff and making the area prone to debris flow development. The XGJ Gully is an area of high precipitation in northwestern Sichuan; the average annual precipitation is 1086.4 mm. This abundant rainfall provides one of the conditions necessary for debris flow development in the XGJ Gully.

Before the Wenchuan earthquake, the vegetation growing in the XGJ catchment was healthy. For example, the coverage rate of trees, shrubs, and grass across the entire area exceeded 90%. There was no debris flow activity during the previous 100 years. However, the Wenchuan earthquake induced numerous landslides and rock avalanches upstream of this area.

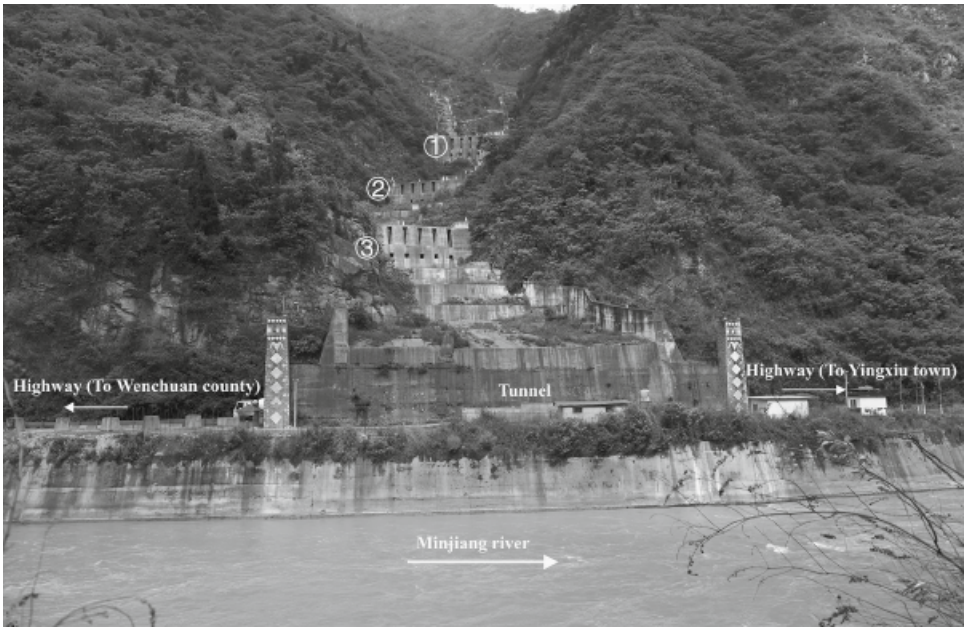

Figure 14.5 Cascade check dams with orifices of various sizes in Shaofang gully, China.

@seismicisolation

The collapsed materials moved down into the gully at high speeds and accumulated at the bottom of the gully. The deposits volume up to a total of $800 \times 10^3\,m^3$. Ten debris flows occurred between 12 May 2008 and 5 September 2011. The landscape changed radically, particularly at the outlet of the gully (Figure 14.6). The old accumulation body was downcutted and reached 35 m. The total volume of solid materials that rushed out of the gully was $500 \times 10^3\,m^3$, including the materials from the old accumulation platform ($400 \times 10^3\,m^3$) and those from the upstream collapses ($100 \times 10^3\,m^3$).

The area that was directly affected by the debris flows at the gully outlet was $3 \times 10^4\,m^2$, including Mianmao Road in front of the gully. The major hazards were the blockage and siltation of the main road and river, the formation of a dammed lake, the inundation of the upstream road, and the riverbed rise and burry of the road downstream by high-intensity sedimentation. Mianmao Road was buried by a debris flow that occurred on 26 July 2010, and traffic was interrupted for 18 days. Another debris flow occurred on 13 August 2010, blocking the road at the gully outlet and forming a dammed lake that flooded the upstream road.

14.4.2. Planning Method for Debris Flow Mitigation in the XGJ Gully

To protect the safe passage of the Mianmao highway before the new construction tunnel is completed, debris flow hazard mitigation engineering needs to be built.

The design standard of the debris flow mitigation measures (Figure 14.7) was to resist debris flows with a

Figure 14.6 The landforms of the XGJ Gully after a debris flow.

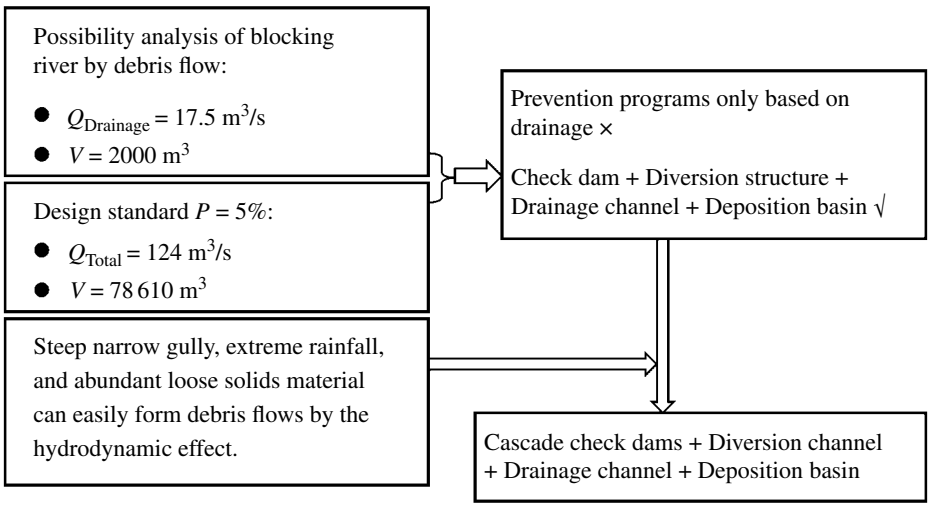

Figure 14.7 Planning method for debris flow mitigation in the XGJ Gully.

@seismicisolation

20-year return period. The geologic, geomorphologic, hydrologic, and meteorological conditions were considered in the project design. The main river transport capacity was considered during the design, and the Mianyuan River was blocked if the debris flow discharge entering the river exceeded $Q_{Drainage} = 17.5\,m^3/s$. Based on the hydrological calculation method for a small watershed of Sichuan Province, the peak discharge of a debris flow with a 20-year return period is $Q_{Total} = 124.1\,m^3/s$, and the corresponding debris flow volume is $78\,610\,m^3$. Because $Q_{Total} > Q_{Drainage}$, a drainage channel is not sufficient.

On the left side of the XGJ Gully, there is a tributary with a catchment area of $0.61\,km^2$, a main channel length of 1540 m, and an average longitudinal gradient of 62.5%. To reduce runoff into the main channel, a water channel was constructed on its left bank to discharge the flood with a discharge of $9.6\,m^3/s$, which was diverting measure and reduced the debris flow discharge in the main gully to $Q_{Total} = 90.3\,m^3/s$ [19, 20].

A group of check dams was used to raise the erosion base level and stabilize the inner bank slope. An analysis of the geologic and geomorphologic conditions determined that five check dams could be built in the gully. Based on a slope stability analysis, these dams could mitigate a peak discharge of $Q_{Block} = 31.3\,m^3/s$. Because $Q_{Total} > Q_{Drainage} + Q_{Block}$, a deposition basin was located to accommodate the additional debris flow peak discharge, the total volume of the deposition basin was equal to the discharge multiplied by the flow time, and the storage capacity of the check dam was calculated by the same method. To avoid blocking the river, the deposition basin should be capable of accepting a peak discharge of $Q^*_{Deposit} = Q_{Total} - Q_{Drainage} - Q_{Block} = 90.3 - 17.5 - 31.1 = 41.7\,m^3/s$. Additionally, the design volume of the deposition basin should not be less than $26\,414\,m^3$.

In summary, the design of an engineering project based on the allocation of the debris flow peak discharge and the total volume of a single debris flow event is as follows: the peak discharge $Q^*_{Drainage}$ of the debris flow that can be drained to the main river is $17.5\,m^3/s$; the reduction in peak discharge Q_{Block} that can be produced by check dams is $31.1\,m^3/s$; and the peak discharge $Q^*_{Deposit}$ that can be accepted by the deposition basin is $41.7\,m^3/s$, with a minimum volume of $26\,414\,m^3$.

14.4.3. Debris Flow Mitigation Engineering

14.4.3.1. Check Dams with Various Opening Sizes

Five check dams with various opening sizes are constructed in the XGJ Gully, as shown in Figure 14.8. The sequence of the dams from upstream to downstream is as follows: the first dam is 14.5 m high with a maximum opening of 0.8 × 5.0 m (width × height); the second dam is 11.5 m high with a maximum opening of 0.8 × 4.5 m; the third dam is 12.5 m high with a maximum opening of 0.8 × 3.0 m; the fourth dam is 10.0 m high with a maximum opening of 0.4 × 4.0 m; and the fifth dam is 9.0 m high with a maximum opening of 0.5 × 0.6 m.

14.4.3.2. Composite Foundation for Dams

In a narrow and steep gully, deficiencies in the foundation bearing capacity of a check dam and excessive erosion downstream of a dam are common problems. It is difficult to use traditional foundations of check dams with sufficient bearing capacity and resistance to erosion given the restrictions of a typically narrow gully, large longitudinal slope, and practical limits on the extent and depth of excavation. These geomorphic conditions created a dangerous working environment, and mechanical excavation induced a high degree of risk and could not meet the required conditions for equipment and site layout. Hence, constructing large piles in a narrow and steep gully is difficult.

Small-diameter steel pipe piles are an effective foundation style that is based on the use of a string of such piles. They have the benefits of minimal excavation, high efficiency, safe construction, and high strength when they are part of a composite foundation formed by the addition of grout. Based on these advantages, the technique was applied in XGJ debris flow prevention projects. A composite foundation with steel pipe piles improved the bearing capacity of the foundation by creating an interaction between the piles and the soil. Additionally, a soil arching effect between the piles was achieved by the rational design of the pile spacing, thus improving the overall stability of the soil and preventing headward erosion from the dam toe to the basement.

For example, check dam No. 3 is a gravity dam with a base plate 2 m wide. The height and length of the dam are 12.5 and 38.2 m, respectively. A composite

@seismicisolation

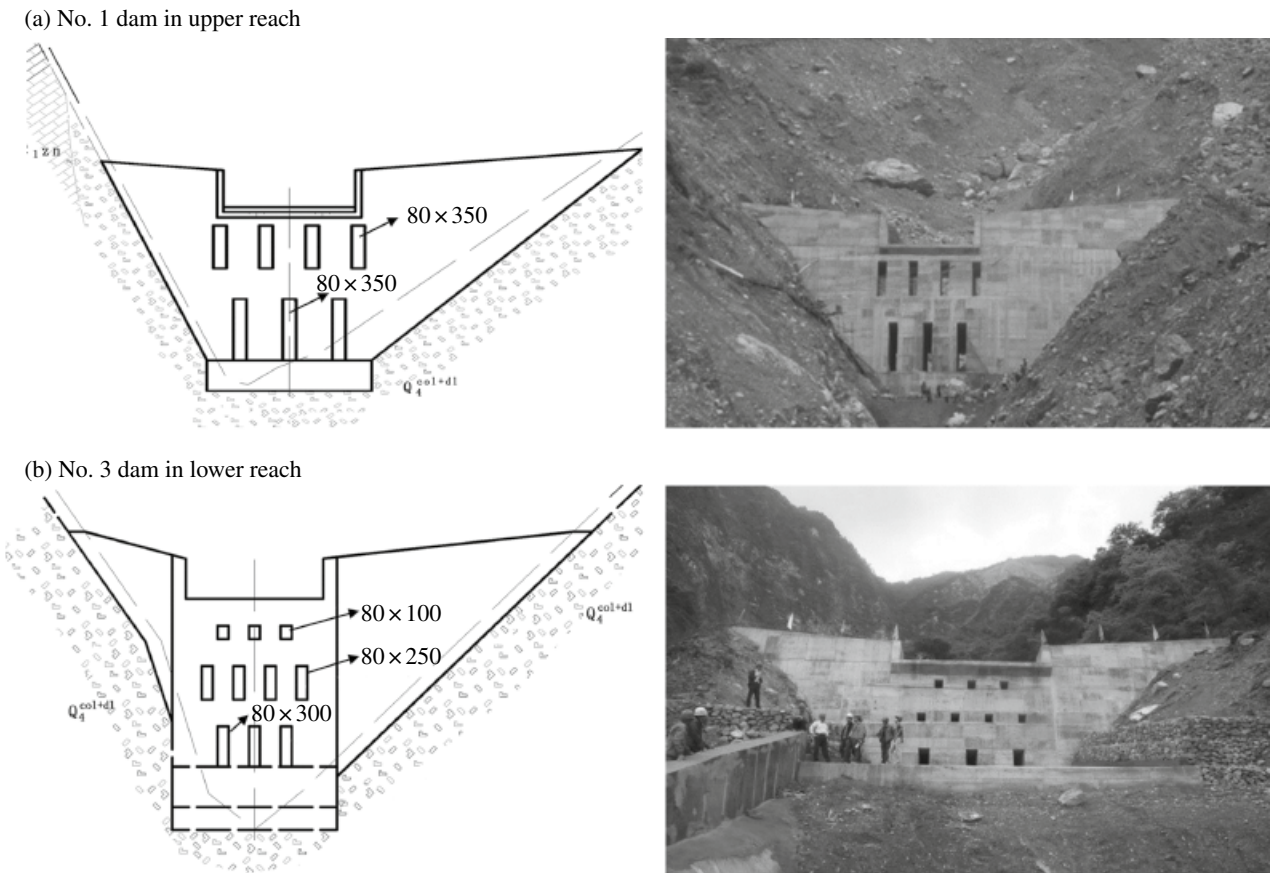

Figure 14.8 Check dams with various opening sizes.

foundation consisting of small-diameter steel pipe piles was used in the No. 3 check dam. Twenty steel pipe piles were used. The lengths of the steel pipe piles were 8.0 m, and their diameters were 0.15 m. The average spacing between the steel pipe piles was 1.0 m. Three lengths of reinforcing steel with diameters of 25 mm were placed in the steel pipe piles to increase their vertical bearing capacities.

14.4.3.3. Engineering Application

Based on a systematic plan and key techniques application, the following engineering structures were constructed: four check dams with various opening sizes and heights ranging from 9.0 to 12.5 m in the main gully; one deposition basin between the highway and the river with a capacity of twice the expected debris flow volume, a total basin area of 24 233 m^2, and a design deposit volume of 52 818 m^3; one drainage channel with a length of 131.7 m at the left bank of the No. 4 check dam; and one open tunnel to serve as the debris flow overpass over the highway. The layout of the mitigation project is illustrated in Figure 14.9.

14.4.4. Application Effect Analysis

Mitigation engineering was completed in May 2012. On 26 July 2012, a debris flow was triggered by a rainstorm in the XGJ Gully. The rainfall recorded was 132 mm from 16:00 to 18:30, representing rainfall with a 50-year return period. The debris volume was $22 \times 10^3\,m^3$.

From 13 to 18 August 2012, seven debris flows were triggered with a total volume of $232\times10^3\,m^3$. On 18 August 2012, the debris flow impacted and scoured the gully bed behind the check dam, a scour hole was formed at the outside of the steel pipe pile foundation, and the scour hole was planar and vertical cliffs. The steel pipe pile foundation effectively blocked the

@seismicisolation

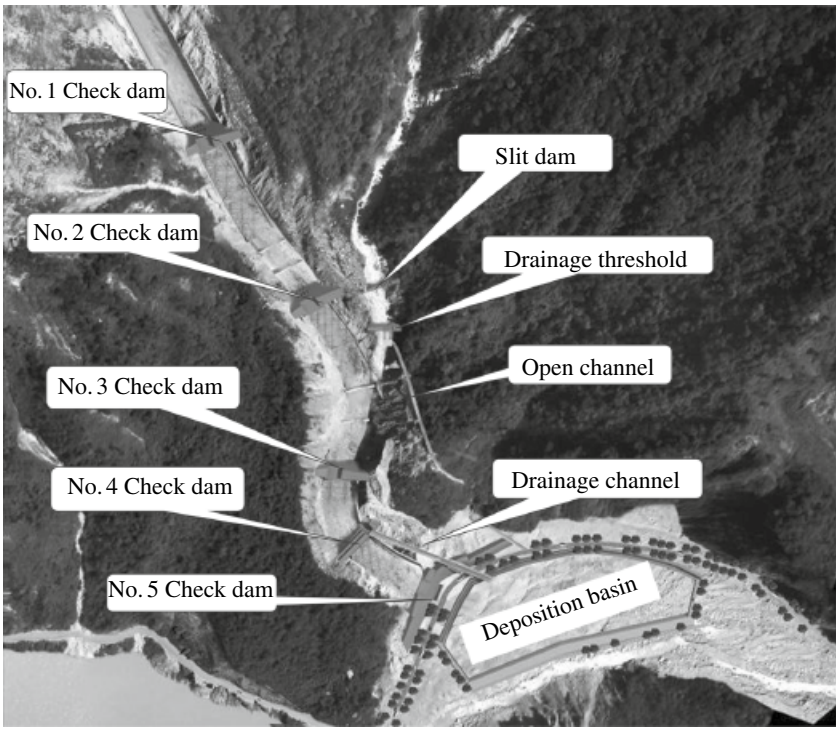

Figure 14.9 The layout of the mitigation project in the XGJ Gully.

development of headward erosion of the scour hole, and the soil between the pipe piles was not washed away.

The mitigation project effectively prevented debris flows, the debris flow did not cause a disaster, and traffic and highways were also successfully protected. This outcome indicates that the debris flow mitigation strategies in this gully were rational and that construction of the mitigation system was feasible. In general, the strategy of controlling debris flows using check dams, drainage channels, and debris flow deposition basins is effective for protecting mountainous highways.

14.5. CONCLUSIONS

The abundant loose source material triggered by the Wenchuan earthquake was conducive to debris flow formation. In the past decade, debris flows have continuously occurred in earthquake-affected areas. According to extensive field work and numerous discussions, we realized the difficulties of debris flow hazard mitigation in strong earthquake-affected areas, including when to construct, how to determine the design standards, how to realize systematic planning in a watershed, and how to develop new technology. Then, we proposed a systematic planning method for debris flow hazard mitigation at the watershed scale based on the sediment transport capacity of the main river. Finally, the proposed planning method was applied in the XGJ Gully, which has a small watershed area and steep slope. The mitigation system in the XGJ Gully effectively resisted a debris flow with a 50-year return period triggered by rainfall on 26 July 2012. Several subsequent debris flow events proved that the system effectively protected the highway and minimized losses. However, whether this hazard mitigation system can effectively prevent large-scale debris flows needs to be verified by continuous prototype observations.

REFERENCES

1. Huang, R.Q. and Li, W.L. (2009). Analysis of the geohazards triggered by the 12 May 2008 Wenchuan earthquake, China. *Bulletin of Engineering Geology & the Environment 68*: 363–371.
2. Parker, R.N., Densmore, A.L., Rosser, N.J. et al. (2011). Mass wasting triggered by the 2008 Wenchuan earthquake was greater than orogenic growth. *Nature Geoscience 4* (7): 449–452.
3. Cui, P., Chen, X.Q., Zhu, Y.Y. et al. (2011). The Wenchuan earthquake (12 May 2008), Sichuan Province, China, and the resulting geohazards. *Natural Hazards 56*: 19–36.

@seismicisolation

4. Zhang, L.M., Zhang, S., and Huang, R.Q. (2014). Multihazard scenarios and consequences in Beichuan, China: the first five years after the 2008 Wenchuan earthquake. *Engineering Geology 180*: 4–20.
5. Zhang, M. and Yin, Y.P. (2013). Dynamics, mobility-controlling factors and transport mechanisms of rapid long-run out rock avalanches in China. *Engineering Geology 167*: 37–58.
6. Wang, Z.Y., Qi, L.J., and Wang, X.Z. (2012). A prototype experiment of debris flow control with energy dissipation structures. *Natural Hazards 60*: 971–989.
7. Xu, Q., Zhang, S., Li, W.L. et al. (2012). The 13 August 2010 catastrophic debris flows after the 2008 Wenchuan earthquake, China. *Natural Hazards and Earth System Sciences 12*: 201–216.
8. Chen, X.Q., Cui, P., You, Y. et al. (2015). Engineering measures for debris flow hazard mitigation in the Wenchuan earthquake area. *Engineering Geology 194*: 73–85.
9. Liu, C.Z. (2012). Analysis on genetic model of Wenjiagou debris flows in Wenchuan earthquake area, Sichuan. *Geological Review 58* (4): 709–716. (in Chinese).
10. You, Y., Chen, X.Z., and Liu, J.F. (2011). "8.13" extra large debris flow disaster in Wenjia Gully of Qingping Township, Mianzhu, Sichuan Province. *Journal of Catastrophology 26* (4): 68–72. (in Chinese).
11. Ma, D.T. and Qi, L. (1997). Study on comprehensive controlling of debris flow hazard in Sanyanyu Gully. *Bulletin of Soil and Water Conservation 17* (4): 26–31. (in Chinese).
12. Hu, K.H., Cui, P., and Zhang, J.Q. (2012). Characteristics of damage to buildings by debris flows on 7 August 2010 in Zhouqu, Western China. *Natural Hazards and Earth System Sciences 12* (7): 2209–2217.
13. Hu, X.D., Wang, G.L., Zhao, C. et al. (2011). Analysis of chatacteristic values for Sanyanyu debris flow in Zhouqu county on August 8, 2010. *Northweatern Geology 44* (3): 44–52.
14. Tang, C., Zhu, J., Ding, J. et al. (2011). Catastrophic debris flows triggered by rainfall on 14 August 2010 at the epicenter of the Wenchuan earthquake. *Landslides 8*: 485–497.
15. Li, D.J. (1997). *Debris Flow Mitigation Theory and Practices*, 132–148. Beijing: Science Press (in Chinese).
16. He, Y.P. (2003). Influence of debris flow on the evolution of river bed in mountain areas. Doctor thesis. Graduate School of Chinese Academy of Sciences (in Chinese).
17. Liu, J.F., You, Y., Chen, X.Q. et al. (2016). Mitigation planning based on the prediction of river blocking by a typical large-scale debris flow in the Wenchuan earthquake area. *Landslides 13* (5): 1231–1242.
18. Yang, D.X., Chen, X.Q., You, Y. et al. (2012). Debris flow development trend in Xiaogangjian Gully in Mianzhu County, Wenchuan earthquake zone. *Journal of Mountain Science 30* (6): 701–708. (in Chinese).
19. Gong, X.L., Chen, K.T., Chen, X.Q. et al. (2020). Characteristics of a debris flow disaster and its mitigation countermeasures in Zechawa Gully, Jiuzhaigou Valley, China. *Water 12* (5): 1256.
20. Zhao, W.Y., You, Y., Chen, X.Q. et al. (2020). Case study on debris-flow hazard mitigation at a world natural heritage site, Jiuzhaigou Valley, Western China. *Geomatics, Natural Hazards and Risk 11* (1): 1782–1804.

@seismicisolation
@seismicisolation

15

Prevention and Mitigation Against Debris Flow and Woody Debris in Japanese Design Using a Steel Pipe Open Sabo Dam

Toshiyuki Horiguchi[1] and Hiroshi Kokuryo[2]

15.1. INTRODUCTION

Japan is one of the most volcanic and earthquake-prone countries in the world, with detrimental geological features. Most of Japan's territory is covered by mountains, hills, and steep streams. Therefore, over 1000 cases of natural disasters, such as landslides, slope failures, and debris flows, occur every year due to earthquakes, typhoons, and localized torrential rainfall. Debris flow is a phenomenon in which part of the boulders and sediment making up a hillside and riverbed is intermingled with water due to torrential rain and carried downstream at an extremely fast velocity, causing devastating losses to the houses and facilities located in the downstream area. Additionally, disasters caused by woody debris, such as houses being destroyed or rivers flooding due to blocked bridges owing to woody debris flowing down together with the sediment, are increasing. In these circumstances, climate change also becomes a factor that increases damage due to sediment-related disasters. For example, in urban areas, there is an increase in the prevalence of areas prone to sediment disasters owing to residential development on the foothills and hillsides and an increase in the frequency of record-breaking rainfall due to climate change. Such a torrential rainfall event occurred in July 2017 in the northern Kyushu area of Japan, dislodging a significant volume of large woody debris and causing approximately 40 fatalities in Oita and Fukuoka [1]. Moreover, a torrential rainfall event occurred in central-western Japan, which was suffering from Typhoon Prapiroon that hit Hiroshima in July 2018, resulting in the instant collapse of a masonry check dam and the injury of more than 200 people [2, 3].

As structural measures to protect people and properties from sediment disasters such as debris flow, Sabo dams are installed in various places to prevent and mitigate sediment disasters with the purpose of depositing sediment. Their function is to (i) prevent the triggering or aggravation of hillside collapse through mountain foot fixation; (ii) reduce longitudinal riverbed erosion; (iii) reduce the runoff of unstable sediment accumulated on the riverbed; (iv) trap debris flow and woody debris; and (v) regulate sediment discharge [4, 5]. Therefore, check dams are installed in places where large amounts of sediment are discharged. Such places include streams with blighted mountainous regions in their headwater areas, vulnerable streams or prone to sediment disasters occurring, or places and their nearby areas where sediment disasters occurred in the past.

Sabo dams can be broadly classified into two types: closed-type and open-type Sabo dams (hereinafter, referred to as closed Sabo dam and open Sabo dam, respectively), as shown in Figure 15.1. The closed Sabo dam is a river-crossing structure installed to intercept the stream on both the upstream and downstream sides, and a gravity-type concrete structure is mainly

[1] *Department of Civil Engineering, National Defense Academy, Youkosuka, Japan*
[2] *Nippon Steel Metal Product Co., Ltd., Tokyo, Japan*

Check Dam Construction for Sustainable Watershed Management and Planning, First Edition.
Edited by Zhanbin Li, Peng Li, Yang Yu, Peng Shi, and Guillaume Piton.
© 2022 John Wiley & Sons, Inc. Published 2022 by John Wiley & Sons, Inc.

@seismicisolation

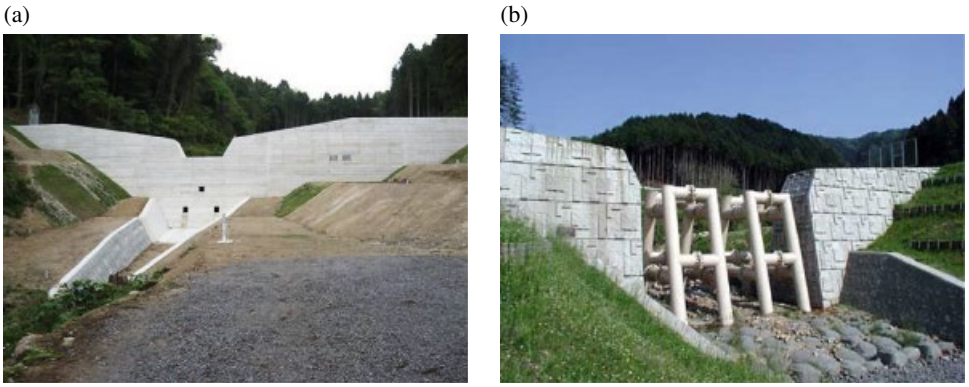

Figure 15.1 Types of check dams. (a) Closed Sabo dam (Concrete). (b) Open Sabo dam (Steel pipe).

used for this purpose. Most of the conventional Sabo dams used to be, historically, this type of concrete-made closed Sabo dam and contributed significantly to the prevention and mitigation of debris flow disasters. However, certain functional and environmental problems, stemming from lack of permeability, have been identified. Their sediment trapping capacity, which shall be the provision until debris flow occurs, decreases for sedimentation under normal conditions, and the continuity of the stream is destroyed owing to the interception of the stream. On the other hand, the steel pipe open Sabo dam is made of steel and has been developed since the 1970s with the main goal of trapping the debris flows and woody debris. Its dam body has a wide opening, with the steel pipe frames placed in a lattice pattern in the opening. This structure allows the sediment to flow down naturally and preserve the continuity of the stream under normal conditions and to trap boulders and woody debris at the occurrence of debris flow. The Sabo dam type to use is determined based on factors such as planed function, natural conditions including geographical and geological features, and watershed characteristics.

Currently, the application range of the steel open Sabo dam has been expanded to comprehensive control of the sediment transport mechanism and stream environment conservation. Steel open Sabo dams have been used in Japan for over 40 years, and their ability to trap debris flow while also being environmentally friendly are highly respected, resulting in over 2000 application sites.

This study reports on the functions and features of the steel open Sabo dam and examples of its application in Japan. Additionally, the applicability of small catchments is discussed with respect to the structure and availability of an open Sabo dam.

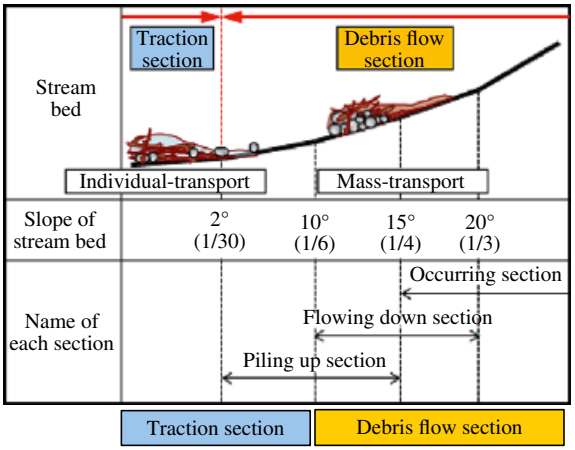

Figure 15.2 Gradation of mountain stream bed in sediment displacement morphology.

15.2. STEEL PIPE OPEN SABO DAM FUNCTIONS

15.2.1. Sediment and Driftwood Trapping Capacity of Steel Pipe Open Dam

Debris flow and woody debris countermeasure structures should be planned based on sediment transport within the stream. Figure 15.2 shows the criteria for sediment transport by the gradation of the riverbed [4]. Sediment transport modes can be largely divided into debris flow and traction sections, depending on the gradient of the streambeds. The debris flow section is a steep section with a streambed gradient greater than 2°. This is where many boulders are gathered at the front line of the debris flow and where sediment discharge is done during mass transportation. This section can be further classified into three subsections: the debris flow occurring section (with a streambed gradient greater than 15°), the flowing down section (between 10° and

@seismicisolation

(a) (b)

Figure 15.3 Open steel pipe Sabo dam. (a) Example of trapping boulder debris flow. (b) Example of trapping large driftwood.

20° streambed gradient), and the piling up section (with a 2°–15° streambed gradient). Conversely, the traction section is a low-gradient section with a streambed gradient below 2°. This is where the sediment is discharged by flowing water in an individual transport (also called bedload transport) and where woody debris is predicted to be discharged at the occurrence of flood or debris flow due to torrential rain. Therefore, the steel pipe open Sabo dam to be installed in each section needs to be a structure with a trapping function suitable for each debris flow condition. More specifically, it needs to have a debris flow section of the Sabo structure, which is aimed at trapping debris flow and woody debris to be discharged together with the sediment, and woody debris trapping works for a traction section of the Sabo structure, which is specifically aimed at trapping driftwood (Figure 15.3).

Subsequently, the dam possesses a natural ability of automatic maintenance of the sediment trap. Figure 15.4 shows the condition of a steel pipe open Sabo dam installed over 20 years ago. A steel pipe open Sabo dam is a dam with a wide dam body opening interval. This opening interval allows it to let sediment safely flow down under normal circumstances or in small- to medium-sized flow conditions without blocking the stream and allows it to have enough sediment trapping space (space to accumulate sediment at the upstream side to trap debris flow) to manage the occurrence of debris flow. Therefore, the steel pipe open Sabo dam can be estimated to have a planned trapping volume (debris flow trapping capacity) that is approximately two to three times higher than that of closed Sabo dams. Moreover, since the opening interval allows sediment to naturally flow downstream, it contributes to the prevention of riverbed degradation in the downstream area, receding coastline, and other related problems. In other words, it is a structure that contributes to the comprehensive sediment control of the entire stream, from the mountain area to the river channel and to the coastline.

Figure 15.4 Entrapment function.

15.2.2. Woody Debris Trapping Effect

Boulders, sediment, and woody debris usually happen together when debris flow occurs. When floods occur, woody debris flows down while floating near the water surface. In addition to boulders and sediment flowing down, a whole host of woody debris also

@seismicisolation

flowing down deepens the damage to downstream areas. Although a closed Sabo dam can trap boulders and sediment, it lets woody debris floating near the water surface overflow together with the flowing water, making it difficult to trap it. Conversely, the steel pipe open Sabo dam traps debris flow and has a higher woody debris trapping effect. This is because the structure can allow flowing water to pass through rather than atop. Figure 15.5 illustrates the planned sediment trapping capacity concept [5]. For the steel pipe open Sabo dam, the woody debris trapping capacity represents 30% ($X_o \times 30\%$) of the planned total trapping capacity, whereas it represents only 2% ($X_c \times 2\%$) for the closed Sabo dam. Taking this difference in the planned trapping capacity into consideration, we can expect the steel pipe open Sabo dam to have an approximately 15 times higher woody debris trapping effect compared to the closed Sabo dam.

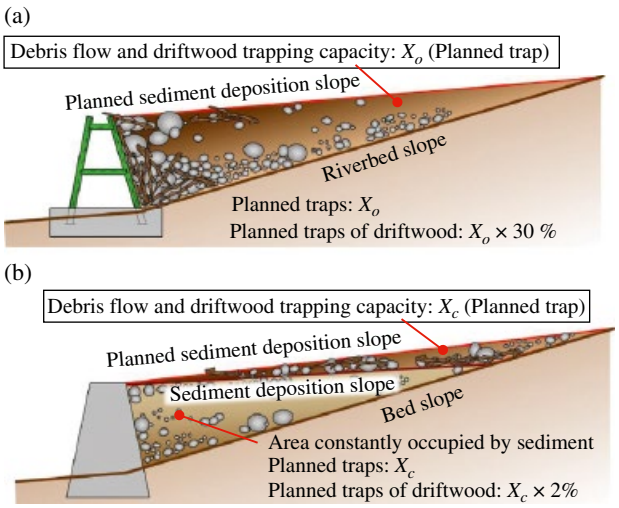

Figure 15.5 Planned traps. (a) Open Sabo dam. (b) Closed Sabo dam.

15.2.3. Trap Function of Debris Flow

Figure 15.6 shows the debris flow and woody debris trapping function concept of the steel pipe open Sabo dam, which is also called a clogging type dam. The dam traps and decelerates the debris flow by trapping boulders and woody debris at the front line of the debris flow by intertwining them at its permeable cross section of its opening and blocking them. The permeable cross section is formed by the horizontal (W_h) and vertical (W_v) net intervals. By setting these intervals up at a suitable width, it can enable the trapping of debris flow while letting sediment, under normal conditions, flow downstream. Figure 15.7 shows the boulder trapping surface conditions. Figure 15.7a shows the inside of the dam at the actual site after the debris flow was trapped. Figure 15.7b shows the boulders trapping surface condition by the dam model when performing debris flow trapping experiments at the flume. It can be understood from these photos that both boulder trapping conditions and debris flow trapping surfaces are extremely similar. Through these forms of trapping, it was found that elements such as pillars or beams and boulders are intertwined for the boulders to be trapped. We thus confirmed that, for the

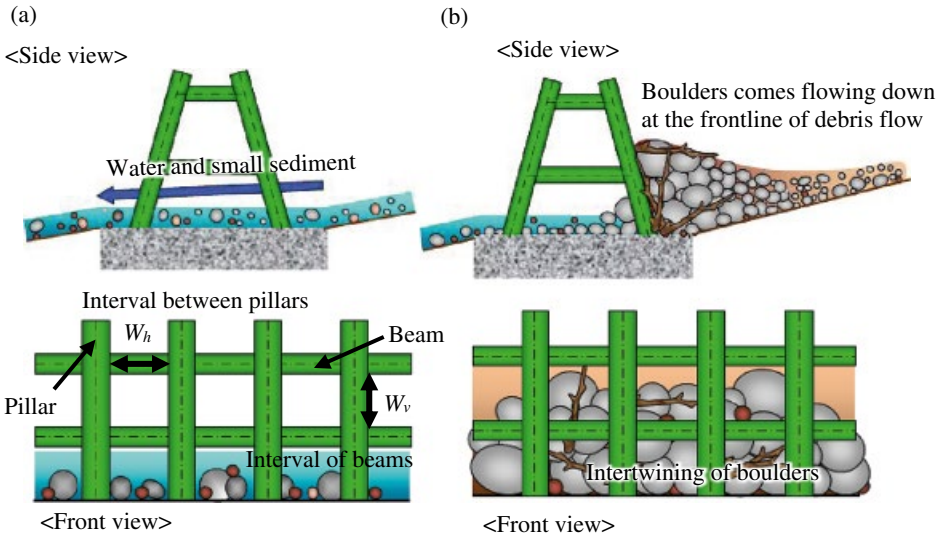

Figure 15.6 Trapping function of open Sabo dam. (a) Normal condition. (b) Occurrence of debris flow.

@seismicisolation

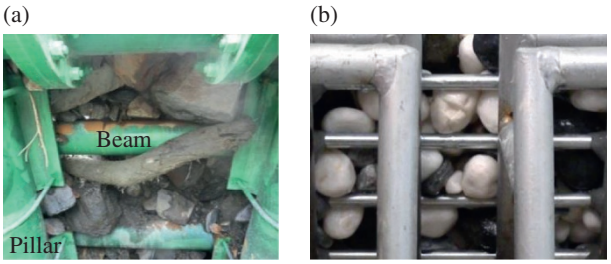

Figure 15.7 Trapping conditions. (a) On-site. (b) Flume experiment.

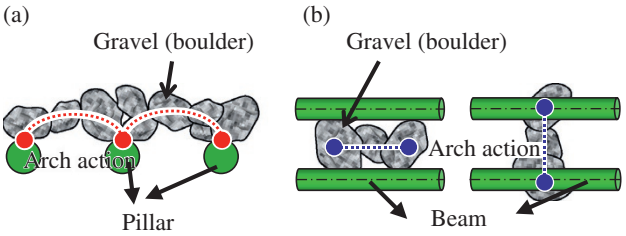

Figure 15.8 Arch action. (a) Vertical member. (b) Horizontal member.

open Sabo dam using steel pipe, the arch action by boulders, as shown in Figure 15.8, is displayed, the dam opening interval is blocked, trapping debris flow, and vertical and horizontal elements stabilize the intertwine between the boulders to control the remobilization of the trapped sediment [6].

15.2.4. Permeable Cross Section

Figure 15.9 shows the permeable cross section of the steel open Sabo dam used to trap the debris flow and woody debris. Here, a permeable cross section refers to the opening interval between elements (functional elements) placed within the opening to trap debris flow and woody debris. The permeable cross section has a horizontal and vertical net interval of 1.0 (or approximately 1.5) times the reference boulder diameter (the grain diameter equivalent to 95% of the cumulative value from the cumulative curve by measuring the diameter of the gravel carried in the debris flow at a 200 m upstream and downstream distance around the position of the dam: D_{95}). Conversely, when the objective of the dam is to only trap woody debris, its net interval between vertical elements (horizontal net interval) should be less than half of the maximum woody debris length (the maximum length estimated from the relationship between maximum tree height discharged from the

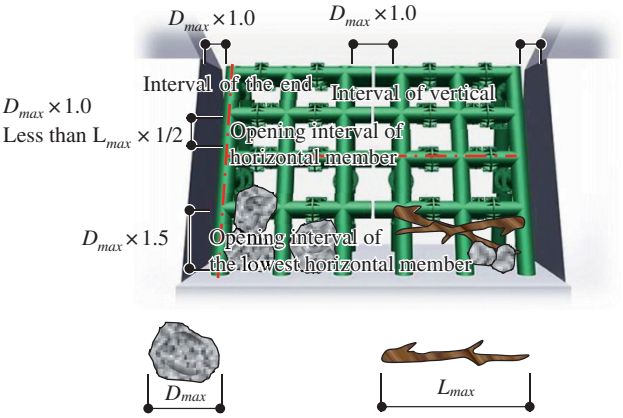

Figure 15.9 Cross-section and member arrangement.

upstream and the channel width of debris flow) but no shorter than twice the reference boulder diameter, to avoid clogging the dam with boulders.

15.3. STRUCTURE FEATURE OF STEEL PIPE OPEN SABO DAM

15.3.1. Structure Overview

Figure 15.10 shows an overview of the structural features of the steel pipe open Sabo dam, which consists of a steel portion and a base concrete. The dam height ($H = H_s + H_c$) is the total of the steel portion height (H_s) and the base concrete thickness (H_c). The bottom part (foundation) of the steel portion is embedded into the base concrete, to unite it as one structure. The embedded depth of the steel portion is usually determined by designing the external force acting against the steel portion, but approximately 1.0 m is commonly used. The steel portion is a hollow steel pipe frame structure formed by combining steel pipes. The diameter and thickness of the steel pipe used are determined based on external forces such as the impact of boulders and debris flow load acting against the steel portion. In previous studies, steel pipes with diameters greater than 400 and 12–25 mm thickness were mainly used. The main elements, including the steel pipes, are combined by shop fabrication, so only bolt connections at the flanges of each unit are necessary on site, leading to high workability.

Steel pipes are used as the main elements because of their high processability, nondirectional weakness (strong or weak axis) against design external forces, and high energy absorption force against boulders collision [7, 8].

@seismicisolation

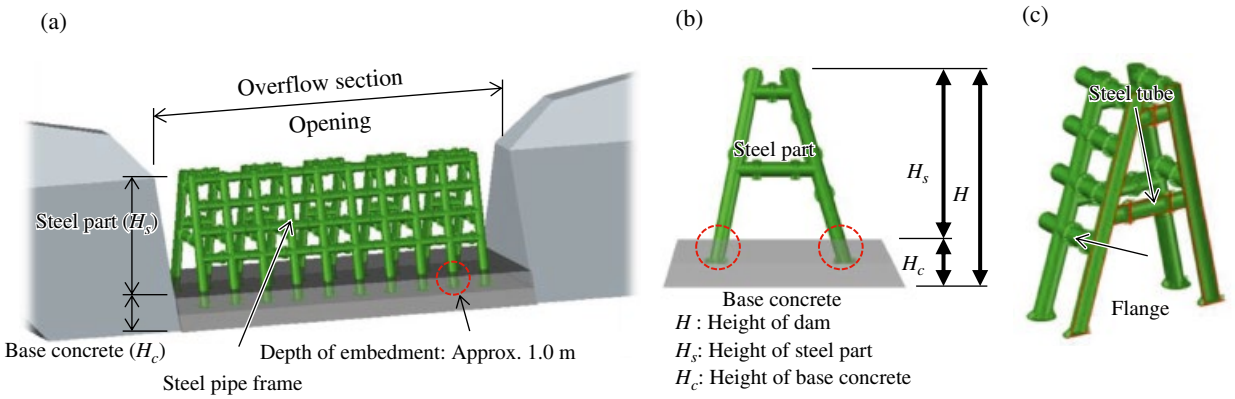

Figure 15.10 Structure overview of steel pipe open Sabo dam. (a) Front view. (b) Side view. (c) Steel pipe frame.

15.3.2. Steel Pipe Minimum Thickness

The minimum steel material thickness used for the open dam was set at 8.0 mm. However, the thickness against steel pipe diameter for steel pipes used as main elements is calculated to ensure sufficient safety against local buckling of the steel pipe below.

$$t_{\min} = \frac{D - 2 \times \Delta t}{80} + \Delta t \tag{15.1}$$

where t_{min} is the minimum steel pipe thickness, Δt is the corrosion plus additional allowance, *and D* is the outer diameter of the steel pipe.

Additionally, the diameter to thickness ratio (ratio of thickness t to outer diameter D of the steel pipe: D/t) for the steel pipe of the uppermost stream element, where boulders collide, should be set to a minimum of 40–60 as a standard.

15.3.3. Corrosion Allowance

The steel pipe thickness used for the open Sabo dam adds to the structurally necessary designed thickness t_1 an additional allowance t_2 for the decrease in the thickness of the effective cross section due to abrasion and impact by sediment and flowing water and a corrosion allowance t_3 for the decrease in the thickness of the effective cross section due to rust generation (Figure 15.11). Therefore, the steel pipe thickness shall be expressed as

$$t = t_1 + t_2 + t_3 \tag{15.2}$$

where t is the total steel pipe thickness, t_1 is the calculated structural design thickness, t_2 is the additional allowance, and t_3 is the corrosion allowance. Table 15.1 lists the standard for the additional and corrosion allowances. In this table, the minimum corrosion allowance t_3 is set at 0.5 mm. This corrosion allowance should be appropriately set based on the installation environment of the structure.

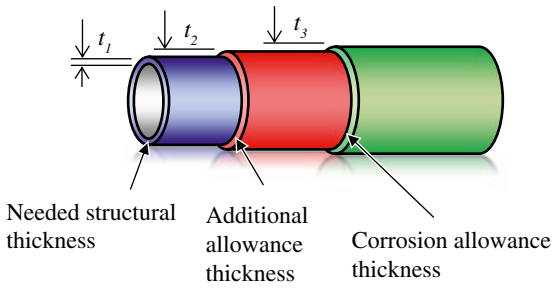

Figure 15.11 Corrosion allowance.

Table 15.1 The standard of corrosion allowance.

Part	Corrosion allowance (t_3)	Additional allowance (t_2)
Uppermost stream element	0.5 mm (~1.5 mm)	3.5 mm
Element near the bottom part	0.5 mm (~1.5 mm)	3.5 mm
Other elements	0.5 mm (~1.5 mm)	0.0~3.5 mm
Joint (Flange)	0.5 mm	1.0 mm

Here, the designed working life is expressed as being equal to designed corrosion allowance/annual corrosion rate. The annual corrosion rate in the atmosphere is considered approximately 0.01–0.02 mm/year. Moreover, there are reports indicating that corrosion progress is below 0.1 mm for a steel open dam installed over 40 years ago. Therefore, when a corrosion allowance of 0.5 mm is considered for the steel material, we

@seismicisolation

can secure the designed thickness through the corrosion allowance for approximately 50 years, which is the working life of general civil engineering structures, as long as it is not installed in a particularly challenging environment such as an acidic river.

15.4. STEEL OPEN DAM DESIGN

15.4.1. Spillway Design and Opening Determination

Figure 15.12 shows the design flow of the steel pipe open Sabo dam. The spillway is the section where the crown of the dam is partially lowered to concentrate the overflow running water. In principle, the spillway is designed such that the center is positioned at the center of the riverbed, and the bottom width of the spillway is based on the bottom width of the riverbed but not narrower than 3.0 m [4, 5]. Moreover, for the steel pipe open Sabo dam, the bottom width of the spillway should be as large as the width of the opening. The cross section of the spillway also must be designed to flow down the peak debris flow safely even after the opening is completely blocked by debris flow. Furthermore, the width of the opening should be as large as possible to take full advantage of the function of the steel open dam and should be designed to a width almost equal to the channel width of the debris flow expected to flow down, taking into consideration the geographical features on site (Figure 15.13).

15.4.2. Stability Analysis

Table 15.2 shows the combination of the external forces used for the stability analysis of the steel open dam to be installed in the debris flow section [4, 5]. When the steel pipe open Sabo dam with a wide opening traps debris flow, ponding does not occur in the sedimentation area because the water within the sediment goes through the space between the boulders and the sediment. Therefore, the external force used for the stability analysis of the steel pipe open Sabo dam shall not calculate the static water pressure but the sediment pressure in the area below the sediment surface and the fluid force of the debris flow in the area above it (Figure 15.14). In this case, the height of the sediment surface was designed such that the total sediment pressure and fluid force of the debris flow became the largest. The stability calculation method is the same as that of a gravity structure and to verify its stability against overturning, sliding, and subgrade bearing

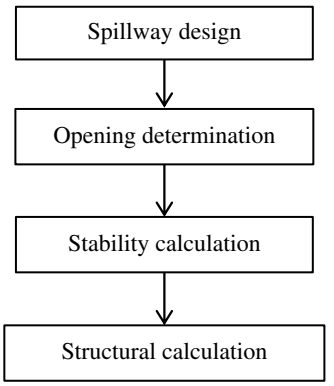

Figure 15.12 Design flow of open Sabo dam.

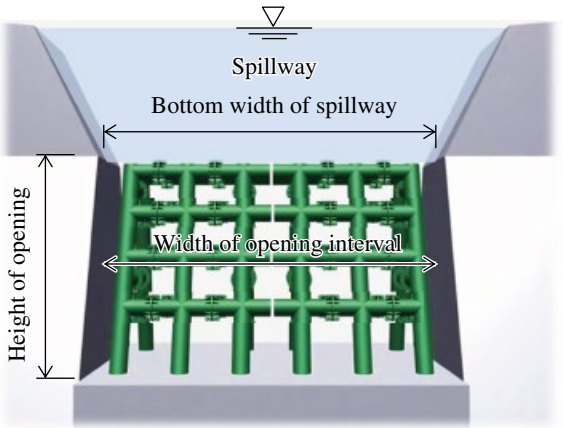

Figure 15.13 Spillway and opening interval.

Table 15.2 External forces for stability analysis.

Case	Normal	Debris flow	Flooding
Self-weight	—	∘	—
Fluid force of debris flow	—	∘	—
Sediment pressure	—	∘	—

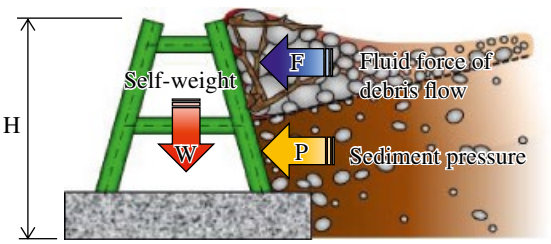

Figure 15.14 External forces for stability analysis.

capacity, the conditions for stability are as follows: (i) the bonding point of the resultant force from the self-weight and the external force of the dam is within 1/3 of the distance from the center of the dam bottom, (ii) sliding must not occur between the dam bottom and

@seismicisolation

Table 15.3 Combination of design external forces for structural calculation.

	Debris flow			
Case	Non-full	Full	Full sediment	Changes of temperature
Self-weight	∘	∘	∘	∘
Fluid force of debris flow	∘	∘	—	—
Sediment pressure	—	—	—	—
Temperature stress	—	—	—	—
Extra coefficient for allowable unit stress	1.5	1.5	1.0	1.15

the foundation ground or within the foundation ground, and (iii) the maximum load strength applied to the foundation ground must be within the allowable bearing capacity of the ground [9].

15.4.3. Structure Analysis

Table 15.3 shows the combination of the external forces used for the structural analysis [10]. The design external forces for structural evaluation are self-weight, fluid force of debris flow, sediment pressure, and temperature stress. Because the steel pipe open Sabo dam is a steel pipe structure connecting panel points by rigid connection, a change in temperature may influence it. Therefore, a structural evaluation considering temperature changes is necessary. The evaluation of temperature influenced stress for the steel pipe frame is carried out, and the change to the cross section of elements that divide the length of its frame are used as measuring standards. Furthermore, debris flow may occur when the upstream side of the dam is not filled with deposited sediment. Therefore, the structural evaluation at the time of debris flow should be performed under both fully and not fully deposited sediment conditions, as shown in Figure 15.15.

The structural calculation verifies the stress intensity of each element, joint portion, and embedded pipe portion of the base concrete by calculating the element forces when the largest stress is working against the design external force and applying the ordinary allowable stress method to these element forces based on the elasticity theory [11]. Additionally, when the fluid force of the debris flow acts eccentrically against the structure, it is designed to be safe against these eccentric loads.

In addition to the evaluation of the dam elements against the design external forces, an evaluation of safety against collision by boulders or woody debris from the debris flow is also carried out, as shown in Table 15.3 (Figure 15.16).

The evaluation of the steel pipe elements against boulder collision is carried out through the mechanics

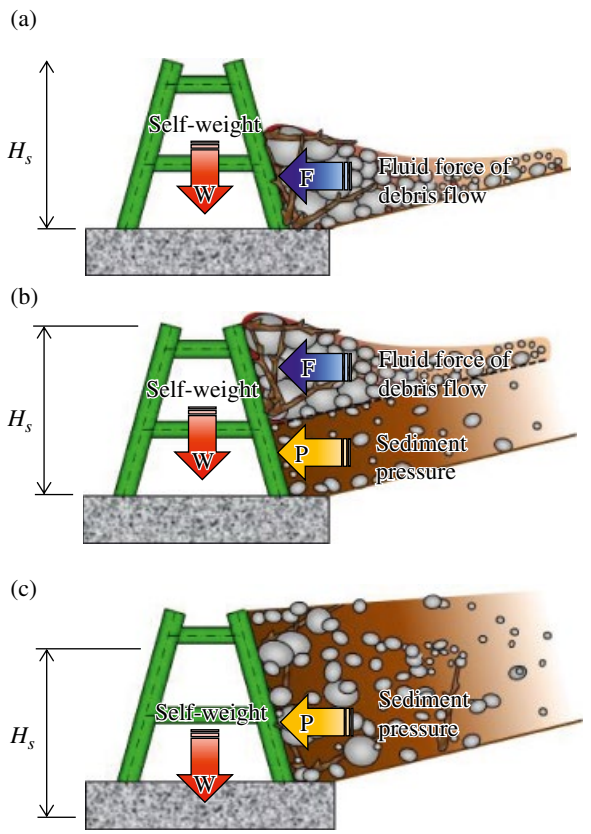

Figure 15.15 Design external forces for elements of open Sabo dam. (a) Debris flow [Non-full sediment]. (b) Debris flow [Full sediment]. (c) Full sediment.

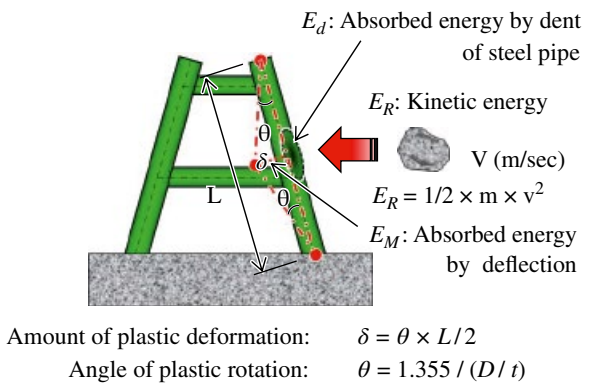

Figure 15.16 Design external forces.

@seismicisolation

of plasticity method, stating that one boulder with an expected maximum diameter will collide with the center portion of the element at the flow velocity of the debris flow, and the kinetic energy of the boulder at that time will be absorbed by the deformation of the steel pipe element. Here, the energy absorption by the steel pipe element is the sum of the dent deformation around the boulder collision point and the plastic deformation (beam deformation) of the element (*e.g.* [12]). Its safety evaluation calculation is expressed as

$$E_R \leq E_d + E_M \tag{15.4}$$

where E_R is the kinetic energy of the boulder, E_d is the absorption energy of the dent deformation of the steel pipe element, and E_M is the absorption energy by plastic deformation of the steel pipe element. As a premise, the kinetic energy of the boulder is fully transmitted, and no energy loss is caused by the collision.

15.4.4. Maintenance

When a steel pipe open Sabo dam is hit by boulders or driftwoods, it may be damaged. Because it is a structure that absorbs the impact force of boulders or driftwoods by the deformation of the entire structure or the local deformation of an element, the deformation itself does not directly become a safety issue of the structure. However, when the damage is significant, the functional reduction of the structure needs to be considered. Therefore, after the debris flow trapping, removal of boulders and woody debris, as well as structural inspections, need to be carried out to recover the dam's function and to evaluate and preserve its structural soundness. Subsequently, the repairing or reinforcement of elements needs to be carried out as necessary. Table 15.4 shows the criteria for repairing based on degree of damage. The soundness of the steel pipe elements was evaluated by the ratio (δ/D) of the dent δ against the steel pipe diameter D. When δ/D is over 40%, the elements are repaired, as shown in Figure 15.17.

Table 15.4 Element repair standards.

Damage level	Rate of dent deformation of steel pipe	Judgment
Level 1	Less than 10%	Healthy
Level 2	10–40%	Repair if necessary
Level 3	More than 40%	Repair, reinforcement or replacement

15.4.5. Debris Flow and Woody Debris Trapping Scenarios

Steel open Sabo dams trap many types of debris flows and woody debris, as shown in Figure 15.18, and their outstanding trapping effect has been widely reported. Based on past debris flow and woody debris trapping scenarios, they can be categorized into four types: (a) boulders + sediment [13], (b) boulders + woody debris + sediment, (c) woody debris + sediment, and (d) woody debris only [14], as shown in Figure 15.18. This shows that trapping results that include woody debris make up most of the trappings, meaning that the debris flow mostly includes woody debris. When taking into account the frequent woody debris disasters that have occurred in recent years, steel open Sabo dams with high woody debris trapping functions can be said to be an extremely effective structure to prevent sediment-related disasters, as shown in Figure 15.19.

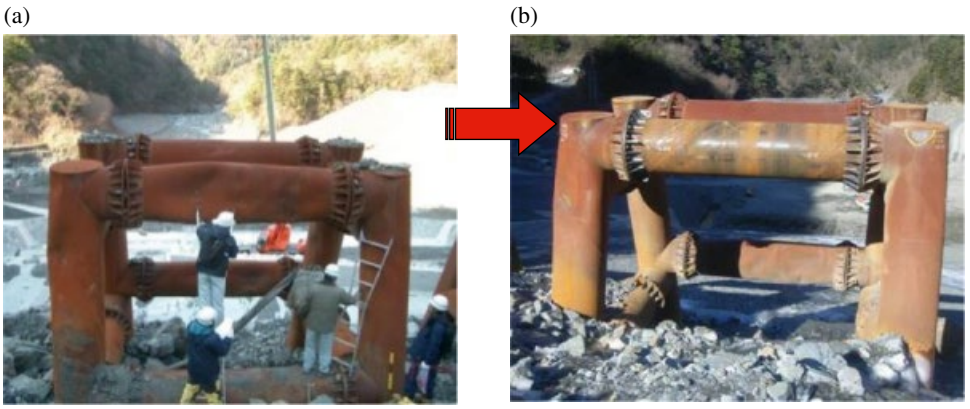

Figure 15.17 Maintenance – element replacement. (a) Element inspection. (b) Replacement.

@seismicisolation

Figure 15.18 Debris flow and woody debris scenarios. (a) Boulders + sediment. (b) Boulders + driftwood + sediment. (c) Driftwood + sediment. (d) Driftwood only.

Figure 15.19 Izu-Oshima Island, 2013.

15.5. CONCLUSIONS

This study examines steel-pipe open Sabo dams and their structure, design, and utilization. The reason steel material is used for Sabo structures, compared to other types of Sabo structures, is its many superb features, such as high material strength and tenacity, stability and uniformity in quality, easy on-site installation, short construction period, easy transportation, and environmental friendliness. Hence, it has been studied not only in Japan but also overseas for debris flow and woody debris trapping functionality, mountain stream ecosystem conservation, and high environmental load reduction effect [15, 16]. The actual debris flow trapping effect is also being recognized for the steel open Sabo dam. In recent years, there has been concern that the intensification of the debris flow, such as an increase in the occurrence frequency, change in the timing of the occurrence, or increase in scale of occurrence due to the increase in typhoon strength and influence of climate change. Therefore, we plan to conduct research and development on a new technology for steel pipe open Sabo dams and develop an application field to contribute to debris flow and sediment disaster prevention and mitigation.

REFERENCES

1. Marutani, T. Kaibori M, Jitousono T et al. (2017). Sediment-related disasters by a heavy rainfall in the northern part of Kyushu-Island, Japan in July 2017, *Journal of the Japan Society of Erosion Civil Engineer*, *70*(4), 31–42. DOI: https://doi.org/10.11475/sabo.70.4_Pict04_1.
2. Ministry of Land, Infrastructure Transport and Tourism, SABO department (2018a). Occurrence report sediment disaster due to torrential rain disaster in July 2018 (25th/Sep.). http://www.mlit.go.jp/river/sabo/jirei/h30dosha/H30_07gouu_180925.pdf.
3. Ministry of Land, Infrastructure Transport and Tourism, SABO department (2018b). The whole country sediment disaster occurrence report in 2018. http://www.mlit.go.jp/river/sabo/jirei/h30dosha/H3005dosyasaigai.pdf.
4. NILIM (2016a). Manual of Technical Standard for establishing Sabo plan for debris flow and driftwood, technical note of national institute for land and infrastructure management. National Institute for Land and Infrastructure Management, Ministry of Land, Infrastructure and Transport. No.904. http://www.nilim.go.jp/lab/bcg/siryou/tnn/tnn0904pdf/ks090402.pdf.
5. NILIM (2016b). Manual of Technical Standard for designing Sabo facilities against debris flow and driftwood, technical note of national institute for land and infrastructure management. National Institute for Land and Infrastructure Management, Ministry of Land, Infrastructure and Transport. No905. http://www.nilim.go.jp/lab/bcg/siryou/tnn/tnn0905pdf/ks090502.pdf
6. Tabata, S., Moriyama, H. (2010). History and futures assignment of technology for open type steel SABO dams, *Journal of the Japan Society of Erosion Control Engineering 62*(6), 47–51. DOI: https://doi.org/10.11475/sabo.62.6_47.
7. Horiguchi, T. and Katsuki, S. (2018). Load evaluation of debris flow against steel open Sabo dam using DEM. *Symposium Proceedings of the INTERPRAENENT 2018 in the Pacific Rim*, Toyama (1–4 October 2018), 228–235.

@seismicisolation

8. Horiguchi T. & Komatsu Y., (2018). Method to evaluate the effect of inclination angle of steel open type check dam on debris flow impact load, *International Journal of Protective structure*, *10*(1), 95–115. DOI: https://doi.org/10.1177/2041419618789702.
9. Research Association for Steel Sabo Structures (2005). Current of the evolving steel Sabo structures. *Journal for Civil Engineers 46* (6): 66–71.
10. Sabo & Landslide Technical Center (2009). Steel Sabo structure designing manual.
11. Hoshikawa, T., Ishikawa, N., Hikosaka, H., Abe S. (1995). Impact response displacement of fixed steel pipe beam considering local deformation and strain rate effect, *Journal of Japan Society Civil Engineering*, *513*(31), 101–115. DOI: https://doi.org/10.2208/ jscej.1995.513_101
12. Sonoda, Y., Tsuchiya, Y., Tamai H., Shima, J. (2016). A fundamental study on the load carrying capacity of steel frame check dam, Japan Society of Civil Engineer, *Journal of structural Engineering*, Vol. *62A*, 1019–1030. DOI: https://doi.org/10.11532/structcivil.62A.1030.
13. Horiguchi T., Richefeu V. (2020). Post-analysis simulation of the collapse of an open sabo dam of steel pipes subjected to boulder laden debris flow, *International Journal of Sediment Research 35*(6), 621–635, DOI: https://doi.org/10.1016/j.ijsrc.2020.05.002.
14. Horiguchi T., Katsuki S., Ishikawa N., Mizuyama T. (2019). Method for evaluating the trapping effects of woody debris using a distince element method, *International Journal of Erosion Control Engineering 12*(1), 1–12, DOI: https://doi.org/10.13101/ijece.12.1.
15. Kokuryo, H., Chen, S.C., An, S.P., and Wang, C. (2014a). A study on debris flow capture effect of open-type steel sabo dam in Taiwan. *Journal of the Japan Society of Erosion Control Engineering 67*(3): 36–42.
16. Kokuryo, H., Moriyama, H., Yamaguchi, M., et al. (2014b). Consideration on the high functionality of closed type concrete Sabo dam, Japan Society of Erosion Control Engineering Publication, (72), B242–243.

@seismicisolation

16

Determining the Optimal Distance of Check Dams, Case Study: Shirkuh River, Iran

Mohammad Ebrahim Banihabib[1], Ali Mohammadi[2], and Mahmoud Piri Ardakani[3]

16.1. INTRODUCTION

Check dams are used around the world in water and soil conservation project to control riverbed slopes and to stabilize rivers [1–3]. Determining the optimal distance of check dams has a leading role in minimizing the cost of the riverbed stabilization projects. Increasing the distance will reduce the number of check dams and ultimately reduce the cost for riverbed stabilization projects. In contrast, reducing the distance between check dams leads to an increase in the cost. Being buried under sedimentation is a long-term impact of short distance between check dams. The equilibrium slope of riverbeds represents their stable state; thus, it can be used to determine the distance between check dams. Methods of Simons and Albertson [4], Shields [5], Gessler [6], and Shields–Manning, Garde and Hasan [7] are important equations for determining the equilibrium slope, and the permitted velocity method also can be used to stabilize riverbed [8]. However, none of them has been used to determine the distance between check dams. Currently, there are several studies discussing the issues about predicting equilibrium bed slope, design of sediment traps, and determining the distance of check dams [9–12]. In this research, the possibility of using the theory of stable channels to determine the check dams' distance is investigated. The equations presented for stable channels are using the characteristics of flow and sediment. In Colorado, United States, Heede and Mufich [10] introduced an equation for distancing check dams, in which only the slope of the river plays a decisive role in determining the check dams distance. In the case of Heede and Mufich [10] equation, for slopes less than 20%, the equilibrium slope proposed 30% of the canal initial slope and for slopes greater than 20%, the equilibrium slope proposed 50% of the canal initial slope which is consistent with the trends observed in the fields and discussed in Piton and Recking [11]. The given Heede and Mufich equation can be used as a general rule to determine the distance between check dams [10].

16.2. MATERIAL AND METHODS

Shirkuh area is one of the mountainous regions of Yazd province, Iran. Floods cause significant damage to agricultural land and orchards, as well as roadsides along rivers, by eroding riverbeds and walls, every year. Determining the optimal distance of dams is important for maximum dam's cost efficiency as the check dams are crucial to stabilize riverbeds. There are more than 300 check dams in the Shirkuh river. Moreover, there are thousands check dams across Iran with almost similar conditions to Shirkuh River's check dams. This

[1] *Department of Water Engineering, College of Aburaihan, University of Tehran, Pakdasht, Iran*

[2] *Department of Water Engineering, College of Aburaihan, University of Tehran, Pakdasht, Iran*

[3] *Department of Rangeland and Watershed Management, Faculty of Natural Resources and Desert Studies, Yazd University, Yazd, Iran*

Check Dam Construction for Sustainable Watershed Management and Planning, First Edition.
Edited by Zhanbin Li, Peng Li, Yang Yu, Peng Shi, and Guillaume Piton.
© 2022 John Wiley & Sons, Inc. Published 2022 by John Wiley & Sons, Inc.

@seismicisolation

issue highlights the importance of check dams in Iran. In this study, data on the equilibrium slope of existing riverbeds between check dams in Shirkuh region were obtained through surveying. In this regard, the slope obtained from the previous stable channel equations can be compared with the observed equilibrium slope in the studied river reaches, and then average error (E) or relative mean error (RME) can be calculated through Equations (16.1) and (16.2):

$$E = \frac{\sum |S - S_c|}{N} \tag{16.1}$$

$$RME = \frac{\sum \left| \frac{S - S_c}{S} \right|}{N} \tag{16.2}$$

where E is the average error, S and S_c are the observation equilibrium slope and calculated equilibrium slope, respectively, N is the number of data, and RME is the relative mean error.

Based on data collected from India and Pakistan channels from 1930 to 1958, Lacey introduced following equations for equilibrium slope, Equation (16.3) [13]:

$$S_c = \frac{f}{\sqrt[6]{1830 \cdot Q}} \tag{16.3}$$

where Q is the discharge (ft^3/s), and f is the silt factor [14]. Simons and Albertson [4] categorized five types of channels 1–5. These channels are channels with: sandy riverbed and bank, sandy bed and adhesive bank, adhesive bed and bank, nonadhesive coarse materials, and adhesive bed river and bank but with a high suspended load (2000–8000 ppm), respectively. Simons and Albertson [4] proposed following equation for equilibrium slopes:

$$\frac{C^2}{g} = \frac{V^2}{g \cdot y \cdot S} = K_4 \left(\frac{V \cdot B}{v} \right)^{0.37} \tag{16.4}$$

where V is the velocity (ft/s), y is the water depth (m), C is the Chezy coefficient, g is the gravitational acceleration, and K_4 is the kinematic viscosity. B is the width of wet area (m) that can be considered equal to the width of the waterway for wide rivers in which the depth of the flow is less than the width of the river. Gessler's studies of particle motion showed that the line indicates the motion threshold in the Shields diagram that needs to be modified a bit, especially for a state where the flow is completely turbulent and the bed is rough. Therefore, based on this modification, the Shields parameter for $R_e^* > 400$ is equal to 0.047. R_e^* is the Reynolds number. Given the possibility of a stream or river tendency to form the armor layer, the equilibrium slope as the Equation (16.5) by considering the value of critical stress based on the diameter of 90% of the bed material (D_{90}) is determined by [6]:

$$S_c = \frac{0.047 \cdot (G_s - 1) \cdot D_{90}}{y} \tag{16.5}$$

where G_s is the sediment particles' density. The equilibrium slope is obtained from the following equation if the critical shear stress based on the Shields curve can be combined with the Manning equation:

$$S_c = \frac{\left(0.047 \cdot (G_s - 1) \cdot D_{90}\right)^{1.428}}{(n \cdot q)^{\frac{6}{7}}} \tag{16.6}$$

where q is the discharge in per unit width, and n is the Manning coefficient.

In many cases, the erosion process can be naturally stopped by the formation of armor or protective layer. This condition is possible in beds composed of sand and gravel materials. In this condition, D is considered equal to be D_{90} [15]. The permitted velocity can be used to determine the equilibrium slope for rivers if there is no cross-sectional change in the river reach. Furthermore, the flow can be considered uniform in the reach. The equilibrium slope in such conditions is calculated based on Equation (16.7):

$$S_c = \frac{(\alpha \cdot V)^{\frac{10}{3}} \cdot B^{\frac{4}{3}} \cdot n^2}{Q^{\frac{4}{3}}} \tag{16.7}$$

where α is the ratio of the average flow velocity in a waterway to the velocity of water at its bottom (this ratio is usually considered 1.3–1.5). In this study, two methods were tested to determine the permitted velocity in Equation (16.7):

A: The permitted velocity was determined using the average grain diameter. Then, through Equation (16.7) and the previously determined roughness coefficient, the equilibrium slope is calculated. Equation (16.7) was tested with K = 1.3 and K = 1.5 velocity coefficient, which K = 1.5 had less error.

@seismicisolation

B: Using the Equation (16.8), first the water depth was calculated, and then the water velocity was determined using flow continuity equation:

$$y = \left[\frac{12.9 \cdot Q^2 \cdot n^2}{B^2 \cdot D_{90}}\right]^{\frac{3}{7}} \tag{16.8}$$

Garde and Hasan [7] method is proposed if the river has reached the armoring condition and the river profile archives to equilibrium condition. It is assumed that the river profile does not change due to the achievement of the equilibrium condition in this method. In the Shields equation, the final shear stress (τ_{cf}) can be calculated from the following equation [14]:

$$\tau_{cf} = 0.05 \cdot (\gamma_s - \gamma) \cdot D_{50f} \tag{16.9}$$

where γ_s and γ are sediment- and water-specific weights, respectively.

The following equation is obtained by combining the Manning equation with the final shear stress. Here, the final shear stress means the shear stress in the equilibrium condition:

$$S_c = \left(\frac{1}{q \cdot n_f}\right)^{\frac{6}{7}} \cdot \left(\frac{\tau_{cf}}{\gamma}\right)^{\frac{10}{7}} \tag{16.10}$$

In the above equation, n_f is the final Manning coefficient of the river. Here, the final Manning coefficient means the Manning coefficient in the equilibrium condition.

In 1977 in Colorado State, United States, Heede and Mufich [10] provided an equation to distancing check dams as follows:

$$L = \frac{H}{K \cdot S_{init} \cdot cos\varnothing} \tag{16.11}$$

where L is the distance between two check dams, H is the effective height of the check dam, Ø is the angle of the riverbed with horizontal, and S_{init} is the slope of the river ($S_{init} = tan\varnothing$). K is also an empirical coefficient where $S_{init} \leq 0.2$, $K = 0.3$, and where $S_{init} \geq 0.2$, $K = 0.5$ are used. Therefore, Heede and Mufich [10] have proposed that if the slope is less than 20%, the equilibrium slope is 30% of the initial bed slope of the river, and if the bed slope is more than 20%, the equilibrium slope is 50% of the initial slope of the canal.

16.3. RESULTS

16.3.1. Examination of the Existing Equations to Determine the Equilibrium Slope

The equilibrium bed slope was calculated using the above equations. It is compared with the observed bed slope in examined river reaches between check dams which achieved equilibrium bed slope. This comparison is carried out for different flood peak flows (Figure 16.1). Then, the mean error and the relative mean error of the calculated equilibrium bed slope were computed using the calculated value with different equilibrium bed slope

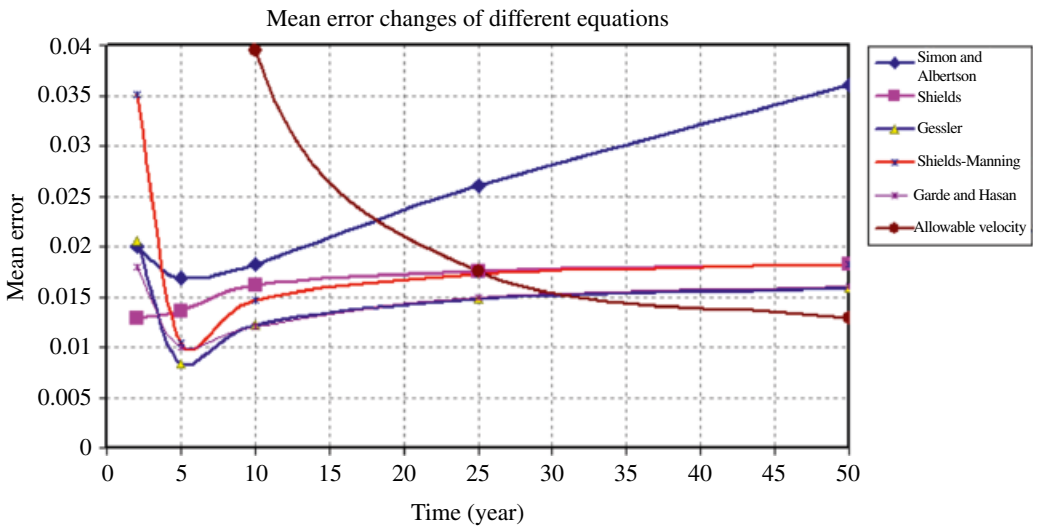

Figure 16.1 Mean error changes of different equations for various time return period of the discharge used in the computation.

@seismicisolation

equations and observed ones. The results showed that the appropriate discharge is the flood peak flow with five years return period for determining the equilibrium bed slope (Figure 16.1). The values of the mean error and the relative mean error were determined by examining the Garde and Hasan [7] equation, calculating the equilibrium slope of the river, and comparing it with the equilibrium slope of the observed stable river reaches. The results of this section also emphasized in desirability of five-year discharge for dams distancing. In addition, the mean error and relative mean error values were calculated based on the Heede and Mufich [10] equation, as shown in Table 16.1. The errors analysis indicates that the error of the Heede and Mufich equation is high. Therefore, the Heede and Mufich equation must be modified as it is earlier explained. The mean error and relative mean error values were calculated after the permitted velocity calculation. Results revealed that the discharge used in the permitted velocity equation with a return period of 50 years is more appropriate. Therefore, it is recommended to use this return period for determining the design discharge in the permitted velocity equation.

16.3.2. Modification of the Heede and Mufich Equation

According to the Heede and Mufich [10] recommendation, the value of K coefficient should be determined regarding the sediment size of the riverbed that has reached the equilibrium slope. In fact, a value should be suggested for study area and other areas with similar conditions. In this regard, the initial slope, the height of the dam, and the K value of the study area were calculated based on the longitudinal profile. This profile is obtained from the intervals where the dams were filled with sediment and upstream bed slope reached the equilibrium slope. Then, a regression is carried out between the parameters of S_{init} (initial slope), D_{90} (grain diameter that 90% of particles is equal to or less), D_{50} (median diameter of sediment particles), D_{50}/D_{90} ratio, and K_0 (determined based on field data), using SPSS software. Finally, four multivariate equations were obtained, as shown in Table 16.2. The mean error and the relative mean error values are shown in Table 16.3.

Table 16.1 Error values of Heede and Mufich equation.

Equation	Mean error	Relative mean error
Heede and Mufich	0.0123	0.555

Table 16.3 Error values of modification Heede and Mufich equation.

Type of error	Equation (16.12)	Equation (16.13)	Equation (16.14)	Equation (16.15)
Mean error	0.002 80	0.002 83	0.002 80	0.002 82
Relative mean error	0.11	0.111	0.111	0.109

16.4. CONCLUSION

1. The return period of design discharge is not defined in the equations proposed by Shields [5], Gessler [6], Garde and Hasan [7], and Simons and Albertson [4] for determining an equilibrium bed slope. Equations with discharge of different return period have been examined in this study, and the results showed that discharge with a return period of five year results the least error for determining the equilibrium bed slope.

2. In the equations examined to modify the K coefficient, the proposed Equation (16.15) is better than the other equation as it has the lowest error. Also, the equation is more appropriate and has acceptable accuracy. This equation requires less data. Thus, Equation

Table 16.2 Proposed equations for the modification factor of the Heede and Mufich equation.

Equation no.	The modified factor of the Heede and Mufich equation (K)	Correlaton coefficent
16.12	$K = 0.048\,775 \cdot S_{init} + 0.303\,882$	$R = 0.95$
16.13	$K = 0.049\,291 \cdot S_{init} + 0.015\,115 \frac{D_{50}}{D_{90}} + 0.2941$	$R = 0.951$
16.14	$K = 0.04939 \cdot S_{init} + 0.51 \frac{D_{50}}{D_{90}} - 0.00141 D_{50} + 0.29192$	$R = 0.952$
16.15	$K = 0.054672 \cdot S_{init} + 0.367236 \frac{D_{50}}{D_{90}} - 0.00424 D_{50} + 0.00129 D_{90} + 0.1805$	$R = 0.96$

@seismicisolation

(16.12) can be proposed to be used practically. To use Equation (16.12), the value of K coefficient can be determined by measuring the initial slope of the riverbed. Then the distance between the dams can be determined using the Heede and Mufich equation, the modified value of K coefficient from Equation (16.12).

3. The Gessler [6], Shields [5], Garde and Hasan [7], and Shields–Manning equations are equal in terms of the amount of required data and have no superiority to each other. However, Gessler equation has less error than other equations. Moreover, other equations are not recommended due to their high error.

4. The modified Heede and Mufich equation in this study has less error than the other equations. Therefore, this modified equation is recommended to optimal distancing of check dams.

ACKNOWLEDGMENT

This chapter was first written and submitted by Prof. Banihabib who unfortunately passed away in 2021. The second author and the editing team agreed to revise and publish it nevertheless to disseminate this last work. The chapter is dedicated to the memory of Prof. Banihabib.

REFERENCES

1. Abbasi, N.A., Xu, X., Lucas-Borja, M.E. et al. (2019). The use of check dams in watershed management projects: examples from around the World. *Science of the Total Environment 676*: 683–691.
2. Piton, G., Carladous, S., Recking, A. et al. (2017). Why do we build check dams in alpine streams? An historical perspective from the French experience. *Earth Surface Processes and Landforms 42* (1): 91–108.
3. Polyakov, V.O., Nichols, M.H., McClaran, M.P., and Nearing, M.A. (2014). Effect of check dams on runoff, sediment yield, and retention on small semiarid watersheds. *Journal of Soil and Water Conservation 69* (5): 414–421.
4. Simons, D. and Albertson, M. (1960). Uniform water conveyance channels in alluvial materials. *Journal of the Hydraulics Division 86* (5): 33–71.
5. Shields, A. (1936). Anwendung Der Aehnlichkeitsmechanik Und Der Turbulenzforschung Auf Die Geschiebebewegung. *Technology 26* (1): 26.
6. Gessler, J. (1970). Self-stabilizing tendencies of alluvial channels. *Journal of the Waterways, Harbors and Coastal Engineering Division 96* (2): 235–249.
7. Garde, R.J. and Hasan, S.M. (1967). Experimental investigation of degradation in alluvial channels. *Proceedings of the 12th Congress, International Association for Hydraulic Research Delft*, Netherlands (11–14 September 1967), 38–45.
8. Chang, H.H. (1992). *Fluvial Processes in River Engineering*. Krieger Publishing Company.
9. Ferro, V. and Porto, P. (2011). Predicting the equilibrium bed slope in natural streams using a stochastic model for incipient sediment motion. *Earth Surface Processes and Landforms 36* (8): 1007–1022.
10. Heede, B.H. and Mufich, J. (1977). Gully control structures and systems. In: *Guidelines for Watershed Management*, 181–220.
11. Piton G, Recking A. 2016. Design of sediment traps with open check dams. I: hydraulic and deposition processes. *Journal of Hydraulic Engineering 142*: 07016009. DOI: https://doi.org/10.1061/(ASCE)HY.1943-7900.0001207.
12. Porto, P. and Gessler, J. (1999). Ultimate bed slope in calabrian streams upstream of check dams: field study. *Journal of Hydraulic Engineering 125* (12): 1231–1242.
13. Lacey, G. (1930). Stable channels in alluvium (includes appendices). *Minutes of the Proceedings of the Institution of Civil Engineers 229* (1930): 259–292. DOI: https://doi.org/10.1680/imotp.1930.15592
14. Geyik, M.P. (1986). FAO watershed management field manual - gully control. http://www.fao.org/docrep/006/AD082E/AD082e00.htm#cont (accessed 6 May 2022).
15. Bahadori, F. (1995). River bed control methods. *Proceedings of the Hydraulic Association*, Iran (11 June 1995).

@seismicisolation

INDEX

Abhandlung von den Überschwemmungen in Tyrol, 235
access track, 254, 255, 259, 260
active mitigation measures, 240
adaptation (of a structure), 241, 254, 259
additional allowance thickness, 290
afforestation, 8, 34, 236
amount of plastic deformation, 292
angle of plastic rotation, 292
antierosion, 47
arch, 237, 257, 289
average infiltration depths, 99

backbone dams, 11
bank reinforcements, 247, 250
barrier backwater, 240, 254
barrier self-cleaning, 237, 262
bedload transport, 240, 254, 262, 287
Beiluo River, 74
Beitagou, 16
bidding contract system, 20
body responsible, 19
buffer effect, 240, 247, 254, 261
burst time, 173

^{137}Cs, 55
capacity equilibrium degree, 217
cascade check dam, 278, 280
Cascade Modes, 49
catchments with check dams, 91
catchments without check dams, 102
cavitation damage, 155
cavitation erosion, 147
cavitation number, 160
cellar, 189
Chabagou, 78
change process of energy, 103
channel bank expansion, 23
channel bed roughness, 100
Channel Connectivity, 19
channel erosion, 24, 103, 192
channel morphology, 100
channel network, 95
channel shape, 28, 38, 91
channel straightening, 247–249
channels, 18
check dam crest, 247
check dam damage, 80
check-dam managed streams, 247
check land for farmland, 141
China seismic intensity scale, 180
clay, 11
closed Sabo dam, 285
coarse sediment area, 190
coefficient of variation, 101
collapse mechanism, 141
combined use of water resources, 189
composite foundation for dams, 280
comprehensive level, 185
comprehensive risk, 183
computer-aided design system, 20
concrete, 31, 237
connected nodes, 29
consistency test, 218
consolidation, 11
consolidation check dams, 245–249
construction supervision system, 20
construction unevenness, 160
controlling flooding, 102
convergence node, 41
conveyance, 240
corrosion allowance thickness, 290
criterion layer, 178
critical peak discharge, 276
cross sections, 103, 128
culvert, 143
cutting a slit, 263

D_{50}, 44
daily management risk, 210
Dali River, 74
dam breach, 142, 177, 181, 184
dam breach warning time, 181
dam-cellar water storage project, 203, 208
dam damage, 80
dam-dominated block, 138
dam expansion, 130
dam field, 9, 23
dam sediment couplet soil, 53, 56, 61
dam system, 3
dam system layout evaluation, 217
dammed farmland, 41
danger event, 255
dead gourd dams, 13
debris basins, 253, 276
debris flood, xii
debris flow basin, 276, 280–282
debris flow section, 286, 287, 291
debris flows, 237, 246, 253, 273, 285
deflection, 240
deposition, 6
deposition basin, 240, 254, 255, 280, 282
design criterion, 178
designed storage capacity, 119, 127
design event, 242, 255, 273, 291
design standard, 7, 13, 78, 143, 197, 203, 206, 241, 275
design standards of engineering, 276
design standards of the control measures, 275
detain floods, 24, 38
detention efficiency, 123, 124, 126
development history, 146
dikes, 254, 255, 258, 264, 265, 268
direct sedimentation efficiency, 127
discharge capacity, 82
discharge structure, 14
diversion, 138
diversion pipe, 204, 205
dosing, 237
downstream branch, 107
downstream economic losses, 180
downstream economic risk, 210
downward erosion, 23
drainage channel, 159, 160, 282
drainage facility damage, 178
drainage threshold, 282
dredging cost, 253, 258, 259, 263
drinking water, 18

Check Dam Construction for Sustainable Watershed Management and Planning, First Edition.
Edited by Zhanbin Li, Peng Li, Yang Yu, Peng Shi, and Guillaume Piton.
© 2022 John Wiley & Sons, Inc. Published 2022 by John Wiley & Sons, Inc.

@seismicisolation

drought resistant and moisture-preserving farming techniques, 189
drought-tolerant crops, 189
dry stone masonry, 237
Duile, Josef, 235
dynamic emergency management, 185

earthquake disaster, 178
ecological environment risk, 180
ecology-ecological soundness, 221
economic risk, 178, 180, 185
efficacy/efficiency, 6, 123, 127, 297
emergency risk, 187
emergency warning, 178
energy dissipation well, 147
engineering risk, 178, 184, 186
ensure flood control, 222
environment risk, 179, 185, 186
equilibrium bed level, 247
eroded sediment, 58
erosion base level, 58, 132, 142, 186, 279
erosion/deposition mass, 132
erosion dynamic, 91
erosion modulus, 8
erosion rainfall, 57, 58
erosion reduction, 33
erosion sediment, 53
erosive rainfall, 43
evaluation index system, 186
excavated lateral basin, 265
excavated material, 259
excess flood, 179
excessive rainfall, 145
extreme rainstorm, 38

Fabre, Jean Antoine, 235
failure (of a structure), 63, 117, 141, 177, 186, 210, 237, 255
Fen River, 191, 193
Fengjiachagou, 143
field investigation, 83
field ONF-RTM officers, 253
filtration, 240
fine sand, 41, 43, 48, 56
fingerprint, 53
fish farming, 189
flat arable land, 189
flood control capacity, 13
flood control risks, 177, 184, 213
flood control safety, 177, 219, 222
flood detention, 25
flood detention and silt retention, 141
flood detention risk, 210
flood disaster, 141
flood discharge risk, 209
flood discharge tunnel, 160
flood lag time, 27
flood peak, 12
flood risk, 169
flood severity, 181
flood simulation, 97
flood storage coefficient, 210
flood storage risk coefficient, 210
flow pattern, 103
flow spreading, 254
flow velocity distribution, 156, 160–162
flowing down section, 286
fluid force of debris flow, 291, 292
flume experiment, 289
flushing, 249
forest-shrub land, 58, 63–65
fractal dimension, 41
full-body check dams, 245
full storage capacity, 105
fully silted check dams, 194, 197, 198
furrow irrigation, 201
fuzzy analytic hierarchy, 177, 181
fuzzy theory, 181

Gaoshegou, 78, 80, 86
Graham method, 181
graphic processing unit (GPU), 93, 94
grass planting, 34, 203
grassland, 10
gravel and sand, 43
gravitational erosion, 23
gravity wall, 237
Guandigou, 16
gully erosion, 58
gully walls, 54, 57, 62, 68

Handbook of watershed hydrology calculation, 277
hazard coefficient, 209
headwater, 91
heavy rain, 77
heavy silting stage, 118
Hejiagou, 78
high-efficiency agriculture, 198
highlight project, 24
hillslope consolidation, 247
hole irrigation, 201
Hongchun Gully, 274, 275
Hongqi Reservoir, 146
Hongshishaigou, 145
horizontal bars and a basal slot, 238, 257, 263
horizontal pipes, 48, 203, 204
horizontal terraces, 33
horizontal tube, 148, 204, 205
Huangbaigou, 16
Huangfuchuan, 77
hungry water effect, 246
hydraulic control, 255, 268
hydraulic filling method, 77
hydraulic radius, 28, 29, 103, 105, 109
hydraulic slope, 109
hydrodynamic parameters, 93, 108
hydrological forecasting, 185
hydrostatic pressure, 93, 238

impact force, 278
in-channel structures, 35, 37
incision, 253, 274
index layer, 178, 209, 210, 212
indicator weight, 181, 182, 184
indirect erosion reduction efficiency, 127, 129, 132
individual-transport, 286
infiltration rates, 25
infiltration volume, 26
InHM, 118
initial bed slope, 247, 299
inlet hole shapes, 159
inorganic colloid, 48
instability coefficient, 209
intercept sediment, 23
intertwining of boulders, 288
interval between pillars, 288
interval of beams, 288
irrigation, 14

Jialu River, 191, 193
Jinghe River, 74, 191
Jiuyuangou, 5
Jiuyuangou dam system, 9, 12, 77

Kanghegou, 8
key dam, 8
Kuye River, 191, 193

landslide, 246, 273
large check dam, 7
large sand, 53
lateral connectivity, 250
Lichtenhahn, 238
light silting stage, 118
Lijiazhai, 27
limit equilibrium method, 163
Linjian, 78, 86
Liujiawa and Wangjiamao in Fugu County, 143

@seismicisolation

Liushugou, 78, 86
livestock breeding, 206
Loess hilly and gully areas, 11, 13, 74
the Loess Plateau Check Dam Project, 23
Loess Plateau World Bank Loan Project, 23
longitudinal connectivity, 95, 247, 249, 250
long-term regulatory effects, 38
loss of life, 181
low design standard, 16
Luo River, 191
Luoyugou, 72

Madizui, 16
magnitude, 16
main channel, 51
maintenance, 66
Majiagou, 69
malfunctions, 253
Maliangou, 18
management risks, 179, 184, 186
management system, 4
masonry dams, 274
mass-transport, 286
maximum discharges, 8, 12
mechanical control, 255, 268
medium check dam, 14
Mianyuan River, 273, 275, 280
microspray irrigation, 201
middle channel, 105, 106
middle of the dam, 42, 45, 57
Ming and Qing Dynasty, 4
mitigation engineering construction, 275
mobile pumping station, 201
monitoring risk, 210
morphology, 100
multivariate analysis, 163

Nachrichten von den Eisbergen in Tyrol, 235
Nash efficiency factor, 25, 97, 122
natural accumulation, 4
needed structural thickness, 290
Nianyangou, 166
normative construction stage, 146
numerical simulation method, 141

obstructive nodes, 29
occurring section, 286
one-dam-and-one-pond project, 205, 208
ONF-RTM, 253
ONR technical standards Series 248xx, 241
on-site, 8, 10, 289, 294
onsite survey, 184
open channel, 282
open check dams, 238
open Sabo dams, 265
operation and management mechanism, 19
organic colloid, 48
outburst of collapsed accumulation, 274
Overflow Weir Treatment, 94
over-standard storm flood, 144
over-topping collapse, 141

parameter, 27
passive measures, 239
peak cutting, 123, 124, 186
peak cutting flood detention, 186
peak discharge, 29
peak discharge lag time, 99
peak location, 92, 93
peak-shaving, 123, 126
Peijiamao, 27
perimeter hydraulic engineering, 236
personnel on duty, 178, 182
piling up section, 286, 287
point estimation method, 142
point irrigation, 201
pond, 189
poor construction quality, 143, 146, 174
poor slope management, 144, 145, 174
population at risk, 181
potential energy, 103, 104, 109
potential operation risks, 186
poultry farming, 206
primary or secondary pumping, 198
primary reservoir, 200
primary risk, 183, 184
project legal person responsibility system, 20
proportion of large dams, 217, 218
protected elements, 258
PSD analysis, 42

Qingjian River, 191, 193
qualitative analysis, 163

rainfall frequency, 177
rain-flood events, 117, 122
"7.15" rainstorm, 110
rainstorm calculation method, 277
rainstorm flood, 82
real-time risk assessment, 142
recreational fishing, 206
regression analysis, 47
remaining storage capacity, 15
removal of flow obstructions, 247
replacement, 293
RESCDAM method, 181
retaining wall, 274, 282
retention, 5, 10, 23, 29, 79, 83, 118, 144, 229, 240, 245, 254
retrogressive erosion, 23
rich and coarse sediment area, 190, 191, 197, 200
rich sediment areas, 190
risk assessment, 142
risk assessment index system, 177, 178, 185
risk calculation, 183
risk damage, 185
risk index, 178
risk level, 179, 184
risk-level division, 212
risk-level standard, 184
risk loss rate, 187
risk score, 212
risk value, 177
river damming, 279
routine event, 255
runoff characteristics, 7
runoff coefficient, 27
runoff depth, 27
runoff ending time, 99, 100
runoff erosion power, 24
runoff impoundment, 99
runoff kinetic energy, 104
runoff lag time, 99, 111
runoff process, 24
runoff shear stress, 27
runoff velocity, 42
runoff volumes, 5

Sabo dams, 285, 286
safety-check event, 255, 268
safety distribution, 209
safety factor, 145
safety stability, 163
Saint-Martin torrent, 254, 259, 262, 263
sand blocking effect, 82
sand-rich areas, 12, 13
sandy loam, 43
Sanyanyu Gully, 274
saturated hydraulic conductivity, 26
scale development stage, 146–147
scour hole, 246–248, 281, 282
scouring protection, 254

@seismicisolation

Seckendorff, 236, 237
secondary reservoir, 200
secondary risk, 183, 184
sediment balance, 120
sediment carrying capacity, 83, 276
sediment connectivity, 112, 238, 245, 257
sediment flux, 120
sediment interception efficiency, 120
sediment pressure, 291, 292
sediment redistribution, 41
sediment retention, 5
sediment sources, 38
sediment storage capacity, 13, 15
sediment transport modulus, 27
sediment trapping efficiency, 120, 127, 128
sediment traps, 253
sedimentary wedge, 246–250
sedimentation process mainly, 136
sediment-retaining effect, 118
seepage failure, 141
self-pressure, 200, 201
self-weight, 291, 292
series rate, 217, 218
shaft, 29
shallow water equations, 93
sharp reduction, 105
Shuiyangou, 78, 80, 86
side effect, 257, 266
Sidizui, 16
silt and clay, 41
silt area design, 217, 218
silt loam, 43
silt soil, 43
siltation-erosion-silting, 136
siltation situation, 31
siltation storage capacity, 15
siltation thickness, 14, 138
silting and reclaiming land, 189
silting scenario, 119
simulating the hydrodynamic process, 103
simulation, 66
slit barrier, 254
slit dam, 257
slope (of deposition), 257
slope break, 254, 255, 264, 267
slope engineering measures, 33
slope land, 43
slope stability, 163, 164, 186, 274, 279
sloping farmland, 26
slot barrier, 257, 265
slot dam, 257
small check dam, 4
small-diameter steel pipe piles, 280, 281
small tube irrigation, 201
small watershed, 3
social economy, 178
soil aggregates, 41
soil and water conservation, 3
soil and water conservation stations, 5, 6
soil and water loss, 56, 70, 72
soil degradation, 45
soil erodibility, 24, 41, 46, 47
soil erosion, 41, 43
soil from the sediment source area, 53
soil infiltration, 25
soil nutrient loss, 65
soil organic carbon (SOC), 46
soil particle, 41
soil particle composition, 41, 43
soil sedimentation, 51
soil texture, 25
Soil & Water Assessment Tool (SWAT), 24
soil water content, 46, 58, 164
solid transport regulation areas, 256
sorting, 43
source-sink, 53
spatial distribution, 38
spillway, 5, 13, 24, 48, 77, 118, 144, 255, 291
spontaneous construction, 146
stability analysis, 163
stabilization, 23, 91, 240, 245, 257, 277, 279, 297
starvation (of sediment), 257, 269
steel pipe minimum thickness, 290
steel pipe open dam, 298
steep channels, 113, 236, 245, 256, 280, 285
storage and seeding in parallel, 13
storage capacities, 38
storage capacity threshold, 123, 124, 126
stored water, 99
structure analysis, 292–293
successive blocking measures, 278
Suide Water Conservation Station, 145
supplement groundwater, 34
surface-stored water, 98

tailwater, 117
Tao Ke, 5
target layer, 178
Telagou, 56, 58
temporal and spatial distribution, 53
terraced fields, 9
time-averaged pressure, 156
time dimension, 197
TOC, 54
torrent control, 235, 248, 258
torrential barriers, 235
total volume, 273
traction section, 286, 287
transformation, 29
transport capacity, 93, 128, 136, 240, 254, 276
transportation and sedimentation, 43
trapping boulder, 257, 287, 288
trapping capacity, 255, 286
trapping large driftwood, 287
Treatment of the Yellow River, 4
Tuwei River, 191, 193

uplift of the dam, 120

vegetation types, 41
vertical connectivity, 250

Walcher, Joseph, 235, 236
wall pressure distribution, 156
Wangjiage Cave, 4
Wangjiagou, 73
Wangmaogou Watershed, 66
Wangtagou, 16
warning ability, 186
warping dam systems, 177
WaTEM-SEDEM model, 38
water and soil conservation, 23
water and soil loss, 45
water and soil resources, 23
water cellar, 189
water damage, 7
water depth distribution, 160
water diversion irrigation, 14
water lifting facility, 200
water-lifting pump station, 200, 201
water regulation and storage project, 198
water resources, 3
water-retaining effect, 118
water–sand process, 120
water saving, 222
water-saving irrigation, 198
water source project, 200
waterlogging pond, 189
Wei River, 191

@seismicisolation

Wenchuan earthquake area, 273
Wenjia Gully, 273
Western Zhou Dynasty, 4
wooden crib walls, 237
woody debris, 237, 240, 246, 254, 258, 285
Wuding River, 35

Xiangtagou, 27
Xiaogangjian Gully, 278
Xiaohaizi reservoir, 142
Xiaqiaogou, 78
Xiheidai Small Watershed, 9
Xiyanguo, 86

Yanhe River, 66
Yellow River, 3
the Yellow River Soil and Water Conservation Ecological Project, 23
yield ensuring risk, 210
Yuanzigou, 53

Zallinger zum Thurn, Franz Seraphin von, 235
zero deposit and lump sum, 141
Zhaizimao, 53
Zhaojiajian, 143
Zhejiagou, 80
Zhuanglang County, 9

@seismicisolation